

CRANFIELD UNIVERSITY

Costas Velis B.Sc., M.Sc., DIC, GradMCIWM, AMInstP

SOLID RECOVERED FUEL PRODUCTION THROUGH THE
MECHANICAL-BIOLOGICAL TREATMENT OF WASTES

SCHOOL OF APPLIED SCIENCES

Ph.D. THESIS

CRANFIELD UNIVERSITY

SCHOOL OF APPLIED SCIENCES

Ph.D. THESIS

Academic Year 2009-2010

Costas Velis

Solid recovered fuel production through the mechanical-biological treatment of
wastes

Supervisor: S J T Pollard

February 2010

This thesis is submitted in partial fulfilment of the requirements for the degree of
Doctor of Philosophy

©Cranfield University 2009. All rights reserved. No part of the publication may
be produced without written permission of the copyright owner

To my beloved parents, Thanasi and Lola

Abstract

This thesis is concerned with the production of solid recovered fuel (SRF) from municipal solid waste using mechanical biological treatment (MBT) plants. It describes the first in-depth analysis of a UK MBT plant and addresses the fundamental research question:

are MBT plants and their unit operations optimised to produce high quality SRF in the UK?

A critical review of the process science and engineering of MBT provides timely insights into the quality management and standardisation of SRF use in Europe. Quantitative fuel property data for European SRFs are collated and analysed statistically in a detailed examination of the fuel quality achievable from MBT-derived SRF.

The experimental research herein applies statistical sampling, analytical characterisation and materials flow analysis to a new generation, fully operational SRF-producing MBT plant. To the author's knowledge, this is the first detailed analysis of this kind for a UK plant. Individual process flows from mechanically processed waste are characterised using a series of fuel properties in line with the European product standards for SRF, and confidence limits in these properties quantified. New data on SRF quality, including biogenic content, is provided. In seeking to understand the variability in waste heterogeneity and its impact on SRF production in an MBT plant, material flow analysis is applied across the MBT flowsheet to compute transfer coefficients for individual unit operations. This provides a basis for critically evaluating the performance of this specific MBT and the extent to which it is optimised for SRF production.

Among the trace metal contaminants in SRF, Cu and Pb show the highest potential to exceed established criteria (upper 75% of medians: 448 mg kg_d^{-1} and 208 mg kg_d^{-1} respectively). For UK-produced SRF, the biogenic content, calculated on a dry ash-free basis, was $55.5 \pm 2.7\% \text{ w/w}_{\text{daf}}$, meeting the minimum operational requirement set by cement operators seeking to utilise SRF. The net calorific value, quantified on as-received basis, approximates to European class 3 and 4 ($17.5 \pm 1.8 \text{ MJ kg}_{\text{ar}}^{-1}$) and may be insufficient for primary firing in cement kilns. However, the total chlorine content, estimated on a dry basis ($0.71 \pm 0.06\% \text{ w/w}_d$) can be tolerated by most thermal recovery applications.

The UK MBT plant evaluated is well optimised. The transfer coefficients (TC) for the SRF processing section of the plant demonstrate most of the combustible materials are concentrated in the SRF product. The bulk of the plastics are incorporated into the SRF (TC: 92.3%). A considerable portion of the chlorine load is also transported to the SRF (TC: 78.9%), with plastics, along with shoes, contributing considerably. The plant is slightly less effective in concentrating the paper in the SRF (TC dry basis: 80.0%), with the residual paper not gaining sufficient lift in the air classifier (TC to heavy air classifier output, as-received: $18.1 \pm 5.0\%$). The process implications of these findings are discussed with a view to the modest improvements that could optimise the plant further.

The thesis concludes that both European and UK MBT plant are capable of producing SRF to a performance standard close to the specified quality standards for most fuel properties. This is significant step forward for the UK which has recently struggled to achieve this outcome because of poor waste segregation. There remains a requirement for an improved understanding of what constitutes suitable quality for each thermal recovery option within the alternative fuels market.

The extensive dataset reported in this thesis is of value to SRF producers, users and regulators. Specific outcomes from this research include the ability to predict MBT-derived SRF quality, the opportunity to inform the better design of future MBT plants, and the generation of unique quantitative input for material flow evaluations at similarly configured MBT plants.

Costas Velis, 20th October, 2009

Acknowledgements

“Our words are the children of many people” George Seferis

I would lie if I claimed I could even just list here all the people that have in one way or another contributed to this piece of research. Not even those whose contribution proved critical. And if I miss anyone this very last moment of panic, be assured that they enjoy my life-long gratitude.

In the hard years of Cranfield I was fortunate to enjoy the insightful guidance, positive feedback and endless drive of my supervisor Prof. Simon Pollard, Head of Sustainable Systems – Simon thank you, without your decisiveness and focus this would have never progressed that far. Dr Phil Longhurst, Head of Centre for Resource Management and Efficiency, has been a constant source of wise advice, always supportive and with the most kind and effective open doors policy I have ever seen - Phil, your intervention in critical moments has saved the situation, thank you so much for the never-ending encouragement, the mild negotiation capability and and... I am also grateful to my initial supervisor, Dr Richard Smith, for selecting and trusting me in what proved a more than challenging piece of work. Cranfield personnel were just more than fabulous. This thesis would have never taken shape without the inspired problem solving of Deborah Hiscock IT trainer and the limitless help on every possible level of Heather Woodfield: cannot thank you enough. In the labs, the contribution of Jane Hubble, Maria Biskupska, Paul Barton, Rukhsana Ormesher, and that of the lab managers Dr Richard Andrews and Dr Keith Richards was critical, both in terms of practical work and willingness to share their precious time and expertise. Tony Parker, Ian Seymour if I was your line manager I would have doubled your remuneration next hour – thanks so much for always delivering solutions irrespective of how troublesome or impossible they seemed. Edna Holliday, Delia Parker, Rebecca Roy and Jess Greenwood, many thanks for all the help with the orders. Energy Technology Centre

led by Prof John Oakey has provided important support in moments of need: thanks to Dr Nigel Simms, and to Buz. All the personnel of the Centre of Resource Management and Efficiency, for the humane, friendly, always accommodating attitude. The university services, all the fantastic people in Library from Sharon Hinton in the inter-library loans, to Tricia, Heidi Smart, Morag Llewellyn, Cathy Carr, Emma Turner... Ms Pat Bellamy, for essential support in statistics and for laughing at everything. Cranfield Security, Tony and every single one of you guys there, it was great knowing that if I ever collapsed at the Fedden container you would be there to save me. Thanks for the good mood, on every encounter. Melanie Severin, for tolerating my unrealistic work demands and delivering under pressure. Outside Cranfield a series of people and organisations made this work feasible. Deep thanks to the management of the waste company running the UK MBT plant for offering the seldom opportunity to do real-life research on a hot topic. Manager and Deputy Manager at the MBT plant your input was critical, despite the hardship of a waste treatment plant – thanks for tolerating my endless requests for assistance. The plant personnel for conducting the sampling in spite of the difficult conditions. Prof. Ing. Susanne Rotter for kindly hosting and training me on SRF characterisation at the Technical University of Berlin, providing time and technical guidance, and sharing expertise without wanting anything in return: Susanne, thanks for all this valuable openness – thank you. Also all the fantastic people I met there: Flo, Perrine, Anne-Katrine. The other critical training week was at WRc, where Dr Any Godley and Jane Tyrrel offered their knowledge, expertise, and good friendly working atmosphere and access to waste characterisation facilities Similarly Tina Onu, and Simon. All the friends for life I have made in the PhD room Roland, Brian, Gareth, Angus, Alsi, Mirka, and and... My very Cranfield people for all the good and bad times we had together, Giorgio, Adina, Katerina, Dimitri, Kwsta, Petro, our CSA president Mina. Tens of academics and researchers all over the world who shared their expertise, provided advice, directed me to solutions, or encouraged me and supported

me in tough times, and were source of hope and inspiration. Particular thanks to Prof. David Wilson for all the great qualities he has been constantly bringing in our collaboration and Dr Chris Cheeseman at Imperial College for training and getting me deep into waste. Last but not least, my former supervisor Prof. Costas Helmis, Head of School of Physics at the University of Athens who insightfully directed me to the seemingly plain, yet exciting world of waste. For my parents the least I can say is that I owe them all I might have achieved.

Table of Contents

Abstract.....	vii
Acknowledgements.....	ix
List of Figures.....	xvii
List of Tables.....	xxxiii
ABBREVIATIONS.....	xxxix
GLOSSARY: REFERENCE GUIDE.....	xliv
1 INTRODUCTION.....	1
1.1 Waste management and sustainable resource management.....	2
1.2 Advent of MBT plants.....	3
1.3 Sustainable resource management and MBT plants.....	4
2 LITERATURE REVIEW.....	11
2.1 MBT characteristics, classification and design objectives.....	12
2.2 Mechanical processing for MBT.....	15
2.2.1 The role and objectives of mechanical unit operations.....	16
2.2.2 Waste characterisation for mechanical processing.....	17
2.3 Comminution processes.....	23
2.3.1 Size reduction in MBT plants.....	24
2.3.2 Process control and performance of comminution processes.....	25
2.3.3 Hammermill shredder.....	28
2.3.4 Rotary shear.....	31
2.3.5 Flail mill.....	32
2.3.6 Cascade/ball mill.....	33
2.3.7 Other comminution processes.....	35
2.3.8 Comparison of PSDs of comminution processes.....	36
2.4 Classification and separation.....	37
2.4.1 Function of classification and separation operation units.....	37
2.4.2 Separation and classification processes in MBT plants.....	38
2.4.3 Performance evaluation of classification and separation processes ..	39
2.4.4 Performance of separation and classification units for RDF/SRF	
production.....	52
2.4.5 Mechanical processing overview.....	93
2.5 RDF/SRF quality management initiatives.....	94
2.5.1 Importance of quality management for RDF/SRF marketability.....	94
2.5.2 Standards and quality assurance/control for RDF/SRF.....	98
2.5.3 SRF classification and specification by CEN.....	104
2.5.4 SRF product quality standards for specific end-uses.....	106
2.6 Statistics for SRF quality.....	127
2.6.1 Statistics for solid waste and SRF properties.....	127
2.6.2 Plant production quality control.....	129
2.6.3 Compliance statistics.....	132
2.6.4 CEN approach to SRF classification and specification compliance....	
.....	134
2.6.5 Compliance rules for end-user SRF specifications.....	138
2.7 Literature review summary.....	139

2.7.1	Appropriate descriptors for evaluating unit process operations	139
2.7.2	Performance of process units and implications for output quality and MBT design	140
2.7.3	SRF quality management	141
3	AIM AND OBJECTIVES	143
3.1	Knowledge gaps	144
3.2	Research aim	145
3.3	PhD research question.....	145
3.4	PhD objectives	145
4	METHODOLOGY	147
4.1	Methodology overview	147
4.2	Description of the UK MBT plant A.....	149
4.3	Variability in waste-related properties measurement.....	154
4.4	Material flow analysis (MFA) for MBT plants - general.....	155
4.5	Selection of properties (goods/substances) to be determined	158
4.6	Sampling plans	165
4.6.1	Sampling plan for an MBT plant according to the theory of sampling (ToS)	165
4.6.2	Sampling plan for UK MBT plant A – an example ToS application	166
4.7	Sample preparation and sub-sampling.....	174
4.8	Material composition of MBT plant flows by manual sorting.....	177
4.9	UK MBT plant A: material flow analysis	188
4.9.1	UK MBT plant A: mass balance model	189
4.9.2	UK MBT plant A: material component balances	196
4.9.3	UK MBT plant A: balances of fuel properties: mass-based specific loads	204
4.10	UK MBT plant A: transfer coefficients of unit operations	204
4.11	Methodology: UK MBT plant A: simulation of SRF properties.....	205
4.12	Computations and statistical analysis	207
4.12.1	Statistics computed and evaluation of compliance for results/discussion sections.....	207
4.13	Measurement of physical/chemical properties	219
4.13.1	Moisture content (M)	219
4.13.2	Ash content (A)	222
4.13.3	Total carbon, nitrogen and hydrogen content	224
4.13.4	Calorific (heating) value	226
4.13.5	Biogenic content by selective dissolution.....	228
4.13.6	Total chlorine content.....	233
5	RESULTS.....	237
5.1	European MBT-derived SRF: statistical overview of quality.....	238
5.2	UK MBT plant A: material composition and characterisation of flows	245
5.2.1	UK MBT plant A: overview of material composition of flows	246
5.2.2	UK MBT plant A: biodried material characterisation	248
5.2.3	UK MBT plant A: oversized heavy rejects characterisation	254
5.2.4	UK MBT plant A: SRF material characterisation.....	257
5.3	UK MBT plant A: material flow analysis (balances of mass, waste components and fuel properties)	260

5.3.1	UK MBT plant A: mass balance model	261
5.3.2	UK MBT plant A: material component balances	269
5.3.3	UK MBT plant A: balance of fuel properties: mass-based specific loads	296
5.4	UK MBT plant A: transfer coefficients of unit operations	303
5.5	UK MBT plant A: simulation of SRF properties	308
5.5.1	UK MBT plant A: concentrations and specific loads per waste component	309
5.5.2	UK MBT plant A: simulation of SRF moisture content	313
5.5.3	UK MBT plant A: simulation of SRF total chlorine content.....	314
5.5.4	UK MBT plant A: simulation of SRF ash content	316
5.5.5	UK MBT plant A: simulation of SRF net calorific value	318
5.5.6	UK MBT plant A: summary of SRF properties simulation	319
5.6	UK MBT plant A: SRF properties characterisation	321
5.6.1	UK MBT plant A: SRF characterisation - overall results and statistics	321
5.6.2	UK MBT plant A: SRF moisture content	327
5.6.3	UK MBT plant A: SRF total chlorine content.....	331
5.6.4	UK MBT plant A: SRF ash content	337
5.6.5	UK MBT plant A SRF: biogenic content.....	340
5.6.6	UK MBT plant A: SRF total carbon and total hydrogen content....	345
5.6.7	UK MBT plant A: SRF calorific values	346
5.6.8	UK MBT plant A: SRF total nitrogen content	352
6	DISCUSSION.....	355
6.1	European MBT-derived SRF: statistical overview of quality.....	356
6.2	UK MBT plant A: material flow analysis (balances of mass, waste components and fuel properties)	360
6.2.1	UK MBT plant A: mass balance model	362
6.2.2	UK MBT plant A: material composition balances.....	368
6.2.3	UK MBT plant A: balance of fuel properties: mass-based specific loads	382
6.3	UK MBT plant A: transfer coefficients of unit operations	386
6.4	UK MBT plant A: simulation of SRF properties	387
6.4.1	UK MBT plant A: concentrations and specific loads per waste component	387
6.4.2	UK MBT plant A: simulation of SRF moisture content, ash content, total chlorine content and net calorific value.....	390
6.5	UK MBT plant A: SRF properties characterisation	392
6.5.1	UK MBT plant A: SRF characterisation - overall results and statistics	392
6.5.2	UK MBT plant: SRF moisture content.....	394
6.5.3	UK MBT plant A: SRF total chlorine content.....	401
6.5.4	UK MBT plant A: SRF ash content	410
6.5.5	UK MBT plant A: SRF biogenic content.....	415
6.5.6	UK MBT plant A: SRF total carbon and total hydrogen content....	421
6.5.7	UK MBT plant A: SRF calorific value	421
6.5.8	UK MBT plant A: SRF total nitrogen content	426
7	CONCLUSIONS AND FUTURE WORK.....	431

7.1	Critical review conclusions	432
7.2	UK MBT plant A material flow analysis conclusions.....	434
7.3	Future research suggestions.....	442
	REFERENCES.....	445
	APPENDICES	469
	Appendix A - Terminology for MBT-derived fuels.....	470
	Appendix B - Statistical approaches and descriptors	473
	B.1 Variability in the measurement of waste-related properties.....	473
	B.2 Measurement error, uncertainty and propagation	475
	Appendix C – Computations and statistical details for fuel characterisation properties	485
	C.1 Moisture content (M)	485
	C.2 Ash content (A)	488
	C.3 Calorific (heating) value	489
	C.4 Biogenic content by selective dissolution	491
	C.4.1 Standard operating procedure: Method for the determination of the biogenic content of solid recovered fuels (solid waste) in percent by weight using the selective dissolution method.....	494
	C.5 Total chlorine content.....	497
	Appendix D – Sampling plan for UK MBT plant A	498
	D.1 Introduction to the Gy’s theory of sampling (ToS)	498
	D.2 Application of theory of sampling to the UK MBT plant A.....	499
	D.2.1 Calculation of lot sizes	499
	D.2.2 Calculation of the composite sample mass according to ToS: desirable vs. achievable precision.....	500
	D.2.3 Parameters with critical impact on Ms.....	503
	D.3 Calculation of trommel input lot.....	504
	D.3.1 Refining the estimates of sample masses through an iterative process	505
	D.3.2 Incremental sampling frequency	506
	D.3.3 Number of increments.....	507
	D.3.4 Temporal random stratified sampling.....	508
	D.3.5 Contingency sampling.....	509
	D.4 Sampling plans prepared for the UK MBT plant A	509
	Appendix E – Analytical determinations and quality control	530
	E.1 Cl determination by ion chromatography (IC).....	530
	E.2 Calorific value determination by oxygen bomb combustor	531
	Appendix F - Material flow analysis of UK MBT plant A.....	532
	Appendix G - SRF characterisation – UK MBT plant A.....	583
	Appendix H – Publications.....	586
	Appendix I – Biodrying: critical review	588

List of Figures

- Figure 1-1** General research scope and aim. Investigating how SRF-producing MBTs manage the material flows can inform the wider sustainable resource management agenda. 4
- Figure 1-2** Key areas of investigation regarding the management of (solid) material flows through SRF-producing MBT plants. Investigating these topics could clarify this significant aspect of the contribution of SRF-producing MBT plants and the demand for sustainable resource management. Note that the scope of the research excludes air and liquid flows, along with energy flows, which are integral part of a wider, holistic evaluation. 7
- Figure 2-1** Simplified schematic of potential flow-line options for mechanical-biological treatment plants: different position for the core biological unit and the refuse-derived fuel/solid recovered fuel (RDF/SRF) production stage. B-M-T: biological-mechanical treatment. Adapted from Enviros⁵ 14
- Figure 2-2** Particle-size distribution (PSD) of components of raw mixed household waste, in semi-logarithmic diagram. Each type of material spreads over a characteristic range of sizes, potentially allowing selective screening through the selection of suitable screen aperture. For example, a screening unit with 25 mm openings could theoretically concentrate all of the paper card and plastic in the overflow fraction. Redrawn from Ruf⁹⁶, cited in Hasselriis⁷⁶ 26
- Figure 2-3** Particle-size distribution (PSD) of components of single-shredded MSW, in semi-logarithmic diagram. After shredding each waste component (e.g. paper) tend to occupy a wider range of sizes, compared with before size reduction (see Figure 2-2). This could restrict the potential for selective screening of certain waste components after shredding. Redrawn from Ruf⁹⁶, cited in Hasselriis⁷⁶ 27
- Figure 2-4** Schematic diagrams and operation principles for two typical comminution equipment in MSW: (a) hammermill; (b) rotary shear. Adapted from Tchobanoglous et al.⁷⁸ 28
- Figure 2-5** Schematic diagram of a vertical section of a ball mill, demonstrating its operating principle: as the drum rotates at a low speed around its horizontal axis the grinding balls in contact with the drum walls are lifted by the centrifugal force. At a certain point they lose contact and fall (cascade), impacting on the materials. Adapted from Faculty of Chemical Technology, University of Split¹¹⁷ and Suryanarayana¹¹⁸ 34
- Figure 2-6** Secondary comminution of SRF, before pelletising, by different types of size reduction equipment (see legend); comparative results for the

mass distribution of the shredded output. Data from Jackson ¹²⁴ , cited in Porteous ⁸¹	36
Figure 2-7 Simplified flow-chart and mass balance of the Nehlsen bio-drying MBT plant in Stralsund, Germany. Adapted from Breuer ¹⁰²	53
Figure 2-8 Effect of comminution and screening on the relationship of net calorific value $O_{p,net}$ and the energy based yield to the screen overflow, for different aperture sizes. Data points within each series from top to bottom correspond to the screen overflow product using 40, 80 and 150 mm apertures. Data from the MBT plant at Quarzbilchl, Germany. Redrawn from Soyez and Plickert ⁷¹	57
Figure 2-9 Histogram of cumulative mass of the organic fraction of German residual domestic waste after comminution in a Loesche-Hese cascade mill. Data from Koch et al. ¹¹⁹	60
Figure 2-10 Cumulative mass fractions reporting at the screen undersize for various types of pre-treated domestic waste. Curves: (1) feed material; (2) comminution and drum screen at 100 mm; (4) and (5): ball-mill and 40 mm trommel underscreen; (6) ball mill-trommel and separation <5 mm organic-rich fraction. Characteristic particle size $d_{63.2}$ values are provided (63.2% w/w total mass smaller in size). From Koch et al. ¹⁵⁷ , with permission	61
Figure 2-11 Histogram of cumulative mass of the organic fraction of German residual domestic waste after comminution in a Loesche-Hese cascade mill. Data from Koch et al. ¹¹⁹	65
Figure 2-12 Mass balance data from the Brandenburg Recycling Park, using a Hese ball mill. SWB: stabilised bio-waste. For legend refer to Figure 2-7. Data from Schade-Dannewitz ¹²¹	66
Figure 2-13 Schematic diagram showing the operating principle of a cross-flow air separator with pneumatic transport of the low-gravity material. Redrawn from Timmel ⁷⁵	76
Figure 2-14 Schematic diagram showing the operating principle of a ballistic separator: (1) waste objects drop onto conveyor; (2) rotating metal conveyors follow an eccentric circular movement; (3) light fraction is carried upwards: e.g., paper, corrugated cardboard, plastic sheets and bags (4) heavy fraction rolls down: e.g., bottles, metals, hard plastics; (5) screen fraction falls through: e.g., sand, discarded food. Adapted from Mitsubishi Rayon Engineering ¹⁷³	80
Figure 3-1 PhD aim and objectives.....	146
Figure 4-1 Experimental design roadmap. OBJ: study objectives (Section 3.4); QC/QA: quality assurance/quality control; GAS: general analysis sample. M: methodology; R: result deliverable; TCs: transfer co-efficients.....	149

Figure 4-2 Technical drawing of the processing section of the UK MBT plant A. For a schematic diagram representing this refer to Figure 4-5.....	151
Figure 4-3 General MFA method, with loops indicating its iterative nature. After Brunner and Rechberger ²⁸ . Here, balancing of goods such as the waste components was used in a loop to verify the mass flows determination (sensitivity analysis) and the necessary corrections imposed upon the model data input.....	157
Figure 4-4 Typical sample preparation procedure followed in this thesis, exemplified for the case of biogenic content measurement. Adopted from Séverin ²⁹⁴ , as detailed in Séverin et al. ²⁹⁵	175
Figure 4-5 Model of the processing section of the MBT plant A flowsheet, as created for the material flow management software STAN2 [®] . The flowsheet is shown in Figure 4-2. Abbreviated descriptive identification codes, numbers and corresponding sampling points (SP), where applicable, are given for each flow (F). Input flow is denoted by I, and output by E ('export') (programm settings). Process units operations are shown as transparent squares, named inside. Grey squares denote mixing points. The flows to the APC residue output, the stock of batteries, the batch re-circulation of the E_C rejects to the input and any non-solid flows are ignored as insignificant for the overall material flows. System boundaries are depicted as a dotted line. Conventions of STAN2 ^{®279} are followed throughout.....	193
Figure 5-1 Results of descriptive, non-parametric statistical analysis on European MBT-derived SRF data: comparison of the of location values of $Q_{p,net}$ expressed on an as received (_{ar}) and dry (_d) basis. Box-plot conventions: (1): lower and upper lines of the boxes denote the 25 th and 75 th percentiles (Q1 and Q3 respectively); (2) lower outlier limit and upper outlier limit, denoted by whiskers, define the non-outlier range. This is here defined as the range of values that do not differ from the median more than the Q1 or Q3 plus 1.5 times the interquartile range (IQR = Q3-Q1) (height of box); (3) extreme values, presented as asterisks, exceed the Q1 plus 3 times the IQR. The values upon which statistics were computed are also plotted (raw data).	241
Figure 5-2 Results of descriptive, non-parametric statistical analysis on MBT-derived SRF data: 1. Location values of moisture content (M) expressed on an as received basis (_{ar}); and 2. Location values of ash content (A) expressed on a dry basis (_d). For box-plot conventions see Figure 5-1.	242
Figure 5-3 Results of descriptive, non-parametric statistical analysis on MBT-derived SRF data: comparison of location and p_{80} values of chlorine concentration [Cl], expressed on a dry basis (_d). For box-plot conventions see Figure 5-1.....	242
Figure 5-4 Results of descriptive, non-parametric statistical analysis on MBT-derived SRF data: comparison of location of concentration of trace elements,	

expressed on a dry basis (_d). As, Cd and Hg are further compared in Figure 5-5 using a suitable axis scale. For box-plot conventions see Figure 5-1..... 243

Figure 5-5 Results of descriptive, non-parametric statistical analysis on MBT-derived SRF data: comparison of location of concentration of certain trace elements, expressed on a dry basis (_d). See Figure 5-4 for comparison with more elements. For box-plot conventions see Figure 5-1. 243

Figure 5-6 Results of descriptive, non-parametric statistical analysis on MBT-derived SRF data: comparison of location and p_{80} values of mass-based mercury concentration [Hg], expressed on a dry basis (_d). For box-plot conventions see Figure 5-1. 244

Figure 5-7 Results of descriptive, non-parametric statistical analysis on MBT-derived SRF data: comparison of location and p_{80} values of energy-based mercury concentration [Hg], expressed on an as received basis (_{ar}). For box-plot conventions see Figure 5-1. 244

Figure 5-8 Material composition of the input and output flows of the UK MBT plant A processing section. Values are average specific (per component) mass load (_{ar}), out of ca 100 overall components mass input. Final results based on statistical analysis of the initial manual sorting results and subsequent modelling: (i) adjusting for changes during processing (e.g., increase of Fines <10 mm after trommel separation or secondary shredding) and (ii) balancing (reconciling) the flows through the material flow management software STAN2[®]. See Figure 4-5 and Table 4-7 for notation, assumptions and computation methodology..... 247

Figure 5-9 Material composition of the input and output flows of the UK MBT plant A processing section. Values are average mass percentages per component load (_{ar}). Final results based on statistical analysis of the initial manual sorting results and subsequent modelling: (i) adjusting for changes during processing (e.g., increase of Fines <10 mm after trommel separation or secondary shredding) and (ii) balancing (reconciling) the flows through the material flow management software STAN2[®]. See Figure 4-5 and Table 4-7 for notation, assumptions and computation methodology..... 248

Figure 5-10 Material composition of the input to the processing section of the UK MBT plant A (residual MSW, shredded at 150-300 mm, and biodried) (SP1). Values (_{ar}) of individual incremental samples, as indentified by manual sorting. The between-samples variability is readily visualised. 249

Figure 5-11 Non-parametric statistics on material composition of the input to the processing section of the UK MBT plant A (residual MSW, shredded at 150-300 mm, and biodried) (SP1). Values (_{ar}), as indentified by manual sorting. The median describes more robustly the average of components with sufficiently high percentage, but underestimates components with low percentage (i.e., those which constitute rare occurrences within the magnitude of sampled mass). 250

Figure 5-12 Material composition of the input to the processing section of the UK MBT plant A (residual MSW, shredded at 150-300 mm, and biodried) (SP1). Values are average mass percentages per component ($_{ar}$) and total extended uncertainty (U_{95}). Final results based on statistical analysis of the initial manual sorting results and subsequent modelling (balancing (reconciling) of all the flows through the material flow management software STAN2[®]). A result of the reconciliation is the narrowing of the U_{95} . See Figure 4-5 and Table 4-7 for notation, assumptions and computation methodology..... 251

Figure 5-13 Average moisture content ($\langle M_T \rangle$), ash content ($\langle A \rangle$) and biogenic content ($\langle X_B \rangle$) and total extended uncertainties ($U_{95,v}$) expressed on various reporting bases for: (i) the of the biodried residual MSW (input to the processing section) ($v = 5$); and (ii) the oversized heavy rejects output of the UK MBT plant A ($v = 2$). Results for the A and M on dry basis, for X_B on dry, ash-free basis. Entire samples (no indication) and combustible (shreddable) part ($_{SHR}$)..... 252

Figure 5-14 Average calorific values ($\langle Q \rangle$), and total extended uncertainties ($U_{95,v}$) expressed on various reporting bases for: (i) the combustible (shreddable) part of the biodried residual MSW (input to the processing section) ($v = 5$); and (ii) the oversized heavy rejects output of the UK MBT plant A ($v = 2$). Results for the net calorific value on as received basis are presented for both before ($\langle Q \rangle_{net,p,ar}$) and after ($\langle Q \rangle_{REC,net,p,ar}$) (**Figure 5-53**) the reconciliation procedure for all the plant flows. A side-effect of the data reconciliation is the narrowing of the uncertainty related to the average value, i.e., higher precision is achieved. All rest values without data reconciliation. The calorific value in the oversized heavy rejects is enriched compared to that of the processing section input, revealing a concentration of high-CV combustible waste components in this plant output. 253

Figure 5-15 Average total chlorine content ($\langle [Cl] \rangle$), and total extended uncertainties ($U_{95,v}$) expressed on dry bases ($_d$) for: (i) the combustible (shreddable) part ($\langle [Cl] \rangle_{SHR,d}$) and (ii) the entire sample ($\langle [Cl] \rangle_d$) of the biodried residual MSW (input to the processing section) ($v = 4$); and the oversized heavy rejects output of the UK MBT plant A ($v = 2$). The concentration for the biodried material is within the range anticipated for MSW. Enrichment is evident to the oversized heavy rejects. The high variability of the oversized heavy rejects and the insufficient number of samples considered do not allow to precisely quantifying this. 254

Figure 5-16 Material composition of SRF (SP13). Values ($_{ar}$) of individual incremental samples, as indentified by manual sorting. The between-samples variability is readily visualised..... 255

Figure 5-17 Non-parametric statistics of oversized heavy rejects (SP16). Values ($_{ar}$), as indentified by manual sorting. The median describes more robustly the average of components with sufficiently high percentage, but underestimates components with low percentage (i.e., those which constitute rare occurrences within the magnitude of sampled mass). 256

Figure 5-18 Material composition of the oversized heavy rejects (SP16). Values are average mass percentages per component ($_{ar}$) and total extended uncertainty (U_{95}). Final results based on statistical analysis of the initial manual sorting results and subsequent modelling (balancing (reconciling) of all the flows through the material flow management software STAN2[®]). A result of the reconciliation is the narrowing of the U_{95} . See Figure 4-5 and Table 4-7 for notation, assumptions and computation methodology..... 257

Figure 5-19 Material composition of SRF (SP13). Values ($_{ar}$) of individual incremental samples, as indentified by manual sorting. The between-samples variability is readily visualised..... 258

Figure 5-20 Non-parametric statistics of SRF (SP13). Values ($_{ar}$), as indentified by manual sorting. The median describes more robustly the average of components with sufficiently high percentage, but underestimates components with low percentage (i.e., those which constitute rare occurrences within the magnitude of sampled mass). 259

Figure 5-21 Material composition of SRF (SP13). Values are average mass percentages per component ($_{ar}$) and total extended uncertainty (U_{95}). Final results based on statistical analysis of the initial manual sorting results and subsequent modelling (balancing (reconciling) of all the flows through the material flow management software STAN2[®]). A result of the reconciliation is the narrowing of the U_{95} . See Figure 4-5 and Table 4-7 for notation, assumptions and computation methodology. Clear differences are evident from the raw manual soting data Figure 5-20 260

Figure 5-22 Mass balance model for the processing section of the MBT plant A. Based on operational plant output data for the sampling period (7/07-9/08) and selected literature values. Computed (reconciled) by iterative application of the material flow management software STAN2[®]. The width of the flows illustrates their relative magnitude. 263

Figure 5-23 Sensitivity analysis for balances of the adjusted (modelled) waste components. Sum of modelled output specific mass load, as a percentage of the measured input specific mass load, per component ($_{ar}$ values). Specific mass loads computed using reconciled mass balances and un-reconciled mass fractions at each plant output stream. The 3 examined scenarios, vary the percentage of the oversized heavy rejects (SP16): L: low (current computations), M: medium, H: high..... 264

Figure 5-24 Shankey diagram of the processing section of the UK MBT plant A for dry matter (entire mass, expressed on a dry basis ($_d$)). The width of the flows illustrates their relative magnitude. Result based upon the reconciled as received ($_{ar}$) mass balance (Figure 5-22) converted to $_d$ values, which were reconciled using the material flow management software STAN2[®]. Conversion from $_{ar}$ to $_d$ values, was accomplished using the ratio of shreddable to non-shreddable manual sorting data and the $\langle M_T \rangle$ results per SP. Uncertainty was propagated throughout the computations. This balance can be used in the

computation of properties determined for the entire sample at each flow, expressed on a dry mass basis. 266

Figure 5-25 Shankey diagram of the processing section of the UK MBT plant A for the shredded mass fraction on a dry basis (d). The width of the flows illustrates their relative magnitude. Result used in balancing of properties determined on the shredded part of the samples (GAS), expressed on a dry mass basis. The balance was based upon the reconciled as received (ar) combustible mass balance (Figure 5-27). Conversion from ar to d values was accomplished using the ratio of shreddable to non-shreddable manual sorting data and the $\langle M_T \rangle$ results per SP. Reconciled using the material flow management software STAN2[®], in two stages: (1) simplified, omitting flows leading to Fe-mixing; and (2) full model. Uncertainty was propagated throughout the computations. 267

Figure 5-26 Shankey diagram of the processing section of the UK MBT plant A for the shredded mass fraction expressed on a dry and ash-free basis (daf). The width of the flows illustrates their relative magnitude. Result used in balancing of properties determined on the shredded part of the samples (GAS), expressed on a daf mass basis, such as the biogenic content ($\chi_{B,SHR,daf}$). Balance was produced by deducting the reconciled ash content balance (Figure 5-51) from the reconciled entire shreddable mass balance (Figure 5-25). Uncertainty was propagated throughout the computations. 269

Figure 5-27 Shankey diagram of the processing section of the UK MBT plant A: model of flows for the sum of combustible waste components. The width of the flows illustrates their relative magnitude. For any processing sub-system, the ratio of any output flow to the sum of input flows provides the transfer coefficient (TC) to this output. Values are average specific (per component) mass load (ar), out of ca 10,000 overall components mass input, plus/minus the total extended uncertainty (U_{95}) (confidence intervals around the average at 95% confidence). Results were balanced (reconciled) by iterative application of the material flow management software STAN2[®], based on sampling and operational plant output data. See Figure 4-5 and Table 4-7 for notation, assumptions and computation methodology. 271

Figure 5-28 Shankey diagram of the processing section of the UK MBT plant A: paper/card waste component model of flows. Values are average specific (per component) mass load (ar), out of ca 10,000 overall components mass input, plus/minus the total extended uncertainty (U_{95}) (confidence intervals around the average at 95% confidence). Results were balanced (reconciled) by iterative application of the material flow management software STAN2[®], based on sampling and operational plant output data. The width of the flows illustrates their relative magnitude. See Figure 4-5 and Table 4-7 for notation, assumptions and computation methodology. 272

Figure 5-29 Shankey diagram of the processing section of the UK MBT plant A: sum of paper and like waste component model of flows. Values are average specific (per component) mass load (ar), out of ca 10,000 overall components

mass input, plus/minus the total extended uncertainty (U_{95}) (confidence intervals around the average at 95% confidence). Results were balanced (reconciled) by iterative application of the material flow management software STAN2[®], based on sampling and operational plant output data. The width of the flows illustrates their relative magnitude. See Figure 4-5 and Table 4-7 for notation, assumptions and computation methodology. 273

Figure 5-30 Shankey diagram of the processing section of the UK MBT plant A: plastic film waste component model of flows. Values are average specific (per component) mass load (a_r), out of ca 10,000 overall components mass input, plus/minus the total extended uncertainty (U_{95}) (confidence intervals around the average at 95% confidence). Results were balanced (reconciled) by iterative application of the material flow management software STAN2[®], based on sampling and operational plant output data. The width of the flows illustrates their relative magnitude. See Figure 4-5 and Table 4-7 for notation, assumptions and computation methodology. 274

Figure 5-31 Shankey diagram of the processing section of the UK MBT plant A: other packaging plastic waste component model of flows. Values are average specific (per component) mass load (a_r), out of ca 10,000 overall components mass input, plus/minus the total extended uncertainty (U_{95}) (confidence intervals around the average at 95% confidence). Results were balanced (reconciled) by iterative application of the material flow management software STAN2[®], based on sampling and operational plant output data. The width of the flows illustrates their relative magnitude. See Figure 4-5 and Table 4-7 for notation, assumptions and computation methodology. 275

Figure 5-32 Shankey diagram of the processing section of the UK MBT plant A: durable plastics waste component model of flows. Values are average specific (per component) mass load (a_r), out of ca 10,000 overall components mass input, plus/minus the total extended uncertainty (U_{95}) (confidence intervals around the average at 95% confidence). Results were balanced (reconciled) by iterative application of the material flow management software STAN2[®], based on sampling and operational plant output data. The width of the flows illustrates their relative magnitude. See Figure 4-5 and Table 4-7 for notation, assumptions and computation methodology. 276

Figure 5-33 Shankey diagram of the processing section of the UK MBT plant A: composite waste component model of flows. Values are average specific (per component) mass load (a_r), out of ca 10,000 overall components mass input, plus/minus the total extended uncertainty (U_{95}) (confidence intervals around the average at 95% confidence). Results before balancing with STAN2[®], based on sampling and operational plant output data. The width of the flows illustrates their relative magnitude. See Figure 4-5 and Table 4-7 for notation, assumptions and computation methodology. 277

Figure 5-34 Shankey diagram of the processing section of the UK MBT plant A: composites waste component model of flows. Values are average specific (per component) mass load (a_r), out of ca 10,000 overall components mass

input, plus/minus the total extended uncertainty (U_{95}) (confidence intervals around the average at 95% confidence). Results were balanced (reconciled) by iterative application of the material flow management software STAN2[®], based on sampling and operational plant output data. Figure 5-33 shows data before reconciliation. The width of the flows illustrates their relative magnitude. See Figure 4-5 and Table 4-7 for notation, assumptions and computation methodology..... 278

Figure 5-35 Shankey diagram of the processing section of the UK MBT plant A: sum of plastic waste components model of flows. Values are average specific (per component) mass load (a_r), out of ca 10,000 overall components mass input, plus/minus the total extended uncertainty (U_{95}) (confidence intervals around the average at 95% confidence). Results were balanced (reconciled) by iterative application of the material flow management software STAN2[®], based on sampling and operational plant output data. The width of the flows illustrates their relative magnitude. See Figure 4-5 and Table 4-7 for notation, assumptions and computation methodology. 279

Figure 5-36 Shankey diagram of the processing section of the UK MBT plant A: sum of textile and like waste components model of flows. Values are average specific (per component) mass load (a_r), out of ca 10,000 overall components mass input, plus/minus the total extended uncertainty (U_{95}) (confidence intervals around the average at 95% confidence). Results were balanced (reconciled) by iterative application of the material flow management software STAN2[®], based on sampling and operational plant output data. The width of the flows illustrates their relative magnitude. See Figure 4-5 and Table 4-7 for notation, assumptions and computation methodology. 281

Figure 5-37 Shankey diagram of the processing section of the UK MBT plant A: treated wood waste components model of flows. Values are average specific (per component) mass load (a_r), out of ca 10,000 overall components mass input, plus/minus the total extended uncertainty (U_{95}) (confidence intervals around the average at 95% confidence). Results were balanced (reconciled) by iterative application of the material flow management software STAN2[®], based on sampling and operational plant output data. The width of the flows illustrates their relative magnitude. See Figure 4-5 and Table 4-7 for notation, assumptions and computation methodology. 282

Figure 5-38 Shankey diagram of the processing section of the UK MBT plant A: biological waste component model of flows. Values are average specific (per component) mass load (a_r), out of ca 10,000 overall components mass input, plus/minus the total extended uncertainty (U_{95}) (confidence intervals around the average at 95% confidence). Results were balanced (reconciled) by iterative application of the material flow management software STAN2[®], based on sampling and operational plant output data. The width of the flows illustrates their relative magnitude. See Figure 4-5 and Table 4-7 for notation, assumptions and computation methodology. 283

Figure 5-39 Shankey diagram of the processing section of the UK MBT plant A: fines <10 mm waste components model of flows. Values are average specific (per component) mass load ($_{ar}$), out of ca 10,000 overall components mass input, plus/minus the total extended uncertainty (U_{95}) (confidence intervals around the average at 95% confidence). Results were balanced (reconciled) by iterative application of the material flow management software STAN2[®], based on sampling and operational plant output data. The width of the flows illustrates their relative magnitude. See Figure 4-5 and Table 4-7 for notation, assumptions and computation methodology. 284

Figure 5-40 Shankey diagram of the processing section of the UK MBT plant A: sum of non-combustible waste components model of flows. Values are average specific (per component) mass load ($_{ar}$), out of ca 10,000 overall components mass input, plus/minus the total extended uncertainty (U_{95}) (confidence intervals around the average at 95% confidence). Results were balanced (reconciled) by iterative application of the material flow management software STAN2[®], based on sampling and operational plant output data. The width of the flows illustrates their relative magnitude. See Figure 4-5 and Table 4-7 for notation, assumptions and computation methodology. 286

Figure 5-41 Approximate Shankey diagram of the processing section of the UK MBT plant A: composites waste component model of main flows. Values are average specific (per component) mass load ($_{ar}$), out of ca 10,000 overall components mass input, plus/minus the total extended uncertainty (U_{95}) (confidence intervals around the average at 95% confidence). Results were balanced (reconciled) by iterative application of the material flow management software STAN2[®], based on sampling and operational plant output data. The width of the flows illustrates their relative magnitude. See Figure 4-5 and Table 4-7 for notation, assumptions and computation methodology. 287

Figure 5-42 Shankey diagram of the processing section of the UK MBT plant A: measured adjusted un-reconciled flows for the hazardous waste component: input to the material flow management software STAN2[®]. Values are average specific (per component) mass load ($_{ar}$), out of ca 10,000 overall components mass input, plus/minus the total extended uncertainty (U_{95}) (confidence intervals around the average at 95% confidence). The width of the flows illustrates their relative magnitude. See Figure 4-5 and Table 4-7 for notation, assumptions and computation methodology. See Figure 5-43 for the reconciled model results. 288

Figure 5-43 Shankey diagram of the processing section of the UK MBT plant A: glass waste component model of flows. Values are average specific (per component) mass load ($_{ar}$), out of ca 10,000 overall components mass input, plus/minus the total extended uncertainty (U_{95}) (confidence intervals around the average at 95% confidence). Results were balanced (reconciled) by iterative application of the material flow management software STAN2[®], based on sampling and operational plant output data. The width of the flows illustrates their relative magnitude. See Figure 4-5 and Table 4-7 for notation, assumptions and computation methodology. 289

Figure 5-44 Shankey diagram of the processing section of the UK MBT plant A: measured adjusted un-reconciled flows for the batteries waste component. Values are average specific (per component) mass load (a_r), out of ca 10,000 overall components mass input, plus/minus the total extended uncertainty (U_{95}) (confidence intervals around the average at 95% confidence). The width of the flows illustrates their relative magnitude. See Figure 4-5 and Table 4-7 for notation, assumptions and computation methodology..... 290

Figure 5-45 Shankey diagram of the processing section of the UK MBT plant A: measured adjusted un-reconciled flows for the glass waste component: input to the material flow management software STAN2[®]. Values are average specific (per component) mass load (a_r), out of ca 10,000 overall components mass input, plus/minus the total extended uncertainty (U_{95}) (confidence intervals around the average at 95% confidence). The width of the flows illustrates their relative magnitude. See Figure 4-5 and Table 4-7 for notation, assumptions and computation methodology. See Figure 5-46 for the reconciled model results.291

Figure 5-46 Shankey diagram of the processing section of the UK MBT plant A: glass waste component model of flows. Values are average specific (per component) mass load (a_r), out of ca 10,000 overall components mass input, plus/minus the total extended uncertainty (U_{95}) (confidence intervals around the average at 95% confidence). Results were balanced (reconciled) by iterative application of the material flow management software STAN2[®], based on sampling and operational plant output data. The width of the flows illustrates their relative magnitude. See Figure 4-5 and Table 4-7 for notation, assumptions and computation methodology. 292

Figure 5-47 Shankey diagram of the processing section of the UK MBT plant A: stones/ceramic waste component model of flows. Values are average specific (per component) mass load (a_r), out of ca 10,000 overall components mass input, plus/minus the total extended uncertainty (U_{95}) (confidence intervals around the average at 95% confidence). Results were balanced (reconciled) by iterative application of the material flow management software STAN2[®], based on sampling and operational plant output data. The width of the flows illustrates their relative magnitude. See Figure 4-5 and Table 4-7 for notation, assumptions and computation methodology. 293

Figure 5-48 Shankey diagram of the processing section of the UK MBT plant A: non-ferrous metal waste component model of flows. Values are average specific (per component) mass load (a_r), out of ca 10,000 overall components mass input, plus/minus the total extended uncertainty (U_{95}) (confidence intervals around the average at 95% confidence). Results were balanced (reconciled) by iterative application of the material flow management software STAN2[®], based on sampling and operational plant output data. The width of the flows illustrates their relative magnitude. See Figure 4-5 and Table 4-7 for notation, assumptions and computation methodology. 294

Figure 5-49 Shankey diagram of the processing section of the UK MBT plant A: ferrous metal waste component model of flows. Values are average specific

(per component) mass load (a_r), out of ca 10,000 overall components mass input, plus/minus the total extended uncertainty (U_{95}) (confidence intervals around the average at 95% confidence). Results were balanced (reconciled) by iterative application of the material flow management software STAN2[®], based on sampling and operational plant output data. The width of the flows illustrates their relative magnitude. See Figure 4-5 and Table 4-7 for notation, assumptions and computation methodology. 296

Figure 5-50 Closures of input-output balances for the UK MBT plant A processing section, for a series of fuel properties, as measured on the shreddable/combustible part of samples. Sum of mass-specific load of the property for all plant outputs, expressed as a percentage of the specific load present in the processing section input (biodried material flow). The specific loads were computed multiplying the average measured properties for each output sampling point, with the suitable reconciled mass balance (shreddable mass d or d_{daf}). The satisfactory closures serve as a direct validation for the accuracy of sampling, measurement, statistical treatment, and the correctness of the produced reconciled mass flows. They allow the application of data reconciliation software STAN2[®] to compute TCs and inner flows, and fully reconcile the balances..... 297

Figure 5-51 Shankey diagram of the processing section of the UK MBT plant A: model of flows for ash content (A), shredded part of samples, expressed on d basis. The width of the flows illustrates their relative magnitude. Values are average specific A load (a_r), out of ca 10,000 overall dry shredded mass input, plus/minus the total extended uncertainty (U_{95}) (confidence intervals around the average at 95% confidence). Results were balanced (reconciled) by iterative application of the material flow management software STAN2[®], based on sampling and operational plant output data. Ash loads computed using the reconciled shredded mass balance (d) (Figure 5-25). See Figure 4-5 for notation and assumptions. 299

Figure 5-52 Shankey diagram of the processing section of the UK MBT plant A for the biogenic content specific load of the shreddable part of the samples, expressed on a dry, ash-free basis (d_{daf}). The width of the flows illustrates their relative magnitude. Values are average biogenic content ($X_{B,SHR,daf}$) specific load, out of ca 10,000 overall dry, ash-free shredded mass input, plus/minus the total extended uncertainty (U_{95}) (confidence intervals around the average at 95% confidence). Results were balanced (reconciled) by iterative application of the material flow management software STAN2[®], based on sampling and operational plant output data. Biogenic content loads computed using the reconciled shredded d_{daf} mass balance (Figure 5-26). Uncertainty was propagated throughout the computations..... 300

Figure 5-53 Shankey diagram of the processing section of the UK MBT plant A: model for the specific load of net calorific value of the combustible part of the samples, expressed on a as received basis, under constant pressure ($Q_{net,p,ar}$). The width of the flows illustrates their relative magnitude. For any processing sub-system, the ratio of any output flow to the sum of input flows provides the

transfer coefficient (TC) to this output. Values are average $Q_{net,p,ar}$ specific load, plus/minus the total extended uncertainty (U_{95}) (confidence intervals around the average at 95% confidence). Results were balanced (reconciled) by application of the material flow management software STAN2[®], based on sampling and operational plant output data. $Q_{net,p,ar}$ loads computed using the reconciled sum of combustible components $_{ar}$ mass balance (Figure 5-27). Uncertainty was propagated throughout the computations..... 301

Figure 5-54 Shankey diagram of the processing section of the UK MBT plant A: model for the specific load of total chlorine content of the combustible part of the samples, expressed on a dry basis $TCI_{SHR,d}$. The width of the flows illustrates their relative magnitude. For any processing sub-system, the ratio of any output flow to the sum of input flows provides the transfer coefficient (TC) to this output. Values are average $TCI_{SHR,d}$ specific load, plus/minus the total extended uncertainty (U_{95}) (confidence intervals around the average at 95% confidence). Results were balanced (reconciled) by iterative application of the material flow management software STAN2[®], based on sampling and operational plant output data. $TCI_{SHR,d}$ loads computed using the reconciled sum of shreddable components $_d$ mass balance (Figure 5-25). Uncertainty was propagated throughout the computations..... 302

Figure 5-55 Results for moisture content ($\langle M_T \rangle_{ar}$) characterisation of biodried waste components, and percent contribution of each component to the overall moisture load of the average SRF produced by the UK MBT plant A. Average composition of the SRF was modelled from the results of the reconciled waste component balances throughout the plant (Figure 5-21). For details on the material composition of each component category refer to Table 4-5..... 313

Figure 5-56 Results for total chlorine content ($\langle [Cl] \rangle_d$) characterisation of biodried waste components, and percent contribution of each component to the overall total chlorine load of the average SRF produced by the UK MBT plant A. For non-shredable components typical literature values are shown. Average composition of the SRF was modelled from the results of the reconciled waste component balances throughout the plant (Figure 5-21). For details on the material composition of each component category refer to Table 4-5..... 315

Figure 5-57 Results for ash content ($\langle A \rangle_d$) characterisation of biodried waste components, and percent contribution of each component to the overall ash load of the average SRF produced by the UK MBT plant A. For inert components 100% ash content was assumed. Average composition of the SRF was modelled from the results of the reconciled waste component balances throughout the plant (Figure 5-21). For details on the material composition of each component category refer to Table 4-5..... 316

Figure 5-58 Results for net calorific value ($\langle Q \rangle_{net,p,ar}$) characterisation of biodried waste components, and percent contribution of each component to the overall net calorific value load of the average SRF produced by the UK MBT plant A. Average composition of the SRF was modelled from the results of the reconciled waste component balances throughout the plant (Figure 5-21). For

details on the material composition of each component category refer to Table 4-5. 319

Figure 5-59 Validation for SRF properties simulation. Relative bias as a percentage of the measured value. Results are shown for two sets of samples (L123-L3outl: typical plant operation from winter to summer; L3-outl: typical plant operation for summer; for details refer to Table 4-9). For statistical significance comparisons refer to Table 5-11. 321

Figure 5-60 Residual moisture determined on the GAS of L3 set of SRF samples. 327

Figure 5-61 Total moisture content and uncertainty for L1+2+3 SRF samples. L1_INC1: SHR-only sample fraction. L2_INC1-7CM: composite, not incremental, sample. 329

Figure 5-62 Total moisture content ($\langle M_T \rangle$) ar, of SRF: box-plots of non-parametric statistics for 4 sets of samples (A-D) (refer to Table 4-9 for explanation), along with SRF end-use specification limits (CK: cement kilns). Box-plot conventions: (1): lower and upper lines of the boxes denote the 20th and 80th percentiles (denoted p_{20} and p_{80} respectively); (2) lower outlier limit and upper outlier limit, denoted by whiskers, define the non-outlier range. Here this is defined as the range of values that do not differ from the median more than the Q1 or Q3 plus 1.5 times the height of box ($p_{80}-p_{20}$); (3) extreme values, presented as asterisks, exceed the Q1 plus 3 times the interpercentile $p_{80}-p_{20}$ range. 330

Figure 5-63 Total chlorine content ([Cl]) of SRF and total extended uncertainty $U_{95,v}$, on a dry mass basis (% w/w_d) for each of the L1+2+3 SRF samples, estimated by 3 replicates (d.f. = 2). L1_INC1 estimated through components of variance experiment at d.f. = 7; The value for L2_INC1-7CM entire sample reconstructed from analysis of the shreddable part excluding fines, fines and purity (contraries) measurements. L3_INC 10 and L1_INC8 estimated by 2 replicates. CK: cement kilns; PP: power plants. 332

Figure 5-64 Total chlorine content of SRF from the UK MBT plant A: box-plots of for 2 sets of samples (A-B) (refer to Table 4-9 for explanation) and 2 statistical approaches (1: non-parametric; -2: normality-based), along with SRF CEN classification ranges. For non-parametric box-plot conventions refer to Figure 5-62; for normality-based to Figure 5-73. 334

Figure 5-65 Total chlorine content of SRF from the UK MBT plant A: box-plots of for 2 sets of samples (C-D) (refer to Table 4-9 for explanation) and 2 statistical approaches (1: non-parametric; -2: normality-based), along with SRF CEN classification ranges. For non-parametric box-plot conventions refer to Figure 5-62; for normality-based to Figure 5-73. 336

Figure 5-66 Ash content and uncertainty for L1+2+3 SRF samples. L1_INC1: SHR-only sample fraction (overall sample reconstructed value at 17.47% w/w_d).
 338

Figure 5-67 Ash content ($\langle A \rangle_d$), of SRF (3 replicates per GAS): box-plots of non-parametric statistics for 4 sets of samples (A-D) (refer to Table 4-9 for explanation), along with SRF end-use specification limits (PP: power plants; CK: cement kilns). Number of observations included (n1 x n2): n1: incremental samples, n2: replications on the GAS of each incremental sample. For box-plot conventions refer to Figure 5-62..... 339

Figure 5-68 Split of ash content in SRF samples into dissolving and not dissolving parts during the selective dissolution process 341

Figure 5-69 Impact of correction of the non-shreddable/combustible fraction (100% w/w ash) in the determination of $\langle \chi_{B,daf} \rangle$ and its uncertainty estimate. 342

Figure 5-70 Biogenic content (dry, ash-free) ($\langle \chi_{B,daf} \rangle$) and uncertainty for L1+2+3 SRF samples..... 344

Figure 5-71 Biogenic content (dry, ash-free) ($\langle \chi_{B,daf} \rangle$) of SRF: box-plots of non-parametric statistics for 4 sets of samples (A-D) (refer to Table 4-9 for explanation), along with SRF end-use specification limits (CK: cement kilns). For box-plot conventions refer to Figure 5-62..... 345

Figure 5-72 Calorific value (net, under constant pressure, as received) ($\langle Q_{net,p,ar} \rangle$) and uncertainty for L1+2+3 SRF samples..... 349

Figure 5-73 Calorific values (3 reporting basis) of SRF: box-plots of for 2 sets of samples (A-B) (refer to Table 4-9 for explanation) and 2 statistical approaches (1: non-parametric; 2: normality-based), along with SRF end-use specification ranges (CK: cement kilns; PP: power plants). For box-plot non-parametric conventions refer to Figure 5-62. Normality-based box-plot conventions: (1) centre: arithmetic mean; (2) lower and upper lines of the boxes denote the mean \pm standard error (SE) around the mean; (3) upper and lower 95% confidence limits around the mean ($UCl_{95,v}(\langle Q \rangle)$ and $UCl_{95,v}(\langle Q \rangle)$), computed for v d.f., are denoted by whiskers. Here this is defined as the range of values that do not differ from the median more than the Q1 or Q3 plus 1.5 times the height of box ($p_{80}-p_{20}$); (3) outlier and extreme values outside the 95% CI are presented as circles and asterisks respectively..... 350

Figure 5-74 Calorific values (3 reporting basis) of SRF: box-plots for 2 sets of samples (C-D) (refer to Table 4-9 for explanation) and 2 statistical approaches (1: non-parametric; 2: normality-based), along with SRF end-use specification ranges (CK: cement kilns; PP: power plants). For non-parametric box-plot conventions refer to Figure 5-62. For normality-based box-plot conventions refer to Figure 5-73. 351

Figure 5-75 Total nitrogen of SRF and uncertainty for L1+2+3 SRF samples. Comparison with indicative ranges for characteristic biofuels, and upper limit for combustion without air pollution control (APC) measures²¹⁵. 353

Figure 5-76 Total nitrogen of SRF: box-plots of non-parametric statistics for 4 sets of samples (A-D). Comparison with characteristic ranges for typical biofuels and upper limit for combustion without air pollution control (APC) measures²¹⁵. Number of observations included (n1 x n2): n1: incremental samples, n2: replications on the GAS of each incremental sample. For box-plot conventions refer to Figure 5-62..... 354

List of Tables

Table 2-1 Main bioconversion reactors commonly used in MBT plants	13
Table 2-2 Potential outputs and uses for MBT processes.....	15
Table 2-3 Indicative mechanical equipment currently used in MBT plants.....	17
Table 2-4 General features of comminution equipment - typical values.....	27
Table 2-5 Indicative classification/separation equipment used in MBT plants .	38
Table 2-6 Descriptors and formulas for the characterisation of the mechanical processing performance.....	43
Table 2-7 Results on material flow management performance of size classification; overflow product stream intended to concentrate components suitable for RDF/SRF production in MBT plants.....	68
Table 2-8 Air separators (air classifiers) for SRF production in MBT plants....	72
Table 2-9 Results on material flow management performance of air classifiers (ACs); low-gravity product stream intended to concentrate components suitable for RDF/SRF production in MBT plants	78
Table 2-10 Results on material flow management performance of ballistic separation; low-gravity product stream intended to concentrate components suitable for RDF/SRF production in MBT plants.....	83
Table 2-11 Existing and provisional national and trade quality assurance/quality control systems and standards for RDF/SRF in Europe	99
Table 2-12 Overview of limit values for existing European SRF quality standards.....	102
Table 2-13 CEN classification codes for SRF	105
Table 2-14 Properties for sufficient characterisation of WDFs according to end-use specifications	107
Table 2-15 Quality parameters for SRF according to end-use	110
Table 2-16 Quality standards for SRF use in cement kilns	114
Table 4-1 Unit operations in the processing section of the UK MBT plant A and role within plant flow-line	152
Table 4-2 Types of variability pertaining to MBT process streams characterisation and relevant sections addressing them.....	155

Table 4-3 Substance and goods selection, relevant to SRF production within UK MBT plant A and SRF thermal recovery; (metals are not reported in this thesis).....	161
Table 4-4 Sampling points at the UK MBT plant A.....	171
Table 4-5 Categories into which process streams samples were manually sorted. The compatibility with other breakdown categorisations of proposed methodologies is shown. However, the exact interpretation and application is inevitably research- and even individual sorter-dependent.	182
Table 4-6 Scenarios of mass balances examined for modelling the UK MBT plant A material flows	194
Table 4-7 Computation steps taken to develop a model for balanced component flows and TCs	201
Table 4-8 Background information on data series used for the statistical evaluation of the European MBT-derived RDF/SRF.....	211
Table 4-9 Notation and type of SRF production represented by each statistically analysed dataset for UK MBT plant A	213
Table 5-1 Results on statistical analysis of MBT-derived RDF/SRF data-series	239
Table 5-2 Characterisation of biodried material and oversized heavy rejects for fuel properties. Arithmetic means (<>) and total extended uncertainty ($\pm U_{95,v}$)	251
Table 5-3 Results on UK MBT plant A outputs mass balance and comparison with literature	262
Table 5-4 Selected transfer coefficients (TC) per waste component (and sums of) or fuel property, for the entire processing section of the UK MBT plant A to the SRF output	304
Table 5-5 Transfer coefficients (TC) per waste component (and sums of), for the process unit: trommel screening (T_SCR). See Figure 4-5 for notation and relative position within the UK MBT plant A flow-line. Average values plus/minus the total extended uncertainty (U_{95}) (confidence intervals around the average at 95% confidence). Computed using data from flows balanced (reconciled) by iterative application of the material flow management software STAN2 [®] , based on sampling and operational plant output data.....	304
Table 5-6 Transfer coefficients (TC) per waste component (and sums of), for the process unit: air classification (A_CL 1). See Figure 4-5 for notation and relative position within the UK MBT plant A flow-line. Average values plus/minus the total extended uncertainty (U_{95}) (confidence intervals around the average at 95% confidence). Computed using data from flows balanced (reconciled) by	

iterative application of the material flow management software STAN2[®], based on sampling and operational plant output data..... 305

Table 5-7 Transfer coefficients (TC) per waste component (and sums of), for the process unit: oscillating screening (Flip-flop screen) (O_SCR). See Figure 4-5 for notation and relative position within the UK MBT plant A flow-line. Average values plus/minus the total extended uncertainty (U_{95}) (confidence intervals around the average at 95% confidence). Computed using data from flows balanced (reconciled) by iterative application of the material flow management software STAN2[®], based on sampling and operational plant output data. 306

Table 5-8 Transfer coefficients (TC) per waste component (and sums of), for the process unit: air drum separator (A_CL 2). See Figure 4-5 for notation and relative position within the UK MBT plant A flow-line. Average values plus/minus the total extended uncertainty (U_{95}) (confidence intervals around the average at 95% confidence). Computed using data from flows balanced (reconciled) by iterative application of the material flow management software STAN2[®], based on sampling and operational plant output data..... 307

Table 5-9 Transfer coefficients (TC) per waste component (and sums of), for the process unit: eddy current separator (E_C_S). See Figure 4-5 for notation and relative position within the UK MBT plant A flow-line. Average values plus/minus the total extended uncertainty (U_{95}) (confidence intervals around the average at 95% confidence). Computed using data from flows balanced (reconciled) by iterative application of the material flow management software STAN2[®], based on sampling and operational plant output data..... 308

Table 5-10 Fuel properties characterisation of biodried MBT process flows . 311

Table 5-11 Comparison of simulated average values for properties of modelled average SRF composition produced by the UK MBT plant A with the measures of central tendency (median and mean with confidence limits at 95% confidence) for these properties as measured on 2 sets of SRF samples 320

Table 5-12 Statistics computed for selected fuel properties, for sets of SRF samples from the UK MBT plant A 323

Table 5-13 Statistics on the coefficient of variation of for selected fuel properties, for sets of SRF samples from the UK MBT plant A..... 326

Table 5-14 Results on bulk, residual and total moisture content of SRF samples from the UK MBT plant A, along with statistical information, including uncertainty estimates. 328

Table 5-15 Results on total chlorine content of SRF samples (dry basis) ($[Cl]_d$) from the UK MBT plant A, along with statistical information, including uncertainty estimates. 331

Table 5-16 Results on ash content of SRF samples from UK MBT plant A, along with statistical information, including uncertainty estimates.	337
Table 5-17 Results on biogenic content of SRF samples from UK MBT plant A, along with statistical information, including computation of uncertainty estimates.	343
Table 5-18 Results on calorific values of SRF samples from UK MBT plant A, along with statistical information, including computation of uncertainty estimates.	348
Table 5-19 Results on total nitrogen content of SRF samples from UK MBT plant A, along with statistical information, including computation of uncertainty estimates.	352
Table_App D-1 Explanation and notes on the ToS sample mass formula ...	500
Table_App F-1 UK MBT plant A: raw results of manual sorting of process flows components. Starting point for developing the corrected (modelled) values serving as input to the STAN2 [®] modelling. Sampling point 1 (SP1)	533
Table_App F-2 UK MBT plant A: raw results of manual sorting of process flows components. Starting point for developing the corrected (modelled) values serving as input to the STAN2 [®] modelling. Sampling point 2 (SP2)	534
Table_App F-3 UK MBT plant A: raw results on manual sorting of process flows components. Starting point for developing the corrected (modelled) values serving as input to the STAN2 [®] modelling. Sampling point 3 (SP3)	535
Table_App F-4 UK MBT plant A: raw results on manual sorting of process flows components. Starting point for developing the corrected (modelled) values serving as input to the STAN2 [®] modelling. Sampling point 4 (SP4)	536
Table_App F-5 UK MBT plant A: raw results on manual sorting of process flows components. Starting point for developing the corrected (modelled) values serving as input to the STAN2 [®] modelling. Sampling point 5 (SP5)	537
Table_App F-6 UK MBT plant A: raw results on manual sorting of process flows components. Starting point for developing the corrected (modelled) values serving as input to the STAN2 [®] modelling. Sampling point 6 (SP6)	538
Table_App F-7 UK MBT plant A: raw results on manual sorting of process flows components. Starting point for developing the corrected (modelled) values serving as input to the STAN2 [®] modelling. Sampling point 7 (SP7)	539
Table_App F-8 UK MBT plant A: raw results on manual sorting of process flows components. Starting point for developing the corrected (modelled) values serving as input to the STAN2 [®] modelling. Sampling point 10 (SP10)	540

Table_App F-9 UK MBT plant A: raw results on manual sorting of process flows components. Starting point for developing the corrected (modelled) values serving as input to the STAN2 [®] modelling. Sampling point 11 (SP11)	542
Table_App F-10 UK MBT plant A: raw results on manual sorting of process flows components. Starting point for developing the corrected (modelled) values serving as input to the STAN2 [®] modelling. Sampling point 12 (SP12)	543
Table_App F-11 UK MBT plant A: raw results on manual sorting of process flows components. Starting point for developing the corrected (modelled) values serving as input to the STAN2 [®] modelling. Sampling point 13 (SP13)	544
Table_App F-12 UK MBT plant A: raw results on manual sorting of process flows components. Starting point for developing the corrected (modelled) values serving as input to the STAN2 [®] modelling. Sampling point 14 (SP14)	545
Table_App F-13 UK MBT plant A: raw results on manual sorting of process flows components. Starting point for developing the corrected (modelled) values serving as input to the STAN2 [®] modelling. Sampling point 15 (SP15)	547
Table_App F-14 UK MBT plant A: raw results on manual sorting of process flows components. Starting point for developing the corrected (modelled) values serving as input to the STAN2 [®] modelling. Sampling point 16 (SP16)	548
Table_App F-15 Comparison of two different statistical estimates of the average percent mass fraction for each component and sampled process flow (SP)	562
Table_App F-16 UK MBT plant A process flows: average (<>) component mass percentages (w/w_{ar}) and their $U_{95,v}$; corrected (modelled) values, input data to the initial stage of STAN2 [®] (R1) for data reconciliation, and rest internal flows and TCs computation with uncertainty propagation	565
Table_App F-17 Results of sensitivity analysis for balances of the adjusted (modelled) waste components – UK MBT plant A	568
Table_App F-18 UK MBT plant A process flows: average (<>) dry mass percentages (w/w_d) and U_{95} , before and after reconciliation by STAN2 [®]	569
Table_App F-19 Reconstructed SRF material composition on dry mass basis for the UK MBT plant A	581
Table_App G-1 Results on SRF characterisation for TC TH TN	585

ABBREVIATIONS

AC	Air classifiers
AD	Anaerobic digestion
APC	Air pollution control
AR	Aspect ratio
BCPP	Brown coal power plant
BMT	Biological-mechanical treatment
CBA	Cost-benefit analysis
CEA	Cost effectiveness analysis
CEN	European Committee for Standardisation
CF	Correction factor
CFD	Computational fluid dynamics
CHP	Combined heat and power
CLO	Compost-like output
CRM	Certified reference material
CV	Calorific value
DBB	Dry bottom boiler
DD	Draft for Development
DDW	De-ionised distilled water
EC	Energy content
EfW	Energy-from-waste
EIA	Energy Information Administration
ERA	Environmental risk assessment
EU-ETS	EU emission trading scheme
FBC	Fluidised bed combustion
FE	Fundamental sampling error
GAS	General analysis sample
GUM	Guide to the expression of uncertainty in measurement
HCB	Hexachlorobenzene
HCPP	Hard coal power plant
HHW	Household hazardous waste

HPIC	High performance ion chromatographer
IC	Ion chromatography
IEA	International Environment Agency
INC	Increment
IQR	Inter-quartile range
IR	Infrared
LCA	Life cycle assessment
LCL	Lower control limit
LFD	Landfill Directive
LHV	Lower heating value
LoD	Limit of detection
LoQ	Limit of quantification
LSL	Lower specification limit
MBT	Mechanical-biological treatment
MC	Moisture content
MEC	Material enrichment coefficients
MFA	Material flow analysis
MP	Melting point
MPE	Minimum practical error
MSW	Municipal solid waste
MCV	Net calorific value
NIR	Near-infrared
NCV	Net calorific value
OBJ	Objective of this research
OFMSW	Organic fraction of municipal solid waste
PCB	Polychlorinated biphenyls
PCDD/F	Polychlorinated dibenzodioxins/dibenzofurans
PDF	Probability density function
PE	Polyethylene
PFA	Pulverised fly ash
POP	Persistent organic pollutant
PP	Polypropylene

PSD	Particle-size distribution
PTE	Potentially Toxic Element
PVC	Polyvinylchloride
QA	Quality assurance
QC	Quality control
QMS	Quality management systems
R&D	Research and development
RDF	Refuse derived fuel
ROC	Renewables obligation certificate
RRSB	Rosin Rammler Sperling Bennet function
RSD	Relative standard deviation
SBW	Stabilised biowaste
SCR	Selective catalytic reduction
SD	Standard deviation
SDM	Selective dissolution method
SE	Segregation error
SOP	Standard operating procedure
SP	Sampled process stream
SP	Softening point
SRF	Solid recovered fuel
S-W	Shapiro-Wilk test
TC	Transfer coefficients
TGA	Thermogravimetric analysis
ToS	Theory of sampling
UCL	Upper control limit
WDF	Waste-derived fuel
WEEE	Waste electrical and electronic equipment
WID	Waste Incineration Directive
WIP	Waste incineration plant
W/S	Welch-Satterswaite method

GLOSSARY: REFERENCE GUIDE

Through the text a series of acronyms are used. Here, a reference guide to them is provided, along with guidance to spot where exactly they are defined in detail and explained in the wider context of research.

- Sampling points (example: **SP12**), process flows (example: **F5**), unit operations (example: **T_SCR**) are all illustrated in **Figure 4-5**.
- Unit operations (example: **T_SCR**) are detailed in **Table 4-1**.
- Acronyms denoting sets of samples (example: **L123-L3outl**) are detailed in **Table 4-9**.
- Acronyms denoting waste component categories (example: **P/C**) as identified by manual sorting (or sets of them) are presented in **Table 4-5**.
- Symbols of quantities describing material flow performance are defined in **Table 2-6**. (example: **TC**). This symbols/acronyms are applied in the results/discussion sections (example: $TC(P/C)_{A_CL\ 1\ HG} = 17.7 \pm 4.7\%$ meaning: the arithmetic mean of the transfer coefficient (TC) of the waste component paper and card (P/C) for the high gravity output (HG) of unit operation air classifier one (A_CL 1) is 17.7 percent units, plus minus, a total extended uncertainty, at 95% level of confidence, of 4.7 percent units).
- Statistical symbols (example: $U_{95,veff}$) are covered in **Section 4.12** and relevant details, including symbols and equations, are provided in **Appendix B**.

1 INTRODUCTION

1.1 Waste management and sustainable resource management

Waste management is steadily gaining importance within the wider sustainability and environmental debate. Historically, management of the unwanted solid material streams became particularly imperative after the industrial revolution and urbanisation prevailed. The contemporary phase of waste management started approximately 200 years ago¹, and despite the rapid societal and technological changes since, many of its core aspects have remained essentially unchanged².

Recent developments in waste management re-emphasise its role as a part of the material flow cycles within the anthroposphere and the environment³⁻⁴. Municipal solid waste management (MSW) has historically been the most visible part of the discarded solid flow streams, and remains a major challenge for the 21st century, both for the prosperous and technologically advanced nations and the economically and environmentally developing ones.

Modern MSW, whilst advocating avoidance and minimisation of waste production, has a strong focus on recycling and recovery. However, even with the most successful source separation schemes, there remains a significant quantity of residual waste. The environmentally acceptable options for this residual MSW stream have been: (1) direct thermal treatment, mainly combustion, either with energy/ heat recovery ('EfW') or without ('incineration'), along a series of less commercially established technologies (gasification, pyrolysis, plasma); (2) disposal in various types of engineered landfills ('sanitary landfills'); and (3) further processing through a series of mechanical and biological steps, such as 'dirty composting' or refuse derived fuel (RDF) production plants (until around 15 years ago, when they developed into the so called mechanical-biological treatment (MBT) plants).

1.2 Advent of MBT plants

Over the last 15 years, interest in mechanical and/or biological treatment methods has seen a significant increase in research and development (R&D) and commercial application. The overarching term of MBT has prevailed, describing what in fact is a great variety of treatment process configurations. Waste treatment plants defined as MBT integrate mechanical processing, such as size reduction and air classification, with bioconversion reactors, such as composting or anaerobic digestion⁵. MBT technologies were developed in Germany and Italy, with the first plants established in 1995. Similar systems exist, to a lesser extent, in Australia and the US. Over the last 15 years, a considerable capacity of MBT has been installed within Europe⁶⁻⁷. In Germany, more than 6.35 million tonnes of residual waste are treated through MBT plants per year⁸.

Internationally, MBT technologies are being adopted for treating residual MSW waste^{6-7, 9-13}. This reflects an intentional move away from disposing of untreated residual waste in landfill, in the face of simultaneous persisting public opposition to usethermal recovery technologies (dismissingly addressed under the umbrella term 'incineration'). Interest has been strongest in Germany^{8, 14}; Austria¹⁵⁻¹⁶, Italy and Spain. Other countries starting to follow: for example, the UK^{5, 17-18}, France¹⁹, Greece²⁰ and Portugal²¹. In the European Union (EU) this turn towards MBT has been highly supported by the Landfill Directive (LFD) (99/31/EC)²². The LFD requires a phased reduction in the amount of biodegradable waste disposed of to landfill, because of its potential to produce landfill gas and leachate. MBT is also a potential option for environmentally developing countries²³⁻²⁴: e.g., Brazil²⁵, south-east Asia²⁶ and China²⁷.

1.3 Sustainable resource management and MBT plants

A fundamental question for the role of MBTs in the emerging waste and resources merged agenda is: how does MBT serve the need for the effective management of material flows, as an integral part of sustainable resource management (**Figure 1-1**)? At the point of being discarded, waste maintains both potential utility (residual value) but also may contain potentially hazardous properties. The elemental and biological composition of waste constituents is the critical factor for extracting value from it, rather than its origin²⁸. The EU thematic strategy²⁹ has re-orientated efforts at recovery according to waste properties. Discarded waste streams still contain residual value. The emerging challenge in exploiting this value lies in extracting relatively homogeneous fractions of known properties, and at fit-for-purpose contamination levels and degree of variability, starting from inevitably heterogeneous input matrices, harbouring potentially harmful biological and chemical constituents³⁰.

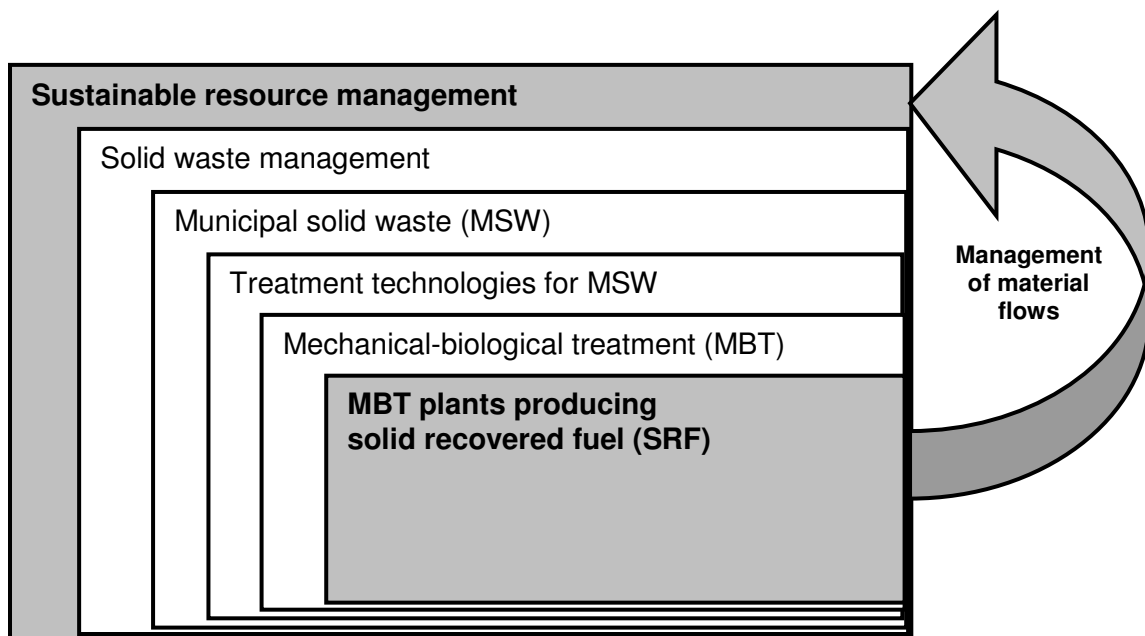


Figure 1-1 General research scope and aim. Investigating how SRF-producing MBTs manage the material flows can inform the wider sustainable resource management agenda.

Using process technology to secure relatively homogenous output materials of a specified composition and degree of variability should enable: (i) the concentration of contaminants for onward disposal or treatment (typically in a highly polluted 'reject' process output) and (ii) production of recyclate/ recoverable streams to a desired quality, prolonging their utility³¹ in either technological or nutrient material cycles³². MBT plants are, in principle, designed for effective material flow management. They use integrated mechanical processing and biological reactors to convert and separate residual waste into output streams of suitable quality. Typical outputs include biostabilised material, dry recyclate, waste-derived fuels (WDFs), contaminated solid reject fractions, and controlled releases to liquid media and air⁵.

A major option for MBT plants is to produce a waste-derived fuel (WDF) (termed refuse-derived fuel (RDF) or solid recovered fuel (SRF))^{13, 18, 33-39}. The MBT-derived RDF/SRF concentrates the combustible, high calorific value (CV) fraction, enabling thermal recovery in a series of potential end uses, such as cement kilns and power plants³⁴ as an alternative to fossil fuels. Indeed, this occurs whilst the indirect thermal recovery of waste through production of WDFs has gained significant impetus^{37, 40-50}

There is need for a timely account of MBT plants that produce RDF/SRF from municipal solid waste (MSW), focusing on material flow and performance. Important aspects of MBTs such as generic assessment¹³, or optimising the processes for the production of a compost-like output (CLO) to be applied on land, have recently been reviewed elsewhere¹². An assessment of the science and process technology of MBT is needed, including the performance of unit processes within MBT plants, so that plant operators, waste managers, regulators and policy makers can assess the strategic contribution that MBT can make to sustainable waste management. An assessment of the policy-related aspects of MBT and SRF adoption is made elsewhere³⁴.

Specific key questions pertain to the contribution of SRF-producing MBT plants to sustainable resource management:

- What is the desired quality of RDF/SRF, and how can this be monitored through quality management schemes? RDF/SRF marketability is increasingly dependent on compliance with existing and emerging quality standards⁵¹⁻⁵². Different end-uses pose different challenges for the desired quality.
- How choices over mechanical processing unit operations (such as air classifiers and ballistic separators) and their arrangement in the process flow sheet affect final RDF/SRF quality? The design of waste processing plants largely remains semi-empirical⁵³⁻⁵⁴ and limited modelling has been attempted. Published information should be collated for the material management performance of typical mechanical processing equipment.
- What descriptors and tools are suitable for evaluating the material flow performance of MBT plants? Established approaches such as yield and purity are covered, along with the application of material flow analysis (MFA) to MBT⁵⁵⁻⁵⁶. Can the required RDF/SRF quality be achieved by MBT plants? Previous experience in the mechanical processing of waste identified a limited ability to generate outputs of the desired chemical composition^{55, 57}. First generation RDF production plants that operated on mixed municipal solid waste (MSW) failed in both the US and Europe because of high levels of contaminants and a high degree of variability in RDF quality^{55, 58}. This failure is also attributable to the prevailing economics that were driven by widespread availability of low-

cost landfill. The quality and yield of RDF/SRF also impacts on the quantity and properties of residual (reject) fraction(s), which will determine the overall economic success of MBT plants producing RDF/SRF.

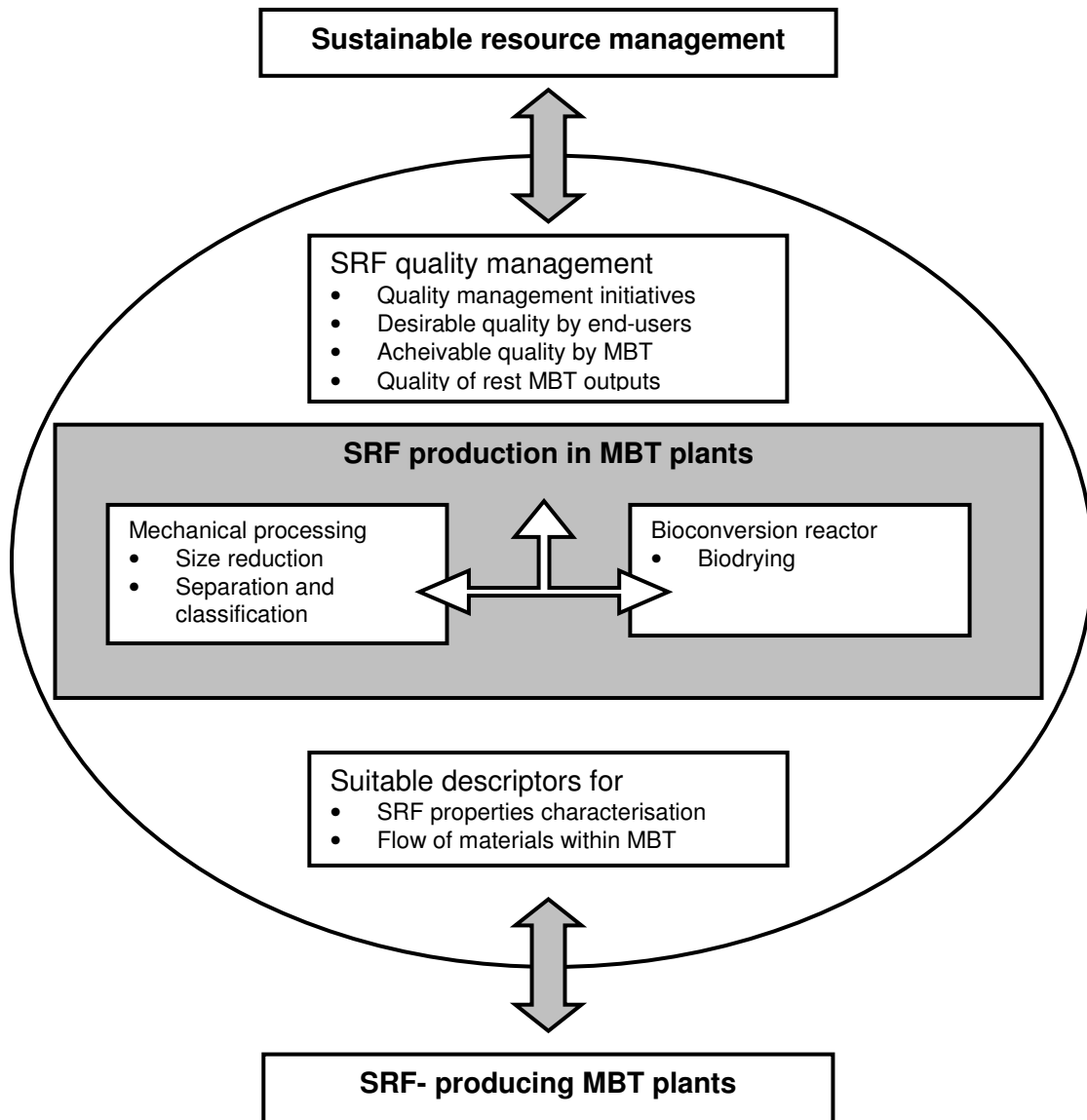


Figure 1-2 Key areas of investigation regarding the management of (solid) material flows through SRF-producing MBT plants. Investigating these topics could clarify this significant aspect of the contribution of SRF-producing MBT plants and the demand for sustainable resource management. Note that the scope of the research excludes air and liquid flows, along with energy flows, which are integral part of a wider, holistic evaluation.

Amongst various MBT configurations able to produce RDF/SRF, biodrying MBT plants are optimised towards this aim. Biodrying is a form of aerobic decomposition (composting) that can be used for drying and partly stabilising waste before subsequent mechanical separation⁵⁹. This is attractive for MBT plants established to produce solid recovered fuel (SRF) as their main output, because removing the excessive moisture of the input waste facilitates mechanical processing and improves its potential for thermal recovery⁶⁰, and partial stabilisation could enable mid-term storage. A significant quantity of readily biodegradable substances is contained within residual waste (ca 68% w/w in England)⁶¹. In biodrying MBT plants, most of the biomass content from the input can be incorporated into the RDF/SRF, reducing the biodegradable material for landfill and producing a partly renewable, low in CO₂ specific emission loading⁶²⁻⁶³ (biomass is carbon dioxide (CO₂)-neutral), alternative energy source⁶⁴⁻⁶⁶, potentially mitigating the waste management contribution to climate change. As result, there is a high level of interest in biodrying MBT plants: 20 commercial references are currently operational in Europe, having an overall capacity of ca 2,000,000 Mg a⁻¹ ⁶⁷⁻⁶⁸.

However, biodrying remains a relatively new technology and relevant published research is limited. Experience from commercial full-scale application of biodrying MBT plants spans only over the last decade. The first plants that became operational were the Eco-deco in Italy (1996), using the 'BioCubi[®]' aerobic drying process; and the Herhof process in Asslar, Germany (1997), using the 'Rotteboxes[®].' Despite having been subject to research ⁶⁹⁻⁷⁰, biodrying has neither been fully understood, nor optimised ⁵⁹: for example regarding the fundamentals of drying and the abatement of within matrix gradients. Thus, the process science and engineering available for optimal SRF production through biodrying in MBT plants should be evaluated. It could be useful to place biodrying in the context of composting and similar bioconversion

applications and incorporate experiences from full-scale biodrying in commercial MBT plants.

Regarding the structure of and particular choices within this thesis, a clarification may be necessary. **CHAPTER 2** serves two purposes. First, it provides a critical assessment of the material flow management performance of SRF-producing MBT plants, by trying to answer the general questions posed above; and second, it functions as a generic literature review, enabling the identification of specific relevant research gaps, leading to the formation of the specific research objectives (**CHAPTER 3**) addressed in the subsequent research. In order to understand the science and engineering of MBT processes adequately, it is necessary to make reference to commercially available technologies and the grey literature. Technologies are described according to the manufacturer or trade name. The author has no interest in promoting or endorsing specific technologies. The use of terminology in this field, especially pertaining to fuels, is clarified (**Appendix A**).

2 LITERATURE REVIEW

2.1 MBT characteristics, classification and design objectives

MBT is a generic term that encompasses a range of waste technologies. Most MBT unit operations have been employed in predecessor treatment plants operated on mixed waste, such as highly-mechanised in-vessel composting ('dirty' composting) and RDF production plants. In its most advanced role, MBT is a material flow management facility. Their flowsheets comprises unit operations employed to split and bio-convert waste; and process the substances present in waste into suitable outputs, and preferably, marketable products⁷¹. In this sense, MBT plants are at the forefront of sustainable resource management, enabling a re-direction of substances contained in the waste to the most appropriate intermediate or final sinks.

Overviews of the current state-of-the-art regarding geographical expansion, roles and perspectives of MBT technologies are available^{6-8, 13, 35}. Key distinguishing features of MBT plants are^{5, 13}: (1) the input (mixed or residual MSW) includes a biodegradable fraction; (2) each plant integrates biological (e.g., aerobic composting, biodrying, anaerobic digestion (AD)) and mechanical unit operations (e.g., size reduction, separation); (3) plants are configured and optimised to produce an array of marketable outputs (secondary products) or at least a stabilised biowaste (SBW) fraction, suitable for disposal in a 'final storage' quality landfill; and (4) plants are enclosed and equipped with air emission control systems e.g., operating under negative pressure and biofilters.

The key objectives of biological waste treatment processes vary significantly. A distinction exists between processes configured for pre-treatment before landfill, and those attempting to add value to the waste stream by producing marketable outputs, such as SRF, biogas, or a CLO³⁰. When MBT processes are used as a pre-treatment to landfill, the objectives should relate to minimising the adverse consequences of

disposal, including volume reduction, biodegradability reduction to minimise landfill gas and odour emissions, and immobilisation of leachate pollutants. According to Juniper¹³ one of the most important differentiating features of MBT processes is the type of main bioconversion reactor (**Table 2-1**).

Table 2-1 Main bioconversion reactors commonly used in MBT plants

Main bioconversion reactor	Sub-category	Description
Aerobic composting	Tunnel	Long enclosed chambers, operated as either continuous or batch flow, some with mechanical agitation
	In-vessel/enclosed halls	Materials are composted on the floor of an enclosed building (hall), usually contained in long beds, i.e. windrows or series of parallel bays or tunnels
	Continuously agitated bays	Rows of long rectangular beds where material is enclosed between two walls and is continuously agitated by turning machines – continuous flow
	Maturation	Maturation stage, usually without aeration or agitation
Biodrying		Use of heat released during aerobic decomposition, supported by controlled aeration, to dry and partially biostabilise waste
Percolation		Washing with water within a reactor to transfer organic material into the liquid phase
Anaerobic digestion	Wet single-stage mesophilic	Use of anaerobic fermentation reactors, operated in a variety of modes
	Wet single-stage thermophilic	
	Dry single-stage mesophilic	
	Wet multi-stage mesophilic	
	Wet multi-stage thermophilic	

Adapted from: The Composting Association⁷², Enviro5⁵, and Juniper¹³

Other approaches take into account the possible differentiations in the series of mechanical and biological unit operations, diversifying between the terms MBT and biological-mechanical treatment (BMT)⁵. **Figure 2-1** provides a schematic for different flow line approaches to MBT plants. Distinction is made regarding the positioning of core biological treatment in the overall flow chart of MBT plants and the stage of RDF/SRF production. Alternatively, MBT processes can be classified according to their primary outputs¹³.

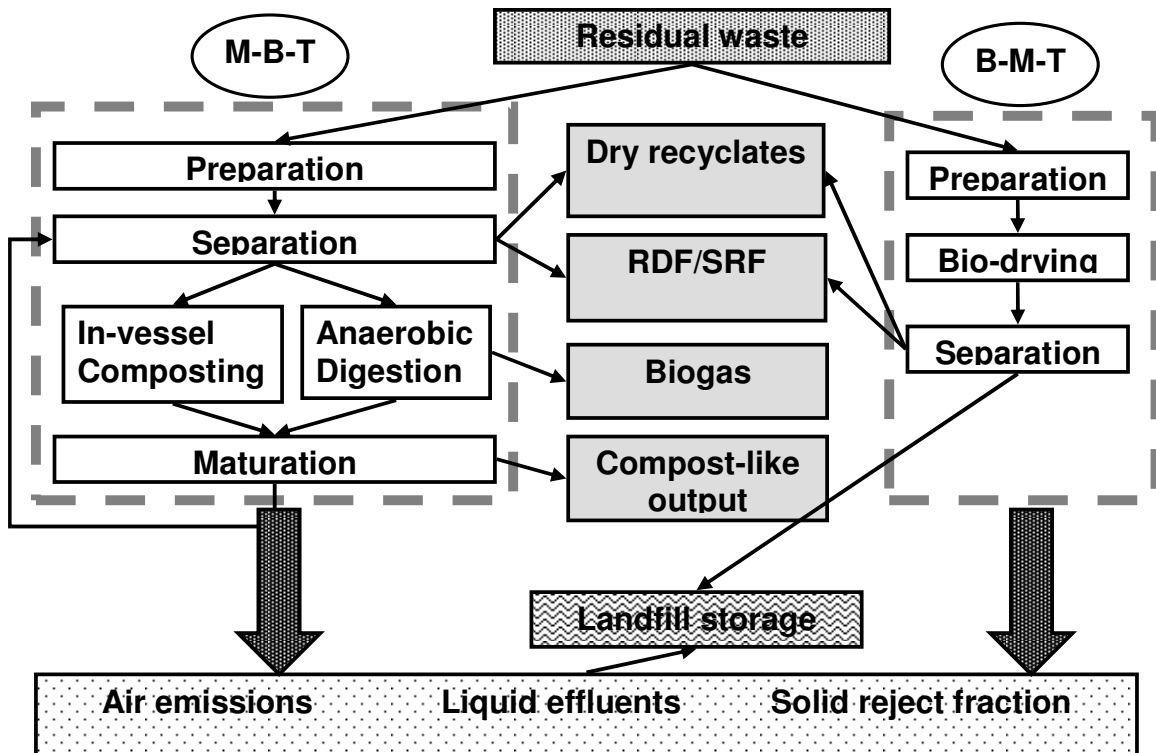


Figure 2-1 Simplified schematic of potential flow-line options for mechanical-biological treatment plants: different position for the core biological unit and the refuse-derived fuel/solid recovered fuel (RDF/SRF) production stage. B-M-T: biological-mechanical treatment. Adapted from Enviro5⁵

MBT processes may be designed and optimised for the production of one or more primary outputs: (1) biostabilised output, to be disposed of in landfill; (2) WDFs, such as RDF or SRF; (3) biogas, for energy and heat production; and (4) CLO for application to land. Dry recyclates (ferrous and non-ferrous metals, aggregates, glass) are co-products found in most process configurations. Products may be marketable subject to creating and securing viable market outlets. If they are not, as is predominantly the case, they may render zero or negative value or end up in landfill. Biostabilised output is intended for landfill disposal: despite not being a product, it has to meet quality criteria. Juniper¹³ provide an extensive list of potential end-uses for MBT process outputs (**Table 2-2**). Most of these combinations of MBT outputs with

end-uses still have to overcome significant technical, legal, and market barriers, if they are to be successfully adopted.

Table 2-2 Potential outputs and uses for MBT processes

Type of output	Application
Compost-like outputs (CLO) (Soil conditioners, low-grade soil improver, etc)	Food crops
	Forestry
	Energy crops
	Improve soil structure and moisture retention in arid areas of poor soil quality
	Pasture land
	Horticultural applications
	Domestic gardens
	Verges and amenity land
	Landscaping during road construction and similar civil engineering projects
	Brown-field sites (contaminated land)
Waste-derived fuel (WDF) Refuse derived fuel (RDF) Solid recovered fuel (SRF) Plastic-rich fraction	Co-fuel for direct combustion in power plants (various technologies e.g. with pulverised fuel, fluidised bed, grate firing, etc)
	Fuel for indirect thermal recovery through gasification and/or pyrolysis for use in power plants
	Co-fuel in bonding agent industries (e.g. cement kilns, lime and gypsum production, asphalt mixing, etc)
	Co-fuel in industrial boilers (e.g. iron and steel, paper industries)
	Fuel for a dedicated incinerator (e.g. fluidised bed)
	Fuel for a dedicated gasification/pyrolysis facility
	Co-fuel for an existing incinerator
Biogas applications	Produce electricity (and heat)
	Blend with landfill gas and/or syngas from waste gasification
	Produce a transportable fuel
Output intended for disposal options	Landfill daily cover
	Biostabilised residue, suitable for depositing in landfills
	Landfill cap
Digestate (liquor as fertiliser)	Liquid fertiliser
Liquor from dewatered digestate	Liquid fertiliser
Fibrous dewatered digestate	Potential as bulking agent or fuel
Ferrous metal	Secondary raw material
Non-ferrous metal (aluminium)	Secondary raw material
Aggregates	Construction and land-filling
Glass	Secondary raw material
Textiles, paper and light plastics	Potential as secondary material

Adapted from: Juniper¹³, and Beckmann *et al.*⁵¹

[†] Unclear if it constitutes disposal or recycling by on-land application

2.2 Mechanical processing for MBT

A variety of mechanical equipment is used in MBT plants. Historically, most unit operations were developed in the mining industry (e.g., coal and ore processing) and adapted for waste stream inputs⁷³⁻⁷⁵. Process units, such as hammermills and trommel screens, have been used for treating mixed MSW e.g., for size reduction before disposal in landfill, recovery of a high CV fraction for RDF production and recycling of materials such as metals and aggregates. There is significant experience of RDF production plants in the US⁷⁶ and Europe⁷⁷ from the 1980s. However, in the case of

MBT plants, these unit operations are fed with new inputs (residual rather than mixed or source separated waste). In this section an introduction to mechanical unit operations for MBT plants is provided with a review of the main waste characterisation properties necessary to evaluate the performance of mechanical processing. Within this review, emphasis is on performance relating to material flow management. Other aspects, such as energy efficiency, or processing that does not change the final chemical composition of the fuel, such as pelletisation, are not covered. The main equipment used for size reduction in MBT plants is presented, including operating principles and performance results where available.

2.2.1 The role and objectives of mechanical unit operations

Mechanical unit processes change the physical characteristics of waste, so as to facilitate removal of constituents, specific components and contaminants from waste streams⁷⁸. Functions served by mechanical unit operations in MSW include size reduction (comminution), mixing and homogenisation, classification and separation (sorting), densification (compaction), and materials handling, including transport, loading and storage^{76, 78-79}. As-received, residual waste usually undergoes an initial mechanical preparation stage (typically bulky item removal, bag splitting or comminution, size separation) before further mechanical or biological treatment steps. Additional mechanical handling and processing steps can be placed both before (pre-treatment) and after (post-treatment) the core biological unit. The throughput rate of individual processing lines of MBT plants is in the range of 20-30 t h⁻¹⁷⁵. In some instances, mechanical units form part of the core biological step e.g., bucket wheels used for turning at in-vessel composting systems.

The key objectives for mechanical unit operations are to^{5, 13}: (1) prepare the input waste for the core biological treatment unit (pre-conditioning); (2) maximise

resource recovery by separating out recyclable/recoverable fractions; (3) remove input waste constituents that may inhibit the effectiveness of further processing steps (contraries), or are inappropriate for the outputs; (4) serve specific process control purposes as part of the core biological unit; and (5) refine the outputs so they are fit for the intended use. The processing objectives for each facility are site-specific and influenced by legislative and market demands for outputs. Juniper¹³ provide an overview of the policy, legal, and market issues affecting mechanical processing in an EU and UK context. **Table 2-3** lists typical mechanical operation units employed in MBT plants.

Table 2-3 Indicative mechanical equipment currently used in MBT plants

Pre-treatment Comminution	Separation Classification Homogenisation	Compaction	Wet processing
Bag identification crusher	Air knife	Baler (baling press)	Flotation tank
Bag splitter	Air-drum separator	Pelletiser	Sand-filter
Cascade/ball mill	Ballistic separator		Sedimentation
Hammermill	Cross-wise air classifier		Settling tank
Hydro-pulper	Cyclone		Sludge centrifuge
Pulper	Disk screen		
Pulveriser	Drum screen (trommel, drum sieve)		
Rotary shear (shear shredder)	Eddy current separator		
Washer	Electromagnet		
	Heavy-solids trap		
	Hydro-cyclone		
	Image detection		
	Inert separator (stoner)		
	Kinetic streamer		
	Magnetic drum		
	Manual picking line		
	NIR separator		
	Over-band magnet		
	Rotating drum mixer		
	Vibrating screen		
	Zig-zag air classifier		

Source of information: Juniper¹³

2.2.2 Waste characterisation for mechanical processing

Waste characterisation refers to the quantities, composition and physical and biochemical properties of waste. A thorough understanding of these properties for input and output streams is vital for effective design and operation of MBT plants⁵⁴. Important descriptors of the physical-mechanical state and behaviour of waste include, but are

not limited to^{78, 80}: waste material composition; moisture content (MC); density descriptors (e.g. bulk density, particle density, etc); elastic properties (material stress and strain descriptors); granulometric descriptors (particle shape, size and particle size distribution (PSD)); electromagnetic behaviour; CV descriptors; and optical properties (colour, texture). These aspects of mechanical processing have been partially reviewed elsewhere^{54, 76, 81-82}. Barton⁸³ provides a qualitative review of selected properties for recyclable municipal waste components. The focus of the work presented here is on the elastic and granulometric properties of waste.

2.2.2.1 Elastic properties of waste and comminution

Comminution (size reduction/shredding) behaviour of waste depends largely on its elastic properties⁸⁴. Schubert and Bernotat⁸⁴ investigated the basic distinction between brittle and non-brittle (i.e. more ductile) materials during shredding. Brittle waste materials include rubble, glass, cast iron and cast non-ferrous metal scraps. Non-brittle materials show little deformation and high stresses in their stress-strain characteristics. These materials include “rubber-elastic” materials, elastic-plastic materials, and elastic-viscous materials. Mixed MSW, residual waste and the organics fraction tend to exhibit predominantly non-brittle behaviour. The current scientific understanding of the micro-processing behaviour of non-brittle materials does not allow these processes to be effectively modelled.

2.2.2.2 Granulometric waste properties

Granulometric properties, such as waste particle size and distribution of waste components or fractions, are conventionally the most significant descriptors⁵³. These properties are used to describe the performance of comminution and separation equipment, to model and simulate their operation, for process control of biological treatment units, and for developing sampling protocols for waste characterisation and

quality control. There is no universally accepted approach to defining waste particle size, due to the irregularity and variability of waste particles. An overview of the possible types of particle shape, morphology, texture and angularity descriptors, and measuring techniques applicable to the mining industry is provided by Pourghahramani and Forssberg⁸⁵. Tchobanoglous et al.⁷⁸ proposed formulas that attempt to account for the three-dimensional, non-isotropic forms of waste particles by estimating an effective particle size (d_e). Material-specific shape categories and characteristic size indicators have been proposed for waste materials, such as metallic scraps and shredded plastics⁵³. Hogg et al.⁸⁶ discuss the role of particle shape in size analysis and evaluation of mining comminution processes through the measurement of an equivalent sphere diameter.

There is a good understanding of particle size measurement methods. Extensive information on application to fine materials such as powders is available⁸⁷. A standard method for sieving waste methods was developed by ASTM in 1985⁸⁸. Detailed guidance on particle size measurement pertaining to SRF has recently been released by CEN, covering both manual and automated sieving for particles >25 mm⁸⁹. Nakamura et al.⁹⁰ applied optical determination and image analysis to enable accurate determination of the waste particle size, as well as shape factors such as aspect ratio (AR), roundness (circularity) and sphericity⁹⁰⁻⁹¹. This method is potentially useful for modelling combustion behaviour of WDFs and evaluating comminution performance. Nevertheless, the practical determination of waste particle size through screening has encountered many restrictions⁵³. For example, ductile materials (about 75% of MSW) can exhibit a significantly lower “projected” particle area, depending on the forces acting on them (e.g., a 1 m x 1 m piece of textile can be forced through a 10 cm opening). The operating mode and performance of the screening apparatus can affect the results. Waste items may not move along the sieving surfaces as expected,

resulting in the maximum particle size passing through an opening that is less than the actual size of the screen. Furthermore, the wide range of sizes can cause fragmentation of the measurement process⁹², producing results that are not directly comparable. For instance, separate size identification for items above and below a certain size, e.g., 40 mm, is not uncommon⁵³. Measurement apparatus and software is commercially available for the fines range, with the CEN SRF standard suggesting machine sorting for samples <25 mm, and more specialised methods, such as laser detection, for samples <1 mm⁸⁹. However, certain sieving standards do not cover oversized items, for example, the German mining standard DIN 22019 (part 1) only covers up to 80 mm⁹³. In addition, the particle equivalent diameter can be geometric or hydrodynamic/aerodynamic, depending on the measurement method⁷⁴. Furthermore, the heterogeneity and high water content of waste can result in fines adhering to coarse fractions and thus being measured as coarser fractions⁹². The CEN guidance addresses this by proposing air drying of SRF samples with moisture contents greater than 20% w/w⁸⁹. As a result of lack of standardisation and the technical challenges outlined above, a certain degree of improvisation on methods for determining particle size has occurred.

PSDs (**Equation [2-1]**) have been extensively used in minerals processing, but have had limited application in solid waste management. The cumulative weight percent of oversize or undersize, in relation to the size of the particles, is most frequently used⁵³. Appropriate graphical representation of PSD data can disclose valuable information about the performance of mechanical processing and enable informed decisions on the configuration of downstream unit operations.

There is evidence that PSDs for both raw mixed and shredded waste may be fitted, at least partially, to a Rosin Rammler Sperling Bennet function (RRSB function)⁵³,⁹⁴. RRSB is suitable for materials that do not exhibit a well defined upper size limit, but

that can describe with accuracy the cumulative weight fraction above a certain sieve size. RRSB distributions plot as a straight line in RRSB grid diagrams (or Weibull diagrams).

$$Y(d) = 1 - \exp \left[- \left(\frac{d}{d_{63.2}} \right)^n \right] \quad [2-1]$$

where,

Y(d) cumulative fraction finer than d

d aperture size

$d_{63.2}$ characteristic particle size $d_{63.2}$ corresponding to $Y(d) = 0.632$

n a measure of uniformity (breadth) of the PSD

Trezek and Savage⁹⁵ discussed the effect of size reduction, air classification and screening on PSDs of ferrous metal, aluminium, glass, paper and plastic. Ruf⁹⁶ studied PSDs of the main components of MSW (unprocessed and comminuted) and provided a general indication of the size ranges of comminuted waste constituents. Hasselriis⁷⁶ described how with mixtures of materials, such as mixed MSW, the RRSB graphs are determined by the relative amounts of the materials and the degree to which their PSDs overlap.

Another approach for graphical representation is the proposed method for analysis of waste deposited in landfills, stemming from geological applications⁹⁷. According to Pfannkuch and Paulson⁹⁸, logarithmic-phi units could be used, enabling the calculation of common statistical measures, such as arithmetic and geometrical mean, median, standard deviation, skewness and kurtosis of the distributions.

Typically defined quantities in PSD determination are explained:

1. cumulative fraction finer than d_x , where x is the percentage (undersize fraction, underflow) passing through the screen/sieve with aperture size d ;
2. characteristic particle size $d_{63.2}$ corresponding to $Y(d) = 0.632$; i.e., the particle size for which 63.2% of the cumulative fraction is smaller than (63.2% cumulative passing)
3. nominal product size d_{90} (i.e., aperture/particle size with 90 % cumulative passing) or nominal top size d_{95} , which can be used to define the product size of comminution process or the upper size of a fraction retained between two consecutive sieves; and
4. measure of uniformity (breadth) of PSD n , calculated as the slope of the linear fit trend in a RRSB grid diagram. The steeper the slope of the line, the tighter the size range of the particles. A narrow size range indicates finer shredding and grinding than coarser cutting, leading to a larger proportion of fine material⁷⁶.

PSDs have been criticised for not producing meaningful results for solid waste management, because of the problems in size determination and measuring. Instead, particle mass distributions have been proposed, which initial evidence suggests can adequately describe the distribution of unit masses (weight fractions of different materials)⁵³.

The size reduction ratio $\eta_{d_{\text{mesh}}}$ (**Equation [2-2]**) is a performance descriptor for comminution unit processes. This is defined as the ratio of the mass of the comminuted product to the mass of the input material, given that the particle size of the comminuted product is lower than the size of the mesh and that of the input material is larger than mesh size⁹⁹.

$$\eta_{d_{mesh}} = \frac{m_{P < d_{mesh}}}{m_{I > d_{mesh}}} \quad [2-2]$$

where,

- $n_{d_{mesh}}$ size reduction ratio
- $m_{P < d_{mesh}}$ mass of the comminuted product
- $m_{I > d_{mesh}}$ mass of the input material

2.3 Comminution processes

Comminution is a unit operation used to reduce the size of materials. Within the waste field, comminution equipment is generally referred to as ‘shredders’ or ‘granulators.’ Primary size reduction refers to comminution of as-received waste; whereas secondary shredding refers to further comminution of a waste stream that has undergone primary shredding⁸⁰.

Objectives met by comminution include^{76, 78, 84, 100}: (1) meeting (commercial) product specifications in terms of particle size and shape, e.g., compost standards or RDF particle specifications to suit the intended method of thermal recovery; (2) fracturing and reducing the size of particles to increase their biochemical reactivity, e.g., lignocellulosic material in anaerobic digestion processes; (3) dismantling assemblies of items into their subcomponents, or cutting them into pieces, enabling separation of desirable and undesirable constituents by downstream mechanical treatment, e.g., closed cans; (4) reduce the bulk of materials for better handling or disposal; (5) disaggregating materials to enable effective separation, e.g., magnets cannot effectively remove metals from a mixture of other large objects; and (6) partially homogenising heterogeneous mixtures. For RDF/SRF production purposes, the

combustible fraction should be comminuted finely enough to enable it to be conveyed, stored, retrieved, fed and air-classified⁷⁶.

2.3.1 Size reduction in MBT plants

Size reduction is commonly one of the first unit operations in MBT processes. Secondary shredding is employed during RDF/SRF processing or to adjust final product size. Typical mechanical unit operations that serve as the initial treatment step for the input waste, along with their operating principles are reviewed by Enviros⁵. Shredding has conventionally been the first unit operation in most separation systems designed to produce RDF, but in the 1980s some systems that employed trommels as the first processing step appeared¹⁰¹. The first biodrying MBT plants resorted to primary shredding of the as-received input, possibly after removal of bulky/unsuitable items. The shredded discharge (e.g., Eco-deco: 200-300 mm; Herhof: <200 mm or 150 mm) was directly fed into the biodrying stage. At the Nehlsen plant in Stalsund, Germany, after pre-shredding and ferrous material separation, only the underflow of a 65 mm disk sieve is fed into biodrying cells¹⁰². However, other recent approaches that avoid initial comminution exist. In addition, Eco-deco and Nehlsen use secondary shredding in the post-treatment stage, with Eco-deco using comminution as the final refining stage to produce an SRF with the appropriate PSD, and Nehlsen as part of the material separation process of the biodried output.

In MBT plants that do not use biodrying, but are able to produce a WDF fraction, comminution is also important. MBT processes that use aerobic composting as the core biological unit usually have shredding as their first unit operation, followed by trommel separation (e.g., commercial reference sites of MBT providers such as Biodegma, Horstmann, Linde, or New Earth)¹³. Different size reduction solutions may be employed by other technology providers; for example, Hese uses a cascade-ball mill

merged with a trommel; Sutco uses a crusher to feed a sieve drum; Wright Environmental uses a pulveriser, followed by a magnetic separator and then a trommel; and Wastec uses a bag splitter to feed their proprietary kinetic streamer.

Some companies that provide MBT processes that use AD or percolation as the core biological unit, use size reduction equipment for primary shredding (e.g., Hese uses a cascade ball mill, and OWS uses a shredder) or at the material recovery/pre-conditioning stage that precedes the AD/percolation unit(s). For example, shredding is used by BTA and Grontmij. Shredders are also used in wet pre-treatment processes such as Arrowbio and STB.

2.3.2 Process control and performance of comminution processes

Comminution operations for the mining and food industries have been widely modelled¹⁰⁰ and the PSDs from various types of shredding equipment can be predicted by computer simulation of the comminution process¹⁰³. Mathematical modelling and simulation of comminution processes in minerals processing and in general have been summarised elsewhere¹⁰⁴⁻¹⁰⁵. However, modelling of size reduction in waste management processes is still under-developed. Van Schaik et al.¹⁰⁶ modelled the recycling rate of secondary metals during shredding of end-of-life vehicles, drawing from minerals processing theory, using particle size reduction distributions and liberation as key model parameters.

Size reduction performance in MBT plants should be measured against their ability to deliver the desired output characteristics, which depend on the unit position in the overall process flow and the plant configuration. For example, primary shredding will have different goals from shredding for up-grading a final output, and different waste particles size ranges are optimal for composting, fermentation, and RDF/SRF thermal recovery purposes. Selective comminution can be beneficial for material flow

management in MBT plants, particularly when different categories of materials, contained in the size reduced output, concentrate in different size ranges. Each type of material tends to occupy a characteristic range of sizes in the as-received waste^{76, 96}, (**Figure 2-2**) and comminuted materials with different properties also tend to concentrate in certain size ranges. This could be useful for separation unit operations, such as screens, to separate out fractions rich in certain materials⁷⁸.

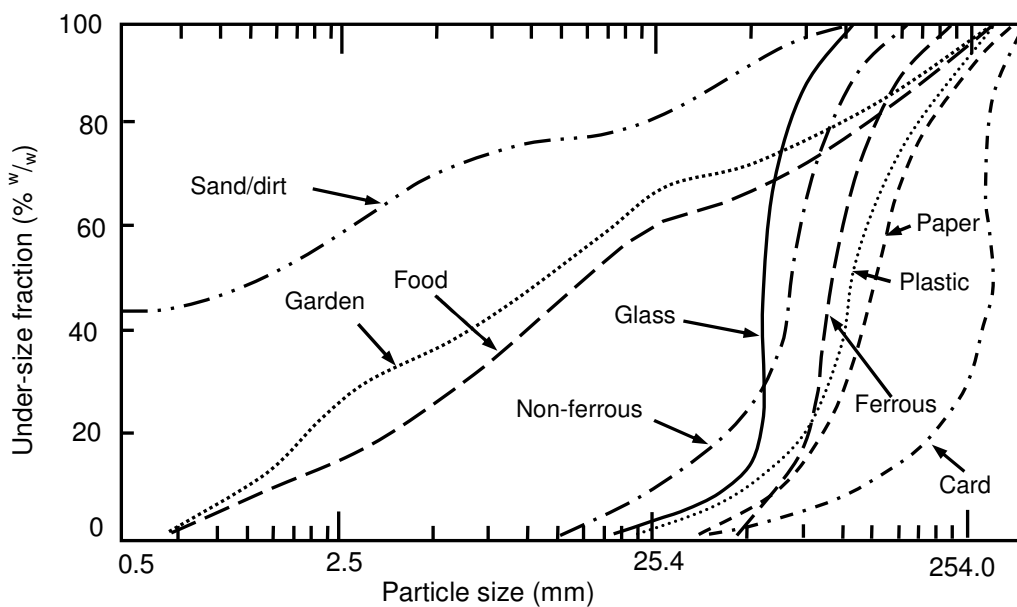


Figure 2-2 Particle-size distribution (PSD) of components of raw mixed household waste, in semi-logarithmic diagram. Each type of material spreads over a characteristic range of sizes, potentially allowing selective screening through the selection of suitable screen aperture. For example, a screening unit with 25 mm openings could theoretically concentrate all of the paper card and plastic in the overflow fraction. Redrawn from Ruf⁹⁶, cited in Hasselriis⁷⁶

Shredding can also cause problems such as cross-contamination of materials, and trade-offs are inevitable in downstream processing⁷⁶⁻⁷⁷. Comminuted output PSDs and liberation/concentration of certain substances, or set of components within defined size ranges, could be used as characteristic performance indicators for comminution machinery. However, there is evidence that the spread of waste component PSDs

generally increases after comminution (**Figure 2-3**) making classification on an item basis by particle size (screening) increasingly difficult.

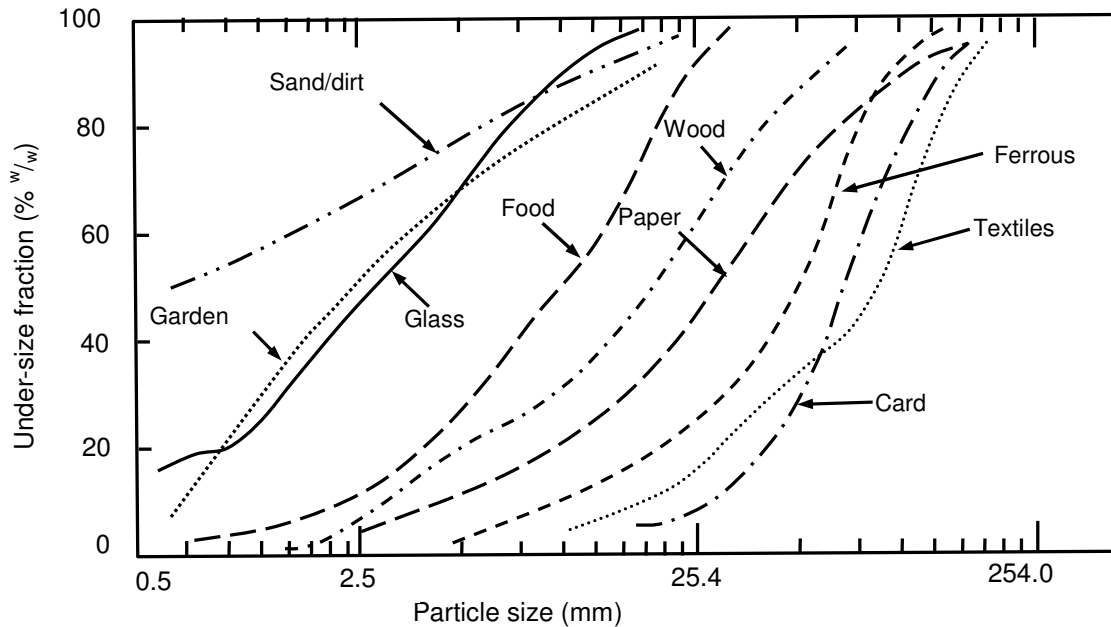


Figure 2-3 Particle-size distribution (PSD) of components of single-shredded MSW, in semi-logarithmic diagram. After shredding each waste component (e.g. paper) tend to occupy a wider range of sizes, compared with before size reduction (see **Figure 2-2**). This could restrict the potential for selective screening of certain waste components after shredding. Redrawn from Ruf⁹⁶, cited in Hasselriis⁷⁶

Table 2-4 General features of comminution equipment - typical values

Equipment	Rotation speed	Power	Through-put	Material processed	Output size
Hammermill shredder	700-3000 rpm	500-700 kW	20-30 t h ⁻¹	Versatile, clay to leather or steel, can process very low density material	Pulverised
Rotary shear/shear shredder	60-190 rpm	100-800 kW		Tyres, refuse bags, bulky waste	25-250 mm
Flail mill				Card and paper	Coarse
Cascade/ball mill	ca 10 rpm			Mixed and residual MSW	Coarse (35-80 mm) [*] Fine (<35 mm) [*]

Source of information: Tchobanoglous and Kreith¹⁰⁷, Pretz and Onasch⁵⁴, and Enviros⁵
^{*} Ball mill coupled with trommel

The most important options for (primary) comminution are hammermill shredders, rotary shears, flail mills and cascade-ball mills. Their operating principles,

performance in relation to material flow management, and results from MBT plants are discussed below. **Table 2-4** summarises their main features.

2.3.3 Hammermill shredder

Hammermill shredders are commonly used for MSW comminution (**Figure 2-4**) and are highly varied in energy requirements, and specific configuration (**Table 2-5**). Hammermill shredders, initially developed for crushing of minerals, are versatile in processing different materials: from sticky clay to tough fibrous solids like leather or steel¹⁰⁰. Their performance is specific to the input material composition and machinery configuration. The important input properties are ductility, moisture content, temperature, bulk density, and shear strength⁷⁸⁻⁷⁹.

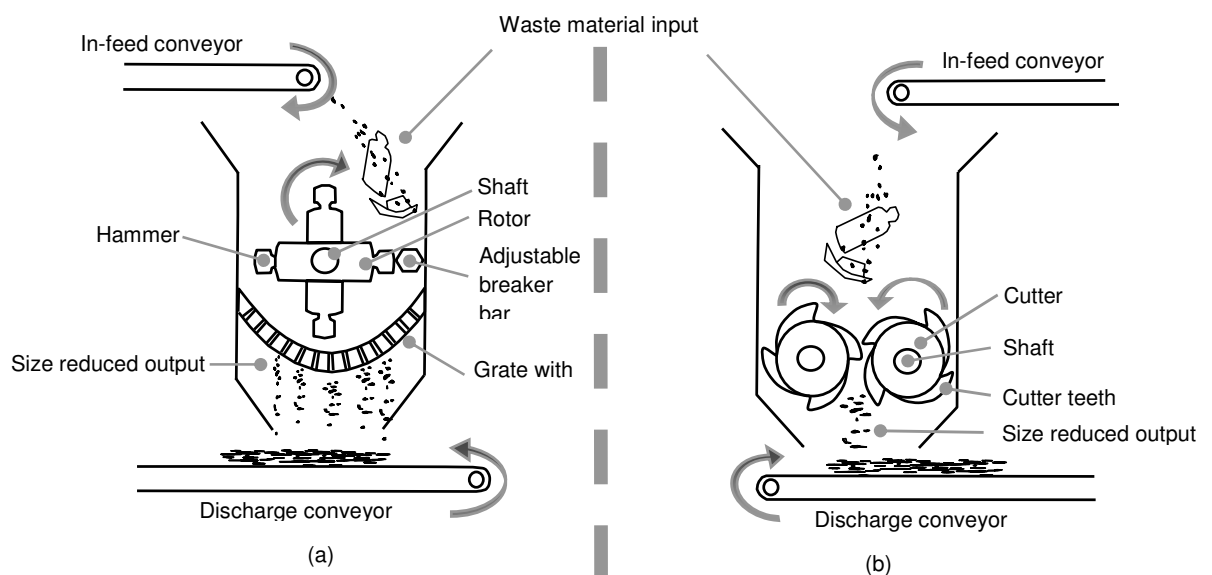


Figure 2-4 Schematic diagrams and operation principles for two typical comminution equipment in MSW: (a) hammermill; (b) rotary shear. Adapted from Tchobanoglous et al.⁷⁸

Hammermills can be designed either in horizontal-shaft or vertical-shaft configurations. Horizontal-shaft hammermills have a bottom discharge grate with specific sized openings. Shredded waste remains within the chamber and comminution continues until it reaches the appropriate size to pass through the

openings. Vertical-shaft hammermills have a cone-shaped housing that narrows down to a throat section⁸⁰. Vertical-shaft hammermills can be fed with very-low density materials due to associated windage⁷⁹. The swinging hammers create a vortex/fan effect (windage; towards product flow) that complements gravity in pulling the waste down into the unit chamber. Grinding occurs more in the lower part beneath the neck section. The ground product is usually comminuted to such a degree that no screening discharge grate is needed.

Vertical-shaft hammermills were specifically designed for MSW processing⁷⁹, but the majority of hammermills in place use the horizontal-shaft configuration. A hammermill shredder is a heavy duty cylindrical or tapered casing, equipped with a number of hammers extended radially to form a rapidly rotating central shaft or disc. Size reduction is achieved by the combined actions of impaction and tearing by the swinging steel hammers. To avoid damage to equipment, hammers can be mounted flexibly on the shaft, allowing for rotation over bulky or very dense waste components. Input waste components enter the mill from the top and move downwards under gravity. A component entering the shredding zone will inevitably be struck by the hammers, imposing sufficient force to crush items. Size reduction is continued by waste being struck against stationary breaker plates or cutting bars fixed around the inner housing wall of the grinding chamber.

Hammermills are versatile, suitable for production of specific PSDs and for the liberation of assemblies of waste component parts⁸⁴. Comminution of mixed waste by a hammermill shredder significantly changes the PSD of input constituents, enabling subsequent screening of selective fractions. Despite the spreading effect for some component PSDs, it can be beneficial for others; for instance, brittle materials such as glass, sand and rock form a higher proportion of the fine particles range, compared

with ductile materials, such as ferrous and non-ferrous metals. Barton et al.⁷⁷ provide data on selective shredding for UK RDF production at the former Byker plant, showing the concentration of the non-combustible and putrescibles in the <10 mm fraction (with the exception of metals).

However, a higher degree of size reduction is not always desirable. High-speed rotation and impaction within hammermills pulverises materials, which may compromise RDF/SRF quality by cross-contamination⁷⁷. Fine particles can become embedded in softer materials, such as paper and textiles, contaminating these with unwanted substances. Despite the beneficial use of shredders for selective reduction, the shredding of highly polluted waste components, such as electronic equipment, batteries and composite materials, should be avoided, as it results in contamination of the less polluted items^{13, 55}. If glass is contained within the input waste, paper items may become laden with shards of glass that contribute to the ash content⁷⁷. Additionally, fine glass particulates can fly in a subsequent air classifier and become incorporated into the RDF stream, increasing its ash content⁷⁶. The organic fraction of MSW can also be contaminated with minerals^{78, 80}. In addition, over-pulverisation is not desirable in the case of material intended for biostabilisation through composting.

The modelling of impact crushers for mining applications is long-established and satisfactory simulation has been achieved (e.g., Nikolov¹⁰⁸). Modelling aspects of primary comminution of MSW has been attempted¹⁰⁹⁻¹¹⁰: the single most important parameter affecting the shredded output PSD is the mean residence time (T), defined as the time a feed particle remains within the shredder. Testing results imply that a longer residence time could lead to a smaller characteristic particle size. A smaller output product size can be achieved by operating the hammermill fully loaded (choked). Selection of the size of discharge grate openings in horizontal-shaft hammermills allows for more accurate control over the upper limit of the ground-waste

overall PSD. However, tests on MSW commercial scale shredding showed a consistently unpredictable PSD for the output¹¹⁰⁻¹¹¹. Validation of the hammermill unit operation of the GRAB¹¹²⁻¹¹³ computer model of 1985 by data from UK RDF plants showed unsatisfactory results¹¹⁴. Parameters used were residence time, residence time distribution, selection function and breakage function, with the last two exhibiting problematic behaviour.

2.3.4 Rotary shear

Rotary shears or shear shredders are commonly used in waste management operations, including RDF/SRF production plants⁷⁵ (**Table 2-4**). Rotating knives or hooks rotate at a slow speed with high torque, the shearing action tears or cuts most materials.

Multi-rotor types are the most common^{78, 80}, with two or four parallel counter-rotating shafts each equipped with a series of perpendicularly mounted disks with comminution tools. Shafts are arranged alternately so that the rotors overlap and the cutting tools act as scissors. Different types of tool geometry may be used, to allow for different feedstock and shredding objectives. In radial-gap rotary shears comminution occurs in the radial gap between the rotor knives and the appropriately adapted stator, resulting from shearing stress¹¹⁵. The cutting tools are usually indexable knives of rectangular, triangular or circular shape. In axial-gap machines the comminution process takes place both in the axial and radial gaps. The shredded output of radial-gap shear rotors typically consists of smaller fragments than the multi-rotor axial-gap, due to the greater number of rotor knives, defined comminution geometry and the use of discharge grates in the radial-gap rotary shears¹¹⁵. Shredding of particles that exhibit elastic-plastic deformation behaviour can improve if they are stressed at low temperatures⁸⁴.

Feeding devices (force feeders) can be employed, especially for oversized bulky waste and for radial-gap machinery, usually pushers, swivel arms, feed rollers, and feed conveyors. The shredded output drops or can be pulled through the unit. In most cases the rotating shafts can be automatically reversed in the event of obstruction, resulting in reduced down time due to blockage.

Shear shredders tend to produce a more uniformly sized output and lower contamination than hammermills⁷⁸, because of the lower rotation speed and absence of impact as a comminution mechanism. Hence, they are preferred over hammermill in RDF/SRF production lines⁷⁵. The cutter spacing between the shafts can be adjusted, ranging from several mm to cm; this may allow glass and other items to fall through the rotors without being shredded⁸⁰. Qualitative data concerning rotary shear fed with mixed MSW, including tyres and oversized materials, showed that a ca 5 cm cutter spacing reduced the size of glass without pulverising it; and a ca 10 cm spacing allowed several bottles and cans to pass through the rotors and report to the output unbroken¹⁰¹.

Limitations of rotary shears include the production of a coarsely shredded output and the need to remove large steel and other durable items prior to shredding, as they may cause excessive wear and tear. Mathematical modelling of rotary shears performance is thought by some authors to be virtually impossible, due to the large number of variables involved⁷⁹.

2.3.5 Flail mill

The flail mill is similar to the hammermill, providing coarse shredding as input passes only once through the comminution chamber. There are some important differences⁷⁸. Instead of hammers, comparatively thin flail arms, spaced farther apart, are mounted on the rotating shaft, with their thickness ranging from

ca 1 cm to ca 2.5 cm⁷⁹. They are usually single-pass machines, with the input material being shredded only during the passage from the rotor area, as they have no discharge grate. Input material is stricken by the flails and smashed against the anvil plates on the inner side of the comminution chamber. Sufficiently small input particles can pass through the mill without undergoing size reduction. Comminution of paper and card rich fractions is thought to be better achieved by flail mills than by hammermills⁷⁹. Another design variation operates with two counter-rotating shafts. Flail mills have increasingly being used for shredding of the combustible fraction in RDF production plants and as bag openers⁷⁸⁻⁷⁹.

2.3.6 Cascade/ball mill

A cascade mill equipped with grinding balls (or ball mill) is a type of tumbling mill, which has been widely used for mechano-chemical processing operations, from minerals processing to advanced materials production (**Figure 2-5**)¹¹⁶.

Rotating drums use heavy balls to break up or pulverise waste. Tumbling mills have been widely used for intermediate and fine reduction of abrasive materials¹⁰⁰. In a typical tumbling mill, a continuously or batch-fed cylindrical or conical steel chamber with tapered ends, appropriately lined in the inner side, rotates slowly around a horizontal axis, with about half its volume filled with a solid grinding medium¹⁰⁰. In ball mills metallic balls cascade within the shell and centrifugal forces lift the balls, in contact with the shell walls and each other, up to where they lose contact and fall. Falling balls and other hard substances contained within the input waste impact on waste feedstock, mainly whilst striking the bottom of the milling chamber. Pressure and shear stresses imposed on the waste constituents result in differentiated comminution, according to their physical-mechanical properties.

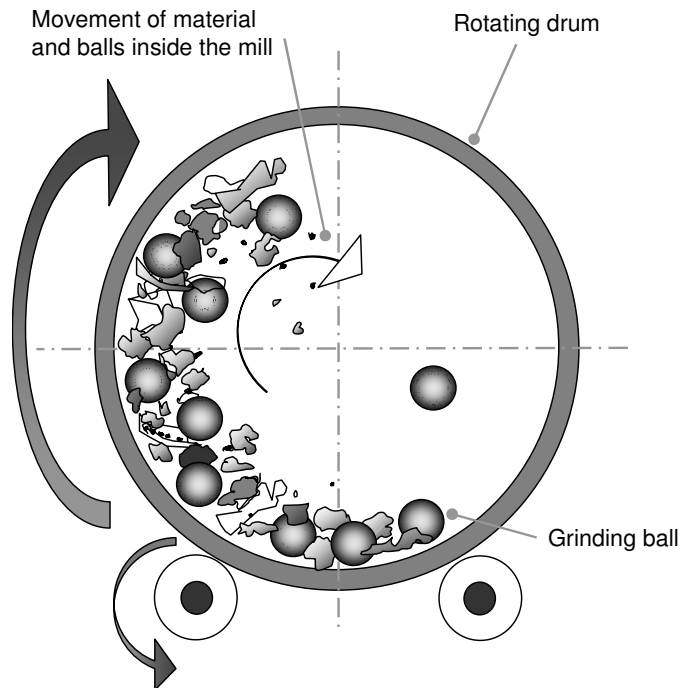


Figure 2-5 Schematic diagram of a vertical section of a ball mill, demonstrating its operating principle: as the drum rotates at a low speed around its horizontal axis the grinding balls in contact with the drum walls are lifted by the centrifugal force. At a certain point they lose contact and fall (cascade), impacting on the materials. Adapted from Faculty of Chemical Technology, University of Split¹¹⁷ and Suryanarayana¹¹⁸

In MBT processes cascade/ball mills have been used for primary shredding. An early European example of a ball mill use is the Loesche GmbH case, operated from the mid-1980s by the Waste Management Association of Kaiserslautern (ZAK), Germany. Another ball mill based process operates on residual waste in Brandenburg. In 2005 a plant was under construction at the Nentzelsrode landfill to treat the residual waste from Norhtren Thuringia, Germany ($140,000 \text{ Mg a}^{-1}$). In the UK, an $180,000 \text{ Mg a}^{-1}$ nominal capacity plant that accepts residual waste began operating in Leicester in 2005¹¹⁹.

Performance data have been published for the Loesche-Hese cascade mill¹¹⁹⁻
¹²¹ and for an Outukumpu-Hese cascade mill, similar to the Harding type, operated in cataract mode¹²². The attached trommel separates two output size ranges, namely

underscreen (fine and intermediate fraction, 5-40/35 mm) and overscreen (coarse fraction, 35/40-80 mm). For the Loesche-Hese mill, the degree of size reduction is in the order of organic portion < paper/cardboard < plastics/glass/batteries < wood/stones/metals¹¹⁹. For the Outukumpu-Hese mill, the order is organic portion < sand < paper/cardboard < plastic films/glass < stones < visco-plastic/tenaciously plastic/shoes/rubber¹²².

Cascade mill action has been found to have a selective effect on different waste constituents. Organic material is crushed or torn and disaggregated, whilst for wood and textiles the action primarily concentrates the coarser fraction (40-80 mm). Ferrous (Fe) material and batteries mostly deform, compress and become rounded at the edges, but do not reduce in size, whilst non-Fe materials deform slightly. This observation is in agreement with the wider experience of the behaviour of ductile, laminated materials in ball mills⁸⁶.

In terms of suitability of the output for further treatment, the two-dimensional deformation of non-ferrous material is beneficial for effective separation in eddy-current separators. Operators claim that metallic material is cleaned, enhancing its saleability after separation. Mechanical energy input transformed into heat flow because collisions within the mill lead to temperature rise up to an average of 50-60°C, resulting in grinding having a drying effect on waste¹²¹. Drying particularly takes place with respect to coarser, hydrophobic plastics, facilitating downstream separation¹¹⁹.

2.3.7 Other comminution processes

Rotating drums use gravity to tumble, mix, and homogenize waste. Within rotating drums, material is lifted up the sides of a rotating drum and then dropped back into the centre. Dense, abrasive items such as glass or metal help break down the softer materials, resulting in considerable size reduction of paper

and other biodegradable materials. In wet rotating mills with knives, waste is wetted, forming heavy lumps that break against the knives when tumbled in the drum. In bag splitters, such as flail mill or shear shredders, a more gentle shredder is used to split plastic bags whilst leaving the majority of the waste intact.

2.3.8 Comparison of PSDs of comminution processes

Preliminary results on the PSDs of various comminution methods¹²³ allow ranking of the processes. More intensive comminution (i.e., higher cumulative mass passing, d_{20}) was found for ball mills ca 68%; mixing drum; hammermill ca 26%; and screw mill ca 21%.

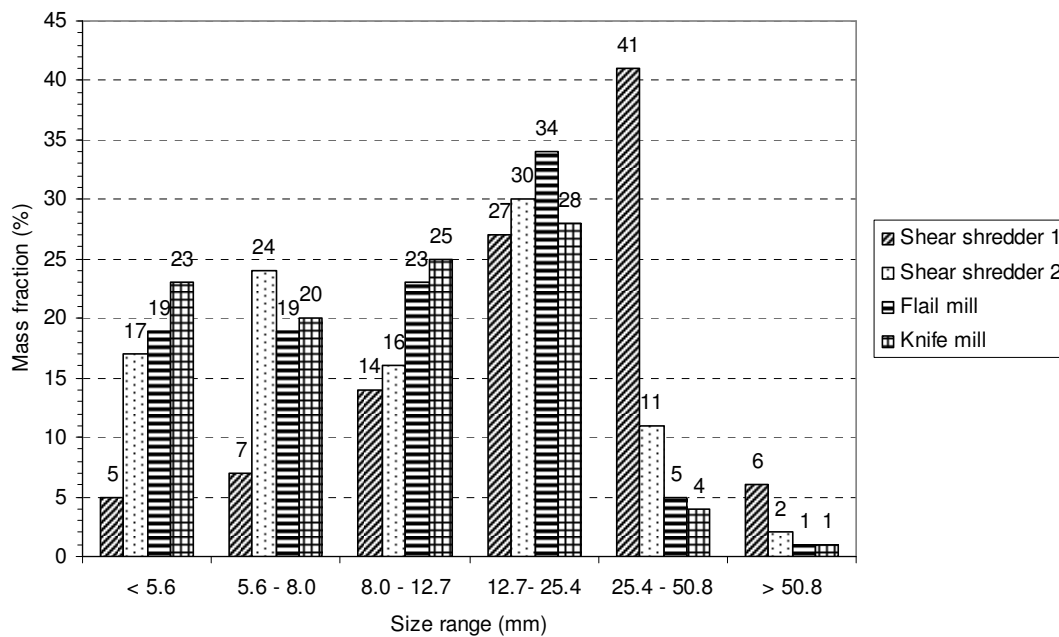


Figure 2-6 Secondary comminution of SRF, before pelletising, by different types of size reduction equipment (see legend); comparative results for the mass distribution of the shredded output. Data from Jackson¹²⁴, cited in Porteous⁸¹

Results on the size reduction ratio for primary and secondary comminution of residual waste in MBT plants were reported by Zwisele⁵⁶. Results on comparative

performance of different secondary size reduction of SRF for subsequent pelletising can be found in Porteous⁸¹, with the knife mill showing the best performance in terms of PSD (**Figure 2-6**). Vertical-shaft hammermills can achieve a higher degree of pulverisation compared to horizontal ones⁸⁰.

2.4 Classification and separation

Mechanical units for the classification and separation of waste streams are central to the material flow management of MBT processes. The appropriate splitting of input waste into outputs with desirable characteristics is a challenging task. Trade-offs are inevitable, and must be resolved according to what is technically and economically feasible, satisfying both legal and market requirements. This section discusses classification and separation units, emphasising RDF/SRF production processes. An assessment of the most appropriate formulas, descriptors and tools for performance evaluation of classification/separation units is included. Some mechanical solutions of emerging importance are presented in more detail than conventional options such as screening and air classification.

2.4.1 Function of classification and separation operation units

Separation and classification unit processes are used to segregate input streams into output sub-streams with desirable characteristics. **Table 2-5** lists some types of equipment used in MBT plants. Pretz and Onasch⁵⁴ and Diaz and Savage⁸² reviewed operations of mechanical processing equipment suitable for MBT plants.

Output streams can either contain sorted desirable items, for example, paper and card in the light fraction of an air knife (termed 'separation'); or can be separated out on the basis of their size, for example, fine fraction of a trommel under-flow (termed 'classification'). Possible objectives include separation of certain size fractions, concentration of certain materials, separation of fractions with specific properties (e.g.,

organic fraction of municipal solid waste (OFMSW), high CV fraction), and removal of undesirable particles. From a material flow management point of view, separation/classification leads to a redistribution of properties/materials, enabling their enrichment or dilution in output streams.

Table 2-5 Indicative classification/separation equipment used in MBT plants

Processing type	Equipment	Operating principle
(Size) classification	Trommel (Drum sieve, Drum screen)	Tabular rotating screen, inclined slightly downwards, lifters help lift materials up
	Disc screens	Horizontal rotating bars across the screen, perpendicular to the material flow carry the material and bounce it into the air
Separation	Air classifiers *	Material is fed into a horizontal air stream: lighter is carried further/up and denser drops, based on density and aerodynamic properties. Advanced designs try to use mainly density properties or to include others, such as elastic
	Ballistic separators	Waste is fed to the middle of sloped vibratory screen, with under-flowing air stream that fluidises the bed: lights flow and heavies are transported by the vibrations, based on density and elasticity
Metal separation (Fe and non-Fe)	Magnetic separation of ferrous metals	Magnetic drums, over-band magnets and head pulleys are available. Magnets are either permanent or electromagnetic
	Eddy-current separation of non-ferrous metals	Application of electric field separates conductive from non-conductive materials. Systems with centric design are prevalent – systems with eccentric pole design are also available
Optical separation	Image detection devices	Picture analysis by sophisticated cameras and software
	Near-infrared detection (NIR) devices	Fast scanning spectrometer analyses identifies molecular structure; air nozzles blow selected items into bunkers; it enables separation based on chemical composition
	X-ray detection	Operates with transmission of X-rays: can distinguish between organic and inorganic materials (e.g. plastics and stones) and between light and heavy metals (e.g., Al and Cu)

Source of information: Tchobanoglous and Kreith¹⁰⁷, Pretz and Onasch⁵⁴, Enviros⁵, and Kohaupt¹²⁵
 * Refer to **Table 2-8** for detailed coverage

The operating principles of separation/classification units depend on the physical properties of the input waste materials or items. Categories of equipment according to main operating principles are¹⁰⁷ size (and shape) separation, density/elastic properties separation, magnetic separation, electric conductivity separation, and optical/image properties separation (chemical properties are also involved). Each of these categories can be further sub-divided.

2.4.2 Separation and classification processes in MBT plants

Input into separation/classification units is usually a previously comminuted waste stream, either sorted or prior to size reduction. As-received waste can also pass

directly through classification to avoid contamination of fractions by subsequent comminution (**Section 2.3.3**), or because the separation unit does not demand a comminuted input, as might be the case for ballistic separators. Classification as the initial treatment unit is common in plants that use AD technology, such as the Iska, Buchen plant; Linde, Barcelona plant; Ros Roca, Avila plant; SBT, Heerenveen plant; and Whehrle¹³. More frequently, classification/separation units are placed downstream in the flowsheets. Most data refer to the combination of comminution and classification, such as hammermill followed by screens or ball-mill followed by trommel.

Other typical functions in MBT flowsheets include post-treatment within biodrying plants aimed at separating combustible high CV materials low in minerals and chemical pollutants, to form RDF/SRF (**Figure 2-1**); pre-treatment of input material (comminuted or not) for composting/AD to separate out a high CV fraction and concentrate the organic-rich, contamination-free fraction; post treatment of composted/anaerobically digested material for CLO production; and separation of dry recycle fractions, typically Fe and non-Fe metals and aggregates.

2.4.3 Performance evaluation of classification and separation processes

2.4.3.1 Conventional performance descriptors

The performance of mechanical processing unit operations can be assessed in different ways and by using various descriptors. For instance, considered as heat engines, the efficiency of energy conversion of machinery can be defined as the ratio of the useful mechanical energy produced over the total energy consumed¹²⁶. Whilst a mechanical and energy efficient approach is significant for both financial and sustainability considerations, we focus on descriptors appropriate to evaluate the material flow performance of MBT plants.

Two main approaches can be identified. The first approach stems from the mining industry, where the performance of a classification of different size fractions is most important during processing (e.g., sharpness of cut, selectivity). Klumpar¹²⁷ discusses these aspects in detail in relation to the performance of air separators. The second approach originates from separation of phases or fractions according to other material properties. As there is no uniformity in the related performance terminology, two clarifications are necessary. Firstly, in the literature the term 'efficiency' is often misused to denote various descriptors of performance¹²⁶. Rather than accurately being used to refer to the ratio of effective use of resources over the overall spent resources, efficiency is used to describe the degree to which an operation is effective: e.g., the segregation of items achieved by a separation process relative to the ideal. In this work the view is taken that the term 'effectiveness' should be preferred for the descriptors that try to measure 'what is achieved vs. what could be, or would be desirable to have been achieved', similar to the approach used by Hasselriis⁷⁶. The term 'efficiency' could be reserved for descriptors that measure the degree of losses in conversion processes. Other relevant terms, such as 'yield,' 'recovery' and 'purity' are clarified and discussed below. Secondly, variety and inconsistency in the terms used to describe the outputs of classification and separation processes often leads to confusion. The input (or in-feed) stream is split into two or more output streams (fractions). In the case of one main useful output fraction, which concentrates the desirable component(s) at the highest purity of all outputs, this can be referred to as the 'product' or 'extract' or 'accepts,' whilst the rest of the output fraction(s) can be referred to as 'reject(s).'

In the case of an air separator with only two output streams, used in RDF production, the material carried away and separated from the air stream would be the extract, and the other stream the reject. For these outputs the historic terms 'lights' or 'low-gravity' fraction vs 'heavies' or 'high-gravity fraction,' 'combustibles' vs

'incombustibles,' and 'organics' vs 'inorganics' have been used respectively. These terms all denote a principal feature, commonly shared by the items in the streams separated and they either refer to the separation operating principle (e.g., low-gravity) or to a desirable property of the stream (e.g., combustibility, or organics). All constitute simplifications which, if taken literally, can be misleading. To illustrate, the separation in an air classifier does not solely depend on density, but on aerodynamic and sometimes elastic waste particle properties. The term 'organics' reflected unrealistic early expectations from air separators and has been proven wrong, because the air separators cannot effectively separate organic from inorganic materials.

In the case of size classification into two streams, the terms 'overscreen fraction,' 'overflow' or 'overs' and 'underscreen fraction' or 'underflow' or 'unders' or 'fines' have been used. However, modern equipment typically has more than two output streams and none of them may be considered useless (i.e., a reject stream), as they are part of a continuing material flow management process, depending on their position in the overall flow-chart of the plant. Hence, all output streams should be called 'products' and, if possible, suitably identified by terms that approximately describe their anticipated constituents. These complexities suggest that careful interpretation of the existing literature on performance is imperative.

The performance of each process unit should be evaluated against the role it plays within the material separation process. No single parameter can describe all aspects of a mechanical unit operation performance. The most important descriptors for material flow management are defined below. The varying nomenclature that is evident in the literature is expressed in symbols compatible, by large, with the MFA according to Rotter et al.⁵⁵. Conventional descriptors of separation unit operations performance are yield, recovery, purity, and overall effectiveness^{74, 76, 126-130}. These are defined for the generic case of a separation unit with multiple input and output streams

(products). The mode of operation of the separation or classification equipment affects the results. During measurements effort should be taken to achieve a constant state of operation over a given time frame¹³¹.

The purity (cleanness or composition) evaluates the degree of contamination by undesirable impurities, or denotes the mass-based material composition (input)⁷⁴. Purity $C(CM)P_i$ is defined as the ratio of the mass of a component (or set of components) in the product over the total mass of the product (**Table 2-6**).

Table 2-6 Descriptors and formulas for the characterisation of the mechanical processing performance

Performance descriptor	Designation	Formula	Comments / References
Yield (mass basis) [of a product P _i]	Y _m (P _i) or Y(P _i)	$Y(P_i) = \frac{m_{P_i}}{\sum_j m_{I_j}}$	mP _i : total mass of product P _i m _l : total mass of the input $\sum_i Y(P_i) = 1$
Yield (energy basis) [of a product P _i]	Y _e (P _i)	$Y_e(P_i) = \frac{m_{P_i} \cdot LHV_{P_i}}{\sum_j m_{I_j} \cdot LHV_{I_j}}$	
Purity (or cleanness) [of product P _i in certain waste component(s) (CM)]	C(CM)P _i	$C(CM)_{P_i} = \frac{m(CM)_{P_i}}{m_{P_i}}$	m(CM)P _i : mass of a particular waste component (or set of components) (CM) in product P _i ; mP _i : total mass of product P _i $\sum_{(CM)} m(CM)_{P_i} = m_{P_i}$
Recovery [of a waste component (or set of components) (CM) into a product P _i]	R(CM)P _i	$R(CM)_{P_i} = \frac{m_{P_i} \cdot C(CM)_{P_i}}{\sum_j m_{I_j} \cdot C(CM)_{I_j}}$	$\sum_j m_{I_j} \cdot C(CM)_{I_j} = \sum_i m_{P_i} \cdot C(CM)_{P_i}$
Recovery [typical case of: one input I, two products (P _{CM} and P _{NCM}) and two sets of components (CM) and other-than-CM (NCM)]	R(CM)P _{CM}	$R(CM)_{P_{CM}} = \frac{m_{P_{CM}} \cdot C(CM)_{P_{CM}}}{m_I \cdot C(CM)_I} = \frac{[C(CM)_I - C(CM)_{P_{NCM}}] \cdot C(CM)_{P_{CM}}}{[C(CM)_{P_{CM}} - C(CM)_{P_{NCM}}] \cdot C(CM)_I}$	
Total effectiveness [according to Rietema ¹²⁶]	E	$E(CM, NCM)_{I, P_{CM}, P_{NCM}} = \left \frac{m_{P_{CM}} \cdot C(CM)_{P_{CM}}}{m_I \cdot C(CM)_I} - \frac{m_{P_{CM}} \cdot C(NCM)_{P_{CM}}}{m_I \cdot C(NCM)_I} \right $ $E(CM, NCM)_{I, P_{CM}, P_{NCM}} = \left \frac{m_{P_{NCM}} \cdot C(CM)_{P_{NCM}}}{m_I \cdot C(CM)_I} - \frac{m_{P_{NCM}} \cdot C(NCM)_{P_{NCM}}}{m_I \cdot C(NCM)_I} \right $	Single overall performance descriptor. Satisfies the full list of the requirements proposed by Rietema ¹²⁶ . Note that no single parameter can describe all performance aspects of a mechanical unit operation.

Performance descriptor	Designation	Formula	Comments / References
Total effectiveness [according to Worrell and Vesilind ¹²⁸]	E	$E(CM, NCM)_{I, P_{CM}, P_{NCM}} = \left[\frac{m_{P_{CM}} \cdot C(CM)_{P_{CM}}}{m_I \cdot C(CM)_I} \cdot \frac{m_{P_{NCM}} \cdot C(NCM)_{P_{NCM}}}{m_I \cdot C(NCM)_I} \right]^{1/2}$	Single overall performance descriptor. Not verified that satisfies it the full list of the requirements proposed by Rietema ¹²⁶ . Note that no single parameter can describe all performance aspects of a mechanical unit operation.
Transfer coefficient (or transfer factor) [of substance (s) to product P _i]	$TC(s)_{P_i}$	$TC(s)_{P_i} = \frac{m_{P_i} \cdot c_m(s)_{P_i}}{\sum_j m_{I_j} \cdot c_m(s)_{I_j}} \quad \text{and}$ $TC(s)_{P_i} = \frac{c_m(s)_{P_i} \cdot m_{P_i}}{c_m(s)_I \cdot m_I} = MEC_m(s)_{P_i} \cdot Y_m(P_i)$	$\sum_i TC(s)_{P_i} = 1$
Material enrichment coefficient (mass basis) [of substance (s) from input I _j to the product P _i]	$MEC_m(s)_{P_i I_j}$	$MEC_m(s)_{P_i I_j} = \frac{c_m(s)_{P_i}}{c_m(s)_{I_j}}$	Concentrating, enrichment, MEC>1 Diluted, depletion, MEC<1
Material enrichment coefficient (energy basis) [of substance (s) from input I _j to the product P _i]	$MEC_e(s)_{P_i I_j}$	$MEC_e(s)_{P_i I_j} = \frac{c_e(s)_{P_i}}{c_e(s)_{I_j}} = \frac{c_m(s)_{P_i} / LHV_{P_i}}{c_m(s)_{I_j} / LHV_{I_j}}$	$c_e = \frac{c_m}{LHV}$
Grade efficiency (or selectivity) [of a narrow size range d _{NF} (portion of waste particulates of given size range) into a product P _i]	$G(d_{NF})_{P_i}$	$G(d_{NF})_{P_i} = \frac{m(d_{NF})_{P_i}}{\sum_j m(d_{NF})_{I_j}}$	Klumpar ¹²⁷ Schweitzer ¹³²
Sharpness of cut [of a grade efficiency curve]	$k_{25/75}$	$k_{25/75} = \frac{d(G = 25\%)}{d(G = 75\%)}$	Klumpar ¹²⁷ Wang et al. ¹³³ Other percentages may be prove more relevant in a waste management application context
Table notation	Symbol	Description	
Main symbols	c	Concentration of substance: i.e. $c_m(s)$ mass based concentration of substance s	
	C	Purity: mass fraction of waste component (or collection of components), i.e. $C(S)$ or $C(B)$	
	E	Total effectiveness	

Performance descriptor	Designation	Formula	Comments / References
	<i>G</i>	Grade efficiency (or selectivity)	
	<i>k</i>	Sharpness of cut (of a grade efficiency curve)	
	<i>m</i>	Mass or mass flow rate	
	<i>MEC</i>	Material enrichment coefficient	
	<i>R</i>	Recovery	
	<i>TC</i>	Transfer coefficient (or transfer factor)	
	<i>Y</i>	Yield	
	<i>LHV</i>	Lower heating value	
Stream symbols	<i>B</i>	Combustible waste components	
	<i>CM</i>	Component (or collection of components) in a stream: e.g. S or B	
	<i>I</i>	Input stream	
	<i>NCM</i>	Set of components other-than-CM	
	<i>NF</i>	Narrow range fraction (portion of waste particulates that fall within a defined size range)	
	<i>P</i>	Product (output stream)	
	<i>s</i>	Substance (according to the definition of MFA, an element or chemical compound that is preserved through a process)	
	<i>S</i>	Waste component (or collection of components) containing substances of concern	
Indices	<i>e</i>	Energy basis of ratios	
	<i>i</i>	Running index of product stream	
	<i>j</i>	Running index of input stream	
	<i>l</i>	A certain product, a value of <i>i</i>	
	<i>m</i>	Mass basis of ratios	

Adapted from: Rotter et al.⁵⁵

It denotes the mass fraction of certain useful waste component(s), such as the combustible items, suitable for RDF/SRF production, present in the corresponding product. An ASTM standard covers the determination of purity¹³⁴. The numeric values measured for purity are affected by the exact determination process that is followed, for example, with Fe materials, manual sorting for waste characterisation or proximate analysis are both plausible.

The yield $Y(P_i)$ of a product P_i is defined as the ratio of the mass (or mass flow rate) of the product over the total mass (or mass flow rate, respectively) of the input (**Table 2-6**). It denotes the overall mass fraction, irrespective of its composition, which is transferred to a certain output stream, and characterises the separation process⁷⁴.

The recovery $R(CM)P_i$ of a waste component (or set of components) into a product is defined as the ratio of mass (or mass flow rate) of these component(s) in the product, over the overall mass (or mass flow rate) of these components in all the input streams (**Table 2-6**). It denotes the mass fraction (or percent if multiplied by 100) of a set of components present in the input that reports in a certain product^{74, 127}. An ASTM standard covers the determination of recovery¹³¹. In continuous processes, purity is easier to determine than the mass (or mass flow rates). Hence, the recovery in the typical case of one input, two products and two sets of components (CM) and other-than-CM (NCM) can be estimated in practice through the measured purities (**Table 2-6**)^{74, 127, 131}.

The minimum requirements to describe the performance of a material separation device are that purity and recovery should be identified¹³¹. However, the idea of combining elements of the above descriptors to produce a single overall performance descriptor is established. More than one total effectiveness formula (in the case of binary separation) that combines recovery and purity can be found in the

literature. Rietema¹²⁶ reviewed the literature for the definitions of overall efficiency E , and assessed them according to a list of mandatory and desirable requirements that such a formula should fulfil, proposing the most appropriate formula (**Table 2-6**). Worrell and Vesilind¹²⁸ proposed another formula that results in similar values. However, it has not been verified as to whether it satisfies the full list of certain requirements proposed by Rietema¹²⁶.

In the case of size classification, i.e. screening, the effectiveness of the separation can also be assessed through the grade efficiency (or partitioning, classification) curve^{127, 132}. The mass based grade efficiency (or selectivity) $G(d_{NF})P_I$ is the recovery descriptor of the portion of waste particulates of a given size (narrow size range d_{NF}) into a product P_I (**Table 2-6**). It expresses the mass fraction of these waste particulates of given size range that reports into a product. For example, this descriptor can be used to evaluate the effectiveness of the separation of a screen for a waste component(s) for which there is evidence that it occupies a certain range of sizes after selective comminution or in the as-received waste.

The grade efficiency curve is the plot of the grade efficiency for the consecutive narrow size range d_{NF} that input can be divided into vs the waste particle size. The main portion of the curve is anticipated to be roughly linear and determines the sharpness of cut. Sharpness of cut $k_{25/75}$ can be conventionally defined as the ratio of the waste particle sizes that correspond to certain selectivity points, typically 25 % and 75 % (**Table 2-6**)^{127, 133}.

In practice, performance descriptors always take values below the unit. Composite items (e.g., complex domestic appliances) or composite materials (e.g., fibre-reinforced plastics) are constituents that cannot be fully liberated during the comminution that typically precedes separation and/or classification⁷⁵. Contamination

effects are particularly important in waste processing because of input heterogeneity and possible comminution.

A lower than expected performance in air separation units can be attributed to stochastic effects introduced by solid particles that interact with each other or with process unit walls. Additionally, unsteady air velocities occur¹³⁵. These effects restrict the effectiveness of separation. As a result, trade-offs are inevitable and isolated use of any descriptor regarding effectiveness can result in misleading conclusions about material flow management performance¹²⁶. For example, the above overall effectiveness relationships can be used in any separation process that sorts out two different output streams. However, in real systems one performance objective may be more important than the other. The need for high purity of a product may necessitate a low product yield, or vice versa⁷⁶. Data from the SRF plant in Neuss, Germany, illustrated the inverse relationship between purity and yield³⁸. Advanced processing with the objective of lowering the chlorine (Cl) content of SRF, (i.e., prioritising purity) resulted in a lower SRF yield. Overall efficiency formulas cannot allow for this varying relative importance of purity and yield.

2.4.3.2 Mass flow modelling and simulation for waste processing plants

The need for an accurate and comprehensive picture of material flows within a processing system has led to the development of system descriptions based upon mass balances¹³⁶. These were particularly applied to RDF production plants. Diaz et al.¹³⁷ developed a system of recovery transfer function matrices to describe each unit operation, based on waste components found in input and output materials. Hasselriis, in a similar approach, developed spreadsheets describing the split of waste components into output streams⁷⁶. For both prediction and design purposes, modelling of processing units and overall plants has been attempted. In the 1980s, Argonne National Laboratory in the US developed the computer programme GRAB, for

simulating the operation of MSW processing plants¹¹²⁻¹¹³. Warren Spring Laboratories produced a detailed evaluation of the software using data from the former RDF plants at Byker and Doncaster in the UK¹¹⁴. However, satisfactory simulation was not achieved.

A recent application in general SRF production can be found in Caputo and Pelagagge¹³⁸, suggesting that, mixing of a high calorific waste such as scrap tires with the stream of household waste is a prerequisite to meet the heating value target specified for RDF. Chang et al.¹³⁹ developed regression analysis models based on mass balances of waste components and chemical elements (ultimate analysis) to predict the heating value of RDF product for a specific production line. Chemical composition models exhibited better prediction capability. Zwisele et al.¹⁴⁰ developed the software interface and the initial version of a simulation tool of mechanical processing for waste treatment plants such as MBT. This includes a material database of input waste properties, computing algorithms describing unit operations, calculation of flows, and quantifying the statistical uncertainty. Mass flows, average material composition and PSD are used for each of the substance sub-groups of light solids, high-gravity solids, minerals, ferrous metals and non-ferrous metals. The limited published validation data shows an acceptable goodness of fit; parameterisation was done with empirical data of the specific plant and a stationary plant model was assumed. Zwisele et al.¹⁴⁰ recognised that dependencies on time (residence time), capacities (load), moisture content, etc. have to be taken into account in future developments and that the model has still to be validated with other case studies.

2.4.3.3 Novel material flow analysis approaches

MFA constitutes a systematic analysis of the flows (inputs and outputs) and stocks of materials both spatially and temporally as defined by Brunner and Rechberger²⁸. As well as providing a systematic approach, descriptors are adapted for

combination with societal evaluation methods such as cost benefit analysis^{3, 28}. In MFA, transfer coefficients (TC) (or transfer factors) describe the partitioning of a substance into the outputs of a process²⁸. The transfer coefficient of a substance into a product is defined as the ratio of mass (or mass flow rate) of the substance in the product, to the overall mass (or mass flow rate) of the substance in all the input streams. Practically, TCs are equivalent to the mass-based recoveries of conventional performance descriptors, with the mass fraction of waste components C(CM) being replaced by the mass-based concentrations of substances $c_m(s)$ (**Table 2-6**).

The TCs can depict the partitioning of a preserved property, such as overall mass and absolute element quantities, over the various output streams of a process. Generally TCs are substance-specific and depend on the input characteristics and the process conditions, such as the unit operation design and operating regime. The moisture content of the waste matrix is affected by both bioconversion (e.g., biodrying) and mechanical processing (e.g., comminution). Therefore, calculations or measurements of TCs should reflect this.

In addition to the use of TCs, Brunner and Stämpfli⁵⁷ and Rotter et al.⁵⁵ advocated the use of material enrichment coefficients (MEC). The MEC (on a mass basis) is defined as the ratio of the mass concentration of a substance over the mass concentration in the input (**Table 2-6**). MECs indicate whether the content of a substance, such as mercury (Hg), is increasing (concentrating, enrichment, $MEC > 1$) or decreasing (diluted, depletion, $MEC < 1$) in an output stream of a process compared to the input. MECs can also be expressed on an energy content (EC) basis, which is in accordance with the CEN approach to classification for trace elements of concern (**Section 2.5.3**). In another approach based on MFA principles, distributions of properties of sets of waste components are plotted against their size range^{56, 99}. The MFA framework enables an expansion of the description of waste processing units,

plants and systems beyond the conventional mass based descriptors of yield, recovery and purity. Contradicting objectives such as high yield and low pollutant content require a quantification of recoveries⁵⁵.

There is little published MFA-based experimental data for MBT-related SRF production. Data is available for construction waste sorting plants^{28, 57, 141} and EfW plants¹⁴²⁻¹⁴³, enhancing our understanding of substance flows. However, limited MFA research has been conducted on the performance of classification/separation for MBT plants and RDF/SRF production lines. Rotter et al.⁵⁵ experimented with urban and rural residual waste in an attempt to identify suitable mechanical processing units for SRF production, in terms of yield, recovery, CV and pollutant loads. Yield, MEC and TCs, reported on a mass and energy basis, were measured for various combinations of separation and classification unit operations, including screening, air classification, ballistic separation and magnetic separation. Pre-treatment was restricted to bag openers and removal of oversize items, without comminution. This restricts the applicability of the conclusions regarding the current MBT configurations, as most of them use primary comminution. Theoretical mass balance results from MFA studies for German MBT plant variants have been reviewed by Fehring et al.¹⁴⁴. In most cases, the data reliability cannot be assessed, as results are based on theoretical models and assumptions derived from existing practical experience.

The combination of conventional performance descriptors with MFA related formulas can convey a more detailed and accurate description of separation and classification unit operations, and mechanical processing plant in general. These descriptors of mechanical processing performance are summarised in **Table 2-6**.

2.4.4 Performance of separation and classification units for

RDF/SRF production

Almost every MBT plant configuration is capable of separating a RDF/SRF product. In 1985, Barton *et al.*⁷⁷ in a detailed overview accounted for the earlier phase of RDF production plants in Europe, covering plant flowcharts, mass balances and detailed operating experiences from commercial references processing mixed MSW. Thomé-Kozmiensky¹⁴⁵ has summarised both recent MBT and mechanical processing plant designs for RDF/SRF production. For MBT plants a main distinction can be made between plant configurations⁵¹. Those in which production of SRF is their principal objective, which employ an initial biodrying step coupled with downstream extensive mechanical processing; and those where RDF is a by-product of only mechanical pre-treatment, with the aim to optimally separate the OFMSW fraction for subsequent biogas production through AD or stabilisation through composting; for indicative process configurations see Hüttner¹⁴⁶. Additional variations with minor capacities exist. For instance the Nehlsen Stralsund biodrying plant (**Figure 2-7**) directs the >65 mm pre-shredded material directly to the SRF mechanical refining part and mixes it with the suitable fractions of undersize which is biodried¹⁰².

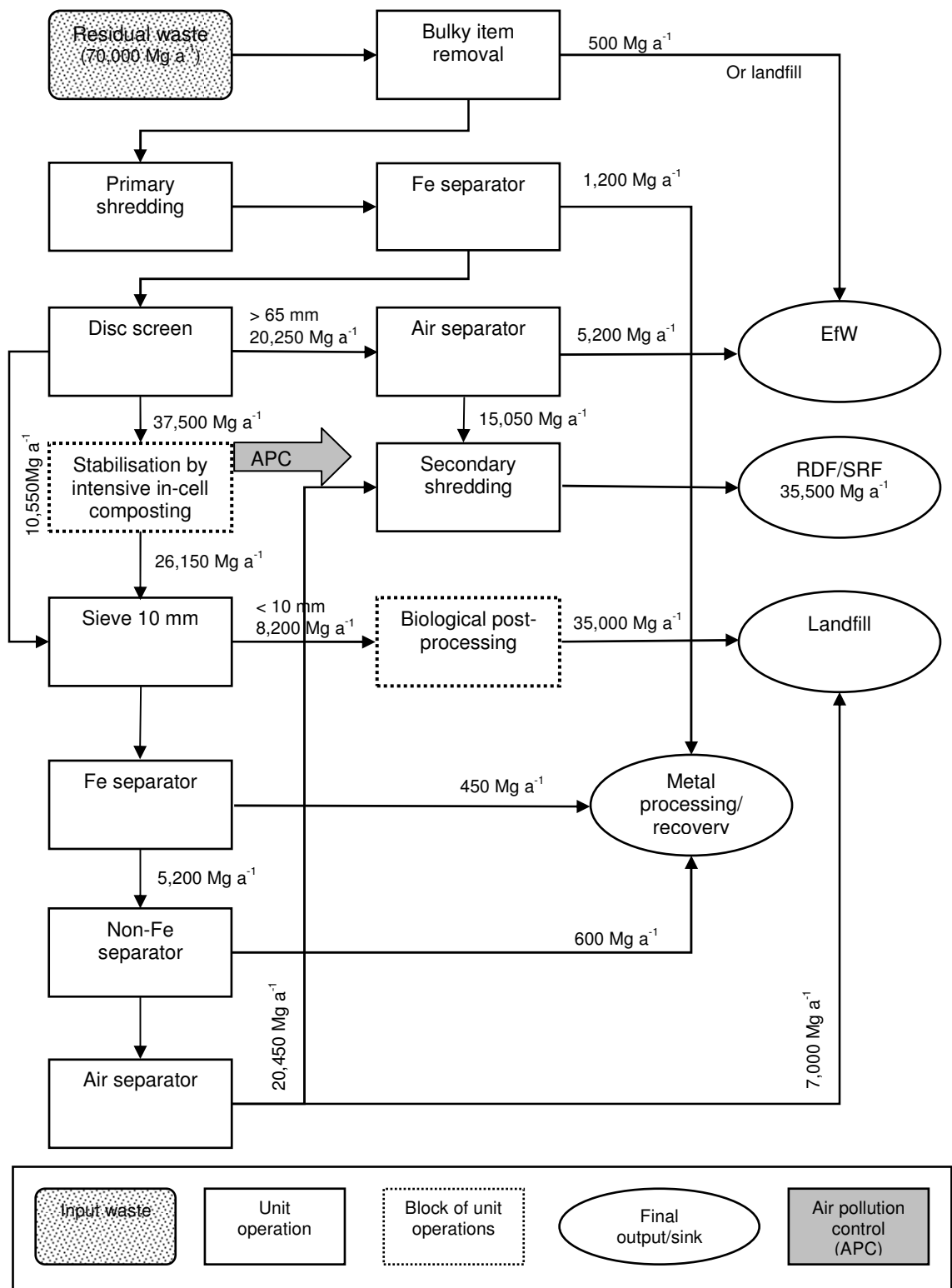


Figure 2-7 Simplified flow-chart and mass balance of the Nehlsen bio-drying MBT plant in Stralsund, Germany. Adapted from Breuer¹⁰²

Another possibility is the inclusion of dewatered and dried digestate residue from an AD process into the RDF product¹⁴⁷.

The SRF output should be produced to a specification that is increasingly subject to specific commercial agreements with the end-user, in addition to national and international quality assurance and control (QA/QC) procedures. From the perspective of an MBT plant operator, this translates into three objectives⁵⁵. The first is to achieve a high yield of the SRF product. It has been estimated that ca 20-30% w/w of the German residual household waste in urban areas and ca 18% w/w in rural areas, could be recovered as a fuel, without the inclusion of the OFMSW, after separation and possible drying losses⁵⁵. Pretz and Onash⁵⁴ estimated lower values of ca 10-15% w/w and Thomé-Kozmiensky¹⁴⁵ estimated 25-50% w/w, possibly including part of the OFMSW and before any losses. Experience from biodrying MBT plants suggests an upper limit at ca 40-50% w/w_{ar} of input residual waste, if most of the biogenic content is incorporated.

Secondly the operator seeks to raise the heating value, compared with the plant input; and thirdly to reduce the chemical (e.g., volatile trace elements of concern, such as Hg) and physical contamination (stones, glass, porcelain, ceramic, concrete, Fe and non-Fe metals) of the RDF/SRF fraction. In order to achieve high recovery rates for the RDF/SRF fraction effective concentration of combustible particles, such as plastics (excluding long-lasting plastic products), papers and cardboard, packaging composites, textiles, and wood, is needed.

In the case of biodrying, inclusion of the biomass fraction is attempted, with the possible exclusion of any particulates that fall in the fine fraction (e.g., <10 mm). Incorporation of the biogenic content into the SRF can be highly desirable in an EU/UK environment (see **Section 2.5.4.7**). Biodrying concurrently serves the main target of

diverting biodegradable content away from landfill, and results in a secondary fuel high in biogenic content, which in certain cases qualifies for a subsidy as an alternative to fossil fuel derived sources of energy.

Achieving high net calorific value (NCV) can be crucial for RDF/SRF marketability – hence its selection as the financial indicator for SRF quality by the CEN classification system (**Section 2.5.3**). NCV of the biodried output has already been increased by removing a significant percentage of the moisture. Mechanical processing can further improve this by separating out the incombustible mineral fraction, which largely constitutes of dry recyclables such as Fe and non-Fe metals, and secondary aggregates (stones, sand, glass, ceramics, porcelain, etc.).

2.4.4.1 Size classification (screening) performance

Screening unit operations are the most established processing units in waste management¹⁴⁸⁻¹⁴⁹. They are used in MBT plants to sort waste particles, mainly according to their size. From the great variety of classification equipment designs, rotating drum screens (or trommels) are the most widespread, followed by vibrating screens and disk screens⁸². Typical applications are immediately downstream of the primary comminution; or even as the first unit operation to exclude items from the primary comminution that do not need size reduction. They can also be used at many other process points. For example, use of trommels to remove the fine fraction contamination (e.g., <10 mm) from the low-gravity output of air-classifiers, intended for SRF production⁹⁵; or for removal of batteries¹⁵⁰.

Trommels are reported as the most proven type of classification equipment, regarding effectiveness and reliability, especially with inputs high in moisture content, ‘stringy’ material and with PSDs widely spread over both fine and coarse sizes⁸². A common performance problem of trommels is caused by plugging of the screening

media, especially in the case of coarse screening. Material that fills and obstructs the openings can restrict their effective aperture size and reduce the mass flow rate able to report to the underflow⁵⁴.

Aspects of the design, function and performance of trommels have been modelled empirically or from the first principles^{112, 151-154}. Earlier theoretical attempts to predict performance of trommels, such as the GRAB¹¹²⁻¹¹³ model, have been criticised as generally unsatisfactory¹¹⁴. Empirical modelling of recovery of the input sizes fractions 20-40 mm, 10-20 mm, and <10 mm of mixed household waste to the underflow product for a 50 mm aperture size trommel was attempted through the development of a 'feed-rate index', defined as the flow-rate of the true oversize particles divided by the trommel cross-sectional area¹⁵¹. Model predictions were close to actual values when the trommel was operated around the specified operation regime; but at lower feed rates, model predictions were much higher. It was suggested that the model did not account for the different characteristics of the comminuted output upstream of the trommel.

2.4.4.2 Screening performance without upstream comminution

Screening before comminution (typically after a mild bag splitting unit) has been proposed as a simple solution to problems caused by front end pulverisation, such as cross-contamination. However, research by Rotter et al.⁵⁵ showed that simple screening as a first and single step for mechanical pre-treatment before the biological stage cannot effectively separate the easily degradable organic fraction from the high CV fraction. This is particularly evident for residual waste that has a low initial CV and that is produced in areas with effective recycling schemes based on source separation. On the one hand, increased source segregation in Germany has led to a lower potential energy based yield for SRF/RDF fraction streams⁵⁵. On the other hand, other separation units performed much better in the same comparative test runs. One

possible partial explanation is that for screening at 40 mm this could be anticipated; experience with the use of trommels has shown that significantly different aperture sizes result in different sets of components reporting to the overflow. Coarse screening at 200 mm concentrates mainly paper, textiles and film-shaped plastics; whilst screening at the range of 40-60 mm, will in addition contain metals, dense particles and putrescibles¹⁵¹.

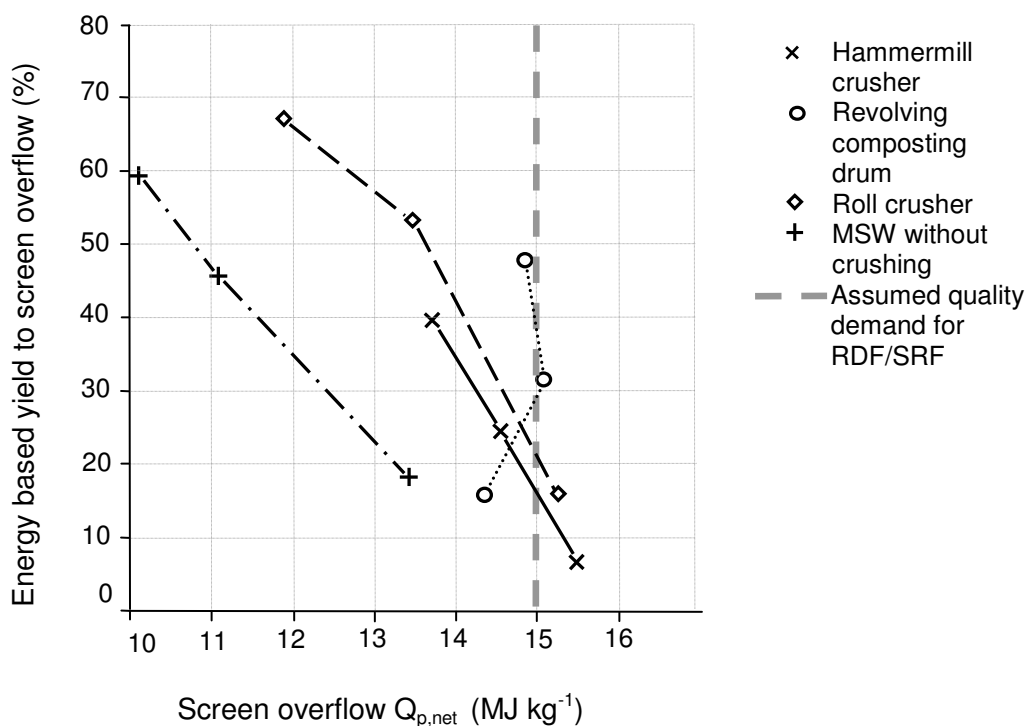


Figure 2-8 Effect of comminution and screening on the relationship of net calorific value $O_{p,net}$ and the energy based yield to the screen overflow, for different aperture sizes. Data points within each series from top to bottom correspond to the screen overflow product using 40, 80 and 150 mm apertures. Data form the MBT plant at Quarzbilchl, Germany. Redrawn from Soyez and Plickert⁷¹

However, in agreement with Rotter et al.⁵⁵, Soyez and Plickert⁷¹ reported results for the CV of uncomminuted residual waste, showing that for coarser screening, the increase in the CV content of the overflow, was small: even for screening at 150 mm, the CV remained relatively low, below 14 MJ kg^{-1} (**Figure 2-8**).

Hence, Soyez and Plickert⁷¹ believe that a comminution stage may be unavoidable for the separation of a high CV fraction, because no screen overflow of uncomminuted waste was able to meet an indicative German market threshold of 15 MJ kg⁻¹. However, as Rotter et al.⁵⁵ have shown, other separation techniques, such as ballistic separation, may be effective without preliminary size reduction.

In terms of chemical purity of the SRF product, Rotter et al.⁵⁵ suggested that the insufficient reduction of pollutants in the SRF product implies that PSDs do not correspond well to the distribution of hazardous chemicals, rendering screening unsuitable for selective removal of highly chemically polluted waste particulates.

2.4.4.3 Performance of comminution followed by screening

The simplest configuration for mechanical processing before a core biological stage of in-vessel composting consists of comminution followed by screening, as illustrated at the Biodegma, Neumunster plant and Linde, Linz plant¹³. A usual objective of this configuration is to separate a high CV coarse fraction from a rich-in-organics fine fraction. Organic compounds present in the OFMSW can contribute to the overall potentially recoverable energy present in the waste and to the biogenic content of the RDF/SRF. However, a higher yield for the coarse fraction achieved by a higher inclusion of organic matter may lead to a lower overall CV. The optimal compromise between the options should be informed by input characteristics and market requirements. Fricke and Mueller¹⁵⁵ and Soyez and Plickert⁷¹ have exemplified the relevant complexities.

Soyez and Plickert⁷¹ examined the performance of comminution followed by screening. German law (No. 30 BImSchV) sets maximum limits for the CV of waste to be landfilled to 6 MJ kg⁻¹, and the minimum for energy recovery of RDF/SRF at 11 MJ kg⁻¹. An indicative market minimum, adopted for illustration purposes could be 15 MJ

kg⁻¹. From an RDF/SRF production point of view, the revolving composting drum performed best. Energy based yield to the RDF output reached up to 48% w/w for the 40 mm screen overflow, whilst CV was only slightly below the assumed quality demand of 15 MJ kg⁻¹. For the 80 mm screen overflow, the respective values were 31% w/w and slightly above the CV limit. Despite the highest CV values being reached by the hammermill and the roll crusher whilst screening at 150 mm, their energy based yield was only 7% w/w and 16% w/w respectively. The combination of a revolving composting drum with screening at 40 mm provided acceptable results. The load of organic dry matter from biological origin in the underflow almost doubled compared to non-crushed MSW. The slightly higher values reached by the hammermill crusher were negligible compared to the large difference in the quality of RDF output.

Hammermill comminution followed by screening at 25 mm is used in the Linde MBT processes¹⁵⁶. Results verified a selective size reduction, with maximum content in hard and vegetable matter between 2-6 mm; and in paper at ca 10 mm. However, a low recovery rate (only 8-10% w/w) was evident for the plastics to the overflow (>50 mm), used for RDF production¹²⁰. The rest of the plastic mass, down to the very fine size of 2-5 mm, did not enable a maximum recovery of high CV material in the coarse fraction.

Knowledge of the input PSD and the size ranges in which waste particles concentrate can enable more effective use of the screening units by informing the appropriate separation size. Pretz and Onash⁵⁴ reported on an example of successful screening (of unknown boundary conditions, e.g. type of input) after appropriate selection of the aperture size by use of PSD. A 60 mm squared hole drum screen enabled the enrichment of OFMSW in the underflow and a fraction intended for SRF production in the overflow.

2.4.4.4 Performance of cascade-ball mill with flanged trommel

In such process configurations the emphasis is on separating an OFMSW optimised for subsequent AD or composting. The PSD of size-reduced output of the ball mill-trommel combination is generally log-normal and does not strictly follow RRSB distribution. Results from Koch¹²⁰ show that the cumulative weight fractions plotted in a RRSB diagram give a straight line only for the finer ground materials, with an interruption commencing at ca 15-40 mm.

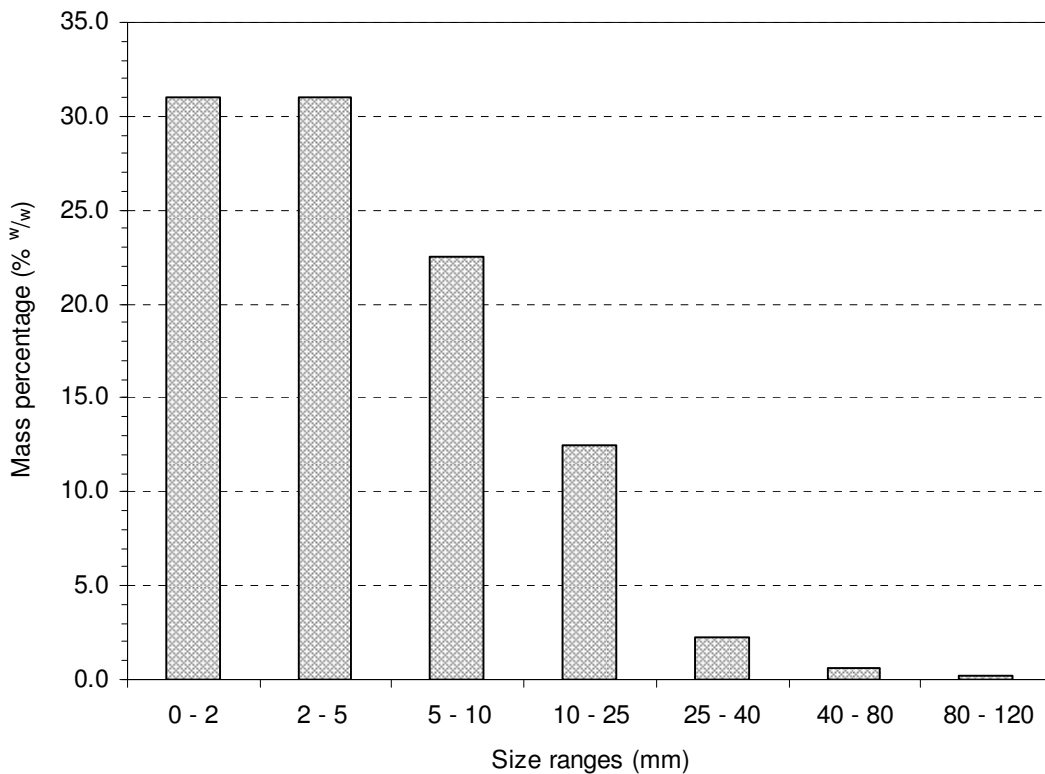


Figure 2-9 Histogram of cumulative mass of the organic fraction of German residual domestic waste after comminution in a Loesche-Hese cascade mill. Data from Koch et al.¹¹⁹

PSD results for the similar Outukumpu-Hese ball mill site were compared to other comminution processes coupled with screening. The histogram of cumulative mass frequency distribution (**Figure 2-9**) indicates that organic-origin material was effectively concentrated in the <40 mm fraction, with less than 3% w/w being above 25

mm¹¹⁹. Around 64% w/w of the organic material reported to the 0-5 mm screenings and 35% w/w to the 5-40 mm fraction.

Similarly, the 0-40 mm fraction, processed by a Outukumpu-Hese cascade mill, concentrated 97% w/w of the organic material contained in the input waste¹²². Operators of the process claimed that compared with the size reduction achieved by hammermills, the fraction 0-40 mm contained lower levels of metals, inert material and textiles contamination¹²². Recoveries to the 0-40 mm underscreens were plastics 33% w/w, cardboard and paper 80% w/w, nappies 80% w/w, and textiles 4% w/w.

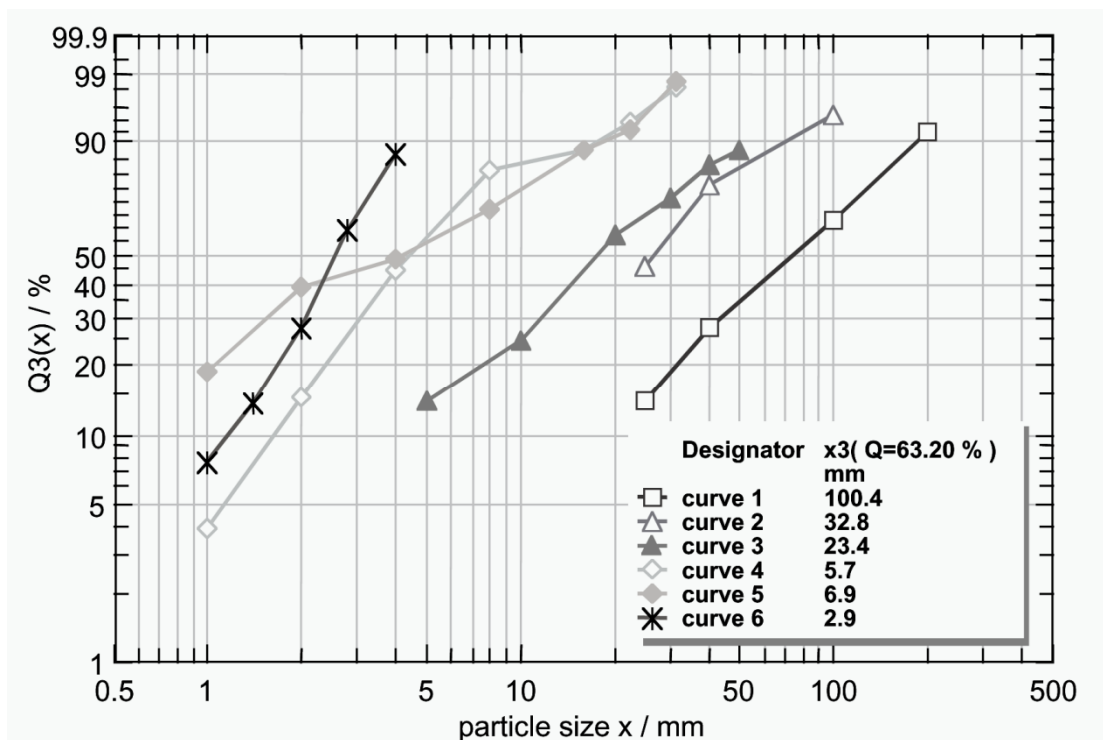


Figure 2-10 Cumulative mass fractions reporting at the screen undersize for various types of pre-treated domestic waste. Curves: (1) feed material; (2) comminution and drum screen at 100 mm; (4) and (5): ball-mill and 40 mm trommel underscreen; (6) ball mill-trommel and separation <5 mm organic-rich fraction. Characteristic particle size $d_{63.2}$ values are provided (63.2% w/w total mass smaller in size). From Koch et al.¹⁵⁷, with permission

Koch¹²² suggested that concentration of the maximum amount of organic mass in the fine fraction (<5 mm) could be favourable for the two fractions intended for

RDF/SRF production (e.g., 5-40 mm and 40-80 mm). Such a fine size range OFMSW could beneficially concentrate the bulk of material that is high in moisture content. This stream would have to be adjusted to higher moisture content levels during the upstream aerobic composting or anaerobic digestion, whilst its separation could free fractions intended for RDF/SRF production from unwanted water content. Advocates of such a process configuration consider it to be more energy efficient than processes that employ less sophisticated mechanical pre-treatment and resort to drying of the total waste input for RDF/SRF¹²². Plastic films, paper and cardboard are distributed in the particle size range of 10-40 mm, reporting in the intermediate output fraction (5-40 mm). As this fraction is intended for RDF/SRF production it should not be finely ground. The 40-80 mm product constitutes ca 25% w/w, before separation. It primarily concentrates wood and textiles, hard plastics, and metals. Metal and inert materials can be easily separated out downstream.

2.4.4.5 RDF production and optimisation of the PSD of organic fraction for subsequent bioconversion

One of the important objectives of comminution in MBT plants that use bioconversion processes, is to optimally pre-treat OFMSW for the subsequent biological process. The OFMSW should be concentrated in the fines range, leaving the material in the coarser stream for either RDF production, or for direct landfill disposal. The yield and quality of RDF is affected by the specific mechanical pre-treatment choices for the intensity of primary comminution and the aperture in the subsequent screening. Conflicts between RDF production and optimal OFMSW bioconversion may arise⁷⁹. Significantly different capabilities and restrictions for separation of the RDF fraction exist for AD and composting configurations of MBT plants. Much more extensive mechanical pre-treatment is necessary for the preparation of a suitable OFMSW for AD. In turn, this choice results in MBT plants being equipped with

sophisticated mechanical processing unit operations, capable of effective separation of the RDF fraction. However, as there is evidence that fine comminution of the OFMSW is beneficial for biogas yield and effective fermentation, an initial pulverisation step might be included, which could result in contamination of the RDF fraction with finely comminuted impurities.

MBT plants using composting to biostabilise the input for landfill disposal or CLO production, need much less sophisticated mechanical pre-processing and the need for size reduction of the OFMSW is lower. The objective of this MBT type is to minimise the capacity of the composting unit and the yield to be landfilled, which may necessitate complex mechanical pre-processing. However, objective conflicts may also arise because some of the waste components could be included in both the OFMSW and RDF fractions. To illustrate this point, wood is of high CV, but can also have a beneficial role in aerobic decomposition, functioning as structural material. Legislation stemming from national waste policies can specify the appropriate split of materials, in terms of biodegradability or CV implications for the final MBT outputs.

Substrate particle size affects (amongst many other parameters) the performance of bioconversion. For composting biostabilisation, primary size reduction is generally sufficient, whilst for AD an additional maceration stage may be attempted upstream of the separation of the OFMSW, usually not affecting the RDF product. Many possible mechanisms exist, through various aspects of the bioconversion, which are dependent on the particle size, shape and condition of the substrate. Generally, the objectives to be met by optimising the PSD of the substrate are to obtain a more extensive degree of bioconversion and to reduce the process time. For instance, in the case of AD these could be exemplified by achieving higher biogas yield, reducing the digestion time, and minimising the amount and improving the quality of the digestate¹⁵⁸.

Optimal size ranges for substrate particulates are significantly different for the anaerobic and aerobic types of bioconversion. Smaller particles are thought to be optimal in the case of AD, where size reduction through mechanical pre-treatment is able to accelerate the bioconversion, possibly through increasing the available specific surface¹⁵⁹⁻¹⁶⁰; especially for substrates of low biodegradability¹⁵⁸. However, the relevant mechanisms are complicated and the PSD of the substrate is not the only, or necessarily, the most influential parameter affected by comminution that may impact on the bioconversion performance. Another factor that has not yet been investigated is the cutting principles (type of loading mechanism)^{84, 161}. Comparative results on the influence of different degrees of substrate size reduction pre-treatment¹²³ (shredding at 14 mm and maceration at 1.7 mm) showed virtually no difference on the biogas yield of laboratory scale anaerobic digestion of OFMSW for organic loading rates from 2 to 5 kg_{VS} m⁻³ d⁻¹.

Organic material comminuted in a cascade mill exhibits a relatively large active surface and is optimally homogenised for subsequent AD treatment, compared with other combinations of size reduction pre-treatment¹¹⁹. Further separation at d (mm) ($d=3, 5$ or 8) has been proposed to provide a fine fraction (0- d) rich in organics intended for biological treatment¹²⁰. However, whilst a 0-10 mm fraction could concentrate around 86% w/w of organics, a 0-3 mm fraction could achieve only an estimated 45% w/w. This seems to be in agreement with the relatively low biogas yield for laboratory tested anaerobic digestion of the >3 mm fraction of residual waste, pre-treated with a Loesche-Hese cascade mill-trommel combination, followed by flip-flop screening, in comparison to average values for biowaste input¹²¹. A similar <5 mm fraction containing mainly paper and inert material in addition to the organic mater, had a 30% w/w yield and a characteristic particle size at ca 3 mm¹²². This material flow approach biostabilises only a small fraction of the input waste (30% w/w). However, the

success of such an MBT configuration depends on securing markets for the two types of RDF that are produced from the 5-40 mm and 40-80 mm mechanically separated outputs (**Figure 2-11**).

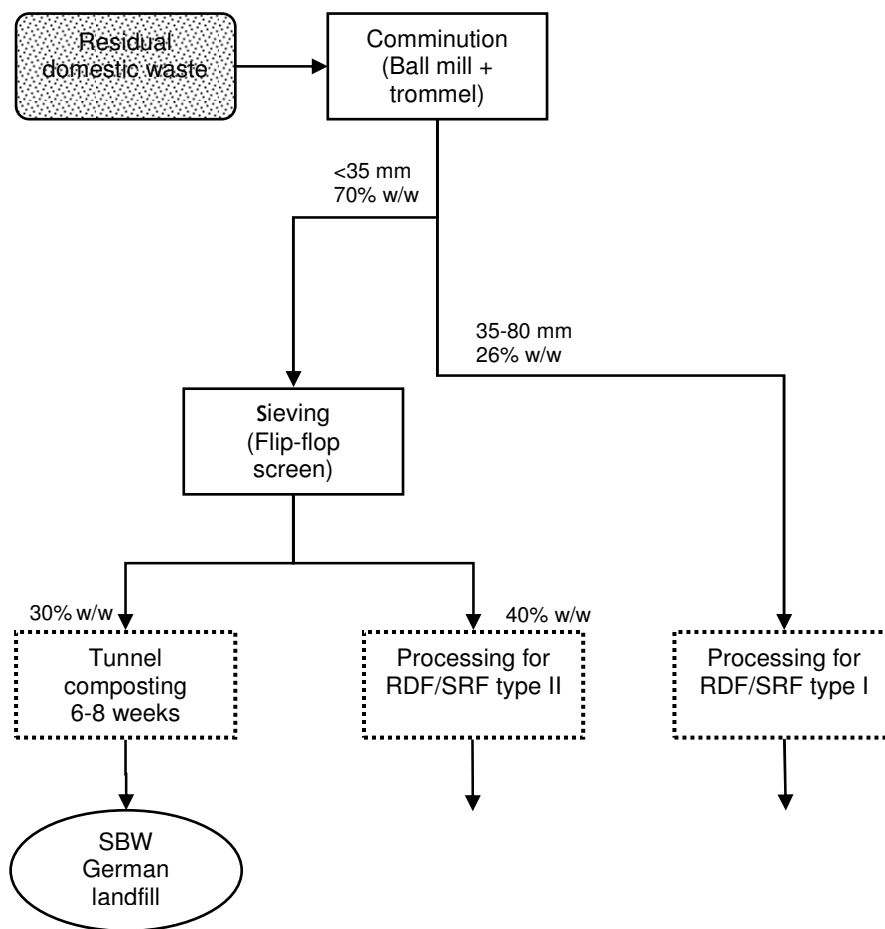


Figure 2-11 Histogram of cumulative mass of the organic fraction of German residual domestic waste after comminution in a Loesche-Hese cascade mill. Data from Koch et al.¹¹⁹

Other typical MBT approaches resort to limited, or different, types of mechanical pre-treatment and aerobically stabilise significantly larger mass percentages of the input waste. Koch¹²² showed that biostabilisation through composting of a fine fraction (<5 mm) after comminution by a ball mill reduced treatment time to achieve the German legal stipulations for landfill storage. This outcome is partially surprising, as

optimal ventilation in composting is enhanced by larger particle sizes with a higher volume of void spaces. If structural conditioning did not take place in this specific process, the result might be explained by enhanced oxygen diffusion transport, anticipated for particle sizes of about 10 mm or lower¹⁶². Additional results from the Brandenburg Recycling Park Hese cascade-mill indicated effective biodegradation reduction by a short intensive composting stage (**Figure 2-12**).

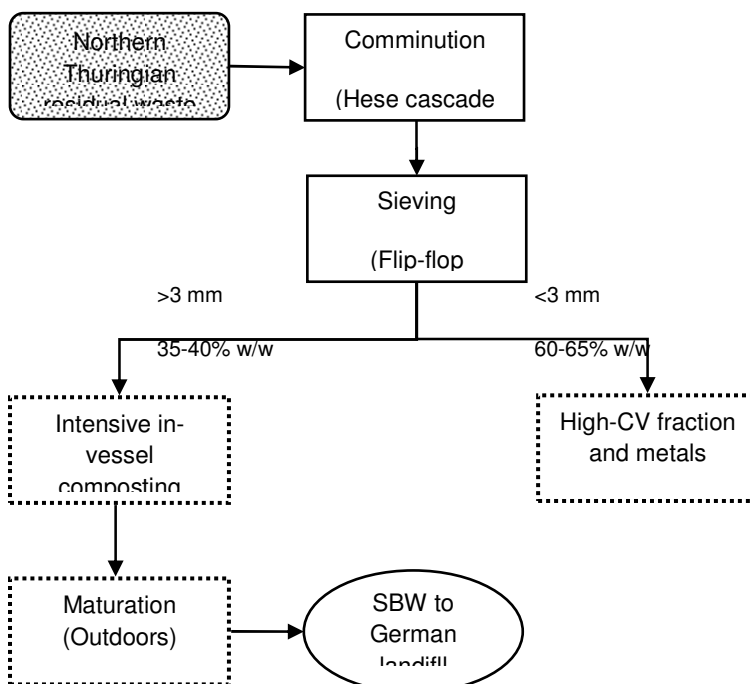


Figure 2-12 Mass balance data from the Brandenburg Recycling Park, using a Hese ball mill. SBW: stabilised bio-waste. For legend refer to **Figure 2-7**. Data from Schade-Dannewitz¹²¹

Silvestri et al.¹⁶³ investigated the performance of comminution by hammermill shredding followed by trommel at 80 mm, with the objective of optimally concentrating the organic fraction in the underflow for aerobic stabilisation, enabling in parallel the separation of an overflow with sufficiently low biodegradability potential, suitable for direct disposal. The input was residual MSW from three areas (Trento, Zucllo and Isclodi Taio) in the Province of Trento, Italy, after source segregation of recyclables, including kitchen and green waste. Results showed that an overflow with respiration

index lower than the legal limit of $1300 \text{ mg O}_2 \text{ kg}_{\text{VS}}^{-1} \text{ h}^{-1}$ was not always achievable at 80 mm, possibly because of a high content of paper and card in the overflow, in addition to the organics (**Table 2-7**).

It was speculated ¹⁶³ that screening at larger apertures (e.g., at 100 mm) could be effective in lowering the biodegradability content of the overflow. However, if the overflow material was used for RDF production this would be counterproductive, as it would lead to higher quantities of high CV materials, such as paper, reporting to the underflow.

Table 2-7 Results on material flow management performance of size classification; overflow product stream intended to concentrate components suitable for RDF/SRF production in MBT plants

	In-feed material composition	Overflow product (OF)			Underflow product (UF)	
		Yield to overflow product	Recovery of CM to OF	Purity of OF in CM	Recovery of CM to UF	Purity of UF in CM
	$C(CM)_I$	$Y(P_{OF})$	$R(CM)P_{OF}$	$C(CM)P_{OF}$	$R(CM)P_{UF}$	$C(CM)P_{OF}$
Set of waste components (CM)	(% w/w)	(% w/w unit operation input)	(%w/w)	(%w/w)	(%w/w)	(%w/w)
Unit operation input		64 (56 % w/w plant input) ^{a,†}				
		n.r. (47 % w/w plant input) ^{a,††}				
		28.3 ^b				
		n.r. (36 % w/w plant input) ^{c,†††}				
		n.r. (26 % w/w plant input) ^{c,†}				
		n.r. (26+40 % w/w plant input) ^{c,††}				
		61 ^d				
Paper	23.6 ^d	80 ^d			80 ^e	
Paper and card				15.1 [†]		5.5 [†]
				34.56 ^{g,†††}		8.08 ^{g,†††}
				39.98 ^{g,††}		7.08 ^{g,††}
				24.93 ^{g,††}		8.56 ^{g,††}
Plastics - body shaped				6.6 [†]		1.3 [†]
Plastics - foil shaped				8.9 [†]		2.0 [†]
Plastics	3.6 ^d	61 ^d	8-10 ^h		33 ^e	
Ferrous metals	4.5 ^d	39 ^d		4.9 [†]		1.8 [†]
Non-ferrous metals	0.4 ^d	0 ^d		0.5 [†]		0.5 [†]
Aluminium	0.3 ^d	8 ^d				
Ash						
Wood	5.7 ^d	78 ^d		5.2 [†]		1.1 [†]
Textiles	15.9 ^d	80 ^d		18.8 [†]	4 ^e	1.1 [†]
Diapers				22.5 [†]	80 ^e	2.9 [†]

	In-feed material composition	Overflow product (OF)			Underflow product (UF)	
		Yield to overflow product	Recovery of CM to OF	Purity of OF in CM	Recovery of CM to UF	Purity of UF in CM
		$C(CM)_I$	$R(CM)P_{OF}$	$C(CM)P_{OF}$	$R(CM)P_{UF}$	$C(CM)P_{OF}$
Set of waste components (CM)	(% w/w)	(% w/w unit operation input)	(%w/w)	(%w/w)	(%w/w)	(%w/w)
Rubber	0.4 ^d	30.5 ^d				
Glass	18.5 ^d	1 ^d				
Stone	3.9 ^d	0 ^d				
Food	2.0 ^d	73.5 ^d				
Yard waste	5.6 ^d	11 ^d				
Organics				2.5 [†]		5.8 [†]
OFMSW				8.26 ^{g,†††}	97 ^e	24.01 ^{g,†††}
				5.22 ^{g,†}		44.67 ^{g,†}
				11.90 ^{g,††}		37.99 ^{g,††}
Fines	15.8 ^d	3 ^d				
Rest > 40 mm				15.0 [†]		6.7 [†]
Rest < 40 mm				0.0 [†]		71.1 [†]

^a Rotter et al.⁵⁵: All values % w/w_{air} of initial input waste. Pilot scale testing. For residual, uncomminuted waste. Input after bulky item removal (1% w/w input). Relevant specific notes:

^{*} Urban waste input: 56% suitable for SRF of plant input: removal upstream: 1% input bulky items and 7% downstream metal separation

^{**} Rural waste input: 47% suitable for SRF of plant input: removal upstream: 1% input bulky items and downstream metal separation

^b Mueller et al.¹⁶⁴: Drum screen at 100 mm, after hammermill comminution in the Linkenbach, aerobic stabilisation MBT plant treating residual domestic and commercial waste

^c Koch¹²²: MBT plant. SRF yields as % w/w of plant input. Relevant specific notes:

^{***} Plant configuration: pre-crushing, Fe and non-Fe metal separation, underflow <100 mm to biostabilisation by composting

[†] Plant configuration: as above, screening at 40 and 100 mm: +40-100 to composting biostabilisation, -40 fraction to AD

^{††} Plant configuration (**Figure 2-11**): cascade mill flanged with trommel, flip-flop screening, underflow to tunnel composting with continuous agitation

^d Hasselriis⁷⁶: Non-MBT, historical data, shown for comparison purposes. All values d. MSW processed through a primary trommel, operated at nominal throughput at former Recovery I test plant, the US. Variation between runs was reported, maximum for the food, rubber, leather, textiles, wood and yard waste and lowest for fines (<6.4 mm), glass and stones. Paper and plastics showed low variation

^e Koch¹²²: Outukumpu-Hese cascade mill flanged with trommel two stage screening at 40 mm and 80 mm. Results for <40 mm undersize.

^f Pretz and Onasch⁵⁴: Drum screen at 60 mm, with squared holes, used for enrichment of OFMSW in the underflow and combustibles in the overflow. No information on composition of input and materials and methods of the research.

^g Silvestri et al.¹⁶³: Residual MSW Province of Trento, Italy, after source segregation of recyclables including kitchen and green waste with 42% effectiveness, affected by tourist activities. Comminution in hammermill and screening at 80 mm in trommel, with the objective of optimal concentration of the OFMSW in the underflow for subsequent aerobic stabilisation and direct landfill disposal of the overflow. Relevant specific notes:

^{†††} Trento, treatment landfill site

[†] Zuclo, treatment landfill site

^{††} Iscle di Taio, treatment landfill site

^h Koch¹²⁰: MBT plant. Hammermill shredding followed by screening at 50 mm, overflow to RDF production, underflow to AD.

The Nehlsen biodrying plant in Stralsund, Germany, has input of residual domestic, commercial and bulky waste. A 65 mm disk sieve is employed to separate the pre-shredded material into overflow that goes directly to SRF processing from the underflow that is biodried; the finest fraction of biodried output (<10 mm, 27% w/w of input) is further stabilised before landfill disposal¹⁰².

2.4.4.6 Air-flow (or pneumatic) separation

Air-flow separators (or air classifiers, AC) are typically present in RDF/SRF production lines of MBT plants. Air classifiers have long been established in industrial applications, such as agriculture and minerals processing, where they are used to separate components from dry mixtures^{74, 76, 78}. In solid waste management (SWM) they were applied as a key part of conventional RDF production plants, operated initially on MSW and later commercial or source-separated waste⁷⁷. Expectations for AC performance were initially high but a phase of scepticism followed in the 1990s. This can be attributed to off-the-shelf applications of ACs proven in other industrial operations, but not adapted or optimised to waste, combined with unrealistic expectations (e.g. separation of organic from inorganic items, despite their similar densimetric properties)^{76, 78, 165}. Currently the confidence in the effectiveness of ACs has been re-established in practice⁷⁵.

Within MBT plants, ACs are mainly used for concentrating the high CV combustible fraction in their low-gravity product⁷⁵. Other specialised uses include the separation of a high-plastic film and paper fraction for subsequent material recovery, and for the removal of plastic from waste intended for landfill disposal in Germany, where legislative upper limits apply on the CV of landfilled material⁷⁵. Application of AC for compost product refinement, with emphasis on the removal of plastics, has recently been considered, with limited success¹⁶⁶. Timmel⁷⁵ reported a typical throughput rate of ACs after the preceding classification at less than 15 Mg h⁻¹.

Shapiro and Galperin⁷⁴ provided a thorough overview of modern classification applications, including operation principles, features and performance parameters. However, their emphasis was not on waste separation, but on particle size separation applications. Timmel⁷⁵ focused on residual and commercial waste treatment and an older RDF-production related overview can be found in Hasselriis⁷⁶ **Table 2-8** provides relevant data from Timmel⁷⁵ and other publications.

Table 2-8 Air separators (air classifiers) for SRF production in MBT plants

Type of air separator	Separation principle	In-feed type and flow line point applicable to	Particle size range (mm)	Materials separated	Air load ($\text{kg}_{\text{waste}} \text{m}^{-3}$ classifying air)	Comments
Zig-zag classifier	Cascade, baffled-column of cross-flow separators	High CV fraction from residual waste	10-40	Low-gravity material is carried by the air current upwards and has then to be separated. High-gravity items repost to the chute downwards	0.4-2.0	<p>Relatively well studied, proven effective for various cases, such as construction waste and cable scrap</p> <p>Relatively small maximum feed size, but good separating effectiveness</p> <p>In the high-gravity chute an air-knife can separate more streams ^a</p> <p>Other type of baffled-column classifiers are the stacked V-shaped ^b</p>
Cone classifier	Multiple cross-flow separation	High CV fraction from bio-dried or thermally dried waste. (including re-sorting of the high-gravity material with pneumatic processing tables)	3-40		0.3-0.8	<p>Relatively small maximum feed size</p> <p>Secondary air-classification can be added at each separation stage to increase the effectiveness</p>
Cross-flow separators with pneumatic transport of the low-gravity material		<p>High CV fraction separation: (1) relatively low CV requiremen</p> <hr/> <p>High CV fraction separation: (2) relatively high CV requirement:</p> <hr/> <p>Pre-separation of high CV stream with subsequent re-sorting of the low gravity fraction and/or the low-gravity fraction</p>	<p>60-110</p> <hr/> <p>110-220</p> <hr/> <p>60-300</p>		0.2-1.0	Capable of separating bigger in-feed particles than cone and zig-zag separators and suitable for a more complex material mix

Type of air separator	Separation principle	In-feed type and flow line point applicable to	Particle size range (mm)	Materials separated	Air load (kg _{waste} m ⁻³ classifying air)	Comments
Cross-flow separators without pneumatic transport of the low-gravity material		(1) Cleaning of metal fraction produced during residual waste processing (separation of entrained film, paper, and textile pieces)		Rotating drum version	0.2-0.8	Suitable for simple separation applications. For enhanced effectiveness a second downstream drum and blower nozzle can be applied to the intermediate-gravity material
		(2) Removal of films from the screen overflow of the first classifying stage	>200	(1) high-gravity material chute: high-gravity items fall directly into it; plus items like glass and ceramics that fall initially against the rotating drum and report to either chute depending on contact time.		
		(3) Production of high CV fraction from biodried waste,	Indicative ranges: 10-65 and 65-250 or 15-35 and 35-85	(2) Low-gravity materials (textiles, cardboard) are transported through the rotating drum.		
Impact classifier	Cross-flow air separation with sorting based additionally on elastic behaviour of particles	High CV fraction from residual waste comminuted in semi-autogenous mill	3-40 or 40-80	(1) Low-gravity material fraction: directly report the low stationary settling rate items (e.g. plastic film, paper) and through a belt the high-gravity, medium stationary settling rate, soft, deformable items (e.g. cardboard packaging and textiles) (2) High-gravity, medium stationary settling rate, hard, dimensionally stable particles (e.g. bricks, pieces of concrete) report to high-gravity material discharge	0.2-0.8	Increased effectiveness for low-gravity material separation
Bench belt separator	Cross-flow air separation with sorting based additionally on elastic behaviour of particles.	High CV fraction from coarse residual waste fraction, low requirements for fuel product	60-300	(1) High-gravity material discharge: directly report the large pieces of waste of high density (e.g. sheet metal packing); and roll to it the compact pieces (e.g. stones) (2) Low-gravity material belt: deformable and/or flat pieces (e.g. drink cartons) and low terminal settling velocity items through the settling chamber	n.r.	
		High CV fraction from commercial waste	0-60			

Source of information, if not mentioned otherwise: Timmel⁷⁵

^a Hasselriis⁷⁶

^b Tchobanoglous and Kreith¹⁰⁷

* Not stated if yield or purity

CV: calorific value

n.r.: not reported

In typical configurations, separation is based on the differences in inertial (such as density) and aerodynamic properties (such as size and shape, i.e. measured as granulometric properties) of the in-feed particles. Air flows through the in-feed waste mixture causing high-gravity waste particles (constituting the reject) to either fall freely or to be deflected towards different chutes or conveyors. The low-gravity particles (being the extract) are either carried away with the off-gasses, to be concentrated downstream in cyclones or fabric filters, or are deposited on spacious settling chambers. Up to 70% of the classifying air can be re-circulated, in cross-flow designs⁵⁴. Within mining processing, separation occurs according to particle size⁷⁴, however, in waste treatment the density-dominant separation is more appropriate and efficient^{130, 135, 167}. Other sophisticated types of ACs have been developed that incorporate additional material properties, such as elastic behaviour⁷⁵. In residual and/or commercial waste separation, only gravity separators are used, and so far, centrifugal separators have not been introduced. Cross-flow separators prevail, in which the classifying air flows perpendicular to the waste and deflects the particles at various distances⁷⁵ (**Figure 2-13**).

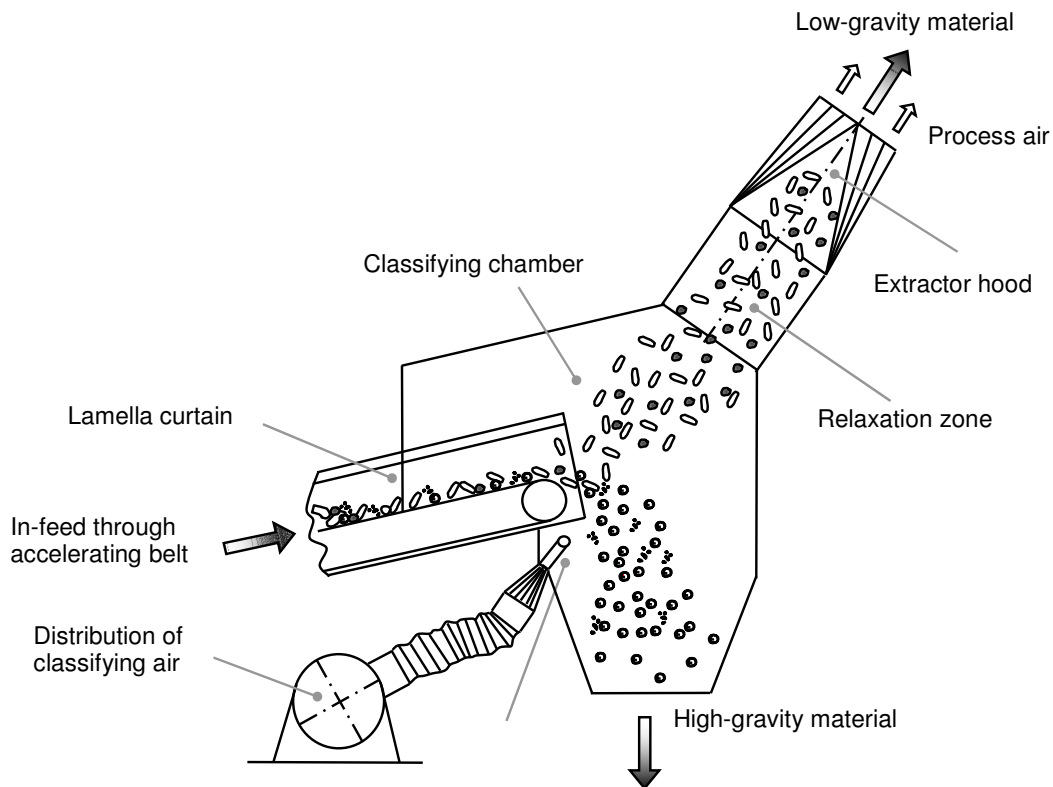


Figure 2-13 Schematic diagram showing the operating principle of a cross-flow air separator with pneumatic transport of the low-gravity material. Redrawn from Timmel⁷⁵

The performance of ACs depends on the particular design, the mode of operation and the characteristics of the in-feed stream. Generally, for optimal separation the following are desirable⁷⁴⁻⁷⁵: (1) sufficiently narrow particle size ranges in the in-feed; (2) constant, and if possible, isolated feed of the individual particles; (3) well-defined and stable air-flow and reduced turbulence; (4) pneumatic conveying through pipelines applied to the low-gravity material; (5) separation of the low-gravity material from the classifying air; and (6) repeated cleaning of all fractions.

Hasselriis⁷⁶ and Everett and Peirce¹³⁰ summarised the research that preceded the development of pulsed air classification. Bartlett¹⁶⁸ showed that the performance of a zig-zag air classifier is compromised at high moisture content of the input, and the amount of adsorbent materials present in the input was identified as an important

parameter. The main effect was on paper density and agglomeration, although plastics were also affected and reported to the low-gravity product. The composition of the feed, such as the paper-glass ratio, is also important¹⁶⁹.

Both first principles and empirical modelling of the performance of air classifiers has been attempted, particularly outside waste management. For example, Wang et al.¹³³ used computational fluid dynamics (CFD) simulation of cross-flow AC performance for size classification and Klumpar¹²⁷ examined performance optimisation of air classification in closed circuits with grinding. There is little research that is directly relevant to waste sorting. However, the principles for density-dominant separation through pulsed air classification are discussed in Vesilind¹³⁵ and Everett and Peirce¹³⁰. Validation of the air classifier unit operation of the GRAB¹¹²⁻¹¹³ computer model using data from UK RDF plants showed adequate results for the raw mixed waste at that time, but different coefficients would be necessary for pulverised waste¹¹⁴. Parameters used were air flow, particle size and density, shape, and coefficient of variation. He et al.¹⁶⁷ showed that non-waste simulation of airflow patterns within passive pulsing air classifiers can raise total effectiveness by 6-8% compared with conventional ACs. Biddulph and Connor¹⁷⁰ used effective diffusivity to model and evaluate the performance of low-gravity and high-gravity products for different duct designs of ACs, operated at high values of air/solid ratio, reporting better performance for lower values.

The exact performance of air-separators has to be evaluated by pilot tests, as accurate design calculations are thought to be impossible because of the problems associated with the granulometric description of waste particles⁷⁵. The selection criteria for the appropriate air-separation equipment include waste composition, particle size of waste stream to be sorted, required throughput rate and required performance⁷⁵.

Table 2-9 Results on material flow management performance of air classifiers (ACs); low-gravity product stream intended to concentrate components suitable for RDF/SRF production in MBT plants

Set of waste components (CM)	In-feed material (I) composition C(CM)I (%w/w)	Low-gravity product (LG)			High-gravity product (HG)	
		Yield to LG product	Recovery of CM to LG	Purity of LG in CM	Recovery of CM to HG	Purity of HG in CM
		Y(P _{LG}) (%w/w unit operation input)	R(CM)P _{LG} (%w/w)	C(CM)P _{LG} (%w/w)	R(CM)P _{HG} (%w/w)	C(CM)P _{HG} (%w/w)
Unit operation input		>70 ^a 40 ^b				
Combustibles				60-99 ^c		
Paper				<1-99 ^c		
Paper and card	50.7 ^d		66.6 ^d	73.7 ^d		27.1 ^a
Plastics	11.8 ^d		85.2 ^d 1-65 ^c	11.8 ^d		1.5 ^a
Paper and plastics			85-99 ^e	55-80 ^e		
Ferrous metals	19.3 ^d		2-50 ^e	0.1-1 ^e 1.1 ^d	98.0 ^d	38.0 ^d
Non-ferrous metals	3.2 ^d		45-65 ^e	0.2-1 ^e 0.1 ^d	99.1 ^d 85-99 ^c	6.6 ^d
Fines			80-99 ^e	15-30 ^e		
Ash			45-85 ^e	10-35 ^e		
Wood	4.7 ^d		13.1 ^d	1.6 ^d		7.8 ^d
Textiles	14.7 ^d		32.2 ^d	11.6 ^d		17.8 ^d
Glass	0.4 ^d			0 ^d	100.0 ^d	0.7 ^d
Vegetable matter	0.8 ^d			0.1 ^d	90.0 ^d	0.5 ^d

^a Pretz and Onasch⁵⁴: General estimate for cross-flow ACs operated with partial air-recirculation (up to 30%) and density of load <35 g m_{AIR}⁻³ h⁻¹. Related specific notes:

^b Mainly: plastic foil, thin-body type plastics and dry paper.

^c Vesilind¹³⁵: Non-MBT, historical data, shown for comparison purposes. The non-ferrous metal is aluminium only. Varying in-feed properties and operating mode affect performance.

^d Data from Flitton¹⁷¹, cited in Porteous⁸¹: Non-MBT, historical data, shown for comparison purposes. Results on a conical rotating AC designed by Newell-Dunford Engineering. In-feed of overscreen product after screening at 25 mm of possibly comminuted commercial waste.

^e Hasselriis⁷⁶: Non-MBT, historical data, shown for comparison purposes. Review of seven commercial references in the US, of horizontal, vertical and vibratory inclined AC types, fed with varying mixed MSW. Generally operated to a typical range of air/solids ratio of 2-7. Values given as 'typical' ranges, not statistically defined. No detailed description for the 'fines' and 'ash' set of components.

Rotter et al.⁵⁵ presented a large scale comparative study on configurations of separation and classification equipment for SRF production for residual waste. This study provided insights into the material flow management performance of ACs. AC unit performance was among the top performing ballistic separation processes, which include air knife and crosswise. They achieved high enrichment in lower heating value (LHV) because of the high plastics percentage. However, this led to a high Cl content. Additionally, failure to incorporate the wet components into the SRF caused a high

enrichment of cadmium (Cd). These results indicate that for the purpose of mechanical post-treatment of biodried output, air-classification may perform closer to ballistic separation both in terms of yield and Cl content, as it would be less difficult to incorporate the paper, card and textile fractions. **Table 2-9** reviews results on air classification performance.

2.4.4.7 Ballistic separation

Ballistic separation has a wide range of applications, including removal of mineral contaminants from grains and nuts, sorting construction waste, concentration of paper and packaging material in MRFs, sorting of plastics¹⁷², conventional mechanical RDF production plants, and various roles in MBT plants¹³. Possible applications within MBT flowcharts include initial separation and classification upstream of the typical primary comminution step (typically performed by a trommel), removal of mineral and metallic contamination from the RDF/SRF fraction (typically performed by air classifiers), and refinement of the biologically treated output for landfill disposal, for example, to meet a maximum CV restriction, or for CLO production¹⁶⁴.

The operating principles of ballistic separators depend on differences in specific density (densimetric separation) in conjunction with other material properties, such as elastic properties (hardness), shape, and size. It combines separation with classification, resulting in at least three output streams. The waste components are separated by following different trajectories as they impact on a series of parallel, inclined, metallic belts (paddle plates) that vibrate by rotating eccentrically and against each other (**Figure 2-14**).

First the low-gravity, soft, flat/foil-shaped (2-D), particles (such as paper, cardboard, textiles, plastic foils and bags) bounce or are moved forwards and upwards in a circular movement by the rotating action of the paddles, reporting to the so-called

'low-gravity material' or 'light fraction'¹⁷⁴. Secondly, the high-gravity, hard, 3-D particles (e.g. minerals like glass and stones, containers such as tins and steel, wood, hard/massive plastic particles) roll or bounce in a downwards diagonal reverse direction, transported to the so-called 'high-gravity material' or 'heavy fraction.' Thirdly, in addition to separation, screening is also achieved by the use of perforated paddles that enable the small-size particles (such as sand, kitchen waste, dust) to fall through and be collected in the 'screenings' or 'underscreens' or 'fine fraction.'

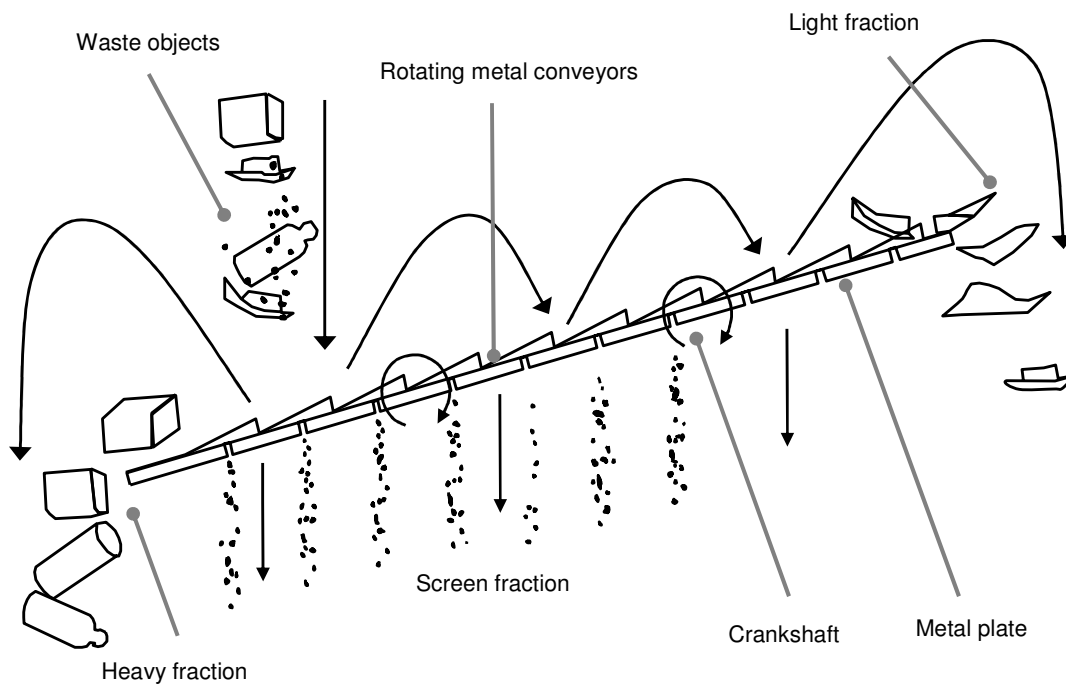


Figure 2-14 Schematic diagram showing the operating principle of a ballistic separator: (1) waste objects drop onto conveyor; (2) rotating metal conveyors follow an eccentric circular movement; (3) light fraction is carried upwards: e.g., paper, corrugated cardboard, plastic sheets and bags (4) heavy fraction rolls down: e.g., bottles, metals, hard plastics; (5) screen fraction falls through: e.g., sand, discarded food. Adapted from Mitsubishi Rayon Engineering¹⁷³

Varying designs options enable optimisation of ballistic separators for specific inputs and objectives. The main distinction can be made between one, two or three

stage designs¹⁶⁴. Additional screens can be added (stacked on top of each other) increasing throughput and the number of screening outputs. Possible adverse impacts on performance aspects are the purity of outputs¹⁷⁵, caused by material falling from the upper screens and interfering with the operation of the lower decks. Different types of paddle perforations (e.g., punched or net-shaped) and aperture sizes can be specified according to the in-feed material composition. Further adaptability is offered by controlling the in-built adjustable angle of inclination of the complete set of paddles¹⁶⁴, and the frequency of paddle rotation⁸².

No detailed modelling of the performance of ballistic separators was found in the literature. However, there is a considerable difference in the density of non-combustible components (stones, glass, ceramic, porcelain and metal) with densities above 2 g cm^{-3} and the combustible components (plastics, wood, paper, textiles) with densities around 1 g cm^{-3} ⁶². Densimetric separation could thus in principle be used for separating combustible from non-combustible waste fractions for RDF/SRF production. However, in a ballistic separator additional physical-mechanical properties are used for separation and classification resulting in the recovery of waste components not being based entirely on their density. In addition, absorbed water may change the density of the waste particles, as is often the case for paper and card.

Experiments on a two-step ballistic separator with horizontal first level paddles in the aerobic stabilisation MBT plant at Linkenbach, Germany (treating residual domestic and commercial waste) were conducted in November 2002¹⁶⁴. The performance of the ballistic separator was measured in the main air classifier role, aiming at the concentration of combustibles in the low-gravity, >45 mm product, by directing minerals in the high-gravity, >45 mm product, with the parallel objective of enriching the organic fraction in the <45 mm screenings for subsequent aerobic stabilisation. In-feed was the overflow of a drum screen with round mesh at 100 mm,

treating comminuted waste. In the first two paddle levels of ballistic separator 45 mm screen apertures were used.

The low-gravity, >45 mm product reached a yield of ca 77% w/w, in which accumulation of the high CV fraction was evident by the high recovery of paper/cardboard (91% w/w), films (97.2% w/w), sanitary products (97.3% w/w), etc). However, the high-gravity fraction accounted for a yield of 13% w/w with a relatively high LHV (9.2 MJ kg^{-1}), resulting in an energy-based yield for the low-gravity product of 83.1% w/w. This was exemplified by the recovery of some high CV materials into the high-gravity product, namely wood (46.0% w/w), plastics (16.2% w/w), composite materials (21.4% w/w), and textiles/shoes (14.7% w/w). According to Mueller et al.¹⁶⁴, this would necessitate a further treatment step for recovery of a light, high CV fraction from the high-gravity stream. A high-gravity solid trap proved effective in this role, rendering a high in LHV low-gravity product at a 55% w/w yield. On the other hand, most of the combustible components that were not satisfactory recovered to the ballistic separator low-gravity product (hard/bottle plastics, composites and textiles/shoes) are generally components of a high specific chemical pollution load, as indicated by Rotter et al.⁵⁵. Hence, the current outcome, despite being partially detrimental to the overall process energy-based yield to the RDF/SRF stream, might be desirable in terms of lowering the level of chemical contamination of the RDF/SRF product. MFA results for the ballistic separation of uncomminuted residual urban waste, with upstream removal of bulky items and metals and screening at 40-150 mm, provided lower values for yields of the unit operation input to the low-gravity product **Table 2-10**⁵⁵.

Table 2-10 Results on material flow management performance of ballistic separation; low-gravity product stream intended to concentrate components suitable for RDF/SRF production in MBT plants

Set of waste components	In-feed material (I) composition	Low-gravity product (LG)			High-gravity product (HG)			Screenings product (SRC)		
		Yield to LG product	Recovery of CM to LG	Purity of LG in CM	Yield to HG product	Recovery of CM to HG	Purity of HG in CM	Yield to SRC product	Recovery of CM to SCR	Purity of SRC in CM
(CM) or property	C(CM)I (%w/w)	Y(P _{LG}) (%w/w unit operation input)	R(CM)P _{LG} (%w/w)	C(CM)P _{LG} (%w/w)	Y(P _{HG}) (%w/w unit operation input)	R(CM)P _{HG} (%w/w)	C(CM)P _{HG} (%w/w)	Y(P _{SRC}) (%w/w unit operation input)	R(CM)P _{SCR} (%w/w)	C(CM)P _{SCR} (%w/w)
Overall input		76.9 ^a 31.8 ^b 36.4 ^c ca. 45 ^e ca. 45 ^d			13.1 ^a 6.4 ^b 11.5 ^c			10.0 ^a 61.8 ^b 52.2 ^c		
Paper and card ^a	17.0		91.1	20.1		6.9	9.2		2.2	3.5
Plastics ^a	9.4		78.6	9.6		16.2	11.7		5.2	5.2
Films ^a	8.8		97.2	11.2		1.4	1.0		1.4	1.4
Textiles and shoes ^a	8.3		85.3	9.3		14.7	9.1		0.0	0.2
Composites ^a	6.9		75.0	6.8		21.4	11.0		3.6	2.3
Sanitary products ^a	18.4		97.3	23.3		2.3	3.4		0.3	0.4
Wood ^a	3.9		42.9	2.1		46.0	13.7		11.1	4.2
Organics ^a	7.6		50.8	5.0		8.9	5.2		40.3	30.9
Glass ^a	0.1		0.0	0.0		0.0	0.0		100.0	1.3
Minerals ^a	5.6		23.1	1.7		53.8	22.8		23.1	12.6
Metals ^a	4.2		63.8	3.5		31.9	10.2		4.3	2.1
Others ^a	6.0		78.6	6.1		5.1	2.1		16.3	10.0
Fines <8 mm ^a	3.7			1.3			0.5			26.1
Net calorific value Q_{p,net} (MJ kg⁻¹ ar)	11.2 ^a	12.1 ^a 11.0 ^b 11.0 ^c			9.2 ^a			6.6 ^a		

^{a,b,c} Mueller et al.¹⁶⁴: Two-step ballistic separator with a horizontally set of first level of paddles in the aerobic stabilisation MBT plant treating residual domestic and commercial waste at Linkenbach, Germany, tests in November 2002. Waste component categories as defined there.

^a Input: overscreens of drum screen at 100 mm, after hammermill comminution; both ballistic separator paddle levels perforation at 45 mm.

^b Input: upstream hammermill comminution. Both paddle levels at 75 mm.

^c Input: upstream hammermill comminution. Both paddle levels at 45 mm.

^{d,e} Rotter et al.⁵⁵: All values % w/w_{ar} of initial input waste. Pilot scale testing. Ballistic separation with paddle perforation at 40 mm.

^d Input: urban residual uncomminuted waste after bulky item removal, overflow of screening at 30 mm and ferrous metal separation (calculated value, supposing 11% w/w of initial residual waste input removed through bulky item and metal separation).

^e Input: urban residual uncomminuted waste after bulky item removal and ferrous metal separation (calculated value, supposing 11% w/w of initial residual waste input removed through bulky item and metal separation).

^f Not yield: absolute NCV values in input and outputs of unit operation

In the same Linkenbach MBT set of tests, glass was entirely directed to the ballistic separator screenings (recovery 100%) in which the organic fraction was also concentrated¹⁶⁴. Although this is beneficial for RDF quality, it would highly contaminate the organic fraction, for non-landfilling or landfill cover uses. Organic content was largely split between the low-gravity product and screenings. A significant percentage of the metal content (63.8% w/w) was recovered in the low-gravity fraction. Effective separation of metals would demand subsequent treatment of both the low and high-gravity fractions.

In a second Linkenbach MBT set of tests, ballistic separator performance was evaluated directly upstream of the primary comminution and compared with an existing drum screen at 100 mm¹⁶⁴. The three-fold aim was to concentrate the RDF-intended fraction in the low-gravity product, achieve high recovery of minerals and metals in the low-gravity product and separate an OFMSW of low LHV in the screenings. In each run identical paddle apertures were used in both decks, at 75 mm and at 45 mm. The low-gravity fraction yield was 31.9% w/w. and 36.4% w/w respectively, comparing favourably to the 28.3% w/w reached by the drum screen. The overall energy-based recovery was also higher for the ballistic separator runs, due to the higher mass yield and only slightly lower LHV (11.9 MJ kg⁻¹ for the drum screen and at 11.0 MJ kg⁻¹ for both the ballistic separator tests). Rough optical inspection indicated that the mineral content of the ballistic separator low-gravity product was composed of smaller particles with planer shape in comparison to the drum screen overflow. It was speculated¹⁶⁴ that this could cause fewer problems during a final size reduction step for control of the RDF PSD than the larger mineral particles apparent in the drum screen output. However, experience from the use of ballistic separators for plastics sorting has indicated that effectiveness as a 'primary' separator of plastics can be low, especially if the input has been compacted in refuse collection vehicles, as plastic bottles that would

normally report to the high-gravity product become flattened after compaction and report to the low-gravity output¹⁷⁵. Nevertheless, for RDF/SRF production purposes this may be desirable, depending on the chemical pollution load of the misplaced components.

Other large-scale MFA tests conducted by Rotter et al.⁵⁵, with similar objectives but with uncomminuted waste, provided evidence for the generally superior performance of ballistic separators as the first sorting unit operation. However, performance on lowering the chemical contamination load for the RDF/SRF intended product was better than on mass yield grounds. Comparative tests included screening at 30 mm, three stage air knife classification, two-stage crosswise air classification, foil suction combined with infrared (IR) plastic detection, and ballistic separator units with paddle openings at 40 mm, with or without upstream screening. In all cases, bulky item removal and magnetic separation took place. Yield on an as received mass basis ranged from 5% w/w_{ar} for foils-suction with IR plastic detection to 60% w/w_{ar} for screening at 30 mm. TC values were in accordance with the identified yields. In most cases, Cl enrichment took place in the final product, up to 70%. Energy-based MECs resulted in lower pollutant elemental enrichment, in comparison to the mass-based.

Apparently contradictory results initially warned against generalisation when dealing with the material flow management performance of separation and classification unit operations. The fact that the yield to the low-gravity output of the ballistic separator (ca 45% w/w_{ar}; of after 11% w/w_{ar} of the test input removal of bulky and ferrous items) was lower than to the 40 mm overscreens of the size classifier (ca 62% w/w_{ar}; after 8% w/w_{ar} of the test input removal of bulky and ferrous items)⁵⁵ seemingly contradicts with the previous results¹⁶⁴. However, the two cases treat waste inputs significantly differently (uncomminuted versus comminuted), the screening is operated at different openings (40 mm versus 100 mm) and different designs of ballistic

separators were used. This apparent contradiction could be explained by the much higher yield anticipated for the overscreen of 40 mm for an uncomminuted waste input, compared with the yield anticipated for the 100 mm overscreen treating a comminuted input.

Tests with ballistic separators were the only way to achieve significant dilution of polluting substances (negative MEC) in the final SRF product, with the best results reported for direct application of ballistic separation, without previous screening⁵⁵. This can be attributed to the greater ability of ballistic separators to incorporate wet high CV items (paper, cardboard and textile) into the low-gravity stream. For example, paper has a CI content lower than 0.5% w/w_d, which is below the average in residual waste. Additionally, high recovery of the highly chemically polluted components in streams other than the low-gravity products enables the concentration of a low-polluted SRF stream. This is in agreement with evidence from Herhof MBT plants, in which reduced specific load for some trace elements of concern was achieved in the low-gravity product of the ballistic separator⁶².

2.4.4.8 Sensor detection and sorting

Various sensor detection and separation technologies are available including optical sensors, image recognition, X-ray fluorescent, X-ray transmission, and IR and near-infrared (NIR), each with different strengths and weaknesses¹⁰⁷. This technological field is currently rapidly developing. Harbeck and Kroog¹⁷⁶ comprehensively reviewed emerging technologies applied in the mining industry, a constant source of technology transfer to the waste processing. They considered as most promising detection methods the X-ray transmission, evaluation of thermographic images and electromagnetic measurements, because they are independent of the item surface, dirt or moisture, qualities similarly desirable in waste sorting. Colour-based sorting devices (optical sensors) have been used for over 20 years. Relatively new

developments are X-ray systems¹⁷⁷, image detection and NIR detection coupled with pneumatic discharge⁵⁴. These technologies offer novel capabilities for chemically-based waste sorting waste, in line with the emerging higher requirements for effective material flow management. If their effectiveness can be demonstrated, this could constitute a major breakthrough in waste handling. Promising combinations of NIR with image analysis, using sophisticated cameras, enable separation of materials based on specialised optical characteristics, such as the surface design⁵⁴.

In NIR, a fast scanning spectrometer analyses the molecular structure of moving objects by NIR light. Spectrums of the most commonly used materials have been developed, enabling selective recovery of materials. Air nozzles, activated for a fraction of a second, blast the identified waste particle, blowing it out of its trajectory to an appropriate discharge gate. Throughputs of 7-9 Mg h⁻¹ are achievable with a machine width of 2000 mm⁵⁴. Recovery percentages as high as 90% for high CV components (e.g., plastics, wood, paper, cardboard, diapers) are thought to be feasible. Nevertheless, cellulose-based items can only be detected at lower percentages of 50-60%.

Use of NIR in MBT plants could theoretically be used for removal of plastics with chlorinated compounds such as polyvinylchloride (PVC). However, this technology is not able to detect chloride salts present in kitchen/yard waste or in other kitchen waste contaminated components¹⁷⁸. The organic-bound chlorine fraction present in plastics (ca 85% w/w of overall Cl) is responsible for most of the high temperature corrosion (attributable to HCl formation)¹⁷⁹. The potential to use NIR to separate out the plastic fraction from RDF/SRF produced via biodrying MBT, so as to increase its biogenic content, has been investigated in Germany¹⁸⁰, with promising results.

However, sensor detection and sorting technologies still need to overcome some challenges. In a large-scale test of a foil suction apparatus combined with IR plastic detection for SRF production from uncominuted urban residual waste, mixed results were reported. Despite the high separation of the components with high chemically polluted content, the yield to the SRF product was just 5% (after bulky items and metal recovery)⁵⁵. Zeiger¹⁷⁷ reported some of the potential limitations of the NIR applications, when used as an alternative or supplement to air classification for RDF/SRF production. The detected and removed output intended for RDF/SRF production contained mainly light-coloured plastics, untreated wood and various textiles ca >50 mm. Many dark plastic components, coated and treated woods, and mixed materials that are difficult to treat cost-efficiently with NIR remained in the residual fraction (0-50 mm and high-gravity items).

Because of the difficulties mentioned directly above, Zeiger¹⁷⁷ proposed the use of X-ray sorting. Typical applications in a RDF/SRF producing MBT could be removal of SRF impurities (inorganic matter and highly chemically polluted matter), and separation of the high-gravity fraction from domestic and commercial waste input, for the effective concentration of the OFMSW.

2.4.4.9 Separation of metals and batteries

Effective processes to separate Fe and non-Fe waste particles are generally available and have been summarised elsewhere¹⁰⁷. Typical equipment for Fe metals are overhead belts and drum magnets, with magnetic separators with alternating pole systems being particularly effective; and eddy-current separators for non-Fe⁵⁴, using either centric or eccentric polar systems. Downstream of these two basic unit operations, sensor sorting systems (inductive, NIR, and X-ray) can also be used for more sophisticated separation¹²⁵. The role and objectives of magnetic separation equipment in MBT plants vary⁸², but include protection of downstream equipment from

wear and tear, extraction of secondary raw material according to end-user specifications (e.g., detinning industry, and iron and steel industry), and removal of contamination from RDF/SRF or the OFMSW stream to be treated in AD.

Recovery of Fe-metals can be up to 95%⁵⁴. Eddy-current separators effectively separate non-Fe metals, particularly for flat and isolated items, which makes screen sizing upstream and feeding with a vibration conveyor beneficial. From the non-Fe metals, aluminium (Al) is the most important, both commercially and as a contaminant for SRF, with achieved yields up to 90%, and purities ca 60-70%, as Al often comes combined with other materials.

Batteries constitute a main source of chemical pollution¹⁸¹. Until effective systems of collection at source are implemented, they will continue to constitute a major challenge for material management in MBT plants. Possible contamination of SRF, OFMSW or secondary raw metals is evident. Avoiding breakage and effective separation are imperative for sustainable resource management. Around 90% of batteries are magnetic or slightly magnetic⁶² and can report to the fine-particle Fe fraction. For example, in the Herhof-Asslar plant, they are manually picked from the ferrous material conveyor and returned to the manufacturers for appropriate recycling. For best results, permanent magnetic neodymium drum separators can be used⁵⁴; however, they do attract weak magnetic items contaminated with organic adhesives.

There is evidence that for certain process configurations, waste particles with high specific loads in trace elements of concern report to the metal product. In experiments with different process configurations for SRF production, Rotter et al.⁵⁵ reported that batteries, electronic waste and other composite materials partially concentrate in the metal stream product, resulting in mainly Cd, and to a lesser extent lead (Pb), enrichment in the metal output. Further evidence from Herhof MBT plants

showed enrichment of the non-Fe metals output with trace elements of concern, possibly because of electronic scrap particles⁶². The contamination of the Fe and/or non-Fe secondary raw products with trace elements of concern creates problems with their quality and marketability. In addition, the problem of the same high-pollution components contaminating the SRF product is not fully avoided by magnetic separation, as some of these items still report to the fuel stream output⁵⁵.

2.4.4.10 Position and performance of unit operations in MBT plant

flow-charts

A challenge observed in RDF production plants during the 1980s using hammermills was to liberate and selectively reduce the size of coarse items, whilst avoiding over-pulverisation that leads to cross-contamination⁷⁷. Recently, rotary shears have been used in preference to hammermills. Another possible partial improvement could include use of screening equipment ahead of the hammermill. Retrofitting the RDF Byker plant, UK, by including a bag splitter followed by a trommel before the primary shredder achieved positive results in the final RDF quality: extensive test results, including impact on downstream operations are available¹⁸².

Screening is often used upstream of other separation processes as a pre-treatment. Experience indicates that a coarse pre-screening of 100-300 mm can be beneficial. If this coarse pre-screening is omitted, screening of mixed MSW input at <100 mm can lead to substantial agglomeration, resulting in contamination of the overflow with material intended for the underflow⁵⁴.

Operating experience from RDF production plants in the 1980s has shown that appropriate feedstock preparation is important for the effective operation of separation units⁷⁷. Whilst comminution is not mandatory, ACs should be at least preceded by a size classification unit operation, such as a trommel, to optimise the sorting effect^{55, 75}.

With air-knife and crosswise air classification, the maximum allowable particle size in the AC in-feed is in the range of 250-350 mm⁵⁵. However, the use of trommels ahead of ACs can affect their performance⁷⁵. Unwanted secondary composites, such as large textile agglomerations, may be formed and lead to AC operational faults. Bar-shaped particles can report to the trommel underflow, even if one of the other dimensions of the particle is larger than the aperture size of the trommel, resulting in items exceeding the maximum desirable size.

In contrast, ballistic separators are non-sensitive to a dispersed PSD of the input stream. When treating residual waste previously screened at 0-150 mm, the performance was slightly worse than treating the unscreened stream⁵⁵, indicating that screening ahead of ballistic separators may not render the desired result.

It is evident that drying of waste can facilitate the flow of waste matrices⁷⁷ and subsequent mechanical processing. Moisture content of the as delivered residual waste (ca 15-40% w/w⁶²; ca 35-55% w/w¹⁴⁵) is unfavourable for efficient screening. Typically, biodried output has moisture content lower than 15% w/w, but fluctuations are common. Reduction of moisture content by biodrying reduces the formation of lumpy material that sticks together and creates problems for efficient separation. Low-gravity yield of air classifiers for RDF/SRF production could benefit from a dried input. For example, eddy-current separators, separating non-Fe metallic material, can particularly benefit from operating with a comminuted dried and disaggregated material^{54, 62} because they are most effective with a mono-layer of single particles. However, ballistic separators can effectively incorporate wet input fractions into the low-gravity product⁵⁵. This fact indicates that if such a unit is used before composting/AD for RDF/SRF production, the output would have increased drying needs. Alternatively, after biodrying, the moisture problem could be avoided. If

processing SRF into hard pellets is necessary, e.g., for subsequent shaft reactor gasification, a moisture content not exceeding 10% should be achieved¹⁴⁵.

2.4.5 Mechanical processing overview

Evolving objectives of material flow management and higher standards determine the needs for mechanical processing in MBT plants that produce RDF/SRF. Segregating out waste fractions with the desired chemical composition progressively becomes more important in the design of these systems. For example, with the objective of high-grade SRF production, it is not sufficient to separate a comminuted coarse fraction just on a PSD basis. The need to obtain the maximum achievable yield in high CV, low in pollutant load and possibly high in biogenic content SRF demands definition and selective separation of waste fractions on the basis of their biochemical properties^{55, 183}.

Specific material flow performance descriptors and overall analytical tools can significantly facilitate the achievement of plant objectives. For example, PSDs can be a useful tool to inform the quality of waste fractions to be processed, if used properly. MFA has recently been employed to accurately map and predict behaviour of MBT systems, along with the conventional performance descriptors of mass-based yield, recovery and purity. MFA can depict the partitioning of preserved properties of waste, such as content in trace elements of concern, into the output fractions. Despite some very promising experimental results reported in recent studies, most of the data comes from theoretical investigations. There is a need for additional experimental MFA research on a test and commercial reference plant scale.

Results on mechanical processing of residual waste in MBT plants are limited, often come from non-peer-reviewed sources, and some lack application of standardised methods and/or statistical analysis. Data from MBT plants comes from a

variety of plant configurations, operated towards different objectives and with specific feedstock; this restricts their comparability and possible wider applicability of results.

Biodrying appears to provide the advantage of optimally preparing the waste for mechanical treatment. Promising results in terms of selective comminution and fast biodegradation were achieved by ball-mill pre-treatment. Overall MFA data verified the difficulty of effective chemical separation solely by mechanical means. Zinc (Zn) and Cl are difficult to dilute in SRF produced from residual MSW, because of the highly diffused distribution within various waste components⁵⁵. Advances in processing equipment, such as ballistic separators or NIR and X-ray sorting, may provide better solutions for specific uses.

2.5 RDF/SRF quality management initiatives

2.5.1 Importance of quality management for RDF/SRF marketability

Quality management for RDF/SRF plays a key role in efforts to establish viable market outlets, not least by creating confidence in suppliers, end-users⁵², and regulators⁸⁹. Quality management is concerned with activities that direct an organisation to fulfil the requirements of involved parties¹⁸⁴. Quality management systems (QMS), consist of: quality planning, quality assurance (QA) and quality control (QC) schemes, and a general framework for a QMS for SRF has been provided by CEN⁸⁹. At the current stage of the development for RDF/SRF this has been largely limited to QA/QC. Quality assurance (QA) addresses the whole range of customer requirements, including the quality of organisation performance (documentation, timing, logistics, and proper use of equipment), and product quality, in terms of reproducible levels of key properties¹⁸⁵. Product requirements can be specified by: the regulator, related institutions, associations, or pressure groups, specific customers; or the producer in anticipation of customer requirements. These may take the form of product

and/or process standards (e.g. product certificates provided on the basis of an assessment guideline), technical specifications, contractual agreements between producers and retailers/end-users, trade and/or involved parties provisional agreements (e.g. quality marks), or regulatory requirements (e.g., permitting regulations)^{184, 186}.

Standardisation, namely the development of classes and specifications for key product features against which fuels can be controlled, is an important part of QA. Market confidence in waste-derived products can be built, when standards are in place and adequate quality control is implemented. Encouraging examples in the UK context are the “Compost Quality Protocol”¹⁸⁷, a quality protocol for the production and use of compost, (a recent update from the previous BSI PAS 100:200, a publicly available standard for composted materials¹⁸⁸); and the code of good practice for landspreading of biosolids, commonly known as the “safe sludge matrix”¹⁸⁹. Lasaridi et al.¹⁹⁰ have argued for EU compost quality standards, which would harmonise the wide range of limit values currently in place within the various member states. According to CEN^{41, 191}, European Standards (ENs) for SRF could potentially guarantee the quality of fuel for energy producers, enabling the efficient trading of SRFs and increasing public trust. Standards could provide access to permits for SRF use; enable the rationalisation of design criteria for thermal recovery units; result in cost savings for co-incineration plants, reducing the need for compliance monitoring; facilitate trans-border movements; aid communication with equipment manufacturers; and ease reporting on the use of fuels from renewable energy sources. However, standardisation in isolation cannot guarantee increased market share¹⁸⁵. The European market for SRF/RDF is still developing and remains unpredictable. For example, in Germany, the ban on landfilling of thermally recoverable and untreated biodegradable fractions of MSW has resulted in an increase in MBT-derived RDF/SRF production, far exceeding the available

utilisation capacity⁵¹. This shortfall in the capacity for MBT-derived RDF/SRF has led to some material being treated in conventional waste incineration plants (WIP), whilst the surplus RDF is temporarily baled and stored in “depositories” in landfill sites¹⁹². From 2008, the RDF/SRF utilisation capacity is anticipated to rise, mainly through the construction of new mono-combustion plants⁵¹. Recent scenarios predicting an overall surplus of RDF availability to at least 2013¹⁹² have been superseded by a predicted shortfall for RDF/SRF during 2011-2012³⁶⁻³⁷.

The marketability of MBT-produced RDF/SRF depends largely on successful implementation of QA/QC schemes, especially, in the light of the wider technical, financial, policy and legislative challenges^{13, 33-34, 36-37, 51, 193-195}. RDF/SRF is anticipated to face high competition from standard fossil fuels and proven substitute fuels, such as biosolids (sewage sludge), used tyres and rubber, used oils and solvents, ground offal, biomass, scrap timber, carpet scraps and bleaching soils^{13, 51}. An analysis of current and future quantities and prospects for these secondary fuels has been compiled by Thomé-Kozmiensky¹⁴⁵. Standardisation and development of guidance on quality assurance plans for the European market of solid biofuels has also advanced recently^{185, 196-197}.

MBT-derived RDF/SRF product quality encompasses three critical aspects; the degree of variability, level of desirable properties and level of contaminants. It is critical for MBT plants to attain and ensure WDFs of acceptable variability. Competitive secondary fuels produced from less variable commercial/industrial waste streams or mono-batches may have an inherently more acceptable profile¹⁹⁸. A quality-certified SRF does not necessarily imply a high fuel quality. Instead, it relates to a more consistent, continuously produced fuel that meets the quality demanded by end-users and their regulators. Producing SRF of known and consistent quality out of the mixed/residual MSW input to MBT processes, characterised by high temporal variability

and heterogeneity, is a major technical challenge^{13, 55}. However, in addition to MBT-derived SRF of invariable quality, the development of specialised SRF products, adapted to specific thermal recovery end-uses, produced by suitably designed MBT plants, could prove similarly critical for its future competitiveness^{33, 47}. The recent retrofitting of the Nehlsen biodrying plant in Stralsund to provide three different qualities of SRF vividly illustrates this need¹⁰².

The RDF/SRF contaminant properties and combustion behaviour critically affects its potential applications. Problems with low quality RDF characteristics, particularly high chlorine and trace metals content, have led to a decline in co-combustion applications in Germany^{55, 58}. The ability of mechanical flow-stream separation in MBT plants to fully achieve the desired low levels of chemical contamination has been questioned^{13, 55, 58}. RDF acceptability problems have been attributed to both unfavourable properties and variability in RDF input¹³. The existing surplus in RDF/SRF production in countries such as Germany is likely to force MBT operators to produce SRF of higher and/or more application-specific quality, leading to lower SRF yield and a higher volume of residual fraction that needs adequate disposal (incineration or landfill). Such a development would imply higher technical difficulties and may demand retrofitting of existing SRF production lines, with more acute dilemmas for material flow management; and increased operational costs for MBT plants⁵¹. One implication of moving towards more technically complex unit processes in order to produce SRF of more consistent and required quality is the additional energy consumption associated with a lower yield of SRF and more reject materials. An optimal balance among the objectives of SRF product quality, cost and overall health and environmental protection, should be sought.

Quality management can build consensus on perceived RDF/SRF quality. Measurements pertaining to the same RDF batch conducted with different sampling

plans and analytical determination, performed at varying points of product life (e.g. within the production plant or just before end-use), by different laboratories, and for stakeholders with partly conflicting interests, may result in surprisingly diverging results, as has been reported for Germany¹⁹⁹. Hence, implementation of appropriate QA/QC for MBT production lines of RDF/SRF based on a sound scientific basis is imperative. In this manner, actual and perceived issues stemming from unfavourable constituents and variability in residual waste input composition can be addressed¹⁹⁸. In addition, the production of a consistent, fit-for-purpose product, that is acceptable to regulatory authorities can be verified, possibly at a reduced cost through avoidance of duplicate, or unnecessarily frequent, QC¹⁹⁶.

2.5.2 Standards and quality assurance/control for RDF/SRF

Quality assurance and control systems for WDF already exist and new ones are under development. In the 1980s, the American Society for Testing and Materials (ASTM) defined classes of RDF based on the form of final product and type of production processes²⁰⁰⁻²⁰¹. In Europe, QA/QC schemes have been applied internally by producers and/or end-users, for example, RWE Umwelt AG¹⁹⁸. Many national initiatives were launched around 2000, achieving different degrees of implementation. Quality control procedures and standards for RDF/SRF have been described and discussed elsewhere^{13, 41, 43-45, 52, 55, 89, 198-199, 202-204}. **Table 2-11** summarises the current QA/QC initiatives for WDFs in Europe.

Table 2-11 Existing and provisional national and trade quality assurance/quality control systems and standards for RDF/SRF in Europe

Country	Legislation/Trade standard	Description and implementation	Reference
Austria	Ö-norm	Joint project launched in 2001 to produce a similar to the German BGS standard. In 2002 founding of association for quality assurance.	European Recovered Fuel Organisation ⁴² Schulz-Eltermann ⁴⁴
Flemish region of Belgium	Standard developed by the European Association of Waste Thermal Treatment Companies for Specialised Waste (EURITS)	Produced by EURITS and adopted by the Flemish region of Belgium; criteria for substitute fuels for co-combustion in cement kilns. Values resulted from calculations based on certain assumptions. Refer to the publication for details. Criticised as too strict by the cement industry, especially for the calorific value threshold.	European Association of Waste Thermal Treatment Companies for Specialised Waste ²⁰² Gendebien et al. ⁴³ Juniper ¹³
Finland	SFS 5875 national standard by Finish Standards Association (FSF)	Based on Finnish separate waste collection system of dry high calorific fractions and specific-target waste processing; created to stimulate SRF market development; extensive co-combustion application in boilers for district heating (CHP); covers whole supply chain, i.e. separation, transport and processing; defines three classes and monitoring of seven parameters – additional ones may be added on contractual agreement; required analytical methods are the International Standards Organisation (ISO) standards for solid mineral fuels; self-monitoring, independent supervision and approval procedures are not identified – provisions of standardisation institute may apply; producer-client agreement on sampling and QC. The standard boosted the use of SRF as a substitute fuel; criticised for absence of control requirements.	Finish Standards Association ²⁰⁵ Cuperus and van Dijk ¹⁸⁶ European Recovered Fuel Organisation ⁴² Schulz-Eltermann ⁴⁴ Wilén et al. ⁴⁵
Germany	2001 RAL-GZ 724-label for SRF Quality and test instructions by the Quality Association for Secondary Fuel and Recycled Wood (BGS) German Institute for Quality Assurance and Certification (RAL)	Initially developed in 1999 by trade organisation BGS and adopted in 2001 by German standard organisation PAL for cement industry and power plants to fulfil the criteria of GZ 724. Establishes a quality label; input oriented, defines two classes: (1) MSW fractions and (2) specific waste, all non-hazardous according to European Waste Catalogue (EWC); no additional diversification with specific intended uses; constitutes of various stages for both internal monitoring and external, independent inspection: (1) initial inspection of production process and product quality by authorised institution to verify capacity for QA, (2) continuous self-monitoring including proximate and ultimate analysis of RDF, individualised sampling plan per plant and regular external control including sampling and analytical determination reporting to BGS, (3) re-inspection. On 30-04-2005 six plants were producing ca. 180,000 Mg a ⁻¹ quality assured RDF, out of which three from MSW fractions. Issue with duplicate monitoring (production plant and internal by end-users) leading to conflicting RDF quality accounts.	German Institute for Quality Assurance and Certification ²⁰⁶ Cuperus and van Dijk ¹⁸⁶ Flamme ¹⁹⁹

Country	Legislation/Trade standard	Description and implementation	Reference
Italy	UNI 9903 Ministerial Decree (5-2-98)	Introduced in 1992 to regulate the Italian “non-mineral” RDF (CDR); specifies RDF classes, sampling and analytical requirements; storage, transportation and documentation aspects are briefly addressed.	European Committee for Standardisation ⁴¹
	Dlgs 152/2006	Introduced new values for chemical-physical properties and CDR (normal quality SRF) and CDR-Q (high-quality SRF).	Schulz-Ellermann ⁴⁴ Zanotta ²⁰⁷
Netherlands		Pre-normative activity for standardisation, research conducted for European Standardisation Organisation (CEN).	Schulz-Ellermann ⁴⁴ Cuperus <i>et al.</i> ²⁰⁸
Norway	Specifikationer	Applies to bio-fuels.	Schulz-Ellermann ⁴⁴
Sweden	SS 18 71 xx	Suite of specifications for bio-fuel and peat.	European Committee for Standardisation ⁴¹
	“Specialbränsle A” and “Lattbränsle”	Specifications for secondary fuels used in cement kilns, two classes.	Gendebien <i>et al.</i> ⁴³ Schulz-Ellermann ⁴⁴
Switzerland	Guideline specifications for cement kilns developed by the Federal Office for Environment, Forest and Landscape (BUWAL)	Two classes; developed with two main objectives: (1) no increase of the entire emission load from the production of cement, and (2) no enrichment of the pollutants in the clinker product.	Kost <i>et al.</i> ⁵⁸ Rotter <i>et al.</i> ⁵⁵
UK	Substitute fuels protocol (SFP)	Industry voluntarily agreement for cement and lime kilns. SFP revised edition published by the Environment Agency (EA) on February 2005. Developed without consideration of MBT-derived RDF/SRF.	Environment Agency ²⁰⁹

Adapted from Schulz-Ellermann⁴⁴

QC: quality control

Attempts at WDF quality management differ substantially: they may apply nationally or regionally; be legally binding or constitute trade provisional agreements; rely upon waste input origin or final product quality; or refer to all or specific end-users. Schulz-Ellermann⁴⁴ provides an overview of the current status of European standards and QA/QC schemes for SRF. **Table 2-12** lists the limits for key properties from existing European SRF quality standards.

Table 2-12 Overview of limit values for existing European SRF quality standards

Parameter	Units	Country							EURITS / Flemish region of Belgium 202 ††	
		Germany ¹⁹⁹		Finland ^{45,*}		Italy				
		Median	80 th percentile	Class I	Class II	Class III	Standard quality (CDR) (2006) 207	Standard quality UNI 9903 (1998) 204		High quality UNI 9903 (1998) ²⁰⁴
Ash content	% w/w _d	***					<15	<20	<15	5 **
Moisture content MC	% w/w _{ar}	***					<18	<25	<15	
Net calorific value Q _{p,net}	MJ kg ⁻¹ ar	***†					>20	>15 min value	>19 min value	>15
Aluminium (metallic) (Al)	% w/w ††			†††	††	††				
Antimony (Sb)	mg kg _d ⁻¹	50 †††	120 †††							
Arsenic (As)	mg kg _d ⁻¹	5 †††	13 †††				<5	<9		
Beryllium (Be)	mg kg ⁻¹									<1
Bromine (Br)/Iodine (I)	% w/w									<0.01
Cadmium (Cd)	mg kg _d ⁻¹	4 †††	9 †††	<1.0	<4.0	<5.0	<3	<7 Hg+Cd	<1 Hg+Cd	
Chlorine (Cl)	% w/w _d	***		<0.15	<0.5	<1.5	<0.7	<0.9% (w/w _{ar})	<0.7% (w/w _{ar})	<0.5
Chromium (Cr)	mg kg _d ⁻¹	125 †††	250 †††				<70	<100		
Cobalt (Co)	mg kg _d ⁻¹	6 †††	12 †††							
Copper (Cu)	mg kg _d ⁻¹	350 †††	***†				<50 soluble	<300 soluble	<50 soluble	
Fluorine (F)	% w/w									<0.1
Lead (Pb)	mg kg _d ⁻¹	190 †††	***†				<100 volatile	<200 volatile		
Manganese (Mn)	mg kg _d ⁻¹	250 †††	500 †††				<200	<400		
Mercury (Hg)	mg kg _d ⁻¹	0.6 †††	1.2 †††	<0.1	<0.2	<0.5	<1			<2
Molybdenum (Mo)	mg kg _d ⁻¹									20
Nickel (Ni)	mg kg _d ⁻¹	80 †††	160 †††				<30	<40		
Nitrogen (N)	% w/w ††			<1.00	<1.50	<2.50				0.7
Sum potassium and sodium (K+Na) ††	% w/w _d			<0.2	<0.4	<0.5				
Sulphur (S)	% w/w ††			<0.20	<0.30	<0.50	<0.3 d	<0.6 w/w _{ar}		0.4
Sum HM	mg kg _d ⁻¹	1049	2460					<1040	<350	
Thalium (Tl)	mg kg _d ⁻¹	1 †††	2 †††							<2
Vanadium (V)	mg kg _d ⁻¹	10 †††	25 †††							
Zinc (Zn)	mg kg ⁻¹									500
As,Se,(Te),Cd,Sb #	mg kg ⁻¹									10

		Country					EURITS / Flemish region of Belgium
		Germany ¹⁹⁹	Finland ^{45,*}	Italy			202 ^{††}
Parameter	Units	Median	80 th percentile	Class I	Class II	Class III	Cement kilns
V,Cr,Co,Ni,Cu,Pb,Mn,Sn [#]	mg kg ⁻¹						200

^{*} Decimal points denote the necessary precision of detection. Classification limits apply to a volume of SRF ≤1000 m³ or to the volume produced or delivered during one month

^{**} Excluding: Ca, Al, Fe, Si. Arbitrary value

^{***} These process-specific parameters should be documented for the purposes of QA/QC: limits specified by each particular end-user contract apply

[†] Both MJ kg_d⁻¹ and MJ kg_{ar}⁻¹ should be reported

^{††} Values result from calculations based on certain assumptions. Refer to publication for details. Necessary basis of report (ar or d) not stated

^{†††} Metallic Al is not allowed, but accepted within the limits of reporting precision (0.01)

^{*†} Metallic Al is removed/minimised by source-separation and by the SRF production process

^{*†} Metallic Al content is agreed separately

^{†††} German values apply to the high-calorific value fractions derived from municipal waste. HM content values are valid as from a NCV of ≥16 MJ kg_d⁻¹. For calorific values falling below, the above-mentioned values need to be accordingly lowered linearly; an increase is not allowed

^{**†} Definition only on the basis of a reliable dataset from the SRF production process

^{††} Total content (K+Na) of water-soluble and ion-exchangeable proportion

[#] Limit values apply to each of the metal separately

HM: heavy metals

QA/QC: quality assurance/ quality control

In the following section the CEN European standard for SRF is briefly presented. This is followed by a discussion of the key properties of SRF that should be taken into account during the design and operation of the MBT processes, from the perspective of specific end-users.

2.5.3 SRF classification and specification by CEN

The CEN technical standard for SRF specification and classes constitutes part of the wider extensive ongoing research and development effort for a European SRF QA/QC system¹⁹¹. Major findings of the pre-normative research were published as a technical report document²¹⁰, where the relative scientific evidence and rationale for final choices is detailed. Development of this standard has been adapted to customer-specific requirements, both technical and legislative, such as meeting the Waste Incineration Directive (WID) emission limits²¹¹. Achievable quality of WDFs has also been considered. It applies at the interface between SRF producer and intended end-user, rather than being input oriented¹⁹¹.

Table 2-13 summarises the recommended classes, descriptors and values. Class codes (1-5), defined by boundary values without overlapping (i.e., closed intervals), have been finally adopted for each of three key fuel properties²¹⁰. These three properties serve as indicators of SRF performance with respect to economics (mean NVC), measured as received); technology (mean chlorine content, measured dry); and environment (median and 0th percentile values for Hg content, measured dry-specific statistics apply depending on the available number of measurements)^{191, 204}. Each property should be determined according to specified sampling plans, including sample preparation and analytical techniques. The degree of chemical contamination

can be expressed either on per mass (mg kg^{-1}) or per energy output (mg MJ^{-1}) basis²⁰⁴,²¹⁰. The most appropriate method depends on the intended information required.

Each property value can fall within five classes. The SRF is assigned a class number for each property and the combination of the three class numbers defines its class code.

Table 2-13 CEN classification codes for SRF

Property category	Classification property	Units	Statistic *	Classes				
				1	2	3	4	5
Economy	Net calorific value $Q_{p,net,ar}$	MJ kg_{ar}^{-1}	Mean	≥ 25	≥ 20	≥ 15	≥ 10	≥ 3
Technology Cl: important in corrosion, slugging and fouling of boilers	Chlorine (Cl)	% w/w _d ***	Mean	≤ 0.2	≤ 0.6	≤ 1.0	≤ 1.5	≤ 3.0
Environment Hg: volatile trace element of concern	Mercury (Hg)	mg MJ_{ar}^{-1}	Median † 80 th percentile †	≤ 0.02 ≤ 0.04	≤ 0.03 ≤ 0.06	≤ 0.08 ≤ 0.16	≤ 0.15 ≤ 0.30	≤ 0.5 ≤ 1.0
Environment Cd: volatile trace element of concern ††	Cadmium (Cd)	mg MJ_{ar}^{-1}	Median † 80 th percentile †	< 0.1 < 0.2	< 0.3 < 0.6	< 1.0 < 2.0	< 5.0 < 10	< 15 < 30

Adapted from: van Tubergen et al.²⁰⁴, European Committee for Standardisation¹⁹¹, and European Committee for Standardisation²¹⁰

* Specified sampling, sample preparation, analytical methods and statistical analysis apply. Classification to be based on at least 10 consecutive data points, collected in a reasonable time according to sampling plans. For Hg specific rules apply, according to number of assays taken

** Net calorific value (NVC) $Q_{p,net}$ is the same as lower heating value (LHV) H_u .

*** Dry reporting basis (d) selected for arbitrarily, because most existing data available are in such form for Cl.

† The higher classification stemming from each of the two statistics specifies the class

†† Proposed classes for Cd were not included in the final proposal of CEN

Four other key SRF descriptors have been proposed, but not included in the final classification scheme for simplicity and practicality reasons. They are ash content ($\% \text{ w/w}_d$), moisture content ($\% \text{ w/w}_{ar}$), and sum of heavy metals (mg kg_d^{-1})^{204, 210}. The sum value of Cd plus thallium (Tl) (Cd+Tl) has also been proposed as an important environmental descriptor. In the final CEN draft, Cd+Tl was rejected on the basis that Hg alone mostly results in a higher or equal classification than the Cd+Tl value of the same SRF, resulting in a more conservative and hence sufficiently environmentally

safe coding, and TI has no influence on the classification of Cd+TI, because of the relatively low value of TI compared to Cd.

2.5.4 SRF product quality standards for specific end-uses

2.5.4.1 Specifications for end uses vs. classification

Class codes are a tool for identifying and pre-selecting SRF by giving an immediate, but inevitably simplifying, image of the SRF quality. However, class codes cannot predict the actual performance of SRF when used (see **Table 2-2**) for a list of possible RDF/SRF uses). Definition of specific SRF properties and value ranges, thresholds and limits most relevant to each SRF utilisation plant in accordance with the particular technical characteristics, and legal demands of each thermal recovery process, is imperative for its marketability⁴⁷.

In order to appropriately characterise SRF, physical-mechanical, chemical and biological descriptors should be identified. Ultimate and proximate analyses are the minimum prerequisite to assess the thermal recovery behaviour and performance of a fuel²¹². Specifying SRF according to the CEN guidance demands a general list of obligatory and voluntary descriptors to be quantified. Properties should be measured according to appropriate, existing, or under development, CEN standard methods²⁰⁴. However, Thomé-Kozmiensky¹⁴⁵ and Beckmann *et al.*⁴⁷ stressed that effective use in varying applications demands the determination of a more complete list of properties (**Table 2-14**).

For example, characterisation of the reaction-related properties is critical, especially for co-combustion applications. For instance, Hilber *et al.*²¹³ have recently developed a method for assessing the process-specific combustion behaviour of low in char-formation RDF/SRF: the de-volatilisation of SRF at specific temperatures is measured by multi-sample thermo-gravimetric analysis (TGA). In the case of biofuel

QA/QC, which has similarities with WDFs, the significance and interrelationships of important physical-mechanical fuel properties have been investigated by Hartmann²¹⁴; and the chemical properties reviewed by Obernberger et al.²¹⁵. Eckardt and Albers⁵² investigated the current use of specification properties and limits proposed by plant operators in various thermal recovery applications of SRF.

Table 2-14 Properties for sufficient characterisation of WDFs according to end-use specifications

Property category	Properties
Chemical	Content of combustible matter Content of non-combustible mater (ash and moisture content) Content of H, C, O, N, (elemental analysis) Trace elements of concern ('heavy metals' or 'minor elements') Major elements: Cl, P, S Content of combined fixed C Content of volatile constituents
Mechanical	Density of the combustible and non-combustible matter Bulk solids properties (bulk density, and angle of repose, flowability) Grindability Particle size distribution Storage properties (biological stability, sanitisation) and dispersability (fluidity)
Calorific	Heating value and calorific value Specific minimum air requirement Specific minimum flue gas requirement Adiabatic combustion temperature Thermal capacity, thermal conductivity and temperature diffusivity
Reaction kinetics	Ignition and burnout behaviour Corrosion potential De-volatalisation ^a

Source of information, if not mentioned otherwise: Beckmann and Thomé-Kozmiensky⁴⁷

^a Hilber et al.²¹³

WDFs: waste-derived fuels

However, even within each specific category of RDF/SRF end-uses, it can be challenging to agree upon specifications that are applicable to every end-use. A wealth of available expertise has been incorporated in the relevant CEN report²¹⁰. Despite this knowlegde, it might still be evident that there is limited understanding of RDF/SRF behaviour within the various possible thermal recovery systems, resulting in the absence of robust technical and environmental criteria for their use as substitute fuel⁵². Furthermore, generalisation on fuel combustion behaviour is not advisable, and plant-specific investigations are preferable, because, for instance, transfer factors for elements of concern are highly process and operation mode-specific^{47, 210, 213}. In

addition, it is usual practice for each plant to prepare its own unique blend of substitute and raw fuels, leading to varying, case-specific contract specifications^{13, 52}.

In co-combustion of RDF/SRF with fossil fuels (and other WDFs), the actual degree of substitution varies, depending on the comparable quality of the RDF/SRF with the rest of the fuels, along with any related legal stipulations. Substitution of the original fuels by RDF/SRF depends on compatibility of the RDF/SRF properties with the thermal recovery process, typically designed for fossil fuels. For example, pulverised hard coal-fired plants with wet bottom boiler types (i.e., with molten slag with cyclones) (WBB) are more tolerant to the shape and dimensions of SRF, in comparison to plants with dry bottom boilers (DBB)²¹⁰. It has been estimated that coal-fired plants may reach up to 20% w/w substitution in the long run²⁰⁴; for cement kilns the percentage may vary between 50-100% w/w. Dedicated fluidised bed combustion (FBC) and gasification/pyrolysis plants are not constrained by such limitations. However, Beckmann and Thomé-Kozmiensky⁵¹ stressed that substitution rates as low as 1% w/w have been established for various thermal SRF recovery applications in the German state of North Rhine Westphalia. Even these low substitution rates have to be proven in future practice and for higher rates process-specific limit values should be convincingly defined for reaction kinetic properties. For confidentiality reasons, contract-based specifications do not often fully reach the public domain; this constrains the development of a wider consensus on what constitutes accepted, fit-for-purpose RDF/SRF quality.

It has been argued that maximum acceptable concentrations of trace elements of concern in SRF may be used to indicate its environmental suitability for each specific end-use²⁰⁴. Maximum values for blending of wastes with fossil fuels exist in national legislation. These values usually apply to the most volatile elements, namely Hg and Cd or Cd+Tl. Standards also apply to the “sum of other heavy metals.”⁴⁴. An indicative

list of SRF environmental classes that could be accepted for key thermal recovery technologies, based on conservative assumptions for trace elements is presented in **Table 2-15**.

van Tubergen et al.²⁰⁴ calculated estimations for the value ranges of SRF class-coding properties that could be accepted for different end-uses; for comparison, Eckardt and Albers⁵² provided data on Cd, Hg and TI limits specified for SRF by certain thermal recovery commercial references in Germany.

Major descriptors and acceptance values/classes for the main SRF end-users, focusing on potential properties of concern, are discussed below. Beckmann and Thomé-Kozmiensky⁴⁷ have detailed the experience in Germany. SRF particle form, size and shape, and NVC are discussed separately.

Table 2-15 Quality parameters for SRF according to end-use

SRF quality parameter	Type of end-use (co-combustion)								
	Power plants			Fluidised bed combustors					
	Cement kiln	Gasification and pulverised coal power plant	Pulverised coal power plant	Hard coal DBB power plant	Hard coal WBB power plant	Brown coal (lignite) power plant	FCB	FCB (with AC)	Industrial firing uses
SRF preparation form and storage requirements^a	1. Bales: Shredding (fluff) Covered storage	1. Bales: Shredding (fluff) Covered storage	1. Bales: Pelletising Storage Pulverisation				1. Bales: Shredding (fluff). Covered storage		
	2. Soft pellets: Covered storage	2. Soft pellets: Covered storage	2. Soft pellets: Covered storage			Soft pellets ^b	2. Soft pellets: Covered storage		
	3. Hard pellets: Simple crushing Covered storage	3. Hard pellets: Simple crushing Covered storage Pulverisation	3. Hard pellets: Covered storage				3. Hard pellets: Covered storage		
Bulk density^c	Range: 0.24-0.35 Mg m ⁻³	Range: 0.24-0.35 Mg m ⁻³	Range: 0.24-0.35 Mg m ⁻³	Range: 0.24-0.35 Mg m ⁻³	Range: 0.24-0.35 Mg m ⁻³	Range: 0.24-0.35 Mg m ⁻³			Range: 0.15-0.25 Mg m ⁻³
Particle size	ca 25-50 ^{e,†} Median 30 ^e <25 mm ^c	ca 10-25 ^{e,†,***} Median 20 ^{e,**} <25 mm ^c	ca 10-25 ^{e,†,***} Median 20 ^{e,**} <25 mm ^c	ca 10-25 ^{e,†,***} Median 20 ^{e,**} <25 mm ^c <20 mm ^b	ca 10-25 ^{e,†,***} Median 20 ^{e,**} <25 mm ^c <20 mm ^b	ca 10-25 ^{e,†,***} Median 20 ^{e,**} <25 mm ^c <25 mm ^b	ca 10-150 ^{e,†} Median 50 ^e	ca 10-150 ^{e,†} Median 50 ^e	Depending on thermal recovery technology: <300 mm grate systems <80 mm fluidised bed systems Length of longest particles <300 mm ^b Range: 50-80 mm ^c
Feeding system				Pneumatic ^b	Pneumatic ^b	Mechanically by conveyor belt ^b			Alkali metals <5% in the remaining ashes ^b
Cl content	Kiln without by-pass ^{b,†} : Mean 0.5-1.0% w/w _{ar}			In general <1% w/w (depending on S content) ^b	In general <1% w/w (depending on S content) ^b	In general <1% w/w (depending on S content) ^b			Median <0.85% ^b

SRF quality parameter	Type of end-use (co-combustion)								
	Cement kiln	Power plants				Fluidised bed combustors			
		Gasification and pulverised coal power plant	Pulverised coal power plant	Hard coal DBB power plant	Hard coal WBB power plant	Brown coal (lignite) power plant	FCB	FCB (with AC)	Industrial firing uses
	Max1-3.0% w/w _{ar} Kiln with by-pass: Max ca 3% w/w _{ar} ^{b,t} Wet process kiln: Max 6 % w/w _{ar} ^{b,t}			Mean 0.6% w/w _d ^{b,†††} Max 1.3 % w/w _d ^{b,†††}	Mean 1.1% w/w _d ^{b,†††} Max 2.5% w/w _d ^{b,†††}	Mean 0.5% w/w _d ^{b,†††} Max 0.6/1.0% w/w _d ^{b,††,†††}	Mean 0.4% w/w _{ar} ^{b,***,†,††} Max 0.5/0.8/1.4 w/w _d ^{b,***,††}	Mean 0.4% w/w _{ar} ^{b,***,†,††} Max 0.5/0.8/1.4% w/w _d ^{b,***,†,††}	
Hg CEN classification classes potentially acceptable (median)^d	1,2,3,4			1,2	1,2	1,2,3	1	1,2,3,4	
Cd CEN classification classes potentially acceptable (median)^d	1,2,3,4			1,2,3	1	1,2	1,2	1,2,3,4,5	
Net calorific value	5/10-12/22 MJ kg _{ar} ^{-1 d,†} Median 21 MJ kg ^{-1 e} Range 15-23 MJ kg ^{-1 e,*}			>20 MJ kg ^{-1 b} Mean 13.5 MJ kg _{ar} ^{-1 d} Range 11-18 MJ kg _{ar} ^{-1 d}	>20 MJ kg ^{-1 b} Mean 17 MJ kg _{ar} ^{-1 d} Range 13-22 MJ kg _{ar} ^{-1 d}	>11 MJ kg ^{-1 b} Mean 13.5 MJ kg _{ar} ^{-1 d} Range 11-18 MJ kg _{ar} ^{-1 d}	Mean 13.5 MJ kg _{ar} ^{-1 d} Range 11-18 MJ kg _{ar} ^{-1 d}	Mean 13.5 MJ kg _{ar} ^{-1 d} Range 11-18 MJ kg _{ar} ^{-1 d}	
		Central tendency value ^{e,†} : Median 17 MJ kg ⁻¹ Range 16-19 MJ kg ⁻¹	Central tendency value ^{e,†} : Median 17 MJ kg ⁻¹ Range 16-19 MJ kg ⁻¹	Central tendency value ^{e,†} : Median 17 MJ kg ⁻¹ Range 16-19 MJ kg ⁻¹	Central tendency value ^{e,†} : Median 17 MJ kg ⁻¹ Range 16-19 MJ kg ⁻¹	Central tendency value ^{e,†} : Median 17 MJ kg ⁻¹ Range 16-19 MJ kg ⁻¹	Median 14.5 MJ kg ^{-1 e,***} Range 6-18 MJ kg ^{-1 e,***}	Median 14.5 MJ kg ^{-1 e,***} Range 6-18 MJ kg ^{-1 e,***}	
		Minimum	Minimum value ^{e,**} : Median 14 MJ kg ⁻¹	Minimum	Minimum	Minimum value			

SRF quality parameter	Type of end-use (co-combustion)								
	Cement kiln	Power plants			Fluidised bed combustors				
		Gasification and pulverised coal power plant	Pulverised coal power plant	Hard coal DBB power plant	Hard coal WBB power plant	Brown coal (lignite) power plant	FCB	FCB (with AC)	Industrial firing uses
		value ^{e,†} : Median 14 MJ kg ⁻¹ Range 11-17 MJ kg ⁻¹	Range 11-17 MJ kg ⁻¹	value ^{e,†} : Median 14 MJ kg ⁻¹ Range 11-17 MJ kg ⁻¹	value ^{e,†} : Median 14 MJ kg ⁻¹ Range 11-17 MJ kg ⁻¹	value ^{e,†} : Median 14 MJ kg ⁻¹ Range 11-17 MJ kg ⁻¹			
Ash content^b				Low	Low	Can be high			
Contrary materials^b				Fe and non-Fe free No 3-D particles	Fe and non-Fe free ³ No 3-D particles	Fe and non-Fe free			Metallic Al <5% in the remaining ashes

^a Glorius et al.⁵⁰

^b Ibbetson and Wengenroth³³: For calorific values not stated: (1) if gross or net; nor (2) the basis (ar/d/dat).

^c Breuer¹⁰²: General SRF production specification (common for both cement kilns and power plants)

^d van Tubergen et al.^{204, 210}: Safety margin exists for all Hg and Cd classes and 100% fuel substitution is assumed in calculations. Actual air emissions will be determined also by raw fuel properties, fuel mix, and transfer coefficients of each specific technology. For hard coal WBB power plant conservative calculations apply, because of limited database. Relevant specific notes:

[†] Mean values; there is no maximum value for NCV if used in clinker kiln

[†] Cl specification depends on the composition of the input: e.g. K, Na content

^{††} The maximum values vary for different companies. Mean and max. values are close for a specific end-user

^{†††} The Cl-concentration of the total fuel mix should be kept <0.2-0.4% to prevent high temperature corrosion. The maximum allowable Cl % (depends on the design and materials chosen): Netherlands (usually) 0.2%; UK 0.4% (plants are designed for coal with a high Cl content)

^e Eckardt and Albers⁵²: Data from end-user requirements. Basis for calorific values not stated (ar/d/dat). Relevant specific notes:

* Readings from graph

** General category of power plants

*** General category for FBC mono-combustion

AC: activated carbon used as absorbent

CEN: European Committee for Standardisation

DBB: dry bottom boiler pulverised coal, dry ash

FBC: Fluidised bed combustor

WBB: wed bottom boiler pulverised coal, molten slag

2.5.4.2 Cement industry

The cement industry has a long-established experience with the use of WDFs²⁰³, especially for wet processes, but increasingly for modern dry ones²⁰⁴. Use of substitute fuels up to 50% w/w has led to changes in the operating features of the cement industry, such as flame characteristics, shape and stability, and ignition properties⁴⁷. The wide range of values for properties of RDF/SRF required by cement kiln operators indicates the resilience of this end-use²¹⁰; but also reflects the variety of cement kiln configurations. NCV is the most important single parameter for substitute fuel selection in the cement industry^{33, 204}. In Germany, compared with other end-uses, the cement industry has the highest median NCV of RDF used (not exclusively MBT-derived), being ca 21 MJ Kg⁻¹. **Table 2-16** provides an overview of existing standards applicable to RDF/SRF used in the European cement industry.

Concerns have arisen from the potential end-users about the possible major technical and environmental problems that relate to SRF fuel properties. These are outlined below and were reviewed in detail by van Tubergen et al.²⁰⁴, the subsequent CEN technical report²¹⁰, and Beckmann and Thomé-Kozmiensky⁴⁷.

(a) Kiln system operation: various possibilities exist for firing SRF in different types of cement production plants, leading to different SRF specifications²¹⁷⁻²¹⁸. For example, SRF clinker firing in a dry method is possible in⁴⁷ kiln exit (primary firing), where only high CV (LHV ca 20 MJ Kg⁻¹), dispersible SRF is suitable to achieve gas temperatures ca 1600 °C and avoid reducing conditions. This is also possible in kiln entrance (secondary firing), which is less demanding in LHV terms. Use in the calcinatory (heating below melting point temperature) is even less demanding^{33, 47}: larger SRF material, of lower LHV and higher ash content can be accepted. Cl, sulphur

(S) and alkali content (Na, K) can form compounds that build up in the kiln system, causing accumulation, clogging and unstable operation²⁰³

Table 2-16 Quality standards for SRF use in cement kilns

Parameter	EURITS/Flemish region of Belgium ^{202,*}	Switzerland ⁴³	UK industry specification ¹³	CEMEX Climafuel ^{216††}	Remondis SBS ^{®2, 42,**}
Bulk density				180 kg m ⁻³ range: 100-300 kg m ⁻³	
Particle size				<30 mm in any 2 dimensions	
Biogenic content				>50% w/w	
Ash content	5% w/w _d ^{***}			15% w/w	<20% w/w _d
Moisture content MC				<15(±0)	<20% w/w
Net calorific value Q _{p,net}	>15		23-29 MJ kg _{ar} ⁻¹	20±2 MJ kg ⁻¹	18-23 MJ kg _d ⁻¹
Antimony (Sb)		0.2 mg MJ _{ar} ⁻¹	<50 ppm	150 mg kg ⁻¹	<120 mg kg _d ⁻¹
Arsenic (As)		0.6 mg MJ _{ar} ⁻¹	<50 ppm	100 mg kg ⁻¹	<13 mg kg _d ⁻¹
Beryllium (Be)	1 mg kg ⁻¹				<2 mg kg _d ⁻¹
Bromine (Br)/Iodine (I)	0.01% w/w			0.25% w/w each	
Cadmium (Cd)				20 mg kg ⁻¹	<9 mg kg _d ⁻¹
Chromium (Cr)		4.0 mg MJ _{ar} ⁻¹	<200 ppm	150 mg kg ⁻¹	<250 mg kg _d ⁻¹
Chlorine (Cl)	0.5% w/w		<0.2% w/w _d	0.8% w/w	1.0% w/w _d
Cobalt (Co)		0.8 mg MJ _{ar} ⁻¹	<100 ppm	75 mg kg _d ⁻¹	12 mg mg kg _d ⁻¹
Copper (Cu)		4 mg MJ _{ar} ⁻¹	<600 ppm	500	<1000 mg kg _d ⁻¹
Fluorine (F)	0.1% w/w			0.5% w/w	
Lead (Pb)		8 mg MJ _{ar} ⁻¹	< 500 ppm	100 mg kg _d ⁻¹	<400 mg kg _d ⁻¹
Manganese (Mn)				150 mg kg _d ⁻¹	<500 mg kg _d ⁻¹
Mercury (Hg)	2 mg kg ⁻¹	0.01 mg MJ _{ar} ⁻¹	<20 ppm	10 mg kg _d ⁻¹	<1.0 mg kg _d ⁻¹
Molybdenum (Mo)	20 mg kg ⁻¹				
Nickel (Ni)		4 mg MJ ⁻¹ ar	<50 ppm	150 mg kg _d ⁻¹	<160 mg kg _d ⁻¹
Nitrogen (N)	0.7% w/w				
Selenium (Se)					<5 mg kg _d ⁻¹
Sulphur (S)	0.4% w/w		<0.3% w/w	1% w/w	<0.8 mg kg _d ⁻¹
Sum Cadmium+Thallium (Cd+ TI)		0.08 mg MJ _{ar} ⁻¹	<4 ppm		
Sum Fluorine+Bromine+Iodine (F+Br+ I)			<0.5		
Sum HM					
Total Group III metals (Sum Sb+As+Cr+Co+Cu +Pb+Mn+Ni+Sn+V)			<1800 ppm	800 mg kg _d ⁻¹	
Tellurium (Te)					<5 mg kg _d ⁻¹
Thallium (TI)	2 mg kg ⁻¹				<2 mg kg _d ⁻¹
Tin (Sn)				50 mg kg _d ⁻¹	
Vanadium (V)		0.12 mg MJ _{ar} ⁻¹	<50 ppm	100 mg kg _d ⁻¹	<26 mg kg _d ⁻¹
Zinc (Zn)	500 mg kg ⁻¹				
As,Se,(Te),Cd,Sb †	10 mg kg ⁻¹				
V,Cr,Co,Ni,Cu,Pb,Mn,Sn †	200 mg kg ⁻¹				
Total Group II metals (Sum As+Co+Cu+Cr(VI))				30 mg kg _d ⁻¹	

* Values result from calculations based on certain assumptions. Refer to publication for details. Necessary basis of report (ar or d) not stated

** Internal standard for the German organisation Remondis; applies to SRF produced from mixed MSW; values for element concentrations determined after microwave digestion of the SRF matrix by aqua regia acid solution mixture

*** Excluding: Ca, Al, Fe, Si. Arbitrary value

† Limit values apply to each of the metal separately

††Metal values: maximum

Research is ongoing regarding the problematic aspects of Cl behaviour during thermal recovery in general^{179, 219-223}. Excessive Cl content in dry processes may block the pre-heater with condensed volatile chlorides, according to end-users' experience, and as acknowledged by specifications from Belgium, Germany and France²⁰⁴. Acceptable Cl content depends on the degree of substitution, K and Na content, and existence of salt bypass. Wet processes are more tolerant, accepting up to 6% w/w_{ar} input Cl content. Recently developed chlorine bypass equipment has been reported to be able to achieve thermal substitution rates of fossil energy above 30%, reducing chlorine content in the hot meal by approximately 50%²²⁴. Nevertheless, in general salt bypass systems result in loss of mass and energy, incurring additional operational costs⁵². High moisture content can reduce the kiln productivity and efficiency. Ash content affects the chemical composition of the cement, and may necessitate adjustment of the raw materials mix²⁰³.

(b) Air emissions: most of the trace elements are absorbed in the clinker product with the exception of the volatile elements Hg and thallium (Tl) that transfer to the raw flue gas, but to a lesser degree compared with other thermal recovery technologies. In the case where RDF/SRF with high ash content is used, the subsequent low NCV (e.g., 3.2-10 MJ kg⁻¹ ar), results in ca ten times higher values of Hg concentrations, expressed on an energy substitution basis (mg MJ⁻¹ ar), compared with low-ash RDF/SRF (NCV ca 11.7-25.5 MJ kg⁻¹ ar)²¹⁰. However, there is evidence that Hg can be virtually removed from off-gasses by electrostatic precipitators in the kiln system. Juniper¹³ reviewed literature on dioxins and furans emissions from cement kilns that substitute fossil fuels with a percentage of WDFs, and found no significant increase in the measured concentrations in the stack gasses due to the use of WDFs. A recent report concluded that co-processing of alternative fuels fed to the main burner, kiln inlet or the preheater/precalciner does not appear to influence or change the

emissions of persistent organic pollutants (POPs), including pesticides, hexachlorobenzene (HCB), industrial chemical polychlorinated biphenyls (PCBs) and PCDD/Fs²¹⁸.

(c) Clinker and cement product quality: the concerns of the cement industry focus around Cl, S and alkali content (affecting overall product quality); phosphate content, which influences setting time; and chromium, which can cause an allergic reaction to sensitive users²⁰³. An investigation of the potential effects of co-combustion of various WDF (other than RDF/SRF) in the cement production industry showed only a slight increase in trace element concentrations (Antimony (Sb), Cd, Zn) in the final product²¹⁷. Cd, Copper (Cu) and Sb stemming from municipal waste-derived fuel contributed to the clinker composition more than the contribution of other fuel sources. Despite the significant differences among individual leaching characteristics of trace elements, it has been established that the release of trace elements from concrete is negligibly small during its operational life-span; and that there is no systematic correlation between the total content of trace elements in cement mortar and the leaching from mortar, even under the worst-case scenario.

With respect to the use of substitute fuels containing elevated concentrations of trace elements in clinker production, Opoczky and Gavel measured a positive effect on its grindability²²⁵. Chromium (Cr), Zn, barium (Ba), nickel (Ni), titanium (Ti), and phosphorus (P) generally improve grindability of clinkers by facilitating the clinker formation process during the molten phase and by forming solid solutions with silicate minerals (alite, belite) during clinker burning.

2.5.4.3 Direct co-combustion in coal-fired power plants

In Europe there is limited recent experience of SRF use for electricity generation, which is mainly restricted to small-scale plants in Germany, the

Netherlands, Italy²⁰⁴, and in the UK²²⁶. RECOFUEL has been a considerable EU research programme that begun in 2004 to investigate the potential use of WDF in large-scale coal-fired power plants^{204, 227}. Deposits of metallic aluminium and aluminium oxides were evident at the beater mill surfaces, which could have resulted from the relatively high Al₂O₃ content of the specific SRF used at the trial²²⁷.

Requirements for SRF co-combustion in coal-fired plants vary according to plant design and coal type, but are generally higher than alternative options for RDF/SRF thermal recovery³³. The Jänschwalde brown coal power plant (BCPP) in Germany uses SRF at an average calculated substitution rate of 1.8% w/w, without any significant impact on operational performance and emissions⁴⁷. However, for a more conclusive evaluation, results from continuous long-term operations are required. More demanding specifications apply for the Werne hard coal power plant (HCPP),²²⁸ as reported by Beckmann and Thomé-Kozmiensky⁴⁷. A summary of the relevant specifications can be found in Beckmann²²⁹, cited by Beckmann and Thomé-Kozmiensky⁴⁷. Specific technical and environmental issues with SRF quality during direct co-combustion with various types of coal, in different boiler technologies have been identified:

(a) Air emissions and air pollution control: it may prove difficult to control emissions of highly volatile trace elements, such as Hg, Cd, and Tl²⁰⁴. Such emissions largely remain in the vapour phase or become absorbed on ultra fine particulates for which air pollution control removal efficiencies are low. Increased capture of volatile trace elements preferentially partitioning in the flue gas will demand use of capital-expensive equipment and create secondary hazardous waste in need of careful management and costly treatment/disposal¹³. In addition, control of nitrogen oxides (NO_x) and sulphur dioxide (SO₂) emissions to WID limits may demand the use of additional air pollution control (APC) equipment. If selective catalytic reduction (SCR) is

used for NO_x abatement, accelerated aging and deactivation of the SCR catalyst should be anticipated in both high and low dust designs, because of the higher RDF/SRF content in alkali metals¹³.

(b) Airborne particulate matter (PM): initial results from test runs of the RECOFUEL project at the Weisweiler RWE power plant, co-combusting Rheinisch brown coal with low LHV (8.15 MJ kg⁻¹) with RDF/SRF of higher LHV (15.4 MJ kg⁻¹) (REMONDIS SBS[®] produced from sorting of residual MSW) at relatively high thermal substitution rate (8.5% of overall thermal input) showed no significant changes of the flue gas emissions that could be allocated to the SRF use²²⁷. Trace elements such as Cd, Cr, Cu, Pb and Zn are of concern for their presence in airborne PM, associated with acute respiratory symptoms in humans. Evidence by Fernandez et al.²³⁰ indicates that concentrations of the above mentioned elements in ash can be higher when MBT-derived RDF/SRF is co-combusted than when German bituminous coal is combusted²³⁰. However, comparison of ash-derived PM of non-MBT RDF co-combusted at 30-34 wt. % substitution rate, with that of German bituminous coal alone, did not reach conclusive results on the health impacts on mice by the long-term exposure to combustion emissions. Exposure to coal/RDF ash particles was found less desirable than exposure to coal ash particles alone. Staged operation mode of coal/RDF co-combustion (leading to low NO_x emissions) exacerbated only short-term lung injury in mice.

(c) Quality of marketable by-products: concerns have been expressed regarding the potentially adverse impact on the quality of marketable by-products i.e. boiler ash, pulverised fly ash (PFA) and gypsum. Their chemical, physical and mineralogical properties may be affected¹³. Possible increases in trace element content and higher contents of unburned carbon and alkaline metal species could result in values that are unacceptable by secondary raw material standards or customer

specifications. However, combustion studies at a pulverised hard coal DBB using dried sewage sludge, which typically has a higher trace element concentration compared with typical MBT-derived SRF, showed insignificant change in the by-product quality²⁰⁴. Bulky contaminants in the RDF/SRF can become incorporated in the by-products lowering their quality. RDF/SRF should be free from bulky undesirable constituents that are incombustible (metal particles) or may not be completely combusted because of insufficient residence time in the combustion chamber (e.g., hard plastics, polystyrene, and wood chips)⁵². Chlorine may adversely influence the ash quality intended as filler in cement, accordingly limiting the acceptable substitution rate.

(d) Plant operation: WDFs have been reported as having lower softening point (SP) and melting point (MP) temperatures than coal, resulting in an increased scaling or corrosion potential⁴⁷. The corrosion potential is enhanced by a lower sulphur (S) content, higher alkali and higher trace elements of concern, estimated as low for $S/Cl > 4$ and as high for $S/Cl < 2$ ⁹³, as cited by Beckmann and Thomé-Kozmiensky⁴⁷. Hence, the Cl concentration of the overall fuel mixture should be restricted to prevent high temperature corrosion. Design and construction materials of the boiler affect the maximum allowable Cl content, estimated up to 0.2% w/w in the Netherlands and 0.4% w/w in the UK²⁰⁴. Alkali metals become molten at combustion temperatures (slagging), increasing the risk of accumulation of fused deposits on the heat transfer surfaces (fouling)¹³. Abrasive RDF/SRF constituents, such as grit and glass particulates, may erode the heat transfer tubes¹³. Heavy wooden and plastic compounds, even at particle size of 20 mm, exhibit different combustion behaviours than pulverised hard-coal and have to be separated out³³. A higher moisture content of SRF (10-20 % wt.) compared with that of coal (ca 5% w/w) could result in increased gas water content and subsequently increased gas volume in the boiler, restricting the substitution rate of SRF to 5-10% w/w¹³. Additional operational end-user issues regarding RDF/SRF storage,

mechanical pre-processing, blending, conveying and feeding have been summarised elsewhere¹³. Because they are not critical for the production of SRF are not detailed here.

2.5.4.4 Co-combustion in industrial boilers

US Department of Environment data indicates that ca 25% of the fuels currently used in industrial boilers, furnaces and process heaters, to satisfy steam and heat production needs, are solid and can potentially be substituted by SRF¹³. In the UK, the most viable cases for SRF use are the paper and pulp, and metallurgical industries. In these cases, potential corrosion of the heat transfer surface by Cl and S can prove critical to the performance of an industrial boiler. In the steel industry, there is a limited possibility for using RDF/SRF, mainly by injecting it directly into the blast furnace to provide additional heating energy. This use may demand low concentrations of Cl, S, major inorganics and trace elements of concern.

2.5.4.5 Indirect co-combustion and dedicated mono-combustion

Thermal pre-treatment of RDF/SRF creates various attractive alternative scenarios for its use^{13, 51-52, 226}. Pre-treatment can be accomplished by: (i) mono-combustion, for example, by fluidised bed combustion (FBC), namely thermal recovery in a dedicated plant that uses RDF/SRF as the only fuel source; and (ii) by indirect thermal recovery of RDF/SRF, by feeding pyrolysis and/or gasification systems, or FBC with RDF/SRF, to introduce the char/syngas to conventional power plants. The term combustion is used here within the terms co/mono-combustion to denote any thermal recovery process (e.g., pyrolysis), following the established terminology which does not restrict it to its accurate scientific definition.

In Germany dedicated mono-combustion plants run in continuous operation, typically using lower quality RDF. Examples include gasification of RDF in circulating

FBC with the produced gas used at the calciner firing of a kiln at the Ruedersdorf cement works, pyrolysis of RDF in a rotary kiln and feeding of the syngas and the appropriately processed char in to the boiler of the power station at Hamm, and combustion of the pyrolysis coke in an FBC⁵¹. Hamel et al.²³¹ reviewed the literature of gasification process configurations with the thermal recovery of SRF derived from biodrying MBT; they have also developed and tested a fit-for-purpose two-stage gasifier, based on a parallel arrangement of fixed bed gasifier and bubbling fluidised bed combustor modules.

Relevant SRF quality standards for mono-combustion are thought to be less demanding than those for co-combustion in power and cement plants^{13, 33, 47, 52}. Ibbetson and Wengenroth³³ have stressed that for dedicated RDF/SRF plants that produce steam and power (FBC or grate fired systems) the important quality parameters are the ones affecting steam temperature and plant availability (particle size, metallic Al, alkali metals content, glass chlorine content), rather than CV.

For circulating FBC, least variable fluidisation behaviour and narrow PSD are required, whilst the process is more tolerant to wider ranges of elemental analysis and LHV⁴⁷. In dedicated gasification for subsequent syngas use in power plant boilers, fouling and corrosion of heat transfer surfaces by compounds of released alkali metals such as Na and K salts, could be a problem. In FBC co-combustion the most problematic elements are Cl and alkali metals causing corrosion and fouling; and Al, which can lead to bed agglomeration and blocking of air injection ports⁴⁵. Kobayashi et al.²³² provided evidence that mixing of calcium compounds into RDF/SRF can effectively remove HCl from the flue gases, even in a high temperature regime, for circulation FBCs; the mechanism of removal has been initially discussed by Liu et al.²²². Volatile matter content was found to be the critical parameter to waste biomass gasification performance for air-stream gasification²³³.

Kilgallon et al.²³⁴ have reviewed the literature and performed thermodynamic modelling on the fate of trace contaminants in various gasification systems co-gasifying coal with biomass-rich fuels. They concluded that fuel gas compositions vary significantly between gasification systems, and most trace and alkali metals exhibit increased volatility when compared with their behaviour in combustion systems, with their volatility being influenced by the S and Cl concentrations. Na and K, and trace elements Pb, Zn, Cd, tin (Sn) (and vanadium (V) in certain systems) can pass to the gas turbine through the fuel gas path at potentially harmful levels; Hg, boron (B), Sb, and selenium (Se) also can pass through the gas turbine.

RDF/SRF can be treated by pyrolysis to produce a homogenised, high CV char fuel²³⁵, with Cl, S and the content of trace elements of concern the most relevant properties in technical and environmental terms. Enrichment of certain trace elements (Cd, Cr, cobalt (Co), Ni, Pb, Zn) has been observed in the char, demanding a more intensive removal of these contaminants during the RDF/SRF production. Similarly, enrichment in the Cl content in the char (char: 1.30% w/w_d, from Herhof dry-stabilate RDF/SRF: 1.05% w/w

_d), because of absorption on inorganic ash compounds after its release, could cause acceptability problems²³⁵. In another case, only the pyrolysis gas from rotary-tube pyrolysis of SRF is fed into the steam generator of a power plant, with the char undergoing additional separate treatment⁴⁷.

2.5.4.6 RDF/SRF particle form, particle size limitations and homogeneity

Particle form and size are obligatory descriptors in the CEN SRF specification. Kock²³⁶ proposed a new modelling method for characterisation of combustion properties of heterogeneous flues as RDF/SRF, relying on the PSD of RDF/SRF. Conveying and dosing of RDF/SRF into the processes, and firing technology, affect the

appropriate delivery form (pellets, bales, briquettes, chips, flakes, fluff, powder, etc), size range and shape of RDF/SRF⁵². **Table 2-15** provides suitable preparation forms and storage for intended uses.

Clear differences exist in the preferred medians and tolerated ranges of the feeding particle sizes appropriate for RDF/SRF⁵². RDF/SRF used in the cement industry should be appropriately small in size to avoid blockage of conveyors. Hard plastic particles should be <15 mm. In addition, contractual practice for cement kilns shows that the fine fraction (typically <10 mm particle size) is not favoured to form part of SRF⁷⁹. Two-dimensional SRF particles have been specified in a recent UK contract for cement kiln use.

In fluidised bed gasification at the Ruedersdorf Cement Works, 3-D WDF size specifications apply²³⁷ (ca 30 x 10 x 5 mm), as cited in Beckmann and Thomé-Kozmiensky⁴⁷. The lowest mean particle size is demanded by the electricity generating plants designed for pulverised coal, so that the required trajectory in the boiler can be achieved, incurring more of a cost than a technical challenge²²⁶. The Jänschwalde BCPP specifications for SRF are maximum permissible particle size of non-pelletised material 25 mm, with 3% w/w allowance for oversize <50 mm⁴⁷. The specifications for the Werne HCPP are higher, with dispersible SRF of particle size <20 mm, suitable for direct injection in to the firing process²²⁸ (cited in Beckmann and Thomé-Kozmiensky⁴⁷).

The case of the Nehlsen biodrying plant in Stralsung, Germany, exemplifies the need for multiple SRF qualities produced to specifications of different end-users. Three SRF qualities are produced¹⁰²: (1) pelletised SRF with bulk densities between 0.25 and 0.35 Mg m⁻³ and particle size <25 mm, suitable for power plants and the cement industry; (2) post-shredded SRF, with bulk density 0.15-0.25 Mg m⁻³ and particle size

50-80 mm, for industrial firing plants; and (3) raw SRF with bulk density 0.15-0.25 Mg m⁻³ and particle size <200 mm, intended for the heat and power plant in Stavenhagen.

The size of RDF pellets was shown to influence the temperature distribution inside the pellet during their combustion in an internal recirculation FBC²³². Eco-deco SRF, used in an FBC plant, has to be shredded to a mean particle size of 100-150 mm¹³. Circulating fluidised bed combustion systems demand a narrow SRF PSD; in the Neumuenster plant, particle sizes <250 mm are accepted⁴⁷. Herhof Stabliate[®] SRF produced in the Dresden plant is pelletised in 20 mm, to be used in a methanol production plant²³⁸. At the Osnabrueck plant, SRF output is post-shredded to 40 mm, pelletised in soft pellets and pressed for loading on trucks, for use in cement kilns²³⁹. It has been speculated that the degree of homogeneity of RDF/SRF can affect performance of APC equipment present in end-use industries. If greater homogeneity is achieved, pollutant emission peak loads, typical in thermal recovery of unsorted waste, may be significantly reduced⁶².

2.5.4.7 Biogenic content of SRF

Advances in alternative and renewable energy fuels aim to reduce reliance on fossil fuels, and mitigate the contribution of waste management in global warming potential. As a result, the biogenic (or biomass) content of waste included in RDF/SRF is becoming increasingly important environmental descriptor, reflecting policy and financial drivers¹⁹³. The draft CEN standard (CEN/TS 15440:2006) defines 'biogenic' as material "*produced in natural processes by living organisms but not fossilised or derived from fossil fuels*"⁸⁹, namely as a characteristic stemming from the origin of the material rather than as a measurable property. CEN has issued guidance on the relative difference between biogenic and biodegradable fractions of SRF, which whilst despite largely overlapping should not be treated as identical (CEN/TR 14980:2004)²⁴⁰. Determination of the biogenic content of SRF is gradually being incorporated into

standard practice, and could prove critical for its marketability as a quality-certified fuel, as well as for earning subsidies. The relative financial importance of biomass content for RDF/SRF use has been discussed by Juniper¹³. The wider policy framework for MBT-derived RDF/SRF use in Europe has been analysed by Garg et al.³⁴.

In terms of renewable energy production in the EU, specialists have agreed a minimum 50% biogenic content for MSW-derived RDF/SRF to qualify as a renewable energy source¹⁸⁰. However, in the UK, the renewables obligation certificates (ROCs) set the threshold values much higher. All electricity that is produced by waste from thermal treatment by gasification and pyrolysis qualifies for ROCs. Additionally, any biogenic percentage of waste-derived fuels qualifies for ROC subsidisation in the case of combined heat and power energy from waste plants (CHP EfW)²⁴¹. The overall biogenic content percentage that has to be met by a fuel to qualify for ROCs has been lowered from 98% to 90%, still a challenging target for MBT-derived SRF, which typically also concentrates high CV materials of fossil fuel origin, such as plastics. A public ROC consultation process was opened with the aim to revisit previous decisions, based on a report on carbon balances²⁴². In the US a report, prepared by the Energy Information Administration (EIA) in 2007, has estimated that 56% of the heating value available in the MSW comes from biogenic sources²⁴³.

In terms of alternative energy sources, carbonaceous emissions released during energy production stemming from the biomass content of fuels are considered by the EU emission trading scheme (EU-ETS) as 'CO₂-neutral' from a global warming potential point of view. Hence, the CO₂ emission factor of fuels is based merely on the fossil carbon content and the biogenic content is ignored⁶⁴. Stipulations for biomass content of waste-derived fuel in order to qualify for ROCs and EU-ETS will determine the processing objectives for the biomass fraction in MBT plants. Enabling implementation could favour concentration of biomass content of residual waste into

RDF/SRF. Currently existing measures clearly favour CHP EfW and not the co-combustion of RDF/SRF in conventional electricity generating plants: no thermal recovery process using SRF has gained ROCs so far (January 2010).

Scientifically appropriate analytical determination of biogenic content of contaminated biomass fuel streams has recently been investigated, with the so called 'selective liberation/dissolution method' being the currently applicable state-of-the-art^{186, 208}. Selective dissolution has been adopted by the CEN QA/QC guidance as normative, along with the manual sorting method, and the informative reductionistic method^{89, 244}. CEN has agreed to further develop another available method for the determination of biogenic content, the carbon isotope method ('¹⁴C method'). It is hoped that the ¹⁴C method will overcome the restrictions faced by the selective liberation method. The ¹⁴C method has been standardised in 2008²⁴⁵. ¹⁴C has the relative advantage that can be applied to either the fuel itself or the off-gasses produced during the thermal recovery. The selective liberation method has been the most practiced the previous years, as confirmed by Flamme⁶⁴, who reviewed European methods; and denoted by the German government adopting it for immediate use. In the UK, the DTI/Ofgem Biomass Fuels Working Group issued sampling guidance in 2007, but has not yet (January 2009) adopted a position on the actual measurement²⁴⁶.

Potential co-combustion of SRF with other fuels (purely fossil or biomass) has led to the development of measurement methods applicable at the location of SRF thermal recovery. Fellner et al.²⁴⁷ proposed the determination of biogenic content during EfW co-incineration using a model based upon typical process/ regulatory monitoring data; Mohn et al.⁶⁵ compared this computational method with the ¹⁴C off-gasses method, finding their results in good agreement. Recently, Staber et al.⁶⁶ provided an up-to-date comparison of the available methods.

2.6 Statistics for SRF quality

An introduction to basic notions that relate to the quantification of uncertainty that pertains every measurement procedure has been compiled in **Appendix A**, where definitions and symbols are introduced. .

2.6.1 Statistics for solid waste and SRF properties

The selection and validity of statistical tools for describing properties of waste either for process design/control or for compliance to legal standards/market specifications is highly debatable. Certain aspects of the ongoing debate have been addressed by Uerkvitz and Goetz²⁴⁸, van Tubergen et al.²⁰⁴, Pehlken et al.⁹² and the PD CEN/TR 15508:2006²¹⁰. Reliable, unbiased estimates for central tendency ('average,' 'expected values,' 'location') (e.g., mean, median), spread of values (e.g., standard deviation, median absolute deviation), scale-free spread of values (e.g., coefficient of variation), and upper/lower limits are needed. Conversely, waste-related results reported as single numbers, without stating the statistical analysis performed, and the uncertainty involved may invoke the misleading impression of accurate knowledge⁹², rather than that of estimates characterised by a level of uncertainty, which is the correct.

The type of the distribution (i.e., normality or not) of a measurand (particular quantity subject to measurement) determines the suitability of applying certain statistical analysis. Investigation on the type of distribution that best fits Cl, Hg, Cu, and Cr concentrations in SRF produced in two MBT plants showed log-normal rather than normal behaviour, with the exception of Hg for the biodrying-MBT, which was normally distributed²⁰⁸. Data reported on SRF from the Eco-deco and Nehlsen biodrying processes¹³ indirectly verify that many properties are not normally distributed. Data-sets for which values of both mean and median are available show varying degrees of

difference between these two statistics, establishing that their distributions are skewed, hence not normal. For instance, Pb and Cr show clear positive skewness in all three available data sets; whilst Hg shows mixed behaviour, including one case of negative skewness.

Further evidence has been reported by Uerkvitz and Goetz²⁴⁸ who have compared the statistical evaluation of data sets of ca 70 incineration slag samples collected at each of 3 plants, by statistics based on normal and log-normal distributions for Cd, Cr, Pb, Zn, and Cl. Using the Chi-square test for goodness-of-fit they showed that for each of the 3 plant data sets Cl and Cr were approximately both normally and log-normally distributed, whilst Cd, Pb, and Zn were better fitted by a log-normal curve. Chang et al.²⁴⁹ have reported the log-normal distribution as best fitting the net heating value of RDF produced by mechanical separation from MSW, as estimated through the K-S test statistic.

Departures from normality can be anticipated for the samples analysed in this research, especially for trace level measurands. This applies with regard to data sets of both (1) the within-GAS variability (See Section 4.7 and 7.3B.1) and (2) the time-sequence of incremental samples representing a wider lot of an MBT material flow (within-lot or between increments variability). Within-GAS variability is anticipated to be less evident for measurands that are more uniformly distributed throughout the GAS mass²¹⁰, such as moisture, ash, and biogenic content, for which a normal distribution for the population of GAS replicates can be reasonably anticipated.

The two main approaches to handle departures from the normality assumption for the PDFs of measurands are to use the non-Gaussian (speculated) distribution (e.g., log-normal) or to resort to non-parametric statistics. Regarding the first option, Uerkvitz and Goetz²⁴⁸ examined on a theoretical level suitable statistics to describe log-

normally distributed waste-derived data-sets. They suggested suitable mathematical formulas, to overcome the bias introduced by the use of the normality-based statistics, mainly for the standard deviation and coefficient of variation; however, the bias for the central tendency was below 7% in all examined data-sets, reflecting the fact that for moderately skewed PDFs the departure from normality is not important. They advocated the comparison of the dispersion measures between datasets observing normally and log-normally PDFs, by using a suitably adjusted coefficient of variation for the log-normal case. Their calculations covered the issue of what constitutes adequate number of samples in order to achieve desired levels of accuracy in determining statistics of log-normally distributed waste measurands, accepting an assumption of a log-normally adjusted %CV at ca 80% for measurands of trace elements in waste samples. Under these conditions, a minimum of 100 measurements are needed to limit the uncertainty in the spread estimate at 20% and in the upper concentrations limit at 80%, necessitating, according to the authors, the use of confidence intervals, rather than single values, for reporting purposes.

The alternative of using non-parametric statistics has been discussed by Pehlken et al.⁹² and is the solution suggested in the pre-normative CEN research on SRF²⁰⁸ and selected for compliance testing in the CEN SRF documents for non-normally distributed measurands, such as the Hg concentrations²¹⁰.

2.6.2 Plant production quality control

Treating SRF as a produce rather than just a processed waste stream could mean that traditional quality control is relevant. For typical production line quality control purposes a suite of statistical tools are well established as described e.g., by Montgomery²⁵⁰. Statistical quality control uses statistics to monitor the performance of production processes. Notably, for the property under examination, control is sought for

both its average and variability. Statistical quality control tools, such as control charts, can deliver an advanced description and understanding of the process. Relevant statistics can be readily computed and plotted by commercially available software programs (e.g., Statistica²⁵¹).

Important controls refer to process stability and process capability/performance, which are two separate notions. The process capability/performance refers to the actual ability of the process to meet the specification limits and target value set. To check for process capability/performance, the process should have already demonstrated sufficient stability. Notably, a 'stable' process does not imply a capable process, i.e., meeting externally set limits on its anticipated performance²⁵².

Process stability assesses if a process is under statistical control, typically using control charts (also known as Shewhart charts). These are a graphical method to evaluate whether the process variability within each minimum production period (e.g., day or batch) is acceptably constant. R-chart plots the range (R) (upper-lower value) for each day/batch data points (e.g., 3 values); and X-bar chart plots their average (X-bar). If the R-chart this is acceptable, the X-bar chart can be used to demonstrate the performance of the average, i.e., the between-day/batch variability.

The process 'sigma'²⁵¹ used is effectively the standard error of the mean, obtained from the individual sets of measurements per each day/batch. Control limits (Upper control limit (UCL) and lower control limit (LCL)) can be correctly computed, using a coverage factor of 3, effectively being confidence limits at the 99.73% level of confidence²⁵⁰. This way of estimating sigma, results in tighter control limits, in comparison to the standard error of the mean of the overall data set, because it accounts only for the so-called 'common cause' variability (i.e., within-day/batch variability, a minimum background level of anticipated variability).

For process capability/performance purposes, nominal or target values T_g and an acceptable level of variability should be specified according to the product user anticipations. The process performance is checked against the upper specification limit (USL) and lower specification limit (LSL). Various capability/performance indices can be computed and reported. The P_p evaluates the potential of the process to meet the specifications, computed as the allowable spread (USP-LSL) over the actual spread (6 times sigma); however it does not account for any deviation from the specified target value. K (Equation 2-3) evaluates the difference of the measured value from the T_g relative to the specified range of values; i.e., it is scale-free²⁵¹:

$$k = abs\left(\frac{T_g - \langle x \rangle}{1/2 \times (USL - LSL)}\right) \quad [2-3]$$

where,

- K non-centering correction
- T_g target value for the examined property
- $\langle x \rangle$ average value of property measured for the product
- USL upper specification limit set
- LSL lower specification limit set

Attention should be paid to correctly estimating the sigma for the capability/performance indices. Estimation of the variability for the capability indices using the common cause variability assumes that the process is under control and can result in a deceptively well-performing (capable) process, if the process is out of control²⁵¹⁻²⁵². Much more sophisticated quality control charts and indices are available²⁵⁰.

Whilst almost every MBT plant producing SRF is assessing its quality, there is no evidence that traditional quality control is applied widely. However, certain SRF producers adhere to basic quality management practices that enable them to demonstrate compliance with quality certifications such, as the German RAL-GZ 724¹⁹⁹, and internally established quality labels (e.g., Remondis SBS^{®253}). Fuel end-users, such as power plants and cement kilns, regularly apply quality control practices to ensure the consistency of fuels utilised. The type of statistical controls just mentioned could be suitable for SRF properties for which a range can be tolerated (rather than a single-sided limit), such as biogenic content and calorific value.

2.6.3 Compliance statistics

Compliance with regulatory or quality management specifications requires incorporating the uncertainty with which the observed value of the measurand has been estimated. Despite the high importance of the subject, it remains highly debatable: a recent review summarises open issues from an analytical chemistry point of view²⁵⁴. Notwithstanding this, a Eurachem/CITAC publication provides up-to-date discussion and guidance on how to best accomplish this²⁵⁵. This publication builds upon previous guidance on the measurement uncertainty notion²⁵⁶⁻²⁵⁷ and incorporates relevant advances in compliance literature brought about in the testing of electrical and mechanical products, as solidified in an ASME document²⁵⁸. Briefly, Eurachem/CITAC recommends along with the upper/lower limits specified for the controlled measurands, the introduction of unambiguous decision rules, describing how the measurement uncertainty would be taken into account in the compliance evaluation.

Specifically, ideally the minimum acceptable level of probability (confidence) that the measured value lies within the set limits should be selected, leading to the creation of acceptance and rejection zones. These zones forming 'guard bands' placed

at around the specification limit, according to the type of the decision to be taken: e.g., for an upper limit demanding a low probability of false acceptance, as in the case of trace level elements of concern, the guard band would be below the limit value. In addition, the document recommends that procedures for dealing with replication (repeated measurements) and potential outliers are included in the decision rules; without, however, further discussing these topics at all.

The size of the guard band is informed by: (i) the desired confidence level; (ii) the estimate of measurement uncertainty available (e.g., combined standard uncertainty) and, (iii) the type of the distribution of the measurand. As, explained above (iii) can be normal, log-normal, or any other type (e.g. rectangular), but typically this is not known. Under these circumstances it is recommended to use the t-distribution, for the specified degrees of freedom to obtain the guard band size. In cases in which the asymmetric distributions of the measurand can lead to asymmetric uncertainty limits, such as inherently asymmetric measurands, measurands close to physical constraints (e.g., zero) or heteroscedasticity (uncertainty correlated to the level of the measurand) the estimates of the guard band can be made using the t distribution for the transformed data and then back transformed to give asymmetric guard bands.

In the case of non-symmetrical measurand PDF the value of the property at which the uncertainty measurement is computed affects the size of the guard band, an issue highly debated²⁵⁵. For example, a decision rule that mandates to calculate the standard uncertainty at the level of the measured value instead of the level of the specified limit can lead to less conservative evaluations in the case of doping control in sports – case of upper limit with high confidence of correct rejection (i.e., wider guard band size for which the measured value is allowed to exceed the limit before a violation is declared). Conversely, the typical case in SRF compliance is that of an upper limit demanding high confidence of false acceptance. Applying the above rationale, by

calculating the guard band using the uncertainty level of the measurand at the level of the limit, would lead to a wider guard band (assuming proportional uncertainty to the level of the measurand (heteroscedasticity)) and thus a more conservative decision rule.

2.6.4 CEN approach to SRF classification and specification

compliance

The CEN compliance documents (initial technical report²¹⁰, final draft for development¹⁹¹, and recent on-going amendments²⁵⁹) do not provide any guidance on the number of replicates necessary for evaluating the central tendency as well as the uncertainty for each composite sample representing a lot. It is indeed mentioned that the 'smaller-scale' variability has to be assessed as well, but no further detail is provided. However, in discussing the origin of the high concentration values (measured within typical 'outlier' or 'extreme' ranges), characteristic of positive skewness of metals at trace levels in the SRF, the variability employed to account for these high level results of a series of incremental samples, the document does not differentiate between the within-GAS and the between-increments variability, leading to confusion.

However, it can be argued that the potentially outlier/extreme values are valid measurements, part of possibly log-normally distributed measurands due to SRF heterogeneity²⁰⁸ and should not be directly excluded from the statistical computations. On the other hand, the rationale employed by CEN argues that any outlier/extreme values, being extreme cases, should not be allowed to artificially inflate the central tendency estimate, as would have happened if non-robust, normality-based statistics were used. Furthermore, because the exact PDF might not be known or other limitations may exist, (such as the distortion of the PDF in the case of Hg because of the lower range values being close to the LoD/LoQ of the analytical techniques

employed), robust statistics are used for Hg (and proposed in general for 'heavy metals'). Because of the long-tailedness evident in the PDFs of measurands present at trace-levels and non-uniformly distributed across the increments/GAS mass, a measure of the upper/lower limit of values is also considered necessary to determine.

The robust statistics adopted by the CEN^{191, 210, 259} are the median and 80th percentile, measures of location and upper limit values respectively. They have the advantages of being independent of the form of distribution and robust to extreme values. They are therefore suitable to describe properties of RDF/SRF that show log-normal distribution or skewness and longtailedness in general. Additionally, they are more suited to describe datasets with few numbers of observations²⁶⁰ (10 suggested as minimum in the CEN classification demands, whilst 100 was identified as a practical minimum for non-robust statistics of log-normally distributed data for an acceptable variability to be achieved²⁴⁸, as discussed before). However, modelling studies of the median, upper and lower confidence limits, showed high uncertainty for as low as 10 data points (with average median at 0.3 mg kg_d^{-1} the upper and lower 95% confidence limits were at 0.1 mg kg_d^{-1} and 1 mg kg_d^{-1} respectively)²¹⁰, with the upper limit converging sufficiently only after at least 50 observations, (values as inferred from graph).

In the case of a normally distributed property, the median is identical to the arithmetic mean. High percentiles, like the 80th percentile (p_{80}), are particularly useful for estimating the upper values of concentrations of trace metals of concern (e.g., Cd), as demanded in practice. Additionally, the CEN/TR 15508:2006²¹⁰ argues that the ratio of the p_{80} over the median can serve as an indicator of the heterogeneity of the SRF measurand, with a typical value of 0.5 used in the relevant CEN modelling computations, but without further justification.

The CEN rules for allocating the class code to an SRF are detailed below. Despite the evidence for cases of log-normality for the Cl concentration, the CEN technical committee draft has opted for [Cl] to be classified by the mean rather than the median, implying a normal distribution would suffice¹⁹¹; indeed there is a certain degree of overlap between the two forms of distribution in the pre-normative research datasets²¹⁰. The decision rule for class code identification for NVC and Cl is based in the creation of a confidence interval around the arithmetic mean. For the Cl the upper limit of the 95% confidence interval around the mean $UCL_{95,v}(<[Cl]>)$ has to be below (or just equal) to the class boundary – conversely the lower 95% confidence limit around the mean has to be above or equal to the class boundary for NCV ($UCL_{95,v}(<Q_{net,p,ar}>)$).

There are many (complimentary) ways to evaluate the type of distribution followed by a population. The Shapiro-Wilk test (S-W)²⁶¹ is arguably one of the most reliable statistics to test for a range of possible departures from normality and can supplement graphical methods such as histogram and box-and-whisker plots²⁶². If the S-W is not significant, it suggests that there is not sufficient evidence for violation of the normality assumption. In this case also the upper or lower confidence intervals at 95% level of confidence ($UCI_{95\%}$ and $LCl_{95\%}$ respectively) around the arithmetic mean can be used to check for compliance.

This approach of the CEN draft standards for SRF classification^{191, 210, 259} whilst similar in the basic rationale, differs from that of the Eurachem/CITAC and ASME. First, the coverage factor used for the computation of the upper and lower 95% confidence limits is that of normally distributed dataset with (1.96). Whilst this is an often encountered practice, it actually corresponds to at least ca 120 d.f. (1.98) of the t-distribution. Instead, the correct approach would have been to use the $t_{95,v}$ for the computation of the extended uncertainty²⁶³, given that the mean ($\langle \rangle$) is estimated

through limited observations. In this case the CEN guidance is for a minimum of 10 numbers of observations, hence the maximum (and most possible to be implemented as it corresponds to less number of analysis, thus minimum cost) coverage factor should have been $t_{95,9} = 2.23$ instead of 1.96. Hence, the CEN guidance is less conservative than the statistically correct by ca 12%. A second difference is that whilst the arithmetic mean plus the upper 95% limit is effectively a decision rule for guard band calculated at the level of the measurement, which leads to less conservative decisions with comparison to guard bands calculated at the classification limits. Thirdly, the effective width of the 'guard band' in this research is not constant, but depends on the actual variability estimate of each data set.

The CEN SRF guidance on sampling plans mandates these 10 minimum data points are test results from analyses performed on composite SRF samples, each consisting of at least 24 mixed incremental samples, and is representative of a lot (population/quantity to be representatively sampled from) of SRF production which has to meet certain mass flow limitations²⁶⁴. However, similar to the Eurachem/CITAC, no guidance is given on the number of authentic replications necessary for each of the 10 data points and classification parameters, nor is it prescribed how the uncertainty measurement pertaining to each individual of the 10 data points can/should be incorporated into the classification decision rule.

Hg is classified using robust statistics, according to both median and p_{80} values, implying that a skewed, long-tailed distribution is anticipated. The classification measurand is expressed on an energy reporting basis ($\text{mg MJ}_{\text{ar}}^{-1}$) which demands to measure independently the concentration of Hg on a mass basis and the NCV and multiply them to get the Hg concentration on an energy basis. The NCV PDF can be reasonably anticipated to be normal, whilst for the Hg the evidence is inconclusive.

Hence, it is not clear how the [Hg] is distributed. In the Hg case, instead of confidence levels around the mean, closed classes for both the median and the p_{80} are used in the decision rule: the worst classification of the two statistics prevails as the assigned class code. When more than 10 (and more than 40) data observations are collected, the CEN guidance suggest the use of the 50% decision rule, which however has not been sufficiently elaborated in the available guidance so far^{210, 259}.

For the exact specification of the SRF relevant properties, the CEN guidance has not proposed any decision rules, apart from clustering the possible measurands as 'obligatory to specify' and 'not obligatory to specify'.

The German quality standard for SRF RAL-GZ -725⁴², established in 1999, also employs non-parametric, robust to outliers statistics, to assure compliance. Limits are set for median values of 20 samples and p_{80} . The limits for medians should be adhered to, whilst the p_{80} must not be exceeded by the 16 out of 20 samples, applying the so-called '4-out-of-5' rule.

2.6.5 Compliance rules for end-user SRF specifications

The existing mutual agreements between SRF producers and end-users in the UK (e.g., CEMEX (Climafuel)^{216, 265}, SRM (Profuel)²⁶⁶ provide some rudimentary guidance on sampling procedures (covering: frequency, mass, composite samples, sub-sampling and sample preparation) and set limit values (upper or lower) for the suitable measurands. However, to the best of my knowledge, there is no reference to any detailed decision rules that are statistically aware. The measurement uncertainty is not considered at all. The CEMEX modification of the permit of the Rugby works in 2006 prescribed values that should be met by every composite sample representing a batch 200 Mg of SRF delivered for thermal recovery - hence no averaging. For long term monitoring the 7-batch rolling average should comply for the most important

quantities: calorific value, ash content, moisture, [Cl], [S]. In a more recent coverage of the CEMEX Climafuel specifications (2008), no explicit reference to statistical treatment has been made, but more stringent values for a series of parameters (e.g., NCV, M, particle size, [Cl], [Pb])²¹⁶ have been set. Similarly, the decision rule for compliance purposes in an agreement between a UK MBT-derived SRF producer and SRM²⁶⁶ is limited to a 7-point rolling average of daily.

Note that, in principle, estimates of the anticipated variability associated to a level of measurand representing a particular lot with unknown but estimable heterogeneity can be produced, e.g., for the sampling part of the variability by the Gy's ToS²⁶⁷⁻²⁷² and for the within-GAS and analytical determination variability for trace-level measurands by the Horwitz formula²⁷³, adjusted for a single laboratory.

2.7 Literature review summary

A significant objective for MBT is to achieve effective material flow management of residual waste that involves extracting homogeneous fractions of known biochemical composition. The benefits of this are twofold: to concentrate contaminants separately and direct them towards appropriate onward disposal or treatment mechanisms; and to produce recyclates to a desired quality, prolonging their useful life.

2.7.1 Appropriate descriptors for evaluating unit process operations

Since MBT is a generic process that can be broken down into many process unit operations, it is important to understand, through characterisation studies, the relative contribution that each unit makes by using appropriate descriptors. Conventional descriptors such as yield and purity of waste components have typically have been applied. PSD, if used appropriately, can be useful in describing comminution results and for modelling size-dependent mechanical processing. The move from a predominantly disposal-led waste sector to one that is more resource

based, demands the use of analytical tools such as MFA. MFA, via TCs and MECs, can provide the ability to map flows of preserved properties of waste, such as trace elements, into the output fractions. This can enable the optimisation of MBT processes to effectively separate waste fractions into outputs of desired quality e.g., known chemical composition. This is of value to waste companies because it provides the basis for a targeted reduction in pollution load of MBT outputs, which could potentially have a positive effect on end-user emissions.

2.7.2 Performance of process units and implications for output quality and MBT design

MFA has recently been employed to accurately map and predict behaviour of MBT plants. Despite some very promising experimental results reported in recent studies, most of the data comes from theoretical investigations. There is a need for additional experimental MFA research on a test scale and full commercial basis.

MFA data have so far demonstrated the difficulty in achieving effective chemical separation solely by mechanical means. The recent application of additional processing technology combined with mechanical methods in MBT plants, such as NIR sorting, 3-stage ballistic separators and x-ray sorting, offers a significant opportunity to improve this situation.

There is invariably a trade off between achieving a high quality of recoverable outputs and the properties of reject material e.g. RDF/SRF with a low Cl content can result in a significant yield of rejects that require subsequent treatment or disposal. The selection of intermediate and final 'sinks' (such as landfill disposal) of materials diverted away from RDF/SRF production therefore needs careful consideration. Additionally, attempting to produce SRF of higher specifications and more consistent quality may

demand resorting to more energy demanding plant configurations, adversely affecting the sustainability of such choices.

Recent studies have provided results for particular aspects of process unit operations. Biodrying systems appear to offer the advantage of optimally preparing the waste for mechanical treatment. Promising results for selective comminution and fast biodegradation were achieved by ball-mill pre-treatment. For RDF/SRF produced from residual MSW, it is difficult to reduce concentrations of Zn and Cl in particular because of their highly diffused distribution in waste components. To achieve higher quality recoverable outputs, there is a need for careful selection of unit operations, appropriate arrangement of them in the flowsheet, and improvements in their design or use of new developments. For example, with the objective of high-grade SRF production, it is not sufficient to separate a comminuted coarse fraction just on a PSD basis.

2.7.3 SRF quality management

The importance of implementing quality management schemes to the SRF production line of MBT plants is gaining recognition. The CEN/TC 343 initiative for harmonisation across Europe is significant in setting a new benchmark. This is exemplified by the requirements for robust sampling plans when dealing with highly heterogeneous material streams such as residual waste. Most of the available drafts for development from CEN are still under validation processes. It is necessary to apply the required quality management schemes in a way that fulfils the intention to avoid duplication of quality control by producers and end-users, whilst achieving optimal, scientifically defensible sampling.

Satisfactory understanding of the exact behaviour of MBT-derived SRF during the many available thermal recovery processes is still to be gained. This would demand

use of characterisation techniques, such as TGA, along with those conventionally used. Biogenic content is becoming an increasingly important descriptor, reflecting the increased recognition of the potential global warming effect of waste. Accurate determination of biogenic content is necessary. Sufficient characterisation and long-term operational data at higher degrees of substitution in co-combustion outlets are necessary in order to estimate the technical feasibility for SRF. Such results could result in more detailed and scientifically defensible specifications becoming available.

Differentiation of SRF production to meet specific end-user requirements is also imperative for the future marketability of SRF. For instance, certain SRF quality criteria for co-combustion in power plants are higher than those applying for cement kilns. It might be technically (and financially) challenging for many MBT process plants to produce suitably high SRF quality, whether achieving desirable levels of properties or low variability, especially for these more demanding applications. From a material flow management point of view, achieving a lower pollution potential for RDF/SRF raises the issue of appropriate intermediate and final sinks for the pollutants that should be directed away from the RDF/SRF stream. The inevitable trade-off questions do not have established or unanimously accepted answers.

3 AIM AND OBJECTIVES

3.1 Knowledge gaps

The review of the literature identified a number of important knowledge gaps for which further investigation could be sought.

- Need for a critical assessment of the various aspects that pertain to the production and quality assurance of SRF from MBT plants
- No or very limited data on the biodried fraction and the MBT outputs regarding fuel properties
- Very limited data on the performance of the contribution of the unit operations of MBTs to the final SRF and rest output fraction quality
- A series of new CEN characterisation standards for SRF quality proposing techniques still not validated and optimised
- No current model able to describe the flow of materials through SRF-producing MBT plants
- Very limited data and understanding on the variability of MBT streams (both input and outputs) and how this is affected by the performance of the unit operations

Given the relatively wide scope of the literature review, it is not feasible or advisable to attempt investigating all these areas within the limitations of a PhD research. The most prominent research question that synthesises various aspects of the research aim has been devised as of below.

3.2 Research aim

To investigate the management of solid material flows of SRF-producing MBT plants, regarding fuel-related properties, in order to enlighten the contribution of such plants to a sustainable resource management.

3.3 PhD research question

Are mechanical-biological treatment (MBT) plants, and their unit operations, optimised to produce high quality solid recovered fuel (SRF) (in the UK)

3.4 PhD objectives

The PhD research question is translated into a suite of PhD research objectives. The objectives of this PhD are (**Figure 3-1**):

1. to review and critically assess the European experience of SRF production from MBT plants;
2. to characterise an SRF-producing UK MBT plant, by analysing the quality of solid input and outputs for properties relevant to its material flow management performance, and gain insights where recently developed characterisation methods are applied;
3. to estimate the variability involved in the measurement of MBT-related material flows, measured through selected prominent fuel quality descriptors;
4. to develop and implement a material flow analysis that describes the material flow management of an SRF-producing MBT plant; and
5. to gain understanding of the relative contribution of MBT unit operations in achieving high quality SRF production.

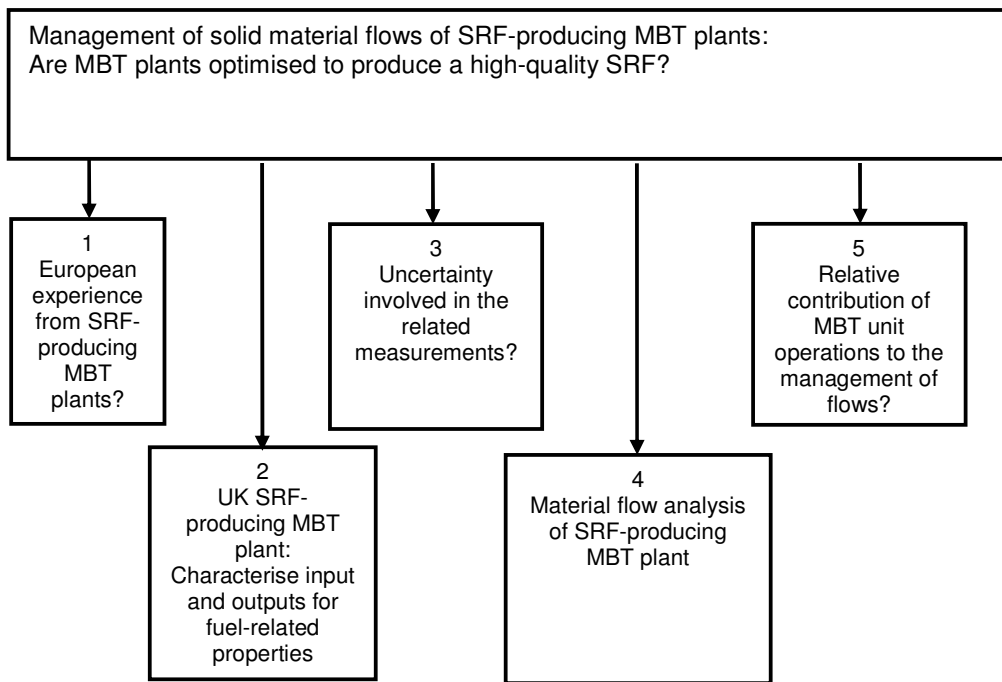


Figure 3-1 PhD aim and objectives

4 METHODOLOGY

4.1 Methodology overview

Figure 4-1 provides an overview of the various part of the methodology and indicates how they interconnect.

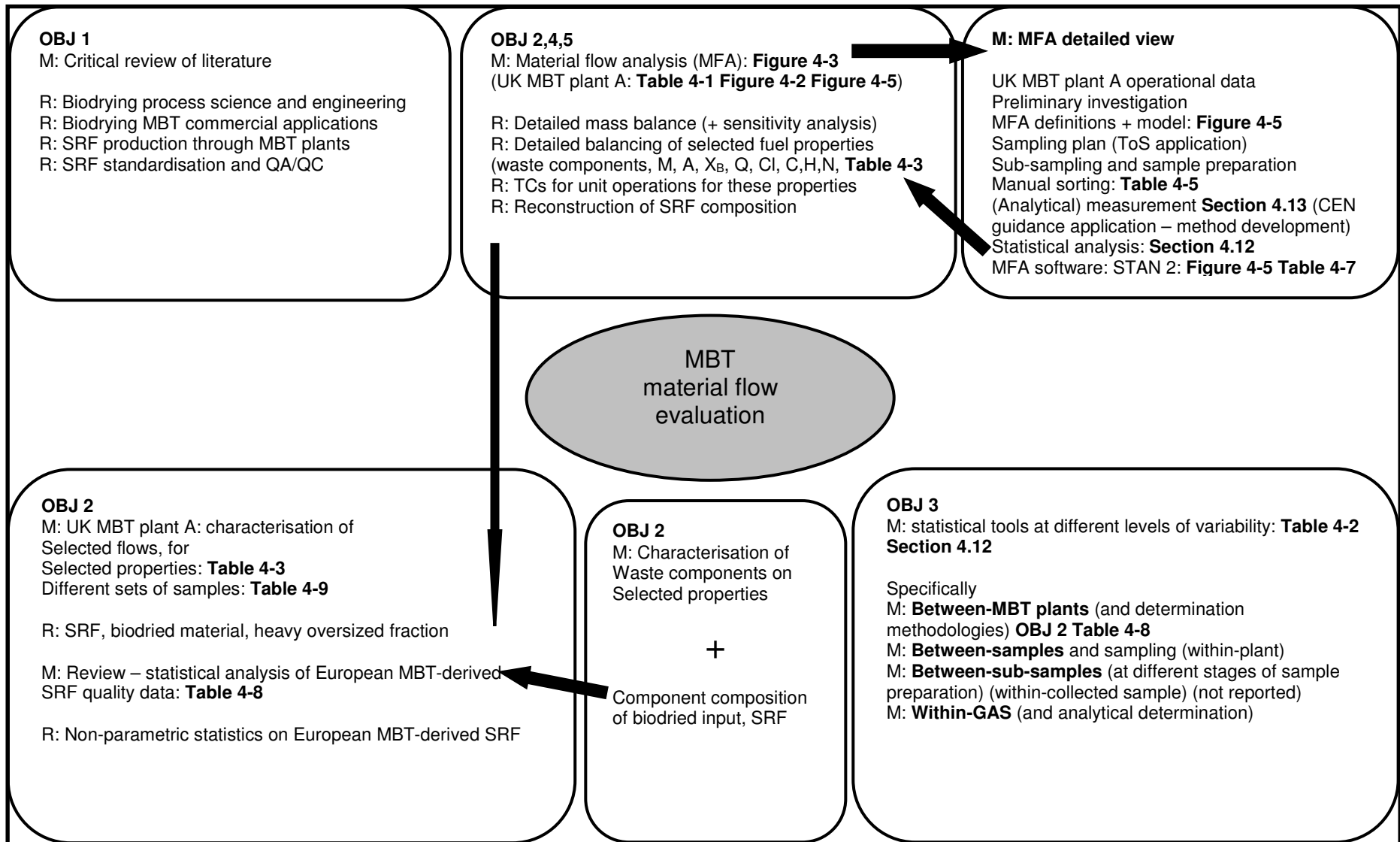


Figure 4-1 Experimental design roadmap. OBJ: study objectives (**Section 3.4**); QC/QA: quality assurance/quality control; GAS: general analysis sample. M: methodology; R: result deliverable; TCs: transfer co-efficients

4.2 Description of the UK MBT plant A

The UK MBT plant A is an example of the latest technological generation of MBTs, although, it belongs to the first generation of MBT plants that were built and operated in the UK. The main objective of the plant design is to produce an SRF. A biodrying reactor is used for the bioconversion stage; hence, it can be called a 'biodrying MBT'. The state-of-the-art regarding process science and engineering of biodrying reactors and their commercial applications within MBT plants is critically reviewed and presented in **Appendix I**. The plant started operating in 2007 and SRF production to suitable end-user specifications commenced towards the end of that year.

The plant receives mainly municipal and commercial waste (MSW). Some of the -areas waste is gathered from, implement separate kerbside collection, but not all. Hence, the input material should be considered as in-between mixed and residual MSW. Occasionally limited amounts of other loads may also be delivered. Any potentially unsuitable items, such as bulky waste, are discharged before any processing. Grab cranes automatically feed the primary shredder from the material deposited in the reception pits. There the input material undergoes light primary shredding (shredded output 150-300 mm, nominal range). The shredder output is deposited into ca 5 m height windrows within the biodrying hall, for approximately 2 weeks. Then the biodried output is transported by means of automated grab cranes to the processing (refinement) section, to produce SRF and other secondary materials (processing section input).

A schematic of the processing section flowsheet is shown in **Figure 4-2**. The configuration of the unit operations aims at producing a secondary fuel to certain

specifications. Other secondary objectives exist: (i) to maximise the yield towards the SRF output, concentrating the desirable combustible waste components in this output; (ii) to minimise the yield of reject fractions (iii) to minimise the biodegradability of the reject fractions to be disposed of in landfill; and (iv) to produce other potentially marketable secondary material outputs (metals, aggregates) of sufficient purity. The main objective has implications for all other secondary objectives. For instance is it desirable to concentrate the entire highly polluting load in the main reject fraction (oversized heavy rejects). Some of the quality specifications the SRF output has to meet may be of higher practical importance (e.g., sufficiently high calorific value or acceptably low total chlorine content) than certain others.

The SRF processing line concentrates in the trommel overs (T_SCR_O) the entire biodried output apart from the <20 mm material, which should consist mainly of putrescible organics and inert (mineralised) components. The windshift air classifier (A_CL 1) is intended to remove any major contraries from the SRF flow-line, directing the heavy items such as stones, metals, and large and/or hard plastics to the heavy gravity fraction. Then, it is feasible to proceed with secondary shredding (S_SH), which is necessary to meet customary dimension specifications for the various potential SRF thermal recovery options. Downstream the flow passes through unit operations to remove any Fe and non-Fe metals (O_M and E_C_S, respectively). Limited material from the 'organics'/'aggregates' processing line (8-10 mm low gravity) is mixed with the main SRF production line, just before the final output, picked by the air drum separator (AC_L 2). **Table 4-1** lists the unit operations in the processing section of the UK MBT plant A and briefly covers their role within plant flow-line.

Refinement section line

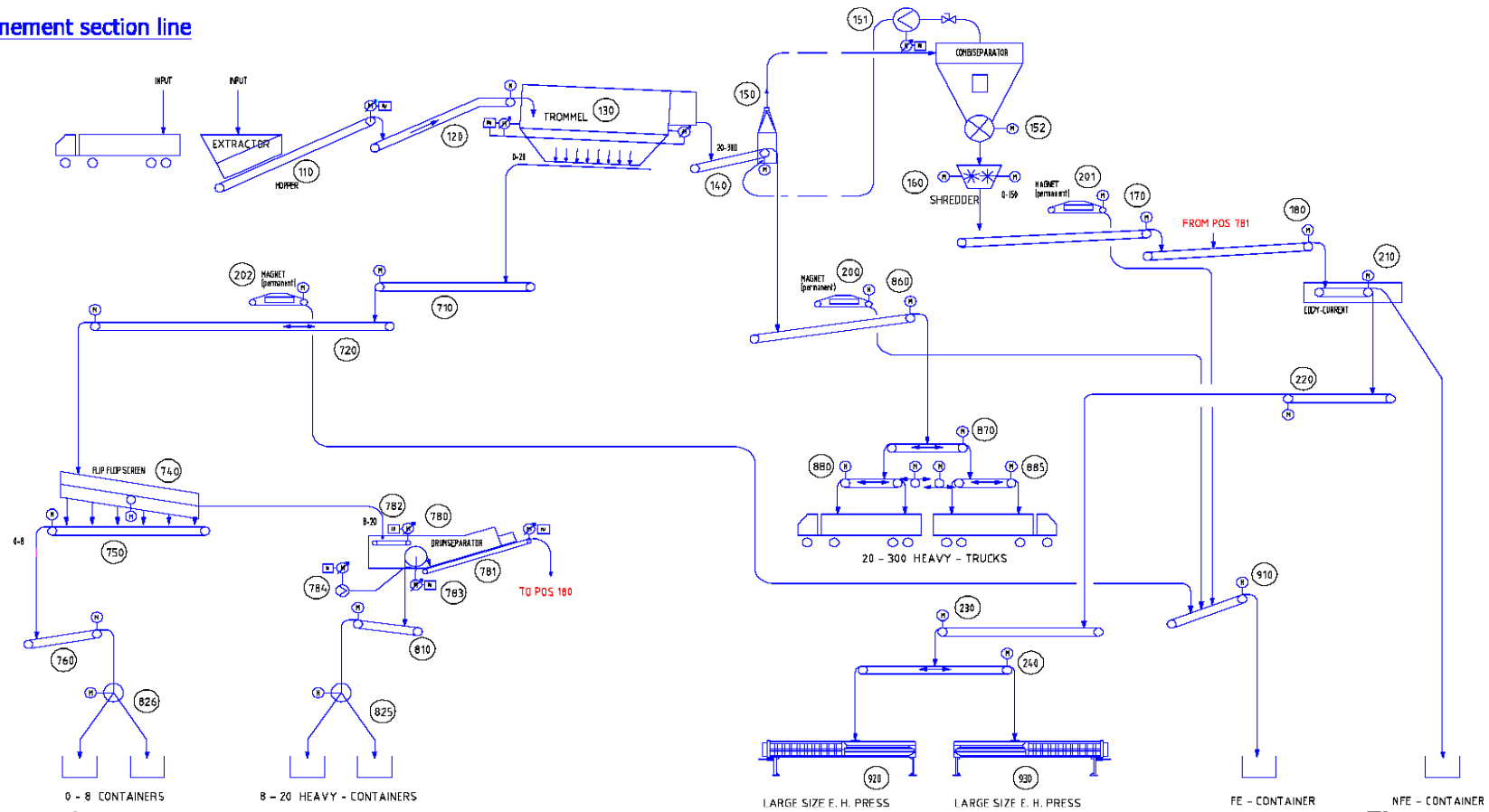


Figure 4-2 Technical drawing of the processing section of the UK MBT plant A. For a schematic diagram representing this refer to Figure 4-5

Table 4-1 Unit operations in the processing section of the UK MBT plant A and role within plant flow-line

Unit operation	Abbreviation	Operating principle and role in the plant	Operating settings
Trommel screen (Rotary screen)	T_SCR	See Section 2.4.4.1 for operating principle. To separate the supposedly high in non-combustible fragments fines <20 mm in under size discharge and the combustibles in the >20mm oversize output.	Aperture: 20 mm Slope (incline): 3° Screen length: 7.5 m Diameter: 3.2 m
Air classification (Windshift, + combi separator)	A_CL 1	On air classification see Section 2.4.4.6 . Separation of the low gravity from the high gravity materials in the adjustable windshift chamber and subsequent separation of the process air from the light gravity material in the combi separator. Most process airflow is re-circulated, a portion directed to the bag-filter APC unit. To concentrate the light combustible items, such as plastics and paper in the low gravity output. To remove the potential contamination of the SRF stream towards the oversized heavy rejects, through the high gravity discharge.	
Secondary shredder	S_SH	On shredding see Section 2.3 . Slow rotation cutting mill. Materials are cut compressed between the static counter-knives attached to the cutting chamber walls and the cutters attached to the rotating shaft. To adjust the dimensions of the SRF flow-line fragments to suitable upper limits for use in cement kilns (or FBC or power plants: different specifications apply).	Rotation speed: 355 rpm (50 Hz) Output d ₉₉ <40 mm
Eddy-current separator	E_C_S	On Eddy-current separation see Section 2.4.4.9 . Uses a strong magnetic field alternating with high frequency. Waste fragments follow different trajectories according to their electric conductivity. 4.2.1 To remove the non-Fe metals (Al-based and other non-Fe, excluding stainless steel) from the SRF flow-line. 3 outputs: SRF, non-Fe metals and rejects.	
Oscillating screen (Flip-flop screen)	OSC_S	To separate a very fine fraction (0-8 mm), concentrating mainly organic, putrescible matter, potentially further compostable, from the intermediate fraction (8 -20 mm) which should concentrate an aggregates fraction. The input comes from the trommel unders (T_SCR_U).	
Air drum separator	A_CL 2	On air classification see Section 2.4.4.6 . The light gravity material is directed away from the conveyor belt. It is discharged by a rotary drum to an expansion chamber for additional separation, where any of the high gravity fragments drop on the conveyor belt underneath. To separate heavy items (aggregates: glass, stones, etc.) from the lighter, which are directed and mixed with the SRF output.	
Overbelt magnets	O_M 1,2,3	On magnetic separation see Section 2.4.4.9 . 4.2.2 3 units. To remove the ferrous materials from the SRF processing line, the oversized reject	

fraction line, and the trommel unders line.

4.3 Variability in waste-related properties measurement

4.3.1.1 Background

“The lack of value [of waste] in many cases can be related to the mixed and, often unknown composition of waste. [...] This inverse relationship between degree of mixing and value is an important property of waste.” McDougal et al.³⁰ “Quality improvement is the reduction of the variability in processes and products.” definition by Montgomery²⁵⁰

Variability, central to waste characterisation and treatment, becomes critical when a quality assured product is the intended output of a treatment process. Hence, **Objective 3** of this study is to estimate accuracy/uncertainty involved in the measurement of MBT-related material flows, measured through selected prominent fuel quality descriptors. This objective spans the whole document and is accomplished by quantifying and discussing the various types of variability involved in the measurements performed.

Lambkin et al.²⁷⁴ discussed the criticality of characterising the heterogeneity of wastes by using suitably designed sampling procedures and reporting results, along with estimates of their uncertainty. This heterogeneity has to be accounted for in the sampling plan, and can be addressed by Gy’s ToS²⁶⁷⁻²⁷². This is developed further in the sampling plan (**Section 4.6**). Here, various forms of variability encountered in the waste processing and product quality characterisation are summarised.

4.3.1.2 Experimental

For MBT plants, relevant forms of variability are: (i) enforced by the processing, in time, of a heterogeneous waste along a processing line; (ii) between-

samples isolated from regular sampling points; (iii) within single samples, during sample preparation and analytical determination. **Table 4-2** summarises key information regarding the form of variability encountered in this research. A more detailed discussion is available in **Appendix B.2**.

Table 4-2 Types of variability pertaining to MBT process streams characterisation and relevant sections addressing them

Type of variability	Importance	Comment
Between-MBT plants (and determination methodologies)	Widest range of potentially anticipated values	Depends on all other smaller-scale variability
Between-samples and sampling (within-plant)	Plant production line variability for the examined stream	E.g., collected as a time sequence of the same process stream. Confounded with sampling, between-sub-samples and between-gas variability
Between-sub-samples (at different stages of sample preparation) (within-collected sample)	Relates to representative sub-sampling a sample preparation	Often neglected. Together with the between-GAS variability might overshadow the plant production variability
Within-GAS (and analytical determination)	Ability of method for sufficiently precise determination	Confounded: within-gas (between aliquots), instrument determination and analyst operation variability

GAS: general analysis sample

During sample preparation the samples underwent a series of alternate shredding and sub-sampling to produce a general analysis sample (GAS), from which aliquots were selected (test samples) for each determination. The considerable sub-sampling necessary (e.g., from 20 kg of biodried material sample to 0.1 g actually used per each test sample for microwave digestion) and the selective shredding among waste components can be a major source of variability. Only limited waste-related studies have so far attempted to quantify variability due to sample preparation²⁷⁵⁻²⁷⁶.

4.4 Material flow analysis (MFA) for MBT plants - general

Background

A definition of MFA is provided in **Section 2.4.3.3**. MFA as a systematic analytical tool offers the advantages of clarity, transparency and completeness, especially over non-systematic approaches to the (environmental) performance evaluation of systems²⁷⁷. Many other analytical tools can generate information

relevant to the performance of environmental systems²⁷⁸: cost-benefit analysis (CBA), cost-effectiveness analysis (CEA); life cycle assessment (LCA); environmental risk assessment (ERA), etc. Such tools employ methodologies to handle data inputs. Eventually, subjective value judgements are necessary to turn input data into evaluation outcomes. MFA, however, is merely a data acquisition methodology, avoiding extensive value judgements, and serving as a basis for subsequent evaluation stages, if coupled with other available tools²⁸.

Brunner and Rechberger²⁸ covered in detail the history of the MFA and the wider range of similar/related applications. Regarding waste treatment plants, MFA can be a valuable tool, suitable for²⁸:

- Determining the elemental composition of wastes: a pre-requisite for the selection of appropriate treatment and design of sustainable waste management systems
- Investigating the substance management of the facility: to show whether given goals have been achieved, e.g., a pre-requisite for estimating the fitness-for-purpose of marketable products
- Identifying the processes and flows with the highest potential for improvement, by conducting MFAs based on total material balance

The application of MFA in MBT plants to date is summarised in **Section 2.4.3.3.**

Experimental

Here the general methodology principles of MFA, according to Brunner and Rechberger²⁸, are followed, adapted to the specific research objectives. The mathematical handling of the raw data is performed using the freely available MFA

software STAN2^{®279}, developed specifically to implement such an approach to the MFA. MFA is applied as general data handling framework, to quantify the flows of materials through the UK MBT plant A.

MFA method consists of several consecutive steps, performed iteratively.

Figure 4-3 illustrates the steps involved and the possible iterations.

The results acquired by the application of the MFA methodology and software are interpreted as such, i.e., without resorting to the further application of any of the potentially suitable environmental performance evaluation tools, such as LCA or statistical entropy analysis³. Notwithstanding this, the results obtained can serve as input to any compatible environmental performance evaluation tool, and in that sense have additional merit.

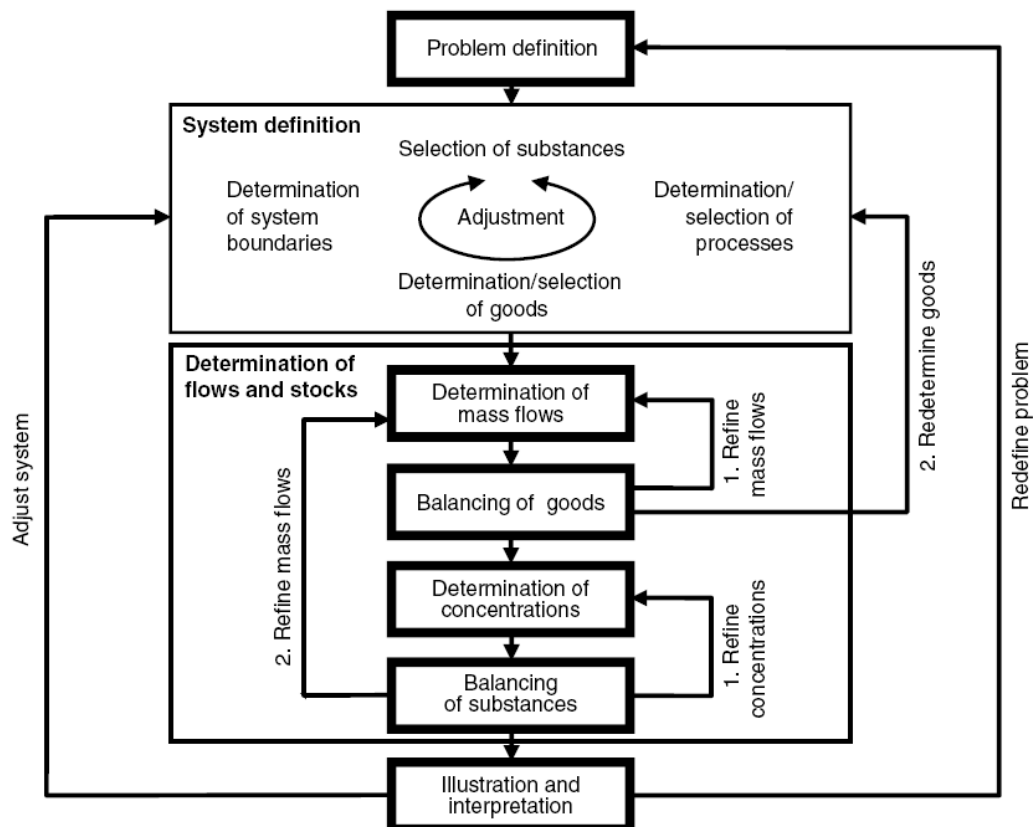


Figure 4-3 General MFA method, with loops indicating its iterative nature. After Brunner and Rechberger²⁸. Here, balancing of goods such as the waste components was used in a loop to verify the mass flows determination (sensitivity analysis) and the necessary corrections imposed upon the model data input.

4.5 Selection of properties (goods/substances) to be determined

Background

Selection of suitable goods/substances for an MFA is important. General guiding principles promote cost-effectiveness and recognise project-led realities. Fehringer et al.¹⁴⁴ advocate the measurement of indicators wherever possible, to maximise information gained about the system being examined, whilst minimising effort and expenses. Indicator goods/substances should: (i) be a significant pointer of the behaviour of the investigated system; and/or (ii) exhibit a physiochemical behaviour representative of a wider group. According to Brunner and Rechberger²⁸, useful selection criteria are: (i) legislation- or standards-driven; (ii) relevance appreciation; (iii) project-set objectives.

Firstly, legal, policy and QA/QC documents contain lists of goods reflecting both existing level of scientific understanding and prevailing socio-economic evaluations, e.g., about what is suitable emission level of controlled substances. This approach guarantees the societal relevance and applicability of results, but also limits their importance to issues already largely addressed. A second approach requires explicitly appraising the relevance of selected goods and substances. This relevance is inevitably process and flow specific. The potential of a chemical substance as a resource or pollutant is an important general selection criterion (e.g., Cu can be a valuable resource as recycled wire, but contaminant if cables are combusted). In the case of chemical substances, an objective way to determine indicator substances can be provided by comparing them in relation to their abundance in the geosphere. The comparison can be done e.g., by establishing ratios of their concentration to geogenic reference concentrations, namely earth crust for solids, hydrosphere for liquids and atmosphere for gases. Despite the elegance and transparency of such an

approach, it might prove misleading, as the selected items may not reflect their relative importance within particular process flows and system outputs in question. Thirdly, selection of substances and goods can be already embedded in the project title and aim, being a material-specific study.

Experimental

Concerning the management of material flows of the processing section of the UK biodrying MBT plant A (the system under examination), the main overarching objective is to produce a secondary fuel to certain specifications, as detailed in **Section 4.2**. Hence, here the focus is upon fuel-related properties, either beneficial or of concern. Nevertheless, the measured properties are highly relevant to the rest outputs as well. To illustrate, the content of the 0-8 mm 'organics' output in selected potentially toxic elements (PTEs) determines whether it is scientifically desirable to apply the produced CLO on land; and the calorific value of the oversized heavy rejects should be below a limit to be allowed to be disposed of in landfill for Germany and Austria (gross calorific value $<6 \text{ MJ kg}^{-1}$).

Table 4-3 lists the properties selected to be measured and briefly underpins the reasons. Selection criteria considered are:

1. properties being identified as important for the existing quality QA/QC of SRF in the literature review (see **Section 2.5**);
2. indicator and mandatory to specify properties in the recently emerged CEN guidance on SRF QA/QC^{210, 259} (see **Section 2.5**);
3. properties specified in the UK cement producing end-user specifications for MBT-derived SRF (currently the single major SRF end-user sector in the UK);

4. properties with the highest potential to exceed specifications agreed with SRF end-users for the first (in-house) data set of UK bio-drying MBT-derived SRF;
5. properties with the highest potential to violate European QA/QC SRF limits among those reviewed in this research for European MBT-derived SRF (see **Section 6.1**);
6. general capability of property to serve as an indicator for a wider set of properties; and,
7. practical limitations (time, human, financial, expertise and equipment resources).

To fully characterise an SRF, a much wider list of properties would have been necessary. For instance, reaction kinetics properties, as determined by TGA, which can inform on the ignition and burnout behaviour of SRF. **Table 2-14** provides a more comprehensive list. Resource limitations led to the selection of the properties investigated and presented in this thesis.

Table 4-3 Substance and goods selection, relevant to SRF production within UK MBT plant A and SRF thermal recovery; (metals are not reported in this thesis).

Substance / Good	Designation	Indicator capacity	Technical – Environmental aspects	UK MBT-derived SRF in-house data ^{q,1}	European MBT –derived SRF statistically analysed (Q3 of median values:)	Δ [(UK MBT-derived SRF in-house value – UK SRF end-user limit)/ UK SRF end-user limit] (%)	UK end-user specifications for MBT-derived SRF (UK cement industry)
Total chlorine	[Cl]	Indicator parameter for technical performance in CEN SRF classification ^a Diffuse, non-uniform load distribution in residual waste. Mechanical processing incapable of meeting certain stringent threshold values; can be used as SRF quality indicator ^k	Cement industry: in dry processes may block pre-heater; Industrial boilers: Corrosion of heat transfer surface ^e	0.612% w/w _{ar}	0.69 % w/w _{ar}	+ 9.2	0.8% w/w _{ar}
Cadmium	[Cd]	Second best indicator parameter for environmental CEN SRF classification ^a Mechanical processing incapable of meeting certain stringent threshold values; can be used as SRF quality indicator ^k	Cement industry: element with most increase in the final product originating from MSW, compared to non-use of SRF (other elements: Cu, Sb) ^d Coal co-combustion: Atmosphere, difficult to control (a). Concerns about ash quality affecting re-use in cement production ^e FBC: causing corrosion and fouling ^h Pyrolysis: Enrichment in pyrolysed SRF char ⁱ	1.1 mg kg _d ⁻¹	2.30 mg kg _d ⁻¹ 0.2 mg MJ _d ⁻¹		20 mg kg _{ar} ⁻¹
Mercury	[Hg]	Indicator parameter for environmental performance in CEN SRF classification ^a	Cement industry: transferred to flue-gas, but can be effectively captured by electrostatic precipitators; similar behaviour as TI ^a Coal co-combustion: Atmosphere, difficult to control ^a	0.4 mg kg _d ⁻¹	0.31 mg kg _d ⁻¹ 0.06 mg MJ _d ⁻¹		10 mg kg _{ar} ⁻¹
Lead	[Pb]	Mechanical processing: incapable of meeting certain stringent threshold values;	Enrichment of Cd, Cr, Co, Ni, Pb, Zn in pyrolysed SRF char ⁱ	91 mg kg _d ⁻¹ 3 rd highest	210 mg kg _d ⁻¹	+ 43.8	200 mg kg _{ar} ⁻¹

Substance / Good	Designation	Indicator capacity	Technical – Environmental aspects	UK MBT-derived SRF in-house data ^{q,1}	European MBT –derived SRF statistically analysed (Q3 of median values:)	Δ [(UK MBT-derived SRF in-house value – UK SRF end-user limit)/ UK SRF end-user limit] (%)	UK end-user specifications for MBT-derived SRF (UK cement industry)
		can be used as SRF quality indicator (k). Incineration: partitioning of intermediate lithophile behaviour: Bottom ash 44±7; APC residue: 45±6 ^p	Key parameter for cement industry and industrial boilers	potential amongst the trace level PTEs to violate limits	14 mg MJ _d ⁻¹		
Zinc	[Zn]	Diffuse and relatively uniform load distribution in residual waste. Mechanical processing: incapable of meeting certain stringent threshold values; can be used as SRF quality indicator ^k	Pyrolysis: enrichment of Cd, Cr, Co, Ni, Pb, Zn in pyrolised SRF char ¹	-	564 mg kg _d ⁻¹ ¹ n.d.		-
Manganese	[Mn]					+ 42.2	
Copper	[Cu]	Lithophile during incineration	Cement industry: element with increase in the final product originating from MSW, compared to non-use of SRF (other elements: Cd, Sb) (d).	290 mg kg _d ⁻¹ Highest potential amongst the trace level PTEs to violate limits	464 mg kg _d ⁻¹ 13.6 mg MJ _d ⁻¹	+ 28.5	500 mg kg _{ar} ⁻¹
Antimony	[Sb]	Representative of oxyanions (Selenium Se, as well), not typically measured, because not extensively regulated, but important to do so ^{m,r} Incineration: partitioning of intermediate to low lithophile behaviour: Bottom ash 12±3; APC residue: 81±6 ^p	Cement industry: element with increase in the final product originating from MSW, compared to non-use of SRF (other elements: Cd, Cu) ^d	13 mg kg _d ⁻¹	n.d.		150 mg kg _{ar} ⁻¹
Carbon Hydrogen Nitrogen	[C] [H] [N]	Ultimate analysis	Essential for combustion behaviour Prerequisite for NCV determination				
Net calorific value	Q _{net}	Indicator for economic performance parameter for CEN SRF classification ^a	Main utility of SRF in replacing other fuels; CEN obligatory to specify; in all	15.71 MJ kg ⁻¹		- 5.4	15 MJ kg ⁻¹

Substance / Good	Designation	Indicator capacity	Technical – Environmental aspects	UK MBT-derived SRF in-house data ^{q,1}	European MBT –derived SRF statistically analysed (Q3 of median values:)	Δ [(UK MBT-derived SRF in-house value – UK SRF end-user limit)/ UK SRF end-user limit] (%)	UK end-user specifications for MBT-derived SRF (UK cement industry)
			producer- end-user specs; defining parameter for SRF use, high differences of type of end use: important in the design and operation control of thermal recovery plants; legislative control in Germany/Austria for material disposed of in landfill				
Moisture content	M	Important parameter for CEN SRF specification ^a	Main measure of biodyring effectiveness; affects mechanical separation performance; among the initially proposed classification parameters for SRF; affects potential for combustion, and intermediate storage; present in all end-user specifications; directly affects potential for energy recovery from SRF; methodological: important in converting between reporting basis for all properties (_d for comparisons, _{ar} more relevant to use), especially for measurands such as calorific value etc.	15.2% w/w _{ar}		- 17.2	<15% w/w _{ar}
Ash content	A	Important parameter for CEN SRF specification ^a		13.2% w/w _{ar}		+ 0.7	<15% w/w _{ar}
Biogenic content	X _B	Carbon-neutral energy source ^b Applies for ROC subsidy for CHP EfW ^c	Importance covered in detail in Section 2.5.4.7 . Limited data on degree of initial residual MWS biogenic content and its preservation in final SRF product ^f	52.2% w/w _{daf}		- 9.2	> 50% w/w _{daf}
Waste components (and sets of)	See Table 4-5 for list of components and for detailed rationale	Indicates on the ability of mechanical processing for material and chemical separation – material flow management	Visualise the origin of certain pollutants in the final products, if simplified material balance is conducted for input constituents.				

ROC: Renewables obligation certificate

FBC: Fluidised bed combustor

APC: Air pollution control

MFA: Material flow analysis

¹ Relative difference (%) of the values (p_{80} for upper limits and Q1 for thresholds, statistical analysis for this study) for UK biodrying MBT-derived SRF (in-house data) from the specified values by the SRF off-taker (cement kiln). Serves as a surrogate measure of the potential to exceed limits.

References: (a): ²⁰⁴; (b): ¹⁹³; (c): ²⁰⁴; (d): ²¹⁷; (e): ¹³; (f): ²⁸⁰; (g): ⁵²; (h): ⁴⁵; (i): ²³⁵; (j): ¹⁷⁸; (k): ⁵⁵; (l): ²⁸¹; (m): ²⁸²; (n): ²⁰³; (o): ²⁸³; (p): ¹⁴³; (q): ²⁶⁶; (r): ²⁸⁴;

4.6 Sampling plans

Background

4.6.1 *Sampling plan for an MBT plant according to the theory of sampling (ToS)*

Sampling of solid streams is necessary for understanding and evaluating the performance of MBT plants to manage the input material flows. The input solid stream of MBT plants is residual municipal waste, characterised by high heterogeneity. A descriptive, intuitive definition of heterogeneity could be: the property of 'consisting of dissimilar or diverse ingredients or constituents'²⁸⁵. Exactly this assorted character of residual waste is one of the reasons that is of reduced value, according to McDougal et al.³⁰. The mechanical processing section of MBT plants aims at producing output fractions of decreased heterogeneity, compared with the input fraction(s), by the use of, mainly, mechanical unit operations, such as classification/separation and size reduction.

Sampling of heterogeneous solid waste has been widely recognised as a challenging exercise, especially compared with the less heterogeneous soils and sludge. A publication that stemmed from a US EPA workshop exemplified related difficulties and reviewed various available statistical tools/approaches²⁸⁵. Recent developments cover the topic in more technical detail. Indicatively, EPA²⁸⁶⁻²⁸⁷ and CEN documents^{264, 288}.

An overview of the Gy's theory of sampling is provided in **Appendix D.1**.

Experimental

4.6.2 Sampling plan for UK MBT plant A – an example ToS

application

4.6.2.1 Sampling plan objectives

The aim of the sampling plan is to characterise the input and output streams and unit operations of the UK MBT plant A for a series of properties relating to fuel quality, for a period satisfactory to gain confidence in the performance of the plant. Information gathered at the end of the measurement process should enable to:

1. reconstruct flow balances for each of the properties through the plant (material flow analysis, MFA);
2. develop empirical transfer coefficients characterising each unit operation, for each of the preserved properties;
3. evaluate the quality of SRF (and potentially other important plant output streams), as far as possible in accordance with the CEN/TS 343 quality assurance and control (QA/QC) stipulations.

The properties selected to be measured are listed in **Table 4-3**

4.6.2.2 Definition of sampling lots - system boundaries

The lot for each flow is the quantity of the material stream for which a representative sample is needed. The system to be described by sampling and sample analysis is confined to the mechanical refinement section of the MBT plant A, upstream the biodrying stage. The flowsheet of the mechanical refinement section is shown in **Figure 4-2**; **Figure 4-4** presents a schematic representation that includes the sampling points.

The starting point of the sampling process is the biodried comminuted output of the primary shredder. This is selected on the basis that: (i) the dried material is much easier to handle for storage, transport and sample preparation purposes (e.g., shredding and sorting); and (ii) the comminution reduces the heterogeneity of the stream and allows representative samples to be achieved with a significantly lower sample mass (see **Appendix D.2.2**). The final point is the plant solid outputs (8 identified). Liquid or gaseous streams are regarded as being insignificant for the properties/analytes measured throughout the refinement section (estimated at <<10% w/w); thus, according to the MFA practice these are not sampled²⁸.

4.6.2.3 Which sampling points for which material flows?

Ideally, all flows within the mechanical refinement section of the plant, upstream and downstream of each unit operation, should be sampled. However, the circumstances encountered do not allow this. Limited access is evident for a series of flows; other flows cannot be sampled in accordance with health and safety (H&S) regulations and/or at an excessive cost. The selected sampling points should enable the reconstruction of mass flows and the development of TCs. Sacrificed is information that could enable to directly check the closing of balances upstream and downstream of certain unit operations. Initially 17 streams were planned to be sampled (**Table 4-4**). These sampling points were grouped according to the type of sampling (drop-flow, static conveyor belt, pile, crane grub) and standard operating procedures (SOPs) were developed to implement the sampling plan (**Appendix D.4**).

For some material flows there is an option to sample as stopped conveyor belts or drop-flows; and as drop-flows or static piles. The relative decision has to be informed by the fact that it is impossible to obtain representative samples from lots that have more than 1 dimension, without homogenising (e.g., mixing) the entire lot. According to the ToS, 'correct' sampling (i.e., sampling that does not introduce systematic bias) is

feasible only for 1-dimension lots (1-D) (e.g., material that flows on a conveyor belt) as it demands (among else)²⁸⁹: “All fragments or groups of fragments, or increments of the lot, must have an equal, non-zero probability of ending up in the sample, while elements foreign to the lot must have a zero probability of ending up in the sample. The increment or the sample must not be altered in any way.” This cannot be achieved for 2, 3 and 4-D lots. A static pile of scale big enough not to allow sampling of full cross-sections and exhibiting segregation, viewed at any moment in time (snapshot), is a 3-D lot. Hence, sampling of static piles is to be avoided, wherever possible. Instead, sampling of stopped conveyor belts and of drop flows can allow for correct sampling, and quantification of the heterogeneity errors.

The lots that are formed by the static piles in time at the UK MBT plant A plant are 4-D lots characterised by high spatial heterogeneity, as visual inspection has verified. Indeed, as materials with different properties fall from conveyor belts that form static piles a series of possible segregation phenomena occur, which have been detailed in the literature²⁹⁰. Moreover, full cross-sections of such lots cannot be obtained. However, the same material flows, while on a conveyor belt or falling in a collection tray/tarpaulin constitute 1-D lots and can be sampled correctly and effectively.

The material flows to be sampled at the UK MBT plant A are highly heterogeneous regarding the spatial and temporal distribution of many of the analytes/properties to be measured; particularly the ones present in trace concentrations. Hence, strict adherence to good practice guidance is necessary for minimising the additional standard deviation introduced by sampling actions; and for avoiding introducing systematic errors (bias), i.e. achieving correct sampling. In any case, the fundamental sampling error (FE) and part of the group and segregation error

(SE) cannot be zeroed, and will constitute the unavoidable minimum practical error (MPE) (quantified as minimum relative standard deviation (RSD)).

4.6.2.4 How many sampling plans for every lot?

Each of the 17 streams constitutes a discrete case in terms of mass flows and degree of heterogeneity regarding properties/analytes to be measured. Ideally, a separate sampling plan should be identified for each of these streams and for each of the properties/analytes to be measured (this would mean 15 sampling plans each for each of the 15 proposed measurands). However, this is not feasible for practical purposes.

In practice, it has to be the heterogeneity of an important property/analyte that is most difficult to representatively sample that can inform the sampling plan details for each sampling point. Such an approach can base calculations on relatively conservative assumptions. This would be a 'micro-analyte' (such as the cadmium (Cd) concentration), because such measurands arguably exhibit much greater heterogeneity than the 'macro-parameters' (such as the lower heating value (LHV))²⁰⁸.

Additionally, for most of the streams each incremental sampling act has to take place in the same time period, which means that the sampling frequencies and number of increments per lot for all these streams have to be the same. Representative samples have to be achieved by differentiating the sample mass acquired for each sampling point.

Cd was selected to perform the initial sampling plan ToS calculations upon, because: (1) it is established that it is an element for which the bulk of its specific load (e.g., in mg Cd / kg waste matrix component) in the residual waste comes from relatively few waste components, i.e. it is unevenly distributed⁵⁵; (2) relevant specific

load data exist in the literature; and (3) it is an important descriptor of the fuel quality^{208,}

210 .

Table 4-4 Sampling points at the UK MBT plant A

SP No.	Stream	Location (engineering plant layout IDs)	Sampling type	Sampling tool	Stream particulates size	Comments
1	Biodried material –primary shredder output	Shredder output [exact point to be indentified]	Crane grub	Crane	-300 mm	Typically grabs Released into container on the floor Cone and quartering to get each incremental sample Sample for belt length (= volume)
2	Trommel 130 underflow (Magnet 202 input)	720 conveyor belt: upstream magnet 202	Stopped conveyor belt	Squeegee repeatedly	-20 mm	Take conveyor guards off Sample for belt length
3	Fe metals (Magnets 202, 201, 200 Fe output)	910_C1	Flowing stream	Machine bucket, under 910 conveyor	Contribution from magnet 200 product: +20-300 mm Contribution from magnet 201 product: +20-30 mm Contribution from magnet 201 product: -20 mm	Remove Fe C1 container Container heap with significant gravitational segregation Sample for time length Final output
4	Magnet 202 reject (Flip-flop 740 screen input)	720 conveyor belt: downstream magnet 202	Stopped conveyor belt	Squeegee repeatedly	-20 mm	Take conveyor guards off Sample for belt length
5	-8 Fines (“Organics”) (Flip-flop 740 screen underflow)	826_C1/2	Flowing stream	Machine bucket, under 826 bi-directional chute	-8 mm	Remove C1/2 0-8 mm container Sample for time length Final output
6	+8-20 Flip-flop 740 screen overflow) (Drumscreen air classifier 780 input)	Small belt (784?)between 740 flip-flop and 780 drumscreen	Stopped conveyor belt	Squeegee repeatedly	+8-20 mm	Take conveyor guards off Sample for belt length: repeat more often if length available not necessary for increment sample (plant on and off, resuming of steady flow necessary)
7	+8-20 Aggregates (“Glass and stones”)	825_C1/2	Flowing stream	Machine bucket, under 825 bi-directional chute	+8-20 mm	Remove Fe C1 container Significant contamination with “organic” material Sample for time length Final output
8*	Trommel M130 overflow (Windshift air classifier 300 input)	140 conveyor belt	Stopped conveyor belt	Squeegee repeatedly	+20-300 mm	Take conveyor guards off (vertical opening from main platform) Sample for belt length: repeat more often if length available not necessary for increment sample (plant on and off, resuming of steady flow necessary) Sample for belt length
9**	Windshift air classifier 300 high-gravity output (Magnet 200 input)	360 conveyor belt	Stopped conveyor belt	Squeegee repeatedly	+20-300 mm	Take conveyor guards off Sample for belt length
10	Windshift air classifier 300 low-gravity output shredded by 160 secondary shredder:	170 conveyor belt	Stopped conveyor belt	Squeegee repeatedly	ca. +20-30 mm	Take conveyor guards off Sample for belt length

SP No.	Stream	Location (engineering plant layout IDs)	Sampling type	Sampling tool	Stream particulates size	Comments
	ca. 30 mm (Magnet 201 input)					
11	Magnet 201 reject	180 conveyor belt: downstream magnet 201, upstream of addition of 781 belt stream	Stopped conveyor belt	Squeegee repeatedly	+20-30 mm	Take conveyor guards off Sample for belt length Not clear if we can sample the output of magnet 201 (as stated here) or the drumscreen 780 high-gravity, 781 belt output
12	Eddy current separator 210 input (Mixed magnet 201 reject and drumscreen 780 high- gravity output – 781 belt)	180 conveyor belt: down stream of addition of 781 belt stream	Stopped conveyor belt	Squeegee repeatedly	Input from drumscreen low- gravity: +8-20 mm Input from magnet 201 rejects: +20-30 mm	Take conveyor guards off Sample for belt length Use of mobile elevated platform
13	SRF (1/3 Eddy current 210 outputs)	240 conveyor belt	Stopped conveyor belt	Squeegee repeatedly	Contribution from magnet 201 rejects: +20-30 mm Contribution from drumscreen low- gravity: +8-20 mm	Take conveyor guards off Sample for belt length Final output
14	Non-Fe metals ("Al")	210_C1	Flowing stream	Machine bucket, under 210 eddy current product	Contribution from drumscreen low- gravity: +8-20 mm Contribution from magnet 201 rejects: +20-30 mm	Remove Non-Fe C1 container Sample for time length Final output
15	Eddy current separator 210 rejects	Eddy current rejects container [not stated in official flow- chart]	Flowing stream	Machine bucket, under 210 eddy current rejects	Contribution from drumscreen low- gravity: +8-20 mm Contribution from magnet 201 rejects: +20-30 mm	Remove container Sample for time length Final output
16	+20-300 Rejects (Magnet 200 rejects)	870 conveyor belt OR landfill site?	Stopped conveyor belt	Squeegee repeatedly	+20-300 mm	Take conveyor guards off Sample for belt length: repeat more often if length available not necessary for increment sample sampling at landfill site may be necessary: however possibly second highest heterogeneity after mechanical processing input stream Final output
17	Dust (APC - de-dusting residue)	Dust pipe [or dust container]	Flowing stream [or container]	Bag attached to pipe OR	Very fine, but fibrous material (ca. -5 mm)	H&S- masks Final output Not in windy conditions Preferably attach bag to pipe end (complexities may

SP No.	Stream	Location (engineering plant layout IDs)	Sampling type	Sampling tool	Stream particulates size	Comments
				Plastic collection film/sheet		occur) [Sample from container: stop operation, detach container.
				OR Scoop		

* Sampling point 8 (SP8) was not successfully sampled, because it eventually proved technically impossible to collect sufficient mass. Hence, SP8 samples were ignored in the analysis of the results.

** Sampling point 9 (SP9) proved technically impossible to sample from. Hence, it is not further mentioned in this thesis.

4.7 Sample preparation and sub-sampling

Background

The importance of appropriate sub-sampling cannot be understated. In the case of household waste scientifically rigorous sub-sampling and homogenisation comminution is imperative to preserve the analytical determination quantity can represent the initially collected sample. Comprehensive guidance has been published by EPA²⁸⁷, following the stipulations of the ToS. Gerlach and Nocerino²⁹¹ published on sub-sampling equipment performance. There is theoretical interest in the field²⁹²⁻²⁹³. Published research on actual procedures followed during waste-related research are limited to a few cases²⁷⁵. Nomographs can be used to achieve an optimal sub-sampling strategy²⁸⁷.

Experimental

In this thesis sample preparation was given utmost attention to guarantee that the procedure introduces the minimum possible variability. An extensive sub-sampling and size reduction programme was followed. The typically flowed procedure is shown in **Figure 4-4**.

After manual sorting, entire samples or reassembled shreddable parts were sub-sampled and reduced in size in accord with the theory of sampling^{287, 296-297}. Samples from SP1, 16 were shredded to <40 mm passing them twice through a slow rotation rotary shear Rodan Engineering CS 3000 (Stoke-on-Trent, UK). All samples were then bulk dried (40°C, 24 h) in advance of dry processing through a slow rotation cutting mill (RETSCH SM 2000, Leeds, UK) to <4 mm.



Figure 4-4 Typical sample preparation procedure followed in this thesis, exemplified for the case of biogenic content measurement. Adopted from Séverin²⁹⁴, as detailed in Séverin et al.²⁹⁵

Where necessary, sample mass was homogenised and further reduced by sub-sampling through an A/S Rationel Kornservice riffle divider (5 L, hinged container type 2, 18 splits; Esbjerg, Denmark), before shredding to <1 mm in a RETSCH ultra-centrifugal mill ZM 200 (12,000 rpm). These final general analysis samples (GAS) were then sub- to 50-100 g, and stored in air-tight bags at ambient temperature, in darkness. Grinding to a size of <1 mm was sufficient for the biogenic content determination. Where fines were constituted mainly of aggregates (SP3, 7, 15), they were excluded from the reassembled fraction as non-shreddable materials and corrections were applied.

Selection of the test quality to be analysed from the finally prepared sample is susceptible to the within-sample variability. Selecting an aliquot of e.g., 0.1 g from a GAS of 50 g that maintains a representative ratio between the grainy and fluffy parts is highly dependent on the analyst skills. To illustrate further, the inclusion or not of a small granule of Cu-based cable can result in huge differences in the Cu concentrations reported. This is less evident for measurands that are more uniformly distributed throughout the GAS mass²¹⁰, such as moisture, ash, and biogenic content, for which a normal distribution for the population of GAS replicates.

The GASs produced generally appear in two forms: (1) very well homogenised soil-like material, e.g., (SP5, fines fractions); and (2) insufficiently homogenised, comprising two fractions with discrete content and behaviour, resulting from the preferential shredding at SH1 and SH0.5 of materials with different elastic properties: (i) high density, hard granules (hereafter “grainy” part), and (ii) soft, fibre-like aggregating material forming cotton-like entities (hereafter “fluffy” part). The grainy part is generally embedded in the fluffy part, but is highly susceptible to gravitational segregation; the grainy particles when liberated accumulate at the lowest part of the GAS storage bags. This is a characteristic case where careless/haphazard effort to

homogenise, e.g., by solely shaking the sample storage bag, can result in an overall less homogeneous lot, as Pitard²⁹⁰ has warned against. Whilst every effort is made to thoroughly homogenise the GAS before selecting an aliquot for each analysis.

To test for the variability introduced during the sample preparation stages, a nested design experiment²⁹⁸⁻²⁹⁹ was conducted to estimate the relative contribution of each sample preparation stage to the variability encountered in the overall measurement procedure (results not reported due to time limitations).

4.8 Material composition of MBT plant flows by manual sorting

Background

The manual sorting of the sampled plant streams (SP1-17) is an inevitable part of the sample preparation procedure and also serves the objective of an independent material characterisation exercise. This characterisation intends to: depict the flow of materials within the plant and provide a basis of primary data suitable for the potential modelling of certain fuel properties for both explanatory and predictive purposes. As a result, explanation/prediction of both beneficial properties, such as the biogenic content and calorific value, and problematic properties, such as the chemical pollutant load of the stream flows, ash and moisture content, can be achieved. Emphasis is on the SRF production stream and final output.

The manual sorting as part of the sample preparation serves to separate out the non-shreddable components ('contraries'). Size reduction of (i) the so-called 'inert' fractions including glass, ceramics, stones, etc, and (ii) the metallic-based fractions cannot be performed with typical shredding equipment. Hence, these fractions have to be identified and separated out before the various stages of shredding takes place to

avoid excessive wear and tear or breakage of the equipment. This practice is standard in MSW sample preparation, as similar works indicate⁵⁵.

The manual sorting as part of the MBT flows characterisation study is a demanding task, regarding both its theoretical conception and application. Of relevance are the many methodologies covering aspects of characterisation of MSW, such as sampling plans and sorting into suitable waste components, and publications reporting on data collected according to them. Dahlén and Lagerkvist³⁰⁰ have recently compiled a comparative critical evaluation of 20 household waste composition methodologies, including those of ASTM³⁰¹, SWA-tool³⁰², CIWMB³⁰³, Maystre and Viret³⁰⁴, Sharma and McBean³⁰⁵, IEA³⁰⁶, Sfeir et al.³⁰⁷, etc. They recognise the inherent difficulties of such attempts, especially in obtaining samples sufficiently representative of the population to be sampled (lot)²⁶⁴, and conclude that the most important relevant choices are: (i) stratification of sub-samples to cover the lot; (ii) sampling location; (iii) sample size; (iv) number of samples; and (v) number and definition of waste categories to sort into. They then discuss the main approaches to each of these methodological aspects.

Varying guidance and practice applies to the sample size, i.e., the sample mass, suitable for waste component identification. As a measure of the standard and suggested best practices, for streams of the variability of mixed MSW, Dahlén and Lagerkvist³⁰⁰ recommend the rule of thumb of 100 kg (and a minimum number of 10 samples, i.e., increments); whilst the most conservative values come from Maystre and Viret³⁰⁴, suggesting 300 kg to be the minimum cumulative sample weight to achieve an almost constant standard deviations for sorting in 47 categories. However, apart from the methodologies of Sfeir et al.³⁰⁷ and of Sharma and McBean³⁰⁵ the other approaches are more or less empirical and are not founded on robust quantitative computations and explicit assumptions as is the ToS. Sharma and McBean³⁰⁵ control the overall sample mass by optimising the number of the increments of 136 kg (300 lb), (an

increment mass selection suggested as the upper limit in the ASTM document, stemming from the initial suggestions put forward by Klee and Carruth³⁰⁸, as explained by Dahlén and Lagerkvist³⁰⁰) and demonstrate converging %CV for 5 increments for the primary waste components of plastics, paper, inorganics and household hazardous, and after 11 increments for organics and paper. Sfeir et al.³⁰⁷ investigated the interaction of the number of the sorting categories with the increment size, concluding that it is necessary to use a sample weight of at least 200 kg if many sorting categories are used in order to avoid bias; alternatively for <10 sorting categories (i.e., only basic primary categories) the minimum recommendation given by ASTM and Klee and Carruth³⁰⁸ of 91 kg (200 lb) could suffice.

Experimental

The determination of material composition of the flows of the UK MBT plant A was accomplished primarily by manual sorting of the collected samples. However, to account for changes in the category into which some materials are allocated because of the processing through the plant flowsheet, modelling-based adjustments were also used for certain flows.

In this research, the choices relevant to obtaining representative samples (i-v, above) were addressed as a part of the sampling plan (**Section 4.6**) designed to cover not only the waste component characterisation, but all of the multiple specific experiments and types of properties to be measured, as dictated by the research objectives. The aspects (i-iv) were chosen with the use of the ToS; note that whilst Dahlén and Lagerkvist³⁰⁰ discuss and advocate the ToS provisions regarding achieving unbiased sampling, they do not refer to the rest, i.e., the quantitative part of this approach. Beyond theoretical stipulations of suggested methodologies, sampling plans inevitably serve the specific objectives and practical limitations of each study, resorting to tailor-made solutions.

The mass quantity of MBT-stream samples collected was initially estimated by application of the ToS. Cd, present at the trace level (ca 1 ppm) in the overall samples at each of the sampling points was used for informing the computations for the mass to be sampled. The selection of Cd was made on the basis that the requirement for representative sampling of 'micro-pollutants,' i.e., of properties present in very small concentrations and not evenly distributed between the components of the lot to be sampled. The sample mass specified in this way should, in principle, lead to conservative estimates, i.e., the mass enabling for representative sampling of Cd should provide for representative sampling of less inhomogeneous properties, such as ash or biogenic content. Computations were based upon literature data and educated guesses, where no suitable information is available.

However, the actual sampled mass at each SP was, in most of the cases, much lower than the estimated minimum representative mass. This was the result of 3 major practical limitations: (i) the material available to be sampled and processed in the particular SP at the plant; (ii) the human working hours available for sorting within the constraints of this research (half of the material was sorted solely by the researcher, with the help of a second sorter for the rest second half); and (iii) the on-campus storage limitations, along with the time and effort involved in the representative shredding and sub-sampling during the subsequent sample preparation, which increased considerably with the sample mass. To compare with the MSW stream guidance, here, the sampled mass of the similarly inhomogeneous biodried fraction (SP1) was at ca 15 kg per increment.

The %CV for each sorting category at each SP can serve as a quantitative measure of the fitness-for-purpose of the eventually sampled quantities, the number of increments (INCs) sampled and analysed, and the accurate and consistent sorting into the selected categories. Visual inspection of stack plots of the sorting categories per

SP for all INCs can reveal any gross departures from a satisfactorily consistent representation of the categories within the sampled mass: all SPs were satisfactory, apart from SP8, which was excluded from subsequent determinations.

The selection of the sorting categories justifies multiple objectives. Firstly, the selection aims to map the material flows within the MBT plant with regard to primary residual MSW constituents. The emphasis is on: (i) the biodried fraction (SP1) because it is the input to the processing section of the plant. Hence, the potential quality of the produced SRF will ultimately depend on the composition of the biodried fraction, for which no data have so far been reported; (ii) the SRF; (iii) the oversized heavy rejects fraction (SP16), because this constitutes the fraction which is designed to concentrate most of the items which are unsuitable for SRF (or any other potentially marketable stream) production and which have to be disposed of in MSW landfill, or through EfW.

The additional intermediate sampled fractions are necessary in order to develop a detailed understanding of the specific unit operations of the plant, and spot potential for improvement. These sampling points provide the necessary degrees of freedom to compute the data reconciliation calculations. To reach conclusions about the material flow performance of the plant and its potential for improvement, the waste components examined should behave consistently whilst treated at each unit operation. For unit operations that depend mainly on the PSD of the waste components (e.g., trommel screening) the rest of the physical-mechanical properties relating to the type of the material are secondary. However, material composition is the main basis to develop a meaningful knowledge base for the behaviour of waste treatment unit operations.

For a basic characterisation, the categories proposed for harmonisation by the International Energy Agency (IEA)³⁰⁶ are covered here (**Table 4-5**), but were judged as not sufficiently detailed for the objectives of this study.

Table 4-5 Categories into which process streams samples were manually sorted. The compatibility with other breakdown categorisations of proposed methodologies is shown. However, the exact interpretation and application is inevitably research- and even individual sorter-dependent.

Categories	Symbol	Main constituents	CEN biogenic content determination standard 309	IEA major categories 306	Rotter et al. 55 In addition: Fines 40-10 mm	Sample preparation sub-fractions
Biological	BIO	Garden (leaves, grass) and kitchen waste (food residues), including non-treated wood	Biological (wood separately)	Kitchen, garden and vegetable	Organic waste	Reassembled shreddable fraction included in GAS Coincides with potentially combustible fraction - with the exception of: (i) some of the household hazardous items, and (ii) the plastic coating of cables
Carpet/mats	C/M		idem	Miscellaneous combustibles	-	
Cartons	CAR	Beverage (e.g., milk/juice) packaging. Several layers of card, plastic film, aluminium	Paper/cardboard	Miscellaneous combustibles	-	
Composites	COM	Combustible composite materials and complex items not fitting in any other categories: e.g. electrostatic cleaning wipes, cigarette filter, sanitary napkin, polystyrene foam, composite food packaging trays, etc. Excluding cartons. Most items consist of or are high in resins.	-	Miscellaneous combustibles	Other composite materials (Packaging composites)	
Durable plastic	D_P	Hard plastic items: e.g., toys, decorative items, consumer appliance casings, PVC tubes, CDs, etc	Rigid plastic	Plastic	(Other plastic products)	
Fines <10 mm	F<10	d ₉₅ ≤10 mm: variable composition including dust, stones, grit, glass shards, biological adhesives, and other items depending of the overall composition of the SP. Identifiable screws and nails in the fines were reassigned to the metal categories.	idem	idem	Fines <10 mm	
Other	OTH	All rare occurrences not fitting elsewhere	-	-	idem	
Fluff	FL	Fluffy mixed material of variable composition according to each SP: mainly textile fibres, plastic films, biological fragments, etc	-	Miscellaneous combustibles	-	
Other packaging plastic	O_P_P	E.g. soft drink bottles/cups of PET: (recycling coding 1), HDPE (recycling coding 2) LDPE, etc. Generally resins of intermediate rigidity.	Rigid plastic	Plastics	(Packaging plastics)	
Paper/card	P/C	All types, apart from tissues	idem	idem	idem	
Plastic film	P_F	Plastic bags and films, soft items (PE, PP)	idem	Plastic	(Packaging plastics) Non-packaging	

Categories	Symbol	Main constituents	CEN biogenic content determination standard ³⁰⁹	IEA major categories ³⁰⁶	Rotter et al. ⁵⁵ In addition: Fines 40-10 mm	Sample preparation sub-fractions
					films	
Rubber/leather	R/L		idem	Miscellaneous combustibles	Rubber Leather	
Sanitary products	S_P	Nappies	Tissue	Miscellaneous combustibles	Diapers	
Shoes	SH		-	Miscellaneous combustibles	idem	
Textile/fabric	T/F	Pieces of clothes, wool fibres	Fabric, idem	idem	idem	
Tissues	TIS	Napkins, toilet paper, etc.	Idem, but also including sanitary products	Paper and card	-	
Treated wood	T_W	Wood treated with chemical substances, e.g. furniture. It may or may not be chromated copper arsenate (CCA) impregnated wood ³¹⁰	Wood	Miscellaneous combustibles	(Wood)	
Batteries	BAT	Various types: e.g., Zn-C, alkaline, Ni-Cd, Hg-free, Li-ion, etc. See: Skutan and Brunner ¹⁸¹	-	Miscellaneous non-combustibles	idem	Not shredded fraction
Cables	CAB	Electric wires, typically Cu, with variable plastic casing (e.g., PVC)	-	Partly fit: Miscellaneous non-combustibles Miscellaneous non-combustibles	-	
Cinders	CIN	Combustion residues, partly burnt or charred pieces of coal	-	Miscellaneous combustibles	-	
Ferrous metal	Fe_M	Any fragment predominantly made of iron or steel	idem	Metals	idem	
Glass	GL	All types of glass (green, brown, transparent); excluding new type electrical bulbs (HAZ)	idem	Miscellaneous combustibles	idem	
Household hazardous	HAZ	Small WEEE (e.g., mobile phones, (fragments of) printed circuit board (PCB), lighting equipment); hazardous chemicals containing bottles, etc.	-	-		
Non-ferrous metal	nFe_M	Any fragment predominantly made of aluminium alloys		Miscellaneous combustibles	idem	
Stones/ceramics	S/C	All stones, ceramics and miscellaneous aggregates other than glass (e.g., construction materials, bricks, concrete etc)		Miscellaneous combustibles		

* As proposed by QUOVADIS (2007)

WEEE: Waste Electric and Electronic Equipment. For a detailed coverage refer to Chancerel and Rotter³¹¹ and Slack et al.³¹²

GAS: general analysis sample

HDPE: high density polyethylene
PET: Polyethylene terephthalate
PP: polypropylene
PE: polyethylene
PVC: polyvinylchloride
CEN: European Organisation for Standardisation
IEA: International Energy Agency

Second, of high interest is to map the pollutant flows through the MBT plant. As explained in the critical evaluation of the literature (**Section 2.4.3.3**), mapping of property flows (e.g., chemical element or ash content) is important and relevant to contemporary waste/resource management. Hence, an attempt was made to sort the samples into suitable material component categories with sufficiently homogenous characteristics. For instance, regarding the chemical composition for the elements under investigation (**Table 4-3**), such as Cl or trace level metals (Cd, Hg, Tl, Zn, Cu, Ni, Pb, Sb, Sn). Creating a suitable categorisation is a challenging aim, for which insufficient data exist and, which still remains an open question, as Dahlén and Lagerkvist³⁰⁰ state in their future research suggestions. Clearly, sorting into categories with sufficiently homogenous chemical composition demands knowledge of the chemical composition of all major items of MSW, and separation into considerably more than just a few primary categories.

Additionally, these optimal categories are different for e.g., different chemical elements. Burnley³¹³ has recently reviewed the limited literature available on the chemical composition of MSW constituents. Other main waste characterisation works were provided by Maystre and Viret³⁰⁴, Rotter et al.⁵⁵, Gidakos et al.³¹⁴, Hansen et al.³¹⁵, Riber et al.³¹⁶, Zhang et al.³¹⁷.

Here, the categories selected reflect the findings of these studies, attempting to separate the major pollutants in suitable categories. This depends on how the specific pollutant load (% of the overall concentration of the element in the sample contributed by the by the specific waste component) is distributed among the potential breakdowns into categories. In selecting the categories the work of Rotter et al.⁵⁵ in particular was used, because it is the only recent study that provides both the physical and chemical composition of wastes, enabling the calculation of the specific loads of waste component categories. The 6 main contributors to the specific load of the combustible

fraction, as reported in Rotter et al.⁵⁵, were (values as read from graphs): (1) Pb: electronic waste (47%), fines 10-40 mm (16%), fines <10 mm (10%), other composite material (6%), other plastic products (5.5%), shoes (5%); (2) Cd: electronic waste (54%), other composite material (17.5%), other plastic products (14.5%), shoes (4%) fines 10-40 mm (2.5%), fines <10 mm (1%); (3) Zn: fines 10-40 mm (16%), electronic waste (16%), other composite material (15%), fines <10 mm (10%), other plastic products (9%), wood (7.5%), (4) Cl: other plastic products (26%), other composite material (12.5%), organic waste (10.5%), shoes (9%), paper and card (8.5), fines 10-40 mm (7%).

Hence, since the plastic resin types and composite materials contribute significantly to the pollutant load for all these elements, it was decided similarly to sort the plastic polymers into more detailed categories, and to maintain a unified category for other potentially highly inhomogeneous primary categories, such as paper and card. The underlying assumption is that of physically similar composition. However, the split into categories containing resins followed in this thesis is different than that of Rotter et al.⁵⁵. The identification of the items in the selected categories was facilitated by the extensive guidance available from CIWMB³⁰³. Despite this detailed guidance, the accurate identification of plastic resins demands the use of portable photo-spectrometric equipment, a solution not applicable to the SRF and the rest of the post-secondary shredding MBT process streams (SP10-12), because of their minute size and the resulting significant delay in the identification time even for the suitably sized items.

Finally, the chosen breakdown of waste components has suitable categories to enable the application of the manual sorting determination method for the biogenic content, as specified by CEN TS 15449:2006³⁰⁹, work complementary to the scope of this research, conducted in parallel, and reported separately²⁹⁵.

The household hazardous waste (HHW) items (see **Table 4-5**) were identified and analysed separately for their properties, including chemical composition. This choice was made because of the limited occurrences of these items in the sample quantities to be sorted, as a preliminary investigation has shown. As a result, the identified HHW items inevitably constitute rare occurrences, but because of their high pollutant concentrations they could potentially distort the overall concentration of the samples in a non-transparent way. Hence, HHW were treated separately, allowing the disaggregation of the information which relates to them from that of the rest of the combustible fraction. The contribution of HHW to the various measurands was allocated for separately, where this was considered as necessary. This handling increases the potential future utility of the plant model results, enabling to potentially account for variable levels of WEEE and rest HHW present in the residual waste input to the MBT plant, reflecting their collection schemes implemented.

The MBT streams to be sorted present challenges. Regarding their general characteristics (i) all the streams are sub-fractions of partly-residual MSW; (ii) most of the plant input material is delivered at the MBT reception as highly compacted waste collection vehicle loads; (iii) it has subsequently undergone limited shredding at ca 300 mm and; (iv) it is the biodried output for ca 2 weeks of processing, resulting in significant losses of moisture and readily biodegradable materials. As a result, waste fragments are highly contaminated by organic adhesives, due to compaction and many components of initially single entities are partly liberated (disassembled) (e.g., parts of small household appliances). Because of the relatively dry status the adhesives, they can be more readily removed during sorting (compared with raw mixed waste). Samples from different SPs produce varying levels of recovery of material by category (reflecting their stage of processing in the plant) and pose different sorting challenges. Large items upstream of the secondary shredder (SP1,16) contain fixed sub-

components of different categories, e.g., plastic and metal and hazardous items, such as printed circuit board. Such complex component parts were separated from one another manually or with scissors, as far as possible.

Samples of SPs downstream of the secondary shredding (SP10-15) at d_{95} ca 40 mm, pose a significant challenge for component identification. Indeed, relative guidance for the application of the biogenic content of SRF by manual sorting recognises this difficulty³⁰⁹. Similarly, a thorough research on RDF production for non-shredded waste has defined the fines fraction at <40 mm, reflecting this difficulty⁵⁵. In this thesis the fines category was defined as $d_{95} < 10$ mm, and all fragments >10 mm were identified. However, it is much more difficult to identify fragments of e.g., shoes, carpets, nappies, cartons, after the secondary shredding. As a result, a bias against such categories is evident for these components, the fragments of which may be counted as parts of other categories (i.e., composites). Most important, the effect of the secondary shredding introduces a bias in the relative importance of the fines fraction in relation to the rest shredded components, which needs to be accounted for: all materials shredded at the secondary shredder are >10 mm (apart from any adhesives), but at the discharge a significant proportion (e.g., up to ca 50% w/w_{ar}) would report to the F<10 mm fraction.

4.9 UK MBT plant A: material flow analysis

The substance flows through the mechanical processing section of the MBT plant A were modelled using experimental and operational information. For the mass balance data from the output weighbridge were utilised. These predominantly correspond to the period under examination (sampling), and were complimented by data dating back to the first operation of the plant in its current configuration.

The substances examined were the waste components categories into which the samples were sorted, and a series of the physiochemical fuel properties, for which each sampling point (and sorting category) was analysed.

4.9.1 UK MBT plant A: mass balance model

Background

Producing a reliable mass balance is the first critical step towards mapping the flows through the MBT plant. Suitable data can be obtained in 3 main ways: (i) by measuring the mass flows (mass over time) at selected sampling points using automatic equipment; (ii) by measuring the mass flow balance by suitably repeated sampling; and (iii) by using the operational data available from the plant input and output process streams. Whilst the need for automatic mass flow measurement (e.g., dynamic weighing by belt scales) has been strongly advocated by waste treatment plant researchers⁹⁹, the reality is that the solid flows in MBT plants are not yet monitored thus. Furthermore, the accuracy of the results of such equipment can be challenged. Instead, Gy²⁶⁷ has proposed the notion of measurement of mass by proportional sampling (case (ii)) as a more accurate alternative to the automated solid mass flow determination. Proportional sampling includes the manual measurement of a series of incremental mass according to the ToS. However, proportional sampling is resource intensive, especially if manual sampling is involved.

The use of operational data (case (iii)) has advantages. Firstly, the data are readily available as monitored for the plant operation logistics. Data include batches of input mass to the plant, input mass to the mechanical processing section (feeding by the automated crane), and batches of the various types of outputs as they leave the plant (weighbridge data). Secondly, operational data can expand over the whole period for which the material flows are examined (assuming a period of at least weeks rather

than hours) and constitute the real mass quantities rather than estimates produced through statistical treatment of samples as in (ii) and (iii). Thirdly, they come already imported in a suitable database (e.g., in MS Excel format).

However, there are certain limitations. Full-time plant operation data include plant operation in non-optimal mode or even during downtime of some unit processes (e.g., without an overbelt magnet or the eddy current separator). Operational data also depend on truthful and correct registering of the types of outputs. Furthermore, these data do not cover any of the internal flows of the plant; a system of equations that describes the mass flows through the plant needs to be resolved to establish internal flows. Because the values constitute the full population data, i.e., not a statistical estimate, no estimation of the anticipated variability can be produced for the overall time period considered. However, the variability on lower time scales can be evaluated. Mass flow rates can be computed only to the degree that the input and/or output data can be assigned to real processing –not calendar– time, which may not be straightforward.

Depending on the complexity of the plant flow-line, only input and output data may prove inadequate in determining all the inner flows, because of insufficient degrees of freedom. This can result from too many internal flows and/or the existence of loops.

Data reconciliation is a mathematical optimisation method that allows handling uncertainty or conflicting data³¹⁸. This field of study has developed for applications like pharmaceuticals and computers industry but recently there has been increased interest for simulating solid flows in the mining and waste sector, with development of suitable software SOLIDSIM^{®319-320}. These ideas have had limited application so far in the waste management sector (e.g., in improving data quality²⁴⁷). STAN2[®] is a relevant material

flow management software with data reconciliation and error propagation capabilities that has been developed and is freely available for use²⁷⁹.

Experimental

Mass balance on as-received basis (ar)

The mass balance of the UK MBT plant A was developed using data of variable sources. Initially, (source 1) operational input-output data became available covering a first period since the plant started operation with its current settings of secondary shredding, optimised for SRF production (21/07/07 to 7/11/07). To get a reliable value for the APC residues (SP17), long-term data covering a period extending over several months were used, because of the very low flow-rate. This input-output balance was used to inform the sampling plan. Whilst the sampling plan included instructions for the measurement of the mass flow rate at each sampling action, this was not achieved in practice due to time limitations (minimising of the plant downtime, necessary for sampling from stopped conveyer belts).

Data source 2 consists of specific flow rate measurements, collected on a single occasion, to identify certain flows. However, the results were incomplete (it was not feasible to determine the conveyer belt speed) and showed high variability. Hence, the solution of using the plant operational input-output data for the overall period within which sampling took place (July 2007 – September 2008) was preferred (source 3). Given that these data were incomplete (missing values for non-Fe metals, E_C rejects and APC residue), values from sources 1 and 2 and literature data (limited to the non-Fe metals output) were also used to estimate these. The E_C rejects flow is re-circulated in the processing section input and not leaving the plant, hence no data was available from the input-output logbooks.

The material flow analysis software STAN2^{®279} was used to compute the values for the inner flows. Given that the plant output flows values cover the whole examined period, no uncertainty estimate is available. Estimates of uncertainty were provided as educated guesses at $<\pm 10\%$, to enable STAN2[®] to effectively reconcile the flows. Hence, these uncertainties do not attempt to simulate the real, but totally unknown, fluctuation of the process flows over a time period of the order of magnitude being examined (approximately half a year). As a result, the reconciled mass flows are indicative only of this particular period and in practice may not be representative of other periods or time scales.

The computation of the reconciled flows was done in two stages. Because the input of the output flows (operational data) (**Table 5-3**) alone do not suffice to compute the inner flows (insufficient degrees of freedom), a simplified model was created. This model ignored the smallest of the mass flows (A_CL 2 lights (F17) and the flows leading to Fe mixing) to establish the gross split of the flows leaving the trommel screening and the air classification. At a subsequent stage, this gross estimate for A_CL 1 lights (along its uncertainty) was included, along with the initially available data to produce estimates for the full model. At a separate subsequent stage, this model was used to estimate the component flows. The initial results indicated that slight departures from the operational data would lead to better balances. Hence, the differences between the operational and the final model (**Figure 4-5**) input data (**Table 5-3**). In the full model the flows to the APC residue output, the stock of batteries, the batch re-circulation of the E_C rejects to the input and any non-solid flows were ignored as insignificant for the overall material flows.

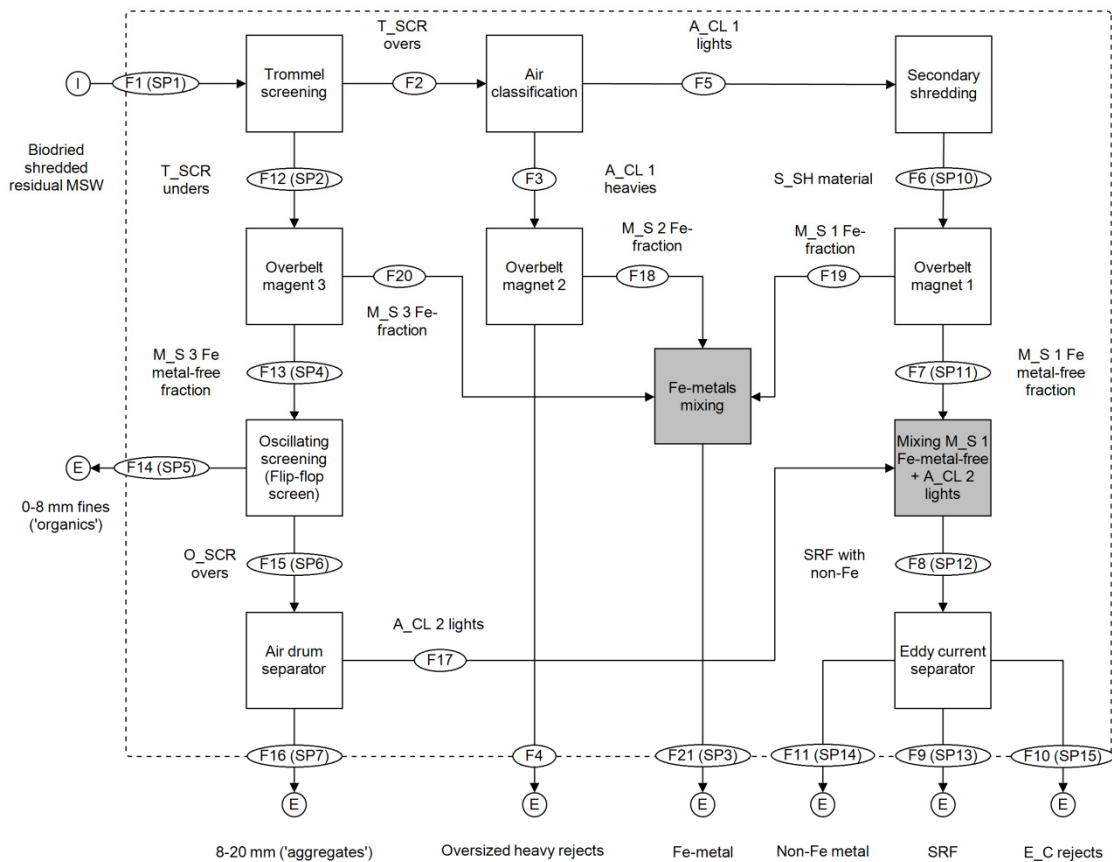


Figure 4-5 Model of the processing section of the MBT plant A flowsheet, as created for the material flow management software STAN2[®]. The flowsheet is shown in **Figure 4-2**. Abbreviated descriptive identification codes, numbers and corresponding sampling points (SP), where applicable, are given for each flow (F). Input flow is denoted by I, and output by E ('export') (programm settings). Process units operations are shown as transparent squares, named inside. Grey squares denote mixing points. The flows to the APC residue output, the stock of batteries, the batch re-circulation of the E_C rejects to the input and any non-solid flows are ignored as insignificant for the overall material flows. System boundaries are depicted as a dotted line. Conventions of STAN2^{®279} are followed throughout.

Sensitivity analysis for the as-received mass balance model

A sensitivity analysis was performed to investigate whether the assumed mass flow model correctly accounts for the material flows, as adjusted after modelling. This is necessary because of the variation on the amount of the heavy oversized reject output (SP16) evident in the available UK MBT plant A and wider literature data (**Table 5-3**).

Given that the data for the mass flows span over a much wider period of plant production time than that of the actual samples, a different mass balance may best represent the collected samples. The scenarios were informed from the data presented in **Table 5-3**, discussed below.

The oversized heavy rejects (SP16) vary from 13% w/w_{ar} to 25% w/w_{ar} of the total outputs. Despite that, the SRF output (SP16) appears relatively steady at 50-55% w/w_{ar}. Instead, the differences in the amount produced as oversized heavy rejects seem to affect the percent outputs of 0-8 mm ('organics') and the 8-20 mm ('aggregates'). This trade-off implies the existence of waste components that would report either at the T_SRC unders or the A_CL 1 heavies. For instance, stones/ceramics: depending on their PSD, one faction would report to the T_SRC unders (<20 mm, nominal) and the bigger in size (and hence generally heavier) would proceed with the T_SRC overs as input to the A_CL1 and (ideally) report to the A_CL 1 heavies, and finally in the oversized heavy rejects. The split of S/C depends on its cumulative passing for d = 20 mm. A variable S/C PSD and/or different trommel apertures would directly impact on the relative balance in the outputs.

Table 4-6 Scenarios of mass balances examined for modelling the UK MBT plant A material flows

Mass balance scenario		L		M		H	
Sampling point	Flow	Set	Rec.	Set	Rec.	Set	Rec.
SP1	Biodried shredded input	100.00	100.00	100.00	100.00	100.00	100.00
SP3	Fe-metals	4.00	4.03	3.50	3.35	3.50	3.35
SP5	0-8 mm fines ('organics')	21.00	20.62	19.00	18.66	16.50	16.16
SP7	8-20 mm ('aggregates')	9.00	8.83	7.00	6.85	5.50	5.35
SP13	SRF	54.00	53.32	54.00	53.39	54.00	53.39
SP14	Non-Fe metals	0.50	0.49	0.50	0.49	0.50	0.49
SP15	E-C rejects	0.10	0.10	0.10	0.10	0.10	0.10
SP16	Oversized heavy rejects	13.00	12.62	17.50	17.16	21.50	21.16
ΣSPoutputs		101.60	100.01	101.60	100.00	101.60	100.00

Set: scenario mass balance values input to STAN2

Rec.: mass balance values as reconciled by the STAN2

L, M, H: L, M, H: mass balance scenarios codes, according to the assumed level of oversized heavy rejects (SP16): low, medium and high accordingly (See also **Table 5-3** for measured and literature data)

The rationale for the scenarios values is informed accordingly. The assumed rounded up values sum up to 101.6% were reconciled by STAN2[®] to a 100% total, used subsequently in the waste components balancing computations (**Table 4-7**, adjustments for averages by MS[®] Excel part). The three variations examined are named after the relative amount rejected as oversized heavies: low, medium and high (**Table 4-6**). In all three scenarios the SRF output is constant at 54%.

Mass balance on a dry basis (d)

To compute balances for data reported on a dry basis (d) (e.g., for total chlorine content), a dry mass balance is necessary. This was computed based upon the reconciled as received (ar) mass balance (**Figure 5-22**). The as-received mass flows were converted to dry values, using the moisture content of each individual sample ($\langle M_T \rangle$) results to correct for their shreddable part of the samples; and the ratio of shreddable to non-shreddable manual sorting data to convert to entire samples. Then data were reconciled using the material flow management software STAN2[®]. Uncertainty was propagated throughout the computations.

Mass balance of the shreddable fraction on a dry basis (SHR, d)

To compute balances for data reported on a dry basis (d) for only the shreddable/combustible part of the samples (e.g., for ash content), a dry, shreddable/combustible mass balance is necessary (SHR,d). The balance was based upon the reconciled as received (ar) combustible mass balance (**Figure 5-27**), Conversion from ar to d values, was accomplished using the $\langle M_T \rangle$ results per SP. Then flows were reconciled using the material flow management software STAN2[®], in two stages: (1) simplified, omitting flows leading to Fe-mixing; and (2) full model. Uncertainty was propagated throughout the computations.

Mass balance of the shreddable fraction on a dry and ash-free basis (SHR, daf)

A suitable mass balance is necessary to compute the mass-specific-loads for balancing of properties reported on a dry, ash-free basis (daf) of the shreddable/combustible part of the samples (e.g., for biogenic content, $\chi_{B,SHR,daf}$). The balance was produced by deducting the reconciled ash content balance (**Figure 5-51**) from the reconciled entire shreddable mass balance (**Figure 5-25**). Uncertainty was propagated throughout.

4.9.2 UK MBT plant A: material component balances

Background

There are many reasons why data on waste component flows collected by sampling of an MBT plant and manually sorted would not balance, considering inputs and outputs for any sub-system of the plant (from single unit operations to the overall plant considered as black-box). In brief:

1. In a fully operational plant it is not feasible to follow the same batch of waste sample in its path through the flowsheet. Hence, inevitably the samples collected at different process flows (SPs) originate from a highly heterogeneous population, and can be considered independent. Given this high heterogeneity regarding the waste components and the various scales of time-related variability, no set of samples, no matter how closely in time might be taken, can be anticipated to result in sufficiently closing balances. Ideally, any set of samples representing various process flows should be sampled within the tightest time scale to guarantee a minimum similarity of the processed material.

2. The mass necessary for representative sampling of the components occurring rarely may be too big to handle during manual sorting. This is discussed in detail in the manual sorting section (**Section 4.8**).
3. The statistical treatment of such data may be difficult, as the normality assumption may not always hold.
4. Balancing of components depends upon successful balancing of the mass flows, which may vary with time.

These limitations are basic reasons for which there are insufficient results on balanced material flows of MBT and similar waste treatment plants. Typically, available data on waste components result from batch-scale tests of (combinations of) unit operations⁵⁵, using real or artificial waste components; are based only upon plant/unit operation output data, without balancing; and do not incorporate any information on their uncertainty.

Available data for unit operations have been summed up in the literature review section (**Section 2.3** and **2.4**). Similarly, efforts to develop semi or fully empirical models with certain degrees of use of spreadsheets or programs are discussed in **Section 2.4.3.2**. Recent publications attempting to model the SRF production SRF³²¹⁻³²² are covered in the relevant discussion sections.

Experimental

In this thesis, balancing of the waste components through every flow of the UK MBT plant A was attempted, in line with **Objective 3 (Section 3.4)**. Furthermore, TCs were computed, as required by **Objective 5**. The aim was to develop a description of the performance of the unit operations and the overall plant in handling the waste component flows, based on real-life empirical data, from a fully operational plant, with

uncertainty considered. Balancing of waste component flows can serve as the basis upon which to predict other properties at each flow and for the SRF output in particular, because of the relatively less inhomogeneous character of these waste components with regard to their properties. The novel solution to overcome the variability, both inherent in the plant flows and induced by the experimental method, was the application of material flow balancing software with the ability for data reconciliation and error propagation. This enabled the apparent incompatibilities for the average-only data to be overcome, leading to balanced flows - assuming absence of gross error.

There was no ambition to develop a first principles or semi-empirical model to describe the operation mechanism of unit operations (e.g., such as in the GRAB¹¹⁴, or SolidSim³¹⁹⁻³²⁰), which would have demanded a different approach in data collection and handling. Hence, the inevitable necessary data adjustments were handled by resorting to the most simplistic assumptions which can perform satisfactorily. Challenges (i-iv) were addressed in this work as follows:

Raw data were made available by sampling and manual sorting. Given the sampling plan implemented, the sets of samples for different flows were anticipated to differ considerably. Hence, no correspondence can be established between the samples from different process streams. Certain flows were estimated by using an increased number of incremental samples (INCs), to account for their higher heterogeneity. Emphasis was put into sufficiently establishing the composition of the most heterogeneous SPs (biodried material: SP1; and oversized heavy rejects: SP16), for which 8 and 9 samples respectively were manually sorted. For the rest SPs, 3-5 observations were considered sufficient. Sampling points covered excluded SP8 where insufficient mass led to non-representative results, and SP17 (APC residue) where manual sorting was not applicable and the mass flow rate was shown to be

comparatively insignificant. Certain SPs from the L1_INC9 set of samples were excluded as non-representative.

The maximum sorted mass per SP (summed over the available INCs) was used to estimate the average mass percentages (percent purity of stream i in component CM_k : $C(CM_k)P_i$, **Table 2-6**) The approach followed assumes that the observations stem from a normally distributed population. The population in this case was the body of every possible sample of mass in line with the sampled sample range, over the time period examined, for each waste component examined, or sums of them. Generally there is no evidence against or for the normality assumption. However, problems concerning the representativeness of the manual sorting result values for the waste component categories that occur in low percentages in any SP had to be addressed. Such relatively 'rare occurrences' may result in misleading average data. This would have been the case if arithmetic means over the INCs have been used. Comparison with the medians over the INCs showed acceptable relative differences. Only components present in low mass concentrations (i.e., $ca < 2\% w/w_{ar}$) in the examined flow, showed very high relative differences, suggesting that summing over the whole INCs was necessary for getting more representative concentrations for these waste components.

The manual sorting data cannot be used directly as input to the material flow model, because of the transformations the waste components undergo in certain unit operations. These result in at some SPs certain waste components to be reported during manual sorting in different than the original categories (**Table 4-7**).

The uncertainty around the average mass concentration of each waste component at each flow it was established using the corrected data. These uncertainties were taken into account into the subsequent computation of the internal

flows and the reconciliation of them, and propagated to the final dataset of flows and TCs. The complete mass balance was resolved independently at a previous stage (**Section 4.9.1**). However, the mass flow uncertainties, were generally assumed relatively small and ignored during the computation of the uncertainties of the specific mass loads. This means that the reported results apply to, and represent, a fixed mass balance, and should be interpreted accordingly.

Table 4-7 details the computation steps taken to estimate the balanced component flows and the TCs. Two the general stages apply: first, the adjustments for averages and estimation of uncertainties in MS[®] Excel, and second a tiered application of the STAN2[®] material flow management software for internal flows computation, data reconciliation uncertainty propagation, and visual representation of both input data and final results in the form of Shankey diagrams.

Flow balances were examined for the individual manual sorting components (**Table 4-5**) and a series of sets of components which gather together components with similar characteristics or constitute wider categories. Sum of:

- Items suitable for combustion: $\Sigma(\text{combustible})$
- Items not suitable for combustion: $\Sigma(\text{non-combustible})$
- Paper/card and similar: $\Sigma(\text{P/C}+\text{TIS}+\text{CAR})$
- Plastics (resins): $\Sigma(\text{COM}+\text{D_P}+\text{O_P_P}+\text{P_F})$
- Textile/fabric and similar: $\Sigma(\text{C/M}+\text{FL}+\text{S_P}+\text{SH}+\text{T/F})$

Table 4-7 Computation steps taken to develop a model for balanced component flows and TCs

Software environment	Computation step	Necessity	Description of computation	Comments
MS [®] Excel	Data processing and statistical data analysis		Establish necessary adjustments (computations) and estimate parameters	
	Average % w/w _{ar} for each component at every SP	Establish central tendency and uncertainties	Manual sorting results used. Average % w/w _{ar} for each component at every SP, established by summing absolute mass over all INCs.	Comparison with the median over INCs approach, can illuminate differences arising from different statistical approaches. Use of overall mass sums before computing percentages allows more accurate estimate for the rare occurrences
	Re-distribution of Fines<10 mm in the post S_SH flows	Correct for initially non-Fines components reported as F<10 mm after S-SH	(1) Re-allocation of the all the F<10 mm % to the rest components, in proportion to their relative mass fraction (excluding FL). Parameter: For SP10-11: 100% of FL re-allocation. For SP13-15 partial re-allocation due to A_CL 2 lights input of F<10 mm (and >8 mm) material. Ca. 10 first terms (iterations) of series considered. (2) Because of different initial PSDs of the components and preferential shredding at S_SH ^{76, 96} (Figure 2-3), T/F least reports as F<10 mm: re-allocation of fraction of T/F to the rest components in proportion to their relative mass fraction Parameter: Fraction of T/F re-allocated: 0.75	Sensitivity analysis for model parameters (trial and error)
	Re-distribution of Fluff in the post-S_SH flows	Correct for initially non-fluff components reported as F<10 mm after S-SH	Re-allocation of F<10 mm precedes the re-allocation of FL. Re-allocation of additional FL generated post S_SH. $\Sigma(\text{FL}) = \Sigma(\text{BIO} + \text{COM} + \text{C/M} + \text{O_P_P} + \text{P_F} + \text{S_P} + \text{T/F})$, in proportion to their relative mass fraction. Parameter: Fraction of FL re-allocated: 0.85	Sensitivity analysis for model parameters (trial and error)
	Re-distribution of Fines<10 mm in the T_SRC unders and downstream flows	Correct for initially non-Fines components reported as F<10 mm after trommel and their subsequent split	SP2,4,5: Re-allocation of additional F<10 mm generated post trommel screening, due to component breakage and liberation. Assumed all reported to T-SCR unders (<20 mm). Additional F<10 mm determined by deduction of SP1 F<10 mm. Computations using all INC averages of F<10 mm. SP6,7: Re-allocation of additional F([8,10]) mm generated post trommel screening, reporting to O_SCR overs, 8-20 ('aggregates') and A_CL 2 lights.	Departures of sum of corrected fines with rest components to 100% mass may result: assumption checked separately and taken into account into the parameter estimation

Software environment	Computation step	Necessity	Description of computation	Comments
			Parameter: Fraction of SP4 actual fines reporting to SP5 (< 8 mm): 0.9253 Part of SP6 actual fines reporting to F21 (A_CL 2 lights): 0.054 Part of SP3 fines originally present in SP1: 0.50	
	U _{95,v} of the average % w/w _{ar} for each component at every SP	Provide data for reconciliation weighting factors and uncertainty propagation	Assuming components percentages in the various INCs constitute a normally distributed population (does not hold for rare occurring components, leads to high standard deviations for these cases) U _{95,v} , using t-value for the d.f. Computations performed on corrected component percentages.	The uncertainties are used as weighting factors in data reconciliation. Use of U _{95,v} allows to incorporate both inherent variability of the components in each flow (SP) and the level of independent data sets (INCs) used to determine this. Whilst STAN2 [®] interprets the uncertainties as standard deviations, the use of extended standard uncertainties is acceptable: only the gross error check function cannot be correctly used- however, this feature of the programme is not necessary for the performed application.
	Specific loads and uncertainties for each component along plant flows	To illustrate and reconcile flows of components with visible their relative importance	Specific mass loads ($\Sigma=10000$) = mass flow balance units ($\Sigma=100$) x mass concentration (purity) of each component in each flow ($\Sigma=100$).	The reconciled mass balance is used in computations. The specific mass loads illustrate directly how many mass units out of 10000 input to the processing section exist for each component at each flow. The 10000 allows for better representation of less heavy components. Division with 100 can express these as %.
	Un-reconciled balances of specific loads for input-output	Gross check of the input-output balancing	The data for SP1 (input to the processing section) are compared against the sum of the corrected (modelled) plant output values for each component (or set of).	Sensitivity analysis can illustrate the trade-offs, in the trommel and air classifier 1 mass splits. Severe departures from 100% suggest either impossible to balance data (sampling/rounding issues and manual sorting issues), or inappropriate statistical analysis, or incorrect/ not suitable adjusted model, or any combination of them.
STAN2[®]	Flows reconciliation	Compute internal flows and transfer coefficients for unit operations; reconcile all flows; estimate uncertainties; illustrate results	Multiple tier approach	
	Illustration of input data flows	To evaluate the potential for flow reconciliation	Built STAN2 [®] model of the processing section of the UK MBT plant A Import reconciled mass balance data from Excel Import specific load and uncertainty data from Excel Test for model validity Run model Obtain and review Shankey illustrations for each component (or,	Certain measured and adjusted by modelling flows may not be reconcilable without too strong reconciliation

Software environment	Computation step	Necessity	Description of computation	Comments
			set of)	
	1 st reconciliation (R1) of flows – inner flows – TCs – illustration	Compute from available corrected (modelled) data: internal flows , transfer coefficients for unit operations; reconcile all flows; estimate uncertainties; illustrate results	Same as above Export data of acceptably reconciled flows and TCs with uncertainty estimates to MS [®] Excel	Applicable to all flows.
	2 nd reconciliation (R2) of flows – simplified inner flows	To correct for logical fallacies of the STAN2 output (incorrect internal loops)	Replace input data average values for certain flows (F1,2,3,5,6,12) from the R1 results. Model ignores flows to Fe metal mixing. Keep original uncertainty values where available. Then, same as above.	Applicable to specific components only, not satisfactorily reconciled in R1
	3 rd reconciliation (R3) of flows – inner flows – TCs – illustration	To correct for logical fallacies of the STAN2 output (incorrect internal loops)	Same as above, use full model	Applicable to specific components only, not satisfactorily reconciled in R2
	4 th reconciliation (R4) of flows – inner flows – TCs – illustration	To correct for logical fallacies of the STAN2 output (incorrect internal loops)	Same as above, use full model	Applicable to specific components only, not satisfactorily reconciled in R3: BIO, D_P, GL, nFe_M, S/C, $\Sigma(C/M+FL+S_P+SH+T/F)$

An example (D_P) of the multiple tier flow reconciliation procedure is provided in **Appendix F**

4.9.3 UK MBT plant A: balances of fuel properties: mass-based specific loads

Balances for the flows of fuel-related properties (ash content, net calorific value, biogenic content, total chlorine content) were created for the mechanical processing section of the UK MBT plant A. Sum of plant outputs was compared to the input to the processing section (biodried fraction). The balances are for mass-specific loads of each property at every flow. The average concentration (content) for the property at each plant output sampling point was established by measuring the properties on the shreddable part of the samples. The sample preparation and analytical determination procedures are detailed in **Section 4.7** and **Section 4.13** respectively. The mass-specific loads were computed by multiplying the average concentrations with the mass rate of the flow, already established for the shreddable dry or dry-ash-free mass balances for the plant (**Section 4.9.1**). Results are presented in **Section 5.3.3**.

For the properties showing sufficient input-output closures, overall fully reconciled balances were created to cover input, all inner and output flows. Reconciliation, computation of inner flows and their uncertainties, and determination of transfer coefficients for each unit operation were accomplished by using the material flow management software STAN2^{®279} (**Table 4-7**). In addition to the input (SP1) and output flows (SP3,6,7,13,14,15,16) all the sampled inner flows (SP2,4,7,10,11,12) were used as input the data reconciliation and error propagation program. Total extended uncertainties were provided as input for each average specific load. Results are presented in typical process flowsheet/Shankey diagrams in **Section 5.3.3**.

4.10 UK MBT plant A: transfer coefficients of unit operations

Transfer coefficients (**Table 2-6**) were computed for the unit operations of the mechanical processing section of the UK MBT plant A. The total extended uncertainty

(U_{95}) around the average values has been determined (i.e., confidence intervals at 95% confidence level) as well. The computation was performed using the material flow management software STAN2^{®279}, in parallel with data reconciliation and inner flow computations. General methodology is described for the waste component categories in **Section 4.9.2** and for full-related properties in **Section 4.9.3**. Results are presented in **Section 5.4**.

4.11 Methodology: UK MBT plant A: simulation of SRF properties

Background

Attempts to simulate the properties of waste are inevitably limited by the inherent heterogeneity. This makes application of literature data problematic, in the sense that they have been possibly derived under a very different set of conditions. This pertains particularly to characterisation exercises, where the definition of waste components has a critical impact upon the result. However, combination of material composition data with characterisation of the components is straightforward yet powerful way to gain an in-depth understanding of the properties of wider more heterogeneous waste-derived flows/products. However, validation is paramount.

Experimental

Fuel properties (moisture content, ash content, net calorific value, and total chlorine content) of the SRF were modelled here, in an attempt to investigate the relative contribution of each waste component category into the average value achieved for the SRF. The model was based entirely on experimental data generated in this research and literature values or simplistic assumptions where necessary. The modelling steps were:

1. Reconstruction of the as-received material composition of the average SRF for the UM MBT plant A (**Figure 5-21**): achieved through balancing each waste component through the material flow software application);
2. Characterisation of the majority of the waste components selected for manual sorting (**Table 4-5**), following identical sample preparation (**Section 4.7**) and analytical determination methods (**Section 4.13**), with those applicable to the entire SRF and rest material flows of the plant. Most components were sourced from the biodried material and the oversized heavy rejects (**Table 4-4**). Because these streams do not undergo secondary shredding, unambiguous identification of the components can be performed. In many cases more than one process streams were sampled;
3. Reconstruction of the dry material composition of the SRF: achieved using the as-received reconstructed composition and the total moisture content, as determined for each waste component category (**Table App F-19**);
4. Computation of the mass-specific loads for each component category: multiplying the relevant SRF mass fraction (as-received or dry) of the waste component category by its concentration;
5. Adjusting to 100 specific load units to gain the percent contribution of each waste component;
6. Summing up the load contributions of each waste component to compute the overall concentration for the SRF (**Table 5-10**);

7. Validation of the simulation by comparison with the average value measured for the SRF. Both the 2 sets of samples representing the typical operation of the plant were considered: L123-L3oult (winter to summer operation) and L3-oult: summer operation (see **Table 4-9**). The evaluation included: (1) computation of the relative bias as a percentage of the measured value to assess the engineering significance of the simulation (**Figure 5-59**); and (2) t-test statistic using the confidence limits computed for the measured value at 95% level of confidence ($\alpha = 0.05$) and the degrees of freedom applicable, to assess the statistical significance of the simulation (**Table 5-11**).

Results are presented in **Section 5.5**.

4.12 Computations and statistical analysis

Background

This section discusses how variability is quantified and reported throughout this thesis. The background to relevant notions and specific choices are detailed in **Appendix B**. Main parts of the topics addressed pertain to general measurement (metrology) and quality management, narrowed down to the specific demands of waste characterisation and waste-derived products quality.

Experimental

4.12.1 *Statistics computed and evaluation of compliance for results/discussion sections*

Here, we evaluate the SRF (and other MBT-streams) quality regarding various properties and for certain cases we assess compliance against industry or

standardisation scheme limits. The statistics employed and the rationale for specific choices is explained.

According to the research objectives, the quality of the European SRF (**Objective 1**) and of the process streams of a UK MBT plant (**Objective 2**) was analysed. As explained, assessment of quality (**Objective 1,2,3**) is not limited to establishing the average quality of a property, but also a series of additional statistically-derived information, covering type of distribution, spread, upper limits, uncertainty propagated throughout the measurement computations.

4.12.1.1 Datasets considered

Regarding the quality of European MBT-derived RDF/SRF, a heterogeneous compilation of existing data, derived through variable measurement conditions, is presented. **Table 4-8** summarises background information on data sources. Available data are mainly found in reports^{13, 43, 204, 208}, along with a few peer-reviewed publications^{62, 235, 323}. These datasets are mostly derived from quality assurance systems internally implemented by MBT plant operators to satisfy end-user contractual requirements and/or to demonstrate compliance with national standards. The RDF/SRF has been produced from varying input materials (different countries/regions and residual or mixed waste collection schemes), treated in MBT plants with different design and operational configurations (but predominantly biodrying), prepared from different fractions of the input waste (e.g., partially including or totally excluding the biomass fraction), and prepared to different national standards and end-user requirements (mainly cement kilns, but also dedicated FBC and power plants).

The potential for meaningful comparison is restricted by many factors. Not all the diversifying methodological details of measurement are clearly stated for each case. Different objectives and methodologies have been applied alongside the entire

measurement process, including sampling plans, sub-sampling and sample preparation, analytical determination techniques, and dissimilar statistical analysis before final reporting of data in the literature (e.g., mean or median to estimate location). The effect of sampling plans on specific data series is anticipated to be critical, and much higher than the uncertainties introduced by differences at the analytical stage. It has been proposed that the number of analyses performed for each data series can cautiously be used to guarantee a minimum reliability of the data²⁰⁴. The majority of the data sets used in our analysis are based on >10 samples/analyses (lower limit proposed by CEN). Differences in all these aspects mandate the use of non-parametric statistics during their further evaluation.

Enhanced reliability can be expected for data series that followed the sampling theory, such as the TAUW investigation²⁰⁸, comply with national quality assurance systems, such as the Italian Eco-deco data¹³, constitute average measurements over long time periods (Nehlsen plant)¹³, and those that have been assessed had independently, such as the Herhof-Stabilate[®] SRF, investigated by Niederdränk et al.²³⁵.

Regarding waste components characterisation of UK MBT plant A, data is produced through manual sorting. Samples collected from the UK MBT plant A are presented in **Table 4-9**, and in detail in **Table_App F-1** to **Table_App F-14**. For the majority of the sampled process streams (SPs) observations exist for a varying number of increments (INCs) of lot 1 (L1). For the biodried materials (SP1), SRF (SP13) and oversized rejects (SP16), supplementary observations come from lot 2 (L2).

L2 comprises two samples: (i) a composite sample created out of 7 consecutive incremental samples (L2_INC1-7CM); and (ii) an individual incremental sample L2_INC8, collected as the next point in the sequence of those 7 incorporated in the

composite L2_INC1-7CM. Hence, L2_INC1-7CM represents the average SRF production during 1.5 spring week, as sampled by daily incremental samples and reduced to a composite sub-sample; and the L2_INC8, represents just the next daily increment in this series. However, they are treated as statistically equal, i.e. as single data points.

Table 4-8 Background information on data series used for the statistical evaluation of the European MBT-derived RDF/SRF

Case number	Data series name (including data period or year of publication)	Country	Type of MBT process	RDF/SRF type/trademark	Type(s) of available statistic	Other background information	Assumptions - limitations	References
1	Herhof (TST) PR2 [1999 publication]	Germany	Biodrying	Trocken stabilat® (TST) or Stabilat®	Mean (arithmetic)	Data from peer-reviewed publication (PR2)	Calorific value assumed net (ar) CI assumed ar	Heering et al. ⁶²
2	Herhof - Asslar plant [2001 publication]	Germany	Biodrying	Trocken stabilat® (TST) or Stabilat®	Mean (arithmetic)		Calorific value assumed net (ar) CI assumed ar	Heering ³²⁴ cited by Gendebien et al. ⁴³
3	Nehlsen (Calobren) [1999-2003 data]	Germany	Biodrying	Calobren®	Mean Median p ₈₀	Data coverage: 10/99-06/03) - use in cement kiln	Calorific values assumed net	Juniper ¹³
4	Nehlsen (Calobren) [2000 publication]	Germany	Biodrying	Calobren®	Mean		Calorific value assumed net (ar) CI assumed ar	Zeschmar-Lahl et al. ³²⁵ cited by Gendebien et al. ⁴³
5	Eco-deco - Montanaso plant [2002-04 data]	Italy	Biodrying	Eco-deco SRF	Mean Median Standard deviation		As received (ar) net calorific values were transformed to dry (d) values following the CEN formula – leading to much higher d values than the ones originally reported Cu: soluble Pb: volatile	Juniper ¹³
6	Herhof (TST) PR1 [2003 publication]	Germany	Biodrying	TST®	Mean	Data from peer-reviewed publication (PR1)		Niederdränk et al. ²³⁵
7	Remondis (SBS 2: for cement kilns) [2003 publication]	Germany	Mechanical sorting of high CV fraction in MBT	Recofuel / SBS® 2	Median p ₈₀	More than 10 data points		van Tubergen et al. ²⁰⁴
8	Remondis (SBS 1: for power plants) [2003 publication]	Germany	Mechanical sorting of high CV fraction in MBT	Recofuel / SBS® 1	Median p ₈₀	More than 10 data points		van Tubergen et al. ²⁰⁴
9	Herhof (TST) Renerod plant [2003 data]	Germany	Biodrying	TST®	Median p ₈₀	Based on 70 samples		Juniper ¹³
10	Eco-deco - Lacchiarella plant	Italy	Biodrying	Eco-deco SRF	Mean Median		As received (ar) net calorific values were	Juniper ¹³

Case number	Data series name (including data period or year of publication)	Country	Type of MBT process	RDF/SRF type/trademark	Type(s) of available statistic	Other background information	Assumptions - limitations	References
	[2003-04 data]				Standard deviation		<i>transformed</i> to dry (d) values following the CEN formula – leading to much higher d values than the ones originally reported Cu: soluble Pb: volatile	
11	Biodrying – TAUW data [2005 publication]	The Netherlands	Biodrying	n.a.	Mean Median p ₈₀ Standard deviation	Independent investigation (Site D)	Sampling plan limitations	Cuperus et al. ²⁰⁸
12	Herhof (TST) - [2005 publication]	Germany	Biodrying	TST®	Median 80th-P	More than 10 data points		van Tubergen et al. ²⁰⁴
13	MBT - high CV fraction - TAUW data [2005 publication]	The Netherlands	Mechanical sorting of high CV fraction in MBT	n.a.	Mean Median p ₈₀ Standard deviation	Independent investigation (Site A)		Cuperus et al. ²⁰⁸
14	Italian SRF average [2005 publication]	Italy	Average including cases of biodrying and mechanical sorting of high CV fraction	Average of TST® (Herhof /Fusina) Eco-deco SRF and Pirelli®	Median p ₈₀	More than 10 data points	Cu: soluble Pb: volatile	van Tubergen et al. ²⁰⁴
15	Herhof – Vesta Fusina plant [2006 data]	Italy	Biodrying	TST®	Mean		Dry basis assumed for ash content	Paoli et al. ³²³

Table 4-9 Notation and type of SRF production represented by each statistically analysed dataset for UK MBT plant A

Dataset notation*	Description of samples (data points)	No. of data points	Statistical analysis ID	SRF production represented
L1+2+3	All samples available from L1, L2 and L3 sampling lots	20	A	Global view of late winter (L1), spring (L2) and summer (L3) samples, including atypical plant operation (25% of data points)
L3	All samples from L3 lot	15	C	Summer (August) SRF production, including atypical plant operation (33% of data points)
L3outl	Group of atypical samples from L3 lot: L3_INC1,3,4,6,9	5		Atypical plant summer operation. Possibly E/C malfunctioning. Not examined separately
L1+2+3-L3outl	All L1, L2 and L3 samples, excluding the 5 atypical of L3 (L3outl)	15	B	'Typical SRF:' global view of late winter (L1), spring (L2) and summer (L3) samples, excluding atypical plant operation:
L3-outl	All L3 samples, excluding (-) the atypical	10	D	'Typical summer SRF:' summer samples (August), excluding atypical plant operation
L2_INC1-7CM	Composite sample, comprising a representative mixture of 7 incremental samples: L2_INC1 to 7	1		Covers 1.5 week of spring production. Analysed separately. Also, included in the statistical analysis as single data point.

*Notation explanation: excluded samples are denoted with a minus (dash) before them
L: discrete period of sampling (sampling lot)

With regard to the SRF characterisation, sourced from the UK MBT plant A, the available number of observations from L1, L2 and L3 has been arranged for the purpose of statistical analysis into four, partly overlapping, sets of data (A-D). Each of them represents different conditions of SRF production. Such a solution is mandated by two main reasons. First, by the set of atypical samples collected during the L3 sampling (denoted L3outl), suspected for problematic operation of the E/C separator and characterised by an unusual plastic to paper ratio. Second, because of the different sampling plans implemented in each of the 3 lots and the practical restrictions encountered, resulting in different number and types of SRF samples are available for each lot. The 15 L3 SRF samples provide a detailed and coherent view of a summertime slot of production, and hence it has a special merit on its own. However, not enough winter samples exist to establish a separate winter quality of the SRF. Because of this difference, in the overall SRF picture statistics, as computed for provided by the L1+2+3-outl (and L1+2+3) dataset, the later winter (L1) early spring

(L2) periods are under-represented regarding data points, when compared with the summer period (L3). The composite sample L2_INC1_CM on its own provides a 1.5 week summary representation of spring SRF production. **Table 4-9** summarises the 4 groupings of samples into datasets.

4.12.1.2 Statistics computed

A number of statistics are computed to sufficiently characterise the measured properties (and the measurement methods). These are in accordance with the theoretical challenges discussed in **Section 2.6** and **Appendix B**. They are briefly presented here.

Both parametric (typically assuming normality) and non-parametric ('robust') statistics are reported and discretionarily used. The S-W statistic²⁶¹ is used to test for departures from the normality assumption, for consecutively collected samples. If not significant at the 95% level of confidence ($\alpha = 0.05$), then the arithmetic mean, standard deviation, coefficient of variation and confidence intervals can be used. Otherwise a non-parametric description is preferred.

Measures of the most probable value to characterise a quantity R of a population (e.g., replicate aliquots from GAS, or collection of incremental samples), are referred to as: average, central tendency, location, expectation. Assuming normality, this is estimated by the arithmetic mean, denoted $\langle R \rangle$. As a robust alternative the median is also used. In certain cases the geometric mean is also reported, because of the widespread evidence of log-normally distributed populations.

Dispersion is evaluated by the standard deviation $s(R)$, coefficient of variation $\%CV(R) = s/\langle R \rangle$ (scale-free, dispersion in relation to the average), range (max-min), and interquartile range $IQR(R) = Q3-Q1$. Note that for small number of observations this $\%CV$ formula does not provide an unbiased estimate and needs to be corrected³²⁶.

Despite that, because typically the number of samples are comparable or/and such a correction is not common in the standard practice we calculated in this way to get results comparable with the literature. If needed, the unbiased estimate can be readily computed. Where normality applies, (or is assumed) the spread around the mean is estimated by standard error (SE) of the mean $s(\langle R \rangle)$; this is used to calculate confidence limits around the mean at 95% level of confidence, using the t-statistic for the actual or effective number of d.f.: $UCI_{95,v}(\langle R \rangle)$ and $LCl_{95,v}(\langle R \rangle)$.

The upper and lower values of the population are indicated by the maximum (Max) and minimum (Min). The non-parametric, robust to outliers percentiles p_{90} , p_{80} , Q3 and p_{10} , p_{20} and Q3 are selected to be reported and/or plotted for certain quantities.

Regarding the evaluation of the uncertainty (**Appendix B.2**), each average measurement on replicates of GAS is reported and plotted along with the measurement uncertainty at the 95% level of confidence $\langle R \rangle \pm U_{95,v_{\text{eff}}}(\langle R \rangle)$ (**Equation [0-4]**). The relative uncertainty $\%U_{95,v_{\text{eff}}}(\langle R \rangle)$ (**Equation [0-7]**) also provides a scale-free measure of the uncertainty and an indirect way to assess repeatability for quantities computed from others. Note that there is not any concrete evidence about the type of distribution (form of PDF) for the population of GAS replicates: normality was assumed and the average and spread were estimated through $\langle R \rangle$ and repeatability (s), respectively. The systematic errors b_R are considered negligible in comparison to the random errors, and hence ignored; they are included in the estimate of U only where there is no random error estimate (see for example the bulk moisture content computation in **Appendix C.1**). Despite being computationally demanding, the effective degrees of freedom are obtained through the W/S method (**Equation [0-6]**), because the simplified Williams method³²⁷ demands more replications than the 2 or 3 encountered throughout this research. For typical example of v_{eff} computation refer to the case of biogenic content (**7.3C.4**).

With regard to compliance with the CEN SRF classification specifications, the rules proposed in DD CEN/TC 343/WG2 N111²⁵⁹ are followed. However, neither in the case of European MBT-derived SRF, nor in the case of SRF from UK MBT plant A the available data have inevitably resulted from a sampling procedure in line with that prescribed in CEN. Hence, this classification is an extrapolation or refers to a hypothetical SRF with the classification property results. The absence of confidence limits in the case of European MBT-derived SRF is case by case commented. For illustrative purposes, the conservative, accurate confidence limits are also computed using the correct coverage factor according the experienced d.f., as explained in **Section 2.6.4** (see application in **Figure 5-64** and **Figure 5-73**).

In order to assess the performance of the SRF properties against the end-user specifications non-parametric statistics is predominantly used. However, the normality-based confidence intervals around the mean are also computed and, if necessary, commented upon. The solution is chosen because of: (i) the absence of any concrete evidence about the form of the PDF for the consecutive increment data sets; (ii) the lack of a simple and defensible way to propagate the each within-GAS variability and incorporate it into a global average of many incremental samples.

Note that where feasible (e.g., for ash content) the computations of statistics and the plots of the summary data for the UK MBT plant A datasets of samples is done on the replicates of determinations for each sample, i.e., not on their average per incremental sample. All available the observations comprise the replicates for each GAS representing an incremental sample collected once daily (2 or 3), times the number of consecutive incremental samples (20, 15, or 10) spanning over the SRF output for certain time periods. By including all these data points in the calculation of the median and p_{80} , the information in the within-GAS variability is propagated. Because the number of replicates (aliquots of GAS) analysed for each incremental

sample is constant (2 or 3, depending on the measurand and the necessity for computations) the contribution of each of the increments is of the same relative weight.

Using the non-parametric statistics to evaluate the compliance of the average SRF has the inherent limitations. Typically just average values or ranges are specified, but no p_{80} or p_{20} . Hence, in the wider absence of compliance decision rules, a surrogate evaluation is attempted. As a conservative measure of compliance, the p_{80} is compared with the upper limit (or the p_{20} with a threshold). Where the W-S test provides no evidence against normality, the $UCI_{95,v}(<R>)$ and $LCl_{95,v}(<R>)$ are computed and used for compliance testing, in the absence of prescribed guard bands.

The individual increment arithmetic mean values and their accompanying measurement uncertainty provide an evaluation suitable for process quality control of the UK MBT plant process streams. These individual incremental and the composite L2_INC1-7CM samples can be directly assessed against desirable levels in a probabilistic way by means of their accompanying uncertainty.

Non-parametric statistics are used to statistically describe and graphically present the quality of the European RDF/SRF. Available statistics of input data is largely limited to: (1) measure of central location of the sample population (arithmetic mean and/or median); (2) measure of the upper limit: (p_{80} and/or max) values; and (3) limited reported values for their spread (typically in the form of s). For each property estimates of the overall average, spread and upper lower values are computed (and presenting in box-plots) for the median and, where available, the p_{80} of the input data.

Preferably statistical analysis should be performed only on medians of input SRF data statistics. However, because median values have not been available for all the cases, as a compromise, mean values have also been used to indicate the location of input data series. Note that for properties that exhibit positive skewness when means

are used instead of medians the overall average of the values is biased towards higher values. However, despite evidence for non-symmetrically distributed properties, the differences between medians and means are not significant, as shown by the cases for which comparative data are available. The number medians which have been replaced by means are shown in **Table 5-1** for each property. For Pb only mean values are used, as there are very limited median values. Given that Pb can exhibit positive skewness, the average location of Pb may have been overestimated.

The significance of the results is also restricted by the fact that data series of different reliability (e.g., values resulting from long and short time series results) are given equal, non-weighted treatment. Similarly, only a low number of data-series on RDF/SRF properties, ranging from 14 to 4 is available; properties with fewer data points available are not analysed. Received (_{ar}) values have been converted to dry basis (_d) for the properties necessary to do so, by using the median(/mean) moisture content values, where available. As received NCV values ($Q_{net,p,ar}$) have been transformed into dry basis ($Q_{net,p,d}$) by applying the proposed CEN formula³²⁸ for the calculation of analyses to different bases³²⁹. This has rendered certain $Q_{net,p,d}$ to have much higher than values reported in the literature (e.g., Eco-deco values¹³), possibly calculated by a different conversion formula. Nevertheless, given the limitations, non-parametric statistics and box-plots provide the most appropriate, accurate and clearly presented account for the RDF/SRF properties.

Trivial computations have been completed in MSExcel[®]. Statistics and graphics are made with Statistica 8^{®251}. Various versions of box-plots are employed to optimally present the data. Typical box-plot conventions are followed; detailed explanations are available in **Figure 5-1**, **Figure 5-62** and **Figure 5-73**.

4.13 Measurement of physical/chemical properties

4.13.1 *Moisture content (M)*

Background on determination

Measurement of the moisture content (M) is a simple and well-established procedure, typically performed in drying ovens, where the loss of mass is reported as moisture content. In the case of SRF relevant guidance has been recently produced as DD. This covers both a reference method DD CEN/TS 15414-1:2006³³⁰ and a simplified one DD CEN/TS 15414-2:2006³³¹. Here, the scope of the measurements justifies the use of the simplified method. In the DD CEN/TS 15414-1:2006³³⁰ it is stressed that the result of the M measurement would not return an absolute value; instead the result depends on the determination conditions, which need to be standardised if comparable results are to be reached. The MC results are expressed as percentages by mass (% w/w).

The overall moisture content M_T is measured in 2 steps (**Equation [4-1]**), for practical reasons. First, in a pre-drying stage, termed 'bulk-drying,' the bulk moisture content M_b is determined on the collected, adjusted for mass, sorted and reassembled (and shredded to <40 mm if applicable (SP1, 16)) samples. Hence the reporting basis of determinations performed on bulk-dried samples, denoted b . Pre-drying serves 3 purposes: (1) it enables the intermediate term storage of the bulk-dried sample if necessary, without risking further biodegradation and significant changes in its moisture content; (2) is a prerequisite for the subsequent shredding at RM 2000 cutting mill, which accepts only sufficiently dry materials; and (3) the total moisture can be determined in without risking potential loss of the volatile elements, which constitute measurands to be determined (Hg, Cd, Tl, etc). The amount of M left until a constant

weight is reached, is determined as residual moisture content M_r , test performed on the GAS. Finally, the M_T is computed in accordance with to the CEN guidance³³⁰:

$$M_T = M_b + M_r \times \left(1 - \frac{M_b}{100}\right) \quad [4-1]$$

where, (all variables are expressed as percentages)

M_T Total moisture content

M_b Bulk drying moisture content

M_r Residual moisture content, determined on the GAS

Materials and method - instrumentation

Bulk drying containers are of plastic or aluminium foil. Same sets of heat-resistant drying containers are used throughout this research on residual M determination on GAS: (i) Perti-dishes, and (ii) silica crucibles, glazed inside-out (where ashing in the same aliquot of the GAS is following directly after). Constant weight of the containers was verified for the drying conditions. The drying is performed in air atmosphere for 24 ± 0.25 h: bulk in drying oven at 40 ± 2 °C; residual drying in drying oven at 105 ± 2 °C. Weights are measured with suitable precision: bulk nearest 0.01 g, residual nearest 0.0001 g.

Quality control

Determination of M_T according to **Equation [4-1]** assumes no changes in the sample M during the various stages between initial sampling at the plant and the two M determinations, i.e. during sample storage, transport, sub-sampling and shredding. The validity of this assumption is discussed.

The moisture content of the samples handled is responding to changes in the environmental conditions. Gain or loss of moisture is partly inevitable, given the time-

scale and types of processing involved. Precautions to mitigate changes introducing bias and limitations are briefly discussed. During the sampling periods of each lot (1,2,3) the samples have to be stored until they are collectively transported to the laboratories. Samples were kept in PP waste bags, which were not moisture-proof. To provide a suitable controlled environment, a cooling container was used to store the sample on-site, at $4\pm 2^{\circ}\text{C}$. Transport time for samples is minimised. Samples were transported on pallets and builder sacks, covered with wrapping plastic, to prevent rain penetrating. For most of the transport, samples were under cover. Effort was made to re-adsorb in the sample any moisture potentially condensed on the bag inner walls before opening the bags. Shredding operations can release heat and result in evaporation of moisture: (i) pre-shredding of SP1,16 was accomplished at very slow rotation speed – hence no temperature built-up has been evident; however, the resultant <40 mm samples looked much more wetter than the initial samples, fact indicating that pockets of liquid still contained in solid items (e.g., plastic bottles with beverages, cosmetics etc) in the initial samples release their moisture which was redistributed over the shredded fragments; (ii) shredding with the SM 2000 caused minimal heat built up, because of the slow rotation rotor used (ca 700 rpm), specifically selected to avoid overheating; (iii) final shredding at the ZM 200 centrifuge mill was performed in 2 stages (SH1: at 1 mm and SH0.5 at 0.5 mm) results in considerable heat built up, despite every effort to minimise this (intermediate rotation speed at 12,000 rpm, enabling a cutting time <2 min) resulting in some condensation formed on the covering lid. This was reintroduced in the sample. However, some moisture loss can have occurred for certain samples. The results of a 2^2 factorial design experiment to test for differences in the M for samples between SH1 and SH0.5 has not revealed any statistically significant difference at the confidence level of 95%.

During bulk drying the whole reassembled shreddable sample was dried. This facilitated the accurate determination of the M_b , which is the greatest part of the moisture content. For the majority of the samples no constant weight can be reached during the bulk drying. In the preliminary investigation the moisture loss during has been recorded over time. Preliminary investigation results (**Figure_App C-1**) suggested that for this SP (SP16) in the residual moisture left after 24h of bulk drying is in the order of 3% w/w. This is in agreement with the results encountered during the main determination tests.

M_r is determined on aliquots (3 replicates) of the GAS. The 24 h is sufficient for constant weight to be reached. DD CEN/TS 15414-2:2006³³¹ raises certain issues with the accuracy of this measurement: (i) the non-absolute value of the test result because of the potential of mass loss due to volatilisation of compounds (extractives), phenomenon particularly evident for biomass components of SRF; (ii) weight accuracy issues related to the hygroscopic nature of the SRF-type of samples: discussed further in the statistical analysis section.

4.13.2 *Ash content (A)*

Background on determination

Determination of ash content (A) follows the recent SRF guidance DD CEN/TS 15403:2006³³². Ashing was performed on bulk dried GAS samples.

Materials and method – instrumentation

Ashing furnace AAF11/118 (Carbolite; Hope, UK) with continuous air-flow of preheated air (4-5 volume changes per min) was used, as suitable for the ashing of materials that produce large volumes of fumes, such as plastics, food, and other hydrocarbons. It was equipped with type K thermocouple and the temperature was controlled through a multi-segment programmer. Crucibles used are described in the

moisture content section. Typically, up to 21 crucibles were processed per batch. Analysis was performed on triplicate aliquots of GAS (minimum of duplicates suggested in the DD), of ca 2.000 g each (1.000 g suggested by DD: double is used to increase the representativeness of the aliquot). Issues of hygroscopic samples were addressed similarly to the M determination. Temperature at the point of removal from the chamber was between 60-70°C. Weight measurement precision at the nearest 0.0001 g. Ash content of the filters and the selective dissolution residue necessary for the $\chi_{B,daf}$ calculation was determined on duplicates. The filters were measured as practically 100% w/w_{ar} in ash content.

Calibration and quality control

The furnace temperature profile has been optimised through initial directions to the manufacturer and subsequent fine-tuning in the laboratory, to achieve close conformance with the specifications stipulated in the recent CEN SRF guidance DD CEN/TS 15403:2006³³². Firstly, the power rate was set and checked by the manufacturer to achieve the 250°C plateau. The slight overshooting observed was addressed in the final settings by introducing a slower rate of temperature increase just before the plateaus to be reached. Hence, eventually the furnace gradient has been set at: 3°C min⁻¹ to 200°C; 15 min plateau; 1°C min⁻¹ to 250°C; 60 min plateau; 3°C min⁻¹ to 520°C; 1°C min⁻¹ to 550, 240 min plateau; progressive cooling to 60°C; further cooling until stabilised in a desiccator (overall ca 24 h), was applied. Visual inspection of the ashes revealed no presence of soot, indicating complete combustion for every type of material fraction used. No sign of ignition was detected. For certain series of determinations, suitable GAS samples were used as internal standards: a consistent performance of ashing was verified.

4.13.3 *Total carbon, nitrogen and hydrogen content*

Materials and method - instrumentation

The concurrent determination of total carbon (TC), total hydrogen (TH) and total nitrogen (TN) was performed by a Vario EL III (Elementar, Hanau, Germany) CHNS-O element analyser instrument, following the guidance of the relevant CEN DD³³³. The advantages of using elemental analysers are high throughput, accuracy, reproducibility and convenience in sample preparation and results monitoring. A rudimentary description of the measuring principle, apparatus configuration and technical specifications can be found in the relevant technical note³³⁴. The determination is achieved through catalytic tube combustion of the samples in an oxygenated CO₂ atmosphere at elevated temperatures (ca 1800°C), which converts the organic substances into combustion products. Gasses flow through the system with the help of helium as the carrier gas. Interfering (“foreign”) gasses such as volatile halogens are removed from the combustion gases and the elements to be measured are isolated by specific adsorption columns and quantitatively determined consecutively by a thermal conductivity detector (TCD). The instrument was operated for simultaneous determination of total quantities of each of C, H, and N.

The amount of samples is limited by the maximum absolute quantities tolerable for these elements, notably C being the limiting factor (30 mg C). This resulted in suitable sample sizes in the order of magnitude of some tens of mg. Typically, aliquots of ca 25 mg were used. An intermediate aliquot of the GAS of less than 500 mg was dried for ca 2 h at 105°C to directly obtain readings on a dry basis and remove any H present as moisture content for which correction can be otherwise difficult, according to the stipulations of CEN/TS 15407:2006³³³. Test portions were sampled from the dried material and rapidly packed into tin boats of suitable size (Elementar, Hanau, Germany), to avoid re-absorbance of moisture of the highly hygroscopic samples. The

loaded boats were packed as air-tightly as feasible, to avoid systematic errors due to the potential inclusion of atmospheric N and H. The net weight of samples was determined by difference (tare) and the value was introduced manually into the Vario EL III software interface, enabling to directly report results of concentrations in the dry sample (d basis of reporting). Each determination took around 15 mins to complete and the overall capacity of the consumables limited the consecutive determinations to ca 70 runs.

Calibration

A matrix-free, multiple-point instrument calibration was used to achieve long-term stability of its performance. As CEN/TS 15407:2006³³³ suggests, acetanilide certified reference materials with increasing concentrations of C,H and N was used as calibration standards.

Quality control

The instrument is capable of automated quality control. Adjustment for the day-to-day performance variability was made through the use of daily correction factors (CF). During the starting up process for each determination day/batch, 5 samples of acetanilide CRM were run, the 3 last of which were used for computing the daily CF values: these are the ratios of the nominal certified values for C, H, and N for acetanilide, over the measured ones. These CFs were subsequently applied to every raw reading to convert it to remove any systematic error introduced by the instrument. The instrument supplier advises the acceptance of 5% tolerances for the C,H,N determination. Practice shows that the particular instrument performs satisfactorily, meeting this criterion. This correction however was made once initially and then applied to all subsequent measurements (as the instrument is meant to be operated), assuming any bias remains unchanged during the whole batch of determinations (up to 70). Hence, in order to check that the measurement process remained under control

throughout the day/batch, additional aliquots of acetanilide were run at regular intervals.

4.13.4 *Calorific (heating) value*

Background on determination

Calorific (or heating) value (Q) is empirically defined (BS 7420:1991)³³⁵ as the amount of heat released during the complete combustion of a fuel under specific conditions, the most useful settings considered at a defined pressure and at a reference temperature. Calorific (or heating) values can be directly determined by calorimetric methods or indirectly computed by inferential methods, such as correlation to ultimate and proximate analysis data³³⁶. The acceptable standard for direct determination is the 'oxygen-bomb' combustion method. In this method, the sample fuel is combusted in a bomb calorimeter immersed in water, and the rise in the water temperature is measured. Note that for the complete combustion of solid samples, such as SRF and the rest MBT-related streams, higher pressures are necessary than the atmospheric: this is accounted for in the instrument calibration computations or it is neglected, if appropriate. So measured a calorific value is determined under constant volume and any water formed is released in the liquid phase. The resultant measurand is termed 'gross calorific value' (or 'higher heating value') (Q_{gr}), at constant volume (denoted $_v$) ($Q_{gr,v}$). The term 'gross' (or 'higher') signifies the liquid phase of water liberation, which means that this quantity includes the water vaporisation latent heat³³⁵.

It is often useful to convert the measured $Q_{gr,v}$ to other calorific value quantities (as defined elsewhere³³⁵), to simulate better the actual fuel utilisation conditions. For example, the thermal recovery of solid fuels takes place under constant pressure, necessitating the conversion to such a basis (denoted $_p$)³²⁸. Typical derived quantity is the 'net calorific value' (or 'lower heating value'), (Q_{net}), in which the formed water is

considered in the gaseous phase; hence it equals the Q_{gr} , the water vaporisation latent heat been deduced. The constant pressure calorific values adds to the constant volume values the sum of energy which would have been released as work done by the atmosphere, under isothermal conditions, given constant pressure³³⁵. Note that the gross and net calorific values are empirical measurements and computations of the thermodynamic quantities 'specific energy of combustion' and 'specific enthalpy of combustion,' respectively.

The moisture content-related reporting basis of the result also can significantly affect the value for Q . Typically, some form of initial drying (bulk or air drying, denoted b or ad , respectively) would have been preceded the determination stage, hence the measurand is reported on this basis (e.g., $Q_{gr,v,ad}$). However, to draw meaningful comparisons a dry basis could be more useful (denoted d) or, to simulate the actual fuel production/use conditions, an as-fired or as-received reporting basis is suitable (denoted af or ar , respectively). Detailed information on the conversion formulas has been initially available for coal and coke (BS 1016-100:1994)³³⁷, and have been also repeated briefly for SRF (DD CEN/TS 15400:2006)³²⁸, directing to the recent draft for development for solid biofuels (DD CEN/TS 15269:2006)³²⁹. The initial standard BS 7420:1991 directs to further literature for the conversion between different reporting bases³³⁵.

The relevant guidance on calorific determination of SRF (DD CEN/TS 15400:2006)³²⁸ extensively covers the calorimeter apparatus and methodological details. The use of automated calorimeters is approved, given specific methodological conditions are met.

Materials and method – instrumentation/Calibration

Gross calorific values ($Q_{gr,v,b}$) of the MBT-related process streams and sub-fractions were determined in Knight Energy Services Ltd (KES) laboratories using an automated bomb calorimeter (IKA, C 7000; Staufen, Germany). Sub-fractions of the prepared GAS (bulk dried, SH0.5) were provided to KES in PP bags, from which aliquots of ca 1.000 g per determination were combusted in duplicate. The method is compatible with various standards including that of CEN for SRF (DD CEN/TS 15400:2006) and that of ASTM covering also soils and high-in-ash materials (ASTM D5865)³³⁸, which is relevant to some of the fractions analysed, particularly SP5 and fines sub-fractions of SPs. An automated calorimeter was used. Details on the apparatus, calibration and SOP followed are presented in the relevant KES document included in **Appendix E.2**.

Quality control

Quality control data for the period covering the determination of the samples available from KES is included in the QC **Appendix E.2**. In addition, determination performance was verified by blind determination of suitable CRM: wood fuel (NJV 945).

4.13.5 Biogenic content by selective dissolution

Background on determination

Because the importance of the biogenic content (χ_B) has just recently emerged, its determination is still subject to research and development. The research efforts of the European Committee for Standardisation (CEN) have progressed through the stages of: (i) pre-normative research on standard development^{186, 208, 339}; (ii) the current practice on determination provided in the two CEN DD documents: DD CEN/TS 15440:2006³⁰⁹, covering selective dissolution and manual sorting methods and DD CEN/TS 15747:2008²⁴⁵, based upon existing standard analytical methods for the determination of the age of carbon by the ¹⁴C radioactivity; (ii) the issue of a 'draft

standard for development' (DD) (European Committee for Standardisation, 2006a; 2007); and (iii) a recently completed validation of the DD methods through the QUOVADIS initiative, but not yet incorporated into formal documents³⁴⁰⁻³⁴¹. The wider growing interest in analytical methods for the determination of biogenic content is reflected in current research output, with Fellner and Rechberger³⁴² developing further the ¹⁴C method; Mohn et al.⁶⁵ and Fellner et al.²⁴⁷ developing a method for in-situ on-line determination in EfW plants; and Staber et al.⁶⁶, 2008) reviewing the development and application of these methods so far.

Here, of practical relevance are the selective dissolution method (SDM) and the manual sorting method (MSM). Despite both methods offering surrogate empirical estimates for χ_B , the SDM is considered the most accurate^{66, 186, 208, 339} and is used in several SRF production plants and/or prior to thermal recovery. The ¹⁴C method is potentially applicable, and has the comparative advantage to provide a less empirical measurement than the SDM, but is not standardised and widely practiced yet in Europe, despite the relevant US ASTM standard³⁴³.

Hence, the SDM according to DD CEN/TS 15440:2006³⁰⁹ is selected here to measure the biogenic content of the MBT-related streams. Since it was developed targeting SRF-type of samples only, the application was investigated in preliminary investigation and in a separate study critically examining the assumed, but non-quantified, correlation between the SDM and MSM two methods for a wide range of MBT-streams plants, results reported elsewhere²⁹⁵.

The SDM stems from a biodegradability method, adjusted for the specific purpose during the pre-normative CEN research by TAUW^{186, 208, 339}. The SDM relies on the fact that biogenic origin materials dissolve and are oxidised more readily in acid

mixtures, whereas non-biogenic matter remains intact and can be recovered gravimetrically.

A clarification is necessary regarding the reporting basis of the biogenic content. Biogenic content χ_B as determined by the SDM can be expressed in a variety of ways, contingent on the specific uses and data demands. The measurement proposed in DD CEN/TS 15442:2006 applies to the concept of ‘pure biomass’ percentage by weight $\chi_{B,daf}$ (% w/w_{daf}), introduced therein. This expresses biogenic content on a dry, ash-free basis (denoted _{daf}), quantity which excludes any of the ash content structurally incorporated into the biogenic components of the sample. Indeed, the DD CEN/TS 15442:2006 B.1 formula can be re-arranged as:

$$\chi_{B,daf} = \left(1 - \frac{m_{res,d}}{m_{ts,d}} - \frac{m_{ts_ashed,d} - m_{res_ashed,d}}{m_{ts,d}} \right) \times 100 \quad [4-2]$$

where, (all variables are expressed as percentages)

$m_{res,d}$ dry mass of dissolution residue

$m_{ts,d}$ dry mass of test sample

$m_{ts_ashed,d}$ dry mass of ashed test sample

$m_{res_ashed,d}$ dry mass of ashed dissolution residue

hence,

$\frac{m_{ts_ashed,d} - m_{res_ashed,d}}{m_{ts,d}}$ part of the ash content of the test sample (denoted _{ts}) that has dissolved during the application of the acids

The rest un-dissolved part of the ash content present in the sample reports in

the residue (denoted _{res}) and is deduced through the term $\frac{m_{res,d}}{m_{ts,d}}$. This correction attempts to overcome the difficulties arising from the fact that the test sample contains

ash content stemming from all three biogenic, non-biogenic and inert sub-fractions, and each of them partly dissolved during the acid digestion, as the evidence verifies (**Figure 5-68**). Whilst the expression of χ_B on a daf basis overcomes the uncertainty pertaining to the ash content, it underestimates the mass percent of the biogenic materials, in the tested sample, which clearly includes an ash residue. Indeed, the ash portion of χ_B is not combustible, not contributing to the energy production during its thermal recovery; however, it constitutes a natural part of the biogenic material, when expressed on a mass basis. These complexities are further elaborated by the researcher elsewhere²⁹⁵.

Other potentially useful ways to express the biogenic content are: (i) in percent by calorific value; and (ii) in percent by total carbon. These demand further testing of the SD residue and are not examined further here.

Materials and method - instrumentation

For the purpose of this research a rig was set up to perform the SM according to the stipulations of the DD CEN/TS 15442:2006³⁰⁹. Any attempted improvements constituting departures from the standard and specific choices are explained. The SDM was performed in duplicate aliquots of the GAS. For each replicate, an aliquot of 5.000 ± 0.050 g from the GAS was weighed to 4 decimal places and inserted into Erlenmeyer flasks. In a fume cupboard, 150 mL of 84% w/w H_2SO_4 (prepared from >95% w/w, analytical grade; Fisher Scientific, Loughborough, UK) was accurately added using a bottle dispenser. The slightly higher concentration than advised by the standard (78% w/w H_2SO_4) has the advantage of being easily prepared from commercially available concentrations. Flasks were gently stirred to impregnate the powder, and the mixture left to react for 16 h under slight continuous agitation achieved using an IKA KS60 mechanical orbital shaker (50 rpm; Staufen, Germany). Hydrogen peroxide (35% w/w analytical grade, Acros Organics, Geel, Belgium) was added by

bottle dispenser in three 10 mL aliquots, separated by ca 10 min, whilst submerging flasks in a 3 cm deep water/ice cooling bath to control the rate of reaction and avoid the deposition of material on the flasks walls. Mixtures were left to digest for 5 h, before 300 mL deionised water was added. The final solution and floating solid residue was filtered through a pre-weighed dried Whatman GF/B \varnothing 90 mm glass microfibre filter (Maidstone, UK) into a Büchner funnel and rinsed with ca 400 mL of deionised water to a final pH of ≥ 3.0 . Whole filters with the residue were dried at $105 \pm 2^\circ\text{C}$ for 24 h according to the M_r determination method (**Section 4.13.1**), weighed, and kept in air-tight plastic containers at ambient temperature before ashing according to the A method (**Section 4.13.2**). The selective dissolution process is described in further detail in the relevant SOP (**Appendix C.4.1**).

Calibration and quality control

Grinding to a size of < 1 mm was sufficient for the SDM. This is supported by both the QUOVADIS validation study³⁴¹, indicating no significant difference for χ_B between samples prepared at < 1 and < 0.5 mm; and our preliminary investigation: (2^2) statistically designed experiment (for fully shredded SRF LOT3, factors: (i) SH, levels: SH1, SH0.5; (ii) level of non-Fe contamination, levels: high (H) and low (L). (Results not reported). In the absence of readily available suitable CRMs no direct evidence can be drawn on the accuracy of the determinations. Certain CRMs have been prepared during the QUOVADIS validation study, but they are not commercially or otherwise accessible. Notably, in QUOVADIS the difficulty of evaluating the method ruggedness in the absence of a reference method is indirectly addressed by comparing the SDM with the MSM. The comparative investigation of the SDM and MSM, performed in parallel with this research²⁹⁵ has shown satisfying agreement for a simplified, dry mass basis χ_B , evidence which supports the general feeling of acceptable accuracy for the SD method, unless both methods suffer a bias of similar direction and magnitude.

4.13.6 *Total chlorine content*

Background on determination

Concentration in chlorine is a key parameter for SRF quality. Elevated levels of chlorine in SRF are a source of concern, particularly for high temperature corrosion, high hydrogen chloride (HCl) emissions and potential formation of dioxins during its thermal recovery^{179, 219, 223}, as explained in **Section 2.5.4**. Hence, [Cl] was selected by CEN as the indicator property for technical performance of SRF²⁵⁹ (**Section 2.5.3**). A determination method adapted to SRF has undergone development²⁰⁸, leading to a draft for development (DD CEN/TS 15408:2006)³⁴⁴, currently under validation³⁴¹. There, oxygen combustion methods³⁴⁵ are proposed for the oxidation of Cl to chlorides and dissolution in an absorption medium, followed by instrumental determination, typically using ion chromatography (IC). IC can determine the Cl along with other anions of interest for secondary fuels, such as sulphides³⁴⁶. The oxygen bomb combustion technique uses high temperature range (1000-1500 °C) and increased gas pressure to completely oxidise the organic chlorine into chlorides. Alternatively, entirely instrumental methods could be used, but suitability has to be demonstrated.

Despite this, there remain challenges with unbiased determination of total chlorine in MSW-derived samples^{58, 178, 347}. Total chlorine content comprises two parts: inorganic salt (e.g., as in common household salt) and organically bound chlorides (e.g., as in PVC plastics). The various determination methods are performing dissimilarly in quantifying these two parts. The combination of oxygen bomb combustion with IC underestimates the inorganic salts, compared to the elution test followed by Schoeninger combustion; the elemental analysers are more accurately determining the organic part^{178, 347}. There remains a need for an accurate, rapid and standardised method to measure total chlorine (and its speciation) in MSW-derived samples, SRF included¹⁷⁹.

Materials/Method – instrumentation

Total chlorine content [Cl] (% w/w_d) on MBT process samples was determined using the established two-step oxygen bomb combustion - IC methodology, in line with the European SRF standard DD CEN/TS 15408:2006³⁴⁴. Oxidation and dissolution was performed by oxygen bomb combustion (Knight Energy Services Laboratories Ltd) using ca 1 g of aliquots of the GAS. This was shredded to 0.5 mm to improve the Cl recovery²⁰⁸ and bulk dried. Three replicates were combusted for the 15 entirely shredded SRF (L3) and the second lot (L2) samples, and 2 replicates for the rest samples (L1, and pure waste components). Given that the anticipated concentrations were <1% w/w high purity de-ionised distilled water (DDW) water was used as the absorbent medium in agreement with DD CEN/TS 15408:2006³⁴⁴. This might have introduced a limited underestimation of the concentration of certain pure waste component samples (plastics and shoes). Solutions were, transferred to 125 mL sterile polypropylene (PP) bottles with polyethylene (PE) screw cap sourced by Fisher Scientific (Loughborough, UK); and stored in darkness, at 4 °C.

Total chlorine content in the solutions was determined as Cl anions using high performance ion chromatographer (HPIC) (DIONEX DX-600; Sunnyvale, USA)³⁴⁸, equipped with a ED50A electrochemical detector (typical background conductivity at ca 24 µS), GS50 low delay series pump, and 4 mm IonPac AS9-HC analytical column operated at 250 µL sample loop volume, using 10.0 mM carbonate/5mM bicarbonate eluent at 1.0 mL min⁻¹. Given the consistent performance of the HPIC, a single determination run was performed per combusted aliquot.

Calibration and quality control

An 8-point external calibration performed satisfactorily lineally ($R^2 > 99.5$), an example is shown in **Appendix E.1**. Calibration standards were prepared from 1000 ppm Cl calibration standard for IC (Fisher Scientific; Loughborough, UK); batch number

was retained to guarantee traceability. Solutions were made using high purity DDW, supplied by an ELGA Ultrapure Genetic purification system (resistivity at 25°C: 18MΩ-cm) (Marlow, UK). Quality control was applied. Method blanks showed no evidence of contamination – the (negligible) average concentration level of the method blanks (0.097 mg L⁻¹) was deducted from the determined values. Limit of detection (LoD) and method limit of quantification (LoQ)³⁴⁹⁻³⁵⁰ were determined using 7 replicate determinations of the method blanks: all samples were well above LoQ. A 5 mg L⁻¹ standard solution was run as an internal quality control standard every 10 determinations to check for consistent HPIC behaviour. Overall recovery (oxygen combustion and HPIC) was checked through the use of CRMs³⁵¹ (Lyophilised brown bread - BCR 191); performance of the HPCI alone was assured through the run of selected spiked sample solutions. Chromatogram peaks were sufficiently symmetrical: examples are provided in **Appendix E.1**.

5 RESULTS

5.1 European MBT-derived SRF: statistical overview of quality

Results related to key technical, environmental and economic aspects of European, MBT-derived RDF/SRF quality are summarised in **Table 5-1**. Box-plots are used to graphically represent the main findings (**Figure 5-1** to **Figure 5-7**). Data collection and statistical analysis methodology is explained in **Section 4.12.1**.

Results are generally within the expected range and mutually consistent. The p_{80} values are higher than the median values, with certain exceptions, such as the maximum values of [Hg] reported on a mass basis. The %CV ranged from 13.1% for the location of $Q_{net,p,ar}$, to 95.9% for the location of [Cu].

The location of median $Q_{net,p,ar}$ (**Figure 5-1**) falls within the range of Class 3 of the proposed CEN classes, with the lower and upper quartiles being at $15.4 \text{ MJ kg}_{ar}^{-1}$ and $16.8 \text{ MJ kg}_{ar}^{-1}$ respectively, showing a narrow spread. The location of M medians (**Figure 5-2**) is at $13.4\% \text{ w/w}_{ar}$, with the maximum value being more than three times the IQR higher than the upper quartile ($Q3 = 14.2\% \text{ w/w}_{ar}$) (hence, depicted as an extreme value (star) in the box-plot). The A location of medians (**Figure 5-2**) is at $21.1\% \text{ w/w}_d$, but the upper quartile reaches as high as $25.1\% \text{ w/w}_d$.

The central tendency of [Cl] median values is at $0.50\% \text{ w/w}_d$, and the maximum reported location value is at $1.05\% \text{ w/w}_d$ (**Figure 5-3**). A hypothetical SRF with the same value would have been classified as Cl class 2.

Table 5-1 Results on statistical analysis of MBT-derived RDF/SRF data-series

Input data property and statistic	Designation of relevant property	Units	Output statistic				Data quality				Equivalent, hypothetical CEN classification
			Max	Q3	Median	Q1	Min	N	Median s-Means	%CV	
Location of moisture content	MC	% w/W _{ar}	24.4	14.2	13.4	12.0	11.7	8	5-3	28.8	
Upper limit (p ₈₀) of moisture content	MC	% w/W _{ar}	31.5	n.a.	19.8	n.a.	15.1	4	n.a.	28.8	
Location of ash content		% w/W _{ar}	26.1	18.7	17.7	16.6	11.9	6	4-2	25.3	
Location of net calorific value _{ar}	Q _{net,p,ar}	MJ kg _{ar} ⁻¹	19.9	16.8	16.3	15.4	13.0	8	5-3	13.1	CEN class for hypothetical SRF with same mean*** value as the median location: 3
Location of net calorific value _d	Q _{net,p,d}	MJ kg _d ⁻¹	28.3	24.33	22.60	20.27	16.50	8	6-2	18.8	
Upper limit (p ₈₀) of net calorific value _d	Q _{net,p,d}	% w/W _{ar}	37.22	n.a.	26.47	n.a.	18.62	5	n.a.	25.7	
Location of chlorine	[Cl]	% w/w _d	1.05	0.72	0.50	0.42	0.29	13	9-4	40.0	CEN class for hypothetical SRF with same mean*** value as the median location : 2
Upper limit (p ₈₀) of chlorine	[Cl]	% w/w _d	1.11	1.00	0.98	0.53	0.39	7	n.a.	36.9	
Location of sulphur	[S]	% w/w _d	0.40	0.33	0.24	0.20	0.18	6	3-3	32.9	
Location of arsenic	[As]	mg kg _d ⁻¹	4.0	3.4	1.1	0.7	0.5	8	4-4	78.6	
Location of cadmium	[Cd]	mg kg _d ⁻¹	2.6	2.2	1.8	1.2	0.4	8	4-4	47.3	
Location of chromium	[Cr]	mg kg _d ⁻¹	192	90	78	60	40	11	6-5	49.8	
Location of copper	[Cu]	mg kg _d ⁻¹	694	448	198	73	14	10	6-4	95.9	
Location of lead	[Pb]	mg kg _d ⁻¹	230	208	152	88	71	8	0-8	48.3	
Location of mercury (mass basis)	[Hg]	mg kg _d ⁻¹	1.50	0.75	0.43	0.33	0.15	12	9-3	71.4	
Upper limit (80th percentile) of mercury (mass basis)	[Hg]	mg kg _d ⁻¹	1.11	0.80	0.53	0.38	0.22	7	n.a.	51.1	

Input data property and statistic	Designation of relevant property	Units	Output statistic				Data quality			Equivalent, hypothetical CEN classification	
			Max	Q3	Median	Q1	Min	N	Median s-Means		%CV
Location of mercury (energy basis)	[Hg]	mg MJ _{ar} ⁻¹	0.040	0.037	0.023	0.014	0.009	6	5-1	53.6	CEN class for hypothetical SRF with same median and 80 th P value: 2
Upper limit (80th percentile) of mercury (energy basis)	[Hg]	mg MJ _{ar} ⁻¹	0.045	n.a.	0.024	n.a.	0.009	4	n.a.	47.7	
Location of nickel	[Ni]	mg kg _d ⁻¹	97	40	28	24	18	9	4-5	66.4	
Upper limit (80th percentile) of GEN SRF sum of "heavy metals"	[Σ(Sb,As,Cd, Cr,Co,Cu,Pb ,Mn,Hg,Ni,Tl ,V)]	mg kg _{ar} ⁻¹	1025	n.a.	795	n.a.	581	4	n.a.	23.5	

* Number of data entries (sets of data) that were used to calculate the related statistics affecting their reliability

** To estimate the location median values were used if available, otherwise arithmetic means: this column provides the exact numbers: depending on the skewness of the initial statistic of a certain property, use of means instead of medians could mean overestimation on the median output location (if the property is positively skewed, as is typical for waste) or vice versa.

*** Note that these classifications are based upon the mean and not the upper confidence interval around the mean, in the absence of the necessary data: hence they are not conservative. n.a.: not available

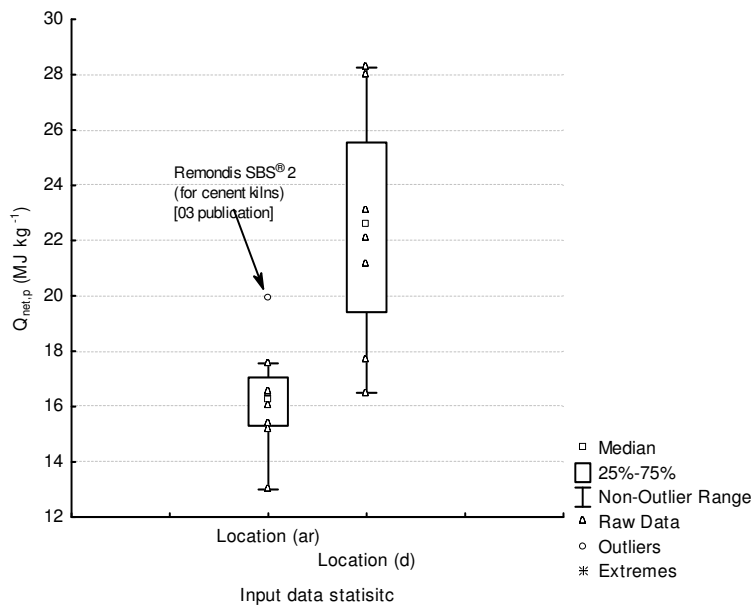


Figure 5-1 Results of descriptive, non-parametric statistical analysis on European MBT-derived SRF data: comparison of the of location values of $Q_{p,net}$ expressed on an as received (_{ar}) and dry (_d) basis. Box-plot conventions: (1): lower and upper lines of the boxes denote the 25th and 75th percentiles (Q1 and Q3 respectively); (2) lower outlier limit and upper outlier limit, denoted by whiskers, define the non-outlier range. This is here defined as the range of values that do not differ from the median more than the Q1 or Q3 plus 1.5 times the interquartile range (IQR = Q3-Q1) (height of box); (3) extreme values, presented as asterisks, exceed the Q1 plus 3 times the IQR. The values upon which statistics were computed are also plotted (raw data).

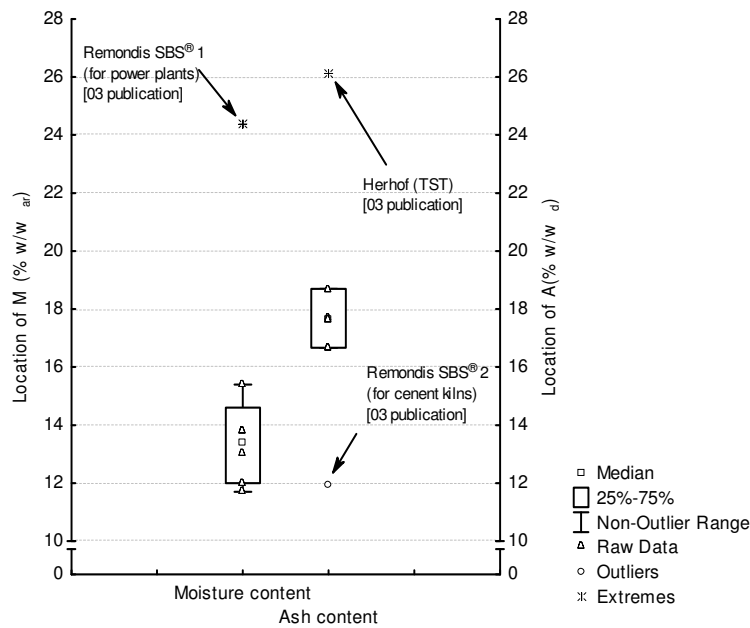


Figure 5-2 Results of descriptive, non-parametric statistical analysis on MBT-derived SRF data: 1. Location values of moisture content (M) expressed on an as received basis (_{ar}); and 2. Location values of ash content (A) expressed on a dry basis (_d). For box-plot conventions see **Figure 5-1**.

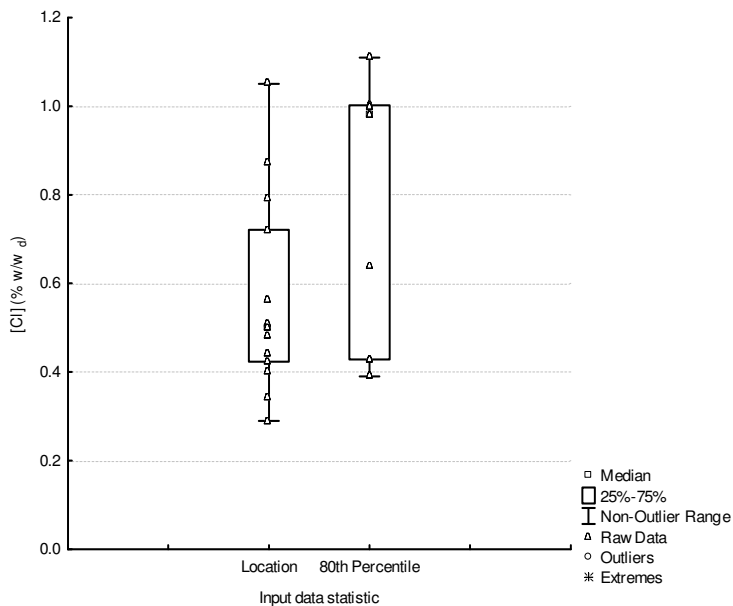


Figure 5-3 Results of descriptive, non-parametric statistical analysis on MBT-derived SRF data: comparison of location and p_{80} values of chlorine concentration [Cl], expressed on a dry basis (_d). For box-plot conventions see **Figure 5-1**.

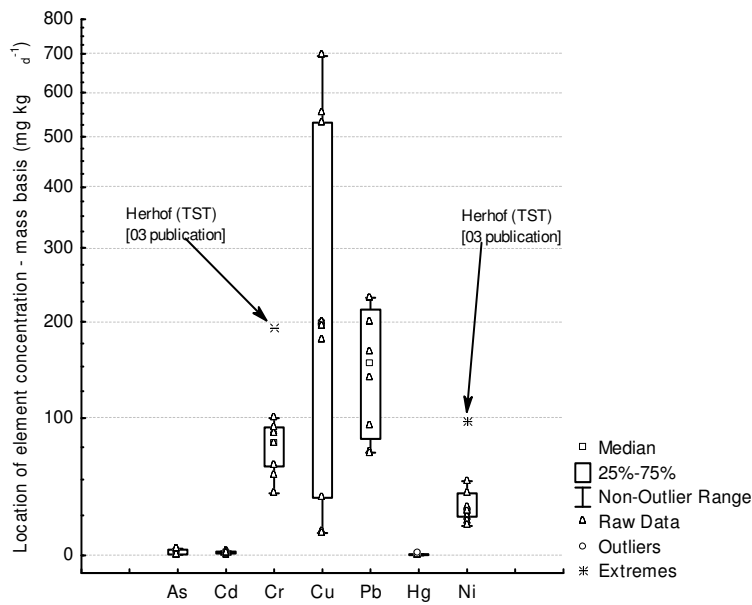


Figure 5-4 Results of descriptive, non-parametric statistical analysis on MBT-derived SRF data: comparison of location of concentration of trace elements, expressed on a dry basis (d). As, Cd and Hg are further compared in **Figure 5-5** using a suitable axis scale. For box-plot conventions see **Figure 5-1**.

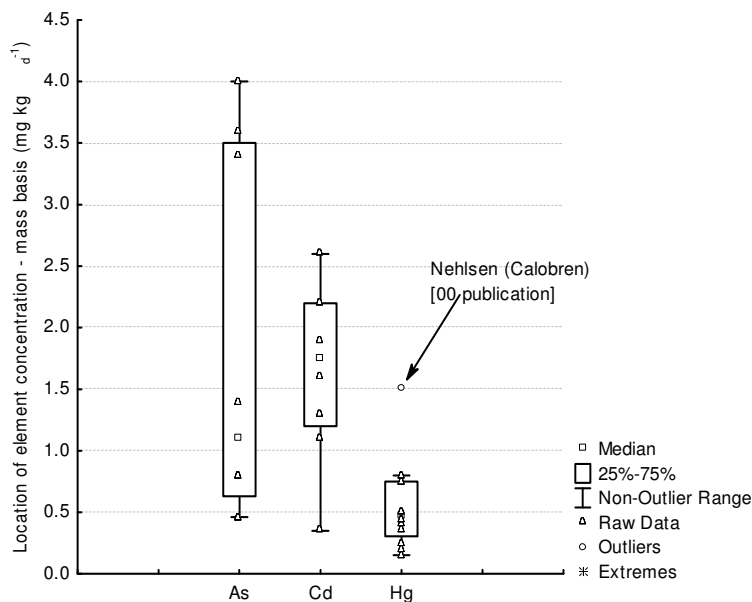


Figure 5-5 Results of descriptive, non-parametric statistical analysis on MBT-derived SRF data: comparison of location of concentration of certain trace elements, expressed on a dry basis (d). See **Figure 5-4** for comparison with more elements. For box-plot conventions see **Figure 5-1**.

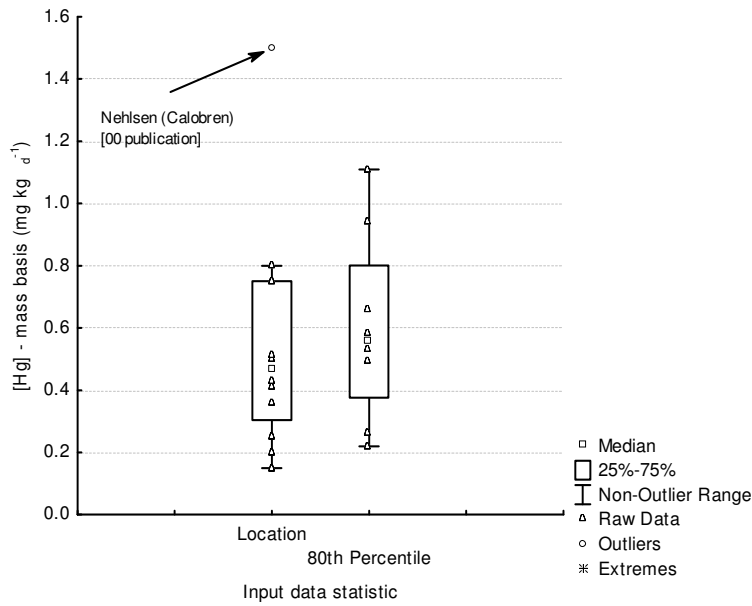


Figure 5-6 Results of descriptive, non-parametric statistical analysis on MBT-derived SRF data: comparison of location and p_{80} values of mass-based mercury concentration [Hg], expressed on a dry basis (_d). For box-plot conventions see **Figure 5-1**.

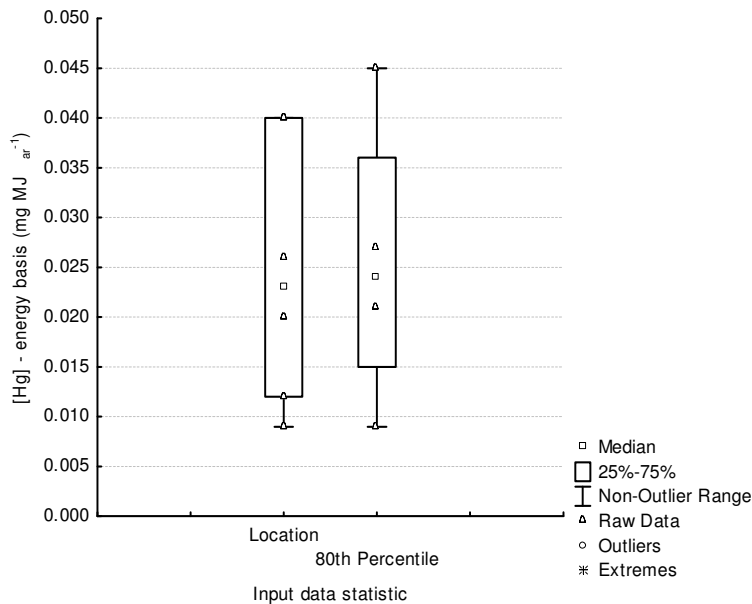


Figure 5-7 Results of descriptive, non-parametric statistical analysis on MBT-derived SRF data: comparison of location and p_{80} values of energy-based mercury concentration [Hg], expressed on an as received basis (_{ar}). For box-plot conventions see **Figure 5-1**.

Trace elements of concern in MBT-derived RDF/SRF (often termed 'heavy metals' or potentially toxic elements (PTE)) is presented in **Figure 5-4 - Figure 5-6** for those elements that enough data points were available. Levels are generally acceptable in most of the cases Indicative upper quartile of the location data: As: $Q3[As] = 3.4 \text{ mg kg}_d^{-1}$; Cd: $Q3[Cd] = 2.2 \text{ mg kg}_d^{-1}$; Cr: $Q3[Cr] = 90 \text{ mg kg}_d^{-1}$; Ni: $Q3[Ni] = 40 \text{ mg kg}_d^{-1}$; with Cu ($Q3[Cu] = 448 \text{ mg kg}_d^{-1}$ and Pb $Q3[Pb] = 208 \text{ mg kg}_d^{-1}$ reaching higher values. The %CVs for the PTEs is least at ca 50%. The spread of values varies considerably from element to element, as can be seen from their IQRs (**Figure 5-4**): e.g., the Cu values spread much greater than that of Cr. For, the p_{80} values are considerably higher than the median in many cases when the data sets for each plant are regarded.

For Hg, reported on mass basis (**Figure 5-6**), the location of medians is at $0.46 \text{ mg kg}_d^{-1}$ and location of p_{80} at $0.53 \text{ mg kg}_d^{-1}$. Reported on an energy basis (**Figure 5-7**), in agreement with the CEN classification system, location of Hg medians is at $0.023 \text{ mg MJ}_{ar}^{-1}$ and location of p_{80} is at $0.024 \text{ mg MJ}_{ar}^{-1}$, showing unexpectedly similar values. Hence, an equivalent imaginary SRF with same median and p_{80} values would have been cautiously classified as CEN Hg class 2.

5.2 UK MBT plant A: material composition and characterisation of flows

Material composition of all the sampled flows of the UK MBT plant A was identified by manual sorting (**Section 4.8**). The results are reported in **Appendix F**, from **Table_App F-1** to **Table_App F-14** and summarised in **Table_App F-16** along with their uncertainty. For flows that a valid material composition can be gained directly by manual sorting (biodried material, oversized heavy rejects) composition and non-parametric statistical analysis are presented. All other flows are affected by the

alteration of the fines by the secondary shredding and the trommel to a lesser degree. For these flows it has been necessary to reconstruct the correct composition through the material flow analysis of the plant. Hence, for these flows results come from the data reconciliation output, as applied to the processing section of the UK MBT plant A, detailed in **Table 4-7**. Identification of material with waste component categories is explained in **Table 4-5**. The processing section of the plant is shown in **Figure 4-2** and a schematic of it denoting flows, unit operations and sampling points according to the notation followed through this thesis in **Figure 4-5**.

In addition, each sample was characterised for a series of fuel-related properties, in line with the methods explained in **Section 4.13** and the results were statistically analysed according to **Section 4.12**.

From these data, here results are presented for the two most important flows, other than SRF: the biodried material which is the input to the processing section and the oversized heavy rejects, which constitutes the main reject fraction of the plant. The rest information is attached in **Appendix F (Figure_App F-1 to Figure_App F-16)**.

These results are not discussed separately, but comments are incorporated into various other sub-sections of the discussion chapter.

5.2.1 UK MBT plant A: overview of material composition of flows

Figure 5-8 presents a detailed breakdown of the material composition for the UK MBT plant A processing section. This summary is presented in detailed in a series of Shankey diagrams (from **Figure 5-27** to **Figure 5-52**), covering each waste component category (or sets of). **Figure 5-9** shows the average reconstructed percent composition of the input and output flows. It is clear the differentiation of the composition according to what materials the plant flowsheet tries to incorporate in each

output flow. With the exception of the oversized heavy rejects, visual inspection reveals that the highly heterogeneous biodried input is split into more homogeneous output fractions – which are the main objective of any MBT mechanical processing section.

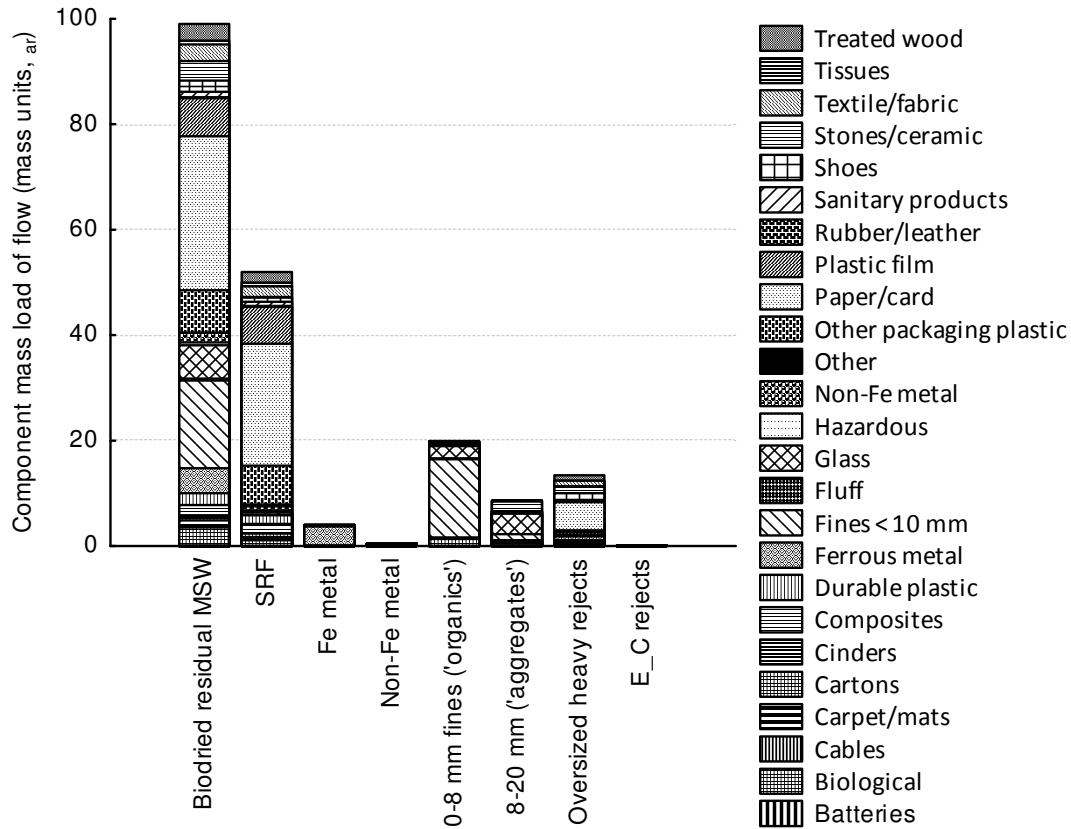


Figure 5-8 Material composition of the input and output flows of the UK MBT plant A processing section. Values are average specific (per component) mass load (a_r), out of ca 100 overall components mass input. Final results based on statistical analysis of the initial manual sorting results and subsequent modelling: (i) adjusting for changes during processing (e.g., increase of Fines <10 mm after trommel separation or secondary shredding) and (ii) balancing (reconciling) the flows through the material flow management software STAN2[®]. See **Figure 4-5** and **Table 4-7** for notation, assumptions and computation methodology.

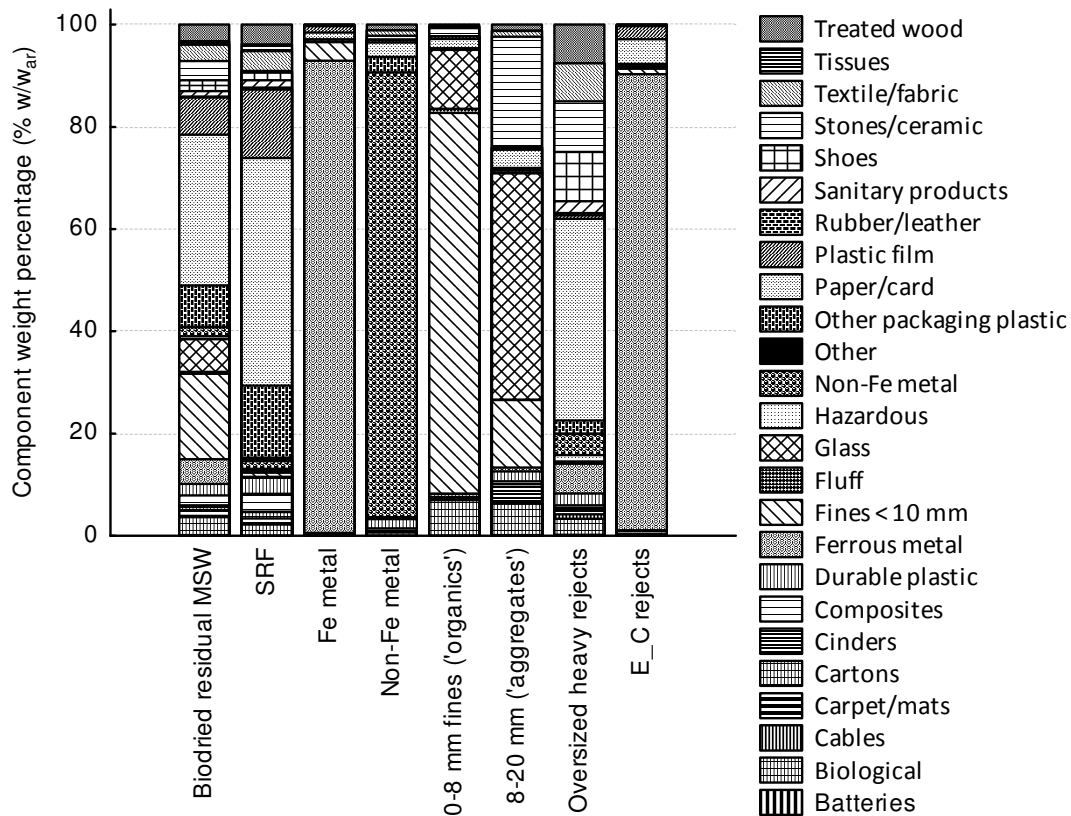


Figure 5-9 Material composition of the input and output flows of the UK MBT plant A processing section. Values are average mass percentages per component load (_{ar}). Final results based on statistical analysis of the initial manual sorting results and subsequent modelling: (i) adjusting for changes during processing (e.g., increase of Fines <10 mm after trommel separation or secondary shredding) and (ii) balancing (reconciling) the flows through the material flow management software STAN2[®]. See **Figure 4-5** and **Table 4-7** for notation, assumptions and computation methodology.

5.2.2 UK MBT plant A: biodried material characterisation

Three descriptions for the material composition of the biodried flow are provided here. **Figure 5-10** shows the raw data, as produced by manual sorting of the biodried flow samples. **Figure 5-11** presents the results of non-parametric statistical analysis of the data plotted in **Figure 5-10**. Notably, the median is capable of describing more robustly the average of components with sufficiently high percentage, but underestimates components with low percentage (i.e., those which constitute rare

occurrences within the magnitude of sampled mass). The paper/card and Fines <10 mm component categories dominate the biodried input.

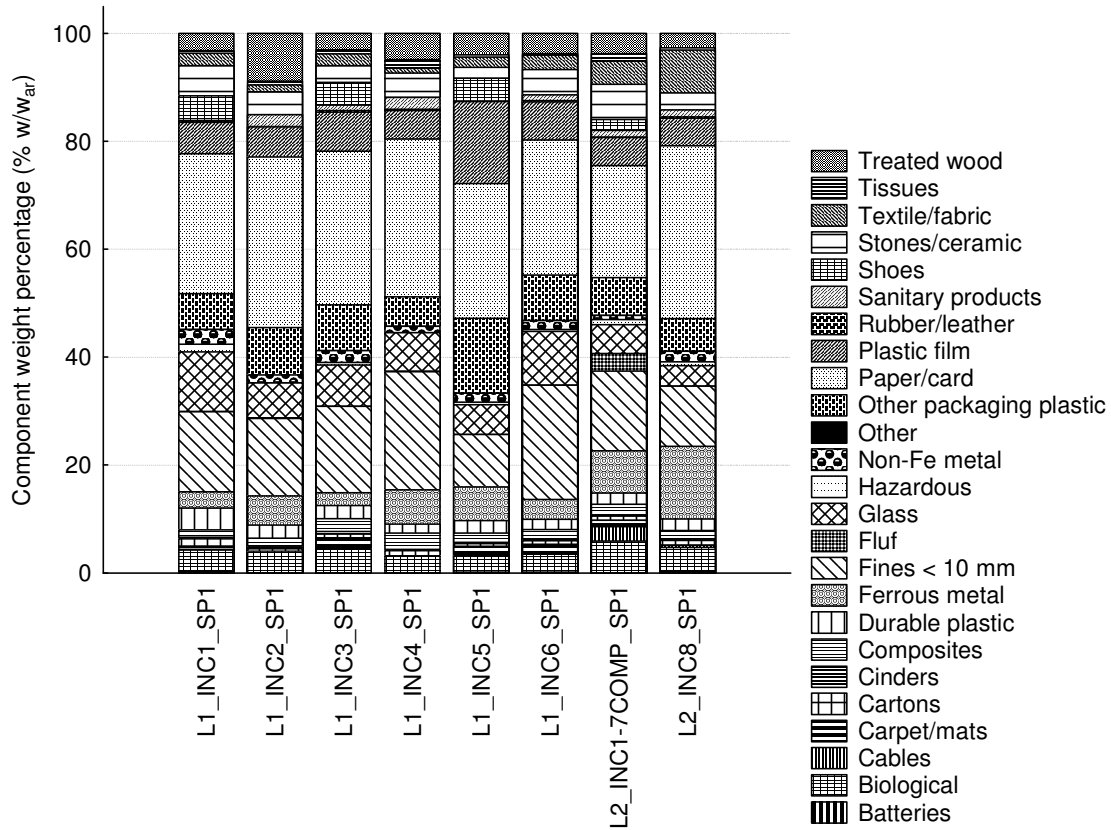


Figure 5-10 Material composition of the input to the processing section of the UK MBT plant A (residual MSW, shredded at 150-300 mm, and biodried) (SP1). Values (\bar{a}_r) of individual incremental samples, as identified by manual sorting. The between-samples variability is readily visualised.

Figure 5-12 presents the final reconstructed composition of the biodried material, which is in agreement with the composition of the all the other flows the plant, inner and output. Values are average mass percentages per component (\bar{a}_r) and total extended uncertainty (U_{95}). Final results based on statistical analysis of the initial manual sorting results and subsequent modelling (balancing (reconciling) of all the flows through the material flow management software STAN2[®]). A result of the

reconciliation is the narrowing of the U_{95} . Comparison with the **Figure 5-11** indicates that the two descriptions are compatible.

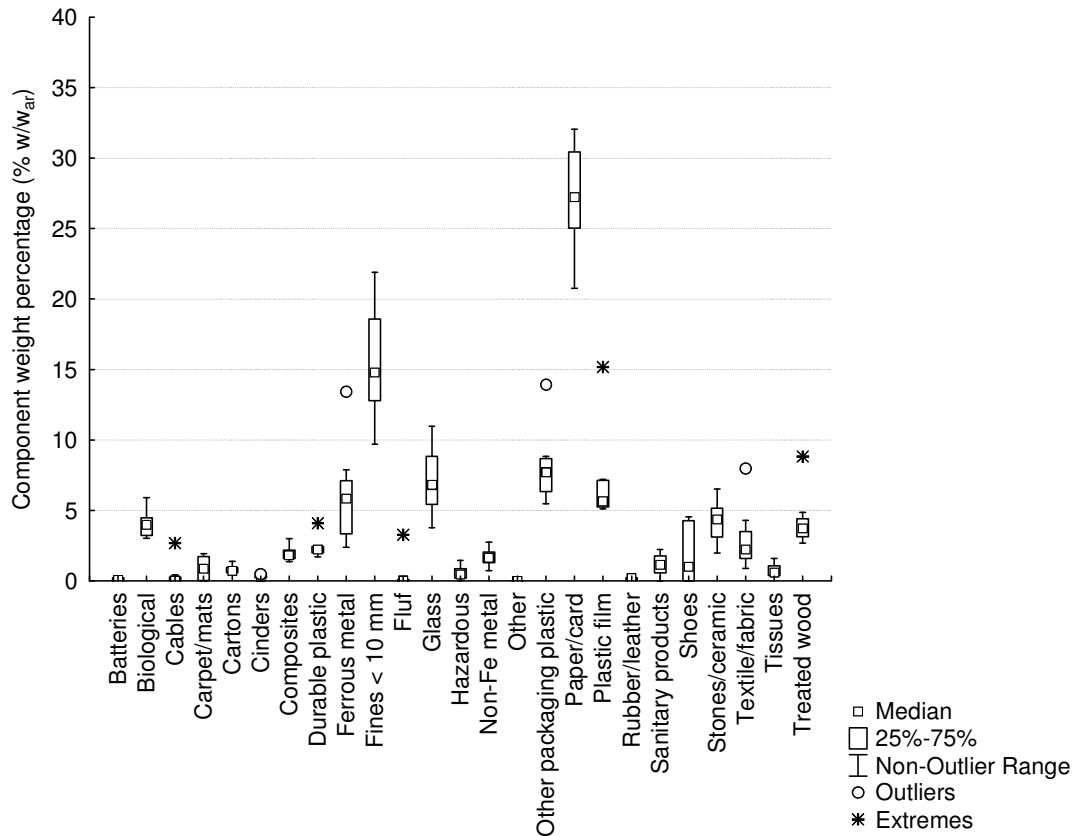


Figure 5-11 Non-parametric statistics on material composition of the input to the processing section of the UK MBT plant A (residual MSW, shredded at 150-300 mm, and biodried) (SP1). Values (w_{ar}), as identified by manual sorting. The median describes more robustly the average of components with sufficiently high percentage, but underestimates components with low percentage (i.e., those which constitute rare occurrences within the magnitude of sampled mass).

Table 5-2 shows statistics of fuel properties characterisation for the biodried fraction and the oversized heavy rejects. **Figure 5-13** to **Figure 5-15** plot and compare these characterisation results.

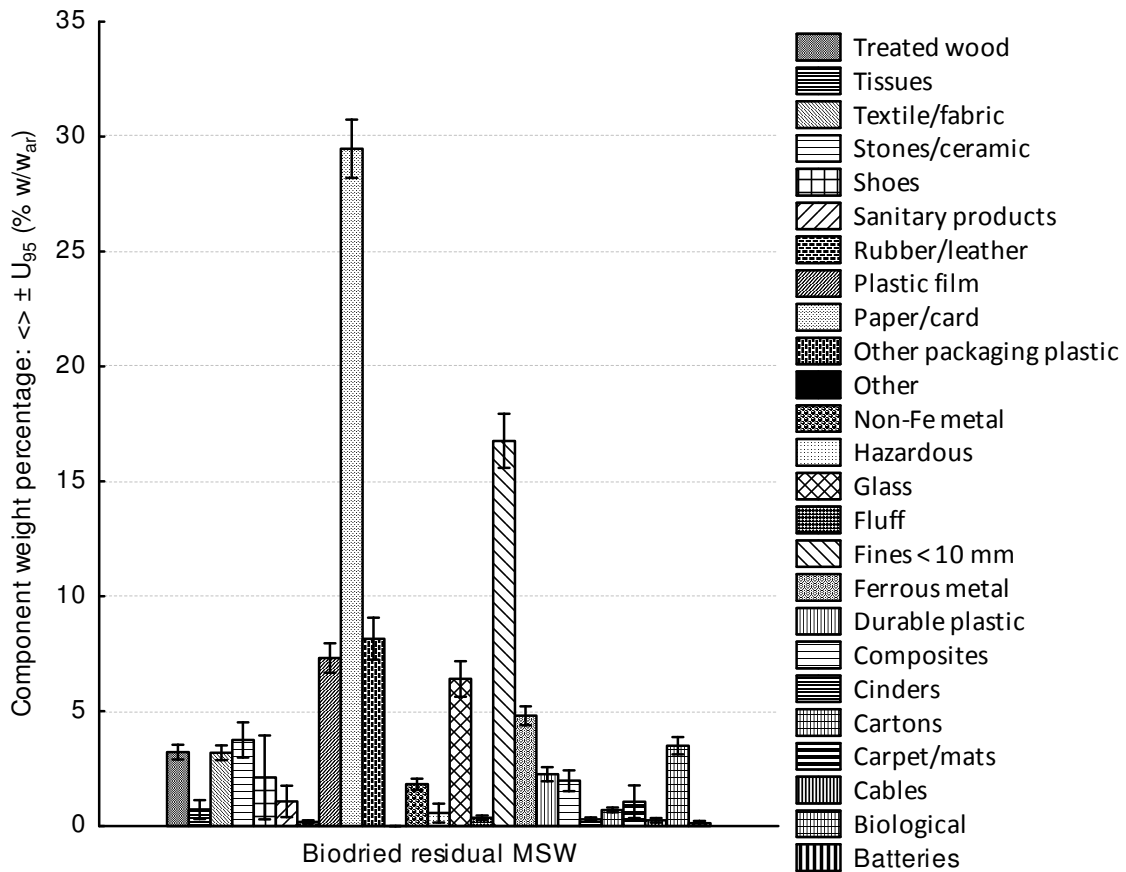


Figure 5-12 Material composition of the input to the processing section of the UK MBT plant A (residual MSW, shredded at 150-300 mm, and biodried) (SP1). Values are average mass percentages per component ($_{ar}$) and total extended uncertainty (U_{95}). Final results based on statistical analysis of the initial manual sorting results and subsequent modelling (balancing (reconciling) of all the flows through the material flow management software STAN2[®]). A result of the reconciliation is the narrowing of the U_{95} . See **Figure 4-5** and **Table 4-7** for notation, assumptions and computation methodology.

Table 5-2 Characterisation of biodried material and oversized heavy rejects for fuel properties. Arithmetic means ($\langle \rangle$) and total extended uncertainty ($\pm U_{95,v}$)

Sampling point		SP1		SP16	
Flow	Units	Biodried residual MSW		Oversized heavy rejects	
		$\langle \rangle$	$\pm U_{95,v}$	$\langle \rangle$	$\pm U_{95,v}$
$\langle M_T \rangle_{SHR,d}$	% w/w _d	14.4	4.6	17.8	6.2
$\langle M_T \rangle_d$	% w/w _d	13.4	5.5	14.8	5.7
$\langle A \rangle_{SHR,d}$	% w/w _d	28.2	8.2	19.8	4.2

Sampling point		SP1		SP16	
Flow	Units	Biordried residual MSW		Oversized heavy rejects	
$\langle A \rangle_d$	% w/w _d	44.4	6.9	35.6	9.9
$\langle X_B \rangle_{SHR,daf}$	% w/w _{daf}	51.1	16.1	67.21	7.49
$\langle X_B \rangle_{daf}$	% w/w _{daf}	39.4	12.2	53.6	15.4
$\langle Q \rangle_{gr,v,b}$	MJ kg _b ⁻¹	16.765	1.835	18.618	5.09
$\langle Q \rangle_{net,p,d}$	MJ kg _d ⁻¹	15.873	1.877	17.862	5.072
$\langle Q \rangle_{REC_net,p,ar}$	MJ kg _{ar} ⁻¹	14.773	1.178	17.165	1.503
$\langle Q \rangle_{gr,v,d}$	MJ kg _d ⁻¹	17.023	1.682	19.127	5.316
$\langle Q \rangle_{net,p,ar}$	MJ kg _{ar} ⁻¹	15.032	2.31	17.32	5.427
$\langle [CI] \rangle_{SHR,d}$	% w/w _d	0.61	0.42	0.93	1.89
$\langle [CI] \rangle_d$	% w/w _d	0.47	0.34	0.71	1.24

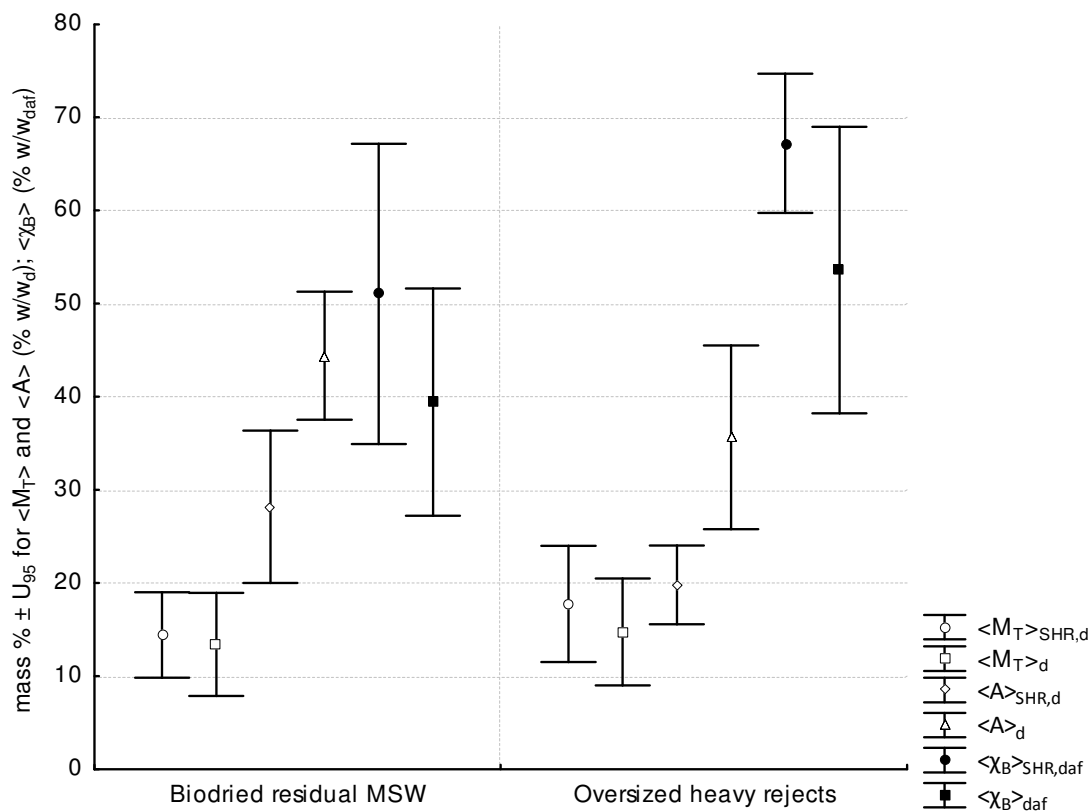


Figure 5-13 Average moisture content ($\langle M_T \rangle$), ash content ($\langle A \rangle$) and biogenic content ($\langle X_B \rangle$) and total extended uncertainties ($U_{95,v}$) expressed on various reporting bases for: (i) the of the biodried residual MSW (input to the processing section) ($v = 5$); and (ii) the oversized heavy rejects output of the UK MBT plant A ($v = 2$). Results for the A and M on dry basis, for X_B on dry, ash-free basis. Entire samples (no indication) and combustible (shreddable) part (_{SHR}).

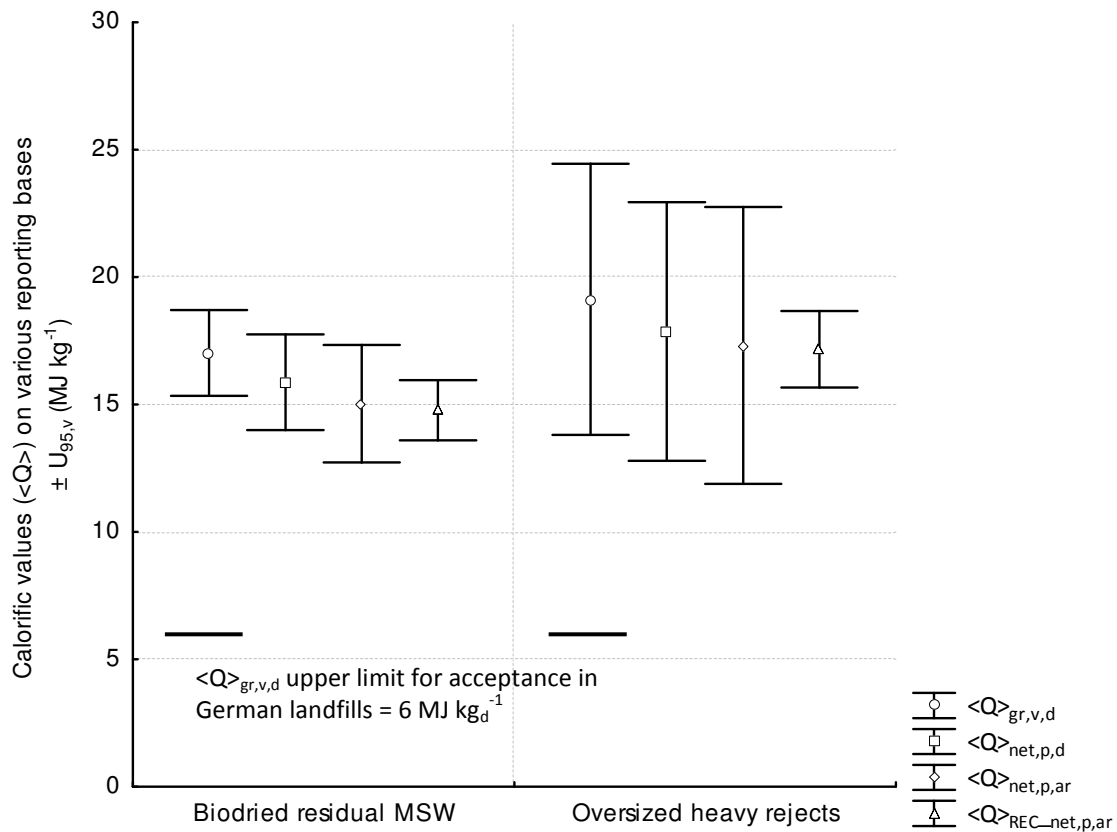


Figure 5-14 Average calorific values ($\langle Q \rangle$), and total extended uncertainties ($U_{95,v}$) expressed on various reporting bases for: (i) the combustible (shreddable) part of the biodried residual MSW (input to the processing section) ($v = 5$); and (ii) the oversized heavy rejects output of the UK MBT plant A ($v = 2$). Results for the net calorific value on as received basis are presented for both before ($\langle Q \rangle_{net,p,ar}$) and after ($\langle Q \rangle_{REC_net,p,ar}$) (**Figure 5-53**) the reconciliation procedure for all the plant flows. A side-effect of the data reconciliation is the narrowing of the uncertainty related to the average value, i.e., higher precision is achieved. All rest values without data reconciliation. The calorific value in the oversized heavy rejects is enriched compared to that of the processing section input, revealing a concentration of high-CV combustible waste components in this plant output.

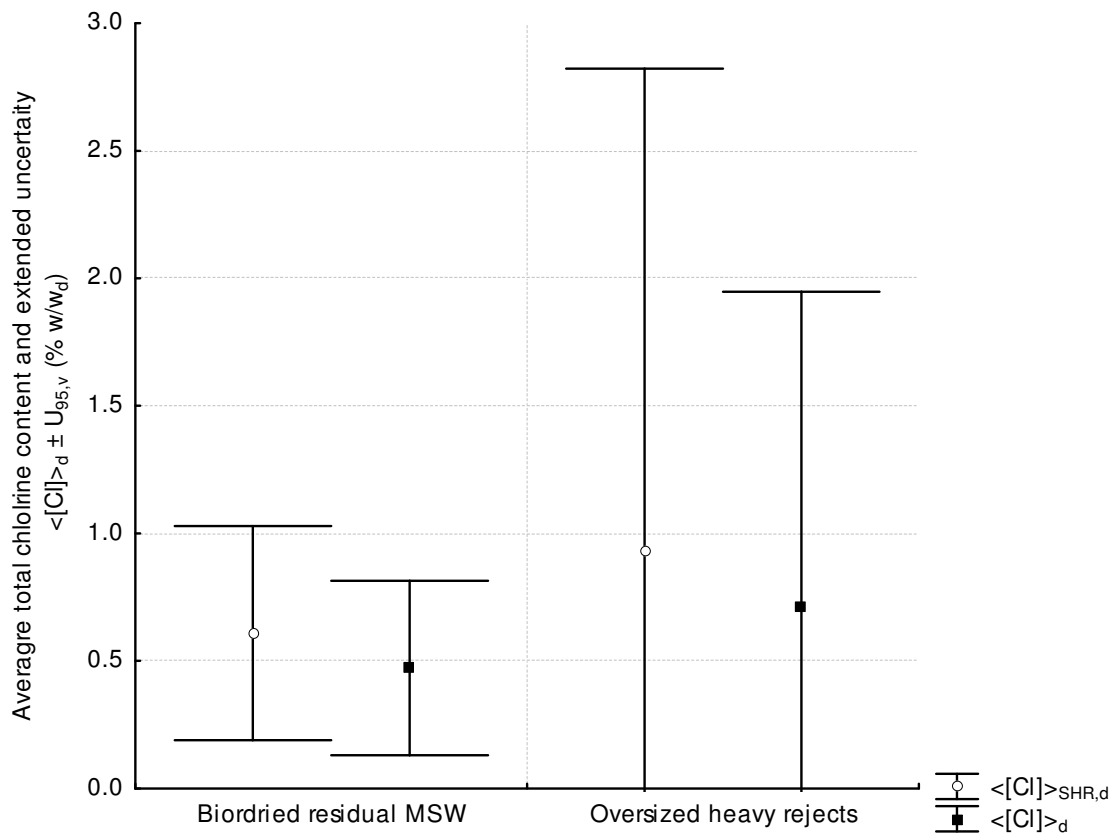


Figure 5-15 Average total chlorine content ($\langle [Cl] \rangle$), and total extended uncertainties ($U_{95,v}$) expressed on dry bases ($_d$) for: (i) the combustible (shreddable) part ($\langle [Cl] \rangle_{SHR,d}$) and (ii) the entire sample ($\langle [Cl] \rangle_d$) of the biodried residual MSW (input to the processing section) ($v = 4$); and the oversized heavy rejects output of the UK MBT plant A ($v = 2$). The concentration for the biodried material is within the range anticipated for MSW. Enrichment is evident to the oversized heavy rejects. The high variability of the oversized heavy rejects and the insufficient number of samples considered do not allow to precisely quantifying this.

5.2.3 UK MBT plant A: oversized heavy rejects characterisation

Similarly to the biodried material and oversized heavy rejects, 3 descriptions of the material composition of the oversized heavy rejects are provided here (**Figure 5-16** to **Figure 5-18**)

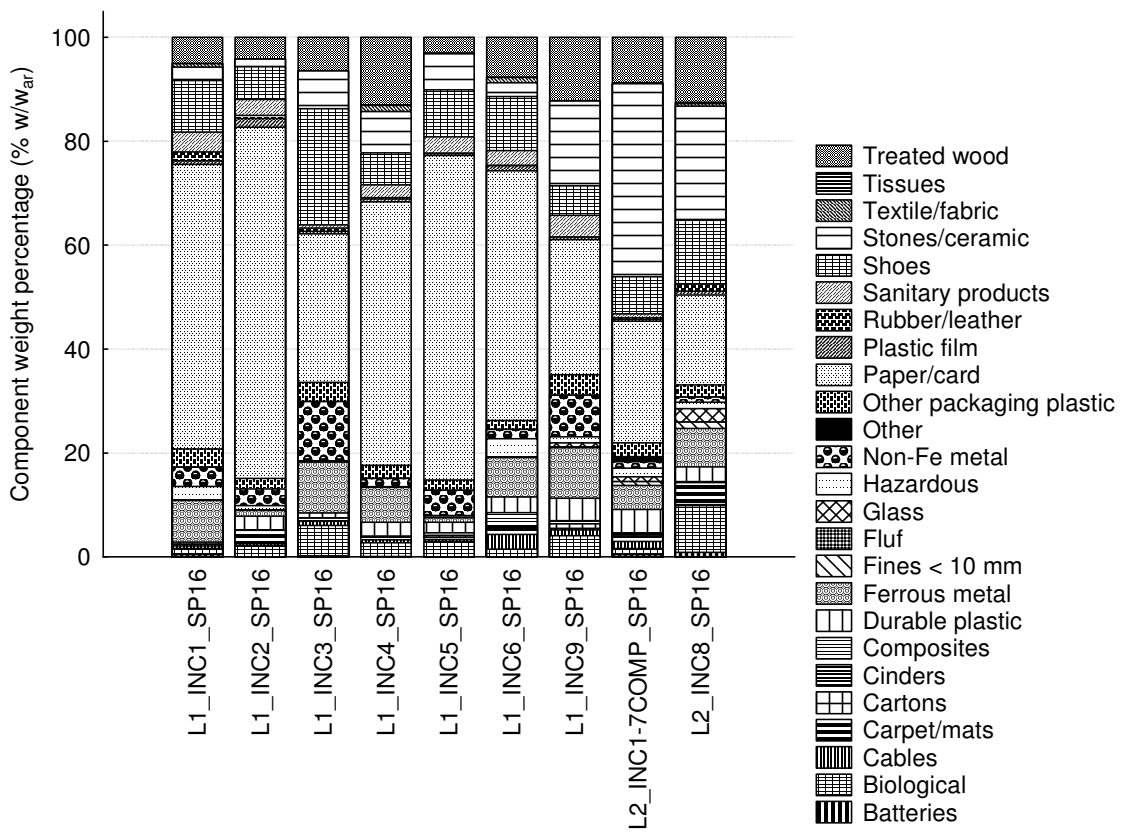


Figure 5-16 Material composition of SRF (SP13). Values (_{ar}) of individual incremental samples, as identified by manual sorting. The between-samples variability is readily visualised.

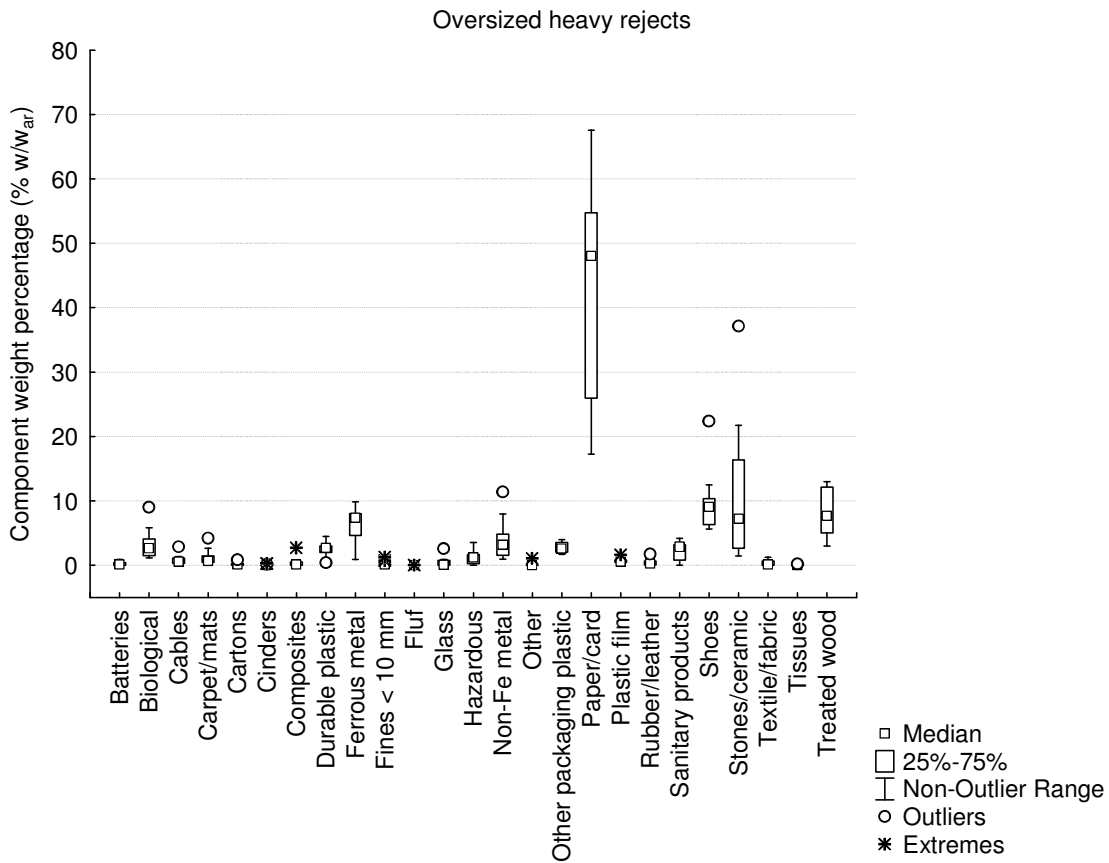


Figure 5-17 Non-parametric statistics of oversized heavy rejects (SP16). Values (w_{ar}), as identified by manual sorting. The median describes more robustly the average of components with sufficiently high percentage, but underestimates components with low percentage (i.e., those which constitute rare occurrences within the magnitude of sampled mass).

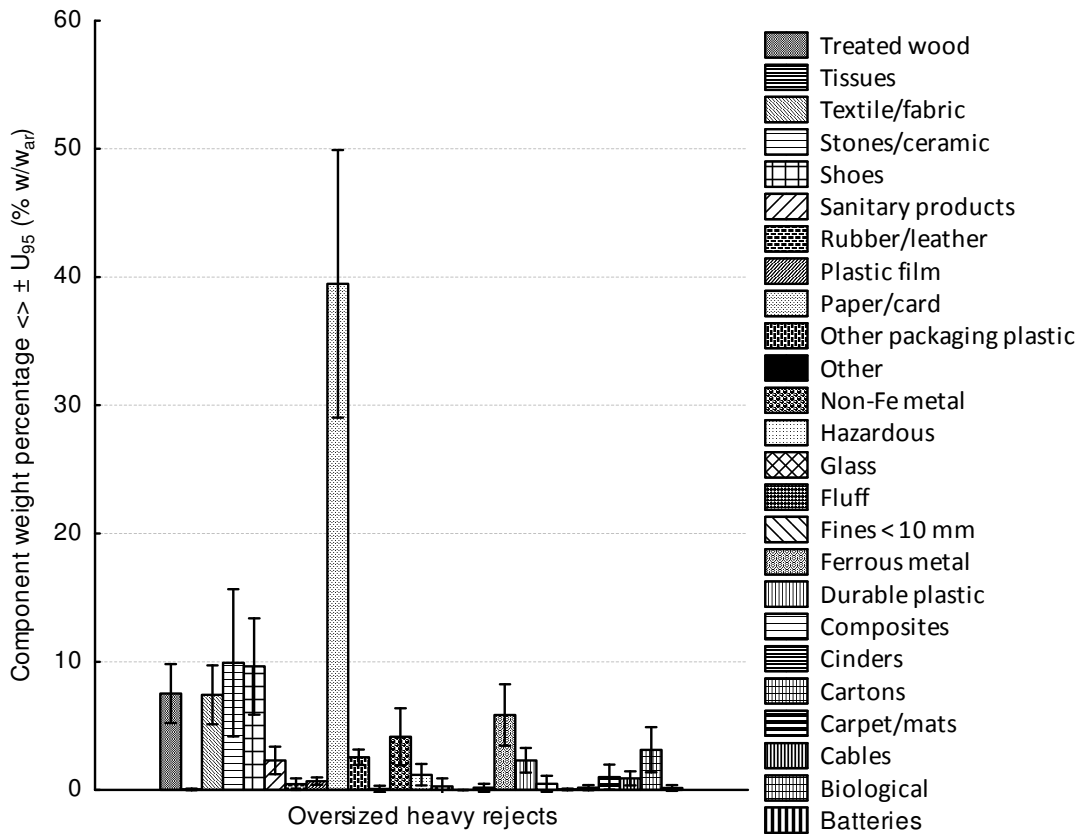


Figure 5-18 Material composition of the oversized heavy rejects (SP16). Values are average mass percentages per component (w_{ar}) and total extended uncertainty (U_{95}). Final results based on statistical analysis of the initial manual sorting results and subsequent modelling (balancing (reconciling) of all the flows through the material flow management software STAN2[®]). A result of the reconciliation is the narrowing of the U_{95} . See **Figure 4-5** and **Table 4-7** for notation, assumptions and computation methodology.

5.2.4 UK MBT plant A: SRF material characterisation

Similarly to the biodried material and oversized heavy rejects, 3 descriptions of the material composition of the SRF are provided here (**Figure 5-19** to **Figure 5-21**)

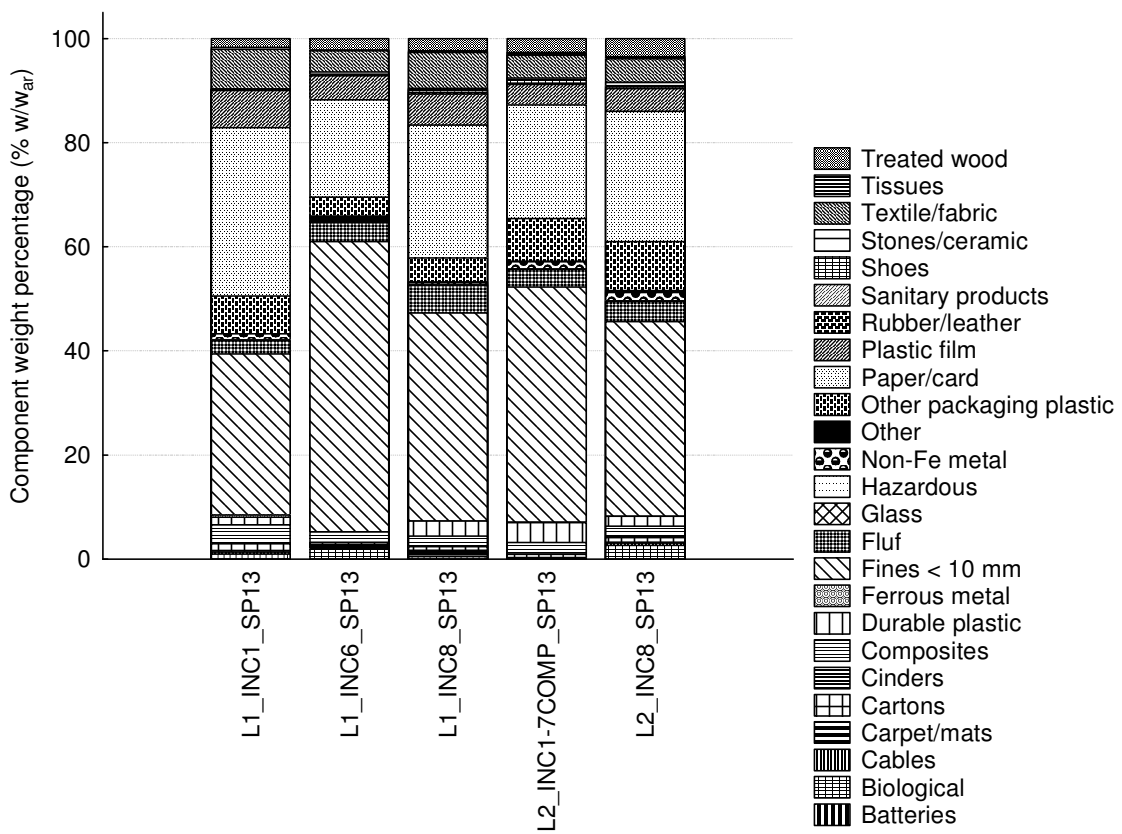


Figure 5-19 Material composition of SRF (SP13). Values (_{ar}) of individual incremental samples, as identified by manual sorting. The between-samples variability is readily visualised.

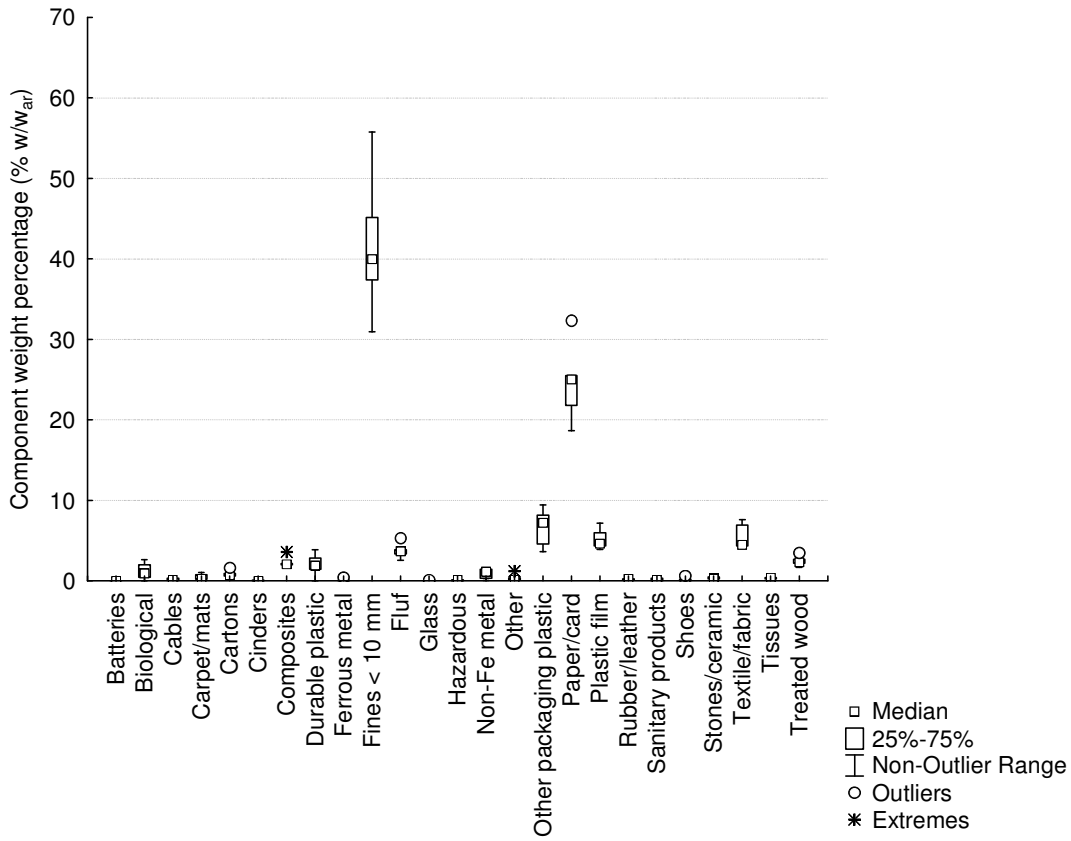


Figure 5-20 Non-parametric statistics of SRF (SP13). Values (_{ar}), as identified by manual sorting. The median describes more robustly the average of components with sufficiently high percentage, but underestimates components with low percentage (i.e., those which constitute rare occurrences within the magnitude of sampled mass).

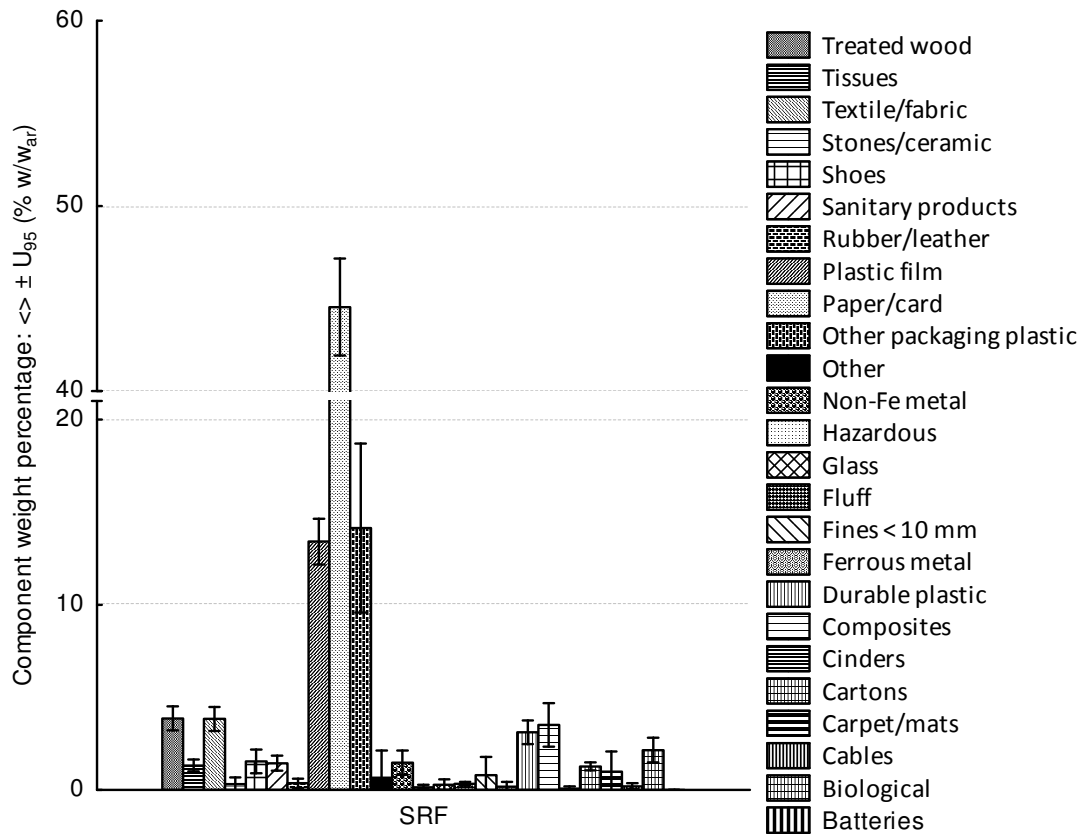


Figure 5-21 Material composition of SRF (SP13). Values are average mass percentages per component (_{ar}) and total extended uncertainty (U_{95}). Final results based on statistical analysis of the initial manual sorting results and subsequent modelling (balancing (reconciling) of all the flows through the material flow management software STAN2[®]). A result of the reconciliation is the narrowing of the U_{95} . See **Figure 4-5** and **Table 4-7** for notation, assumptions and computation methodology. Clear differences are evident from the raw manual sorting data **Figure 5-20**

5.3 UK MBT plant A: material flow analysis (balances of mass, waste components and fuel properties)

In this section results are presented for a material flow analysis performed on the mechanical processing section of the UK MBT plant A (**Section 4.2**), to address the thesis **Objective 4**. Results comprise 3 parts: (i) development of a mass balance model (on various reporting bases), including a sensitivity analysis; (ii) balancing of the flows of waste component categories, identified by manual sorting; and (iii) balancing of the

flows of mass-based loads for fuel-related properties. The general material flow analysis methodology can be found in **Section 4.4**. Specific application to the UK MBT plant A is detailed in **Section 4.9**.

5.3.1 UK MBT plant A: mass balance model

Mass balance on as-received basis (ar)

Methodology can be found in **Section 4.9.1**. The results of the measurement of mass flows of MBT plant A are shown in **Table 5-3**. These include the operational values from the weighbridge for 2 periods, and the estimates of values as reconciled by the application of the STAN2[®] model. Results for all the mass flows, including internal flows, are illustrated in **Figure 5-22**.

The reconciled results for the outputs closely reflect the 7/07-9/08 plant operational data. The SRF flow has been reduced by ca 2% w/w_{ar} units. Comparatively increased are the Fe-metals (ca +1% w/w_{ar}) and 0-8 mm ('aggregates') (ca +2% w/w_{ar}). The contribution of the A_CL 2 lights to the SRF output is very limited (on average <1% w/w_{ar}, although determined with high uncertainty). The APC residue flow (SP17) was established as low as ca 0.04% w/w_{ar} and hence ignored from the mass flow model in further computations. The 8-20 mm ('aggregates') output shows considerably higher percentages than those reported for an initial plant operation period (21/07/07 - 07/11/07) and a biodrying MBT plant of similar configuration³⁵².

Table 5-3 Results on UK MBT plant A outputs mass balance and comparison with literature

Output stream	UK MBT plant A						Shanks/Ecodeco: Frog Island plant***				
	21/07/07 - 07/11/07*		7/07- 9/08*		STAN2® input**		STAN2® final output (reconciled)		2006		
	Absolute mass	Percent mass	Absolute mass	Percent mass	Mass flow rate	Average percent mass	±U ₉₅ percent mass	Average percent mass	Percent mass		
	kg	% w/w _{ar}	kg	% w/w _{ar}	kg min ⁻¹	Mg h ⁻¹	% w/w _{ar}	% w/w _{ar}	% w/w _{ar}	% w/w _{ar}	
SRF	339.68	54.78	4531960	55.29	93.71	5.62	54.00	2.00	53.32	54.17	
Oversized heavy rejects	124.68	20.11	1065790	13.00	22.04	1.32	13.00	1.00	12.62	24.31	
Fe-metals	10.12	1.63	245880	3.00	5.08	0.31	4.00	1.50	4.03	3.61	
Non-Fe metals	5.36	0.86	34861 [†]	0.43 [†]	0.72 ^{†,††}	0.04 [†]	0.50	0.20	0.49	0.42	
0-8 mm fines ('organics')	112.47	18.14	1748470	21.33	36.16	2.17	21.00	1.50	20.62	15.28	
8-20 mm ('aggregates')	27.52	4.44	569260	6.95	11.77	0.71	9.00	1.00	8.83	2.22	
E_C rejects	n.a.	n.a.	n.a.	n.a.	n.a.	n.a.	0.10 ^{†††}	0.02	0.10	n.a.	
APC residues	0.25	0.04	n.a.	n.a.	n.a.	n.a.	n.a.	n.a.	n.a.	n.a.	
Overall	620.08	100.00	8196221	100.00	169.48	10.17	101.60		100.01	100.00	

n.a.: not available

* Data as were made available by the plant manager³⁵³. All percentages as of the processing section input

** Rounded estimates, provided as input to STAN2®

*** Source of data: Scotti and Minetti³⁵²: all percentages as of the processing section input, computed from the overall plant input

† Estimated according to the SRF/non-Fe outputs ratio of the Shanks/Eco-deco Frog Island plant³⁵²

†† Measured flow rate for the UK MBT plant A in a one-off experiment (average of 569 sec): 0.39 kg min⁻¹

††† Gross estimate, from visual inspection of the drop flow at the plant, at the 1/5 of the non-Fe flow rate

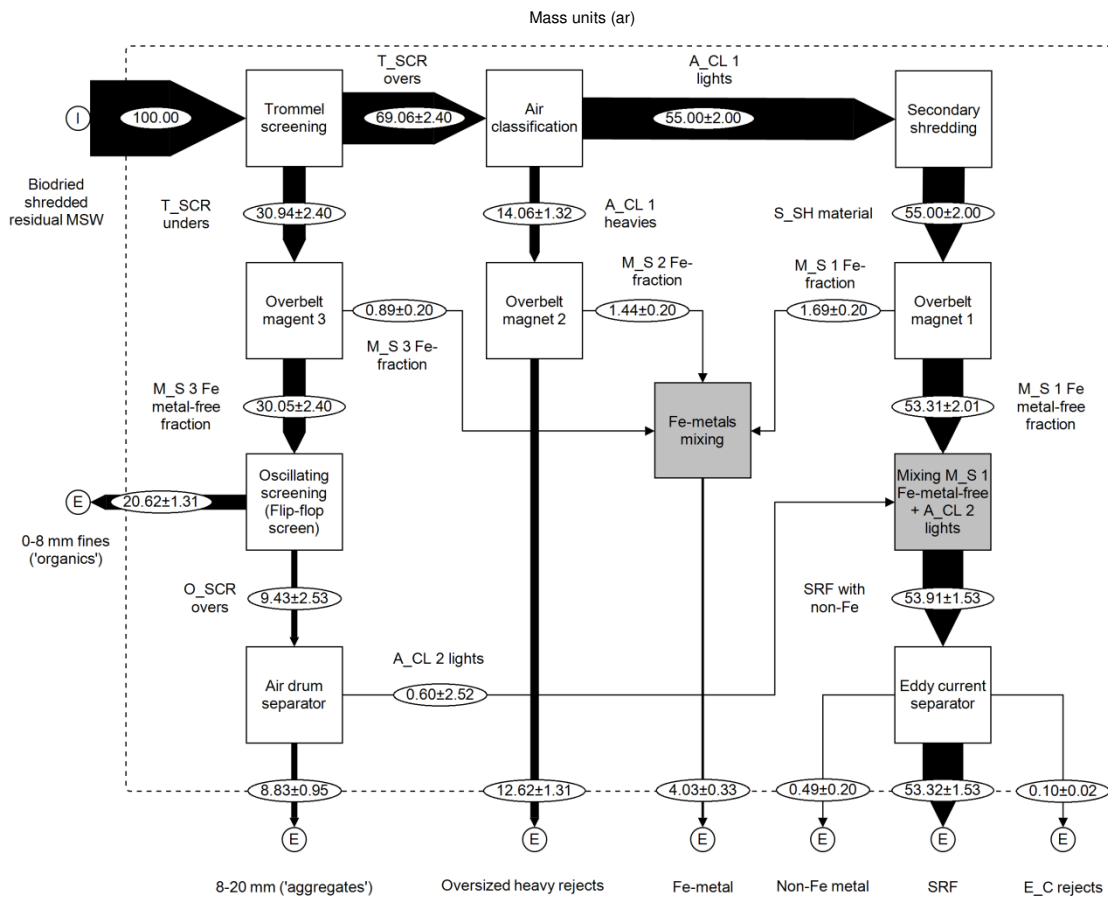


Figure 5-22 Mass balance model for the processing section of the MBT plant A. Based on operational plant output data for the sampling period (7/07-9/08) and selected literature values. Computed (reconciled) by iterative application of the material flow management software STAN2[®]. The width of the flows illustrates their relative magnitude.

Sensitivity analysis for as-received mass balance model

A sensitivity analysis was performed on the mass balance to assess and validate its suitability to produce closing balances for the individual waste components. The necessity, rationale and methodological choices are discussed in **Section 4.9.1**. Numerical results are shown in **Appendix F, Table_App F-17**. Results are plotted in **Figure 5-23**.

For most of the waste component categories it was feasible to establish a satisfactorily closing mass balance between the input and output flows of the UK MBT plant A processing section (85-115% of input), before any data reconciliation is applied. Results for the different scenarios (L, M, H) differ less than 10% (of the baseline scenario), for most of the waste components. Sum of components closes at ca 100%. Best overall fit is achieved for the scenario L. As a result, it was selected for subsequent data analysis, modelling and computations.

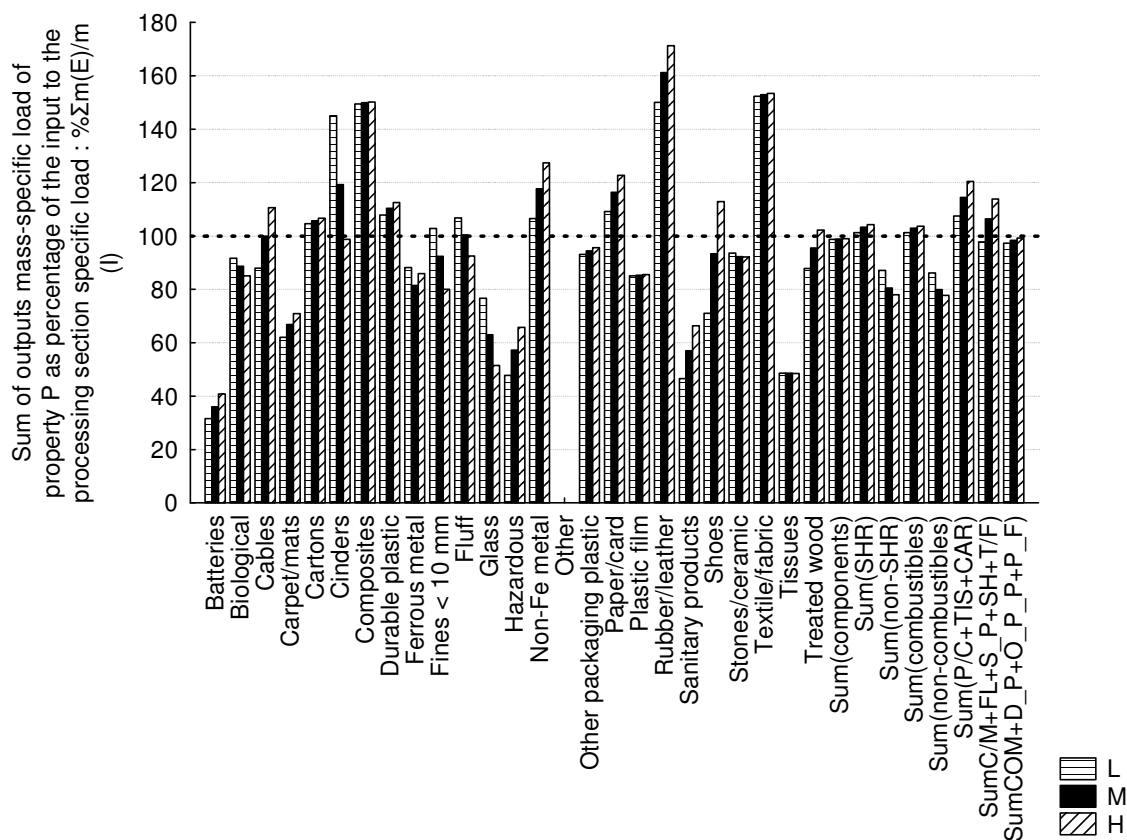


Figure 5-23 Sensitivity analysis for balances of the adjusted (modelled) waste components. Sum of modelled output specific mass load, as a percentage of the measured input specific mass load, per component (\bar{a}_r values). Specific mass loads computed using reconciled mass balances and un-reconciled mass fractions at each plant output stream. The 3 examined scenarios, vary the percentage of the oversized heavy rejects (SP16): L: low (current computations), M: medium, H: high.

Specific waste components categories provide further insight into the relative performance of the scenarios. Each waste component category is examined separately in detailed after the STAN2 data reconciliation software has been applied, using the scenario L settings in **Section 5.3.2**. Certain components such as stones/ceramics and plastic film show only negligible differences. However, glass is affected considerably: The existing deficit for the baseline scenario L (76.64% w/w_{ar}) has been further exacerbated for the M and L scenarios. Paper/card is increasing its over-recovery as the oversize rejects percentage increases. Conversely, for the shoes, hazardous, and treated wood, which are anticipated to mainly report in the oversized rejects (and SRF, which is the same for all scenarios), the H scenario best balances the input-output flows; and the M for cables.

Mass balance on a dry basis (d)

Figure 5-24 illustrates the reconciled mass balance of the UK MBT plant A expressed on a dry basis (d), assuming ca 100 dry mass units as input to the processing section. For methodological refer to **Section 4.9.1**. The input data for the d mass balance are illustrated in **Appendix F, Table_App F-18**, and **Figure_App F-17**. The balance is very similar to the as-received (**Figure 5-22**).

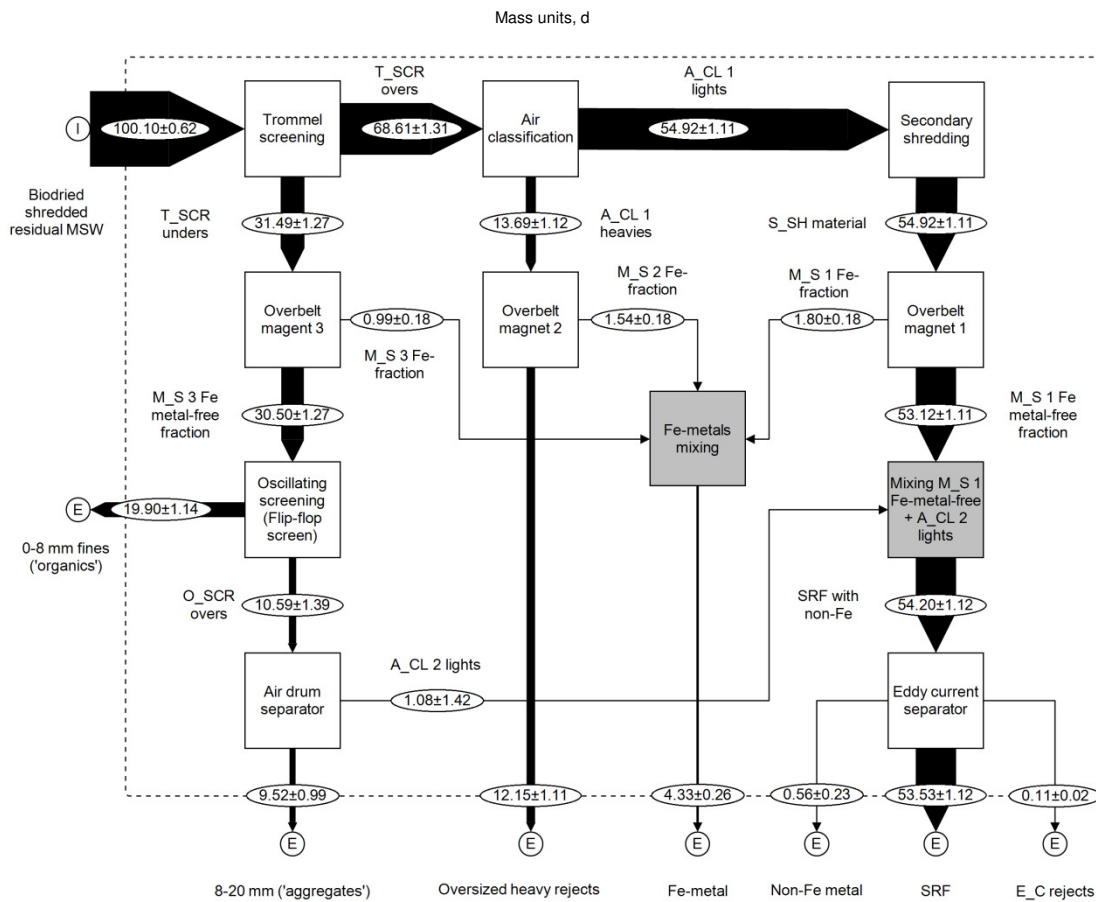


Figure 5-24 Shankey diagram of the processing section of the UK MBT plant A for dry matter (entire mass, expressed on a dry basis (d)). The width of the flows illustrates their relative magnitude. Result based upon the reconciled as received (a_r) mass balance (**Figure 5-22**) converted to d values, which were reconciled using the material flow management software STAN2[®]. Conversion from a_r to d values, was accomplished using the ratio of shreddable to non-shreddable manual sorting data and the $\langle M_T \rangle$ results per SP. Uncertainty was propagated throughout the computations. This balance can be used in the computation of properties determined for the entire sample at each flow, expressed on a dry mass basis.

Mass balance of the shreddable fraction on a dry basis (SHR, d)

Figure 5-25 illustrates the reconciled mass balance for the UK MBT plant A, expressed on a dry basis (d), assuming ca 100 dry shreddable/combustible mass units as input to the processing section. Methodological details are provided in **Section 4.9.1**. For comparison, the as-received, entire sample mass balance is shown in **Figure 5-22**.

A higher percentage of the dry shreddable/combustible mass of the processing section input reports to the SRF output (63.7% w/w_d), than for the entire dry mass (53.5% w/w_d) (**Figure 5-24**). The amounts reporting the 8-20 mm ('aggregates') constitutes contamination with combustible material (3.16±1.03% w/w_d). The amount of contamination removed by the air drum separator is just almost half of it - however, this is a highly uncertain result (1.55±1.91% w/w_d).

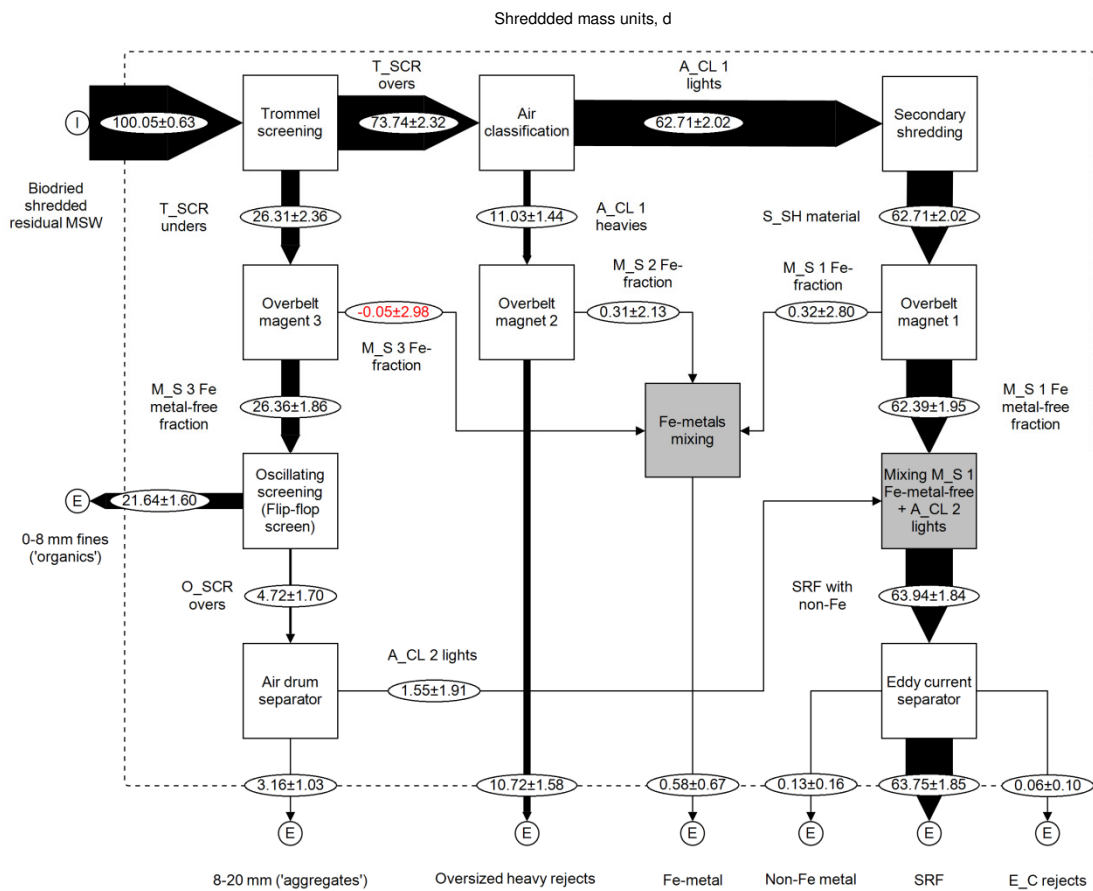


Figure 5-25 Shankey diagram of the processing section of the UK MBT plant A for the shredded mass fraction on a dry basis (_d). The width of the flows illustrates their relative magnitude. Result used in balancing of properties determined on the shredded part of the samples (GAS), expressed on a dry mass basis. The balance was based upon the reconciled as received (_{ar}) combustible mass balance (**Figure 5-27**). Conversion from _{ar} to _d values was accomplished using the ratio of shreddable to non-shreddable manual sorting data and the <M_T> results per SP. Reconciled using the material flow management software STAN2[®], in two stages: (1) simplified, omitting flows leading to Fe-mixing; and (2) full model. Uncertainty was propagated throughout the computations.

Mass balance of the shreddable fraction on a dry and ash-free basis (SHR, daf)

For the first time in the MBT literature, a detailed dry, ash-free mass balance of an MBT processing section is presented here (**Figure 5-26**). It is suitable for computing the mass-specific-loads for balancing of properties reported on a dry, ash-free basis (_{daf}) of the shreddable/combustible part of the samples (e.g., for biogenic content, $X_{B,SHR,daf}$). Methodological details are provided in **Section 4.9.1**. The fact that a satisfactorily closing balance has been achieved before the application of the data reconciliation establishes the mutual compatibility of the ash content balance and the dry mass balance. These two balances were developed using partially independent sets of experimental data (manual sorting and ash content determinations on shreddable part of sample). Their mutual compatibility serves as an indirect validation for both shreddable dry mass and ash content (_d) balances.

A dry and ash-free balance can best reveal how well the processing flowsheet performs regarding concentrating the combustible (oxidise able) mass of the materials present in the input into the intended fuel output (SRF), having removed the chemically inert fraction and the unbound water present. Here, from every 100 units of combustible dry, ash-free mass (_{daf}) in the processing section input of the MBT plant A $12.5 \pm 2.31\%$ w/w_{daf} are lost in the oversized heavy rejects fraction, whilst most of them are successfully incorporated into the SRF product ($75.5 \pm 2.9\%$ w/w_{daf}). Also, $9.24 \pm 2.56\%$ w/w_{daf} report to the 0-8 mm ('organics'). For comparison, the as-received, entire sample mass balance is shown in **Figure 5-22**.

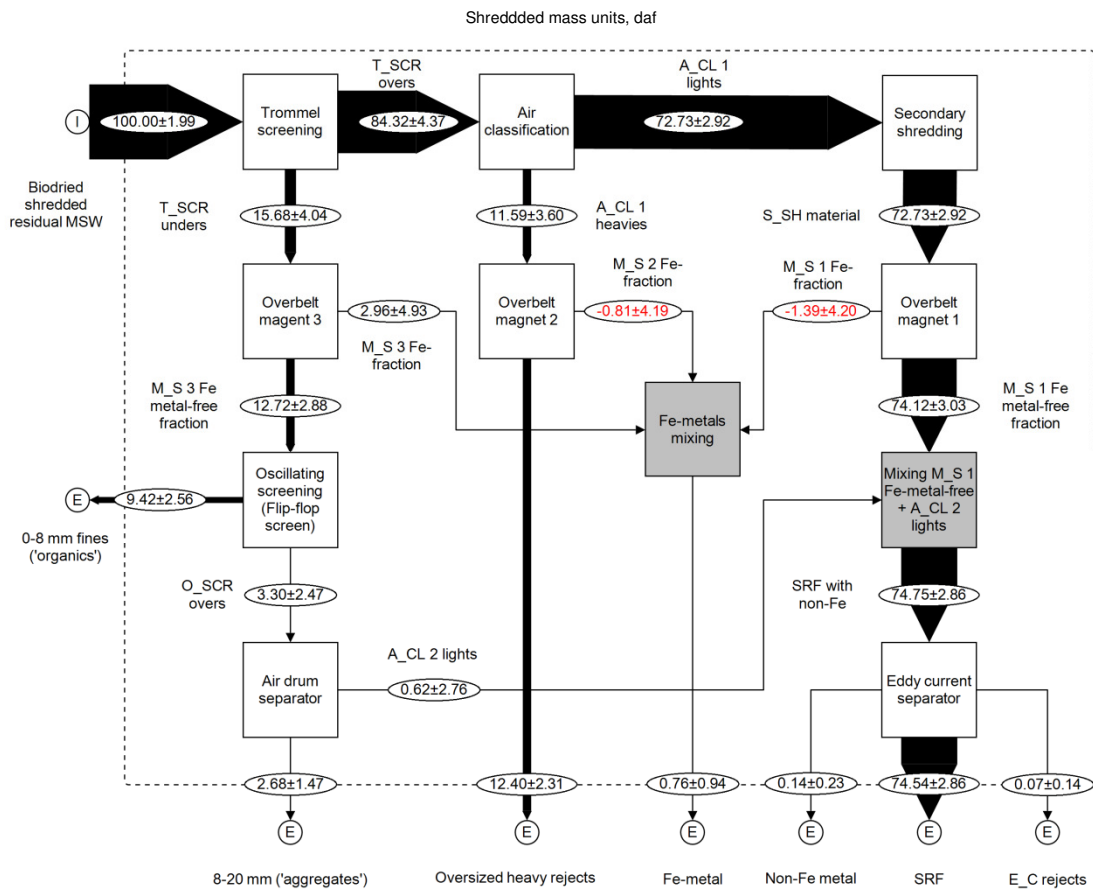


Figure 5-26 Shankey diagram of the processing section of the UK MBT plant A for the shredded mass fraction expressed on a dry and ash-free basis (daf). The width of the flows illustrates their relative magnitude. Result used in balancing of properties determined on the shredded part of the samples (GAS), expressed on a daf mass basis, such as the biogenic content ($X_{B,SHR,daf}$). Balance was produced by deducting the reconciled ash content balance (**Figure 5-51**) from the reconciled entire shreddable mass balance (**Figure 5-25**). Uncertainty was propagated throughout the computations.

5.3.2 UK MBT plant A: material component balances

Balances for waste component categories are presented in a process flowsheet combined and Shankey diagram for the processing section of the UK MBT plant A. For each flow average values of specific (per component) mass load (a_r), out of ca 10000 overall components mass input, plus/minus the total extended uncertainty (U_{95})

(confidence intervals around the average, at 95% confidence level) are provided. The width of the flows illustrates their relative magnitude, assuming a 100% width of the input flow of each diagram. Results were balanced (reconciled) by iterative application of the material flow management software STAN2[®], based on sampling and operational plant output data. Notation, assumptions and computation methodology were explained in the **Section 4.9.2** and summarised in **Figure 4-5** and **Table 4-7** in particular. The results are grouped in two general categories: combustible waste component categories and incombustible or contrary to SRF.

Mass balances for combustible waste components

The maximum sum of the potentially combustible components accounts for $82 \pm 0.1\%$ w/w_{ar} of the biodried input to the processing section (**Figure 5-27**). It is maximum because it includes components such as fines, cables and hazardous, which can be considered in many ways as contraries and, ideally, they should not report to the SRF output. Most of the sum of combustibles ($\Sigma m(\text{Comb})$) is directed to the SRF output (51.9% of entire processing mass input_{ar}); with the rest split between the 0-8 mm ('organics') (17.5%) and the oversized heavy rejects (9.7%).

Regarding the individual combustible components, paper/card (**Figure 5-28**) is the dominant component present in the biodried input: 29.2 mass units (out of 100) (see also **Figure 5-12**). The majority of this is incorporated in the SRF output: 23.1 mass units. But 5.3 mass units are lost (ca 1/6 of the input paper/card), reporting to the oversized heavy rejects. Similar values result for the sum of paper/card, cartons and tissues (paper and like) balance (**Figure 5-29**). The last two components are insignificant compared to the paper/card alone, and not balancing individually (**Figure 5-23**). Most of the paper/card remains in the SRF production line after the trommel screening ($\text{TC(P/C)}_{\text{T_SCR_LG}} = 96.3 \pm 0.7\%$) (**Table 5-5**). It is the next downstream unit

operation of air classification that allows the paper/card to exit the SRF processing line:

$TC(P/C)_{A_CL\ 1_HG} = 17.7 \pm 4.7\%$ (Table 5-6).

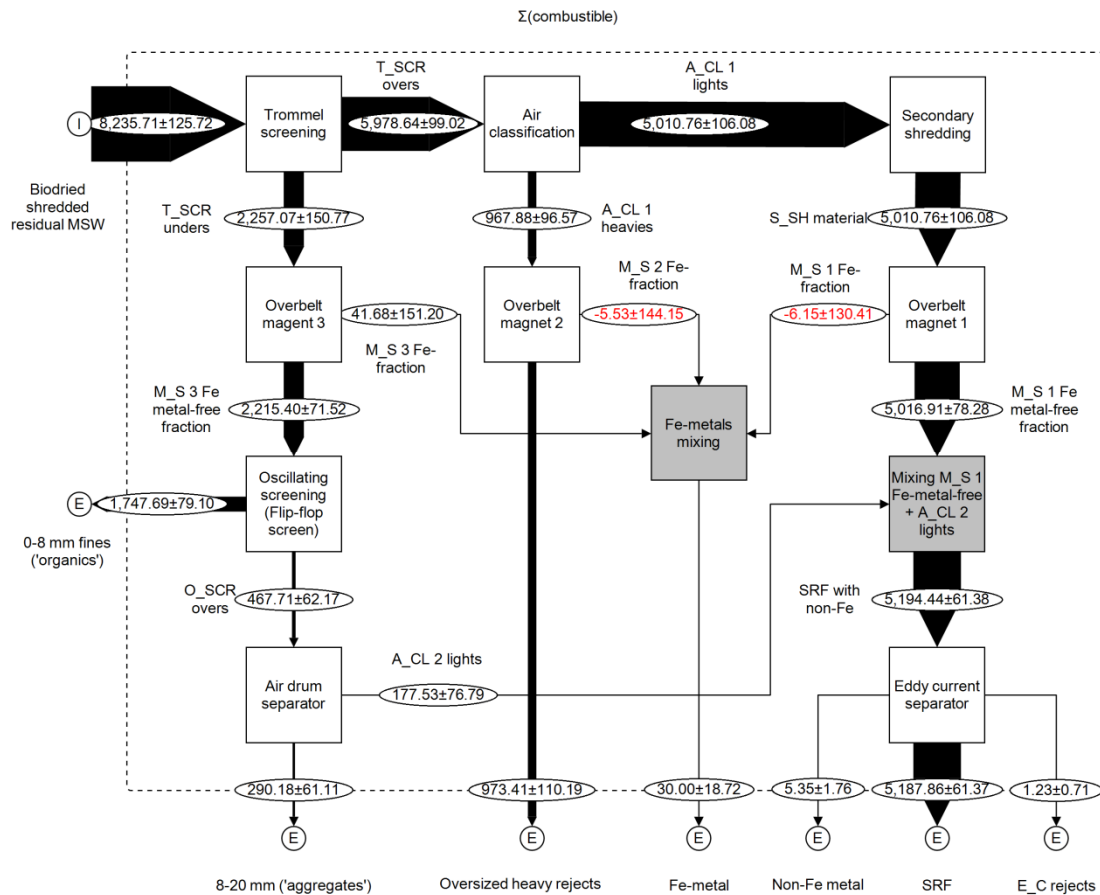


Figure 5-27 Shankey diagram of the processing section of the UK MBT plant A: model of flows for the sum of combustible waste components. The width of the flows illustrates their relative magnitude. For any processing sub-system, the ratio of any output flow to the sum of input flows provides the transfer coefficient (TC) to this output. Values are average specific (per component) mass load (a_r), out of ca 10,000 overall components mass input, plus/minus the total extended uncertainty (U_{95}) (confidence intervals around the average at 95% confidence). Results were balanced (reconciled) by iterative application of the material flow management software STAN2[®], based on sampling and operational plant output data. See Figure 4-5 and Table 4-7 for notation, assumptions and computation methodology.

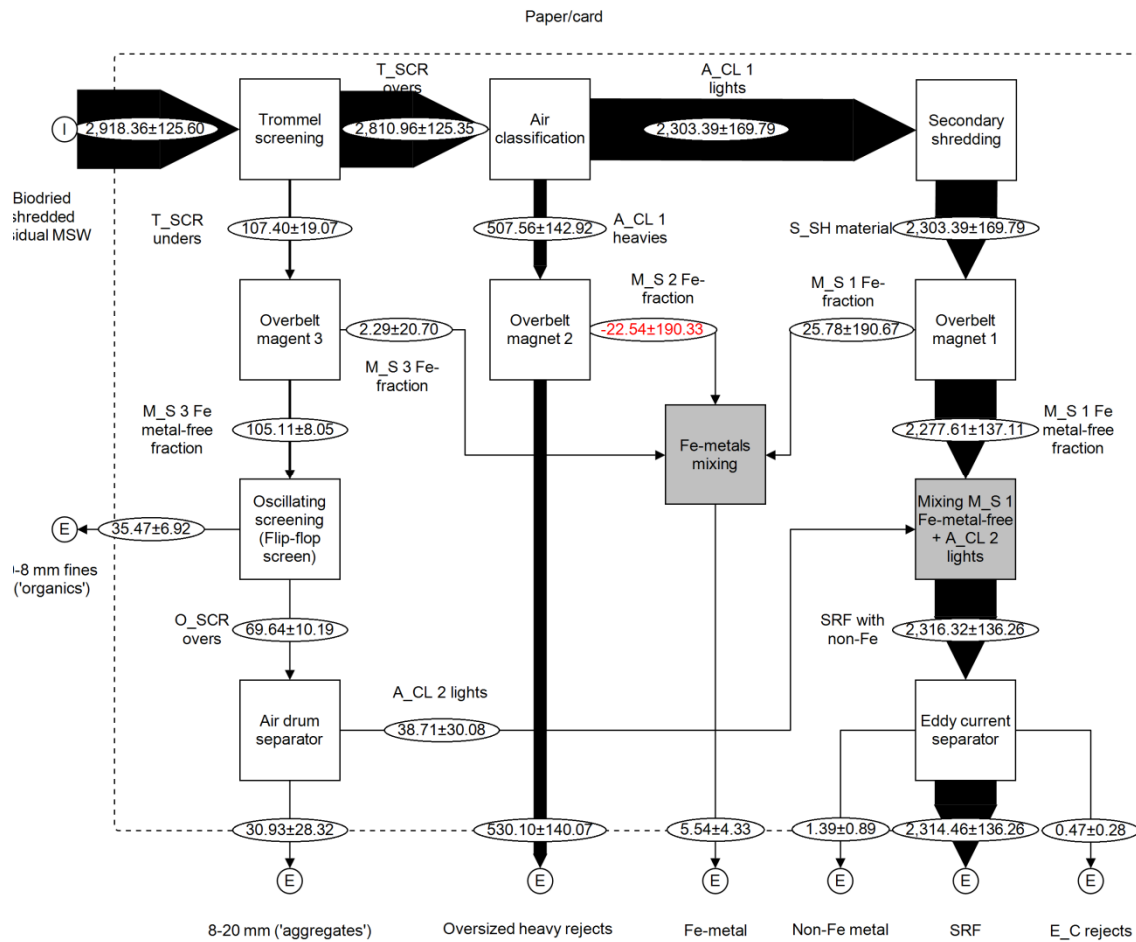


Figure 5-28 Shankey diagram of the processing section of the UK MBT plant A: paper/card waste component model of flows. Values are average specific (per component) mass load (a_r), out of ca 10,000 overall components mass input, plus/minus the total extended uncertainty (U_{95}) (confidence intervals around the average at 95% confidence). Results were balanced (reconciled) by iterative application of the material flow management software STAN2[®], based on sampling and operational plant output data. The width of the flows illustrates their relative magnitude. See **Figure 4-5** and **Table 4-7** for notation, assumptions and computation methodology.

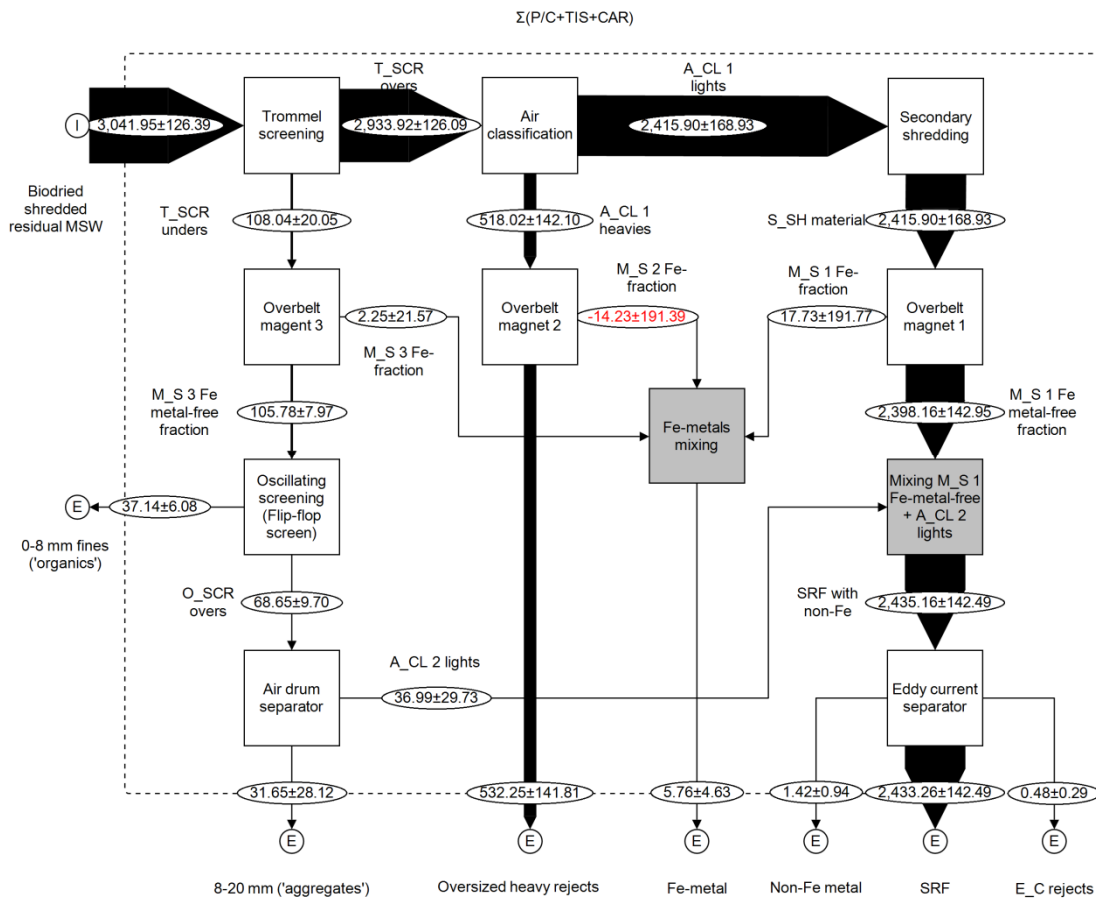


Figure 5-29 Shankey diagram of the processing section of the UK MBT plant A: sum of paper and like waste component model of flows. Values are average specific (per component) mass load (a_r), out of ca 10,000 overall components mass input, plus/minus the total extended uncertainty (U_{95}) (confidence intervals around the average at 95% confidence). Results were balanced (reconciled) by iterative application of the material flow management software STAN2[®], based on sampling and operational plant output data. The width of the flows illustrates their relative magnitude. See **Figure 4-5** and **Table 4-7** for notation, assumptions and computation methodology.

Closing balances were developed for 3 out of the 4 categories of plastics identified during the manual sorting (P_F, O_P_P, D_P, COM) (**Figure 5-30** to **Figure 5-35**). **Figure 5-35** depicts the overall mass balance for the sum of the four plastic categories. This overview shows clearly the dominance of the SRF production line in incorporating the plastics present in the processing section input.

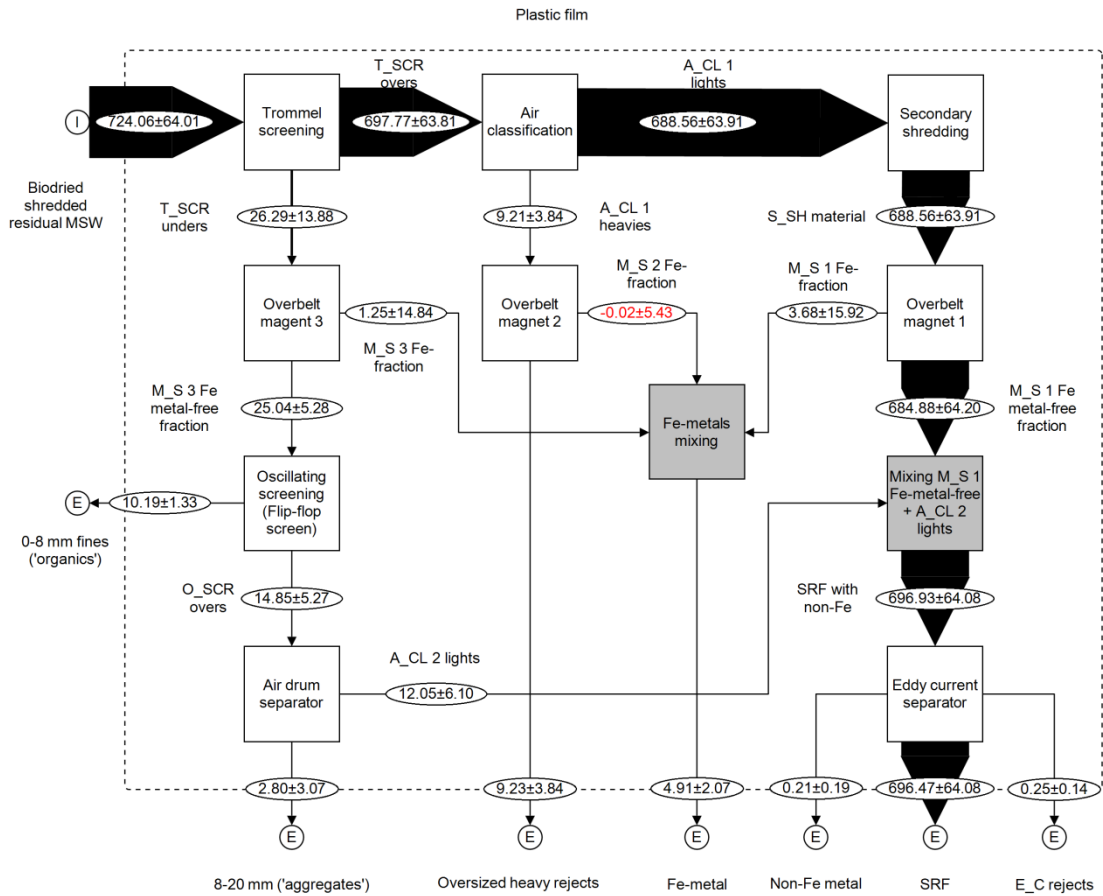


Figure 5-30 Shankey diagram of the processing section of the UK MBT plant A: plastic film waste component model of flows. Values are average specific (per component) mass load (a_r), out of ca 10,000 overall components mass input, plus/minus the total extended uncertainty (U_{95}) (confidence intervals around the average at 95% confidence). Results were balanced (reconciled) by iterative application of the material flow management software STAN2[®], based on sampling and operational plant output data. The width of the flows illustrates their relative magnitude. See **Figure 4-5** and **Table 4-7** for notation, assumptions and computation methodology.

The plastic film and other packaging plastic present in the biodried fraction report almost entirely into the SRF output (**Figure 5-30** and **Figure 5-31**). Most of the durable plastic (2.2% w/w_{ar} or mass units, in the biodried material,) is also incorporated into the SRF stream (**Figure 5-32**) (1.6 mass units). The rest does is split among tree outputs. In addition to the oversized heavy rejects, it is present as contamination in the 0-8 mm ('organics') (0.12 mass units) and the 8-20 mm ('aggregates') (0.17 mass

units). Durable plastic is the only plastic category that does not report entirely to the SRF output.

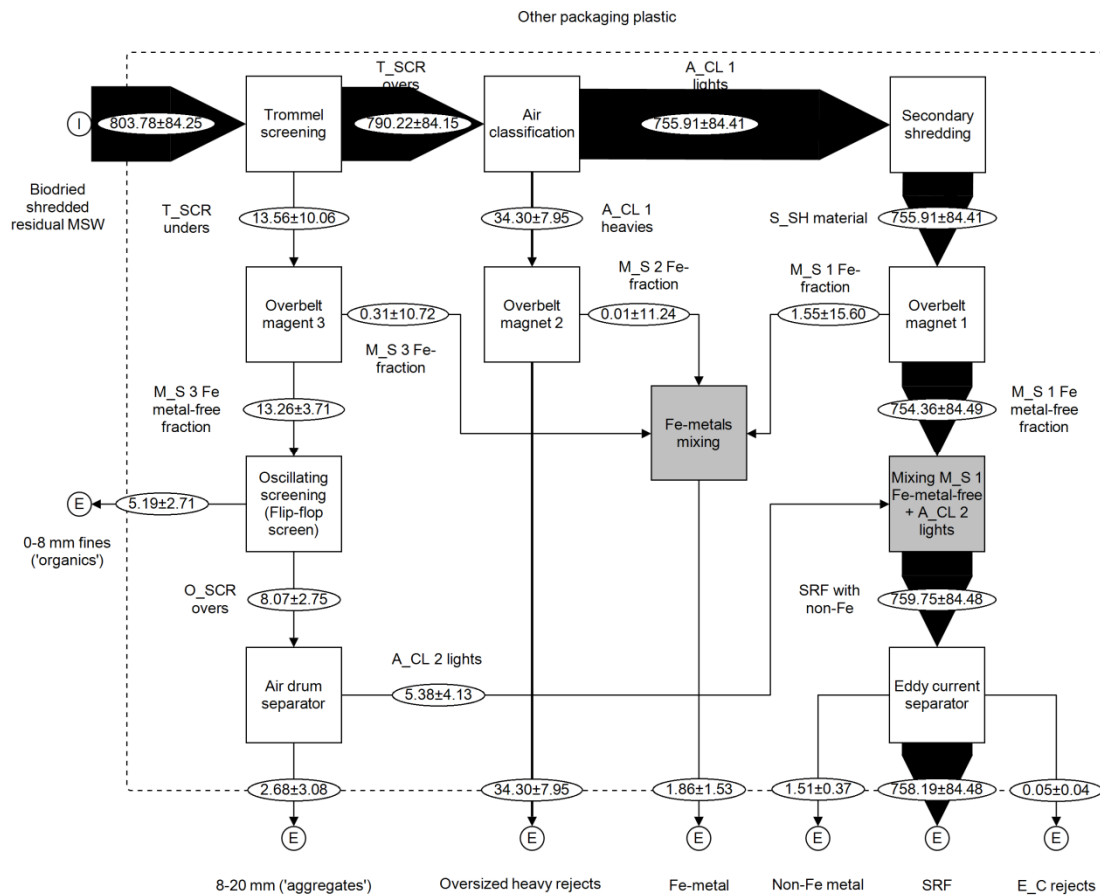


Figure 5-31 Shankey diagram of the processing section of the UK MBT plant A: other packaging plastic waste component model of flows. Values are average specific (per component) mass load (a_r), out of ca 10,000 overall components mass input, plus/minus the total extended uncertainty (U_{95}) (confidence intervals around the average at 95% confidence). Results were balanced (reconciled) by iterative application of the material flow management software STAN2[®], based on sampling and operational plant output data. The width of the flows illustrates their relative magnitude. See **Figure 4-5** and **Table 4-7** for notation, assumptions and computation methodology.

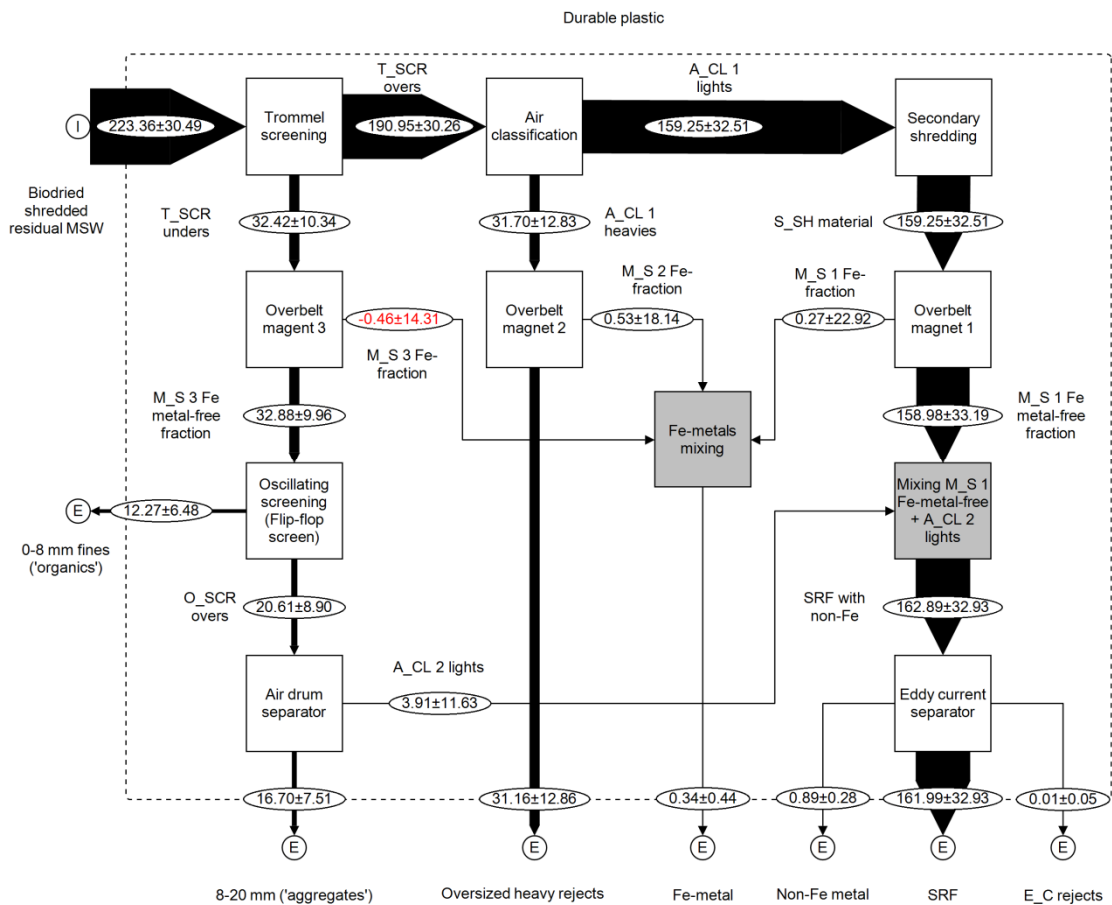


Figure 5-32 Shankey diagram of the processing section of the UK MBT plant A: durable plastics waste component model of flows. Values are average specific (per component) mass load (a_r), out of ca 10,000 overall components mass input, plus/minus the total extended uncertainty (U_{95}) (confidence intervals around the average at 95% confidence). Results were balanced (reconciled) by iterative application of the material flow management software STAN2[®], based on sampling and operational plant output data. The width of the flows illustrates their relative magnitude. See **Figure 4-5** and **Table 4-7** for notation, assumptions and computation methodology.

Composites balance is not closing before reconciliation (**Figure 5-23**). Thus, the data before reconciliation also are shown here (**Figure 5-33**), along with the finally reconciled values (**Figure 5-34**). The composites show high variability, both between flows not anticipated to differ considerably (A_SH material, M_S 1Fe metal-free

fraction, SRF with non-Fe, and SRF) and within each flow, as the high relative extended uncertainties indicate (**Figure 5-33**, data input to reconciliation).

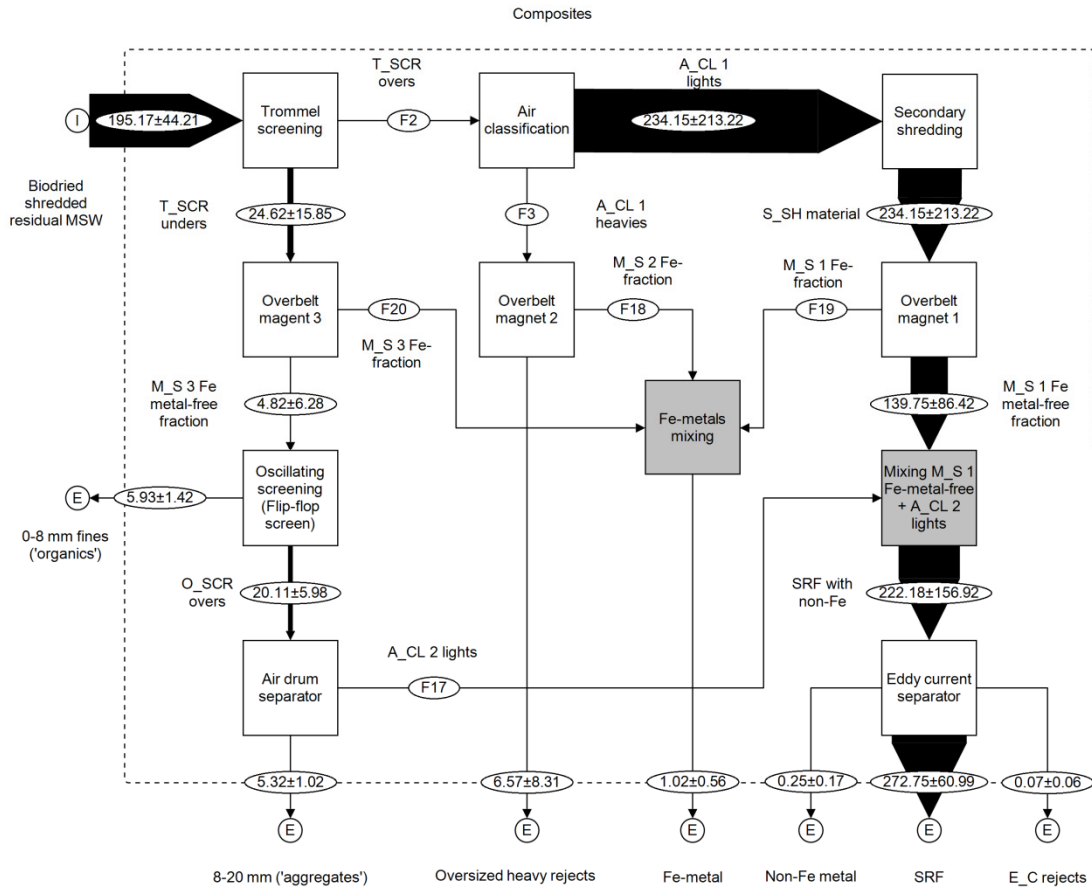


Figure 5-33 Shankey diagram of the processing section of the UK MBT plant A: composite waste component model of flows. Values are average specific (per component) mass load (\bar{a}_r), out of ca 10,000 overall components mass input, plus/minus the total extended uncertainty (U_{95}) (confidence intervals around the average at 95% confidence). Results before balancing with STAN2[®], based on sampling and operational plant output data. The width of the flows illustrates their relative magnitude. See **Figure 4-5** and **Table 4-7** for notation, assumptions and computation methodology.

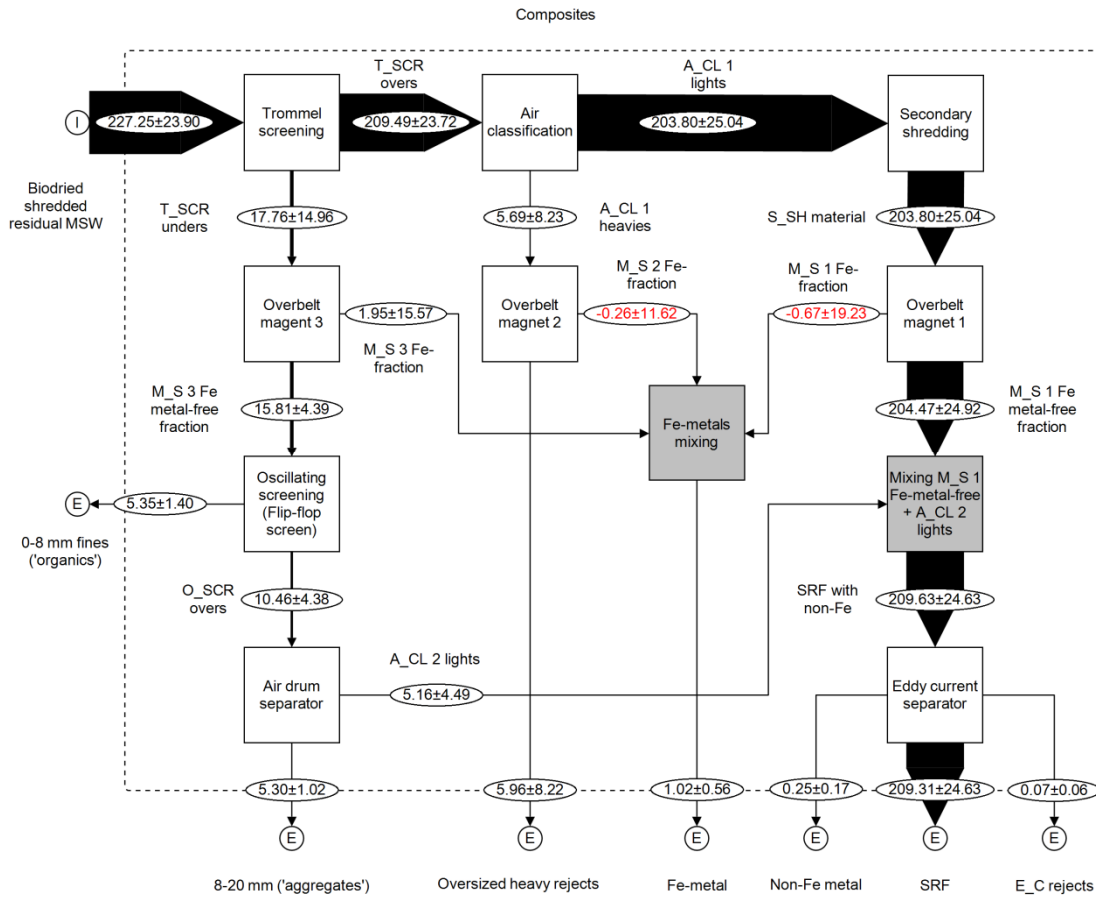


Figure 5-34 Shankey diagram of the processing section of the UK MBT plant A: composites waste component model of flows. Values are average specific (per component) mass load (\bar{a}_r), out of ca 10,000 overall components mass input, plus/minus the total extended uncertainty (U_{95}) (confidence intervals around the average at 95% confidence). Results were balanced (reconciled) by iterative application of the material flow management software STAN2[®], based on sampling and operational plant output data. **Figure 5-33** shows data before reconciliation. The width of the flows illustrates their relative magnitude. See **Figure 4-5** and **Table 4-7** for notation, assumptions and computation methodology.

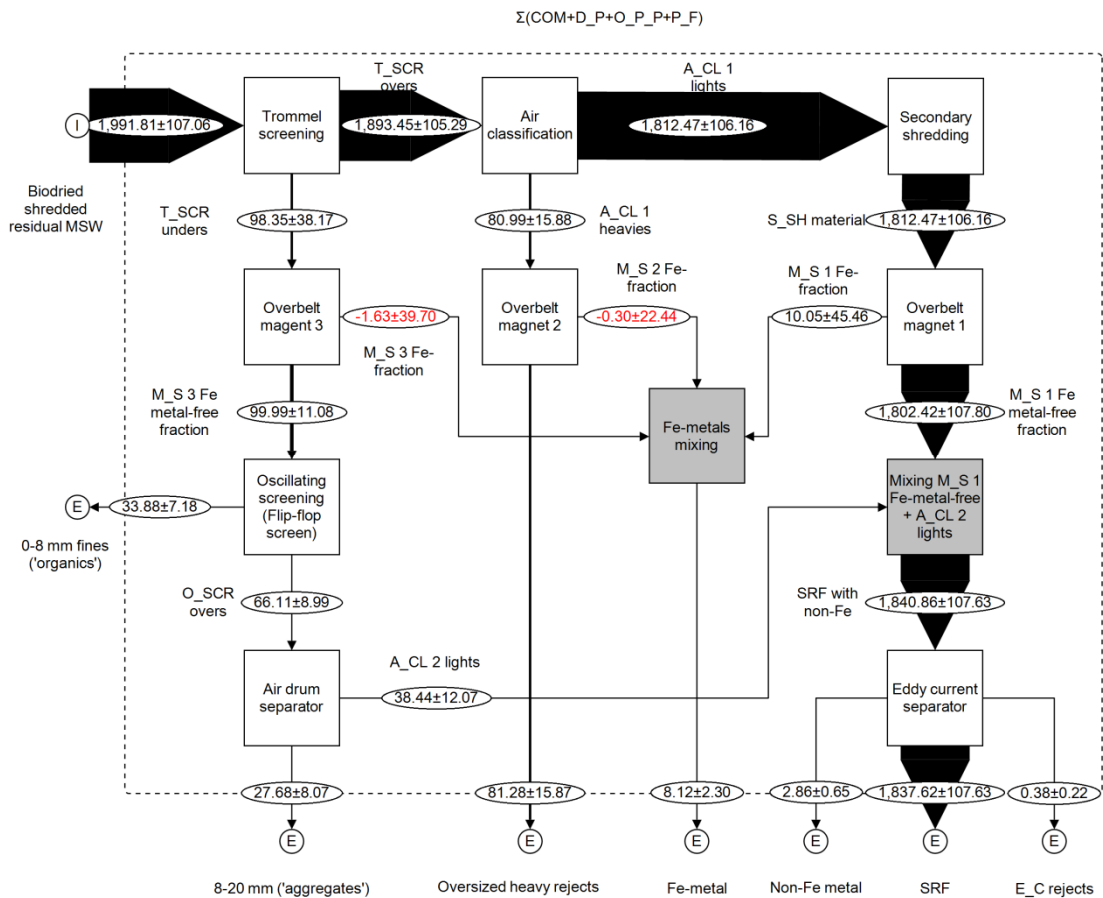


Figure 5-35 Shankey diagram of the processing section of the UK MBT plant A: sum of plastic waste components model of flows. Values are average specific (per component) mass load (a_r), out of ca 10,000 overall components mass input, plus/minus the total extended uncertainty (U_{95}) (confidence intervals around the average at 95% confidence). Results were balanced (reconciled) by iterative application of the material flow management software STAN2[®], based on sampling and operational plant output data. The width of the flows illustrates their relative magnitude. See **Figure 4-5** and **Table 4-7** for notation, assumptions and computation methodology.

Results for balances of a series of waste component categories constituting a wider group are presented here: textile/fabric, carpets/mats, shoes, and sanitary products. They all contain cloth, to varying degrees. The adjusted un-reconciled textile/fabric balance shows a high surplus, whilst carpets/mats, shoes, sanitary products a clear deficit, apart from the fluff which is sufficiently closing (**Figure 5-23**). This could be due to the relatively simplistic data handling adjustment adopted to

account for the post-secondary shredding increase of reported $F < 10$ mm. A deficit could be anticipated for these categories, because in manual sorting they are not easy to recognise as such, being fine fragments. Conversely, they could be mistaken mainly for textile/fabric (and as composites, to a lesser degree). A balance for the sum for these materials is presented (**Figure 5-36**). This accounts for this partly inevitable possible systematic mistake during the manual sorting, not fully corrected by the adjusted model. Reconciled balances for the individual components using adjusted values can be found in **Appendix F**. However, they are just indicative, hence not shown here.

The sum of these components ('sum of textiles and like') exhibits a satisfactorily closing balance. Collectively consisting ca 5.5% w/w_{ar} of the biodried input, these component categories report mainly to the SRF (3.5 mass units) and secondarily to the oversized heavy rejects (1.8 mass units). The air classifier is responsible for directing a around one third of them to the oversized heavy rejects $TC(\Sigma(C/M+FL+S_P+SH+T/F))_{A_CL_1_HG} = 34.3 \pm 7.7\%$ (**Table 5-6**). **Figure_App F-25** indicates that shoes are split between the SRF and oversized heavy rejects. Especially, if the assumption holds that the deficit in the outputs is a manual sorting error.

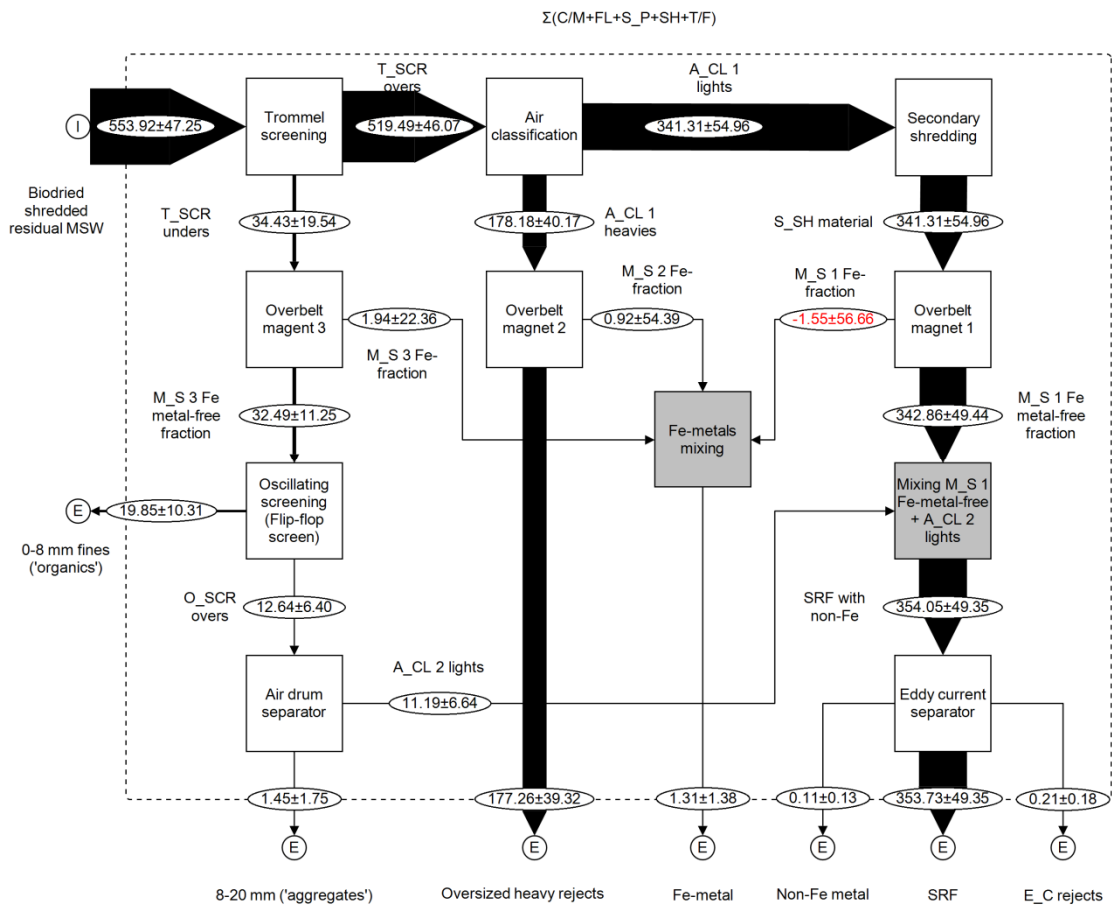


Figure 5-36 Shankey diagram of the processing section of the UK MBT plant A: sum of textile and like waste components model of flows. Values are average specific (per component) mass load (\bar{a}_r), out of ca 10,000 overall components mass input, plus/minus the total extended uncertainty (U_{95}) (confidence intervals around the average at 95% confidence). Results were balanced (reconciled) by iterative application of the material flow management software STAN2[®], based on sampling and operational plant output data. The width of the flows illustrates their relative magnitude. See **Figure 4-5** and **Table 4-7** for notation, assumptions and computation methodology.

Waste component categories containing biogenic combustible materials comprise also the biological, treated wood and fines <10 mm (**Figure 5-37** to **Figure 5-39**). Treated wood is monitored separately from e.g., yard waste such as trees branches which are included in the biological component (**Table 4-5**). Treated wood is directed almost exclusively to the SRF (2.0 mass units, out of 100 biodried material,

containing 3.1 mass units of treated wood) and the oversized heavy rejects (1.0 mass units) (**Figure 5-37**). The split between the two outputs depends largely upon the air classification ($A_CL\ 1$), currently directing around the 1/3 of the T_W to the high-gravity product: $(TC(T_W))_{A_CL\ 1_HG} = 33.5 \pm 10.2\%$ - **Table 5-6**).

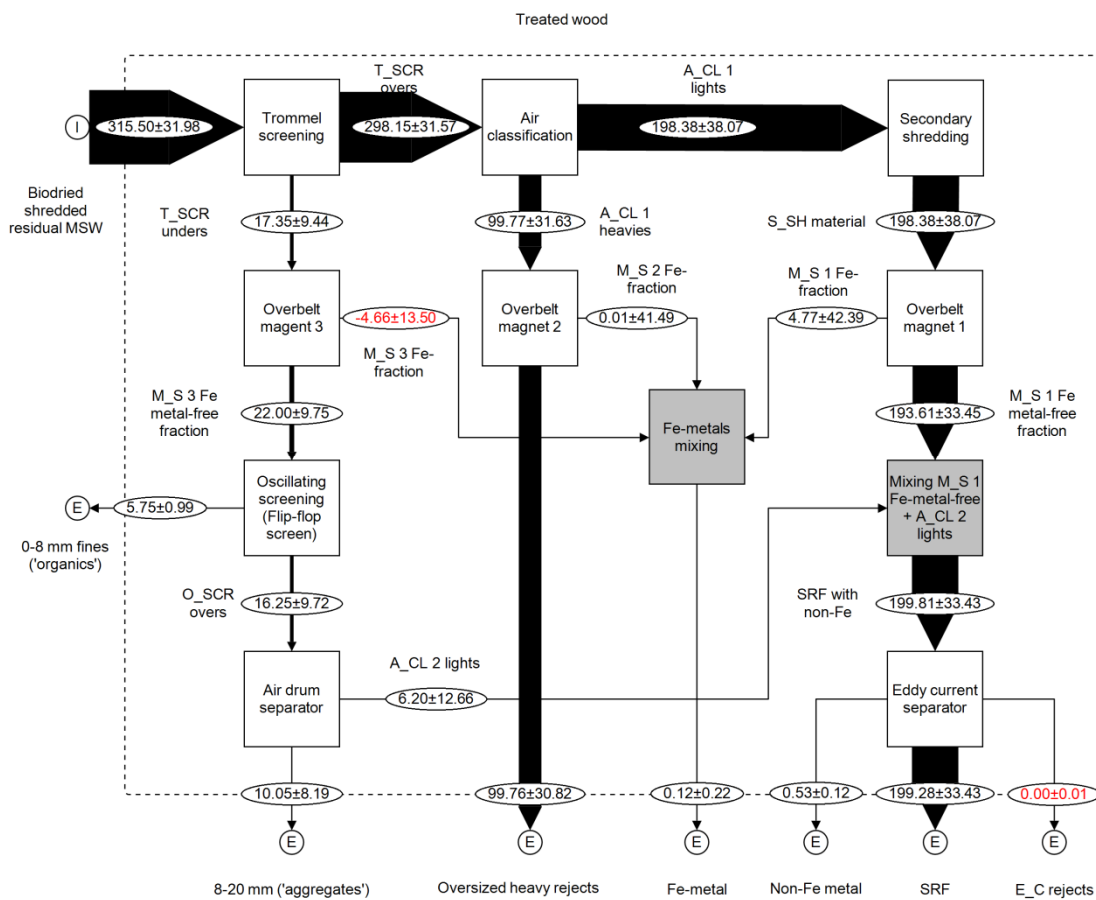


Figure 5-37 Shankey diagram of the processing section of the UK MBT plant A: treated wood waste components model of flows. Values are average specific (per component) mass load (a_r), out of ca 10,000 overall components mass input, plus/minus the total extended uncertainty (U_{95}) (confidence intervals around the average at 95% confidence). Results were balanced (reconciled) by iterative application of the material flow management software STAN2[®], based on sampling and operational plant output data. The width of the flows illustrates their relative magnitude. See **Figure 4-5** and **Table 4-7** for notation, assumptions and computation methodology.

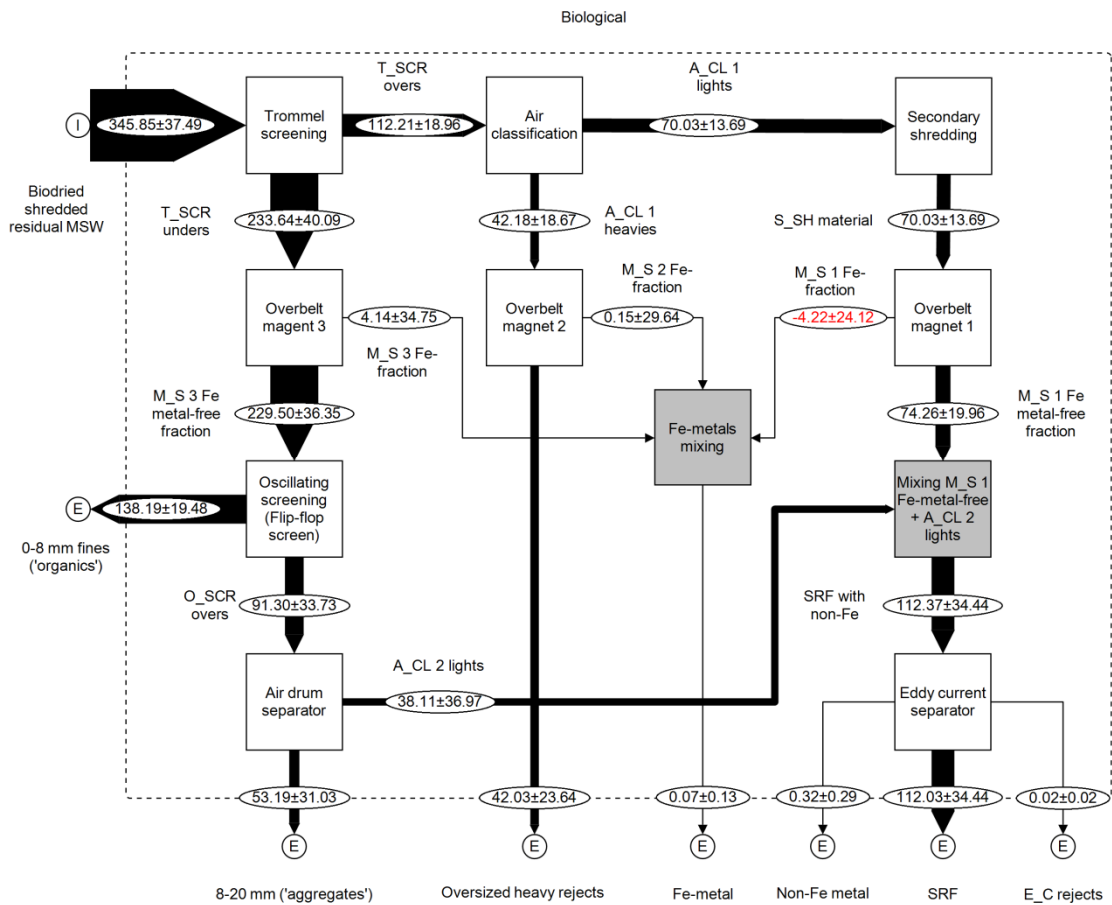


Figure 5-38 Shankey diagram of the processing section of the UK MBT plant A: biological waste component model of flows. Values are average specific (per component) mass load (w_{ar}), out of ca 10,000 overall components mass input, plus/minus the total extended uncertainty (U_{95}) (confidence intervals around the average at 95% confidence). Results were balanced (reconciled) by iterative application of the material flow management software STAN2[®], based on sampling and operational plant output data. The width of the flows illustrates their relative magnitude. See **Figure 4-5** and **Table 4-7** for notation, assumptions and computation methodology.

The biological category of waste components shows a complex flow balance (**Figure 5-38**). Limited amount of BIO is present in the biodried flow (3.5% w/w_{ar}). This is directed predominantly to the 0-8 mm ('organics'), but also reports at a similar level to the SRF and at a lower level at the 8-20 ('aggregates') and the oversized heavy rejects. The trommel screening directs only partly the biological component mass to the

undersize product $(TC(BIO))_{T_SCR_U} = 67.6 \pm 6.2\%$ - **Table 5-5**). Similarly, the air drum separator (A_CL 2) only partly prevents it from reporting to the 8-20 mm ('aggregates'); the re-directed material reports to the SRF output $(TC(BIO))_{A_CL\ 2_LG} = 62.4 \pm 12.7\%$ - **Table 5-8**).

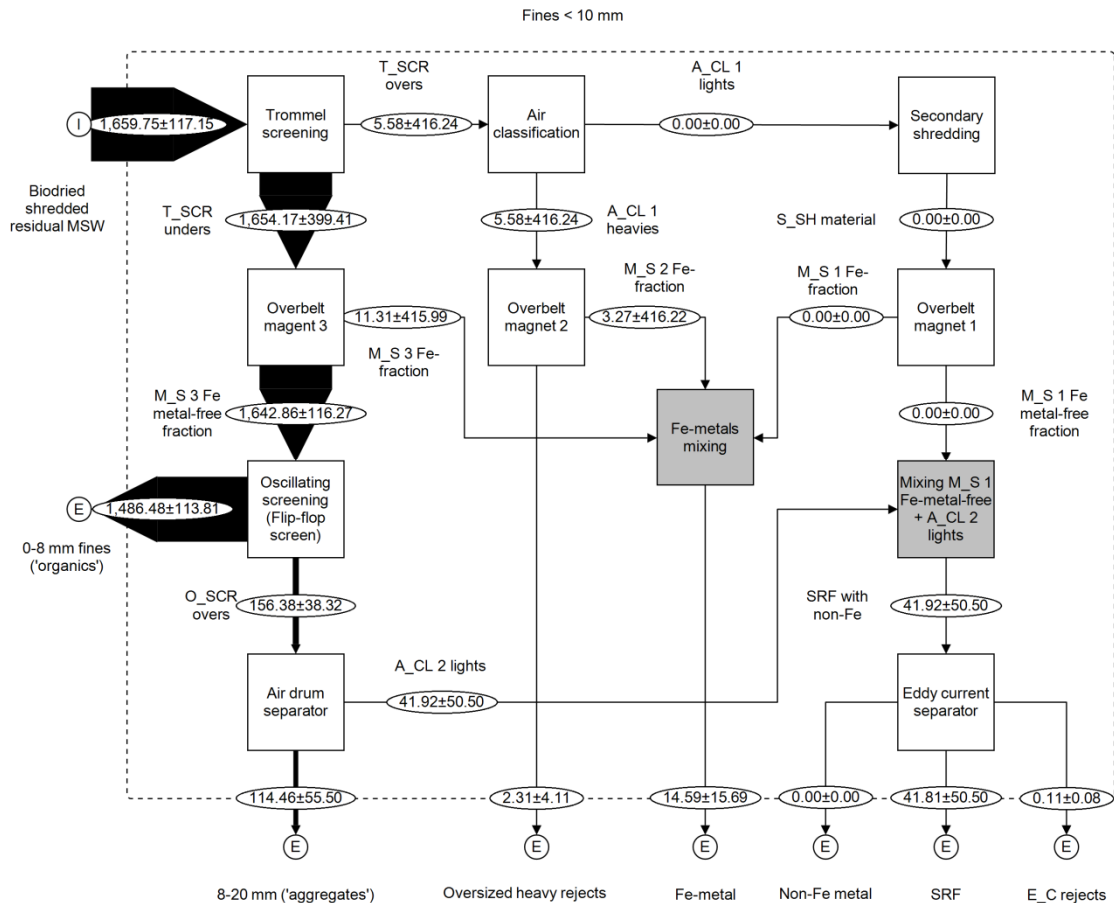


Figure 5-39 Shankey diagram of the processing section of the UK MBT plant A: fines <10 mm waste components model of flows. Values are average specific (per component) mass load (a_r), out of ca 10,000 overall components mass input, plus/minus the total extended uncertainty (U_{95}) (confidence intervals around the average at 95% confidence). Results were balanced (reconciled) by iterative application of the material flow management software STAN2[®], based on sampling and operational plant output data. The width of the flows illustrates their relative magnitude. See **Figure 4-5** and **Table 4-7** for notation, assumptions and computation methodology.

The fines <10 mm waste component category constitute a considerable part of the biodried material (16.6% w/w_{ar}) (**Figure 5-39**). The current modelling adjustments and flows reconciliation lead to a closing balance for the fines <10 mm component (**Table 4-7**). F<10 are effectively concentrated into the 0-8 mm ('organics') plant output. The amount directed to the SRF by the air drum separator operation (A_CL 2 LG) is limited and insignificant for the SRF yield. Only a negligible amount of F<10 is directed to the T_SCR over. This agrees with the absence of F<10 in the oversized reject fraction (just 0.18±0.33% w/w_{ar}).

Mass balance of incombustible or contrary-to-SRF waste components

A reconciled balance for the sum of the incombustible waste component categories is shown in **Figure 5-40**. A complex pattern is evident. The balance is rather indicative, because certain waste component categories such as batteries, or glass are not sufficiently balancing individually. A limited amount of incombustibles is transferred to the SRF output, negatively affecting the ash content of the fuel $TC(\Sigma(\text{non-combustibles}))_{\text{SRF}} = 8.8\pm 3.8\%$ (**Table 5-4**). In the next paragraphs, the waste component categories comprising the sum of incombustibles are presented in detail (**Figure 5-41** to **Figure 5-49**).

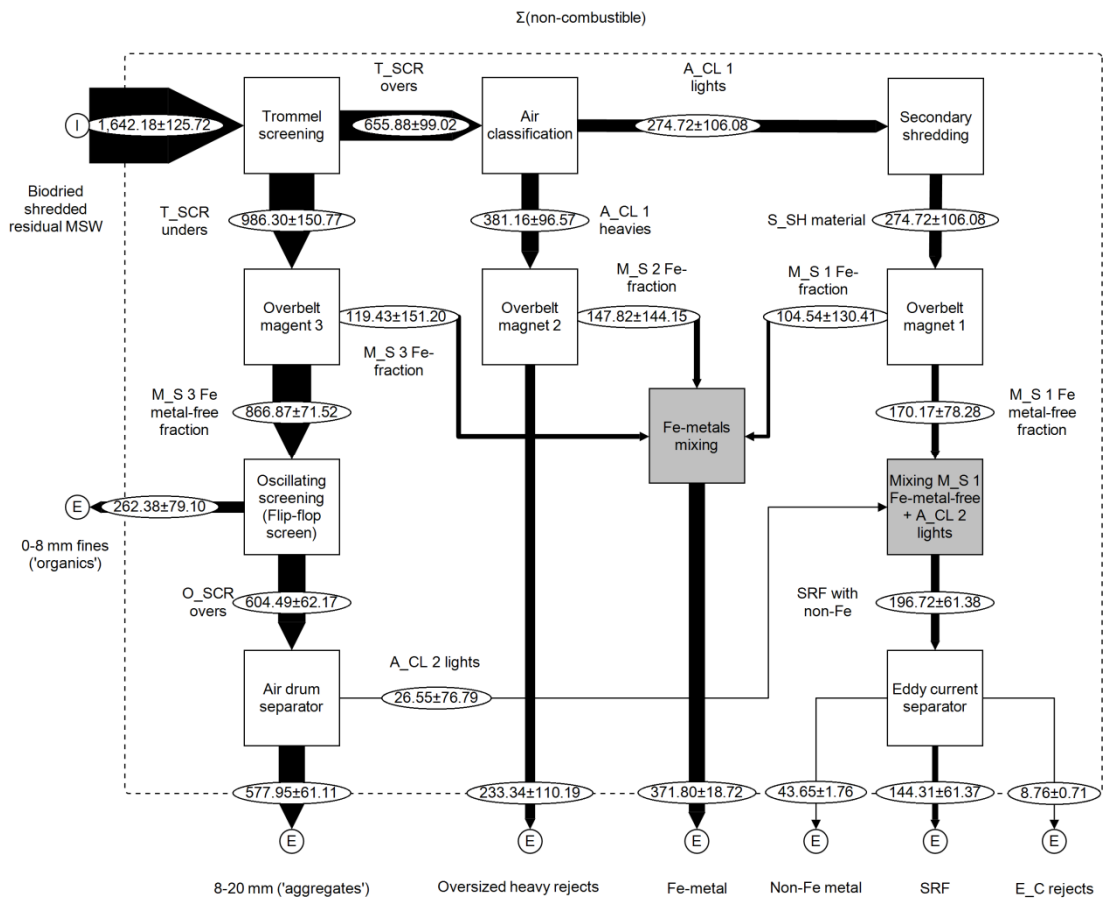


Figure 5-40 Shankey diagram of the processing section of the UK MBT plant A: sum of non-combustible waste components model of flows. Values are average specific (per component) mass load (a_r), out of ca 10,000 overall components mass input, plus/minus the total extended uncertainty (U_{95}) (confidence intervals around the average at 95% confidence). Results were balanced (reconciled) by iterative application of the material flow management software STAN2[®], based on sampling and operational plant output data. The width of the flows illustrates their relative magnitude. See **Figure 4-5** and **Table 4-7** for notation, assumptions and computation methodology.

An approximate reconciled balance was produced for the cables component category (**Figure 5-41**). This result can satisfactorily depict the split of the flows leaving the two main unit operations of trommel and air classifier, enabling to compute the relevant TCs. Cables category is divided between the heavy oversized reject fraction and the SRF. The A_CL 1 allows a considerable amount to enter in the SRF processing line: $TC(CAB)_{A_CL\ 1_LG} = 43.45 \pm 45.1\%$ (**Table 5-6**). The high U_{95} for this TC

partly results from not having been reconciled due to the partial application of the STAN2[®] software in the case of cables. Only a negligible amount of cables is found in the both the non-Fe and rejects outputs for the eddy-current separator, the rest reporting to the SRF output.

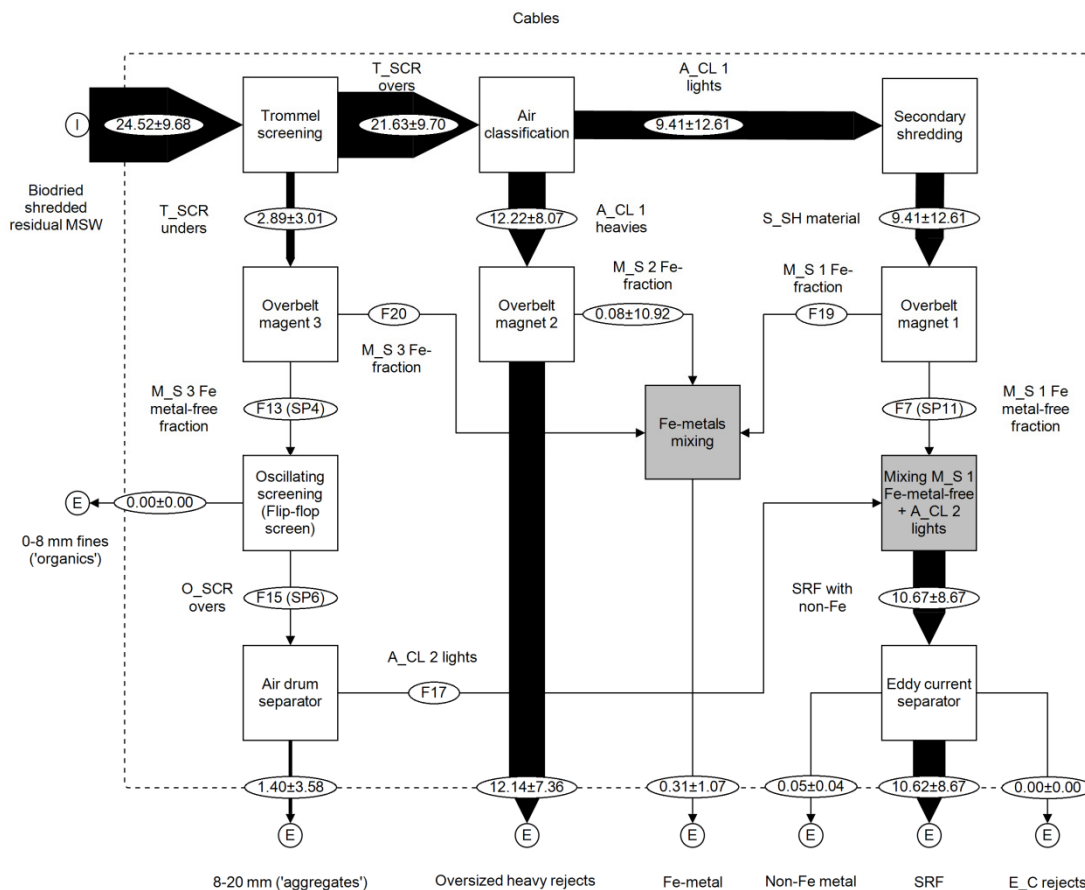


Figure 5-41 Approximate Shankey diagram of the processing section of the UK MBT plant A: composites waste component model of main flows. Values are average specific (per component) mass load (a_r), out of ca 10,000 overall components mass input, plus/minus the total extended uncertainty (U_{95}) (confidence intervals around the average at 95% confidence). Results were balanced (reconciled) by iterative application of the material flow management software STAN2[®], based on sampling and operational plant output data. The width of the flows illustrates their relative magnitude. See **Figure 4-5** and **Table 4-7** for notation, assumptions and computation methodology.

No closing balance is achieved for the adjusted (modelled) flows of the hazardous components (**Figure 5-42**). Around 48% of the input material can be

accounted for by the sum of outputs (**Figure 5-23**). It mainly reports to the oversized heavy rejects and the SRF. A reconciliation of the flows is attempted, but results should be considered as semi-quantitative (**Figure 5-43**). The oversized rejects fraction concentrates most of the HAZ, resulting from the A_CL 1 operation: $TC(HAZ)_{A_CL\ 1_HG} = 81.6 \pm 12.5\%$ (**Table 5-6**). However, the rest is directed mainly to the SRF.

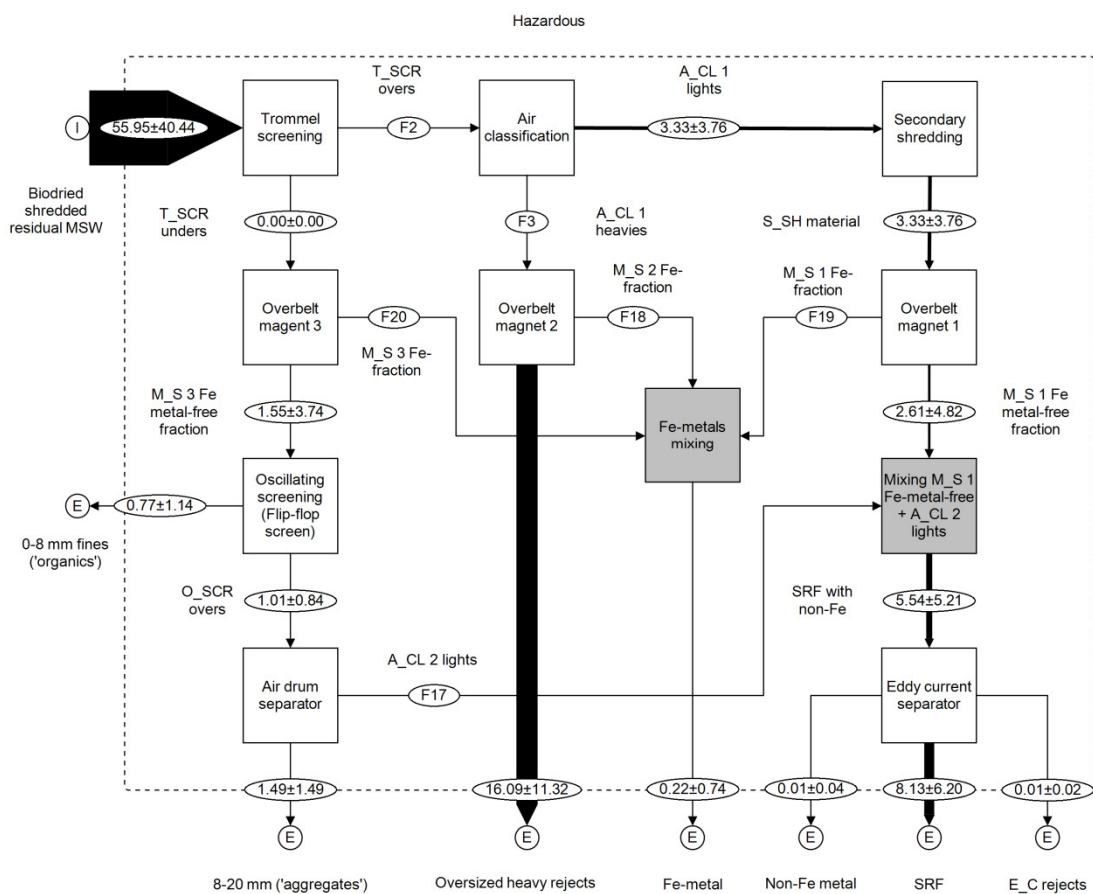


Figure 5-42 Shankey diagram of the processing section of the UK MBT plant A: measured adjusted un-reconciled flows for the hazardous waste component: input to the material flow management software STAN2[®]. Values are average specific (per component) mass load (a_r), out of ca 10,000 overall components mass input, plus/minus the total extended uncertainty (U_{95}) (confidence intervals around the average at 95% confidence). The width of the flows illustrates their relative magnitude. See **Figure 4-5** and **Table 4-7** for notation, assumptions and computation methodology. See **Figure 5-43** for the reconciled model results.

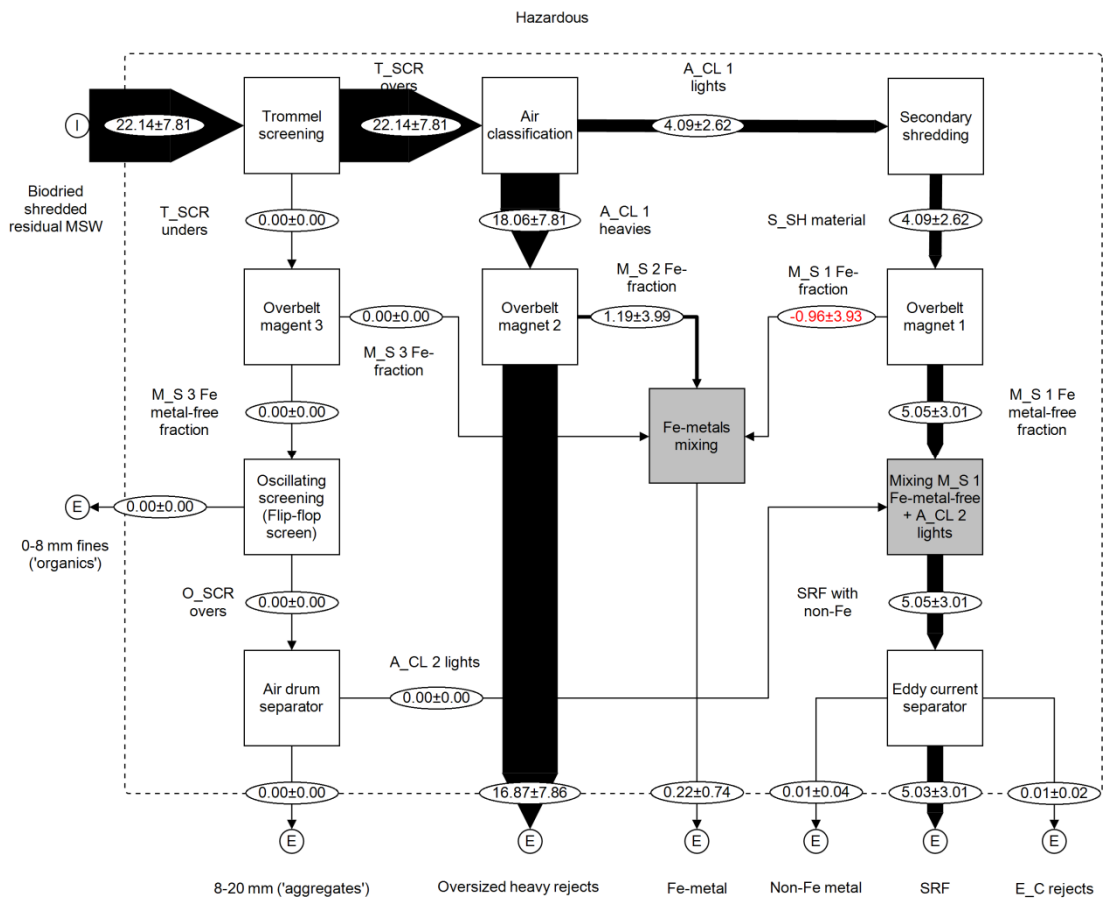


Figure 5-43 Shankey diagram of the processing section of the UK MBT plant A: glass waste component model of flows. Values are average specific (per component) mass load (a_r), out of ca 10,000 overall components mass input, plus/minus the total extended uncertainty (U_{95}) (confidence intervals around the average at 95% confidence). Results were balanced (reconciled) by iterative application of the material flow management software STAN2[®], based on sampling and operational plant output data. The width of the flows illustrates their relative magnitude. See **Figure 4-5** and **Table 4-7** for notation, assumptions and computation methodology.

The balance for batteries exhibits a deficit (**Figure 5-23**). Manual sorting results show that BAT report only to the oversized heavy rejects, the 8-20 mm ('aggregates') and the Fe-metal plant outputs. Altogether, these output streams account for only ca 32% of the amount found in the biodried material. The un-reconciled flow results clearly depict the oversized heavy rejects as the main output (**Figure 5-44**). Batteries are absent from all the flows discharging to the SRF. On-site investigation at the plant

revealed that possibly after the air classification (A_CL 1) batteries are discharged and accumulate, until they are finally disposed manually. Hence, a stock of batteries is created within the plant, comprising mainly various types of AA size. The contamination of the Fe-metal with batteries is estimated as limited, on a mass basis: $0.12 \pm 0.42\%$ w/w_{ar} of the Fe-metal output flow.

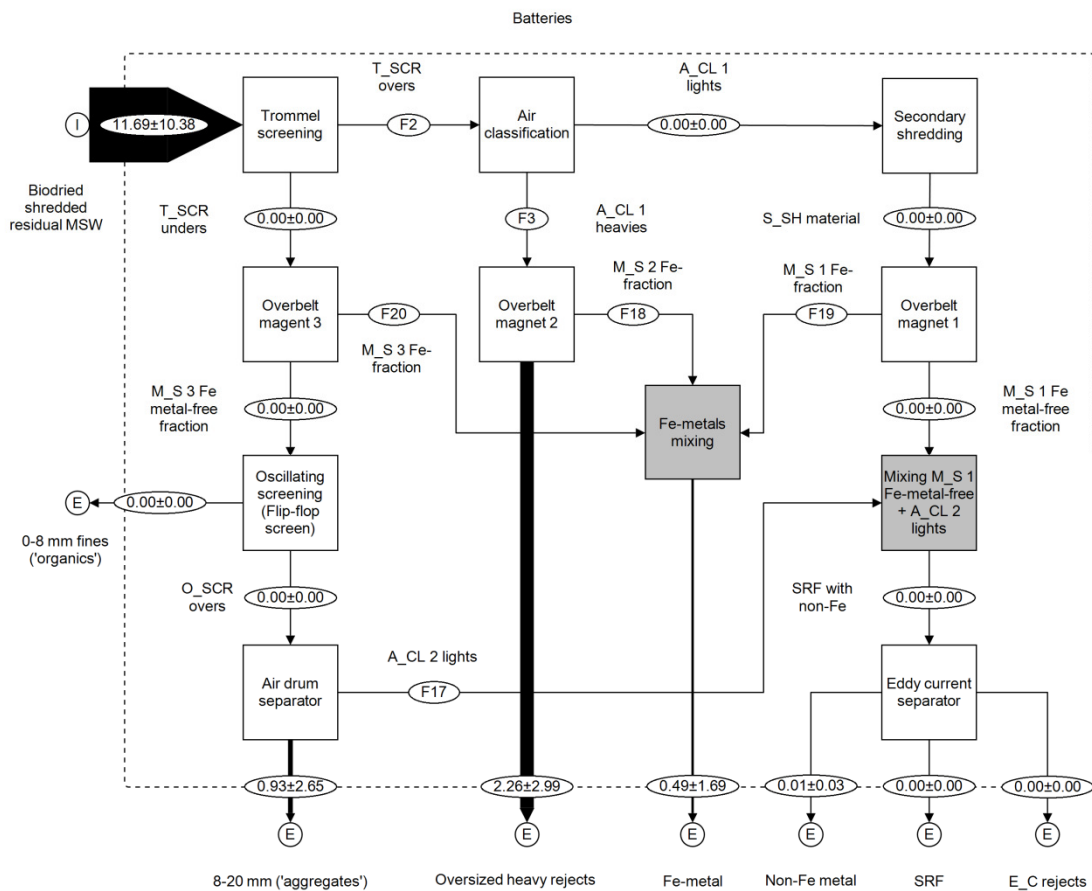


Figure 5-44 Shankey diagram of the processing section of the UK MBT plant A: measured adjusted un-reconciled flows for the batteries waste component. Values are average specific (per component) mass load ($_{ar}$), out of ca 10,000 overall components mass input, plus/minus the total extended uncertainty (U_{95}) (confidence intervals around the average at 95% confidence). The width of the flows illustrates their relative magnitude. See **Figure 4-5** and **Table 4-7** for notation, assumptions and computation methodology.

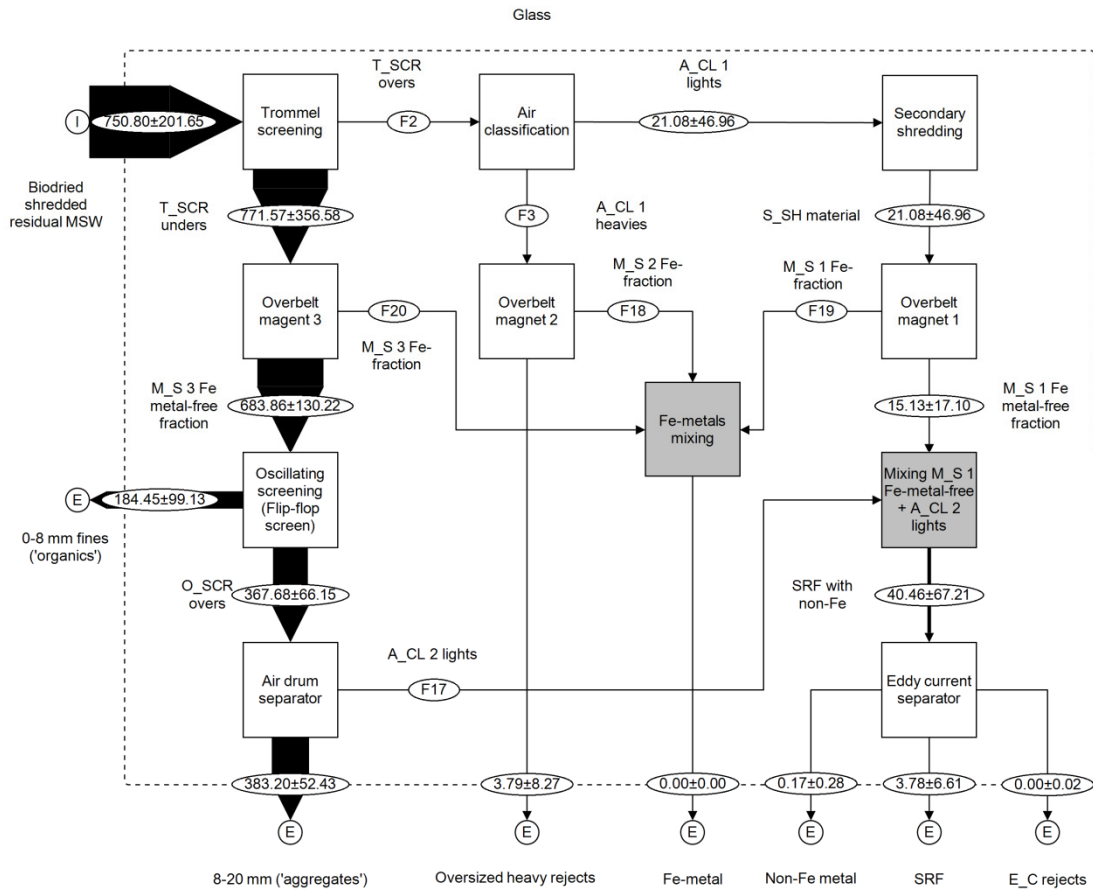


Figure 5-45 Shankey diagram of the processing section of the UK MBT plant A: measured adjusted un-reconciled flows for the glass waste component: input to the material flow management software STAN2[®]. Values are average specific (per component) mass load (\bar{a}_r), out of ca 10,000 overall components mass input, plus/minus the total extended uncertainty (U_{95}) (confidence intervals around the average at 95% confidence). The width of the flows illustrates their relative magnitude. See **Figure 4-5** and **Table 4-7** for notation, assumptions and computation methodology. See **Figure 5-46** for the reconciled model results.

Glass flows, adjusted for the effect of the trommel upon the waste component category of fines < 10 mm, are not balancing (**Figure 5-23**). A deficit in the sum of outputs is evident (**Figure 5-45**). Glass reports almost exclusively to the 8-20 mm ('aggregates') (where it is intended to concentrate) and the 0-8 mm ('organics'). The split is determined by the operation of the oscillating screen (O_SCR). An indicative reconciled balance is reported in **Figure 5-46**. The TCs developed based on this for the

oscillating screen show that around a 60-40 split is achieved for the 8-20 and 0-8 mm discharges respectively ($TC(GL)_{O_SCR_8-20} = 62.6 \pm 8.6\%$) (Table 5-7). Only a negligible amount ends up in the SRF, compared to that present in the biodried flow.

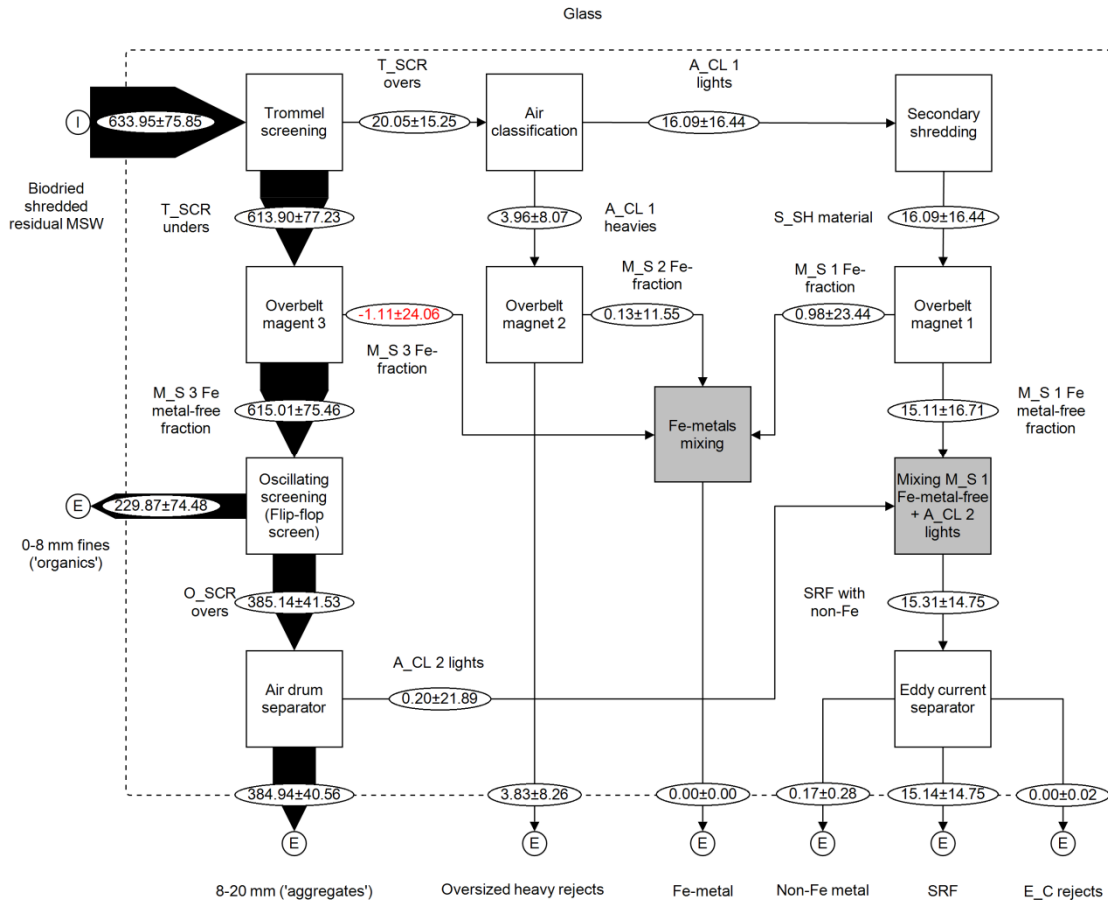


Figure 5-46 Shankey diagram of the processing section of the UK MBT plant A: glass waste component model of flows. Values are average specific (per component) mass load (\bar{a}_r), out of ca 10,000 overall components mass input, plus/minus the total extended uncertainty (U_{95}) (confidence intervals around the average at 95% confidence). Results were balanced (reconciled) by iterative application of the material flow management software STAN2[®], based on sampling and operational plant output data. The width of the flows illustrates their relative magnitude. See Figure 4-5 and Table 4-7 for notation, assumptions and computation methodology.

The balance for stones/ceramic waste component category shows a slight deficit before reconciliation (Figure 5-23). A reconciled balance is presented in Figure

5-47. Two main outlets are the 8-20 mm ('aggregates') and the oversized heavy rejects. A lower amount reports to 0-8 mm ('organics'). The SRF output receives only a negligible amount, at the same order of magnitude of glass is directed to the trommel overs (TC(S/C)_{T_SCR_O} = 45.1±19.7% - **Table 5-5**). The air classifier directs the majority of this input to the oversized heavy rejects.

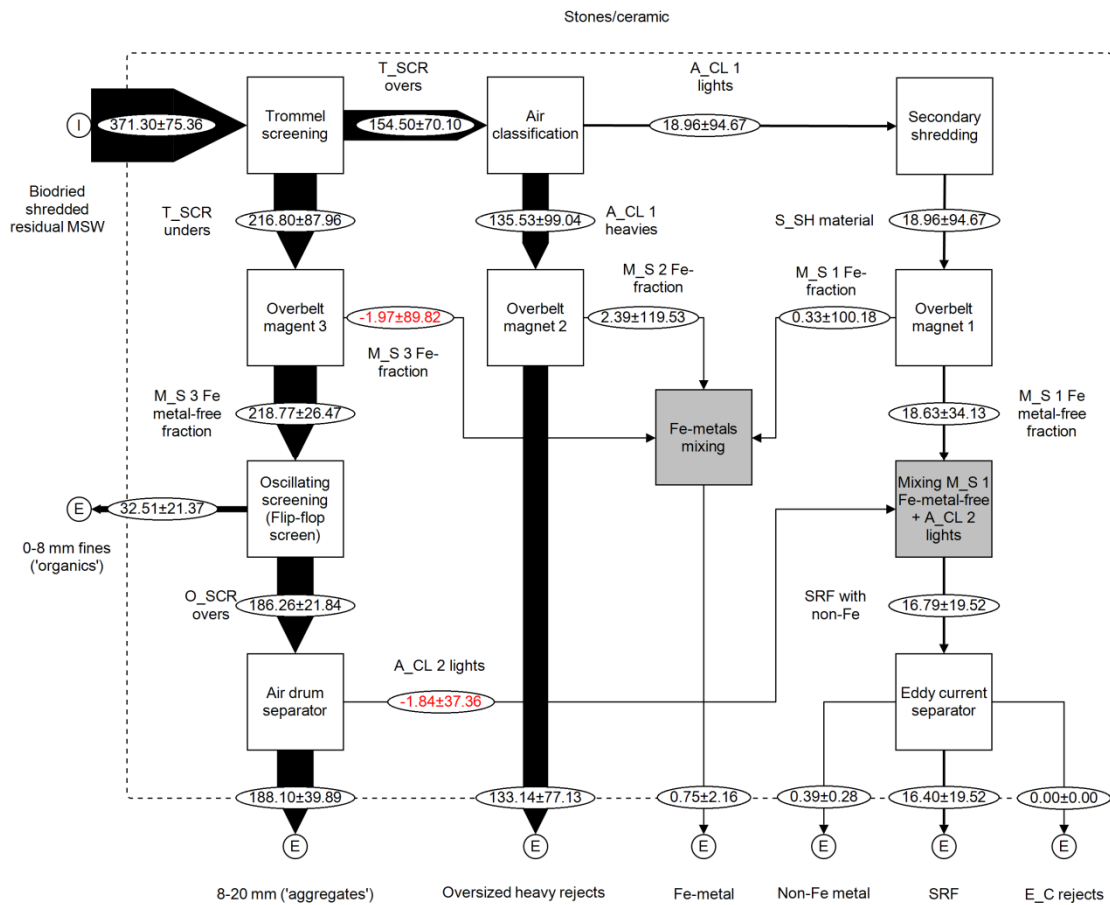


Figure 5-47 Shankey diagram of the processing section of the UK MBT plant A: stones/ceramic waste component model of flows. Values are average specific (per component) mass load (\bar{a}_r), out of ca 10,000 overall components mass input, plus/minus the total extended uncertainty (U_{95}) (confidence intervals around the average at 95% confidence). Results were balanced (reconciled) by iterative application of the material flow management software STAN2[®], based on sampling and operational plant output data. The width of the flows illustrates their relative magnitude. See **Figure 4-5** and **Table 4-7** for notation, assumptions and computation methodology.

The non-Fe metals Shankey diagram (**Figure 5-48**) reveals a limited capability of the existing process flowsheet and individual unit operations performance to direct the component mainly in the intended output. From the 1.80% w/w_{ar} (or mass units) evident in the biodried material, only 0.43 mass units report to the non-Fe plant output, whilst 0.77 mass units to the SRF and 0.56 to the heavy oversized rejects. The validity of this result could be questioned, based on the fact that no reliable operational data on the non-Fe metal were made available for the UK MBT plant A. This is discussed in detail in **Section 6.2.2**.

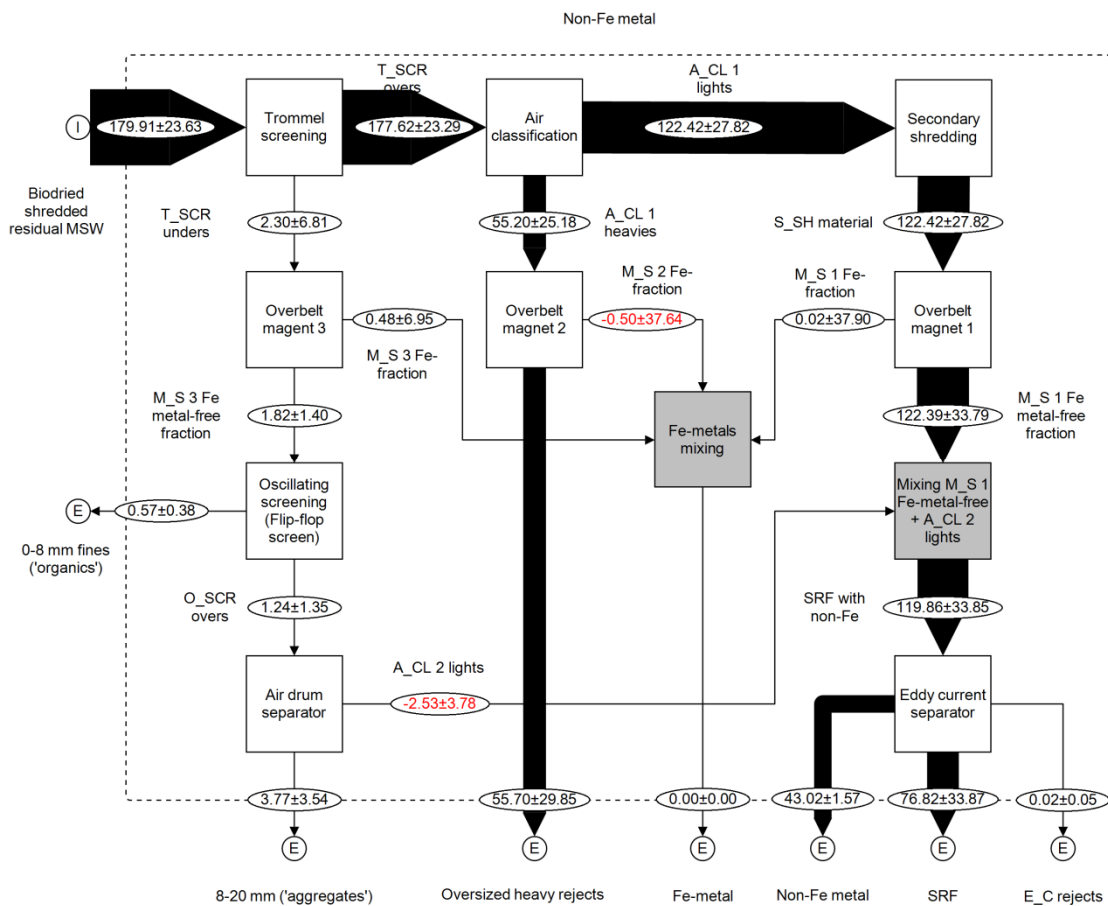


Figure 5-48 Shankey diagram of the processing section of the UK MBT plant A: non-ferrous metal waste component model of flows. Values are average specific (per component) mass load (_{ar}), out of ca 10,000 overall components mass input, plus/minus the total extended uncertainty (U_{95}) (confidence intervals around the average at 95% confidence). Results were balanced (reconciled) by iterative application of the material flow management software STAN2[®], based on sampling and operational plant output data. The width of the flows illustrates

their relative magnitude. See **Figure 4-5** and **Table 4-7** for notation, assumptions and computation methodology.

Assuming the adjusted reconciled balance is correct, the difficulty of concentrating the non-Fe metals in the non-Fe output can be tracked down to the operation of the A_CL 1 and the E_C_S. The A_CL 1 allows a considerable part of the input of non-Fe components to drop in the high gravity fraction ($TC(nFe_M)_{A_CL\ 1_HG} = 31.1 \pm 13.3$) (**Table 5-6**), directing it away from the E_C_S. However, given the poor operation of the E_C_S, this prevents more non-Fe metal to enter the SRF output. Indeed, the E_C_S is not able to prevent the majority of the non-Fe metal components entering the SRF output: $TC(nFe_M)_{E_C_S_nFe_M} = 64.1 \pm 10.2\%$ (**Table 5-9**).

Figure 5-49 presents the reconciled balance for the ferrous metal waste component category. All three overbelt magnets are contributing towards the Fe-metal output of the plant. However, the recovery of the ferrous metal is not complete: a non-negligible amount of ca 20% reports to the oversized heavy rejects ($TC(Fe_M)_{Fe-metal} = 78.1 \pm 8.0\%$). All rest outputs are practically free from metal. The eddy-current separator removes for the SRF stream around half of the Fe-metal present in its input ($TC(Fe_M)_{E_C_S_SRF} = 51.6 \pm 35.2\%$ - **Table 5-9**).

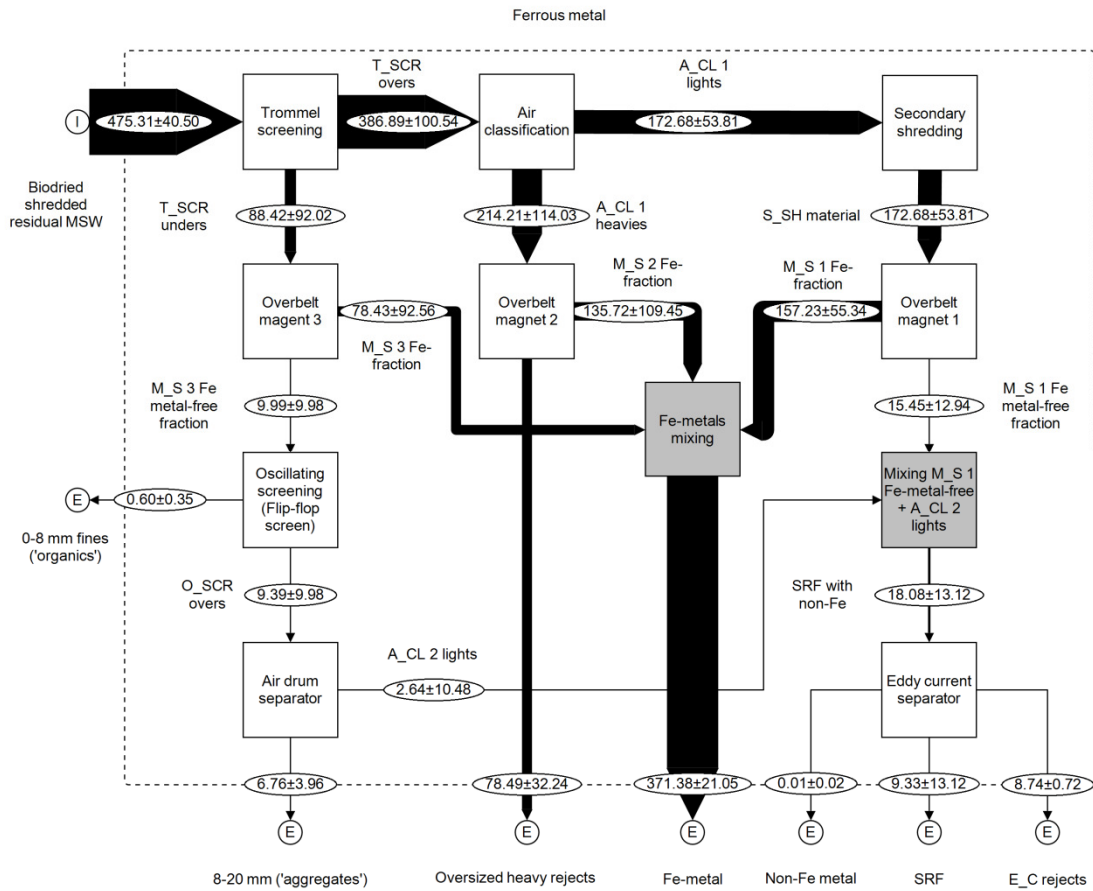


Figure 5-49 Shankey diagram of the processing section of the UK MBT plant A: ferrous metal waste component model of flows. Values are average specific (per component) mass load (a_r), out of ca 10,000 overall components mass input, plus/minus the total extended uncertainty (U_{95}) (confidence intervals around the average at 95% confidence). Results were balanced (reconciled) by iterative application of the material flow management software STAN2[®], based on sampling and operational plant output data. The width of the flows illustrates their relative magnitude. See **Figure 4-5** and **Table 4-7** for notation, assumptions and computation methodology.

5.3.3 UK MBT plant A: balance of fuel properties: mass-based specific loads

Results for balances of key fuel properties are presented in this section regarding the processing section of the UK MBT plant A. Methodology can be found in **Section 4.9.3**. **Figure 5-50** summarises the closures for sum of input and output mass-

specific loads for four properties. Sum of outputs is expressed as a percentage of the input load.

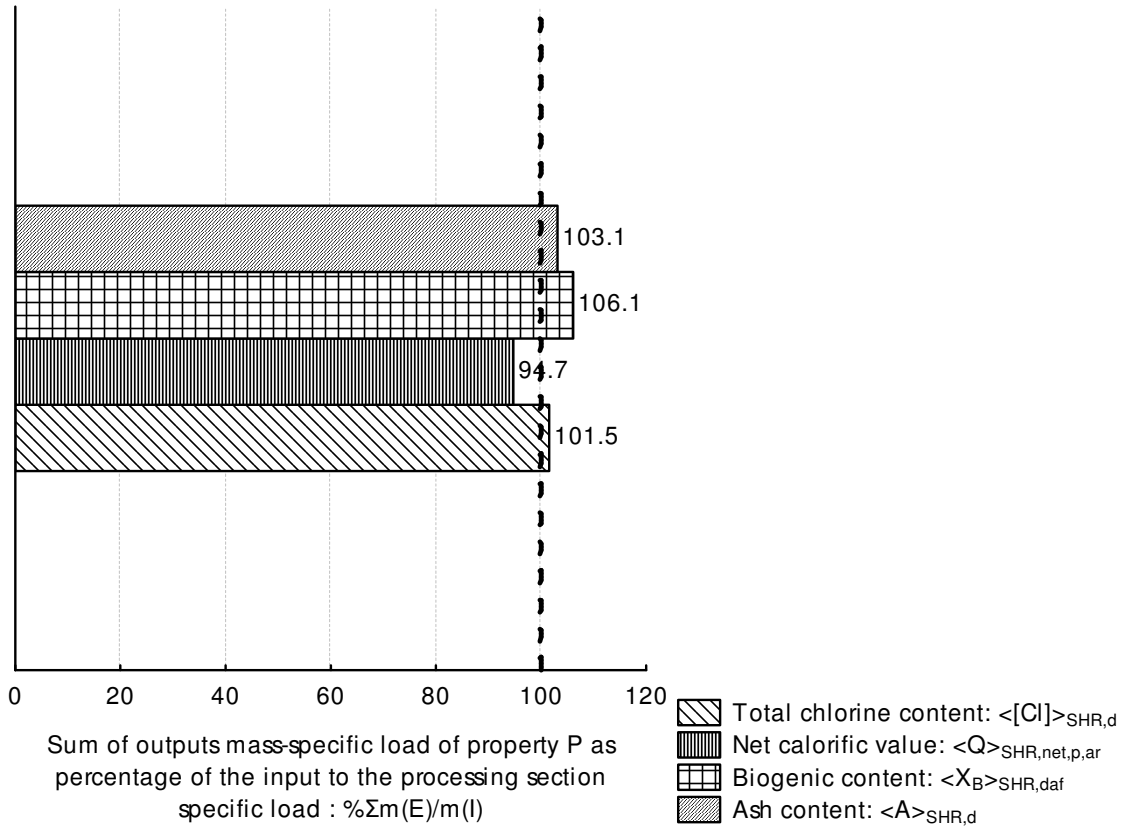


Figure 5-50 Closures of input-output balances for the UK MBT plant A processing section, for a series of fuel properties, as measured on the shreddable/combustible part of samples. Sum of mass-specific load of the property for all plant outputs, expressed as a percentage of the specific load present in the processing section input (biodried material flow). The specific loads were computed multiplying the average measured properties for each output sampling point, with the suitable reconciled mass balance (shreddable mass m_d or m_{daf}). The satisfactory closures serve as a direct validation for the accuracy of sampling, measurement, statistical treatment, and the correctness of the produced reconciled mass flows. They allow the application of data reconciliation software STAN2[®] to compute TCs and inner flows, and fully reconcile the balances.

The results show very good agreement between input and sum of outputs. This validates the overall methodology, including sampling, sub-sampling and sample preparation, analytical determination and statistical analysis. It also verifies the

correctness of the reconciled shreddable mass both on dry and dry, ash-free bases. Given that the input-output data match satisfactorily, the material flow management software STAN2 can be employed to compute transfer coefficients and inner flows, and fully reconcile the balances. Results of the STAN2 application for each of these fuel properties are presented from **Figure 5-51** to **Figure 5-54**.

The ash content load of the shreddable/combustible part of each flows is shown in **Figure 5-51**. The balance reveals that the two main destinations are the 0-8 mm ('organics') output and the SRF. The oscillating screen directs almost all ash content to the organics output. The considerable load reporting to the SRF is added to the non-shreddable, inert part, reporting to it as contamination, they both contribute to its ash content. The transfer coefficient to the SRF is $(TC(\langle A \rangle_{SHR,d})_{SRF} = 37.8 \pm 3.1\%$ - **Table 5-4**).

The biogenic content ($\langle X_B \rangle_{SHR,daf}$) load of the shreddable/combustible part of each flow is presented in **Figure 5-52**. The balance results establish that the bulk of the biogenic dry ash-free load on a mass basis is incorporated into the SRF output ($TC(\langle X_B \rangle_{SHR,daf})_{SRF} = 77.6 \pm 3.4\%$ - **Table 5-4**). The rest load is split between the main relevant outputs, with the oversized heavy rejects gaining the biggest part ($TC(\langle X_B \rangle_{SHR,daf})_{A_CL\ 1_U} = 16.3 \pm 2.3\%$ - **Table 5-6**). The paper reporting there as well can be assumed that it contributes significantly to this outcome ($TC(P/C)_{A_CL\ 1_U} = 18.1 \pm 5.0\%$ - **Table 5-6**).

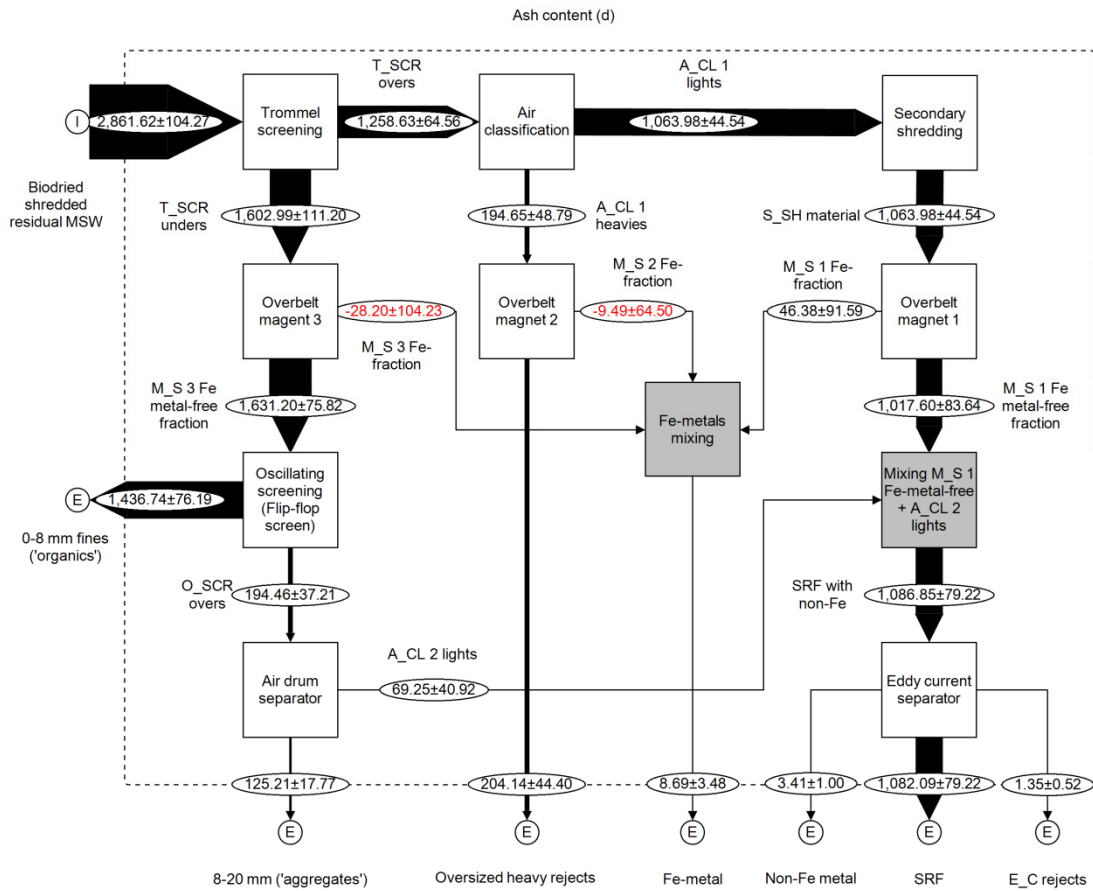


Figure 5-51 Shankey diagram of the processing section of the UK MBT plant A: model of flows for ash content (A), shredded part of samples, expressed on d basis. The width of the flows illustrates their relative magnitude. Values are average specific A load (A_{ar}), out of ca 10,000 overall dry shredded mass input, plus/minus the total extended uncertainty (U_{95}) (confidence intervals around the average at 95% confidence). Results were balanced (reconciled) by iterative application of the material flow management software STAN2[®], based on sampling and operational plant output data. Ash loads computed using the reconciled shredded mass balance (d) (**Figure 5-25**). See **Figure 4-5** for notation and assumptions.

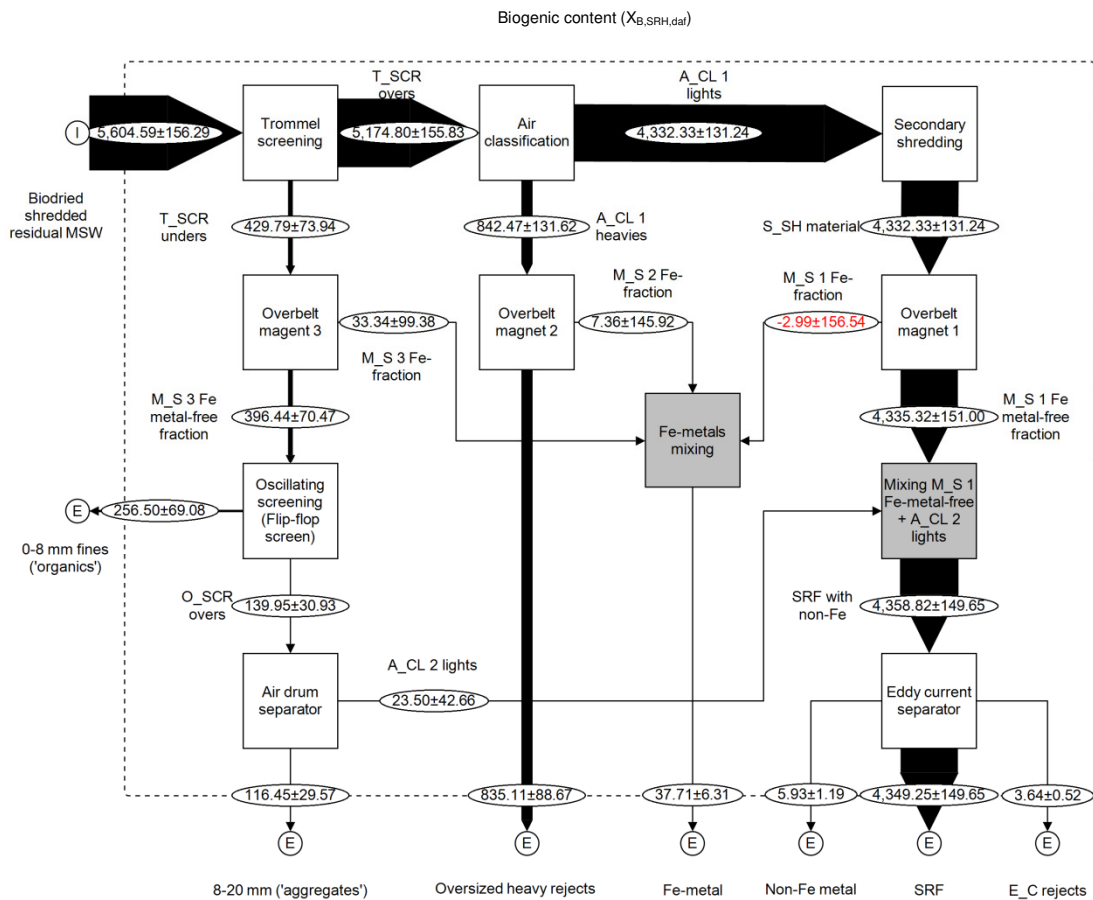


Figure 5-52 Shankey diagram of the processing section of the UK MBT plant A for the biogenic content specific load of the shreddable part of the samples, expressed on a dry, ash-free basis ($_{daf}$). The width of the flows illustrates their relative magnitude. Values are average biogenic content ($X_{B,SHR,daf}$) specific load, out of ca 10,000 overall dry, ash-free shredded mass input, plus/minus the total extended uncertainty (U_{95}) (confidence intervals around the average at 95% confidence). Results were balanced (reconciled) by iterative application of the material flow management software STAN2[®], based on sampling and operational plant output data. Biogenic content loads computed using the reconciled shredded $_{daf}$ mass balance (**Figure 5-26**). Uncertainty was propagated throughout the computations.

Table 5-4). However, energy content equal to almost 1/5th of the amount in the SRF is lost in the oversized heavy rejects output, directed there by the air classifier (TC($\langle X_B \rangle_{SHR,daf}$)_{A_CL 1_U} = 15.4±23.1% -**Table 5-6**). Almost 10% of the biodrying input load amount reports to the 0-8 mm ('organics'). The arguments expressed in the discussion of sum of combustible matter (**Figure 5-27**) apply here as well.

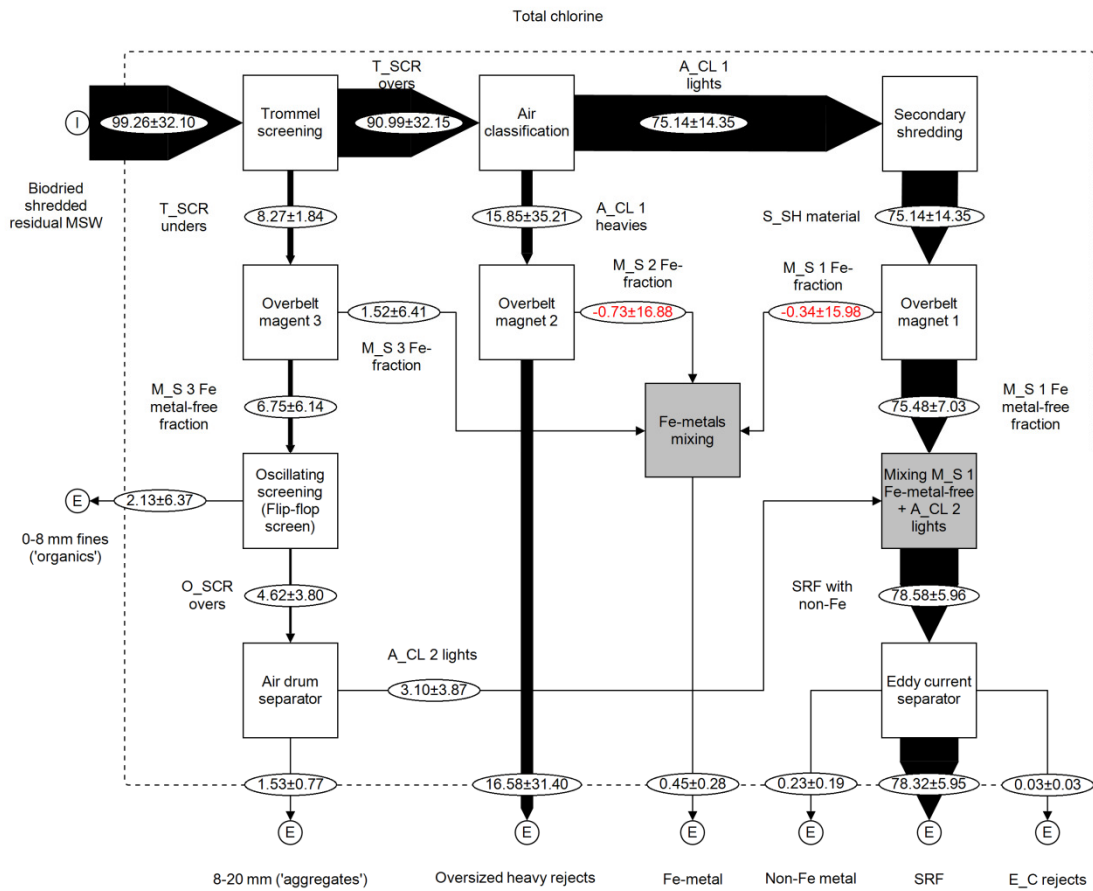


Figure 5-54 Shankey diagram of the processing section of the UK MBT plant A: model for the specific load of total chlorine content of the combustible part of the samples, expressed on a dry basis $TCI_{SHR,d}$. The width of the flows illustrates their relative magnitude. For any processing sub-system, the ratio of any output flow to the sum of input flows provides the transfer coefficient (TC) to this output. Values are average $TCI_{SHR,d}$ specific load, plus/minus the total extended uncertainty (U_{95}) (confidence intervals around the average at 95% confidence). Results were balanced (reconciled) by iterative application of the material flow management software STAN2[®], based on sampling and operational plant output data. $TCI_{SHR,d}$ loads computed using the reconciled sum of shreddable components _d mass balance (**Figure 5-25**). Uncertainty was propagated throughout the computations.

In **Figure 5-54** the balanced flows of the total chlorine content of the shreddable/combustible part is shown. A clear split of the load is evident between the SRF and the oversized heavy rejects. Around 80% of the load is incorporated into the SRF ($TC(\langle [Cl] \rangle_d)_{SRF} = 78.9 \pm 26.2\%$ - **Table 5-4**). This split is determined by the operation of the air classifier ($TC(\langle [Cl] \rangle_d)_{A_CL_1_O} = 82.6 \pm 33.2\%$ - **Table 5-6**). The high uncertainties are propagated from the too high uncertainty of the total chlorine concentration as measured for the biodried and oversized heavy rejects flow characterisation (**Figure 5-15**).

5.4 UK MBT plant A: transfer coefficients of unit operations

Transfer coefficients were computed for a series of fuel properties and materials (components), for mechanical unit operations of the UK MBT plant A: trommel screening, air classification, air drum separator, oscillating screen, and eddy-current separator. Transfer coefficients are defined in **Table 2-6** and discussed in **Section 2.4.3**. Operating principles of the unit processes are presented in **Table 4-1**, and positioning in the flowsheet of the UK MBT A in **Figure 4-2** and **Figure 4-5**.

Computation involved the development of mass-based balances based on the manual sorting data, analytical determination of properties on samples, plant operation data and mathematical adjustments. Then the flows were further balanced and the transfer coefficients computed by applying the material flow management software STAN^{®2}. The detailed methodological steps are described in **Section 4.9** and presented in **Table 4-7**.

Experimental results on are shown in and **Table 5-9**. The TC are visualised in the Shankey diagrams (**Figure 5-42** to **Figure 5-54**), where flows are expressed as specific loads (concentration on mass basis multiplied by mass units of the flow,

corresponding to an input to the processing section of 10.000 mass units). The width of the flows illustrates the relative magnitude of their specific loads. For any processing sub-system, the ratio of any output flow, to the sum of input flows (i.e., ratio of widths) provides the transfer coefficient (TC) to this output.

Table 5-4 Selected transfer coefficients (TC) per waste component (and sums of) or fuel property, for the entire processing section of the UK MBT plant A to the SRF output

UK MBT plant A: processing section to		U ($\Sigma \rightarrow$ (SP13)) Solid recovered fuel	
Component	Symbol	TC	$\pm U_{95}$
Sum of plastics (ar)	$\Sigma(\text{COM}+\text{D_P}+\text{O_P_P}+\text{P_F})$	92.3	7.3
Paper/card (ar)	P/C	79.3	5.8
Sum of Paper-like (ar)	$\Sigma(\text{P/C}+\text{CAR}+\text{TIS})$	80.0	5.7
Ash content (SHR,d)	$A_{\text{SHR,d}}$	37.8	3.1
Biogenic content (SHR,daf)	$X_{\text{B,SHR,daf}}$	77.6	3.4
Net calorific value (SHR,ar)	$Q_{\text{SHR,net,p,ar}}$	73.2	8.6
Total chlorine (SHR,d)	$[\text{Cl}]_{\text{SHR,d}}$	78.9	26.2
Sum of combustible (ar)	$\Sigma(\text{Combustible})_{\text{ar}}$	63.0	1.2
Sum of combustible (daf)	$\Sigma(\text{Combustible})_{\text{daf}}$	74.5	3.2
Sum of non-combustible (ar)	$\Sigma(\text{non-Combustible})_{\text{ar}}$	8.8*	3.8*

*Indicative values due to no sufficient balancing for a series of non-combustible waste component categories

Table 5-5 Transfer coefficients (TC) per waste component (and sums of), for the process unit:

trommel screening (T_SCR). See **Figure 4-5** for notation and relative position within the UK MBT plant A flow-line. Average values plus/minus the total extended uncertainty (U_{95}) (confidence intervals around the average at 95% confidence). Computed using data from flows balanced (reconciled) by iterative application of the material flow management software STAN2[®], based on sampling and operational plant output data.

Trommel screening (T_SCR)		U ($\Sigma \rightarrow$ F12 (SP2)) 'Organics' and 'aggregates' flow-line		O ($\Sigma \rightarrow$ F2) SRF flow-line	
Component	Symbol	TC (ar)	$\pm U_{95}$ (ar)	TC (ar)	$\pm U_{95}$ (ar)
Sum of mass	Σm	30.9	2.4	69.1	2.4
Sum of combustible	$\Sigma(\text{Comb})$	27.4	1.5	72.6	1.5
Sum of non-combustible	$\Sigma(\text{nComb})$	60.1	6.4	39.9	6.4
Sum of paper and like	$\Sigma(\text{P/C}+\text{TIS}+\text{CAR})$	3.6	0.7	96.4	0.7
Sum of plastics	$\Sigma(\text{COM}+\text{D_P}+\text{O_P_P}+\text{P_F})$	4.9	1.9	95.1	1.9
Sum of textiles and like	$\Sigma(\text{C/M}+\text{FL}+\text{S_P}+\text{SH}+\text{T/F})$	6.2	3.4	93.8	3.4
Biological	BIO	67.6	6.2	32.4	6.2
Cables	CAB	11.8	12.5	88.2	12.5
Cartons	CAR	0.7	0.8	99.3	0.8
Cinders	CIN	24.8	37.6	75.2	37.6
Composites	COM	7.8	6.4	92.2	6.4
Durable plastic	D_P	14.5	4.7	85.5	4.7
Fines < 10 mm	F<10	99.7	25.1	0.3	25.1

Trommel screening (T_SCR)		U ($\Sigma \rightarrow$ F12 (SP2)) 'Organics' and 'aggregates' flow-line		O ($\Sigma \rightarrow$ F2) SRF flow-line	
Component	Symbol	TC (ar)	$\pm U_{95}$ (ar)	TC (ar)	$\pm U_{95}$ (ar)
Ferrous metal	Fe_M	18.6	19.4	81.4	19.4
Fluff	FL	64.6	13.1	35.4	13.1
Glass	GL	96.8	2.4	3.2	2.4
Hazardous	HAZ	0.0	0.0	100.0	0.0
Non-Fe metal	nFe_M	0.0	31.0	100.0	31.0
Other packaging plastic	O_P_P	1.7	1.2	98.3	1.2
Paper/card	P/C	3.7	0.7	96.3	0.7
Plastic film	P_F	3.6	1.9	96.4	1.9
Rubber/leather	R/L	1.7	10.9	98.3	10.9
Stones/ceramic	S/C	54.9	19.7	45.1	19.7
Treated wood	T_W	5.5	2.9	94.5	2.9
Dry matter	d.m.	31.5	1.2	68.5	1.2
Shredded dry matter	d.m.-SRH	26.3	2.3	73.7	2.3
Ash content (_{SHR,d})	A _{SHR,d}	56.0	2.5	44.0	2.5
Biogenic content (_{SHR,daf})	$\chi_{B,SHR,daf}$	7.7	1.3	92.3	1.3
Net calorific value (_{SHR,ar})	Q _{SHR,net,p,ar}	13.4	2.8	86.6	2.8
Total chlorine	[Cl] _d	8.3	3.3	91.7	3.3

Values for input flow of residual, shredded at 300 mm and biodried municipal waste. Trommel apertures 20 mm. Notation explanation: transfer coefficient of the component (substance) CP to the output (product) O for the unit operation OU: TC(CP)_{OU,O}

Table 5-6 Transfer coefficients (TC) per waste component (and sums of), for the process unit: air classification (A_CL 1). See **Figure 4-5** for notation and relative position within the UK MBT plant A flow-line. Average values plus/minus the total extended uncertainty (U_{95}) (confidence intervals around the average at 95% confidence). Computed using data from flows balanced (reconciled) by iterative application of the material flow management software STAN2[®], based on sampling and operational plant output data.

Air classification (A_CL 1)		HG ($\Sigma \rightarrow$ F3) Oversized heavy rejects flow-line		LG ($\Sigma \rightarrow$ F5) SRF flow-line	
Component	Symbol	TC (ar)	$\pm U_{95}$ (ar)	TC (ar)	$\pm U_{95}$ (ar)
Sum of mass	Σm	20.4	1.6	79.6	1.6
Sum of combustible	$\Sigma(\text{Comb})$	16.2	1.5	83.8	1.5
Sum of non-combustible	$\Sigma(n\text{Comb})$	58.1	13.7	41.9	13.7
Sum of paper and like	$\Sigma(P/C+TIS+CAR)$	17.7	4.7	82.3	4.7
Sum of plastics	$\Sigma(\text{COM}+D_P+O_P_P+P_F)$	4.3	0.9	95.7	0.9
Sum of textiles and like	$\Sigma(C/M+FL+S_P+SH+T/F)$	34.3	7.7	65.7	7.7
Batteries	BAT				
Biological	BIO	39.8	9.9	60.2	9.9
Cables	CAB	56.5	45.1	43.5	45.1
Cartons	CAR	3.7	4.0	96.3	4.0
Cinders	CIN	6.5	7.9	93.5	7.9
Composites	COM	2.7	3.9	97.3	3.9
Durable plastic	D_P	16.6	7.1	83.4	7.1
Fines < 10 mm	F<10	-	-	-	-
Ferrous metal	Fe_M	55.4	18.1	44.6	18.1
Fluff	FL	0.2	0.4	99.8	0.4
Glass	GL	19.7	41.4	80.3	41.4
Hazardous	HAZ	81.6	12.5	18.4	12.5
Non-Fe metal	nFe_M	31.1	13.3	68.9	13.3

Air classification (A_CL 1)		HG ($\Sigma \rightarrow$ F3) Oversized heavy rejects flow-line		LG ($\Sigma \rightarrow$ F5) SRF flow-line	
Component	Symbol	TC (ar)	$\pm U_{95}$ (ar)	TC (ar)	$\pm U_{95}$ (ar)
Other packaging plastic	O_P_P	4.3	1.1	95.7	1.1
Paper/card	P/C	18.1	5.0	81.9	5.0
Plastic film	P_F	1.3	0.6	98.7	0.6
Rubber/leather	R/L	-5.9	19.1	105.9	19.1
Stones/ceramic	S/C	85.0	70.1	15.0	70.1
Treated wood	T_W	33.5	10.2	66.5	10.2
Dry matter	d.m.	20.0	1.4	80.0	1.4
Shredded dry matter	d.m.-SRH	15.0	1.8	85.0	1.8
Ash content (_{SHR,d})	A _{SHR,d}	15.5	3.3	84.5	3.3
Biogenic content (_{SHR,daf})	$\chi_{B,SHR,daf}$	16.3	2.3	83.7	2.3
Net calorific value (_{SHR,ar})	Q _{SHR,net,p,ar}	15.4	21.3	84.6	21.3
Total chlorine	[Cl] _d	17.4	33.2	82.6	33.2

Notation explanation: transfer coefficient of the component (substance) CP to the output (product) O for the unit operation OU: TC(CP)_{OU,O}

Table 5-7 Transfer coefficients (TC) per waste component (and sums of), for the process unit: oscillating screening (Flip-flop screen) (O_SCR). See **Figure 4-5** for notation and relative position within the UK MBT plant A flow-line. Average values plus/minus the total extended uncertainty (U_{95}) (confidence intervals around the average at 95% confidence). Computed using data from flows balanced (reconciled) by iterative application of the material flow management software STAN2[®], based on sampling and operational plant output data.

Oscillating screening (Flip-flop screen) (O_SCR)		U($\Sigma \rightarrow$ F14 (SP5)) 0-8 fines ('organics')		O($\Sigma \rightarrow$ F15 (SP6)) 8-20 mm ('aggregates') flow-line	
Component	Symbol	TC (ar)	$\pm U_{95}$ (ar)	TC (ar)	$\pm U_{95}$ (ar)
Sum of mass	Σm	68.6	6.4	31.4	6.4
Sum of combustible	$\Sigma(\text{Comb})$	78.9	2.7	21.1	2.7
Sum of non-combustible	$\Sigma(\text{nComb})$	30.3	7.7	69.7	7.7
Sum of paper and like	$\Sigma(\text{P/C}+\text{TIS}+\text{CAR})$	35.1	6.2	64.9	6.2
Sum of plastics	$\Sigma(\text{COM}+\text{D}_P+\text{O}_P+\text{P}_P+\text{P}_F)$	33.9	5.8	66.1	5.8
Sum of textiles and like	$\Sigma(\text{C/M}+\text{FL}+\text{S}_P+\text{SH}+\text{T/F})$	61.1	18.5	38.9	18.5
Biological	BIO	58.3	33.2	41.7	33.2
Cables	CAB	-	-	-	-
Cartons	CAR	35.9	52.7	64.1	52.7
Cinders	CIN				
Composites	COM	33.8	11.8	66.2	11.8
Durable plastic	D_P	37.3	17.4	62.7	17.4
Fines < 10 mm	F<10	90.5	2.3	9.5	2.3
Ferrous metal	Fe_M	-	-	-	-
Fluff	FL	70.3	20.4	29.7	20.4
Glass	GL	37.4	8.6	62.6	8.6
Hazardous	HAZ	-	-	-	-
Non-Fe metal	nFe_M	31.6	27.6	68.4	27.6
Other packaging plastic	O_P_P	39.1	15.4	60.9	15.4
Paper/card	P/C	33.7	6.9	66.3	6.9
Plastic film	P_F	40.7	9.5	59.3	9.5
Rubber/leather	R/L	-	-	-	-
Stones/ceramic	S/C	14.9	8.8	85.1	8.8
Treated wood	T_W	26.2	12.1	73.8	12.1
Dry matter	d.m.	65.3	3.8	34.7	3.8
Shredded dry matter	d.m.-SRH	82.1	5.8	17.9	5.8

Oscillating screening (Flip-flop screen) (O_SCR)		U($\Sigma \rightarrow$ F14 (SP5)) 0-8 fines ('organics')		O($\Sigma \rightarrow$ F15 (SP6)) 8-20 mm ('aggregates') flow-line	
Component	Symbol	TC (ar)	$\pm U_{95}$ (ar)	TC (ar)	$\pm U_{95}$ (ar)
Ash content ($_{SHR,d}$)	$A_{SHR,d}$	88.1	2.2	11.9	2.2
Biogenic content ($_{SHR,daf}$)	$\chi_{B,SHR,daf}$	64.7	8.6	35.3	8.6
Net calorific value ($_{SHR,ar}$)	$Q_{SHR,net,p,ar}$	64.3	10.6	35.7	10.6
Total chlorine	$[Cl]_d$	31.6	72.8	68.4	72.8

Notation explanation: transfer coefficient of the component (substance) CP to the output (product) O for the unit operation OU: $TC(CP)_{OU,O}$

Table 5-8 Transfer coefficients (TC) per waste component (and sums of), for the process unit: air drum separator (A_CL 2). See **Figure 4-5** for notation and relative position within the UK MBT plant A flow-line. Average values plus/minus the total extended uncertainty (U_{95}) (confidence intervals around the average at 95% confidence). Computed using data from flows balanced (reconciled) by iterative application of the material flow management software STAN2[®], based on sampling and operational plant output data.

Air drum separation (A_CL 2)		HG ($\Sigma \rightarrow$ F16 (SP7)) 8-20 mm ('aggregates')		LG ($\Sigma \rightarrow$ F17) SRF flow-line	
Component	Symbol	TC (ar)	$\pm U_{95}$ (ar)	TC (ar)	$\pm U_{95}$ (ar)
Sum of mass	Σm	93.6	25.1	6.4	25.1
Sum of combustible	$\Sigma(\text{Comb})$	62.0	13.8	38.0	13.8
Sum of non-combustible	$\Sigma(n\text{Comb})$	95.6	12.4	4.4	12.4
Sum of paper and like	$\Sigma(P/C+TIS+CAR)$	46.1	41.5	53.9	41.5
Sum of plastics	$\Sigma(\text{COM}+D_P+O_P_P+P_F)$	41.9	13.5	58.1	13.5
Sum of textiles and like	$\Sigma(C/M+FL+S_P+SH+T/F)$	11.5	15.0	88.5	15.0
Biological	BIO	37.6	12.7	62.4	12.7
Cables	CAB	-	-	-	-
Cartons	CAR	58.7	147.1	41.3	147.1
Cinders	CIN				
Composites	COM	50.7	23.4	49.3	23.3
Durable plastic	D_P	81.0	50.5	16.6	50.5
Fines < 10 mm	F<10	73.2	31.4	26.8	31.4
Ferrous metal	Fe_M	71.9	84.7	28.1	84.7
Fluff	FL	13.1	23.3	86.9	23.3
Glass	GL	100.2	3.9	-0.2	3.9
Hazardous	HAZ	-	-	-	-
Non-Fe metal	nFe_M				
Other packaging plastic	O_P_P	33.2	39.8	66.8	39.8
Paper/card	P/C	44.4	41.2	55.6	41.2
Plastic film	P_F	18.8	21.7	81.2	21.7
Rubber/leather	R/L	56.2	93.2	43.8	93.2
Stones/ceramic	S/C	101.1	20.1	-1.1	20.1
Treated wood	T_W	61.9	62.3	38.1	62.3
Dry matter	d.m.	89.8	12.4	10.2	12.4
Shredded dry matter	d.m. _{SRH}	67.1	31.1	32.9	31.1
Ash content ($_{SHR,d}$)	$A_{SHR,d}$	64.4	15.2	35.6	15.2
Biogenic content ($_{SHR,daf}$)	$\chi_{B,SHR,daf}$	83.2	27.9	16.8	27.9
Net calorific value ($_{SHR,ar}$)	$Q_{SHR,net,p,ar}$	66.3	27.5	33.7	27.5
Total chlorine	$[Cl]_d$	33.0	31.8	67.0	31.8

Notation explanation: transfer coefficient of the component (substance) CP to the output (product) O for the unit operation OU: $TC(CP)_{OU,O}$

Table 5-9 Transfer coefficients (TC) per waste component (and sums of), for the process unit: eddy current separator (E_C_S). See **Figure 4-5** for notation and relative position within the UK MBT plant A flow-line. Average values plus/minus the total extended uncertainty (U_{95}) (confidence intervals around the average at 95% confidence). Computed using data from flows balanced (reconciled) by iterative application of the material flow management software STAN2[®], based on sampling and operational plant output data.

Eddy current separator (E_C_S)		$\Sigma \rightarrow$ F9 (SP13) SRF		$\Sigma \rightarrow$ F11 (SP14) Non-Fe metal		$\Sigma \rightarrow$ F10 (SP15) E_C rejects	
Component	Symbol	TC (ar)	$\pm U_{95}$ (ar)	TC (ar)	$\pm U_{95}$ (ar)	TC (ar)	$\pm U_{95}$ (ar)
Sum of mass	Σm	98.9	0.4	0.9	0.4	0.2	0.0
Sum of combustible	$\Sigma(\text{Comb})$	99.9	0.0	0.1	0.0	0.0	0.0
Sum of non-combustible	$\Sigma(\text{nComb})$	73.4	8.4	22.2	7.0	4.5	1.4
Sum of paper and like	$\Sigma(\text{P/C}+\text{TIS}+\text{CAR})$	99.9	0.0	0.1	0.0	0.0	0.0
Sum of plastics	$\Sigma(\text{COM}+\text{D}_P+\text{O}_P+\text{P}_F)$	99.8	0.0	0.2	0.0	0.0	0.0
Sum of textiles and like	$\Sigma(\text{C/M}+\text{FL}+\text{S}_P+\text{SH}+\text{T/F})$	99.9	0.1	0.0	0.0	0.1	0.1
Biological	BIO	99.7	0.3	0.3	0.3	0.0	0.0
Cables	CAB	99.5	0.5	0.5	0.5	0.0	0.0
Cartons	CAR	100.0	0.1	0.0	0.1	0.0	0.0
Cinders	CIN	-	-	-	-	-	-
Composites	COM	99.8	0.1	0.1	0.1	0.0	0.0
Durable plastic	D_P	99.8	14.4	0.2	14.4	0.0	0.0
Fines < 10 mm	F<10	99.7	0.4	0.0	0.0	0.3	0.4
Ferrous metal	Fe_M	51.6	35.2	0.1	0.1	48.3	35.2
Fluff	FL	99.9	0.0	0.0	0.0	0.1	0.0
Glass	GL	96.8	287.4	3.2	287.4	0.0	0.1
Hazardous	HAZ	99.6	0.9	0.2	0.8	0.2	0.4
Non-Fe metal	nFe_M	64.1	10.2	35.9	10.2	0.0	0.0
Other packaging plastic	O_P_P	96.2	33.1	0.2	0.1	3.6	33.1
Paper/card	P/C	99.9	0.0	0.1	0.0	0.0	0.0
Plastic film	P_F	99.9	0.0	0.0	0.0	0.0	0.0
Rubber/leather	R/L	99.5	0.8	0.4	0.7	0.1	0.1
Stones/ceramic	S/C	97.7	3.2	2.3	3.2	0.0	0.0
Treated wood	T_W	99.7	0.1	0.3	0.1	0.0	0.0
Dry matter	d.m.	98.8	0.4	1.0	0.4	0.2	0.0
Shredded dry matter	d.m.-SRH	99.7	0.3	0.2	0.3	0.1	0.2
Ash content ($_{\text{SHR,d}}$)	$A_{\text{SHR,d}}$	99.6	0.1	0.3	0.1	0.1	0.0
Biogenic content ($_{\text{SHR,daf}}$)	$\chi_{\text{B,SHR,daf}}$	99.78	0.03	0.14	0.03	0.08	0.01
Net calorific value ($_{\text{SHR,ar}}$)	$Q_{\text{SHR,net,p,ar}}$	99.9	0.0	0.1	0.0	0.0	0.0
Total chlorine	$[\text{Cl}]_d$	99.7	0.2	0.3	0.2	0.04	0.04

E_C rejects (F10, SP15) balance based upon assumption

Notation explanation: transfer coefficient of the component (substance) CP to the output (product) O for the unit operation OU: $\text{TC}(\text{CP})_{\text{OU},\text{O}}$

5.5 UK MBT plant A: simulation of SRF properties

Results are presented here (**Table 5-10**) for a characterisation of the waste components identified during the manual sorting process (**Section 4.8**), for a series of fuel-related properties. The reconstructed through the material flow analysis as

received composition of SRF (**Figure 5-21**) and its dry basis equivalent (**Table App F-19**) are then used to compute the specific load of the SRF for each of the properties (**Table 5-10** and **Figure 5-55** to **Figure 5-58**). Insights into the contribution of each component are gained. Methodology is detailed in **Section 4.11**. The overall load is simulated and the result is compared with the experimentally determined value, to validate the simulation (**Table 5-11** and **Figure 5-59**).

5.5.1 UK MBT plant A: concentrations and specific loads per waste component

The moisture content measured for the biodried waste components of the UK MBT A process streams spans 55.4-0.0% w/w_{ar} (**Table 5-10** and **Figure 5-55**). However, with the exception of the maximum of 55.4% w/w_{ar} for sanitary products, all rest items were found dried to below 15% w/w_{ar}, with the exception of the biological and paper/card component categories which slightly exceed 20% w/w_{ar}.

The total chlorine content measured for the biodried waste components of the UK MBT A process streams spans 0-6% w/w_d. The highest total chlorine concentrations were measured for sub-categories of plastics or plastic-containing items (**Table 5-10** and **Figure 5-56**). Shoes were the highest (6.0% w/w_d), followed by other packaging plastics and plastic films, both above 1% w/w_d. Average plastic mixture of the modelled average UK MBT plant A SRF composition is 1.19% w/w_d, computed as their mass fraction weighted mean. All other components were measured below 1% w/w_d. Paper and card, the dominant SRF component, was found 0.19% w/w_d. Only negligible concentration of total chlorine was identified in the durable plastics (0.016% w/w_d). The value of cables was assumed at the half of a typical value for high-in-PVC materials (5% w/w_d)³²², using the average mass ratio between cable wires and

insulating plastic coating (ca 50% w/w). Fluff concentration was computed as the non-weighted average of its most prominent components in the SRF process stream.

The ash content measured for the biodried waste components of the UK MBT A process streams spans 1.61-100% w/w_d. (**Table 5-10** and **Figure 5-57**). For the simulation purposes, a value of 100% w/w_d was assumed for chemically inert components (metals, stones, batteries, etc.), as shown in **Figure 5-57**. For the main SRF constituents, the lowest values are evident for the category of other packaging plastics (1.6% w/w_d) and plastic film (7.62% w/w_d). Paper/card shows a value close to the average level evident for the SRF (17.5% w/w_d). In general, relatively few components have ash content values lower than the achieved average SRF as can be seen in **Figure 5-57**.

The net calorific value measured for the biodried waste components of the UK MBT A process streams spans 0-30.7 MJ kg_{ar}⁻¹ (**Table 5-10** and **Figure 5-58**). For the simulation purposes, a value of 0 MJ kg_{ar}⁻¹ was assumed for mineralised components (metals, stones, batteries, etc.), as shown in **Figure 5-58**. For the main SRF constituents, highest values are reached by the plastics, as anticipated (other packaging plastics (26.1 MJ kg_{ar}⁻¹) and plastic film (30.7 MJ kg_{ar}⁻¹). Paper/card has a much lower value (13.0 MJ kg_{ar}⁻¹).

Table 5-10 Fuel properties characterisation of biodried MBT process flows

Waste component	Component ID	Ash content A (% w/w _d)	Ash content (<A> _d) (% w/w _d)	Ash content specific load	% Ash content specific load contribution	Moisture content (<M _T >) (w/w _{ar})	Moisture content specific load	% Moisture content specific load contribution	Q _{net,p, ar} (KJ/kg _{ar})	Net calorific value <Q> _{net,p, ar} (KJ kg _{ar} ⁻¹)	Net calorific value specific load	% Net calorific value specific load contribution	Total chlorine content [Cl] (% w/w _d)	Total chlorine content <[Cl]> (% w/w _d)	Total chlorine content specific load	% Total chlorine content specific load contribution	
Biological	BIO	29.17	27.19	0.53	3.3	21.56	0.46	3.5	10424	10553	228	1.3	0.306	0.301	0.006	0.8	
		34.40								10682				0.386			
		18.01								15646				0.210			
Carpet/mats	C/M	30.15	30.15	0.33	2.1	4.86	0.05	0.4	29672	29672	294	1.6	0.222	0.222	0.002	0.3	
Cartons	CAR	6.92	10.19	0.13	0.8	12.93	0.16	1.2	19836	19836	253	1.4	0.061	0.061	0.001	0.1	
		13.45															
Composites	COM	16.61	16.61	0.60	3.8	10.30	0.36	2.7	22357	19272	676	3.8	0.688	0.531	0.019	2.8	
										16187				0.373			
Durable plastic	D_P	11.43	13.75	0.49	3.1	1.29	0.04	0.3	20719	20719	646	3.6	0.003	0.016	0.001	0.1	
		16.07												0.029			
Fines <10 mm	F<10	65.33	67.09	0.57	3.6	8.44	0.07	0.5	6028	6861	55	0.3	0.128	0.096	0.001	0.1	
		68.84								7695				0.064			
Other Fluff	OTH	50.00	50.00	0.39	2.4	0.00	0.00	0.0	0	0	0	0.0	0.000	0.000	0.000	0.0	
	FL		22.01	0.08	0.5	3.64	0.01	0.1		17966	61	0.3		1.075	0.004	0.6	
Other packaging plastic	O_P_P	1.68	1.61	0.25	1.6	4.01	0.57	4.2	30227	26050	3682	20.6	1.818	1.523	0.239	34.5	
		1.55								21874		0	0.0	1.229			
Paper/card	P/C	19.45	17.52	7.15	44.9	20.63	9.19	68.4	12268	13036	5806	32.5	0.188	0.239	0.098	14.1	
		15.60								13805				0.290			
Plastic film	P_F	7.62	7.62	1.13	7.1	4.60	0.62	4.6	30708	30708	4115	23.0	1.283	1.283	0.189	27.4	
Rubber/leather	R/L		8.72	0.03	0.2	4.95	0.02	0.1		24726	89	0.5		0.756	0.003	0.4	
Sanitary products	S_P	36.03	36.03	0.27	1.7	55.43	0.80	6.0	5942	5942	86	0.5	0.132	0.132	0.001	0.1	
Shoes	SH	18.84	18.84	0.31	2.0	6.42	0.10	0.7	21745	21745	335	1.9	6.048	6.048	0.101	14.5	

Waste component	Component ID	Ash content A (% w/w _d)	Ash content (<A> _d) (% w/w _d)	Ash content specific load	% Ash content specific load contribution	Moisture content (<M _T >) (w/w _{ar})	Moisture content specific load	% Moisture content specific load contribution	Q _{net,p, ar} (KJ/kg _{ar})	Net calorific value <Q> _{net,p, ar} (KJ kg _{ar} ⁻¹)	Net calorific value specific load	% Net calorific value specific load contribution	Total chlorine content [Cl] (% w/w _d)	Total chlorine content <[Cl]> (% w/w _d)	Total chlorine content specific load	% Total chlorine content specific load contribution	
Textile/fabric	T/F	9.82	9.82	0.40	2.5	8.50	0.33	2.4	18744	18744	719	4.0	0.229	0.229	0.009	1.3	
Tissues	TIS		17.52	0.25	1.6	6.94	0.09	0.7		13036	173	1.0		0.239	0.003	0.5	
Treated wood	T_W	2.47	5.98	0.23	1.4	13.78	0.53	4.0	19728	15582	603	3.4	0.364	0.224	0.009	1.2	
		8.49								11414				0.168			
		6.98								15605				0.141			
Batteries	BAT	100.00	100.00	0.00	0.0	0.52	0.00	0.0	0	0	0	0.0	0.000	0.000	0.000	0.0	
Cables	CAB	50.00	50.00	0.12	0.7	0.00	0.00	0.0	10359	10359	21	0.1	2.500	2.500	0.006	0.9	
Cinders	CIN	12.88	12.88	0.01	0.1	7.98	0.01	0.0	26149	26149	19	0.1	0.071	0.071	0.000	0.0	
Ferrous metal	Fe_M	100.00	100.00	0.21	1.3	0.85	0.00	0.0	0	0	0	0.0	0.000	0.000	0.000	0.0	
Glass	GL	100.00	100.00	0.34	2.1	0.02	0.00	0.0	0	0	0	0.0	0.000	0.000	0.000	0.0	
Hazardous	HAZ	39.96	36.41	0.06	0.4	2.86	0.00	0.0	12841	16999	27	0.1	0.128	0.533	0.001	0.1	
		26.78								27155				1.035			
		49.11								17032				0.150			
		31.71								11283				1.429			
		12.98								20227				0.136			
57.91								13458				0.322					
Non-ferrous metal	nFe_M	100.00	100.00	1.69	10.6	1.02	0.02	0.1	0	0	0	0.0	0.000	0.000	0.000	0.0	
Stones/ceramics	S/C	100.00	100.00	0.36	2.3	0.84	0.00	0.0	0	0	0	0.0	0.000	0.000	0.000	0.0	
Total sum				15.93	100.0		13.43	100.0			17887	100.0			0.69	100.0	

5.5.2 UK MBT plant A: simulation of SRF moisture content

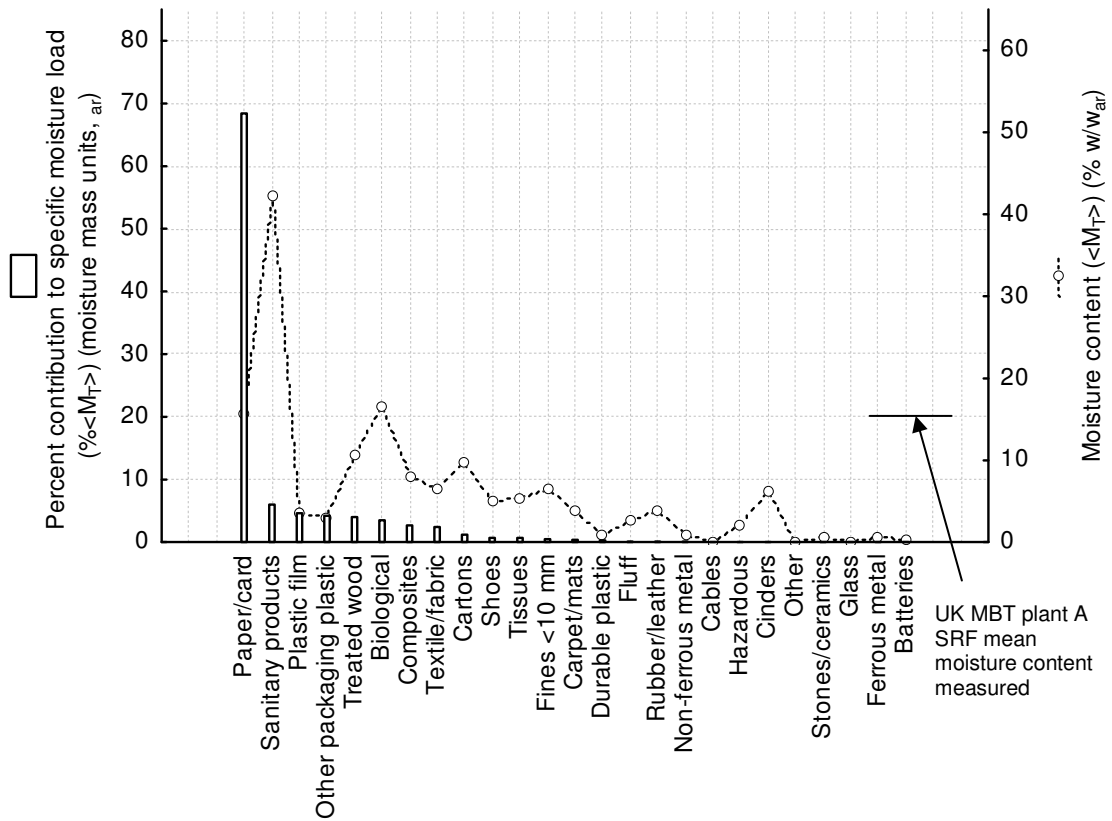


Figure 5-55 Results for moisture content ($\lt;M_T>_{ar}$) characterisation of biodried waste components, and percent contribution of each component to the overall moisture load of the average SRF produced by the UK MBT plant A. Average composition of the SRF was modelled from the results of the reconciled waste component balances throughout the plant (**Figure 5-21**). For details on the material composition of each component category refer to **Table 4-5**.

The central tendency of the moisture content in SRF produced from the UK MBT plant A was simulated with reasonable agreement (**Table 5-11** and **Figure 5-59**). The relative difference between the measured and simulated value, expressed as a percent of the measured value, ranges 10-15%. For the two typical plant operation sets

of samples the underestimation is higher for the summer set of all samples (L3-outl). Because this difference falls well within the confidence limits around the means (d.f. = 9 and 14 respectively, $\alpha = 0.05$), the simulated value cannot be statistically differentiated from the measured mean (at this level of confidence and replication).

The contribution from the paper/card waste component category accounts for the bulk of the simulated moisture specific load (68.4%) (**Table 5-10** and **Figure 5-55**). Despite their relatively low moisture content, the other important contribution comes from the sum of other packaging plastic and plastic films plastics (11.8%), because of their dry mass percentage mass (30.5%) (**Table_App F-19**). The very wet sanitary products (nappies) are also contributing a considerable 6.0%. The readily degradable components (biological, fines <10 mm) contribute only 3.5 % and 0.5% respectively. All other components are responsible for minor parts of the overall simulated moisture load of the SRF.

5.5.3 UK MBT plant A: simulation of SRF total chlorine content

The central tendency of the total chlorine concentration in SRF produced from the UK MBT plant A was accurately simulated (**Table 5-11**). The relative difference between the measured and simulated value, expressed as a percent of the measured value, is less than 3.5%. It falls in-between the averages (mean, median) for the two typical plant operation sets of samples: it slightly overestimates the mean value measured for summer SRF production (L3-outl) and slightly underestimates the mean value measured for winter through to summer set of all samples (L123-L3outl). This difference just within the confidence limits around the means, as constructed for 9 and 14 degrees of freedom respectively, $\alpha = 0.05$. Hence, the simulated value is not statistically different from the measured mean (at this level of confidence and replication).

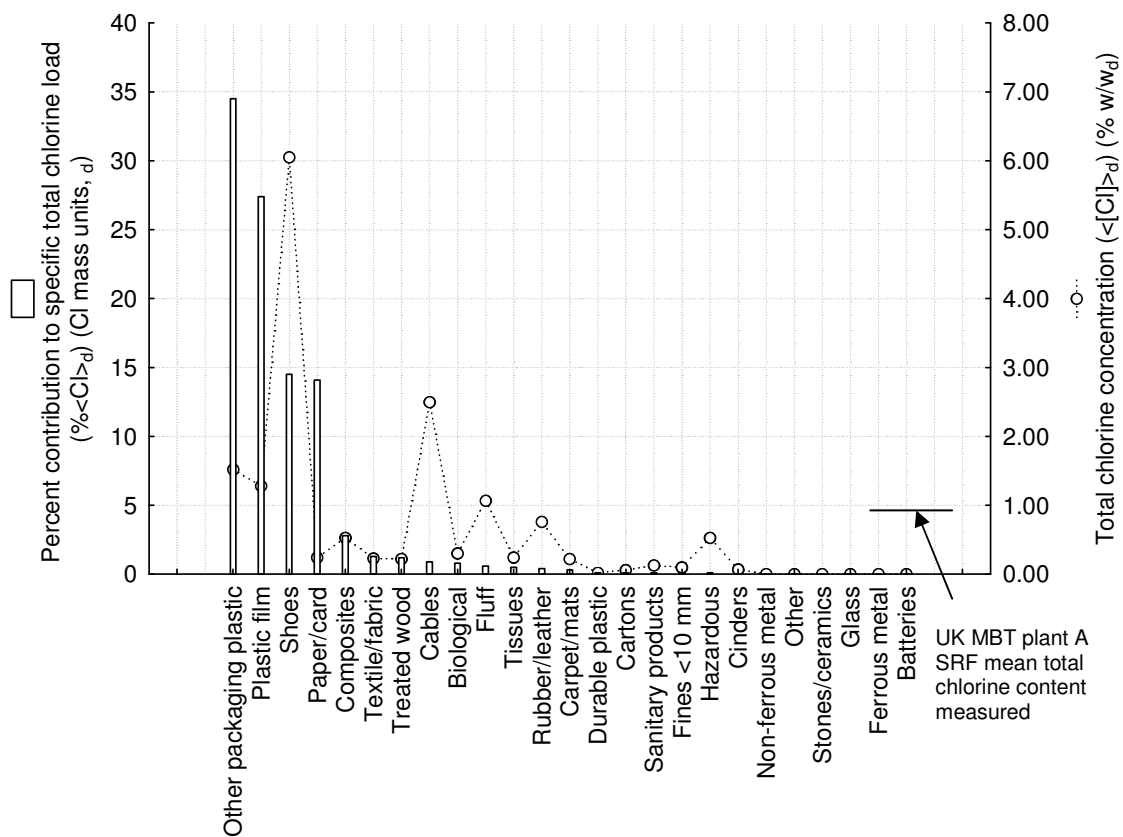


Figure 5-56 Results for total chlorine content ($\langle [Cl] \rangle_d$) characterisation of biodried waste components, and percent contribution of each component to the overall total chlorine load of the average SRF produced by the UK MBT plant A. For non-shredable components typical literature values are shown. Average composition of the SRF was modelled from the results of the reconciled waste component balances throughout the plant (**Figure 5-21**). For details on the material composition of each component category refer to **Table 4-5**.

The contribution from four waste components accounts for 90.5% of the simulated amount of total chlorine present in the average SRF from the UK MBT plant A (**Table 5-10, Figure 5-56**). Due to their high total chlorine concentration other packaging plastic and plastic films are contributing 62% of the specific load in total chlorine, despite comprising only 30% w/w_d of the SRF dry mass (**Table App F-19**). Shoes also contribute 14.5%, having the highest concentration, despite their low mass percentage. Conversely, paper and card material fraction is responsible for only 14% of the total chlorine specific load of SRF, despite being the dominant fraction (42% w/w_d),

This results from its relatively low total chlorine concentration, measured less than one third of the SRF average ($\langle [Cl] \rangle_{d,P_C} = 0.19\% \text{ w/w}_d$ vs. $\langle [Cl] \rangle_{d,SRF(L123-L3out)} = 0.71\% \text{ w/w}_d$).

5.5.4 UK MBT plant A: simulation of SRF ash content

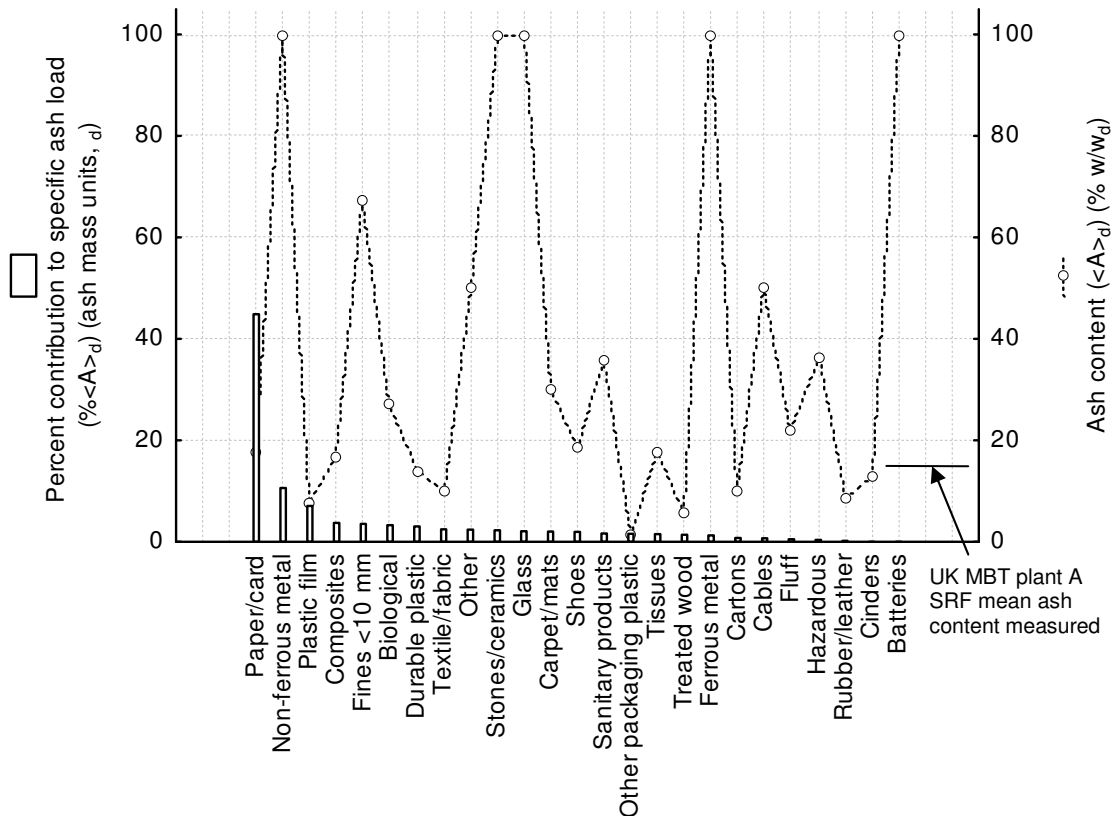


Figure 5-57 Results for ash content ($\langle A \rangle_d$) characterisation of biodried waste components, and percent contribution of each component to the overall ash load of the average SRF produced by the UK MBT plant A. For inert components 100% ash content was assumed. Average composition of the SRF was modelled from the results of the reconciled waste component balances throughout the plant (**Figure 5-21**). For details on the material composition of each component category refer to **Table 4-5**.

The central tendency of the ash content in SRF produced from the UK MBT plant A was simulated (**Table 5-11** and **Figure 5-59**). The relative difference between

the measured and simulated value, expressed as a percent of the measured value, ranges 8.4-11.7%. For the two typical plant operation sets of samples the underestimation is higher for the winter through to summer set of all samples (L123-L3outl). Because this difference falls just outside the confidence limits around the means (d.f. = 9 and 14 respectively, $\alpha = 0.05$), the simulated is statistically different from the measured mean (at this level of confidence and replication). However, regarding engineering significance the difference is reasonably small.

The contribution from the paper/card waste component category accounts for the bulk of the simulated moisture specific load (68.4%). Despite their relatively low moisture content, the other important contribution comes from the sum of other packaging plastic and plastic films plastics (11.8%), because of their dry mass percentage mass (30.5%) (**Table_App F-19**). The very wet sanitary products (nappies) are also contributing a considerable 6.0%. The readily degradable components (biological, fines <10 mm) contribute only 3.5% and 0.5% respectively. All other components are responsible for minor parts of the overall simulated moisture load of the SRF.

Paper accounts for the bulk of the ash content load (44.9%) (**Table 5-11** and **Figure 5-59**). Plastic materials, showing low ash content (plastic film: 7.6% w/w_d; other packaging plastic: 1.6% w/w_d), contribute insignificantly in relation of their mass fraction (11.9%) (**Table_App F-19**). Incombustible impurities in the SRF, despite being relatively low as a mass fraction (measured: 3.5±1.2% w/w_d), contribute considerably to the overall ash load; the non-ferrous metals in particular account for 10%.

5.5.5 UK MBT plant A: simulation of SRF net calorific value

The central tendency of the net calorific value in SRF produced from the UK MBT plant A was simulated least accurately compared to the rest three properties (**Table 5-11**). However, the relative difference between the measured and simulated value, expressed as a percent of the measured value, is still less than 15%, which could be considered as acceptable for the purpose of a general quality evaluation. This difference fall clearly outside the confidence limits around the means, as constructed for 9 and 14 degrees of freedom respectively, $\alpha = 0.05$. Hence, the simulated value is statistically different from the measured mean (at this level of confidence and replication). The prediction overestimates the mean values measured for summer SRF production.

Paper/card, plastic film and other packaging plastic account collectively for 76.1% of the simulated amount of net calorific value present in the average SRF from the UK MBT plant A (**Table 5-10, Figure 5-58**). Due to their high net calorific value, the plastic components of other packaging plastic and plastic films are contributing 43.6% of the specific load, despite comprising only 30% w/w_d of the SRF dry mass (**Table_App F-19**). Next group of waste components that make a non-negligible contribution are textile/fabric, composites, durable plastic and treated wood, all of them around 3.5%.

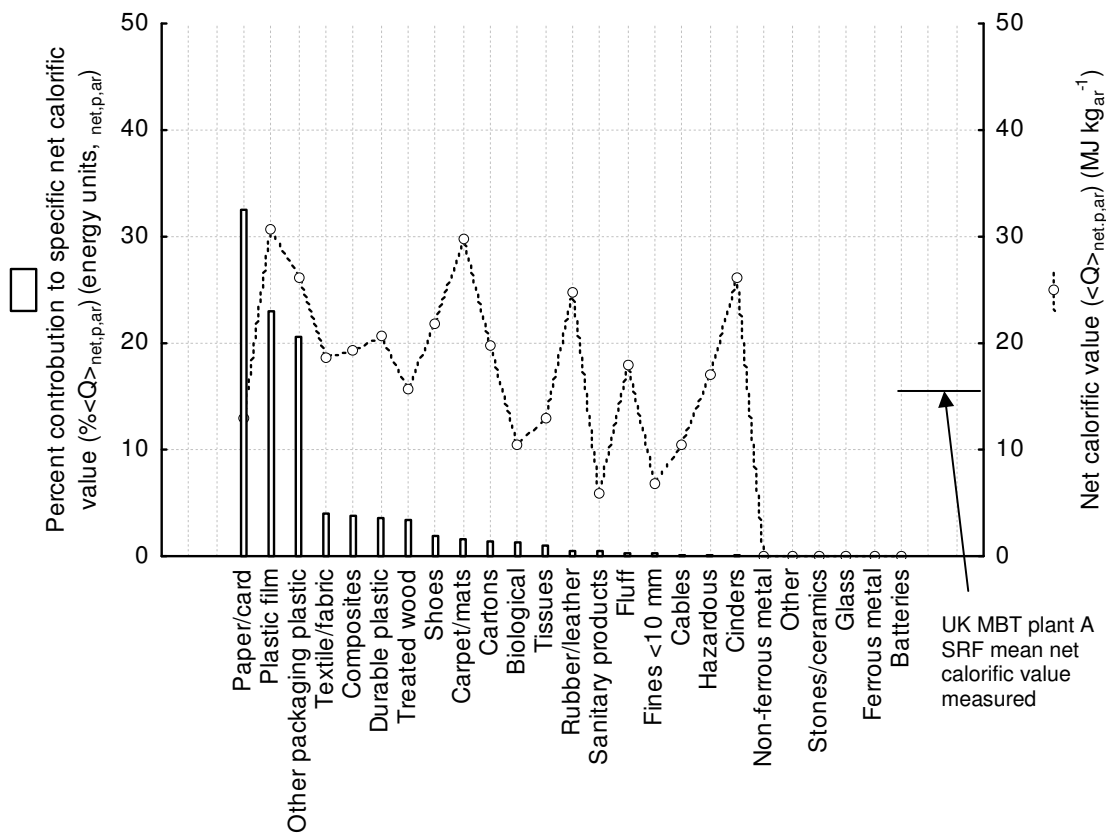


Figure 5-58 Results for net calorific value ($\langle Q \rangle_{\text{net,p,ar}}$) characterisation of biodried waste components, and percent contribution of each component to the overall net calorific value load of the average SRF produced by the UK MBT plant A. Average composition of the SRF was modelled from the results of the reconciled waste component balances throughout the plant (**Figure 5-21**). For details on the material composition of each component category refer to **Table 4-5**.

5.5.6 UK MBT plant A: summary of SRF properties simulation

Table 5-11 summarises the simulation results discussed above. Notably, because of the way the total extended uncertainty has been computed, it allows to perform a hypothesis testing, checking whether the simulated value is statistically identical to the mean value measured with the stated uncertainty (H_0 : identical, H_1 : different, t-test at $\alpha = 0.05$, for 9 or 14 degrees of freedom, depending on the sample size).

Table 5-11 Comparison of simulated average values for properties of modelled average SRF composition produced by the UK MBT plant A with the measures of central tendency (median and mean with confidence limits at 95% confidence) for these properties as measured on 2 sets of SRF samples

SRF property	Ash content (<A> _d) (% w/w _d)		Moisture content (<M _T >) (% w/w _d)		Net calorific value (<Q> _{net,p, ar}) (KJ kg _{ar} ⁻¹)		Total chlorine content (<[Cl]> _d) (% w/w _d)	
	L123-L3outl	L3-outl	L123-L3outl	L3-outl	L123-L3outl	L3-outl	L123-L3outl	L3-outl
Simulated average	15.9		13.4		17887		0.69	
Median measured	17.6	17.3	14.8	16.7	15694	15536	0.72	0.69
Mean measured	18.1	17.4	15.0	15.8	15742	15572	0.71	0.67
± U_{95,v}(mean measured)	1.6	1.1	2.7	2.6	929	1191	0.06	0.07
%Relative bias (as % of measured mean)	-11.7	-8.4	-10.5	-15.0	13.6	14.9	-2.5	3.4

L123-L3outl: set of samples representing typical plant operation from winter to summer: based on 15 samples

L3-outl: set of samples representing typical plant operation in summer: based on 10 samples

(see **Table 4-9** for details)

The amount of overestimation or underestimation are visualised in **Figure 5-59**.

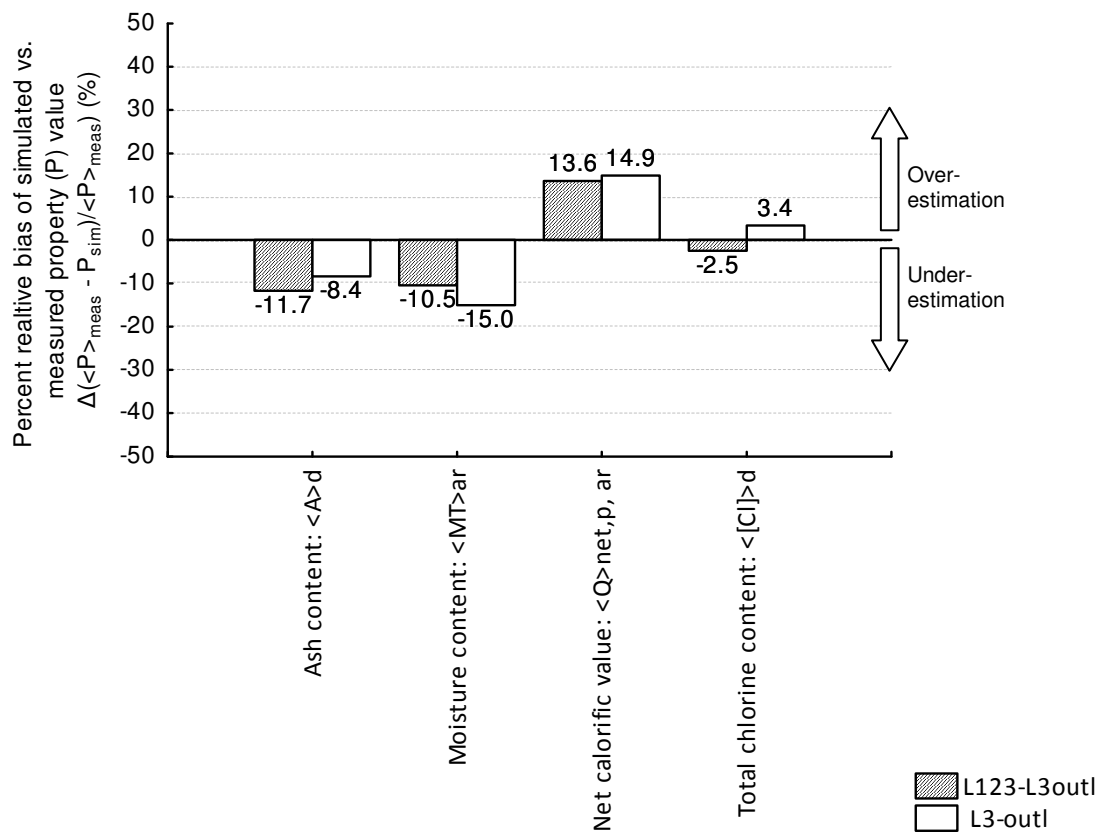


Figure 5-59 Validation for SRF properties simulation. Relative bias as a percentage of the measured value. Results are shown for two sets of samples (L123-L3outl: typical plant operation from winter to summer; L3-outl: typical plant operation for summer; for details refer to **Table 4-9**). For statistical significance comparisons refer to **Table 5-11**.

5.6 UK MBT plant A: SRF properties characterisation

5.6.1 UK MBT plant A: SRF characterisation - overall results and statistics

This section summarises results of properties measured for the characterisation of the SRF produced in the UK MBT plant A. The statistical analysis methodology and the rationale behind it are presented in **Section 4.12**. The following **Sections 5.6.2 - 5.6.8** present these results in detail. Materials and methods employed in the experimental determination of each of these properties are detailed in **Section 4.13**.

Variability from day to day in the plant production can be assessed by the between-incremental sample variability, quantified through the coefficient of variation. All samples considered (L1+2+3), the between-incremental sample variability of the determined quantities ranges from a maximum of 47.3% for $\langle M_T \rangle$ to a minimum of 5.8% for $\langle TH \rangle$. If the atypical SRF samples are excluded these values drop to 31.8% and 4.1%, respectively. In decreasing variability order (%CV, **Table 5-12**): $M_T > TN > \chi_B > A > Q_{net,p,ar} > [Cl] > Q_{gr,v,b} > TC > TH$. Regarding the four combinations of samples examined, ignoring the atypical plant production samples (L3outl) improves considerably the variability, because these form a group with markedly different characteristics than most of the rest samples, for most of the measured quantities. The summer typical only set of samples (L3-outl) shows lesser inhomogeneity than the entire set of typical samples (L1+2+3-L3outl), which is anticipated as they are sampled in consecutive operational days, within the same period (August).

Table 5-12 Statistics computed for selected fuel properties, for sets of SRF samples from the UK MBT plant A

Quantity	Units	Set of observation s	N	Shapiro- Wilk (S-W) W	p _{S-W}	Max	p ₉₀	Q3	UCI _{95%}	Arithmetic mean ↔	SE(↔)	Geometric mean	Median	LCI _{95%}	Q1	p ₁₀	Min	IQR (Q3- Q1)	s	%CV
<M _T >	% w/w _{ar}	L123	20	0.96	0.579	24.4	19.9	17.4	15.43	12.6	1.34	11.1	12.8	9.84	7.7	4.3	3.7	9.7	5.97	47.3
		L123-L3out l	15	0.98	0.935	24.4	21.1	17.9	17.65	15.0	1.23	14.2	14.8	12.37	10.8	8.4	6.9	7.0	4.77	31.8
		L3	15	0.90	0.113	21.1	18.6	17.6	15.55	12.2	1.56	10.5	14.5	8.87	5.9	3.8	3.7	11.7	6.03	49.4
		L3-outl	10	0.94	0.568	21.1	19.9	17.9	18.37	15.8	1.14	15.4	16.7	13.22	14.5	10.0	9.3	3.4	3.60	22.8
<A>	% w/w _d	L123	20	0.95	0.431	25.2	20.6	18.8	18.51	17.1	0.69	16.8	17.0	15.62	14.9	13.4	12.5	3.9	3.09	18.1
		L123-L3out l	15	0.95	0.604	25.2	20.7	19.7	19.67	18.1	0.75	17.8	17.6	17.93	16.3	15.2	12.5	3.4	2.92	16.2
		L3	15	0.97	0.862	20.6	18.6	17.6	17.37	16.1	0.59	15.9	16.3	14.83	13.6	13.3	12.5	4.0	2.29	14.2
		L3-outl	10	0.94	0.589	20.6	19.6	18.2	18.48	17.4	0.47	17.4	17.3	16.35	16.3	15.7	15.6	1.9	1.49	8.5
<TC>	% w/w _d	L123	20	0.85	0.565	56.8	56.2	53.1	51.56	49.8	0.83	49.7	48.3	48.09	46.9	46.2	45.8	6.2	3.71	7.4
		L123-L3out l	15	0.89	0.060	52.8	50.8	48.8	49.01	48.0	0.48	47.9	47.6	46.95	46.7	46.0	45.8	2.1	1.87	3.9
		L3	15	0.90	0.109	56.8	56.4	54.3	52.90	50.8	0.98	50.7	49.2	48.71	47.5	46.7	45.8	6.8	3.79	7.5
		L3-outl	10	0.94	0.564	52.8	51.8	49.2	49.99	48.5	0.65	48.5	48.3	47.07	47.0	46.3	45.8	2.2	2.04	4.2
<TH>	% w/w _d	L123	20	0.96	0.586	7.3	7.2	6.9	6.84	6.7	0.08	6.7	6.7	6.49	6.4	6.1	6.0	0.5	0.37	5.6
		L123-L3out l	15	0.96	0.688	7.3	7.2	6.8	6.81	6.6	0.10	6.6	6.6	6.39	6.3	6.0	6.0	0.5	0.38	5.8
		L3	15	0.94	0.333	7.3	7.3	6.9	6.97	6.8	0.07	6.8	6.8	6.65	6.6	6.4	6.4	0.3	0.28	4.1

Quantity	Units	Set of observations	N	Shapiro-Wilk (S-W)	P _{S-W}	Max	P ₉₀	Q3	UCI _{95%}	Arithmetic mean <->	SE(<->)	Geometric mean	Median	LCI _{95%}	Q1	P ₁₀	Min	IQR (Q3-Q1)	s	%CV
		L3-outl	10	0.92	0.380	7.3	7.3	6.9	6.99	6.8	0.09	6.8	6.8	6.58	6.6	6.5	6.4	0.3	0.29	4.2
<TN>	% w/w _d	L123	20	0.97	0.851	1.3	1.2	1.1	1.02	0.9	0.05	0.9	0.9	0.81	0.7	0.6	0.5	0.3	0.22	24.1
		L123-L3outl	15	0.98	0.965	1.3	1.2	1.1	1.10	1.0	0.05	1.0	1.0	0.90	0.9	0.7	0.7	0.2	0.18	18.2
		L3	15	0.97	0.870	1.2	1.1	1.1	0.98	0.9	0.05	0.8	0.9	0.76	0.7	0.6	0.5	0.3	0.20	22.8
		L3-outl	10	0.97	0.849	1.2	1.2	1.1	1.08	1.0	0.05	1.0	0.9	0.87	0.9	0.8	0.7	0.2	0.14	14.7
<Q _{gr,v,b} >	% w/w _b	L123	20	0.96	0.462	26373	23758	21562	21782	20728	503	20615	20682	19675	19563	17831	16823	1999	2252	10.9
		L123-L3outl	15	0.92	0.205	21737	21386	20934	20592	19799	370	19748	19944	19005	19185	17120	16823	1749	1433	7.2
		L3	15	0.97	0.828	26373	24536	22439	22424	21025	652	20884	20937	19627	19740	17120	16823	2699	2525	12.0
		L3-outl	10	0.89	0.158	21737	21562	20937	21017	19780	547	19708	20323	18542	18543	16972	16823	2394	1730	8.7
<Q _{net,p,d} >	% w/w _d	L123	20	0.96	0.515	25297	22753	20702	20892	19865	491	19751	19848	18837	18706	17061	15866	1996	2196	11.1
		L123-L3outl	15	0.92	0.165	20970	20434	20168	19795	18984	378	18929	19158	18173	18382	16216	15866	1786	1464	7.7
		L3	15	0.97	0.816	25297	23490	21453	21502	20138	636	19997	20168	18774	18916	16216	15866	2537	2463	12.2
		L3-outl	10	0.88	0.148	20970	20702	20168	20210	18954	555	18876	19476	17697	17907	16041	15866	2262	1756	9.3
<Q _{net,p,ar} >	% w/w _{ar}	L123	20	0.94	0.277	24247	21397	18750	18526	17122	671	16886	16300	15718	15203	13764	12641	3548	3000	17.5
		L123-L3outl	15	0.98	0.944	18801	18370	16753	16671	15742	433	15658	15694	14813	14595	13309	12641	2158	1677	10.7
		L3	15	0.95	0.469	24247	22222	20564	19282	17468	846	17194	16317	15654	14941	14218	12641	5623	3275	18.8
		L3-outl	10	0.98	0.969	18801	17842	16317	16763	15572	527	15492	15536	14381	14595	13429	12641	1722	1665	10.7

Quantity	Units	Set of observations	N	Shapiro-Wilk (S-W)	P _{S-W}	Max	P ₉₀	Q3	UCI _{95%}	Arithmetic mean \leftrightarrow	SE(\leftrightarrow)	Geometric mean	Median	LCI _{95%}	Q1	P ₁₀	Min	IQR (Q3-Q1)	s	%CV
<X _{B,daf} >	% W/W _{da}	L123	19	0.88	0.020	60.9	60.9	58.5	55.53	50.9	2.22	49.8	53.6	46.18	45.8	33.6	27.1	12.7	9.70	19.1
		L123-L3outl	14	0.92	0.219	60.9	60.9	59.6	58.21	55.5	1.25	55.3	56.2	52.79	52.8	48.4	45.8	6.8	4.69	8.4
		L3	15	0.87	0.032	60.9	60.9	58.5	56.31	50.4	2.75	49.2	54.4	44.53	44.9	33.6	27.1	13.6	10.64	21.1
		L3-outl	10	0.90	0.234	60.9	60.9	59.6	59.52	56.7	1.24	56.6	58.0	53.89	54.4	51.0	48.4	5.2	3.93	6.9
<cf _d >	-	L12	4		0.949			0.956	0.937	0.0058	0.937	0.937	0.918	0.927					0.0116	1.2
$\Delta(<X_{B,SRH,daf}> - <X_{B,daf}>)$	% W/W _{da}	L12	4		4.3			4.7	3.5	0.36	3.5	3.5	2.4				2.7		0.72	20.4
<[CI]>	% W/W _d	L123	20	0.97	0.767	1.03	0.98	0.86	0.83	0.77	0.032	0.75	0.77	0.70	0.69	0.60	0.46	0.17	0.141	18.5
		L123-L3outl	15	0.91	0.161	0.86	0.78	0.77	0.76	0.71	0.026	0.70	0.72	0.65	0.63	0.60	0.46	0.14	0.100	14.2
		L3	15	0.97	0.882	1.03	1.03	0.89	0.85	0.76	0.042	0.75	0.77	0.67	0.63	0.60	0.46	0.26	0.162	21.3
		L3-outl	10	0.91	0.276	0.78	0.78	0.77	0.74	0.67	0.032	0.66	0.69	0.60	0.61	0.53	0.46	0.16	0.102	15.1

For sets of observations explanations see: **Table 4-9**

Table 5-13 Statistics on the coefficient of variation of for selected fuel properties, for sets of SRF samples from the UK MBT plant A

Quantity (determination repeatability)	Set of observations	N	Shapiro-Wilk (S-W) W	P _{S-W}	Max	P ₉₀	Q3	LCI _{95%}	Arithmetic mean <->	SE (<->)	UCI _{95%}	Geometric mean	Median	Q1	P ₁₀	Min	IQR (Q3-Q1)	s	%CV
%CV(M _r)	L123	19	0.96	0.496	12.0	10.6	7.5	3.48	5.1	0.75	6.62	3.8	4.6	2.4	1.0	0.3	5.1	3.26	64.4
	L123- L3outl	14	0.93	0.277	10.6	8.0	7.5	2.68	4.5	0.85	6.35	3.3	3.7	1.9	1.0	0.3	5.7	3.18	70.4
%CV(A _d)	L123	20	0.87	0.013	4.9	3.8	2.2	1.04	1.6	0.29	2.25	1.1	1.1	0.8	0.5	0.0	1.3	1.29	78.4
	L123- L3outl	15	0.95	0.529	3.1	2.7	1.8	0.85	1.3	0.22	1.80	0.9	1.1	0.8	0.4	0.0	1.0	0.86	64.6
%CV(TC _d)	L123	20	0.92	0.085	3.5	2.6	1.9	0.95	1.4	0.20	1.80	1.1	1.1	0.7	0.4	0.3	1.2	0.90	65.4
	L123- L3outl	15	0.90	0.101	3.5	2.6	2.0	0.83	1.4	0.25	1.88	1.0	0.9	0.6	0.3	0.3	1.3	0.95	70.1
%CV(TH _d)	L123	20	0.93	0.189	3.2	3.0	1.9	1.04	1.5	0.20	1.89	1.2	1.4	0.8	0.4	0.2	1.1	0.91	61.8
	L123- L3outl	15	0.95	0.472	3.0	2.4	1.7	0.85	1.3	0.21	1.75	1.0	1.3	0.6	0.4	0.2	1.1	0.82	62.7
%CV(TN _d)	L123	20	0.83	0.002	13.1	7.5	5.7	2.73	4.1	0.65	5.46	3.3	3.3	1.9	1.5	1.1	3.8	2.92	71.3
	L123- L3outl	15	0.88	0.048	7.6	6.2	4.0	2.14	3.2	0.49	4.22	2.7	2.6	1.7	1.3	1.1	2.4	1.88	59.1
%CV(Q _{gr,v,b})	L123	20	0.84	0.003	0.47	0.35	0.22	0.136	0.19	0.024	0.234	0.16	0.15	0.12	0.08	0.07	0.11	0.105	56.9
	L123- L3outl	15	0.88	0.051	0.47	0.41	0.27	0.143	0.21	0.29	0.269	0.18	0.17	0.13	0.09	0.08	0.15	0.113	55.0
%CV(A _{ts,dis,d/b})	L123	19	0.88	0.019	13.7	11.2	6.0	2.28	4.1	0.88	5.99	2.4	3.0	1.0	0.4	0.2	5.0	3.84	93.0
	L123- L3outl	14	0.90	0.099	13.7	11.2	6.5	2.36	4.8	1.11	7.15	2.8	3.3	1.9	0.4	0.2	4.6	4.15	87.2
%CV([CI] _d)	L3	13	0.94	0.430	23.6	19.3	12.8	6.86	10.7	1.74	14.46	8.9	9.2	7.6	3.0	2.6	5.1	6.29	59.0
	L3- L3outl	9	0.93	0.444	17.2	17.2	9.2	4.55	8.1	1.53	11.60	6.9	8.4	4.4	2.6	2.6	4.8	4.58	56.7

Samples with outlier replicates were not considered in the statistical analysis of the %CV([CI])

5.6.2 UK MBT plant A: SRF moisture content

Results on $\langle M_T \rangle$ and the necessary for its computation M_b , $\langle M_r \rangle$ of individual (incremental) samples, along with assessment of spread and uncertainty are presented in **Table 5-14** and plotted in **Figure 5-61**; and summary data and statistics for all samples are found in **Table 5-12** and **Table 5-13** and presented in **Figure 5-61**. Note that apart from the SRF specifications related $\langle M_T \rangle$, these 3 moisture content measurands are employed to convert the test results of other properties between the 3 possible reporting basis: a_r , b_r , and d_r . The propagation of uncertainty for $\langle M_T \rangle$ is explained in detail in the relevant **Appendix B.2**. The repeatability of the $\langle M_T \rangle$ results on individual GAS (within-sample and analytical determination variability) can be evaluated only indirectly by the $U_{95,veff}(\langle M_T \rangle)$, because it depends upon the independent repeatability of $\langle M_r \rangle$ and the error involved in M_b measurement.

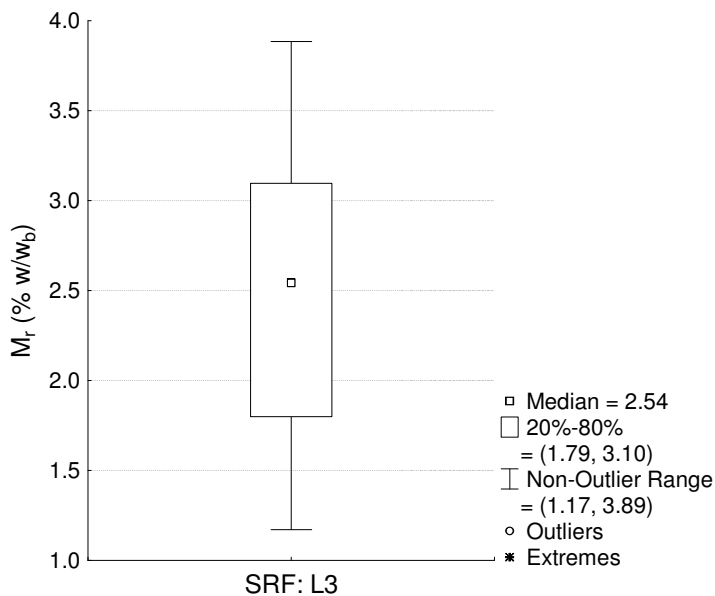


Figure 5-60 Residual moisture determined on the GAS of L3 set of SRF samples.

The uncertainty of the M_b measurement is covered in the experimental section discussion of the $U(<M_T>)$ (**Appendix C.1**). Concerning the reproducibility of M_r determination, the $\%CV(M_r)$ spans over 0.3-12.0% (**Table 5-13**), with a median for the L123 samples at 4.6%, and at 3.7% if the atypical L3 samples are excluded. The between-sample variability of $<M_T>$ can be evaluated by the IQR (Q3-Q1) and the scale-free $\%CV$, because here the normality assumption is not violated. For L123, $IQR(<M_T>) = 9.7\% w/w_{ar}$ and $\%CV(<M_T>) = 47.3\%$; for L123-L3outl it reduces to 7.0% w/w_{ar} and 31.8% respectively.

Table 5-14 Results on bulk, residual and total moisture content of SRF samples from the UK MBT plant A, along with statistical information, including uncertainty estimates.

Sample ID	M_b (% w/w _{ar})	$\pm U_{95}(M_b)$ (% w/w _{ar})	$<M_T>$ (% w/w _b)	$s(M_r)$ (% w/w _b)	$\%CV(M_r)$	$SE(<M_T>)$ (% w/w _b)	$\pm U_{95,2}(<M_T>)$ (% w/w _b)	$\%U_{95,2}(<M_T>)$ (% w/w _b)	$<M_T>$ (% w/w _d)	$\pm U_{95,2}(<M_T>)$ (% w/w _d)	$\%U_{95,2}(<M_T>)$
L1_INC1	5.26	0.210	3.29	0.257	7.8	0.148	0.639	19.4	8.37	0.638	7.6
L1_INC6	22.60	0.904	2.27	0.038	1.7	0.022	0.096	4.2	24.36	0.887	3.6
L1_INC8	12.52	0.501	2.64	0.199	7.5	0.115	0.495	18.7	14.83	0.652	4.4
L2_INC1-7CM	9.08	0.363	2.26	0.046	2.0	0.026	0.114	5.0	11.13	0.370	3.3
L2_INC8	9.15	0.366	1.86	0.019	1.0	0.011	0.046	2.5	10.84	0.362	3.3
L3_INC1	2.20	0.088	1.55	0.104	6.7	0.060	0.259	16.7	3.72	0.268	7.2
L3_INC2	19.04	0.761	2.55	0.067	2.6	0.039	0.167	6.6	21.10	0.754	3.6
L3_INC3	3.37	0.135	1.58	0.067	4.3	0.039	0.167	10.6	4.89	0.208	4.3
L3_INC4	3.95	0.158	2.04	0.126	6.2	0.073	0.314	15.4	5.91	0.339	5.7
L3_INC5	7.97	0.319	2.98	0.073	2.4	0.042	0.180	6.1	10.71	0.351	3.3
L3_INC6	2.55	0.102	1.27	0.152	12.0	0.088	0.379	29.8	3.79	0.383	10.1
L3_INC7	11.55	0.462	3.37	0.230	6.8	0.133	0.571	17.0	14.52	0.674	4.6
L3_INC8	6.11	0.245	3.36	0.011	0.3	0.007	0.028	0.8	9.26	0.238	2.6
L3_INC9	4.60	0.184	2.45	0.088	3.6	0.051	0.218	8.9	6.93	0.275	4.0
L3_INC10	12.98	0.519	3.78	0.104	2.7	0.060	0.258	6.8	16.27	0.548	3.4
L3_INC11	15.47	0.619	2.54	0.118	4.6	0.068	0.293	11.5	17.61	0.652	3.7
L3_INC12	15.31	0.612	3.04	0.056	1.9	0.032	0.140	4.6	17.88	0.605	3.4
L3_INC13	14.97	0.599	2.51	0.125	5.0	0.072	0.310	12.3	17.10	0.640	3.7
L3_INC14	12.80	0.512	2.35	0.189	8.0	0.109	0.470	20.0	14.85	0.646	4.4
L3_INC15	16.53	0.661	2.48	0.264	10.6	0.153	0.656	26.4	18.61	0.846	4.5

The $\pm U_{95}(M_b)$ was estimated at 4% of the M_b

For all four SRF sets of samples the range of $<M_T>$ medians observed is 12.8-16.7% w/w_{ar} , with the all typical-MBT-operation-only samples (L123-L3outl) at 14.8% w/w_{ar} . There is no statistically significant evidence against normality for any of the data sets according to the W-S test statistic at the 95% level of confidence: hence both the $UCI_{95\%}(<M_T>)$ and the p_{80} values could be potentially used to evaluate compliance with

standards. For L123 $p_{80}(\langle M_T \rangle) = 17.75\% \text{ w/w}_{ar}$ and $UCI_{95\%}(\langle M_T \rangle) = 15.43\% \text{ w/w}_{ar}$; whilst for the typical only SRF samples (L123-L3outl) at $18.24\% \text{ w/w}_{ar}$ and $17.65\% \text{ w/w}_{ar}$ respectively.

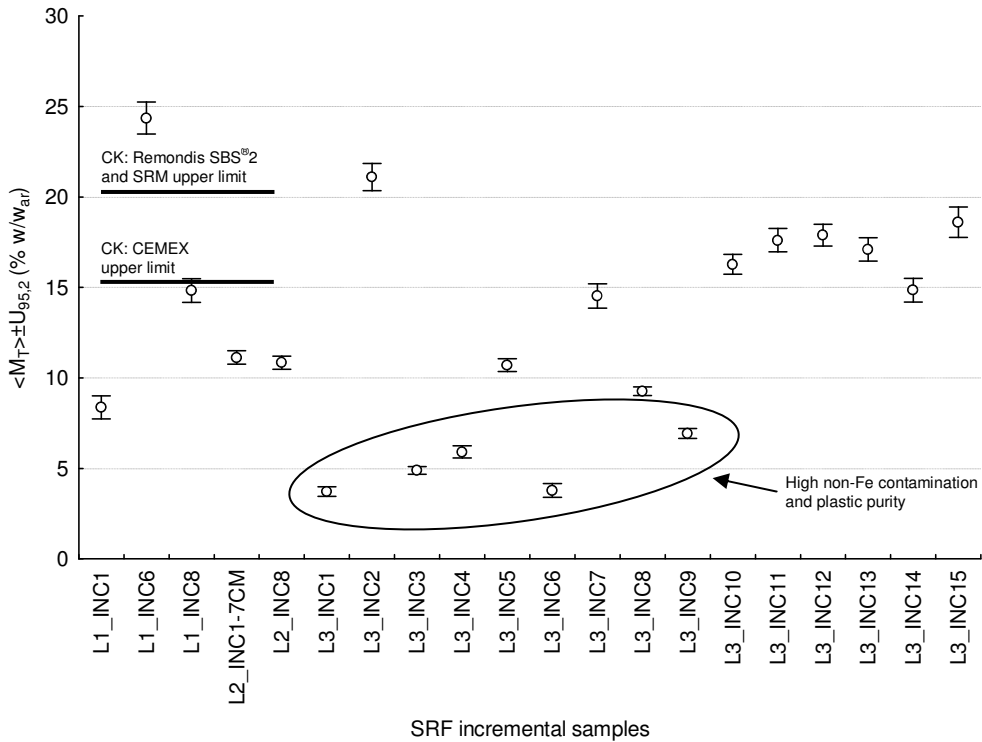


Figure 5-61 Total moisture content and uncertainty for L1+2+3 SRF samples. L1_INC1: SHR-only sample fraction. L2_INC1-7CM: composite, not incremental, sample.

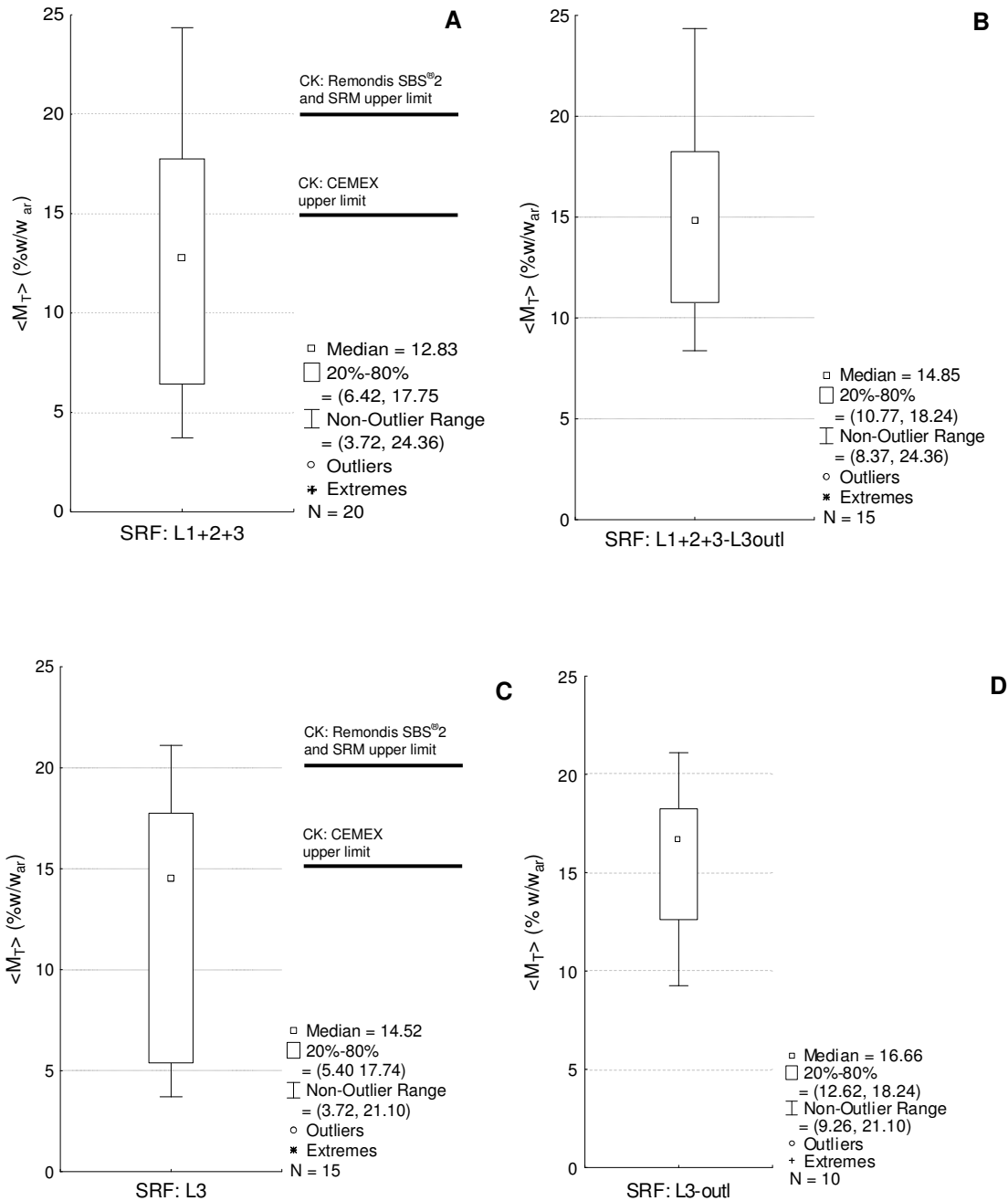


Figure 5-62 Total moisture content ($\langle M_T \rangle$) ar, of SRF: box-plots of non-parametric statistics for 4 sets of samples (A-D) (refer to **Table 4-9** for explanation), along with SRF end-use specification limits (CK: cement kilns). Box-plot conventions: (1): lower and upper lines of the boxes denote the 20th and 80th percentiles (denoted p_{20} and p_{80} respectively); (2) lower outlier limit and upper outlier limit, denoted by whiskers, define the non-outlier range. Here this is defined as the range of values that do not differ from the median more than the $Q1$ or $Q3$ plus 1.5 times the height of box ($p_{80}-p_{20}$); (3) extreme values, presented as asterisks, exceed the $Q1$ plus 3 times the interpercentile $p_{80}-p_{20}$ range.

5.6.3 UK MBT plant A: SRF total chlorine content

Results on total chlorine content ([Cl]) for the individual incremental and composite samples, including assessment of their uncertainty are reported in **Table 5-15** and shown in **Figure 5-63**. Summary statistics are presented in **Table 5-12** and **Table 5-13** and plotted in **Figure 5-64** and **Figure 5-65**. For explanation of the rationale and the abbreviations of the analysed sets of SRF samples refer to **Table 4-9**.

Table 5-15 Results on total chlorine content of SRF samples (dry basis) ([Cl]_d) from the UK MBT plant A, along with statistical information, including uncertainty estimates.

Sample ID	<[Cl]> % w/w _d	s([Cl]) % w/w _d	%CV([Cl])	SE(<[Cl]>) % w/w _d	±U _{95,2} (<[Cl]>) % w/w _d	%U _{95,2} (<[Cl]>)
L1_INC1	0.77	n.a.	n.a.	n.a.	0.15	19.7
L1_INC6	0.72	0.072	10.1	0.042	0.18	25.0
L1_INC8	0.77	0.021	2.7	0.015	0.18	24.0
L2_INC1-7CM	0.76	n.a.	n.a.	n.a.	0.53	70.3
L2_INC8	0.86	0.109	12.6	0.063	0.27	31.4
L3_INC1	0.86	0.073	8.5	0.052	0.181	21.2
L3_INC2	0.72	0.032	4.4	0.018	0.08	11.0
L3_INC3	1.03	0.105	10.2	0.061	0.26	25.4
L3_INC4	0.89	0.114	12.8	0.066	0.28	31.7
L3_INC5	0.78	0.072	9.2	0.042	0.18	22.9
L3_INC6	0.93	0.219	23.6	0.127	0.55	58.7
L3_INC7	0.60	0.071	11.8	0.041	0.18	29.3
L3_INC8	0.69	0.057	8.4	0.033	0.14	20.8
L3_INC9	1.03	0.198	19.3	0.114	0.49	47.8
L3_INC10	0.46	0.298	65.2	0.211	0.74	162.0
L3_INC11	0.63	0.048	7.6	0.028	0.12	19.0
L3_INC12	0.61	0.018	3.0	0.013	0.04	7.3
L3_INC13	0.78	0.066	8.4	0.038	0.16	20.9
L3_INC14	0.77	0.020	2.6	0.012	0.05	6.5
L3_INC15	0.70	0.120	17.2	0.069	0.30	42.7

Refer to **Figure 5-63** for comments on specific samples
n.a.: not available

The repeatability of total chlorine content determination (within-sample and analytical determination variability), as measured on 3 replicate aliquots from the general analysis sample, is assessed by the %CV([Cl]) (**Table 5-15**). As explained in the methodology for total chlorine determination (**Section 4.13.6**), Cl was the only

property for which a limited number of outlier results were evident and discarded as such. For these samples less than 3 replicates were available, and not considered in the statistical analysis of repeatability. The median repeatability for the entire set of samples, excluding the plant production atypical samples, (L1+2+3-L3oult) is at 8.4%, more than double than the second-high property (%CV(M_r) = 3.7%) (**Table 5-13**). This low relatively low repeatability effects high relative uncertainty values (%U_{95,2}(<[Cl]>) - **Table 5-15**), resulting in not satisfactorily precise determination of the total chlorine on each sample. This is visualised in **Figure 5-63**.

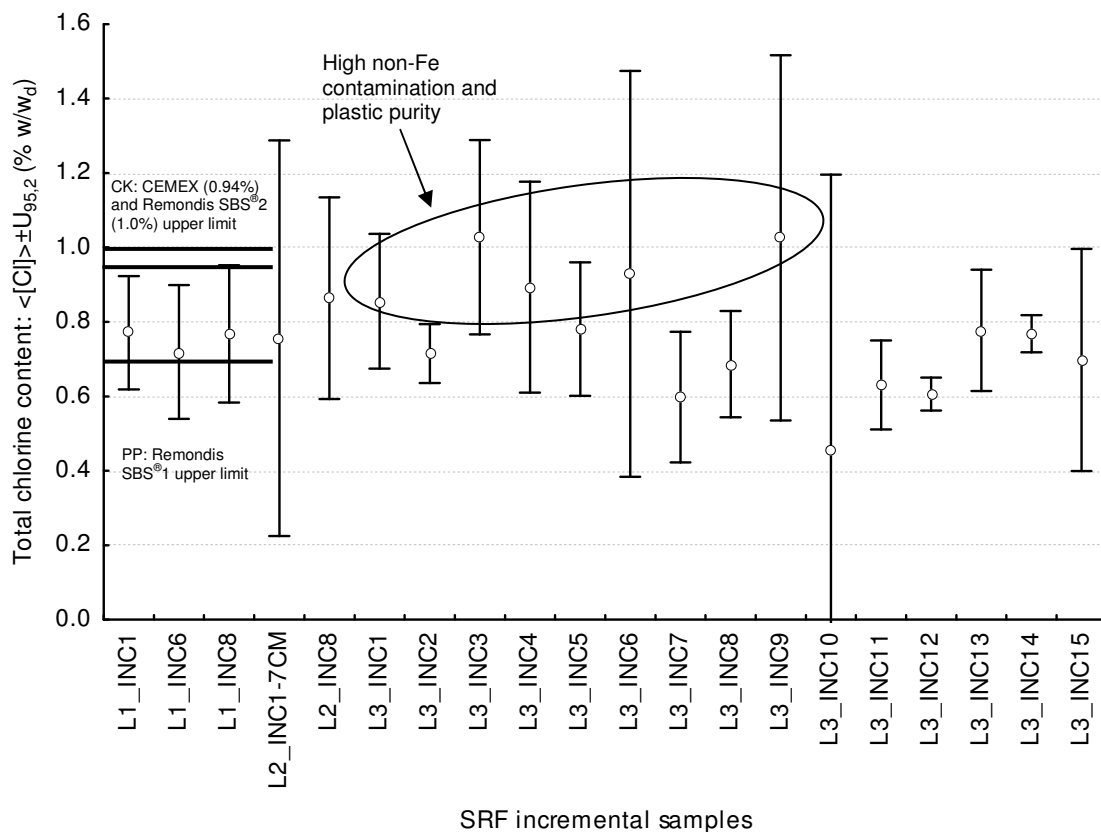


Figure 5-63 Total chlorine content ([Cl]) of SRF and total extended uncertainty U_{95,v}, on a dry mass basis (% w/w_d) for each of the L1+2+3 SRF samples, estimated by 3 replicates (d.f. = 2). L1_INC1 estimated through components of variance experiment at d.f. = 7; The value for L2_INC1-7CM entire sample reconstructed from analysis of the shreddable part excluding fines, fines and purity (contraries) measurements. L3_INC 10 and L1_INC8 estimated by 2 replicates. CK: cement kilns; PP: power plants.

The day-to-day variability in the SRF production for total chlorine content is assessed as the between-incremental samples variability. This can be evaluated by interquartile range IQR (Q3-Q1) (not scale-free): the 50% of the samples differ by 0.14% w/w_d, when all typical production samples are considered (L123-L3outl). Because the normality assumption is not violated ($p_{w-s} > 0.05$ - **Table 5-12**) the coefficient of variation (%CV) is also a valid measure: 14.2% for typical plant production (L123-L3outl); and similarly 15.1% for typical summer plant production (L3-outl). The plat production variability for the total chlorine content of SRF can be visualised as the fluctuation between the average values (circles) in **Figure 5-63**.

However, high within samples and analytical determination variability is of the same order of magnitude with the between-incremental samples, as can be seen in **Figure 5-63** (comparison of the width between the whiskers with the difference between average values of samples), even if the non-typical production samples and the samples with outlier replicates are excluded. Namely, the low precision in the determination of total chlorine overshadows the variability in the plant production line. Hence, a part of the variability measured for the Cl in SRF production, stems from the insufficiently precise analytical determination of the property.

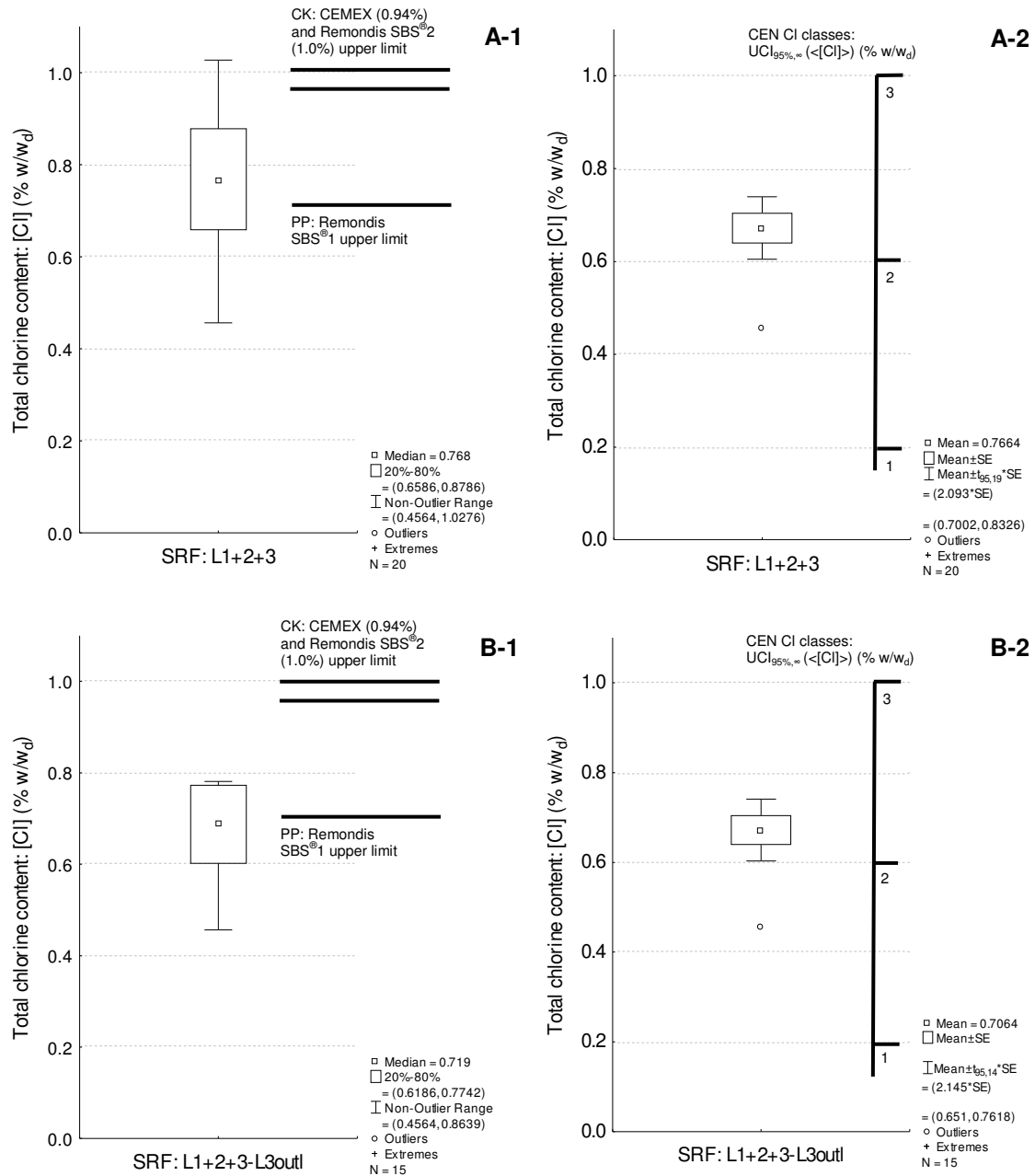


Figure 5-64 Total chlorine content of SRF from the UK MBT plant A: box-plots of for 2 sets of samples (A-B) (refer to **Table 4-9** for explanation) and 2 statistical approaches (1: non-parametric; -2: normality-based), along with SRF CEN classification ranges. For non-parametric box-plot conventions refer to **Figure 5-62**; for normality-based to **Figure 5-73**.

The total chlorine medians for all four sets of samples of SRF considered fall close together (0.69-0.77% w/w_d) (**Table 5-12**), with all the typical plant operation samples median 0.72% w/w_d. Almost no individual samples exceed 1% w/w_d. The

highest values are evident for the atypical August samples, containing high mass percentages of plastics (and aluminium) (**Table 5-15**) - encircled in **Figure 5-63**. The W-S statistic is not significant ($p_{w-s} > 0.05$ - **Table 5-12**); hence there is no evidence against normality. Normality-based statistics are depicted as statistical approach 2 in **Figure 5-64** and **Figure 5-65**. The upper and lower confidence intervals around the mean (95% confidence level) for the set of all typical samples are 0.76% w/w_d and 0.65% w/w_d respectively. For the same set of samples, according to the CEN prescribed statistic for SRF CI classification (**Section 2.5.3** and **Section 2.6.4**) the lower confidence limit is 0.72% w/w_d, rendering it as CI class 3 (**Table 2-13**). Same outcome holds for the all rest 3 sets of samples. The CEN CI classification limits can be seen in **Figure 5-64** and **Figure 5-65**. The 80th percentile of total chlorine for both typical sets of SRF samples (all: L123-L3outl and summer only: L3-outl) is at 0.77% w/w_d. Minimum value encountered is 0.46% w/w_d.

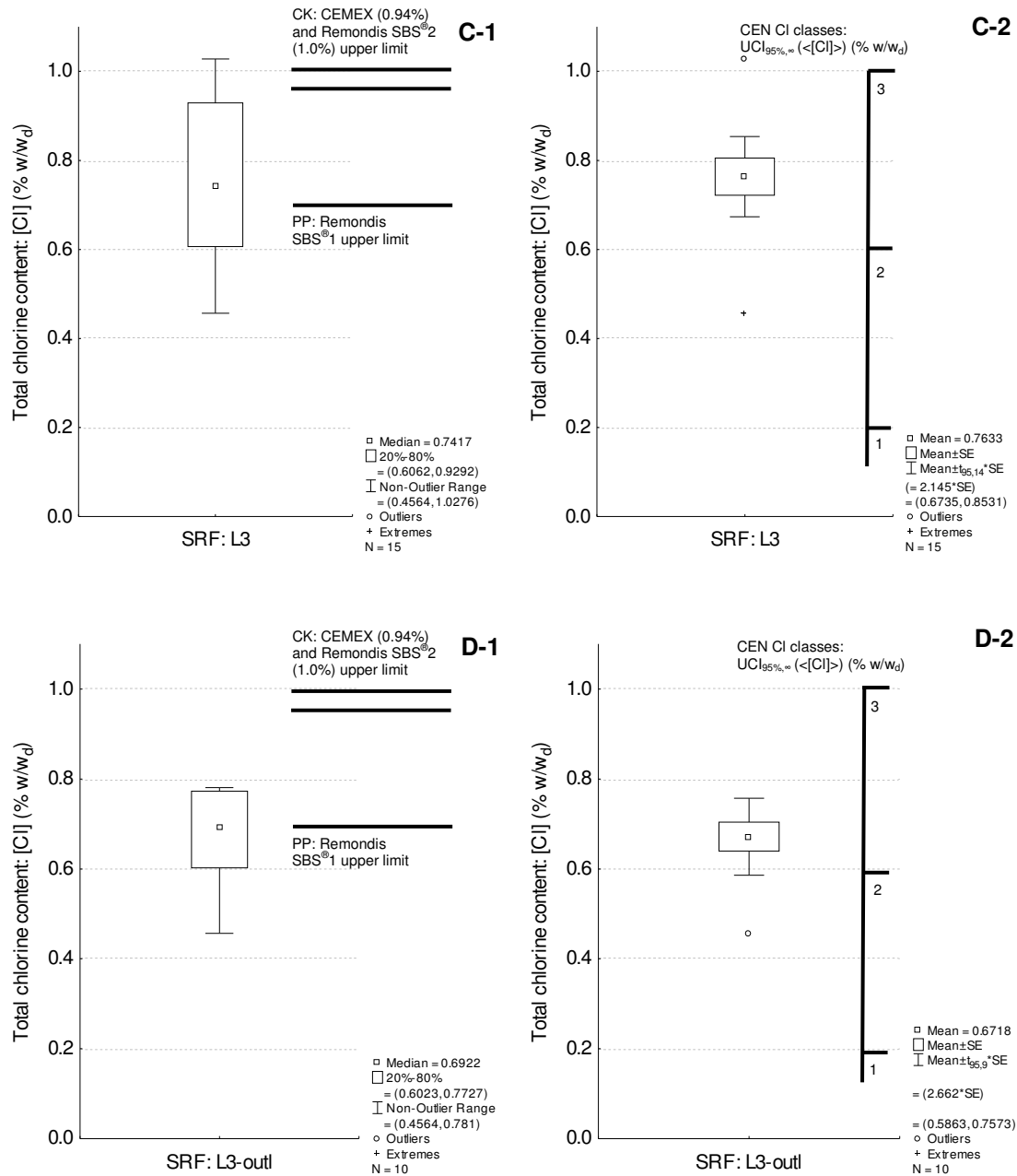


Figure 5-65 Total chlorine content of SRF from the UK MBT plant A: box-plots of for 2 sets of samples (C-D) (refer to **Table 4-9** for explanation) and 2 statistical approaches (1: non-parametric; -2: normality-based), along with SRF CEN classification ranges. For non-parametric box-plot conventions refer to **Figure 5-62**; for normality-based to **Figure 5-73**.

5.6.4 UK MBT plant A: SRF ash content

Results on ash content (A) for the individual incremental and composite samples, including assessment of their uncertainty are reported in **Table 5-16** and shown in **Figure 5-66**. Summary statistics are presented in **Table 5-12** and **Table 5-13** and plotted in **Figure 5-67**. For explanation of the rationale and the abbreviations of the analysed sets of SRF samples refer to **Table 4-9**.

The repeatability of ash content, determined on 3 replicates of the GAS, (within-sample and analytical determination variability) is assessed by the %CV(A): its maximum (4.9%) is for the entire SRF set of samples (L1+2+3) and it is reduced to 3.1% when the sample of non-typical plant performance are excluded (L1+2+3-L3outl). The median values of %CV(A) is for both cases at 1.1%. The between-incremental sample variability of ash content can be evaluated by the interquartile range IQR (Q3-Q1) (not scale-free). Because the normality assumption is not violated, the %CV is also a valid measure. For L1+2+3, $IQR(<A>) = 3.9\% \text{ w/w}_d$ and $\%CV(<A>) = 18.1\%$; for L1+2+3-L3outl it reduces to $3.4\% \text{ w/w}_d$ and $16.2\% \text{ w/w}_d$ respectively.

Table 5-16 Results on ash content of SRF samples from UK MBT plant A, along with statistical information, including uncertainty estimates.

Sample ID	<A> % w/w _d	s(A) % w/w _d	%CV(A)	SE(<A>) % w/w _d	±U _{95,2} (<A>) % w/w _d	%U _{95,2} (<A>)
L1_INC1	15.24	0.169	1.1	0.098	0.420	2.8
L1_INC6	25.24	0.121	0.5	0.070	0.302	1.2
L1_INC8	18.94	0.184	1.0	0.106	0.456	2.4
L2_INC1-7CM	19.72	0.233	1.2	0.134	0.579	2.9
L2_INC8	20.66	0.228	1.1	0.132	0.567	2.7
L3_INC1	13.32	0.071	0.5	0.041	0.176	1.3
L3_INC2	17.63	0.152	0.9	0.087	0.376	2.1
L3_INC3	13.46	0.655	4.9	0.378	1.627	12.1
L3_INC4	13.64	0.601	4.4	0.347	1.493	11.0
L3_INC5	17.46	0.376	2.2	0.217	0.934	5.4
L3_INC6	14.52	0.316	2.2	0.183	0.786	5.4
L3_INC7	15.78	0.069	0.4	0.040	0.172	1.1
L3_INC8	15.57	0.165	1.1	0.096	0.411	2.6
L3_INC9	12.47	0.341	2.7	0.197	0.848	6.8
L3_INC10	20.57	0.642	3.1	0.371	1.595	7.8
L3_INC11	18.21	0.246	1.3	0.142	0.610	3.4
L3_INC12	16.78	0.002	0.0	0.001	0.005	0.0
L3_INC13	17.16	0.140	0.8	0.081	0.349	2.0
L3_INC14	16.31	0.299	1.8	0.173	0.743	4.6
L3_INC15	18.64	0.321	1.7	0.185	0.797	4.3

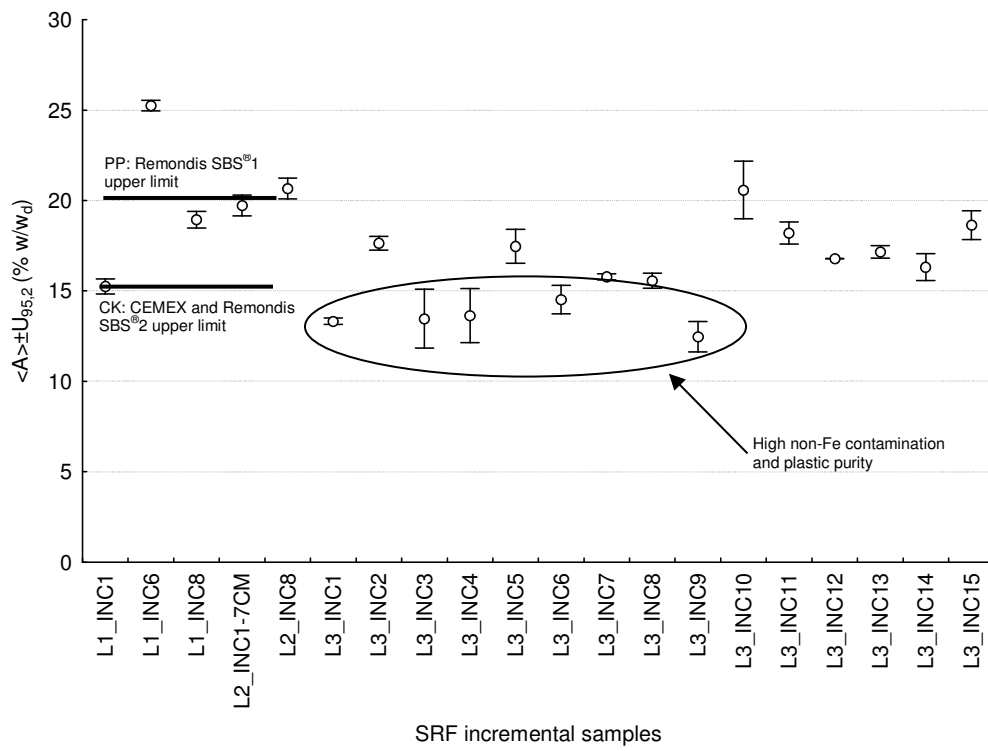


Figure 5-66 Ash content and uncertainty for L1+2+3 SRF samples. L1_INC1: SHR-only sample fraction (overall sample reconstructed value at 17.47% w/w_d).

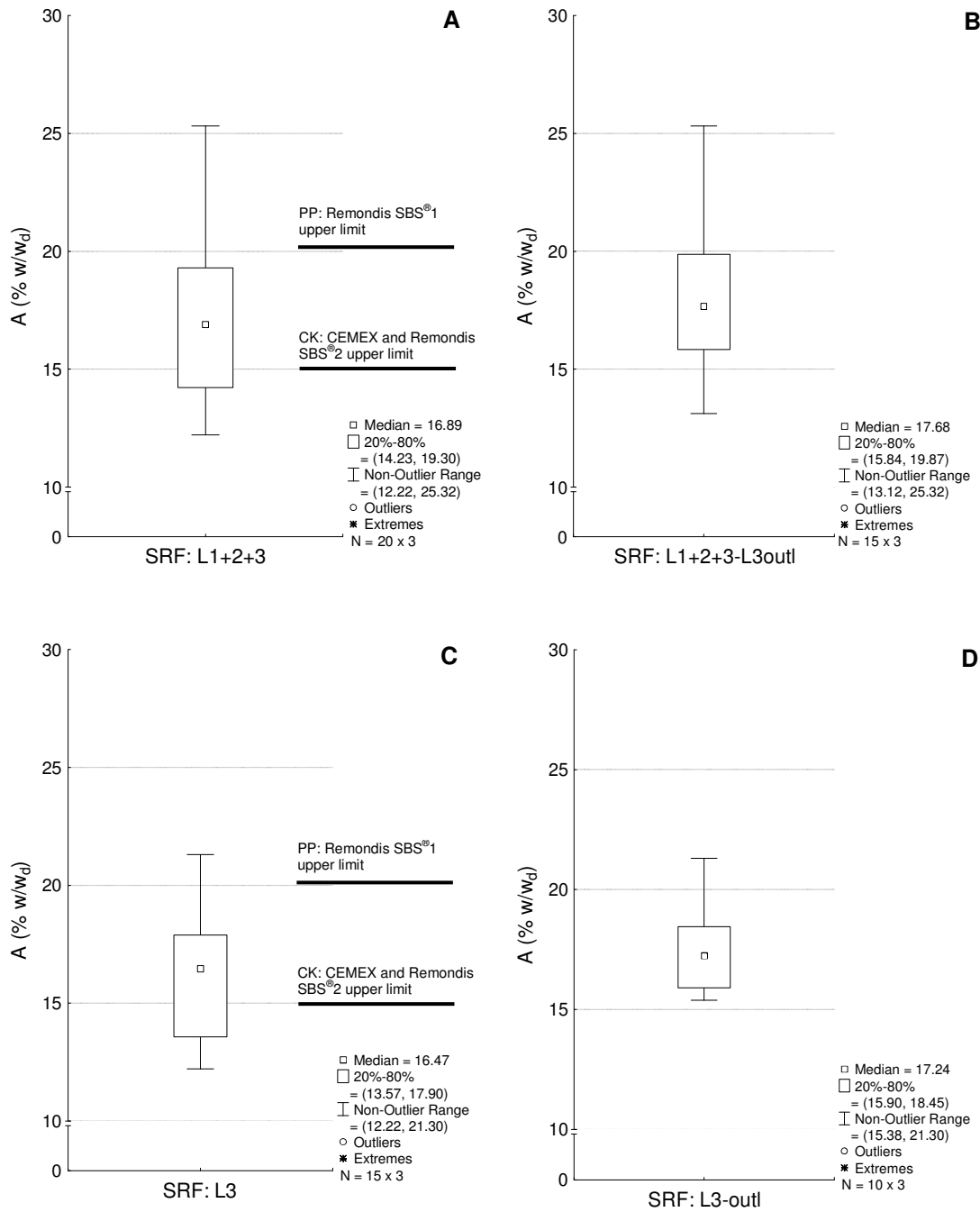


Figure 5-67 Ash content ($\langle A \rangle_d$), of SRF (3 replicates per GAS): box-plots of non-parametric statistics for 4 sets of samples (A-D) (refer to **Table 4-9** for explanation), along with SRF end-use specification limits (PP: power plants; CK: cement kilns). Number of observations included ($n_1 \times n_2$): n_1 : incremental samples, n_2 : replications on the GAS of each incremental sample. For box-plot conventions refer to **Figure 5-62**.

For all four SRF sets of samples the $\langle A \rangle$ medians range is 16.3-17.6% w/w_d (**Table 5-12**), (or 16.5-17.9% w/w_d, if the individual replicates are used for their computation, as plotted in **Figure 5-67**. The typical-MBT-operation-only samples (L1+2+3-L3outl) median is 17.6% w/w_d. For L1+2+3 $p_{80}(\langle A \rangle) = 19.3\%$ w/w_d. There is no statistically significant evidence against normality for any of the data sets according to the W-S test statistic at the 95% level of confidence: hence, the upper confidence limit around the mean $UCI_{95\%}(\langle A \rangle)$ could be potentially as well used to evaluate compliance with standards. For the samples L1+2+3 $UCI_{95\%}(\langle A \rangle) = 18.51\%$ w/w_d; when the atypical operation samples are ignored (L1+2+3-L3outl) is increases to 19.67% w/w_d.

5.6.5 UK MBT plant A SRF: biogenic content

Results of $\chi_{B,daf}$ on individual incremental samples are presented in **Table 5-1** and plotted in **Figure 5-70**; and summary data and statistics are found in **Table 5-12** and **Table 5-13**, and presented in **Figure 5-71**. The reproducibility of the $\chi_{B,daf}$ results on individual GAS (within-sample and analytical determination variability) can be assessed only indirectly through the $U_{95,veff}(\chi_{B,daf})$, because it depends upon the independent repeatability of selective dissolution and residue ashing ($A_{ts,dis,d/b}$), residual moisture M_r , ashing $A_{ts,d}$ (and cf_d , if applicable).

Regarding the repeatability of $A_{ts,dis,d/b}$ determination, the $\%CV(A_{ts,dis,d/b})$ ranges from 0.2-13.7%, with a median for the L123 samples at 3.0%. The between-sample variability of $\langle \chi_{B,daf} \rangle$ can be evaluated by the IQR (Q3-Q1) and the scale-free $\%CV$ if there is no evidence against the normality assumption, which here is the case only for the L123-L3outl set of samples. For L123, $IQR(\langle \chi_{B,daf} \rangle) = 12.7\%$ w/w_d; for L123-L3outl it reduces to $IQR(\langle \chi_{B,daf} \rangle) = 6.8\%$ w/w_d and $\%CV(\langle \chi_{B,daf} \rangle) = 8.4$.

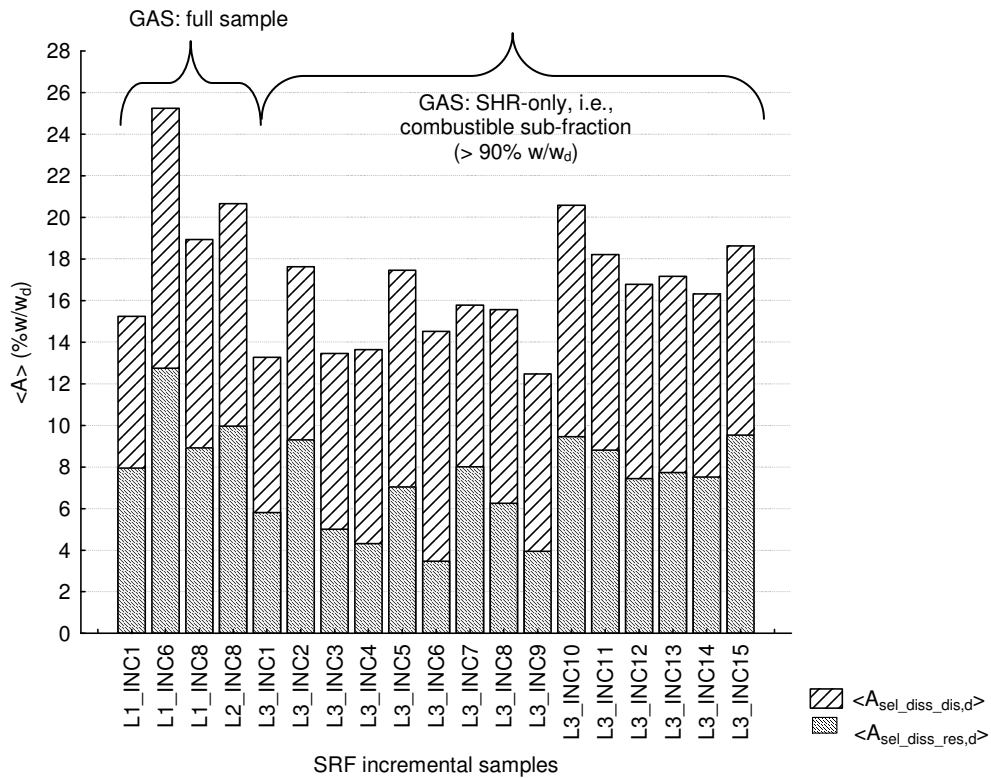


Figure 5-68 Split of ash content in SRF samples into dissolving and not dissolving parts during the selective dissolution process

For all four SRF sets of samples the range of $\chi_{B,daf}$ medians observed is 53.7-58.4% w/w_{daf}, with the all typical-MBT-operation-only samples (L123-L3outl) at 56.22% w/w_{daf}. The L3 samples suspected as atypical form a separate group indicated accordingly, presetting clearly lower values than most of the rest, and rendered the W-S test significant (p=0.020) at the 95% level, indicating that the $\chi_{B,daf}$ L123 samples results are not normally distributed. However, if L3outl are excluded (L123-L3outl), there is no statistically significant evidence against normality any more (p=0.219).

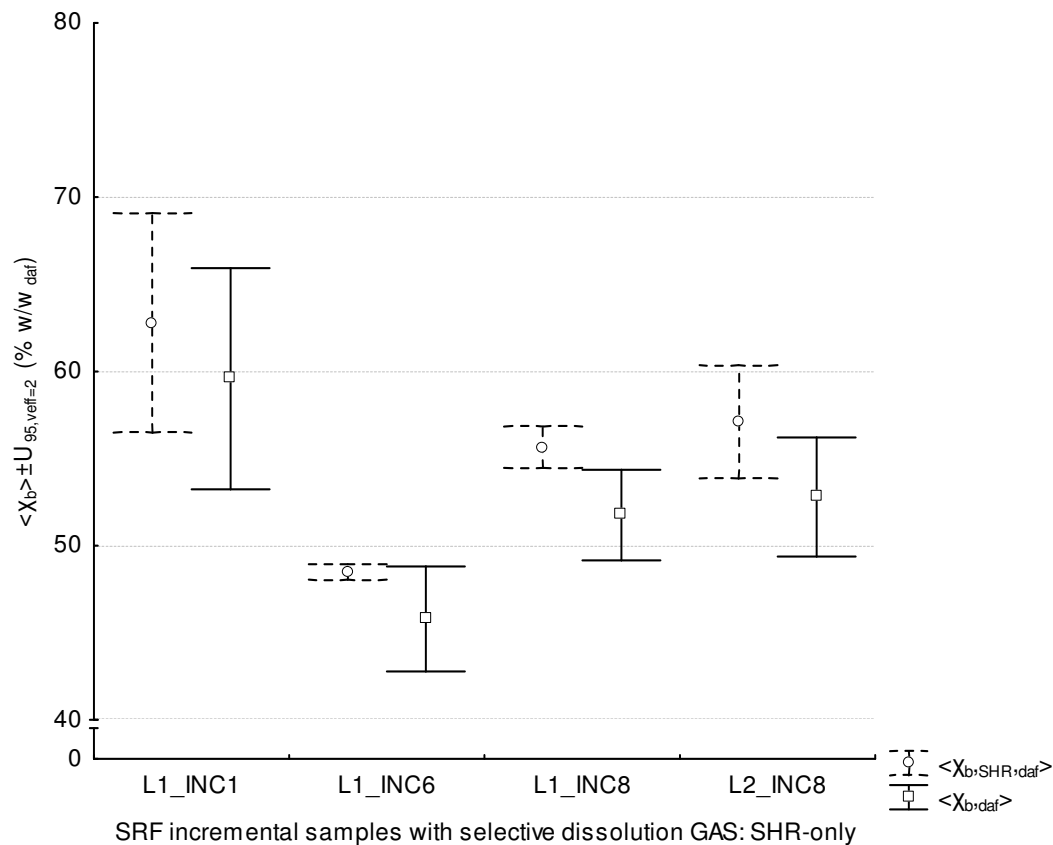


Figure 5-69 Impact of correction of the non-shreddable/combustible fraction (100% w/w ash) in the determination of $\langle \chi_{B,daf} \rangle$ and its uncertainty estimate.

Results support interesting findings for the methodological (analytical and computation-related) choices for the $\chi_{B,daf}$ determination. **Figure 5-68** presents the split of the ash content present in the samples into presumably dissolved $\langle A_{sel_diss_dis,d} \rangle$ and undissolved $\langle A_{sel_diss_res,d} \rangle$ parts after their selective dissolution in acids: around half or more of the A dissolves. **Figure 5-69** illustrates the difference in the computation of $\chi_{B,daf}$ where a correction for the non-combustible part is necessary due to methodological choices; statistical results presented in **Table 5-12**. The median level of reduction $\Delta(\langle \chi_{B,SHR,daf} \rangle - \langle \chi_{B,daf} \rangle)$ is at 3.5% w/w_d, reflecting the high purity of SRF in combustible materials for L1+2 SRF samples (median $\langle cf_d \rangle = 0.973$).

Table 5-17 Results on biogenic content of SRF samples from UK MBT plant A, along with statistical information, including computation of uncertainty estimates.

Sample ID	SH mm	$\langle A_{sel_diss_res,d} \rangle$ % W/W _d	$\langle A_{sel_diss_dis,d} \rangle$ % W/W _d	$\%((m_{res+f,d} \cdot m_{res+f_ashed,d})/m_{ts,b})$ % W _d /W _b	$s(\%((m_{res+f,d} \cdot m_{res+f_ashed,d})/m_{ts,b}))$ % W _d /W _b	$\%CV(\%((m_{res+f,d} \cdot m_{res+f_ashed,d})/m_{ts,b}))$ % W _d /W _b	$s(\%((m_{res+f,d} \cdot m_{res+f_ashed,d})/m_{ts,b}))$ % W _d /W _b	$\langle X_{b,SHR,daf} \rangle$ % W/W _{daf}	$SE(\langle X_{b,SHR,daf} \rangle)$ % W/W _{daf}	$Verff(\langle X_{b,SHR,daf} \rangle)$	$\pm U_{95,verff=z}(\langle X_{b,SHR,daf} \rangle)$ % W/W _{daf}	$\%U_{95,verff=z}(\langle X_{b,SHR,daf} \rangle)$ % W/W _{daf}	$\langle cf_d \rangle$	$s(\langle cf_d \rangle)$	$\langle X_{b,daf} \rangle$ % W/W _{daf}	$SE(\langle X_{b,daf} \rangle)$ % W/W _{daf}	$\pm U_{95,verff=z}(\langle X_{b,daf} \rangle)$ % W/W _{daf}	$\%U_{95,verff=z}(\langle X_{b,daf} \rangle)$ % W/W _{daf}
L1_INC1	1	7.94	7.30	21.3	2.00	9.4	1.41	62.8	1.46	1.01	6.30	10.0	0.949	0.0078	59.6	1.47	6.34	10.6
L1_INC6	1	12.74	12.50	25.7	0.10	0.4	0.07	48.5	0.10	2.62	0.44	0.9	0.944	0.0143	45.8	0.70	3.01	6.6
L1_INC8	1	8.92	10.02	24.7	0.35	1.4	0.24	55.7	0.27	1.37	1.18	2.1	0.930	0.0098	51.8	0.60	2.60	5.0
L2_INC8	1	9.97	10.69	21.8	1.03	4.7	0.73	57.1	0.76	1.06	3.26	5.7	0.925	0.0066	52.8	0.79	3.42	6.5
L3_INC1	0.5	5.81	7.47	58.7	0.21	0.4	0.15			1.00					27.1	0.15	0.66	2.4
L3_INC2	0.5	9.30	8.33	33.1	0.66	2.0	0.47			1.07					48.4	0.49	2.09	4.3
L3_INC3	0.5	5.02	8.45	48.6	0.38	0.8	0.27			3.00					37.2	0.47	2.01	5.4
L3_INC4	0.5	4.33	9.31	39.1	2.15	5.5	1.52			1.10					46.5	1.59	6.85	14.7
L3_INC5	0.5	7.05	10.41	28.1	1.02	3.6	0.72			1.18					53.6	0.78	3.35	6.2
L3_INC6	0.5	3.48	11.04	51.2	0.53	1.0	0.37			1.49					33.6	0.42	1.82	5.4
L3_INC7	1	8.01	7.76	28.5	0.55	1.9	0.39			1.02					54.7	0.40	1.74	3.2
L3_INC8	1	6.26	9.31	29.0	3.97	13.7	2.81			1.00					54.4	2.91	12.51	23.0
L3_INC9	0.5	3.95	8.52	41.6	1.81	4.3	1.28			1.05					44.9	1.33	5.70	12.7
L3_INC10	1	9.46	11.11	19.1	0.57	3.0	0.40			2.47					59.6	0.56	2.41	4.0
L3_INC11	0.5	8.82	9.39	23.5	1.53	6.5	1.08			1.03					57.7	1.12	4.81	8.3
L3_INC12	0.5	7.44	9.35	21.6	1.30	6.0	0.92			1.00					60.9	0.95	4.09	6.7
L3_INC13	1	7.73	9.43	21.4	0.54	2.5	0.38			1.09					60.9	0.40	1.73	2.8
L3_INC14	0.5	7.52	8.79	24.7	2.76	11.2	1.95			1.02					58.4	2.00	8.63	14.8
L3_INC15	0.5	9.54	9.10	22.3	0.03	0.2	0.02			2.02					58.5	0.19	0.82	1.4

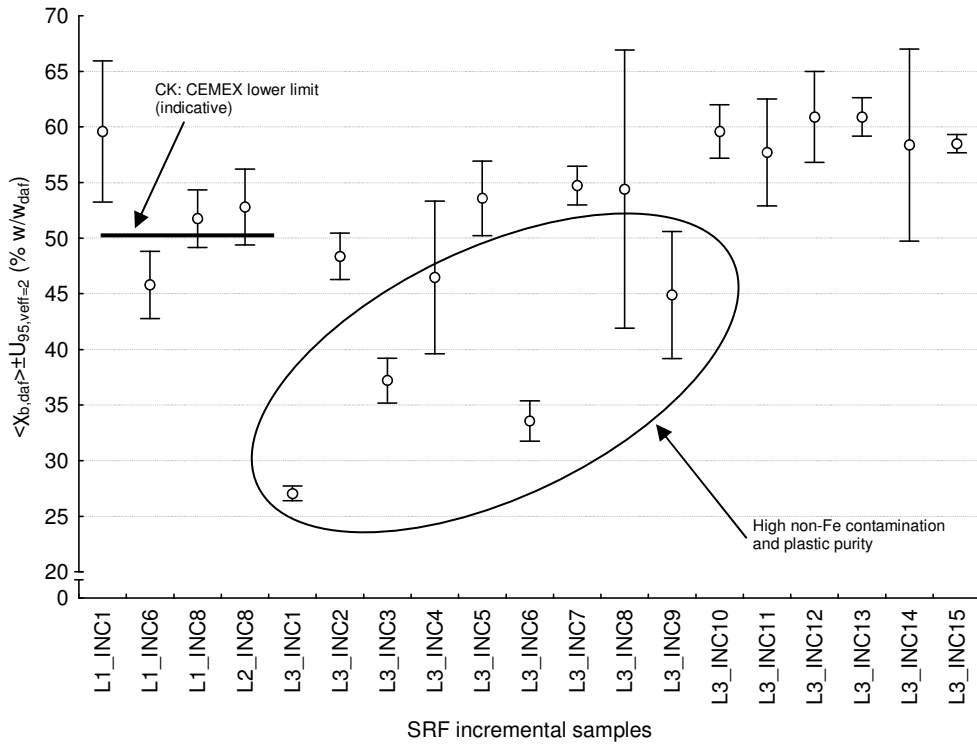


Figure 5-70 Biogenic content (dry, ash-free) ($\langle \chi_{B,daf} \rangle$) and uncertainty for L1+2+3 SRF samples.

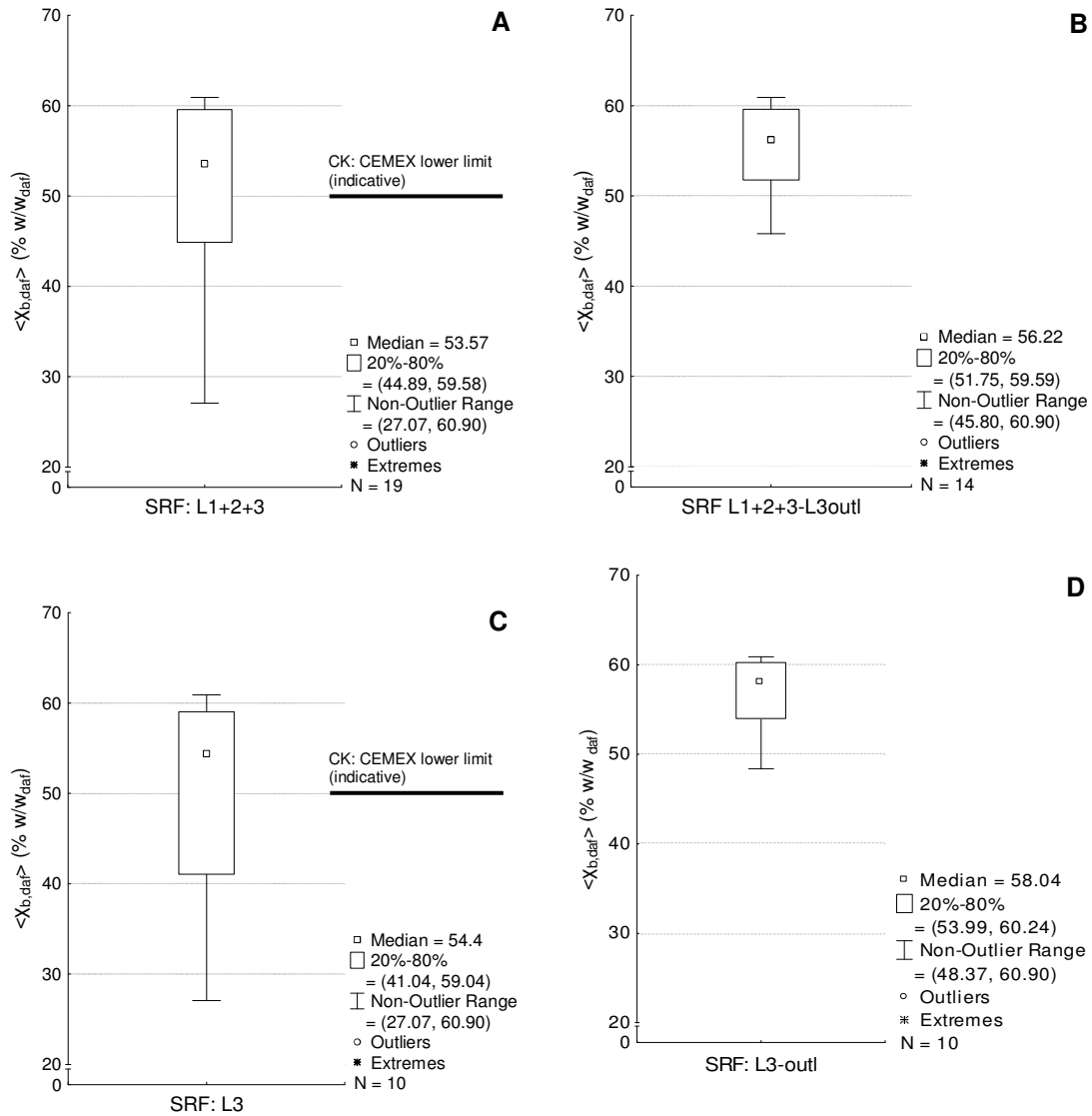


Figure 5-71 Biogenic content (dry, ash-free) ($\langle \chi_{B,daf} \rangle$) of SRF: box-plots of non-parametric statistics for 4 sets of samples (A-D) (refer to **Table 4-9** for explanation), along with SRF end-use specification limits (CK: cement kilns). For box-plot conventions refer to **Figure 5-62**.

5.6.6 UK MBT plant A: SRF total carbon and total hydrogen content

Results on $\langle TC \rangle$ and $\langle TH \rangle$ are part of the proximate analysis of fuels. Average results and statistics are found in **Table 5-12** and **Table 5-13**. Results per sample and their plot are detailed in **Appendix G**.

5.6.7 UK MBT plant A: SRF calorific values

Results of calorific values on individual incremental samples are presented in **Table 5-18** and plotted in **Figure 5-72** and in **Appendix G**; summary data and statistics are found in **Table 5-12** and **Table 5-13**, and presented in **Figure 5-73** and **Figure 5-74**.

The repeatability of $\langle Q_{\text{net,p,ar}} \rangle$ (within-sample and analytical determination variability) can be assessed only indirectly through its uncertainty $\%U_{95,\text{veff}}(\langle Q_{\text{net,p,ar}} \rangle)$, because it depends upon the measurement of other quantities and subsequent computations. The calorific values as determined in the laboratory ($\langle Q_{\text{gr,v,b}} \rangle$), upon which computations for reporting on other bases depend, depict the best variability among all the investigated SRF quantities: the max $\%CV(Q_{\text{gr,v,b}}) = 0.47\%$ (2 GAS replicates) and the median at 0.15%, for the L1+2+3 samples. The max for the computed $\%U_{95,\text{veff}}(\langle Q_{\text{net,p,ar}} \rangle)$ is at 5.4%. The between-incremental sample variability of $\langle Q_{\text{net,p,ar}} \rangle$ can be evaluated by the $\%CV$, because the normality assumption is not violated at the 95% level of confidence, and/or the IQR (Q3-Q1) (not scale-free). For L1+2+3, $IQR(\langle Q_{\text{net,p,ar}} \rangle) = 12.7 \text{ kJ kg}_{\text{ar}}^{-1}$ and $\%CV(\langle Q_{\text{net,p,ar}} \rangle) = 19.7\%$; for L1+2+3-L3outl it reduces to $6.8 \text{ kJ kg}_{\text{ar}}^{-1}$ and 8.4% respectively.

The medians of all four SRF sets of samples for the $\langle Q_{\text{net,p,ar}} \rangle$ range from $15536 \text{ kJ kg}_{\text{ar}}^{-1}$ to $16317 \text{ kJ kg}_{\text{ar}}^{-1}$ (Table 5-12). For the typical-MBT-operation-only samples L1+2+3-L3outl median is at $15694 \text{ kJ kg}_{\text{ar}}^{-1}$ and $Q1(\langle Q_{\text{net,p,ar}} \rangle) = 14595 \text{ kJ kg}_{\text{ar}}^{-1}$. There is no statistically significant evidence against normality for any of the data sets according to the W-S test statistic at the 95% level of confidence, but p value is much higher when the non-typical samples are excluded (L1+2+3-L3outl: $p_{\text{w-s}} = 0.277$ and L3-outl: 0.944): hence, the $LCI_{95\%}(\langle Q_{\text{net,p,ar}} \rangle)$ could be potentially used to evaluate compliance with standards, as suggested by the CEN classification rules. For L1+2+3

$LCI_{95\%}(\langle Q_{net,p,ar} \rangle) = 15718 \text{ kJ kg}_{ar}^{-1}$; whilst for L1+2+3-L3outl at $14813 \text{ kJ kg}_{ar}^{-1}$. Note that these $LCI_{95\%}(\langle Q_{net,p,ar} \rangle)$ values are correctly computed here, using the coverage factor resulting from the available degrees of freedom, i.e., the number of samples examined in each dataset (Figure 5-73 and Figure 5-74). As explained in **Section 2.6.4**, this differs from the CEN rule, which resorts to an 1.96 coverage factor, rendering the $LCI_{95\%}(\langle Q_{net,p,ar} \rangle)$ values: $15807 \text{ kJ kg}_{ar}^{-1}$ and $14893 \text{ kJ kg}_{ar}^{-1}$, respectively.

Table 5-18 Results on calorific values of SRF samples from UK MBT plant A, along with statistical information, including computation of uncertainty estimates.

Sample ID	$\langle Q_{gr,v,b} \rangle$ kJ kg ⁻¹	$S(Q_{gr,v,b})$ kJ kg ⁻¹	%CV($Q_{gr,v,b}$)	$SE(\langle Q_{gr,v,b} \rangle)$ kJ kg ⁻¹	$\pm U_{95,1}(\langle Q_{gr,v,b} \rangle)$ kJ kg ⁻¹	% $U_{95,1}(\langle Q_{gr,v,b} \rangle)$	$\langle Q_{net,p,d} \rangle$ kJ kg ⁻¹	$SE(\langle Q_{gr,v,d} \rangle)$ kJ kg ⁻¹	V_{eff}	$\pm U_{95,veff=1}(\langle Q_{net,p,d} \rangle)$ kJ kg ⁻¹	% $U_{95,veff=1}(\langle Q_{gr,v,d} \rangle)$	$\langle Q_{net,p,ar} \rangle$ kJ kg ⁻¹	$SE(\langle Q_{net,p,ar} \rangle)$ kJ kg ⁻¹	V_{eff}	$\pm U_{95,veff=1}(\langle Q_{net,p,ar} \rangle)$ kJ kg ⁻¹	% $U_{95,veff=1}(\langle Q_{net,p,ar} \rangle)$
L1_INC1	20934	98	0.5	69	877	4.2	20272	81	1.00	1030	5.1	18370	78	1	987	5.4
L1_INC6	19185	16	0.1	11	140	0.7	18382	14	1.00	172	0.9	13309	12	1	154	1.2
L1_INC8	19641	17	0.1	12	152	0.8	18852	30	1.01	377	2.0	15694	27	1	349	2.2
L2_INC1-7CM	19944	59	0.3	42	534	2.7	19158	44	1.00	564	2.9	16753	42	1	532	3.2
L2_INC8	19484	27	0.1	19	241	1.2	18561	20	1.00	259	1.4	16283	19	1	245	1.5
L3_INC1	22439	27	0.1	19	241	1.1	21453	35	1.02	444	2.1	20564	34	1	436	2.1
L3_INC2	21386	23	0.1	16	203	1.0	20434	32	1.03	410	2.0	15608	29	1	366	2.3
L3_INC3	24536	37	0.2	27	337	1.4	23490	38	1.01	488	2.1	22222	37	1	476	2.1
L3_INC4	22981	17	0.1	12	152	0.7	22017	24	1.01	310	1.4	20572	24	1	301	1.5
L3_INC5	17120	28	0.2	20	254	1.5	16216	26	1.00	330	2.0	14218	25	1	312	2.2
L3_INC6	26373	30	0.1	21	267	1.0	25297	33	1.00	419	1.7	24247	32	1	412	1.7
L3_INC7	20866	35	0.2	24	311	1.5	20168	39	1.00	496	2.5	16884	36	1	460	2.7
L3_INC8	21737	34	0.2	24	305	1.4	20970	29	1.00	371	1.8	18801	28	1	353	1.9
L3_INC9	21256	33	0.2	23	292	1.4	20275	28	1.00	359	1.8	18700	27	1	347	1.9
L3_INC10	18543	46	0.2	32	413	2.2	17907	38	1.00	483	2.7	14595	35	1	442	3.0
L3_INC11	16823	21	0.1	15	191	1.1	15866	20	1.00	252	1.6	12641	18	1	230	1.8
L3_INC12	20148	40	0.2	28	356	1.8	19364	30	1.00	383	2.0	15464	27	1	348	2.2
L3_INC13	20937	37	0.2	27	337	1.6	20107	32	1.00	402	2.0	16250	29	1	367	2.3
L3_INC14	20498	83	0.4	59	750	3.7	19589	67	1.00	854	4.4	16317	62	1	789	4.8
L3_INC15	19740	54	0.3	38	483	2.4	18916	51	1.00	643	3.4	14941	46	1	581	3.9

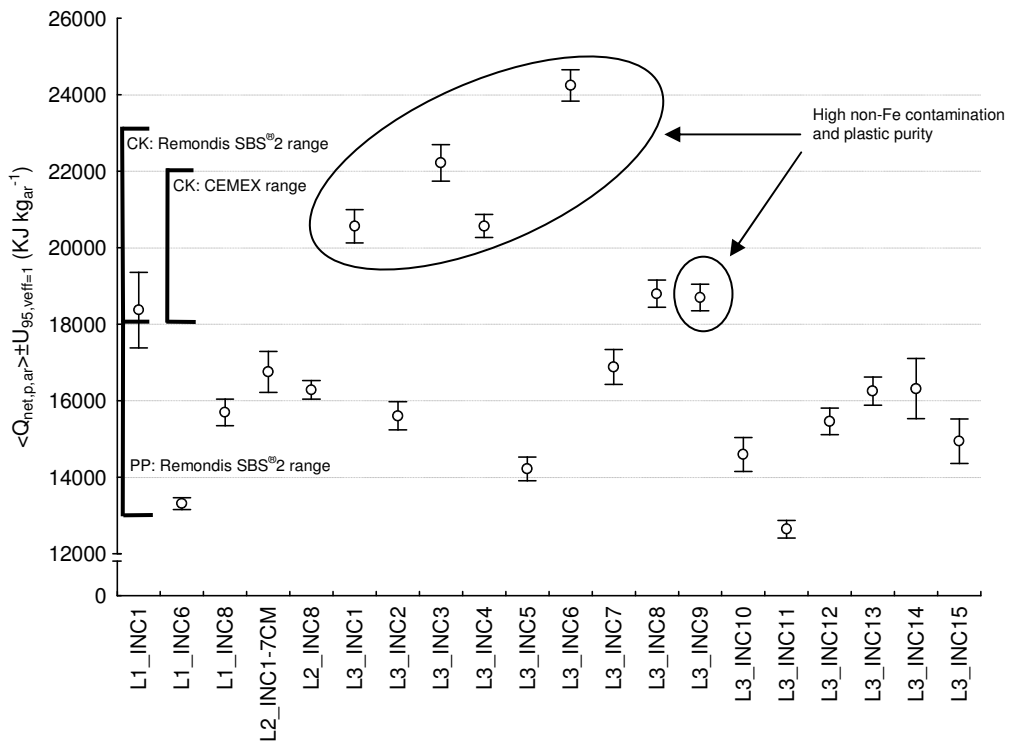


Figure 5-72 Calorific value (net, under constant pressure, as received) ($\langle Q_{net,p,ar} \rangle$) and uncertainty for L1+2+3 SRF samples.

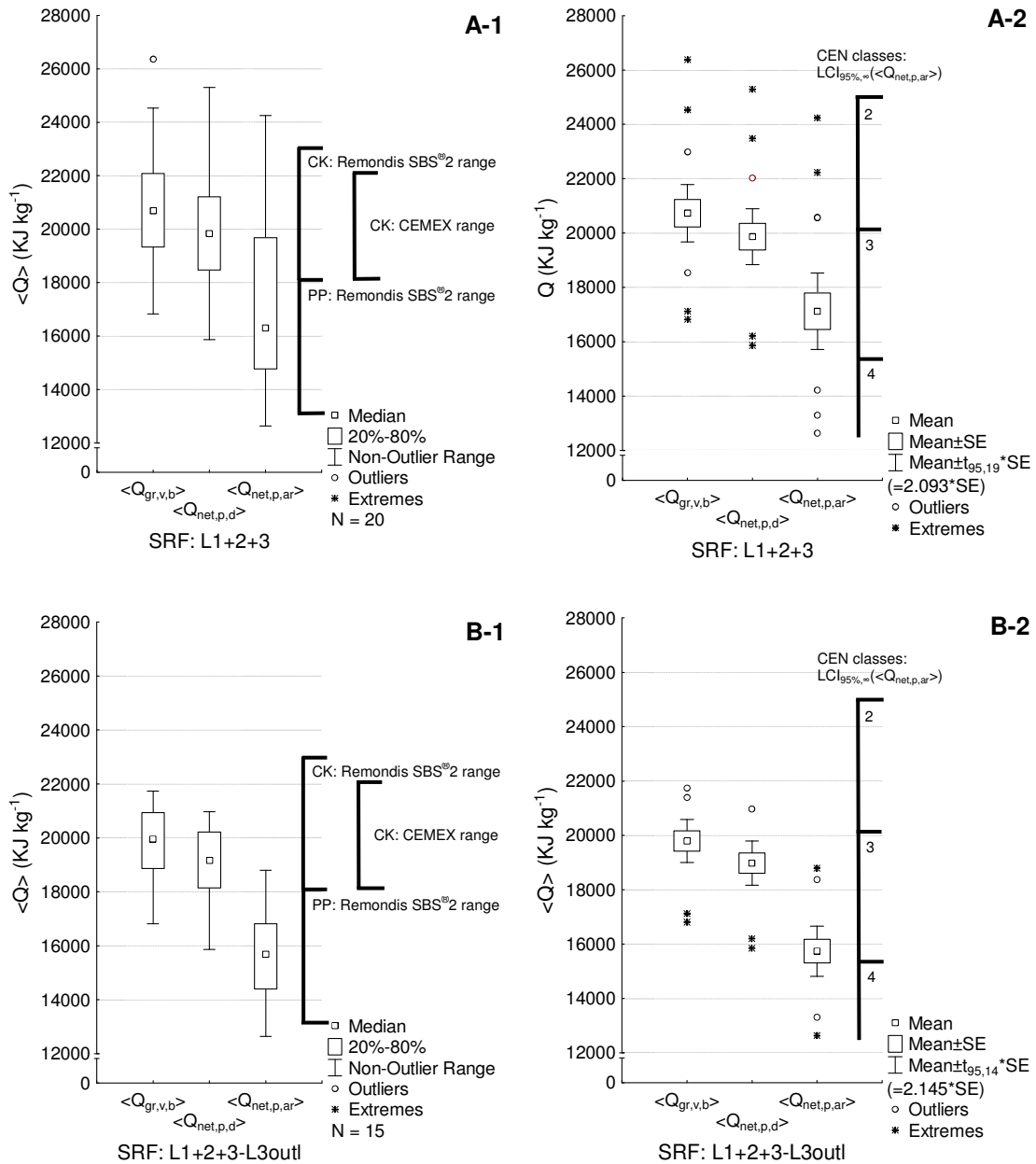


Figure 5-73 Calorific values (3 reporting basis) of SRF: box-plots of for 2 sets of samples (A-B) (refer to **Table 4-9** for explanation) and 2 statistical approaches (1: non-parametric; 2: normality-based), along with SRF end-use specification ranges (CK: cement kilns; PP: power plants). For box-plot non-parametric conventions refer to **Figure 5-62**. Normality-based box-plot conventions: (1) centre: arithmetic mean; (2) lower and upper lines of the boxes denote the mean \pm standard error (SE) around the mean; (3) upper and lower 95% confidence limits around the mean ($UCI_{95,v}(\langle Q \rangle)$ and $LCI_{95,v}(\langle Q \rangle)$), computed for v d.f., are denoted by whiskers. Here this is defined as the range of values that do not differ from the median more than the Q_1 or Q_3 plus 1.5 times the height of box ($p_{80}-p_{20}$); (3) outlier and extreme values outside the 95% CI are presented as circles and asterisks respectively.

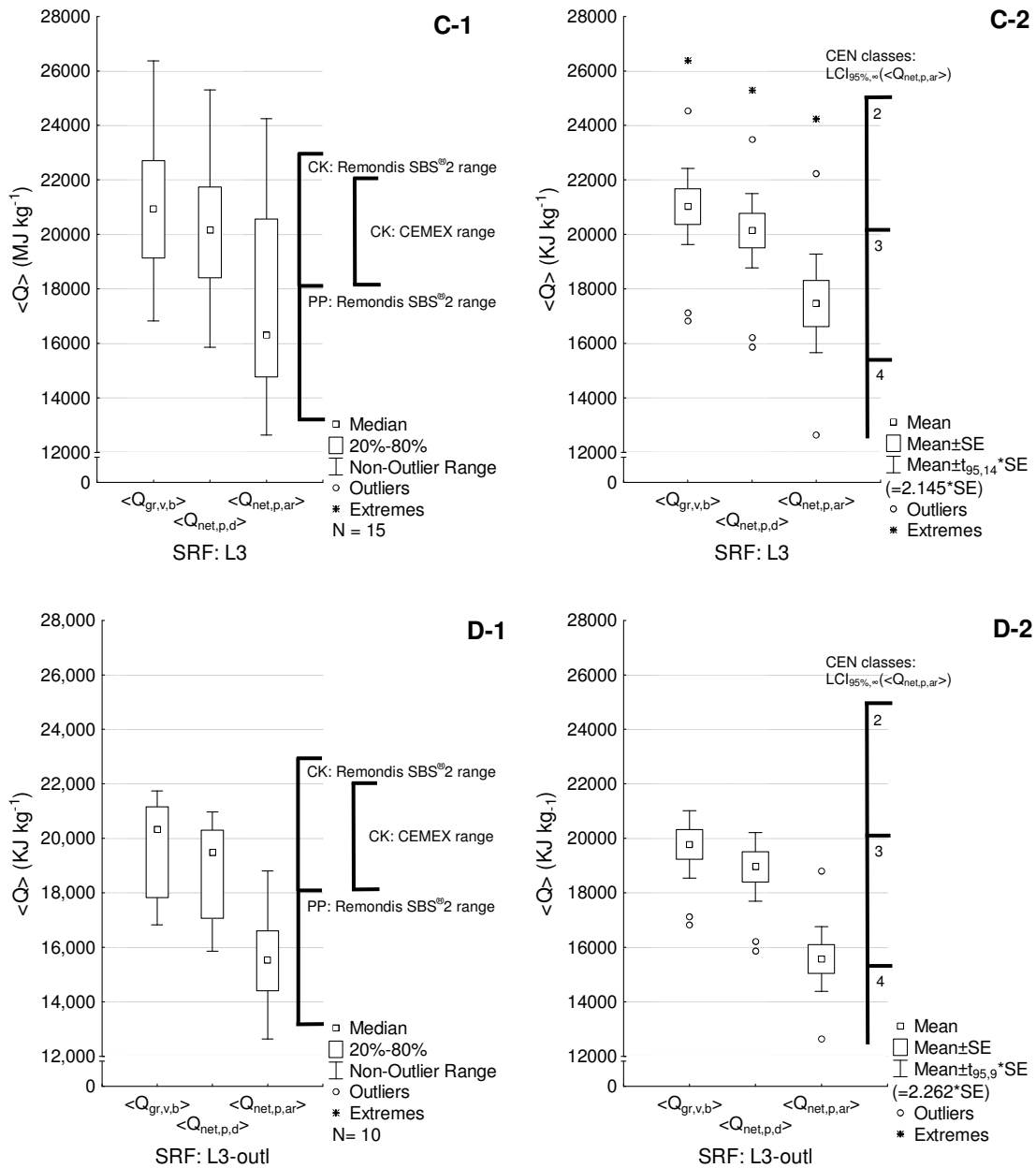


Figure 5-74 Calorific values (3 reporting basis) of SRF: box-plots for 2 sets of samples (C-D) (refer to Table 4-9 for explanation) and 2 statistical approaches (1: non-parametric; 2: normality-based), along with SRF end-use specification ranges (CK: cement kilns; PP: power plants). For non-parametric box-plot conventions refer to **Figure 5-62**. For normality-based box-plot conventions refer to **Figure 5-73**.

5.6.8 UK MBT plant A: SRF total nitrogen content

Results of total nitrogen on individual incremental (and composite) samples are presented in **Table 5-19** and plotted in **Figure 5-72**. Summary data and statistics are found in **Table 5-12** and **Table 5-13**, and presented in **Figure 5-76**.

The repeatability of <TN>, determined on 3 replicates of the GAS, (within-sample and analytical determination variability) can be assessed by the %CV(TN) (**Table 5-13**): it ranges from 13.1% to 1.1% for the L1+2+3 set of samples; and 7.6-1.1% for the L1+2+3-L3outl. The median values are respectively 3.3% and 2.6%. The between-incremental sample variability of <TN> can be evaluated by the %CV, because the normality assumption is not violated ($p_{w-s} > 0.8$) (**Table 5-12**): 18.2% for L1+2+3-L3outl and 14.7% for L3-outl; when the atypical samples are included, higher between-sample variability is experienced (>20%).

Table 5-19 Results on total nitrogen content of SRF samples from UK MBT plant A, along with statistical information, including computation of uncertainty estimates.

Sample ID	<TN> % w/W _d	s(TN) % w/W _d	%CV(<TN>)	SE(<TN>) % w/W _d	±U _{95,2} (<TN>) % w/W _d	%U _{95,2} (<TN>)
L1_INC1	0.66	0.008	1.1	0.004	0.019	2.8
L1_INC6	1.33	0.024	1.8	0.014	0.060	4.5
L1_INC8	1.22	0.020	1.7	0.012	0.050	4.1
L2_INC1-7CM	1.00	0.033	3.3	0.019	0.082	8.2
L2_INC8	1.02	0.034	3.3	0.019	0.083	8.2
L3_INC1	0.54	0.071	13.1	0.041	0.177	32.5
L3_INC2	1.22	0.064	5.2	0.037	0.158	12.9
L3_INC3	0.72	0.050	6.9	0.029	0.123	17.1
L3_INC4	0.71	0.023	3.2	0.013	0.057	8.0
L3_INC5	0.87	0.023	2.6	0.013	0.056	6.5
L3_INC6	0.57	0.042	7.3	0.024	0.104	18.2
L3_INC7	0.94	0.013	1.3	0.007	0.031	3.3
L3_INC8	0.73	0.055	7.6	0.032	0.138	18.8
L3_INC9	0.76	0.028	3.7	0.016	0.069	9.1
L3_INC10	1.06	0.066	6.2	0.038	0.165	15.5
L3_INC11	1.05	0.035	3.3	0.020	0.086	8.2
L3_INC12	0.89	0.015	1.6	0.008	0.036	4.1
L3_INC13	0.92	0.019	2.0	0.011	0.047	5.1
L3_INC14	0.93	0.037	4.0	0.022	0.093	10.0
L3_INC15	1.14	0.029	2.6	0.017	0.073	6.4

All four SRF sets of samples show very similar <TN> medians (0.9-1.0% w/w_d) **Table 5-19** (or 0.9% w/w_d if the individual replicates are used for their computation, as plotted in **Figure 5-76**). Given normality is not violated the UCI_{95%}(<TN>) can be used

to evaluate compliance with standards. For both L1+2+3-L3outl and L3-outl the $UCI_{95\%}(<TN>)$ is similar (1.10% w/w_d and 1.08% w/w_d, respectively); and the $p_{20}(<TN>)$ at 1.16% w/w_d and 1.12% w/w_d respectively.

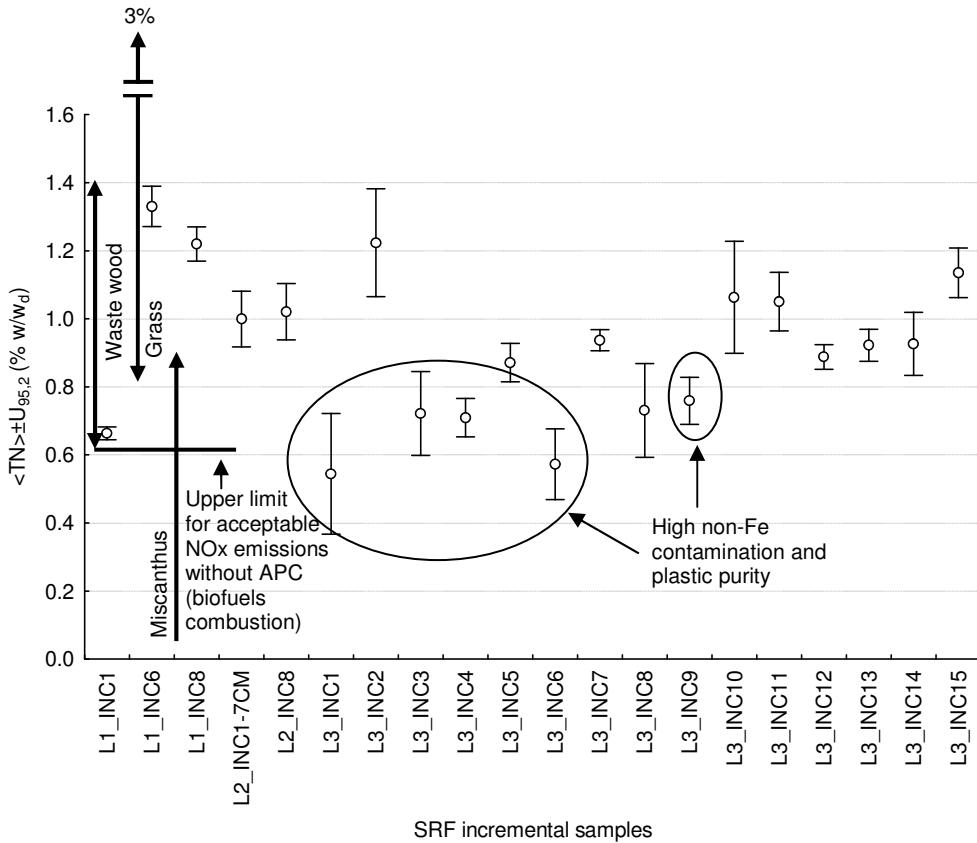


Figure 5-75 Total nitrogen of SRF and uncertainty for L1+2+3 SRF samples. Comparison with indicative ranges for characteristic biofuels, and upper limit for combustion without air pollution control (APC) measures²¹⁵.

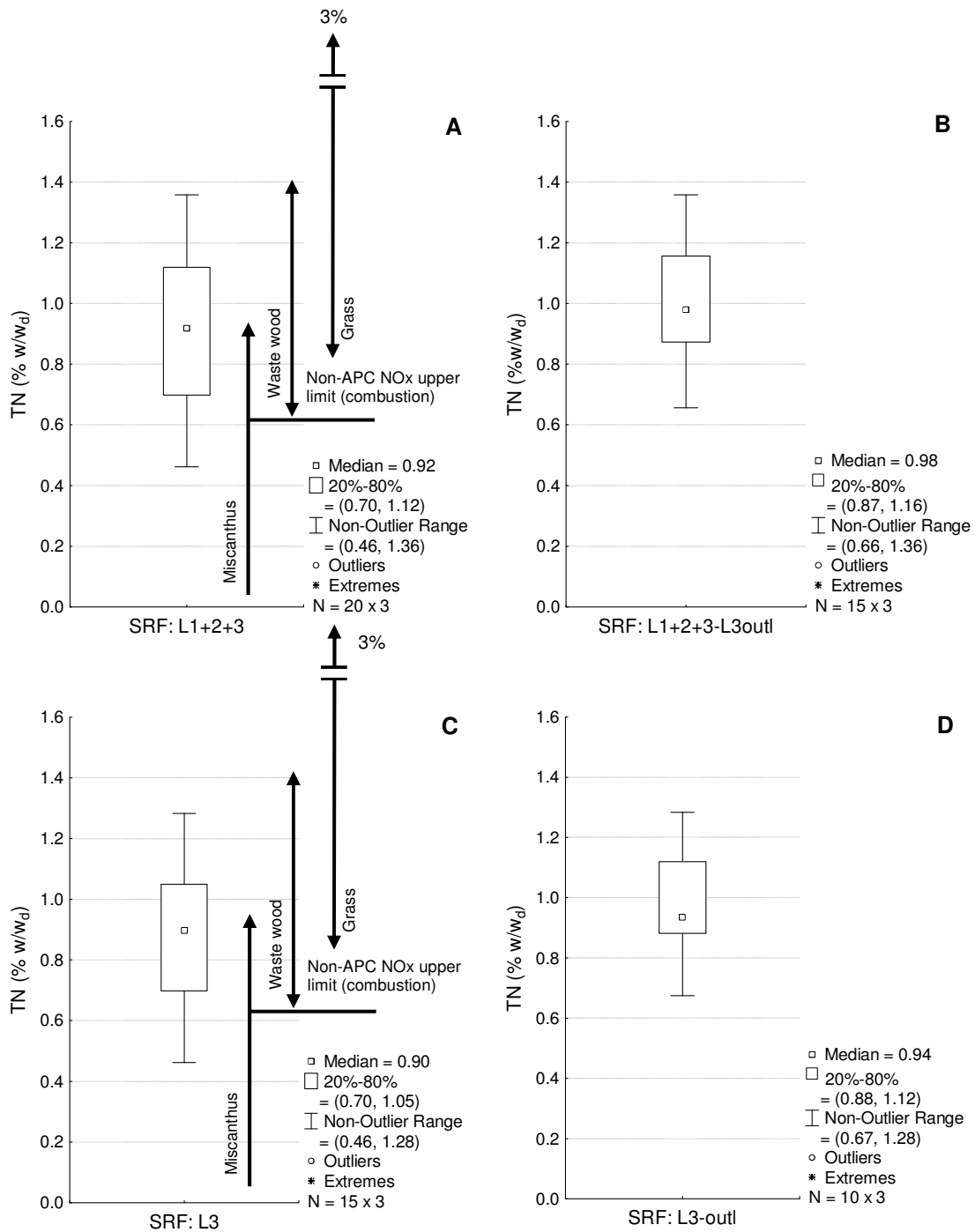


Figure 5-76 Total nitrogen of SRF: box-plots of non-parametric statistics for 4 sets of samples (A-D). Comparison with characteristic ranges for typical biofuels and upper limit for combustion without air pollution control (APC) measures²¹⁵. Number of observations included (n1 x n2): n1: incremental samples, n2: replications on the GAS of each incremental sample. For box-plot conventions refer to **Figure 5-62**.

6 DISCUSSION

6.1 European MBT-derived SRF: statistical overview of quality

Publicly available data on European MBT-derived RDF/SRF (**Table 4-8**) were compiled and statistically analysed to produce the most representative and thorough overview of the quality achieved for RDF/SRF to date (**Objective 1**). As a result, and for the first time, average and upper/lower values and ranges are available for MBT-only RDF/SRF, rather than isolated values for single plants. This allows an evidence base for the quality level that is achievable in practice, and how it relates to expectations. It also creates a quantitative benchmark for evaluating new SRF data, such as the first UK dataset discussed in subsequent sections within this chapter. Results are presented in **Section 5.1**.

The net calorific value of the average SRF (equivalent $Q_{\text{net,p,ar}}$ of Class 3 - **Table 2-13**), is considered acceptable for the less demanding thermal recovery applications, such as dedicated mono-combustion in FBCs, or firing in the secondary system of cement kilns to pre-heat the raw materials. But, only the highest of the SRF calorific value medians reaches the lower level ($20 \text{ MJ kg}_{\text{ar}}^{-1}$) specified by a cement industry company, for use in the primary firing systems (**Table 2-16**). Hence, only SRF of the highest calorific value currently produced by MBTs is marginally suitable for this use. Schirmer et al.³²² recently published review data on SRF production from biodrying-MBT plants in Germany, reporting an average net calorific value of 14 MJ kg^{-1} (moisture level basis not stated) – this value falls within the lower quartile of the SRF cases examined here.

More than 75% of the SRFs considered exceed the upper limit of ash content set for primary firing in cement kilns ($15\% \text{ w/w}_d$) (**Table 2-16**). Hence, the average SRF violates this limit, but it meets the less demanding one suitable for thermal recovery in power plants, as proposed by Remondis ($\text{A} = 17.7 > 20.0 \text{ \%w/w}_d$) (**Figure 5-2**) (**Table**

2-16). For ash content, improvements are required to meet market demands. Notwithstanding this, SRF with unsuitably high ash content for combustion in hard coal power plants could potentially find an outlet as a component of the raw meal in cement kilns, where it could be incorporated into the clinker and final cement product. However, it has to be chemically suitable²⁰³.

Satisfactory total chlorine content quality is reported for the average MBT-derived SRF (**Figure 5-3**) (central tendency of [Cl] medians = 0.50% w/w_d, equivalent to a GEN Cl class 2 - **Table 2-13**). With the maximum chlorine content reported at 1.1% w/w_d, and 75% of the SRF cases at below 0.7% w/w_d it seems that the majority of MBT-derived SRF can be accepted for use in most established thermal recovery processes (**Table 2-12** and **Table 2-16**), including power plants, for which more demanding limits apply (e.g., Remondis SBS[®]2 specification: 0.7% w/w_d).

However, these results should be interpreted cautiously, especially given the central importance of chlorine concentration for the marketability of SRF. Firstly, in the absence of the necessary data, this indicative classification is based upon the mean and not the upper confidence interval around the mean. Hence, it is not conservative. Because the chlorine concentration is relatively close to the class limit (0.5% w/w_d with the upper limit for class 2 at 0.6% w/w_d), it is possible that the resulting Cl classification for a hypothetical average SRF could be 3 instead; a less attractive outcome for SRF marketing.

Secondly, the data series considered here included RDF/SRF with unexpectedly low average values for Cl, especially for measurements reported on a dry basis and stemming from plants that have not incorporated sophisticated sorting (e.g., NIR) to screen out high-Cl components (see **Section 2.4.4** – sensor detection and sorting); the minimum being at 0.29% w/w_d. Calculations by Schirmer et al.³²²

established that the average total chlorine content in MBT-derived RDF/SRF, using a residual MSW input, falls in the range 0.6-0.8% w/w_d. Anticipated values for RDF/SRF produced from biodrying MBTs were computed at ca 0.1% w/w_d higher than values for MBT plants that just mechanically separate RDF/SRF, before biological treatment of the rest of the material. This said, the unexpectedly low values reported in the literature could also reflect difficulties in sampling and analytical measurements. Schirmer et al.¹⁷⁸ have pointed out the particular challenges related to determining total chlorine. Importantly, they stress that combustion digestion methods underestimate the inorganic portion of Cl in samples with high ash content, which is problematic for QA/QC purposes.

In general, for the trace metals examined (PTEs), results have been reported within the tolerable levels (**Table 2-12** and **Table 2-16**), with the exception of certain elements, at the SRF of specific plants. Comparing the average trace element content reached by the upper quartile of all SRF cases (Q3, the range that includes 75% of the population values, from low to high) with, for example, the limits of the German quality certification mark for SRF RAL-GZ 724¹⁹⁹ shows that: Q3[As] = 3.4 mg kg_d⁻¹ < German limit = 5 mg kg_d⁻¹; Q3[Cd] = 2.2 mg kg_d⁻¹ < German limit = 4 mg kg_d⁻¹; Q3[Cr] = 90 mg kg_d⁻¹ < German limit = 125 mg kg_d⁻¹; Q3[Ni] = 40 mg kg_d⁻¹ < German limit = 80 mg kg_d⁻¹. Among the elements for which sufficient data series existed for statistical analysis, only the Cu (Q3[Cu] = 448 mg kg_d⁻¹ < German limit = 350 mg kg_d⁻¹), and Pb (Q3[Pb] = 208 mg kg_d⁻¹ < German limit = 190 mg kg_d⁻¹) showed an upper quartile if SRF cases with average values that exceed the limits.

For data regarding each plant, the 80th percentile values are considerably higher than the median in many cases. This finding supports the need to resort to statistical description and classification of trace metal content with an indication of both location (median) and upper values (p₈₀).

The %CVs for the individual PTEs is least at 47%, which is by and large anticipated for elements present at trace level concentrations, and reflects all the possible sources of variability, from plant inputs and processing, to sampling, sample preparation, analytical determination. The wide spread of the Cu values, leading to the highest %CV here might be due to the presence of Cu in pure form in cables and WEEE components present in residual MSW. If such Cu-containing fragments report to the SRF an extreme heterogeneity could be anticipated. This result is in agreement with the findings of Cuperus et al.²⁰⁸ during the pre-normative research for CEN standardisation of SRF. Copper was found to have the poorest repeatability amongst the examined elements (Cu, Cr, Hg, Cl); it also exhibited considerable between-plants variability. The worst repeatability has been reported for biodrying MBT plants, similarly to the bulk of the data statistically examined in this thesis statistical overview.

However, the picture is slightly less clear for Hg expressed on an energy basis - chosen by CEN as the indicator element for environmental performance of the SRF (**Table 2-13**). An equivalent hypothetical SRF with the same median and p_{80} values would have been cautiously classified as CEN Hg class 2. This is towards the best end of possible qualities. However, it exceeds the limits of the Swiss BUWAL standard⁴³ (**Table 2-11** and **Table 2-16**) (more stringent than the CEN Hg class 1), which, however, has been criticised as over-conservative. According to the CEN pre-normative SRF research²⁰⁴, the average MBT-derived SRF is suitable for all thermal recovery processes, excluding FBCs when activated carbon is not used in the air pollution control suite. However, the unexpectedly similar values of the location of median and p_{80} values for Hg on an energy basis may imply an insufficient number of data points available for the p_{80} : thus, the p_{80} criterion cannot be used with certainty. Given that the Hg concentrations are generally very close to the detection limits²⁰⁸, of

certain analytical determination methods, it is difficult to reach reliable and consistent results.

The difficulties discussed just above, might provide an argument for reconsidering the suitability of Hg concentration as an indicator property, despite being the most difficult PTE to mitigate its emissions, due to its volatility. For instance, Cd also a volatile PTE, bears certain advantages from an analytical determination point of view. It is typically well above the method limits of quantification; and evidence suggests that almost full recoveries can be reached with the use of only nitric acid as the oxidising agent during the digestion analytical step, for certain matrices. In fact, Cd has been considered also as a suitable indicator PTE during the pre-normative research of the CEN SRF standardisation²¹⁰ (**Table 2-13**).

The maximum of the average the mercury concentration (on a mass basis) encountered for the examined MBT-derived SRF cases is at 1.5 mg kg_d^{-1} , which falls within the limits set by the EURITS/Flemish region of Belgium²⁰² (**Table 2-16**), but exceeds other more demanding standards. The 50% of the SRF cases show mercury concentration ($0.43 \text{ mg kg}_d^{-1}$) acceptable for cement kilns (**Table 2-16**) and other applications, apart from the most demanding Class I and II Finish specifications⁴⁵ (**Table 2-12**).

6.2 UK MBT plant A: material flow analysis (balances of mass, waste components and fuel properties)

Results on a detailed material flow analysis, developed for the UK MBT plant A, are discussed in this section (**Objective 4** and **2**). These cover mass on various bases, a series of fuel-related properties, and individual materials (waste components) or wider sets of them. For the first time detailed material flows are presented for a

contemporary, commercial, and fully operational SRF-producing 4th generation MBT plant.

A series of novel methodological approaches were adopted to reach results that cover all major inner solid matter flows, rather than treating the plant as a black-box, and to quantify their uncertainty. Firstly, experimental data were generated for 14 flows, including all inner flows that could be sampled, given the health and safety or technical limitations that inevitably apply. Secondly, an exhaustive sample preparation was followed with every single sample, in line with the stipulations of theory of sampling and the best available practices, to guarantee that the measured value can be considered as representative of the collected flow sample. Thirdly, the uncertainty for each property/waste component, at each flow, was estimated from the experimental data, using the statistically correct total extended uncertainty, i.e., computing confidence limits around the mean values at 95% level of confidence, applying where necessary uncertainty propagation. Fourthly, material flow management software was employed to mutually reconcile all the 14 flows in an optimal way provide estimates for all the flows not sampled, whilst using the redundant degrees of freedom to reduce the uncertainty and applying uncertainty propagation.

The outcome is a detailed mapping of all the flows throughout the plant, accompanied with the uncertainty around the mean values reported, quantified at a = 0.05. This constitutes a major leap forward from MBT flow balances developed only from the output flows of the plant, without description of and validation from the input and inner flows and quantification of the accompanying uncertainty. In addition, this is the first set of data reported for a processing section of biodrying MBT plant. It provides new insights on how the mechanical processing performs with biodried material as input, rather than with wet, untreated (residual) MSW. The results are presented utilising the relevant capabilities of the material flow management software STAN2[®],

combining a schematic of the plant flowsheet with Shankey diagrams that enable to readily visualise the relative magnitude of the flows. Numeric values are incorporated in each graph.

Results are presented in **Section 5.3**, shown in **Figure 5-22** to **Figure 5-54**. They comprise 3 parts: (i) development of a mass balance model (on various reporting bases), including a sensitivity analysis; (ii) balancing of the flows of waste component categories, identified by manual sorting; and (iii) balancing of the flows of mass-based loads for fuel-related properties. The general material flow analysis methodology can be found in **Section 4.4**. Specific application to the UK MBT plant A is detailed in **Section 4.9**.

6.2.1 UK MBT plant A: mass balance model

Mass balance on as-received basis

Results for all the mass flows, including internal flows, are illustrated in **Figure 5-22**. The processing line configuration is effective in allocating to the SRF stream more than half of the biodried matter, fed into the processing section. This corresponds to the ca 37% w/w_{ar} of the plant input (assuming that 32% w/w_{ar} of the plant input is biodrying reactor losses, as estimated by plant input-output operational data balance³⁵³ – an unusually high percentage for losses). This high percentage of the partially dried waste components reporting as SRF is typical of the biodrying configuration plants. Result is in close agreement with those reported for the Frog Island Shanks/Ecodeco biodrying plant³⁵² (**Table 5-3**) and other biodrying configurations, summarised in **Appendix I**. The high percentage for the SRF output flow is tracked down to the T_SRC overs being ca 69% w/w_{ar} of the 100% w/w_{ar} processing section input, and most of it is maintained in the A_CL 1 lights (ca 55% w/w_{ar}).

Because of the very limited contribution of the A_CL 2 lights to the SRF output (<1% w/w_{ar}) compared to the input from the main SRF flow-line (ca 53% w/w_{ar}) (**Figure 5-22**), the air drum separator serves more as a means to increase the purity of the 8-20 mm ('aggregates') output, rather than as an effective way to increase the percentage of the SRF output. The contribution to the SRF is limited despite that the 8-20 ('aggregates') output is unusually high (reported at ca 7% w/w_{ar} modelled at ca 9% w/w_{ar}); otherwise, it would have been even less. Assuming that the main potential of the 0-8 'aggregates' output is for low value applications, the increase of its purity in aggregates by the removal of the lights contraries by the air drum separator, may not be critical.

It is assumed that the A_CL 2 lights is the only contribution to the SRF from the initially existing fines <10 mm, reporting to the nominal range 8-10 mm. Fines that could potentially adhere to components and end up in the SRF stream might be partly liberated in the trommel and report to the T_SRC unders; any limited residual adhesives may be liberated only after the secondary shredding. Despite the positive but limited contribution of to the SRF mass, given the established distaste for the inclusion of the initial fines into any SRF product⁷⁹, this choice could be questioned regarding the possible increase in the pollutant load. The reconciled total chlorine balance (**Figure 5-54**) indicates that ca 4% of the load present in the SRF is contributed by the A_CL 2 lights; however, this result should be regarded with caution, because the flows pertaining to the A_CL 2 lights were too small to be identified with satisfactory precision in this research. In any case, it deserves further investigation.

The limited APC control output (ca 0.04% w/w_{ar}) is not a liability on a mass basis. In other bio-drying plants configurations this flow is incorporated into the SRF output³⁵⁴.

Sensitivity analysis for as-received mass balance model

Sensitivity analysis was performed to assess and validate its suitability to produce closing balances for the individual waste components; results are presented in **Section 5.3.1**.

The increase in the glass deficit for the scenarios M and H (medium and high rejects respectively) (**Figure 5-23**) compared to the baseline scenario L (low rejects) reflects mainly the decrease of 0-8 mm aggregates, given its insignificant presence in the oversized heavy rejects. Paper/card further departs from 100% as the oversized heavy rejects increase: result anticipated given that this flow contains paper at ca 45% w/w_{ar} , whilst the 0-20 mm flow, much lesser. These results indicate that the L scenario behaves best for major waste component categories, such as paper/card and glass. However, these components are subject to heavy adjustment during the correction of the measured data to allow for the re-allocation of the $F < 10$ mm. Hence, the possibility of the scenario L to behave better than the H if a more refined correction is applied cannot be excluded.

Results that do not favour the L scenario are achieved for cables, shoes, hazardous and treated wood. However, even in the L scenario results are acceptable for cables (ca 88% w/w_{ar} of input mass accounted for). For the hazardous all scenarios show great deficit implying not sufficiently representative presence in the collected mass samples or high input variability. Hence, this component category is not suitable for judging. Shoes and treated wood depend on modelling accuracy in a similar way to paper/card. With the currently applied correction attempting to account for the part of shoes manually sorted as fines in post-secondary-shredding streams a deficit rather than a closing balance is anticipated. This is so because the correction is based on the amount of shoes identifiable in the > 10 mm, leading to underestimation.

Given that the scenarios were computed keeping set the waste component adjustment computations and relevant parameters, it is concluded that the Scenario L is the most suitable to describe the results obtained by manual sorting, assuming only limited bias is introduced by the performed adjustments on the waste components alone.

The sensitivity analysis on the mass balance showed that despite all the scenarios being possible, the high percentages experienced for 8-20 mm ('aggregates') and 0-8 mm ('organics') are most compatible with the measured waste components compositions for the UK MBT plant A (L, baseline scenario). This indicates that for plants of this configuration it may be feasible to achieve a relatively low level for the main reject output (oversized heavy rejects). Such a lower level of the main rejects output (ca 13% w/w_{ar} of mechanical processing section biodried input) results in higher percentages for the for 8-20 mm ('aggregates') and 0-8 mm ('organics'). These plant outputs are much less heterogeneous than the main rejects and can potentially be beneficially used, as low value aggregates and CLO (after further biostabilisation possibly) respectively. Conversely, oversized heavy rejects constitute the main liability in terms of output process, having to be disposed of in landfill (UK) or thermally recovered in other European market and legal environments (Germany), and it is desirable to be minimised.

The variability experienced within a plant in the oversized heavy rejects percentage, reflects the variability of the plant input and/or the processing section settings. Primarily, those affecting the PSD of the primarily shredded material, and the trommel operation. If these can be assumed constant, it is then due to input variability. In any case, a comparison of the unit operation settings with those of plants with similar configuration for which much higher main rejects percentage has been reported³⁵²

(**Table 5-3**) could reveal any differences in the operational settings and hint towards their optimisation.

Mass balance on a dry basis (d)

Figure 5-24 illustrates the reconciled mass balance of the UK MBT plant A expressed on a dry basis (d), assuming ca 100 dry mass units as input to the processing section. Methodological details are in **Section 4.9.1**. For comparison, the as-received mass balance is shown in **Figure 5-22**. The input data for the d mass balance are presented in **Table_App F-18** and illustrated in **Figure_App F-17**. The flows very similar with the dry basis mass balance (**Figure 5-22**).

Mass balance of the shreddable fraction on a dry basis (SHR, d)

Figure 5-25 illustrates the reconciled mass balance for the UK MBT plant A, expressed on a dry basis (d), assuming ca 100 dry shreddable/combustible mass units as input to the processing section. Methodological details are provided in **Section 4.9.1**. For comparison, the as-received, entire sample mass balance is shown in **Figure 5-22**.

A higher percentage of the dry shreddable/combustible mass of the processing section input reports to the SRF output (63.7% w/w_d), than for the entire dry mass (53.5% w/w_d) (**Figure 5-24**). The amounts reporting the 8-20 mm ('aggregates') constitutes contamination with combustible material ($3.16 \pm 1.03\%$ w/w_d). The amount of contamination removed by the air drum separator is just almost half of it - however, this is a highly uncertain result ($1.55 \pm 1.91\%$ w/w_d).

Mass balance of the shreddable fraction on a dry and ash-free basis (SHR, daf)

For the first time, a detailed dry, ash-free mass balance of an MBT processing section is presented here (**Figure 5-26**). It is suitable for computing the mass-specific-loads for balancing of properties reported on a dry, ash-free basis ($_{daf}$) of the shreddable/combustible part of the samples (e.g., for biogenic content, $\chi_{B,SHR,daf}$).

The fact that a satisfactorily closing balance has been achieved before the application of the data reconciliation, establishes the mutual compatibility of the ash content balance and the developed using partially independent sets of experimental data (manual sorting and ash content determinations on shreddable part of sample); and it serves as an indirect validation for both shreddable dry mass and ash content ($_d$) balances.

Such a balance can best reveal how well the processing flowsheet performs regarding concentrating the dry oxidisable mass (combustible waste components after removing the chemically inert fraction and the unbound water) of the materials present in the input into the intended fuel output (SRF). For the UK MBT plant A, from every 100 units of combustible dry, ash-free mass ($_{daf}$) in the processing section input $12.5 \pm 2.31\%$ w/ w_{daf} are lost in the oversized heavy rejects fraction, whilst most of them are successfully incorporated into the SRF product ($75.5 \pm 2.9\%$ w/ w_{daf}). The potential to further increase this lies in improving the performance of the air classifier regarding the recovery of the paper into the SRF production flow. Currently, $17.7 \pm 4.7\%$ w/ w_{ar} of paper/card, and waste components of similar composition input to the air classifier is lost, reporting to the high-gravity fraction (**Table 5-6**).

There is no literature data from other SRF-producing MBT plants to compare with. In EfW plants the equivalent percentage is 100%, but there is no scope for wider

conclusions to be drawn without evaluating these results through a systematic assessment tool such as LCA. Whether this loss of combustible matter can be justified by the benefits achieved by the SRF production and utilisation in more technically demanding thermal recovery options, is still to be answered. This, along with other results reported in this thesis, could provide a quantitative basis to address such questions.

6.2.2 UK MBT plant A: material composition balances

The most comprehensive set of data available so far regarding flows of materials through MBT plants is presented in this section. This in-depth investigation provides the necessary data to understand how these materials flow through the plant and where they finally report to, determining the properties of the output fractions. Most waste component categories were balanced successfully and were able to fully reconcile through the application of the material flow software STAN2. However, for some components, no sufficient balancing was evident. These cases either need more sophisticated account for the transformations that occur in the processing section of the plant, or require bigger samples to be collected, because they cannot be representatively be identified with the currently used.

For most items some negative flows appear around the mixing of ferrous materials. This stems from an inherent limitation of STAN2, which allocated optimal flows that included circular routes with some negative flows. It is not feasible to prevent negative flows in STAN2 and the code is not modifiable at the moment. Hence, this issue was addressed by manual iteration of the reconciliation procedure, as explained in **Table 4-7**. The remaining negative flows are of insignificant magnitude and are typically characterised by large uncertainties. The automatic resolution of this issue could deserve more attention in future editions of STAN2.

The successful closures and reconciliation of flows established that the proposed and applied methodology has a great potential to map the material flows within the mechanical processing section of MBT plants or similar applications such as material recycling factories (MRFs).

Mass balances for combustible waste components

Figure 5-27 presents the balance for maximum amount of potentially combustible (sum of combustible, $\Sigma m(\text{Comb})$) components accounts. It is maximum because it includes components such as fines, cables and hazardous, which can be considered in many ways as contraries and, ideally, they should not report to the SRF output. For instance, they are least or marginally combustible due to their relatively higher ash content than others (e.g., plastics). In principle, the desirable outcome for the processing section would be to concentrate the maximum of components with beneficial combustion properties in the SRF stream and the maximum of components with high pollutant load (even if partly combustible) in the oversized heavy rejects output. According to the literature data and researcher views⁵⁵, this would mean to include in the SRF output all paper and likes, plastic film and other packaging plastic (but these may rise the total chlorine content), fabrics and textiles, biological; treated wood (but this may rise the PTEs if it is chemically treated); whilst components of high pollutant load such as hazardous, hard plastic, batteries, cables, shoes, sanitary products, composites should report to the oversized heavy rejects.

The sum of combustible components accounts for $82 \pm 0.1\%$ w/w_{ar} of the biodried input to the processing section. Most of it is directed to the SRF output (51.9% of entire processing mass input_{ar}), with the rest split between the 0-8 mm ('organics') (17.5%) and the oversized heavy rejects (9.7%). As can be seen from other balances, it is predominantly the fines < 10 mm (**Figure 5-39**) and the part of the biological (**Figure 5-38**) which report to the 0-8 mm ('organics') output. The former are typically

intended to be excluded from the SRF output⁷⁹. The latter constitutes only a very limited potential source of combustible matter for the SRF, forming only 3.5% w/w_{ar} of the biodried fraction (**Figure 5-12**). Hence, most of the losses in desirable combustible components yield for the SRF are directed to the oversized heavy rejects output.

Regarding the individual combustible components, paper/card (**Figure 5-28**) is the dominant component present in the biodried input: 29.2 mass units (out of 100) (see also **Figure 5-12**). The majority of this is incorporated in the SRF output: 23.1 mass units leading to an enrichment for paper/card in the SRF compared to the biodried flow (reconstructed SRF composition: 44.5±2.6% w/w_{ar} - **Table App F-19**). But ca 1/6 of the input paper/card are lost (5.3 mass units), reporting to the oversized heavy rejects.

A similar balance results for the sum of paper/card, cartons and tissues (paper and like) balance (**Figure 5-29**). The last two components are insignificant compared to the paper/card alone, and not balancing individually (**Figure 5-23**), possibly because they are mistaken for paper/card in the manual sorting of post-secondary shredding flows, such as the SRF.

Most of the paper/card remains in the SRF production line after the trommel screening ($TC(P/C)_{T_SCR_LG} = 96.3\pm0.7\%$) (**Table 5-5**), indicating that most of the paper/card is >20 mm, despite the primary shredding. It is the next downstream unit operation of air classification that allows the paper/card to exit the SRF processing line: $TC(P/C)_{A_CL\ 1_HG} = 17.7\pm4.7\%$ (**Table 5-6**). The losses occur despite that, at the current operational settings, the A_CL 1 is already creating an updraft air stream capable of capturing ca 80% of the overall input mass to this unit operation ($TC(\Sigma m)_{A_CL\ 1_LG} = 79.6\pm1.6\%$). This fact, along with the >20 mm aerodynamic size, indicates that the lost paper/card comes in the form of big heavy items. This agrees with observations during

manual sorting, showing that the paper/card reporting to the oversized heavy rejects comprises items such as telephone catalogues and whole newspapers left intact by the primary shredding and not showing any sign of biodegradation due to biodrying. Thus, incorporation of more paper/card to the SRF output could be achieved by finer primary shredding and/or stronger upwind suction at the A_CL 1. However, the former could lead to a series of undesirable side-effects, such as higher percentage of combustibles reporting to the T_SCR_U, paper/card included; and the latter could increase the impurities and undesirable combustibles incorporated into the SRF stream.

Closing balances were developed for 3 out of the 4 categories of plastics identified during the manual sorting (P_F, O_P_P, D_P, COM) (**Figure 5-30** to **Figure 5-35**). The plastic film and other packaging plastic present in the biodried fraction report almost entirely into the SRF output (**Figure 5-30** and **Figure 5-31**). Most of the durable plastic (2.2% w/w_{ar} or mass units, in the biodried material,) is also incorporated into the SRF stream (**Figure 5-32**) (1.6 mass units). The rest does not exclusively report to the oversized heavy rejects, but instead is present as contamination in the 0-8 mm ('organics') (0.12 mass units) and the 8-20 mm ('aggregates') (0.17 mass units). Durable plastic is the only plastic component category that does not report entirely to the SRF output, because it contains materials of much higher density (specific gravity) than the rest plastics; thus, they are partly reporting to the unders of either the trommel or the air classifier ($TC(D_P)_{T_SCR_HG} = 14.5 \pm 4.7\%$ and $TC(D_P)_{A_CL\ 1_HG} = 16.6 \pm 7.1\%$, respectively) (**Table 5-5** and **Table 5-6**). This shows that all the other plastics have mechanical/physical characteristics that enable the existing unit operations to direct them to the SRF production line.

Composites balance is not closing before reconciliation (**Figure 5-23**). Thus, the data before reconciliation also are shown here (**Figure 5-33**), along with the finally reconciled values (**Figure 5-34**). The high within-flow relative uncertainty for

composites is possibly due to the fact that they are the least homogeneous component category, when compared with the rest plastics. In practice, they serve as 'other' category for most plastics not covered by the rest categories. Again, the main quantity is directed to the SRF stream - because they are typically low-density materials (e.g., packaging composites, foam, cigarette butts, synthetic cloths, etc). It seems not feasible to direct them in the heavy oversized rejects, even if this was desirable.

Figure 5-35 depicts the overall mass balance for the sum of the four plastic categories. This overview shows clearly the dominance of the SRF production line in incorporating the plastics present in the processing section input. Hence, regarding the plastics, the UK MBT plant A is successful in incorporating these high-CV materials into the fuel product. On the other hand, this is the worst case scenario for the biogenic content, given the fossil origin of the resins. The successful incorporation of the plastics has also positive implications for the ash content (**Figure 5-51**) and negative implications for the total chlorine content (**Figure 5-54**) of the SRF, which are discussed in the relevant sections of the characterisation for the SRF produced from the UK MBT plant A (**Section 6.5.4** and **6.5.3**, respectively).

Results for balances for a group of waste component categories are discussed here: textile/fabric, carpets/mats, shoes, and sanitary products. All of them contain cloth, to varying degrees. The adjusted un-reconciled textile/fabric balance shows a high surplus, whilst carpets/mats, shoes, sanitary products a clear deficit (**Figure 5-23**). With the relatively simplistic data handling adjustment adopted to account for the post-secondary shredding increase of reported $F < 10$ mm, it should be anticipated a deficit for these categories, because in manual sorting they are not easy to recognise as such, being fine fragments. Instead, they could be mistaken mainly for textile/fabric (and as composites to a lesser degree). Hence, to account for this partly inevitable possible systematic mistake during the manual sorting, not fully corrected by the

adjusted model, a balance for the sum for these material is presented (**Figure 5-36**). However, this means that the information for the comprising components is by-and-large insufficient, apart from the fluff which is sufficiently closing. Reconciled balances for the individual components using adjusted values can be found in **Appendix F**. However, they are just indicative, hence not shown here.

The sum of these components ('sum of textiles and like') exhibits a satisfactorily closing balance. Collectively consisting ca 5.5% w/w_{ar} of the biodried input, these component categories report mainly to the SRF (3.5 mass units) and secondarily to the oversized heavy rejects (1.8 mass units). The air classifier is responsible for directing a considerable part of them to the oversized heavy rejects. Notably, from this sum of waste components, the category of shoes should be directed away from the SRF, whilst the textiles/fabric can be incorporated. Hence, the overall balance does not provide sufficient information to evaluate each of them.

A more sophisticated correction should be applied in future applications. For this to be feasible, knowledge of the input (and output) particle size distribution for each waste component category is necessary, along with effective mathematical model for the type of shredder used. Despite efforts in the past (**Section 2.4.3.2**), such as the GRAB model¹¹⁴, and the recent modelling attempts by Zwisele et al.¹⁴⁰ or the capabilities of SOLIDSIM software³¹⁹⁻³²⁰, the correct modelling of shear shredders cannot be guaranteed. In any case, in this research, for the UK MBT plant A it was not technically feasible to sample just upstream of the secondary shredder, which could have generated the necessary data for mathematical modelling of its performance.

Whilst no transfer coefficients were computed for shoes, the un-reconciled flows (**Figure_App F-25**) provides sufficient indication that the component flow is split between the SRF and the oversized heavy rejects. Hence, the highly polluted shoes

are to a considerable degree reporting in the SRF category. This has implications, not least for the total chlorine content, as discussed in **Section 6.5.3**. The air classifier is not optimised for directing the shoes away from the SRF production line. However, it can be speculated that in order to achieve this, less powerful uplifting would be necessary, resulting in negative implications for other important SRF components, such as paper/card, already not reporting entirely in the low-gravity output of A_CL 1.

Major waste component categories containing biogenic combustible materials, in addition to the paper/card, comprise also the biological, treated wood and partly the fines <10 mm (**Figure 5-37** to **Figure 5-39**). Treated wood is monitored separately from e.g., yard waste such as trees branches which are included in the biological component (**Table 4-5**). Treated wood is directed almost exclusively to the SRF (2.0 mass units, out of 100 biodried material, containing 3.1 mass units of treated wood) and the oversized heavy rejects (1.0 mass units) (**Figure 5-37**). Depending on whether T_W is intended to be incorporated into the SRF or not, this may be an acceptable or not outcome. The split between the two outputs depends largely upon the performance of the air classification (A_CL 1), currently directing around the 1/3 of the T_W to the high-gravity product: $(TC(T_W)_{A_CL\ 1_HG} = 33.5 \pm 10.2\%$ - **Table 5-6**). This constitutes a loss of material intermediate in calorific value ($\langle Q \rangle_{net,p,ar}(T_W) = 15.6 \text{ MJ kg}_{ar}^{-1}$ - **Table 5-10**), just above the average measured for the UK MBT plant A SRF (**Figure 5-58**); and 100% biogenic (on a dry mass basis). On the other hand, T_W can be highly polluted in PTEs, if it has been chemically treated (e.g., chromated copper arsenate (CCA) impregnated wood, as discussed by Pedersen et al.³¹⁰).

The biological category of waste components shows a complex flow balance (**Figure 5-38**). Limited amount is present in the biodried flow (3.5% w/w_{ar}). This is directed predominantly to the 0-8 mm ('organics'), but also reports at a similar level to the SRF and at a lower level at the 8-20 ('aggregates) and the oversized heavy rejects.

The 20 mm trommel screening aperture is not wide enough to direct effectively the entire biological component mass to either the undersize product $(TC(BIO))_{T_SCR_U} = 67.6 \pm 6.2\%$ - **Table 5-5**). The air drum separator succeeds only partly in preventing the BIO from reporting to the 8-20 mm ('aggregates'), where it constitutes contamination; the re-directed material reports to the SRF output $(TC(BIO))_{A_CL\ 2_LG} = 62.4 \pm 12.7\%$ - **Table 5-8**). In any case, the BIO available in the biodried flow is low; hence, it can only be of correspondingly limited importance to the SFR output. Thus, it would make sense to attempt to concentrate it to the 0-8 mm ('organics'), which have a potential use as CLO and it is considered to undergo further treatment to limit its potential for biodegradation. Similarly to T_W, it is not desirable in the oversized heavy rejects, because there it contributes to the amount of potentially biodegradable material having to be disposed of in landfill.

The fines <10 mm waste component category constitutes a considerable part of the biodried material (16.6% w/w_{ar}) (**Figure 5-39**). The current modelling adjustments and flows reconciliation lead to a closing balance for the fines <10 mm component (**Table 4-7**). For the pre-adjusted results of manual sorting, a clear surplus of fines is shown. This applies to both the trommel undersize and the post-secondary shredding flows. The modelling adjustment reallocated the additional fines <10 mm generated as a result of material processing to their original components. F<10 are effectively concentrated into the 0-8 mm ('organics') plant output. The amount directed to the SRF by the air drum separator operation (A_{CL 2 LG}) is limited and insignificant for the SRF yield. Only a negligible amount of F<10 is directed to the T_{SCR} over. This is in agreement with by the absence of F<10 in the oversized reject fraction (just $0.18 \pm 0.33\%$ w/w_{ar}) and the limited data available for the T_{CSR} _O (SP8 - not considered in the computations due to insufficient sample mass collected). Hence, all the F<10 measured post the secondary shredding are generated by the comminution,

apart from the contribution of the A_CL 2_LG to the E_C_S input flow. Adjustments were made to the model, before reconciliation, in line with these initial findings, in the iterative application of MFA (**Figure 4-3** and **Table 4-7**).

Mass balances for incombustible or contrary-to-SRF waste components

The indicative reconciled balance for the sum of the incombustible waste component categories shows a complex pattern (**Figure 5-40**). This reflects the heterogeneous mixture of material types included within the sum of combustibles. The balance is indicative, because certain waste component categories such as batteries, or glass are not sufficiently balancing individually. A limited amount of incombustibles is transferred to the SRF output, negatively affecting the ash content of the fuel $TC(\Sigma(\text{non-combustibles}))_{\text{SRF}} = 8.8 \pm 3.8\%$ (**Table 5-4**). Results upon balances and transfer coefficients for the individual waste component categories comprising the sum of incombustibles (**Figure 5-41** to **Figure 5-49**) are discussed.

The approximate reconciled balance produced for the cables component category (**Figure 5-41**) can satisfactorily depict the split of the flows leaving the two main unit operations of trommel screening (T_SCR) and air classifier (A_CL 1). The cables category is divided between the heavy oversized reject fraction and the SRF. Despite being a minor fraction of the biodried flow (before reconciliation: $0.34 \pm 0.77\%$ w/w_{ar} ; after reconciliation: $0.24 \pm 0.10\%$ w/w_{ar}), it is a source of potential contamination with pure Cu fragments (typical wire) and PVC (typical wire coating). Ideally they should concentrate in the oversized heavy rejects fraction. However, the A_CL 1 allows a considerable amount to enter in the SRF processing line: $TC(\text{CAB})_{\text{A_CL 1_LG}} = 43.45 \pm 45.1\%$ (**Table 5-6**). The high total extended uncertainty for this transfer coefficient should not totally undermine the validity of the average, because it is the result of conservative approach to U_{95} - it has not been reduced further due to the partial application of the STAN2[®] software in the case of cables balance. Only a

negligible amount of cables is found in the both the non-Fe and rejects outputs for the eddy-current separator. The E_C_S is not effective in removing the cables from the SRF stream, despite that each individual cable fragment is composed of ca 52% w/w_{ar} non-Fe material (average as measured for this thesis, data not reported).

No closing balance is achieved for the adjusted (modelled) flows of the hazardous components. Only ca 48% of the input material can be accounted for by the sum of outputs (**Figure 5-23**). This is further illustrated in **Figure 5-42**. The main outlets are identified as the oversized heavy rejects and the SRF. This imbalance is possibly the result of the HAZ component constituting a very small mass fraction in all sampled flows, constituting rare occurrences (e.g., $0.17 \pm 0.40\% w/w_{ar}$ of the biodried flow; $0.15 \pm 0.12\% w/w_{ar}$ of the SRF flow, after adjusting for fines). Hence, possibly greater sizes of samples would be necessary to evaluate more accurately the HAZ component. Despite that, a reconciliation of the flows is attempted, but results should be considered as semi-quantitative (**Figure 5-43**). The oversized rejects fraction concentrates most of the HAZ, resulting from the A_CL 1 operation: $TC(HAZ)_{A_CL\ 1_HG} = 81.6 \pm 12.5$ (**Table 5-6**). However, the rest is directed mainly to the SRF. Despite the uncertainty regarding the exact flows of the hazardous waste component category, it has insignificant implications for the quality of the SRF produced in the UK MBT plant A, for the properties of moisture content, total chlorine content, ash content and net calorific value. This is evident from the simulation of the SRF quality, for which results are presented in **Section 5.5** and discussed in **Section 6.4**. However, this should be investigated for PTEs as well.

The balance sheet for batteries shows a deficit (**Figure 5-23** and **Figure 5-44**). Manual sorting results show that BAT report only to the oversized heavy rejects, 8-20 mm ('aggregates') and the Fe-metal plant outputs, together accounting for only ca 32% of the amount found in the biodred material. The un-reconciled flow results clearly

depict the oversized heavy rejects as the main output. Evidently, batteries are absent from all the flows discharging to the SRF. This imbalance could be due to the very low mass fractions of the batteries in every one of these flows (e.g., $0.12 \pm 0.10\%$ w/w_{ar} of the biodried flow), indicating that a more accurate (and precise) measurement would have demanded even bigger sample sizes. However, on-site investigation at the plant revealed that the air classification (A_CL 1) has an output where batteries are discharged and accumulate, until they are finally disposed manually. Hence, a stock of batteries is created within the plant, comprising mainly various types of AA size. It has not been feasible to estimate the magnitude of this stock, so as to check whether it could sufficiently account for the deficit experienced.

The contamination of the 8-20 mm ('aggregates') with batteries seems partly inevitable. This is so because the BAT, being <20 mm, would initially report to the T_SCR_U. It then depends on the performance of the overbelt magnet 3 whether they would continue towards the 8-20 mm ('aggregates') or they would be directed to the Fe-metal output. The O_SCR at 8 mm prevents most BAT from entering the 0-8 mm ('organics') flow, at the expense of reporting to the 8-20 mm ('aggregates'). The contamination of the Fe-metal with batteries is the result of the O_M 3 and O_M 2 OUs: however, the contamination can be –imprecisely– estimated as limited, on a mass basis: $0.12 \pm 0.42\%$ w/w_{ar} of the Fe-metal output flow.

Glass flows, adjusted for the effect of the trommel upon the waste component category of fines < 10 mm, are not balancing (**Figure 5-23**). A deficit in the sum of outputs is evident (**Figure 5-45**). It is difficult to account for this deficit. A more sophisticated modelling of the breakage of the glass items while in the trommel could lead to further insights. However, the way this correction was modelled in this thesis (**Table 4-7**), assuming that the average glass percentage in the biodried flow is accurately estimated by the collected samples, leads inevitably to a deficit.

Alternatively, it could have been assumed that the sum of the glass in the outputs is correct, and adjust upstream, leading to a surplus for the biodried input glass. Because of being present in the form of big, relatively intact heavy items (glass bottles), the glass percentage increases in a stepwise, rather than continuous mode. Hence, bigger sample sizes may be necessary to mitigate this, especially for the biodried flow.

Glass reports almost exclusively to the 8-20 mm ('aggregates') (where it is intended to concentrate) and the 0-8 mm ('organics'). The split is determined by the operation of the oscillating screen (O_SCR). An indicative reconciled balance is reported in **Figure 5-46**. The TCs developed based on this for the oscillating screen show that around a 60-40 split is achieved for the 8-20 and 0-8 mm discharges respectively ($TC(GL)_{O_SCR_8-20} = 62.6 \pm 8.6\%$) (**Table 5-7**). Only a negligible amount ends up in the SRF, compared to that present in the biodried flow.

The slight deficit before reconciliation (**Figure 5-23**) evident for the stones/ceramic waste component category is balanced after reconciliation (**Figure 5-47**). Two main outlets are the 8-20 mm ('aggregates') and the oversized heavy rejects. A lower amount reports to 0-8 mm ('organics'). The SRF output receives only a negligible amount, at the same order of magnitude of glass. A considerable amount of the stones/ceramic are above the >20 mm and are directed to the trommel overs ($TC(S/C)_{T_SCR_O} = 45.1 \pm 19.7\%$ - **Table 5-5**). As a result, it is not feasible to concentrate all of it in the 'aggregates' plant output. Downstream of the trommel, the air classifier directs the majority of this input to the oversized heavy rejects for disposal.

The non-Fe metals Shankey diagram (**Figure 5-48**) reveals a limited capability of the existing process flowsheet and individual unit operations performance to direct the component mainly in the intended output. From the 1.80% w/w_{ar} (or mass units)

evident in the biodried material, only 0.43 mass units report to the non-Fe plant output, whilst 0.77 mass units to the SRF and 0.56 to the heavy oversized rejects.

The validity of this result could be questioned, based on the fact that no reliable operational data on the non-Fe metal were made available for the UK MBT plant A; instead, the value was estimated using literature data from a plant of similar configuration (**Table 5-3**), assuming a constant ratio for the E_C_S products. Nevertheless, the assumed value is favourable for the flow-rate of the non-Fe metal output as modelled (0.72 kg min^{-1}), in comparison to the result of an on-site measurement at the UK MBT plant A (almost half: 0.39 kg min^{-1}). If the measured value has been used, the model output for the non-Fe mass component would have resulted in even lesser percentage reporting in the non-Fe plant output.

Another possible objection would have been to assume a much higher flow of the oversized heavy rejects: the scenarios M and H (**Figure 5-23**) lead to higher absolute amount reporting in the oversized heavy rejects. However, because the SRF yield has been shown to remain relatively stable, these scenarios just lead to surplus of non-Fe metals component in the sum of outputs: yet, the SRF gathers considerable part of it and the non-Fe output collects an even smaller relative percentage. Potential objections could be also raised for the amount of the non-Fe component measured and subsequently adjusted (modelled) in the SRF production line. **Table_App F-16** shows relatively low between-flows variability for the flows that should be exhibiting similar levels of non-Fe metals (A_SH material, M_S 1Fe metal-free fraction, SRF with non-Fe), despite the relatively high within-flow variability, which is, however, conservatively estimated ($U_{95,v}$). Hence, the measured levels can be reasonably considered as representative. The modelling adjustment increases the average non-Fe presence in the SRF from the measured $1.16 \pm 0.92\% \text{ w/w}_{\text{ar}}$ to STAN2[®] input: $1.53 \pm 1.44\% \text{ w/w}_{\text{ar}}$ (ca 32% increase in relation to the measured value). An increase should indeed be

anticipated as most of the non-Fe metal appears in the form of Al-alloy beverage containers, which undergo size reduction during the secondary shredding, generating some amount at <10 mm, as the visual inspection of high-in-non-Fe metals SRF samples (L3outl - **Table 4-9**) has shown.

Hence, assuming the adjusted reconciled balance is correct, the difficulty of concentrating the non-Fe metals in the non-Fe output can be tracked down to the operation of the A_CL 1 and the E_C_S. The A_CL 1 allows a considerable part of the input of non-Fe components to drop in the high-gravity fraction ($TC(nFe_M)_{A_CL\ 1_HG} = 31.1 \pm 13.3\%$) (**Table 5-6**), directing it away from the E_C_S. However, given the poor operation of the E_C_S, this prevents more non-Fe metal to enter the SRF output. Indeed, the E_C_S is not able to prevent the majority of the non-Fe metal components entering the SRF output: $TC(nFe_M)_{E_C_S_nFe_M} = 64.1 \pm 10.2\%$ (**Table 5-9**).

This indicates that the operation of the E_C_S may deserve additional attention. There seems to be space for optimisation, which could remove the non-Fe metal contamination from the SRF stream and collect considerably higher non-Fe material in the right output. Notably, this non-Fe contamination is responsible for the second biggest contribution to the ash content of the SRF (**Figure 5-57**). Eddy-current separator manufacturers claim high recovery rates for contemporary equipment (e.g., > 95%³⁵⁵). The secondary non-Fe metal output stream is the only output with a potential positive financial value, with recent estimate of market prices at 357-857€ per tonne³⁵⁵. Amongst the produced secondary raw materials, it has been the major source of income for waste processing plants in Europe (much more profitable than secondary Fe-metal scrap, valued at 21-57€ per tonne).

The reconciled balance for the ferrous metal waste component category (**Figure 5-49**) shows that all three overbelt magnets are contributing towards the Fe-

metal output of the plant. A non-negligible amount of ca 20% reports to the oversized heavy rejects ($TC(Fe_M)_{Fe-metal} = 78.1 \pm 8.0\%$). Thus, optimisation of the overbelt magnet 2 could be investigated, because of the potential to recover the rest Fe-metal available in its input. All rest outputs are practically free from metal. With the assumed estimate for the mass flow to the eddy current separator rejects, the unit operation removes from the SRF stream around half of the Fe-metal reporting in its input ($TC(Fe_M)_{E_C_S_SRF} = 51.6 \pm 35.2\%$ - **Table 5-9**).

6.2.3 UK MBT plant A: balance of fuel properties: mass-based specific loads

Results are discussed here for four key SRF quality properties: total chlorine content, biogenic content, net calorific value, and ash content. Their importance has been stressed in the literature critical review in **Section 2.5**, summarised in **Table 4-3** where the selection of properties to be analysed is explained, and briefly revisited in the SRF characterisation discussion **Section 6.5**.

Results refer to balances of these fuel properties regarding the processing section of the UK MBT plant A. Methodology can be found in **Section 4.9.3**. **Figure 5-50** summarises the closures for sum of input and output mass-specific loads for four properties. The very good agreement between input and sum of outputs validates the overall methodology, including sampling, sub-sampling and sample preparation, analytical determination and statistical analysis. It also verifies the correctness of the reconciled shreddable mass both on dry and dry, ash-free bases. Thus, it was proven that the methodology followed can lead to the development of closing balances despite the high heterogeneity that characterises the waste. In this way, it can be further used for other properties. It remains to be tested for properties that are present in much

lower concentrations or are less evenly distributed in the fragments constituting the waste samples (e.g., for trace metals).

The closing balances also allow the use of the material flow management software STAN2[®] to compute transfer coefficients and inner flows, and fully reconcile the balances. These results of the STAN2[®] application for each of these fuel properties are presented from **Figure 5-51** to **Figure 5-54**. It can be seen that most of the load for both beneficial fuel (biogenic content and calorific value) and problematic properties (total chlorine content, ash content) present in the shreddable part of input to the processing section is reporting to the SRF output. This by-and-large reflects the similar transfer of the combustible dry mass.

In **Figure 5-54** for the first time a detailed balancing of the total chlorine content load of the shreddable/combustible of an MBT plant flows is shown. A clear split of the load is evident between the SRF and the oversized heavy rejects. Around 80% of the load is incorporated into the SRF ($TC(<[Cl]>_d)_{SRF} = 78.9 \pm 26.2\%$ - **Table 5-4**). This split is determined by the operation of the air classifier ($TC(<[Cl]>_d)_{A_CL_1_O} = 82.6 \pm 33.2\%$ - **Table 5-6**). The high uncertainties are propagated from the too high uncertainty of the total chlorine concentration as measured for the biodried and oversized heavy rejects flow characterisation (**Figure 5-15**).

An almost direct comparison regarding the transfer coefficient of unit operation can be drawn between the trommel in the UK MBT plant A with aperture at 20 mm and the trommel screening of unshredded waste at 30 mm as examined by Rotter et al.⁵⁵ for urban and rural waste. For total chlorine content the UK MBT directs much more chlorine in the SRF flow ($TC(<[Cl]>_d)_{T_SCR_O} = 91.7 \pm 3.3\%$) when compared to the German pilot scale experiment ($TC(<[Cl]>_d)_{T_SCR_O} = 67\%$ (rural) or 77% (urban)). This can be partly explained by the lower yield for the German case, because of the wider

aperture (49% w/w_d and 57% w/w_d yield to the SRF stream, compared to 69.1±2.4% w/w_d for the UK MBT plant A). Hence the two results do not seem incompatible.

These loads can be evaluated as ratios of beneficial/problematic load transported over the yield achievable for the SRF product. Roos and Peters³⁸ have reported theoretical computations and empirical observations for SRF production in plants using NIR to sort out the high-in-total-chlorine-content items such as PVC. They reported a trade-off between increasing SRF yield and decreasing total chlorine concentration. For an SRF yield comparable to that achieved by the UK MBT plant A processing section (53.5% w/w_d - **Figure 5-24**) they considered practically as best achievable a total chlorine content ca 0.5% w/w_d, if advanced optical sorting unit operations are employed. The value measured for the UK MBT plant A is 0.71±0.06% w/w_d, without using advanced optical sorting.

In the large-scale test runs by Rotter et al.⁵⁵ all unit operation configurations led to very low SRF yield; hence they are not of direct relevance. Only the trommel screening of unshredded waste at 30 mm led comparable yield, as explained. In this case the total chlorine content enriched in the SRF product by 35% (assuming an input at 0.75% w/w_d, this results to 1.01% w/w_d in the RDF product); whilst for the UK MBT plant A the enrichment is from 0.61% w/w_d to 0.71% w/w_d, i.e., 16.4%. Hence, it seems that the UK MBT plant behaves better for the scenario that requires high SRF yield. However, the flowsheet of the UK MBT plant extends much further than a simple trommelling. The most successful scenario examined by Rotter et al.⁵⁵ was a ballistic separator which led to a marginally acceptable SRF yield (39%), still enabling a lower enrichment in total chlorine content (28%) in the SRF. Again, the UK MBT Plant seems to outperform this.

This thesis presents for the first time a balance for the biogenic content ($\langle X_B \rangle_{SHR,daf}$) load of MBT flows (**Figure 5-52**). The balance results establish that the bulk of the biogenic dry ash-free load on a mass basis is incorporated into the SRF output ($TC(\langle X_B \rangle_{SHR,daf})_{SRF} = 77.6 \pm 3.4\%$ - **Table 5-4**). The rest of the load is split between the main relevant outputs, with the oversized heavy rejects gaining the biggest part ($TC(\langle X_B \rangle_{SHR,daf})_{A_CL\ 1_U} = 16.3 \pm 2.3\%$ - **Table 5-6**). The paper reporting there as well can be assumed that it contributes significantly to this outcome ($TC(P/C)_{A_CL\ 1_U} = 18.1 \pm 5.0\%$ - **Table 5-6**).

The ash content balance for the shreddable/combustible part of each flow (**Figure 5-51**) reveals that the two main destinations are the 0-8 mm ('organics') output and the SRF. The transfer coefficient to the SRF is ($TC(\langle A \rangle_{SHR,d})_{SRF} = 37.8 \pm 3.1\%$ - **Table 5-4**). This considerable load reporting to the SRF is added to the non-shreddable, inert part, reporting to it as contamination, they both contribute to its ash content.

The net calorific value ($Q_{net,p.ar}$) load balance on as-received basis. (**Figure 5-53**) showed that around 75% of the energy content present in the combustible part of the input to the processing section of the UK MBT plant A is incorporated into the SRF product ($TC(\langle Q \rangle_{SHR,net,p.ar})_{SRF} = 73.2 \pm 8.6\%$ - **Table 5-4**). Energy content equal to almost 1/5th of the amount in the SRF is lost in the oversized heavy rejects output, directed there by the air classifier ($TC(\langle X_B \rangle_{SHR,daf})_{A_CL\ 1_U} = 15.4 \pm 23.1\%$ - **Table 5-6**). Almost 10% of the biodrying input load amount reports to the 0-8 mm ('organics'). Similar arguments as those expressed in the discussion of sum of combustible matter (**Figure 5-27**) apply here as well.

6.3 UK MBT plant A: transfer coefficients of unit operations

The transfer coefficients for a series of fuel properties and materials (waste components) were computed for mechanical unit operations of the UK MBT plant A (trommel screening, air classification, air drum separator, oscillating screen, and eddy-current separator) using experimental data (**Objective 5**). For the first time transfer coefficients are presented for a contemporary, commercial, and fully operational SRF-producing 4th generation MBT plant, with their uncertainty estimated. Furthermore, for the first time the transfer coefficients are measured pertain to a biodried MSW input material, which is supposed to behave in an improved way compared to the undried MSW³⁵⁶. Transfer coefficient data in the literature have been limited to theoretical computations, describing process equipment of previous generations and plant configurations, or based on pilot-scale runs and simplified process flowsheets; all lacking in quantification of their uncertainty. These TCs constitute the backbone of the MBT operation. They allow us to map and interpret the plant operation and can serve as the basis to model its performance, assuming varying input compositions.

A series of novelties adopted in the methodological approach made this computation feasible. The application of data reconciliation software resulted in overcoming the inherent heterogeneity of waste-related flows by combining data from every measured flow – not just before and after single process units. This creates confidence that the reported transfer coefficients are mutually consistent. For effective reconciliation the uncertainty pertaining to data had to be statistically evaluated from the initial experimental data. The data reconciliation modelling procedure allowed computing the uncertainty around the transfer coefficients, by both propagating the input data uncertainty and using the redundant degrees of freedom to reduce uncertainty where feasible, improving the achieved precision. Notably, for such a methodological approach to be applicable, access is needed to suitable sampling

points within the plant – a situation inevitably challenging for any fully operational MBT plant not designed for regular sampling of inner flows, as is almost everywhere the case.

However, transfer coefficients are inevitably specific to input flow and process unit operating settings, which prohibits careless generalisation. The conditions under which these unit operations performed as reported here are presented in **Table 4-1**, including their relative position in the flowsheet of the UK MBT A (**Figure 4-2** and **Figure 4-5**). That said, the function of the unit operations in the UK MBT plant A are typical of the latest trends in SRF-producing MBTs - the plant was commissioned in 2007.

Transfer coefficients are mathematically defined in **Table 2-6** and discussed in **Section 2.4.3**. Results are presented in **Section 5.4**, **Table 5-4** to **Table 5-9**, and visualised through flowsheet/Shankey diagrams (**Figure 5-42** to **Figure 5-54**). The TCs are discussed in the context of the balances developed in the relevant **Section 6.2.2** for waste component categories and in **Section 6.2.3** for fuel properties of the flows, because they constitute a clear way to describe these flows. With regard to their impact on the average SRF quality of the UK MBT plant A they are also discussed in the relevant **Section 6.5**, in the sub-section explaining the contribution of each waste component category to the concentrations observed.

6.4 UK MBT plant A: simulation of SRF properties

6.4.1 UK MBT plant A: concentrations and specific loads per waste component

Relevant results are reported in **Section 5.5.1**. Here, for the first time, characterisation was performed on biodried waste components, rather than the original

waste arisings or inputs to waste treatment plants. Inevitably, the values reflect the definition of each waste category and the effectiveness in correct identification and allocation of the waste fragments to the categories. A series of important details regarding the manual sorting were suitably chosen for characterisation of SRF-producing MBT process flows. Plastics were identified as 3 main grades, with main criterion their specific gravity, which is important for their behaviour during mechanical separation processing. The waste categories included the specified for the determination of the biogenic content by the manual sorting method³⁰⁹. In addition, the fines category was defined as <10 mm, resulting in the allocation of the 10-40 mm waste fragments to suitable waste component categories, despite the relative practical difficulty this entailed.

For the first time here detailed data are presented on the level of dryness achieved by a biodrying MBT reactor (**Table 5-10** and **Figure 5-55**) for individual material components of residual MSW (**Section 5.5.1** and **5.5.2**). As discussed in the critical review of the biodrying process science and engineering (**Appendix I**), the final moisture content achieved by the biodrying reactor is its key measure of its performance, whilst optimal drying is still under investigation, because of gradients evident in the process parameters and final biodried product. The set of data reported provide and insight into a finer level of detail, not previously available. Results were generally consistent with what could be reasonably anticipated, regarding the degree of dryness of each component category, relative to the others. Hygroscopic materials, having also the ability to retain moisture such as nappies were not dried effectively (55.4% w/w_{ar}). Similarly, biological and paper/card categories maintained a relative high degree of moisture (20-22% w/w_{ar}). All rest items were dried to a satisfactory degree, below 15% w/w_{ar}. It is clear that for main categories that biodegrade during biodrying (biological, and fines <10 mm), a considerable degree of dryness is evident, if

they are compared with literature values for wet unprocessed or compacted MSW^{107, 357} or MBT plant inputs³⁵⁸. It has to be noted however, that this material categorisation does not account for items such as glass and plastic bottles which contain liquids, a limited amount of which was found in the biodried fraction during the manual sorting. Because the simulation exercise using these data to reconstruct the moisture content for the SRF produced showed 10-15% underestimation of the measured value (**Figure 5-59**) some of the components might be slightly wetter than actually reported here. Only Nicosia et al.³⁵⁹ have reported on the investigation of drying for individual components for a operational biodrying MBT, but of a different type, using bio-cells rather than in-hall reactors, as is the case for the UK MT plant A; however, they reported only moisture content specific loads rather than concentrations (commented upon in the relevant **Section 6.5.2**), and used limited number of waste component categories (7).

Results for total chlorine concentration (**Section 5.5.1** and **5.5.3**) of waste components are in agreement with the values reported in the literature, given the variability of waste and the differences in the waste component category definitions. The relatively low level for paper and the above 1% w/w_d values for the plastics – the two major SRF components – were verified. The highest value was reached for shoes, in line with other researchers reporting, possibly due to the use of chlorinated plastics in their construction. A series of recent publications reported on values Cl content of MSW components and reviewed older relevant data^{55, 178-179, 347}. In comparison with Rotter et al.⁵⁵ one main difference is spotted, which deserves further investigation. Their category 'other plastic products' could potentially contain materials of partly similar composition to the category of 'durable plastic,' used in this thesis. However, the total chlorine concentration of durable plastic was negligible (0.03% w/w_d) and the lowest amongst the plastics, whilst the 'other plastic products' was identified as the

highest in concentration (ca 8.5% w/w_d), a result explained by Rotter et al.⁵⁵ as a consequence of the use of chlorine in long-lived plastic products.

The ash content of the biodried waste components (**Section 5.5.1** and **5.5.4**) is within what can be reasonable anticipated and in agreement with the values reported in the literature for waste components³⁵⁹. Similar values have been reported in the literature for paper and plastic components of SRF³⁶⁰. Typically low levels are evident for the various categories of plastics, which is beneficial to the SRF as content. Paper/card is at 17.5% w/w_d, which means that would be to achieve very low ash content for an SRF that has considerable paper/card content.

Similarly reasonable were the net calorific values (**Section 5.5.1** and **5.5.5**) measured for the biodried waste components. The biodrying reactor affects the overall calorific value of the waste input and this has received considerable attention in the literature so far^{59-60, 361}, as explained in the biodrying critical review (**Appendix B**). Values are comparable with those available in the literature for MSW components^{212, 362}. Plastics or plastic-containing materials such as carpets/mats and shoes show the highest levels. Also cinders have very high content, but their very low contribution to the SRF makes no difference regarding the calorific load contribution. The relatively high moisture content of the paper/card, negatively affects its net calorific value.

6.4.2 UK MBT plant A: simulation of SRF moisture content, ash content, total chlorine content and net calorific value

Discussion of the relevant results (**Section 5.5.1** to **5.5.5**) is placed the last sections of each relevant SRF property characterisation, as measured for the UK MBT plant A (**Section 6.5.2** to **6.5.7**). Specifically, in the sub-sections entitled: 'property A: SRF concentration vs. its material composition'. There, the quality of the SRF produced in the UK MBT plant A is tracked down to the physical-chemical characteristics of its

material components and the processing performance of the plant flowsheet. The ability to successfully simulate the experimentally measured SRF quality with the followed methodology is commented upon; and novel insights are drawn about how the material composition of the SRF (**Figure 5-21** and **Table_App F-19**) and the characteristics of its material components (**Table 5-10** and **Figure 5-55 -Figure 5-58**) account for the observed levels of each property. This novel set of data make it feasible to explore possibilities for improving each property level; insights from the material and property balances developed (**Section 5.3**), and the transfer coefficients measured (**Section 5.4**) are incorporated. Potential implications of the proposed improvements to the rest SRF properties are also investigated.

As a general comment, the correctness of the simulation exercise is indicated by the reasonable agreement achieved for all four properties examined (**Figure 5-59**). In addition, this serves as strong indication that the reconstructed composition of the SRF (**Figure 5-21** and **Table_App F-19**) is sufficiently accurate. Notably, the reconstruction was necessary because manual sorting cannot depict the material composition of the SRF because of the secondary shredding to <40 mm upstream. It was shown that the original average SRF composition can be established by using of the manual sorting data, simplistic modelling corrections to account for the secondary shredding (and changes through the plant flowsheet) and subsequently applying the reconciliation of all the flows material management software.

The individual waste components characterisation data, novel for biodried waste fractions, can be beneficially applied to perform sensitivity analyses of the relevant SRF properties of the UK MBT plant A, by assuming different material compositions for the produced SRF. Such a sensitivity analysis could be expanded to include, as its starting point, different compositions of the biodried material, if it was

combined with the transfer coefficients reported in this thesis for the individual waste components.

However, successful implementation would depend on the similarity of the physical and mechanical properties of the assumed material compositions with that upon which the transfer coefficients were measured in this thesis. The most critical parameters are particle size distribution and moisture content, because most of the mechanical unit operations of the processing section use size and/or weight to separate the components, as explained in the literature (**Section 2.4**). For instance a lower degree of effectiveness in drying achieved by the biodrying reactor could result in increased moisture content of paper and card, rendering it heavier and less suitable for effective separation through the air classifier, as has been reported for wet, as produced waste⁵⁵.

However, as the produced data are not accompanied by an estimation of the level of uncertainty involved, results could be only indicative of central tendencies, but are unsuitable to establish confidence limits around the predicted values or, even further, to describe the probability density function of these properties in the analysed waste component categories. Such data would be necessary for a more detailed and sophisticated simulation of the relative contributions to the specific loads of biodried MBT process streams.

6.5 UK MBT plant A: SRF properties characterisation

6.5.1 UK MBT plant A: SRF characterisation - overall results and statistics

This thesis presents the first comprehensive, independent evaluation of SRF produced in the UK by a contemporary MBT plant (**Objective 2**). Properties are

determined following the new methodology standards prepared by CEN -still under validation- and are particular to SRF (see **Section 2.5.3**). Thus, this is one of the first cases in which they are applied, enabling methodological insights to be gained.

The properties reported here are central in determining the suitability of SRF for thermal recovery in a series of potential applications. Their importance has been demonstrated in the literature review, where the quality assurance and control schemes for SRF are critically assessed (**Section 2.5**), and summarised in the methodology (**Section 4.5**). For the biogenic content of SRF, which gains considerable interest as a measure of its sustainability and directly affects its financial attractiveness, very limited data have been reported worldwide.

Satisfactory SRF quality means that certain statistics measured for every property should fall within specified limits. As explained in **Section 2.6.2**, in addition to central tendencies (averages), a low variability of the production line (between-samples variability) is central to the good quality of SRF (**Objective 3**). This aspect however, has received very limited attention in the literature. The variability experienced in the determination of the properties is also examined to assess whether it is satisfactorily low and does not overshadow the within-plant production variability.

The main results for the selected fuel properties are found in **Section 5.6**. Insights are produced for different sets of samples, representing different operational conditions and periods of the MBT plant. Sets of samples are abbreviated as: L123, L123-L3outl, L3, L3-outl – for details refer to **Table 4-9**. Emphasis is on L123-L3outl, which represents typical plant operation and corresponds to the widest time period.

6.5.2 UK MBT plant: SRF moisture content

The main objective of the biodrying bioreactor, preceding the mechanical processing in the UK MBT plant A, is to dry the input waste as far as possible, to improve its combustion behaviour (). Commercial biodrying process providers have reported or claim as feasible moisture contents $<15\%$ w/w_{ar} for the biodried material, which is then processed to SRF. Gradients experienced in the performance of the biodrying suggest that the reaching a sufficiently low moisture content for all the mass of the treated waste is not entirely trivial, as discussed in detail in the review of the biodrying engineering and science (**Appendix I**). Many, but not all, thermal recovery processes require SRF of a moisture content $<15\%$ w/w_{ar} as explained in the critical literature overview of the SRF use specifications (**Section 2.5.4**). Here for the first time a detailed investigation on the moisture content of SRF produced from biodried MBT is reported and discussed. Results on moisture content are presented in **Section 5.6.2**. Statistical analysis performed is explained in **Section 4.12.1**.

Variability and methodological insights on moisture content determination

The measurement of residual moisture (M_r), present in the general analysis sample after bulk drying, can be performed with intermediate repeatability when determined in triplicates: median coefficient of variation for all samples ($\%CV(M_r)_{L123}$) is 4.6%; if the atypical samples are excluded it improves further ($\%CV(M_r)_{L123-L3outl} = 3.7\%$). This suggests that together the general analysis sample is satisfactorily homogeneous in residual moisture and that the drying at 105°C heated oven behaves consistently. However, because for certain samples the coefficient of variation is in the order of magnitude of 10%, 3 replications might be the minimum acceptable. The impact of the high relative total extended uncertainty in the determination of residual moisture ($\%U_{95,2}(<M_r>)$) on the overall moisture content uncertainty ($U<M_r>$) is

restricted because to the overall moisture is dominated by the initial bulk drying component.

Moisture content variability during SRF production

The within-sample and analytical measurement variability is low enough in comparison to between-sample variability as can be seen in **Figure 5-61**, posing no problem in the precise evaluation of the plant production variability. The relatively high between-sample variability is exacerbated by the presence of atypical samples with very low overall moisture content (encircled in **Figure 5-61**). The between-sample moisture content variability for the typical plant operation samples is the highest among the properties examined, as evaluated by the coefficient of variation ($\%CV(\langle M_T \rangle)_{L123-L3outl} =$ of 31.8%). This rises to 47.3%, if the atypical samples (L3outl, **Figure 5-61**, encircled), are included. Their invariably low moisture content values are possibly due to their comparatively low paper content, which is the main absorbing medium of the moisture liberated from other waste components (e.g., bottles with remaining liquid) by compaction during waste transport and shredding in the MBT plant).

However, a part of the between-sample variability should not be allocated to plant-production reasons, but accounted for by the inevitable changes in moisture over time, occurring during sample storage, transport and preparation (see experimental **Section 4.7**), despite the detailed efforts to mitigate such effects. The estimated within-sample and analytical measurement variability remains limited, when compared to the between-sample (**Figure 5-61**). Hence, more effort put into additional replication of M_r would not render any practical improvements in the overall accuracy of the $\langle M_T \rangle$ determination. Instead, efforts should be focused around further reducing and quantifying the currently unquantifiable speculated bias related to M changes during sample handling. Lower between-sample variability could benefit the SRF quality.

Average and upper range values of moisture content

Overall, the average moisture content ($\langle M_T \rangle$) and the p_{80} results for all the sets of samples fall close to the average values reported in the literature for MBT-derived SRF (**Table 5-1** and **Figure 5-1**). Regarding compliance with specifications, the most demanding upper limits for cement kilns primary firing are not met; however, less demanding cement kiln specifications are complied with, whilst power plants can in principle tolerate much higher levels than those measured here. The range of medians observed for all four SRF sets of samples, is 12.8-16.7% w/w_{ar}. The median of all the typical plant operation samples ($\langle M_T \rangle_{L123-L3outl} = 14.8\%$ w/w_{ar}) falls towards the upper quartile of the values of non-UK, European MBT-derived SRF (14.2% w/w_{ar}) (**Table 5-1**). For the upper range of moisture content values, the 80th percentile is slightly lower than that of the 50% of the European SRF cases ($p_{80}(M_T)_{L123-L3outl} = 18.24\%$ w/w_{ar} < 19.8% w/w_{ar}, respectively) (**Figure 5-62 B** and **Figure 5-2**). Slightly higher values are reached by the summer-only, set of samples (L3) (**Figure 5-62 C**). However, despite efforts for suitable samples storage, this might reflect the reduced amount of time between sampling and determination for these samples.

The all typical samples are in agreement with in-house data from another commercial biodrying-MBT plant determined on 16 samples showed, especially regarding their average value ($\text{median}\langle M_T \rangle_{\text{in-house_SRF_data}} = 15.2\%$ w/w_{ar}, $p_{80}(\langle M_T \rangle)_{\text{in-house_SRF_data}} = 17.6\%$ w/w_{ar} (data not publically available - statistically analysed for this research²⁶⁶). Recently reported typical SRF values produced from a UK Shanks/Ecodeco biodrying MBT plant³⁶³ (plant origin not indicated) presented a much lower median (ca 13% w/w_{ar}) and upper quartile (ca 17 w/w_{ar}, values as read from graph).

Recently published data for composting-oriented MBTs, producing SRF by mechanical separation, without drying, show a mixed outcome when compared with the

UK biodrying MBT plant A. UK MBT plant A SRF compares favourably with SRF from mechanical processing of Mediterranean mixed urban MSW³⁶⁴, which showed a considerably higher value ($\langle M_T \rangle \pm U_{95,94} = 27.4 \pm 1.2\%$). Notably, this is higher than the maximum evident for the European MBT-derived SRF, as reviewed in this thesis. This difference could be indicative of the beneficial effect of biodrying in reducing the moisture content of the produced SRF. However, SRF moisture content from MSW of a Greek island³⁶⁰, was reported at much lower levels and was apparently highly affected by the seasonal variation. Extremely low values were reported for August at 4.22% w/w_{ar} (for comparison: UK MBT A: median $\langle M_T \rangle_{L3} = 14.5\%$ w/w_{ar}) and for February at 14.61% w/w_{ar} (UK MBT A: median $\langle M_T \rangle_{L12} = 11.3\%$ w/w_{ar}, but showing high variation). Given the different inputs and operating conditions and the contradicting results for the two composting-oriented MBT plants, no definitive conclusion can be drawn regarding how the SRF moisture content compares for these two processing concepts.

Cemex Climafuel²⁶⁵⁻²⁶⁶ for cement kilns specifies the upper limit for moisture content at 15% w/w_{ar}. However, other cement applications⁵² may tolerate up to 20% w/w_{ar} (**Table 2-16**). Indeed, a less demanding upper limit is set for cement kilns at 20% w/w_{ar} by SRM²⁶⁶ and Remondis SBS^{®2}³⁶⁵ (it is not clear whether these apply to secondary firing). The 80th percentile ($p_{80}(M_T)$) and the upper 95% confidence limit around the mean ($UCI_{95\%}(\langle M_T \rangle)$) achieved here (**Table 5-12** and **Figure 5-62**) fall just below the 20% w/w_{ar} limit. The Remondis SBS^{®1}³⁶⁵ upper limit for power plants, set at 35% w/w_{ar}, is met by every individual sample analysed for the UK MBT plant A (**Figure 5-61**). Hence, the moisture content of the UK MBT plant A SRF makes it just marginally attractive for use in primary firing of cement kilns, if the decision rule is simplistically refers to its average value. If, estimates of upper range of values of upper confidence limits around the mean moisture content are used, it becomes attractive only for less demanding cement kiln specifications.

The achieved average level for moisture content of the UK MBT plant A is ca 50% higher than the 9% w/w, reported by Manser and Keeling⁷⁹ as typical for a 3rd generation RDF production plant (post-1985), possibly using a sequence of drier, pre-densifier and pelletiser. However, the anticipated moisture content at the discharge of the drier would be approximately <16% w/w, which is deemed suitable for the subsequent processing stages: this is at a similar level to that measured for the UK biodrying MBT A SRF. However, this value is not totally representative of the as-produced SRF.

Inevitably the as-measured moisture content differs from the as-produced and as-used, i.e., at the moment of thermal recovery, because it is modified during post-production handling. Overall, observations show that the biodried material, SRF and the rest MBT process streams, show at the time of sampling elevated temperatures (40-55°C), having just been removed from the biodrying piles. This enables some of the residual moisture (generally <25% w/w_{ar}) to be further evaporated as the material gradually cools down to ambient temperatures. In a realistic route for the commercial utilisation of SRF, the output is readily compacted in trucks, transported, stored and further shredded before its use in cement kilns. A considerable post-production moisture loss was evident for the latest generation of RDF production plants, as Manser and Keeling⁷⁹ noted. There the dryers were used towards the latest stages of the plant flowsheet and before densification to e.g., 600 kg m⁻³. As a result, sensible heat was trapped in the core of the compacted material of low thermal conductivity (e.g., 80°C). This is gradually transported and released, resulted in cooling and in turn, a drop in the moisture content from e.g., 8% w/w to 4% w/w. In the case of the biodrying MBT plants, the as-produced SRF temperature is approximately the half and the moisture content more than double.

In this research the sampled SRF (as-produced, before compaction) inevitably follows a dissimilar route. It is transported to the cooling storage container, its temperature eventually dropping at $4\pm 2^{\circ}\text{C}$ and then reheated to ambient levels before the analytical determination. Hence, these differences suggest that the total moisture content measured (M_T), underestimates that of the biodrying MBT-streams at their moment of sampling (as-produced). However, because of the inevitable losses during the compaction, transport and intermediate storage of SRF before its thermal recovery, this underestimation is partly desirable. Thus, it might be assumed that the moisture content of an SRF as measured in the laboratory is not too dissimilar to that envisaged just before thermal recovery, which is of practical relevance. However, it is suggested that specific experiments should be conducted to quantify the potential differences between as-produced, as-stored, i.e., awaiting thermal recovery, and as-used, i.e., immediately before thermal recovery (vs. as-analysed), when sampling from any of these SRF lots.

SRF moisture content vs. material composition

The central tendency of the moisture content in SRF produced from the UK MBT plant A was simulated with reasonable agreement (**Section 5.5.1**) (**Table 5-11** and **Figure 5-59**). Chemical characterisation measurements for the biodried waste components of the UK MBT plant A and average SRF composition, as reconstructed through the material flow analysis (0), were used. Thus, a detailed understanding of how the measured moisture content results from the contribution of the individual waste components present in the SRF is achieved. The relative difference between the measured and simulated value, expressed as a percent of the measured value, ranges 10-15%, which is not statistically able to differentiate (d.f. = 9 and 14, for the sets of samples L3-outl and L 123-L3outl respectively, $\alpha = 0.05$).

The underestimation encountered should be in fact partly anticipated for two main reasons. Firstly, the trommel breaks closed glass bottles containing liquid or jars with semi-fluid materials, leading to re-wetting of other component categories. Also plastic bottles with limited amount of liquid may be carried to the air classifier light fraction, leading to the liberation of this moisture after the secondary shredding. Because it is not as accurate to identify the waste components after the secondary shredding the characterisation of the materials was performed for items sourced mainly from the biodried fraction or the oversized heavy rejects. Secondly, individual waste components underwent manual sorting, during which limit air drying is inevitable, whilst the values reported for SRF moisture content were produced from samples not exposed to sorting. Despite that these effects can be reasonably anticipated, it is very difficult to quantitatively correct for.

The contribution from the paper/card waste component category accounts for the bulk of the simulated moisture specific load (68.4%), whilst the readily degradable components (biological, fines <10 mm) contribute only 3.5% and 0.5% respectively (**Table 5-10** and **Figure 5-55**). Paper/card is desirable in SRF; despite being already the main fraction (42% w/w_d), there is potential to further improve the recovery of it to the SRF. Because the moisture content of the paper/card is higher than that of the SRF average ($\langle M_T \rangle_{d,P_C} = 20.6\% \text{ w/w}_d > \langle M_T \rangle_{d,SRF(L123-L3outl)} = 15.0\% \text{ w/w}_d$) any further increase in the mass fraction of it in the SRF would result in a moisture content increase. However, the existing level of moisture content in the SRF just marginally complies with the strictest limits which are applicable for use in cement kilns, as discussed in the previous sub-section.

Hence, improvements in the overall moisture content of the SRF cannot be sought in altering its compositions, (i.e., the relative amount of the waste components reporting to it); instead, further improvement might be necessary for the overall drying

performance of the biodrying reactor should be investigated. Apart from the drying potential of the biodrying reactor discussed in detail in **Appendix I**, other improvements may be feasible. For instance, the amount of liquids reporting enclosed in the processing section, despite not quantified in the simulation, might play a role. This could be avoided if an increased degree of waste component liberation could be achieved by shredding to lower sizes during the primary shredding upstream the biodrying. However, altering the particle size distribution of the waste components reporting to the processing section would have wide implications its performance and cannot be implements without careful investigation.

6.5.3 UK MBT plant A: SRF total chlorine content

Chlorine concentration is a key parameter for SRF quality. Elevated levels of chlorine in SRF are a source of concern, particularly for high temperature corrosion, high hydrogen chloride (HCl) emissions and potential formation of dioxins during its thermal recovery^{179, 219, 223}, as explained in **Section 2.5.4**. Hence, it was selected by CEN as the indicator property for technical performance of SRF²⁵⁹ (**Section 2.5.3**). Results discussed here are presented in **Section 5.6.3**. Statistical analysis performed is explained in **Section 4.12.1**.

Variability and methodological insights on total chlorine content determination

The total chlorine content determination bears the lowest repeatability amongst the properties examined (**Table 5-13**), as evaluated through the coefficient of variation (%CV). This affects negatively the accurate determination of the variability due to plant production. Additionally, chlorine was the only property for which certain replicates of the general analysis samples were discarded as outliers, showing impossibly low values. Cuperus at al.²⁰⁸ has similarly reported poor repeatability results for the total

chlorine determination in SRF samples – though not directly comparable because of a different statistical methodology followed. In this thesis, since determination through the HPIC has been proven precise, the issue can be tracked back to sample homogenisation and/or oxygen bomb combustion performance.

The part of variability that may come from the degree of inhomogeneity of the final general analysis sample is essentially a sampling challenge. When picking aliquots to perform replicate analyses, sampling from the general analysis samples occurs. Hence, the theory of sampling²⁷², explained in **Appendix D**, applies. The two major parameters that affect the variability over which control can be exercised are the maximum particle size and the mass of the replicate. Samples were shredded down to 0.5 mm maximum size. Selective grinding at the 1 mm and 0.5 mm levels has been evident, resulting in fluffy and grainy fractions of the general analysis samples as discussed in **Section 4.7**. The non-typical SRF samples (L3outl) contained high aluminium percentages which served as a grinding aid resulting in more uniform, less selective grinding; notably aluminium oxide is suggested as grinding aid for not enough brittle materials according to BS EN 1482 (method B). However, these samples showed reproducibility (**Figure 5-63**) similarly low to the rest samples, but this could have resulted from the existence of aluminium fragments, of almost zero chlorine content. Cuperus et al.²⁰⁸ found that grinding down to 0.5 mm provided statistically significant improvement in the recovery of total chlorine compared to shredding at 1 mm for SRF samples ($\alpha = 0.05$), leading to a two-fold increase in repeatability. However, finer grinding was deemed as unnecessary, because with 0.5 mm grinding almost 100% recovery of the analyte was achieved.

The other way to improve representativeness when sampling aliquots from the general analysis sample is by increasing the replicate mass. However, this set at ca 1 g, which is already many times higher than the 50-200 mg typically suggested by

classical analytical procedures according to Schirmer et al.¹⁷⁸. Total nitrogen is present in the SRF samples at a similar concentration level (ca 1% w/w_d) with total chlorine, but it proved feasible to determine with 3.3% (median coefficient of variation; 8.4% for Cl) despite that only 25 mg of aliquot samples were used. This illustrates that a much more precisely can an analyte be determined, if the GAS is more homogenised regarding this specific analyte.

In any case, insufficient oxygen bomb combustion for certain runs cannot be excluded either.

Poor total chlorine repeatability constitutes a problem when the uncertainty around the average measurement on a single sample is of the same order of magnitude with the e.g., between-daily collected samples variability, as it happens in this thesis. This is even more the case when the total chlorine in SRF is at critical levels for compliance with standards set. I speculate that more often than not, this could be the case with total chlorine, because reaching levels considerably lower than the specified upper limits is not technically feasible for MBT-derived SRF, using residual MSW as input, as this thesis suggests, in agreement with the literature³²².

Thus, given the wider issues with total chlorine determination mentioned in the methodology **Section 4.13.6**, the accurate and precise determination of total chlorine deserves additional attention. A solution for reducing the total extended uncertainty around the average value per sample, with the same level of repeatability, is by increasing the number of replications. This would result in increased degrees of freedom available, resulting in lower standard error around the mean and lower coverage factor. Discussion of ash content results for the UK MBT plant A SRF includes a relevant numerical example (**Section 6.5.4**). However, increased replications come at additional cost and the decrease achieved for the total extended

uncertainty is not linear; relevant decisions require careful cost-benefit evaluation. In conclusion, if a similar level of repeatability is encountered and it results in a total extended uncertainty per individual sample not considerably lower than the SRF production variability, three replicates could be considered as a minimum requirement.

Total chlorine content variability during SRF production

The between-day variability for total chlorine in SRF samples for the UK MBT plant A is intermediate ($\%CV([Cl])_{L123-L3out} = 14.2\%$), considering the properties examined in this thesis, as presented in **Table 5-12** and explained in **Section 5.6.3**. However, as detailed in the previous sub-section, a part of this variability could have resulted from insufficiently precise analytical determination of the property, and is inevitably cofounded with the variability introduced through sampling.

It is not feasible to judge whether this level of variability is acceptable, because there are no relevant quality control rules available for the existing SRF specifications. If a rolling average is computed (e.g., 7-day/batch point), as specified and applied by the CEMEX²⁶⁵ for SRF, this variability would be smoothed. As a general comment, a coefficient of variation of around 15% seems not unreasonable for a fuel derived from such a heterogeneous input as the residual MSW. However, it remains whether it is fit-for-purpose.

The values reported in this thesis for a series of variability related statistics for biodrying MBT-derived SRF could be used to provide a first evidence base useful in applying a quality control approach to SRF production²⁵⁰, as discussed in **Section 2.6.2**. For instance, the standard error around the mean total chlorine ($SE(\langle [Cl] \rangle)_{L3-out} = 0.032\% \text{ w/w}_d$) could estimate the so called 'common cause' variability (one sigma), for 3-week period production a unit of measurement (lot). If necessary, other statistics can be computed, e.g., using 5 consecutive production days to provide information for

the background, typical part of the variability for a weekly production lot. A systematic evaluation of the temporal variability should be eventually performed to create a variogram³⁶⁶⁻³⁶⁸, using the theory of sampling. This could quantify the level of variability at different time scales, including the minimum inevitable variability due to the inherent heterogeneity of SRF.

Average and upper range values of total chlorine content

Upper limits are specified for the total chlorine content in SRF for all thermal recovery applications, as discussed in **Section 2.5.4**; different tolerances would apply to each specific plant. The fact that almost no average of individual samples exceeds 1% w/w_d (**Figure 5-63**) and the median for all possible 4 sets of samples is clearly below that level (medians: 0.69-0.77% w/w_d - **Table 5-12**), shows that the Cl in SRF of the UK MBT plant A can be tolerated by most thermal recovery options. Specifically, the central tendency of total chlorine for the typical plant operation samples, estimated through either median or mean value is below the ca 1% w/w_d limit specified for cement kilns (**Table 2-16**), as illustrated in **Figure 5-64** and **Figure 5-65** as well. The achieved average and upper range values are not prohibitive for the SRF use as substitute of raw materials in the cement kilns, which could be an alternative, given its relatively high ash content (practical limits of median = 0.77% w/w_{ar} and 80th percentile = 0.82% w/w_{ar} have been reported)²¹⁰.

The tighter upper limit of 0.7% w/w_d, suggested by Remondis as suitable for power plants, is just marginally failed by the UK MBT plant A SRF (**Figure 5-64** and **Figure 5-65**). However, there might be cases of existing thermal recovery plants, such as CHP fluidised bed combustors designed for biofuels in Scandinavian countries, that might not be able to accept this SRF (upper limit for average values 0.4% w/w_{ar})

The relatively higher values measured for the atypical summer samples (L3outl, encircled in **Figure 5-63**) (**Table 5-15**) are possibly due to higher mass percentages of plastics and lower paper percentage. Plastic film and other packaging plastic components of SRF bear concentrations above 1% w/w_d, and are responsible for the bulk of the total chlorine content (61% of Cl dry mass) in SRF samples of typical composition (**Figure 5-56** and **Table 5-10**). Conversely, paper and card has a total chlorine concentration of 0.24% w/w_d, with literature values reported up to 0.5% w/w_d¹⁷⁹. Hence, if for atypical plant input or operation conditions result in SRF with unusually low paper/card and high plastics content this increases the total chlorine content of SRF produced. In the particular case experienced for the available samples, including ca 25% of such atypical samples the median total chlorine increased by ca 0.5% w/w_d (**Table 5-12**, difference between medians [Cl]_{d,L123} - [Cl]_{d,L123-Loutl}).

Given that there is no evidence against the normality assumption (W-S test), confidence limits around the mean are reported to the typical plant operation set of samples (0.76-0.65% w/w_d); and the SRF is identified as potentially a CEN Cl class 3 (**Table 2-13**; **Section 2.5.3** and **Section 2.6.4**).

Comparison with the overview results for European MBT-derived SRF (**Table 5-1**, discussed in **Section 6.1**) shows that the median total chlorine of the UK MBT plant A falls exactly at the upper quartile (Q3), i.e., it is higher than 75% of the European MBT-derived SRF cases. However, as explained, certain low values reported in the European literature should be interpreted with caution.

Total chlorine results are in good agreement with in-house data from another commercial biodrying-MBT plant (median[Cl]_{in-house_SRF_data} = 0.72% w/w_d, determined on 16 samples) (data not publically available - statistically analysed for this research²⁶⁶). Recently reported typical SRF values produced from a UK

Shanks/Ecodeco biodrying-MBT plant³⁶³ (plant origin not indicated) presented comparatively lower median and upper quartile values (ca 0.62% w/w_d and 0.72% w/w_d respectively, values as read from graph). Internal quality control data were made available recently for consecutive production years of Remondis SBS[®] SRF²⁵³. Yearly median total chlorine levels are reported around or below 0.5% w/w_d (2003-2007), which is 28% lower than the typical SRF median total chlorine content of the UK MBT plant A. This low level constitutes an improvement from previous years, achieved using second generation optical sorting (NIR) to remove high-in-chlorine plastic components such as PVC; in addition to residual waste, commercial and other waste inputs are used.

Despite that the encountered total chlorine levels for SRF from the UK MBT plant A can be tolerated by most of the thermal recovery applications, typical problems related with the use of fuels high-in-chlorine can be anticipated, given that these occur for concentrations >0.1% w/w_d²¹⁵. Hence, depending on the exact type of the thermal recovery plant, process design and control measures against corrosion should be implemented (e.g., automatic heat exchanger cleaning systems, suitable material selection and coating of boiler tubes with corrosion resistant layers).

SRF total chlorine concentration vs. its material composition

The average amount of total chlorine measured in the SRF has been satisfactorily simulated (<3.5% relative bias; simulated value not statistically different to the measured, $\alpha = 0.05$) by using chemical characterisation measurements for the biodried waste components of the UK MBT plant A (**Section 5.5.1**) and the average SRF composition, as reconstructed through the material flow analysis (**Figure 5-21** and **Table_App G-18**). This makes feasible a detailed understanding of how the measured total chlorine concentration results from the contribution of the individual waste components present in the SRF.

The contribution from four waste components accounts for 90.5% of the simulated amount of total chlorine present in the average SRF from the UK MBT plant A (**Table 5-10, Figure 5-56**). Due to their high total chlorine concentration other packaging plastic and plastic films are contributing the 62% of the specific load in total chlorine, despite comprising only 30% w/w_d of the SRF dry mass (**Table_App F-19**). Shoes also contribute 14.5%, having the highest concentration, despite their low mass percentage. Conversely, paper and card material fraction is responsible for only 14% of the total chlorine specific load of SRF, despite being the dominant fraction (42% w/w_d). This results from its relatively low total chlorine concentration, measured as less than one third of the SRF average ($\langle [Cl] \rangle_{d,P_C} = 0.19\% \text{ w/w}_d$ vs $\langle [Cl] \rangle_{d,SRF(L123-L3out)} = 0.71\% \text{ w/w}_d$).

Results from other attempts, of varying sophistication, to simulate the total chlorine content of SRF produced by (biodrying) MBT plants have been reported recently^{321-322, 369}. However, none of these publications reports validation results, i.e., comparison of the theoretical computations with empirically gained data. Schirmer et al.³²² conclude that the average total chlorine of MBT-derived SRF spans 0.6-0.8% w/w_d, with the biodrying MBTs SRF just below 0.8% w/w_d. The minimum achievable total chlorine content for MBT-derived SRF was computed at 0.5% w/w_d, even after the removal of the highly halogenated plastics (e.g., PVC) through sensor-based sorting. Whilst the results reported in this thesis are in good agreement with the reported range, the underlying assumptions were pertaining to German residual waste, assuming much higher organic content ('native organics') than experienced in the biodried fraction and the subsequent process flow stream of the UK MBT plant, including the SRF output. Hence, the agreement is more coincidental than mutually verifying. Mrotzek et al.³²¹ simulated SRF properties based upon characterisation and literature data, reporting that the development of a spreadsheet and database able to predict the SRF total

chlorine content. However, no relevant results were shown, other than for calorific values, which are discussed in the relevant **Section 6.5.7**. Ketelhut³⁶⁹ reported on the theoretical aspects of a statistically based, probabilistic approach to predicting the total chlorine content of waste-derived fuels, using probability density functions to describe the concentrations present in various general material groups of waste components. Validation results were anticipated.

Improvement to the achieved average level of total chlorine content in the SRF of the UK MBT plant A might be necessary to make it appealing for power plants and other more demanding applications. Also, a decrease of at least 1.2% w/w_d is necessary in order to be classified as CEN Cl class 2, instead of 3 (assuming same level of variability). This could have a positive impact upon its general market attractiveness. The simulated total chlorine load provides insights on how this is feasible for the SRF produced in this particular plant.

A possible suggestion could be to attempt increasing the mass fraction of paper in the SRF. The material flow balance for paper and card (**Figure 5-28**) revealed potential to do so, showing that 18% w/w_d of the mass present in the biodried fraction reports to the oversized heavy rejects, because it cannot be effectively lifted by the air classifier ($(TC(P/C))_{ACL_1_U} = 18.1 \pm 5.0$ - **Table 5-6**). Because paper and card is by definition biogenic, excluding non-biogenic inert additives, this would positively influence the biogenic content of the SRF as well. Increased mass fraction of paper and card in the produced SRF would not impact significantly its ash content, because it was measured close to the SRF average (**Figure 5-57**). Because ash content is relatively high in the SRF, other means should be sought to improve it, as discussed in **Section 6.5.4**.

Alternatively, additional unit operations, capable of negative sorting of highly-chlorinated plastic polymers, such as second generation NIR, could be installed, as is increasingly the case in newly built SRF-producing MBT plants. Recent positive evidence on the effectiveness of sensor-based sorting devices has been discussed in the previous sub-section. However, counter-evidence has been also made available through test-scale runs⁵⁵ and simulation exercises. Schirmer et al.³²² reported on simulating the reduction in total organic content achievable through the use of NIR, assuming 2.5-10% w/w_{ar} plastics in the input of a biodrying MBT, with 6-25% of these showing very high total chlorine concentration ([Cl] = 5-12% w/w_d); they concluded that the NIR is capable of reducing the total chlorine content of the SRF by only 0.1-0.2 % w/w_d. However, this simulation assumed a very different material composition to that evident for the UK MBT plant A, for both plant input and SRF produced. Hence, it is not clear if this is a practically advisable route for lowering the total chlorine content of the MBT plant A. Currently, 90% w/w_{ar} of the plastics are incorporated into the SRF product stream (**Figure 5-32**), which could allow the application of sensor-based sorting just before the eddy-current separator or the final SRF output.

6.5.4 UK MBT plant A: SRF ash content

Ash content is a very important descriptor of SRF quality. Upper limits are specified in all quality standards, as discussed in **Section 2.5**. Upper limits are summarised in **Table 2-15**, **Table 2-16**, and **Table 2-12**. Results on moisture content are presented in Section 5.6.4. Statistical analysis performed is explained in **Section 4.12.1**.

Variability and methodological insights on ash content determination

The repeatability of the ash content determination on SRF samples following the stipulations of the new SRF standard (DD CEN/TS 15403:2006)³³² (still under

validation). The ashing furnace has been programmed to follow the specific new temperature evolution profile requested in the standard, as explained in **Section 4.13.2**. Repeatability is satisfactory. Coefficient of variation, determined on triplicates, is low for both the sets of all samples and typical-plant-operation-only samples (median $\%CV(A)_{L1+2+3} = \text{median } \%CV(A)_{L1+2+3-L3\text{out}} = 1.1\%$, respectively) (**Table 5-13**). Hence, 2 g aliquots of general analysis samples shredded at 0.5 mm are sufficiently homogenised for SRF ash content determination. The satisfactory repeatability also indicates that the ashing furnace operates consistently. The consistent ashing was also verified by visual inspection of the ashes, showing no evidence of incomplete combustion, in any run. The extended uncertainty (U_{95}) around the average of the triplicates directly reflects the repeatability of the analytical method, because there is no random uncertainty propagation in the determination (**Section 4.13.2**). Hence, repeatability is visualised in the **Figure 5-66**, as the within-sample/analytical uncertainty estimate.

Ash content variability during SRF production

The **Figure 5-66** the between-incremental is dominant, but less than for other quantities, such as $\langle M_T \rangle$. The between-incremental sample variability is clearly higher than the within-sample/analytical variability, as anticipated. However, for certain cases (e.g., L3_INC10), given only 3 replications, the resultant $U_{95,2}(\langle A \rangle)$ is comparable to the variability from plant production and sampling (between-incremental sample variability) (e.g., difference between $\langle A \rangle$ of L3_INC11 and 12, 13, 14). Always assuming normality and standard deviation independent from the number of observations, one additional replication, would increase the d.f. to 3, reducing the uncertainty in the $\langle A \rangle$ determination for each GAS at the 2/3 of the current value, (each uncertainty according to **Equation [0-1]**, for no systematic error and omitting standard deviation, being constant):

$$\left(\frac{t_{95,2}/\sqrt{3}}{t_{95,3}/\sqrt{4}} = \frac{4.303/\sqrt{3}}{3.182/\sqrt{4}} = 1.56 \approx 1.5 = 3/2 \right).$$

The between-sample variability is on the higher range of all the quantities considered; however, still within an acceptable range (below 20%). If the L3 typical samples are considered only, %CV(<A>) reduces to 8.5%, indicating that the SRF output for consecutive summer-period days of trouble-free plant operation can be relatively stable regarding <A>. **Figure 5-66** suggests that both the winter and summer samples are at similar levels (whilst not enough winter samples are available for a statistically quantified comparison).

Average and upper range values of ash content

The typical-MBT-operation-only samples (L1+2+3-L3outl) show a median <A> at 17.6% w/w_d, which reduces slightly to 17.3% w/w_d for the L3-outl set of samples. These values roughly coincide with the average values of the so far reported for the European MBT-derived SRF (**Table 5-1, Figure 5-2**). Comparison with in-house monitoring data of the same plant operator stemming from a different plant (Plant B)²⁶⁶ reveals even lower values, with a median of the combustible fraction of 10 samples at 14.0% w/w_d and p₈₀ at 16.0% w/w_d. Shanks Waste Management Ltd have recently reported typical SRF values (plant origin not stated): median <A> = ca 13% w/w_d and p₈₀ = 14% w/w_d (approximate values, as read from graph)³⁶³. The SRF ash content of an MBT plant located on a Greek island and producing SRF merely by mechanical separation, has been recently reported³⁶⁰ for the months November to April at 15.83% w/w_d (possibly arithmetic mean).

Cemex Climafuel²⁶⁵⁻²⁶⁶ and Remondis SBS^{®2}³⁶⁵ specify an upper limit for <A> for cement kilns at 15% w/w_d. A less demanding upper limit, is set by Remondis

SBS[®]2³⁶⁵ for use in power plants at 20% w/w_d. The p₈₀(<M_T>) and UCI_{95%}(<M_T>) values achieved here fall just below the 20% w/w_d limit (UCI_{95%}(<A>) = 18.51 UCI_{95%}(<A>) = 18.51% w/w_{ar}; whilst for L1+2+3-L3outl at 19.67% w/w_{ar}. Hence, if normally distributed, the <A> just complies with the Remondis upper limit for power plants, but fails to meet the Remondis and Cemex limits for cement kilns. Regarding the individual incremental samples, the bulk of them fall between the two limits (15-20% w/w_d).

The only samples that exhibit values below the 15% w/w_d upper limit are the L3 potential outliers. At first, this is a surprising result: the higher levels of contamination in Al alloys, considered alone, should increase the ash content in comparison with the rest, typical SRF samples. Al content can be safely considered as ca 100% ash, because the melting point of Al is at 660.32°C, whilst the maximum temperature encountered during ashing is 550°C. Possibly the lower <A> values experienced are due to the concurrent unusually high ratio of plastics over paper for these samples as the results of the ash concentrations of these waste verify (**Table 5-10**).

The investigation of the <A> of the waste components has shown for the 2 major plastic components of SRF: (1) other packaging plastic: <A>±U_{95,1} = 1.55±0.03% w/w_d; and (2) plastic films: 7.62±1.73% w/w_d. Much higher values are experienced for the paper and card category, investigated in SRF-type streams (SP11, 12): 15.60±0.20% w/w_d, and in the biodried material (SP1): 19.45±1.40% w/w_d. Thus, the very low content of the paper and card in these samples, combined with the very high film and other packaging plastic content has possibly resulted in a lower <A> in comparison with the typical SRF samples, despite the high Al alloy contamination. As a result, the occurrence of such atypical samples has no detrimental impact on the ash content of the SRF. However, it does not mean that these are desirable, since other specifications might be violated, Al impurities content in particular.

SRF ash content vs. material composition

The ash content of typical SRF samples clearly exceeds the upper limit of 15% w/w_d, suitable for primary firing in cement kilns and is just marginally within the limit of 20% applicable to thermal recovery in certain types of power plants. However, only 37.8±3.1% of the ash content of the combustible part of the biodried input reports to the SRF. Paper is now responsible for the bulk of the load (44.9%); incorporation of more paper would not alter the ash content level considerably, because it is almost identical (17.5% w/w_d). Plastic materials, already fully incorporated into the SRF, have a beneficial impact due to their low ash content (plastic film: 7.6% w/w_d; other packaging plastic: 1.6% w/w_d).

There is potential to lower the ash content by reducing the mass fraction of the incombustible impurities in the SRF, which, despite being relatively low (3.5±1.2% w/w_d), contributes considerably to the overall ash load; the non-ferrous metals in particular account for 10%. For this to be achieved, the performance of the eddy-current separator should improve, currently transferring 64.1±10.2% of its non-ferrous metal input to the SRF output.

The relative ratio between paper and plastic in the plant input affects the final also the finally achieved concentration in the SRF. Because paper and these plastic items are those typically targeted in kerbside collection schemes, the extent of application and success of such schemes for each component could directly influence the resultant ash content. Visual inspection during manual sorting has revealed that most of the paper and card survives intact the biodrying stage, as anticipated.

Another option for lowering the SRF ash content could be to blend the current MBT input with rich-in-plastic film and other packaging plastic commercial waste. However, this would further increase the total chlorine content, if no targeted removal

of high-in-chlorine plastics is effected, possibly through application of sensor-based sorting (see **Section 2.4.4.8**), as has also been reported by Schirmer et al.³²² for German SRF-producing MBT plants. It could also have a direct detrimental impact on the biogenic content, which with the current input and plant operation only marginally achieves the aspired level (**Section 6.5.5**). However, the level of the biogenic content has not a direct technical impact, but affects financial attractiveness and the sustainability profile of the SRF. Conversely, ash content has direct technical implications for the SRF applicability, apart from the indirect financial implications (managing of ashes, or alteration cement quality through its contribution to the mineral content of clinker, in the case SRF is used in the raw meal).

6.5.5 UK MBT plant A: SRF biogenic content

Variability of $\langle \chi_B \rangle$

The propagation of many uncertainties in the determination of the $\chi_{B,daf}$ makes it susceptible to being computed with a high uncertainty, where only 2 replicates are employed in the individual measurements, as can readily seen in **Figure 5-70**. The combination of selective dissolution with subsequent ashing of the residues is able to achieve good repeatability with just duplicate determinations on the SRF GAS (median $\%CV(A_{ts,d,dis,d/b})=3.0$); However, almost in 15% of the cases (3 out of 19), $\%CV$ results in the order of magnitude of 10% (**Table 5-17**), which increases considerably the uncertainty of the final quantity of interest ($\%U_{95,veff}(\chi_{B,daf})$ at 10-23% for these cases). Note that the $U_{95,veff}(\chi_{B,daf})$ can be inflated also by a poor repeatability of the rest measurands it depends upon (M_r , $A_{ts,d}$, and cf_d , if applicable), as it is evident for L3_INC4 and L3_INC9.

For comparison, QUOVADIS³⁴¹ has reported for χ_B of MSW-derived SRF a $\%CV$ of 2.1% w/w_d. However the QUOVADIS values stem from two samples

representing 2 lots of an SRF, with SDM replicated five times; it is not clear if a correction for the ash content has been implemented; hence results might not be directly comparable. If this is the case, the %CV quoted has no scientific meaning for the $\chi_{B,daf}$, because where uncertainty propagation applies only uncertainty can be reported: %CV refers to independent samples or replicate runs and not cases where many expected values are used to compute a final expected quantity. Also it is not clear whether the %CV represents the average of within-GAS and analytical determination variability or global average, i.e., both within- and between-sample variability. Hence, possibly it can be comparable only with the individual values of the %CV($A_{ts,dis,d/b}$) for duplicate determinations.

Here, the between-sample variability of $\langle\chi_{B,daf}\rangle$ for the L123-L3outl set of samples is reasonably low (%CV($\langle\chi_{B,daf}\rangle$)=8.4%), indicating that the MBT SRF production line is capable of producing SRF of sufficiently stable biogenic content quality, given any problems in the production are controlled. However, the between-sample variability almost doubles when the atypical samples are included (as evaluated through the IQR). As a result of the many uncertainty components propagated, $\chi_{B,daf}$ shows a within-sample and analytical determination variability (difference between whiskers of a measurement for a single sample, **Figure 5-70**) (as estimated by the uncertainty at the 95% level of confidence) that is comparable to the between-sample variability (difference between averages of different samples, **Figure 5-70**), when only 2 replications are performed for each of the $A_{ts,dis,d/b}$, M_r , $A_{ts,d}$ resulting in a low v_{eff} and a subsequent high coverage factor. Note that this is despite the highest test sample mass used in the $A_{ts,dis,d/b}$ determination (ca 5.000 g) when compared with other measurands, e.g., TH (ca 0.0020 g), which should mitigate the within GAS variability effect. However, if a much smaller coverage factor could be deemed as appropriate (e.g., 2 as it is the standard practice, instead of 4.303 used here) the

estimated uncertainty would be approximately half, indicating that the between-sample variability overshadows the within-sample and analytical determination, which is in line with the current empirical wisdom for waste measurands. Note that the within-sample and analytical determination variability does not cover the variability from sub-sampling which is examined separately, but for the purpose of this analysis can be ignored, since it has been found sufficiently smaller than the within-sample and analytical determination variability (data not reported).

Average and upper limit of $\langle\chi_B\rangle$

The overall achieved level of biogenic content is just above 50% w/w_{daf}, which is a level currently appealing for use in cement industry applications. The higher plastic/paper mass ratio of the non-typical MBT operation samples results in lower $\chi_{B,daf}$ values (**Figure 5-70**), and lower considerably the 20th percentile, well below 50% w/w_{daf}. The rest typical operation values reach acceptably high values: the only commercial end-user specification that sets limits for χ_B is that of Climafuel by CEMEX²⁶⁵⁻²⁶⁶: $\min(\chi_B) = 50\%$ w/w; however the reporting basis is not stated: we assume it _{daf}. This threshold is met by the 20th percentile (p_{20}) of the typical SRF samples (L3-outl and L123-L3outl), being at 53.99% w/w_{daf} and 52.75% w/w_{daf} respectively (**Figure 5-71**). Note that the $LCI_{95\%}$ can be used for compliance testing only for the data set that excludes the atypical samples (L123-L3outl), because of the violation of normality assumption for the overall data set (L123): $LCI_{95\%}(\chi_{B,daf}) = 52.79$, just above the specified value. The individual incremental samples also meet the specification in most of the cases, apart from cases where threshold is not met either fully (L1_INC6, L3_INC2) or because of high measurement uncertainty (the uncertainty $LCI_{95\%}$ extends below the threshold) (L3_INC8). However, the atypical SRF samples show high between-sample variability and invariably fail to meet the specification.

Very limited literature data are available to compare with the results of this thesis. QUOVADIS³⁴¹ has reported for χ_B of MSW-derived SRF an average of 51.7% w/w_d, with a range of values 53.4-52.6 %w/w_d. This is of similar order of magnitude to our results. However, much higher values have been reported by SRF producers, but lacking in the necessary supportive information to enable a fruitful comparison: Flame⁶⁴ has reported χ_B of a household waste-derived SRF at 62% w/w_d, (inter-laboratory study, average of 8 labs, excluding one measuring at 50%) as measured by a variation of the SDM according to DD CEN/TS 15440:2006³⁰⁹. Reporting basis is weight, but it is not clearly stated whether _d or _{daf}. The considerably higher value than those observed here, where max 80th percentile is at 60.25% w/w_{daf} it is possibly due to the high paper content (57% w/w_d) of the SRF, whilst here it was found at 44.5±2., along with significantly lower plastics (21% w/w_d) and textiles (10% w/w_d) in the SRF. In addition, speculating that this value is not pure biogenic content, i.e., not corrected for ash content, and it is contraries-free ($\chi_{B,SHR}$), could partly also explaining the difference. Similarly, annual average χ_B of the Remondis SBS1[®] (power plant SRF specification) SRF from the Erftstadt plant³⁶⁵ was reported by the producer at 63.4% w/w_d for 2005 and at 75.0% w/w_d for 2006, measured according the SMS as specified in the prCEN/TS 15440: no statistical or other background information for these data is available; for the much higher values the same explanations as for the Flame's data might apply.

The scope of this research does not cover computing the potential greenhouse gas savings when an MBT-derived SRF is substituting a certain fossil fuel for energy production. However, just to grossly illustrate the potential market appeal of the achieved levels of biogenic content, such calculations present are presented here. According to SRF producer Remondis, an SRF with 50% w/w biogenic content can

lead to CO₂ emissions reduction from 0.75 tCO_{2,eq}/tSFR if hard coal is replaced and to 1 tCO_{2,eq}/tSFR if bituminous coal is replaced; the reporting basis of χ_B is not denoted [

More correctly, values of biogenic content on a total carbon basis ($\chi_{B,TC}$) should be used for the emission calculations³⁰⁹. Note that the biogenic content by TC typically results in lower values than when reported on a weight basis: e.g., from the QUOVADIS³⁴¹ study, for an $\chi_{B,d} = 52.6\%$ but $\chi_{B,TC} = 45.8\%$. Veolia Environment⁶³ SRF producer has made some similarly rudimentary calculations on the life-cycle CO₂ balance for SRF, reporting avoided emissions of 0.95 tCO_{2,eq}/tSFR if a mixture of 1/3 black coal, 1/3 lignite, and 1/3 petcoke is replaced by a high-CV (and possibly high-plastic) SRF of 30% by TC in cement kilns; and of 1 tCO_{2,eq}/tSFR, when a 56% by TC SRF is replacing lignite in power plants. Since the order of magnitude of the biogenic content results achieved here is similar to those used in the cited crude modelling emissions attempts, similar anticipations for avoided CO₂ emissions can be speculated. However, these computations should be treated with caution as they have neither been independently researched, nor peer-reviewed.

Shanks Waste Management Ltd³⁷⁰ has recently reported 'typical' values for the $\chi_{B,TC}$ (specific UK plant not denoted): with median of ca 52% w/w_d and an IQR of ca 45-55% w/w_d (values as read from figure). In-house results for biodrying MBT as internally reported by the organisation²⁶⁶, showed $\chi_{B,TC}$ median of 52.5% w/w_d; 80th percentile: 54.0% w/w_d, IQR: 45.4-53.9% w/w_d, based on the shreddable fraction of 9 samples (statistical analysis of data for this thesis).

SRF biogenic content vs. material composition

The material composition of the biogenic content was not simulated through the components in this research. This is because it is not possible to correctly account for the biogenic, non-biogenic and inert parts of the ash content, dissolved during the

selective dissolution. Hence it is not readily feasible to accurately reconstruct a dry ash-free basis biogenic content. In a parallel research by Séverin et al.²⁹⁵, reported separately, it was established that the biogenic content as measured by the selective dissolution method reported on and uncorrected for ash content basis and the manual sorting method correlate sufficiently well. Hence this version of the biogenic content can be sufficiently simulated by manual sorting data.

Methodological insights on determination of $\langle\chi_B\rangle$

Regarding the split of the ash content resulting from the selective dissolution, the considerable quantity dissolving $\langle A_{\text{sel_diss_dis,d}} \rangle$ (ca 50% w/w of overall A, **Figure 5-68**) justifies the necessity for a correction. Part of this $\langle A_{\text{sel_diss_dis,d}} \rangle$ stems from biogenic components. However, is all the dissolved ash in waste components deemed as biogenic or indeed biogenic origin? Significant proportion of the analysed SRF is paper and card (44.5% w/w_d). Typical paper contains chalk as filling mineral matter (i.e., calcium carbonate, CaCO₃), which entirely dissolves during the selective dissolution, as also stated in the TAUW pre-normative research¹⁸⁶. Since this is an inert additive to the biogenic part of the paper/card it is correctly excluded from the computation of the χ_B .

The average difference in the computation of $\chi_{B,\text{daf}}$ where a correction for the non-combustible part is necessary $\Delta(\langle\chi_{B,\text{SRH,daf}}\rangle - \langle\chi_{B,\text{daf}}\rangle)$ is at a non-negligible 3.5% w/w_d lowering (**Table 5-17** and **Figure 5-69**), despite the high purity of SRF in combustible materials (as measured for the L1+2 SRF samples). This correction can be accompanied by widening of the uncertainty involved in the estimation of $\langle\chi_{B,\text{daf}}\rangle$, depending upon the level of uncertainty related to the $\langle M_T \rangle$, which is necessary to compute $\langle cf \rangle$ on an dry basis. Quantifying this difference provides us with a rapid surrogate measure to estimate the $\langle\chi_{B,\text{daf}}\rangle$ from the $\langle\chi_{B,\text{SRH,daf}}\rangle$, where the level of SRF

purity in combustibles it >90% w/w_d, as it is the case for other determinations of <X_{B,daf}>, internally reported for a UK plant of similar configuration²⁶⁶.

6.5.6 UK MBT plant A: SRF total carbon and total hydrogen content

Results (**Section 5.6.6**) useful as typical ultimate fuel characterisation have been reported. They can be used for predicting calorific values directly from the chemical composition, which is feasible for a series of a materials, as has been established in the literature^{336, 371}.

6.5.7 UK MBT plant A: SRF calorific value

Calorific values determine the main utility of the SRF as a fuel, and directly affect the technical feasibility of its use in a series of thermal recovery options as discussed in the literature **Section 2.5.4**. Complexities regarding the meaning and utility of each reporting basis are detailed in the methodology **Section 4.13.4**.

Variability of calorific value

The comparatively highest repeatability of the Q_{gr,v,b} amongst all the determined SRF properties (max %CV(Q_{gr,v,b}) = 0.47%) shows that the SRF samples are sufficiently homogenised for gross calorific value determination and that the bomb calorimeter operates consistently. As a result, the %U_{95,veff}(<Q_{net,p,ar}>) remains within acceptable levels (max at 5.4%), despite the propagation into the result of the <M_T> and <TH> uncertainties. In turn, this results in a low within-sample and analytical variability for the <Q_{net,p,ar}>, in comparison to the between-incremental-sample variability (**Figure 5-72**), which is a desirable outcome for the overall measurement process.

The lack of evidence against the normality for the incremental samples datasets, provides evidence in favour of the CEN choice to assume normality and

propose the $LCI_{95\%}(\langle Q_{net,p,ar} \rangle)$ in the assessment of the calorific value classification rule. However, note that this does not alter our reservations for the selection of the non-conservative coverage factor. The substantial reduction in the between-incremental-sample variability when the atypical SRF samples are excluded ($\%CV(\langle Q_{net,p,ar} \rangle)$ for $L1+2+3-L3outl = 8.4\%$, compared with 19.7% for the $L1+2+3$ dataset) verifies that these samples ($L3outl$) stand out (**Figure 5-72**). In line with the rest properties, the considerably close values of $L2_INC1-7CM$ and $L2-INC8$ provides no evidence of high variability in the performance of the plant production line, during this particular period ($L2$).

Such a between-sample-variability could be considered as being within the anticipated range for waste-derived properties. It is placed in the intermediate to low range of variability for the properties under investigation. The end-user specifications (**Table 2-15** and **Figure 5-73** and **Figure 5-74**) recognise the versatility of the thermal recovery process to accept SRF within a range of Q values. Whilst the reporting basis is not always clear, requested ranges around the median have been reported (kJ kg^{-1}) for CK at 3 or 4 and for PP at 5 or 7. To compare with, here the overall $L1+2+3$ $IQR(\langle Q_{net,p,ar} \rangle) = 12.7 \text{ kJ kg}_{ar}^{-1}$, reducing to $6.8 \text{ kJ kg}_{ar}^{-1}$ for the typical MBT plant operation samples ($L1+2+3-L3outl$). These range results indicate that the achieved between-sample variability might need to be reduced, if the anticipations of the end-users for a relatively constant level of Q are to be met, especially for cement kiln applications.

Average and lower limit of calorific value

The median $\langle Q_{net,p,ar} \rangle$ for the typical-MBT-operation-only samples ($L1+2+3-L3outl$) is at $15694 \text{ kJ kg}_{ar}^{-1}$ and the $Q1(\langle Q_{net,p,ar} \rangle) = 14595 \text{ kJ kg}_{ar}^{-1}$ and the $LCI_{95\%,N-1}(\langle Q_{net,p,ar} \rangle) = 14813$ (**Table 5-12**, **Figure 5-73**); the corresponding values for the $L3-outl$ dataset are slightly lower. This $\langle Q_{net,p,ar} \rangle$ median is lower than the central tendency

of the European MBT-derived SRF data medians ($= 16.3 \text{ MJ kg}_{\text{ar}}^{-1}$) and it just exceeds their lower quartile ($= 15.4 \text{ MJ kg}_{\text{ar}}^{-1}$) (**Table 5-1** and **Figure 5-74**). Shanks Waste Management Ltd³⁶³ have recently reported typical $\langle Q_{\text{net,p},\rangle}$ values for biodrying MBT-produced SRF (plant origin not stated): median $\langle Q_{\text{net,p},\rangle} = \text{ca } 18 \text{ MJ kg}^{-1}$ and Q1 ca 16 MJ kg^{-1} (approximate values, as read from graph; reporting basis not stated whether $_{\text{d}}$ or $_{\text{ar}}$). If these values are $_{\text{ar}}$ then they are considerably higher than those measured here. If they are $_{\text{d}}$, they are lower than those measured here for L1+2+3-13out: median($\langle Q_{\text{net,p,d}} \rangle$) = $19158 \text{ kJ kg}_{\text{ar}}^{-1}$ and Q1($\langle Q_{\text{net,p,d}} \rangle$) = $18382 \text{ kJ kg}_{\text{ar}}^{-1}$.

These two very different scenarios vividly illustrate the considerable affect the conversion between $_{\text{ar}}$ and $_{\text{d}}$ basis has upon the calculation of the Q. Note that these 2 reporting bases represent the two ends of the spectrum regarding optimal and least optimal energy recovery from the SRF, during its thermal recovery. In the case of any form of EfW plant, in the absence of the recovery of energy from heat (CHP) the $_{\text{ar}}$ values apply. However, the current trend is to opt for high energy efficiency CHP EfW plants, where part of the water vaporisation energy, considered lost in the $_{\text{ar}}$ reporting basis, is in practice recovered through the steam cycle. Hence, in the **Figure 5-73** and **Figure 5-74** our results are presented in both reporting bases.

The $\langle Q_{\text{net,p,d}} \rangle = 19158 \text{ kJ kg}_{\text{d}}^{-1}$ falls towards the Q1 of the encountered amongst the investigated European MBT-derived SRF ($= 18.2 \text{ MJ kg}_{\text{d}}^{-1}$) (**Table 5-1**). It is considerably lower than that recently reported by Gidakos and Simantiraki³⁶⁰ for SRF produced by mechanical separation through an MBT located on a Greek island: the yearly average was at $Q_{\text{net,p,d}} = 21268 \text{ kJ kg}_{\text{d}}^{-1}$ (possibly arithmetic mean; converted from $\text{kcal kg}_{\text{ar}}^{-1}$ assuming 4.187 J per cal).

The $\text{LCI}_{95\%,\infty}(\langle Q_{\text{net,p,ar}} \rangle)$ is used in the CEN guidance for SRF classification²⁵⁹. Given $\text{LCI}_{95\%,\infty}(\langle Q_{\text{net,p,ar}} \rangle)$ is at $15807 \text{ kJ kg}_{\text{ar}}^{-1} \geq 15000 \text{ kJ kg}_{\text{ar}}^{-1}$ (for the typical samples

only: L1+2+3-L3outl) an SRF with this value would be of Q class 3, as can be also seen in the Figure 5-73, B-2. However, for the classification a sampling plan using composite samples to represent lots extending over the yearly production should be used, which is not here the case. If the accurate d.f. = N-1 are used in the computation of the $LCI_{95\%}(\langle Q_{net,p,ar} \rangle)$, the value results below the limit of class (= 14813 kJ kg_{ar}⁻¹), i.e., within the class 4. However, despite this being the correct $LCI_{95\%}(\langle Q_{net,p,ar} \rangle)$ for the data set, the computation with the d.f. = infinite, resulting in a coverage factor of 1.96, should be used in accordance with the rule set by the CEN documents²⁵⁹, as discussed in **Section 2.6.4**.

The fact that the plant MBT A-derived SRF is at the verge of class 3 and 4 is shown when the L3-outl samples dataset is used, resulting in $LCI_{95\%,\infty}(\langle Q_{net,p,ar} \rangle) = 14539 \text{ kJ kg}_{ar}^{-1}$ i.e., within the class 4 range. Note that this difference from the L1+2+3-L3outl case is by and large due to the greater $s(\langle Q_{net,p,ar} \rangle)$ value (**Table 5-12**), resulting from the lower number of observations (10 vs. 15). Whilst the CEN guidance mandates a minimum of 10 observations, it allows using more, if this is the case. Differences in the precision with which the standard error is determined can reflect upon the classification outcome when the values are close to any class limit, as it happens here.

For the time periods examined, the average MBT plant A SRF could meet the end-user Q specifications for FBC and hard coal DBB or lignite power plants, but is just below the desirable range aspired for cement kiln applications and had coal WBB power plants (**Figure 5-73** and **Figure 5-74**) (L1+2+3-L3outl median $\langle Q_{net,p,ar} \rangle = 15694 \text{ kJ kg}_{ar}^{-1}$ and the $LCI_{95\%,N-1}(\langle Q_{net,p,ar} \rangle) = 14813 \text{ kJ kg}_{ar}^{-1}$). Most of the available end-user specifications regarding the calorific value of SRF have been summarised in **Table 2-15** and **Table 2-16**. The Italian lower limit for low quality SRF is at 15 MJ kg_{ar}⁻¹ and for high quality at 19 MJ kg_{ar}⁻¹. Most cement kiln related specifications set a lower limit at 18 MJ kg_{ar}⁻¹ for $Q_{net,p,ar}$ (Cemex Climafuel²⁶⁵ and Remondis SBS^{®2365}). However, a

lower threshold at $15 \text{ MJ kg}_{\text{ar}}^{-1}$ has been set by CEMEX²⁶⁵ during the permitting change procedure and specified in a UK off-take agreement²⁶⁶; and if the SRF is directly used in the clinker kiln as both raw material and fuel, then lower values can be tolerated^{42, 210}. Regarding the possibility of using the SRF in EfW with typical grate furnace technology, the values just exceed the maximum tolerable Q of $14 \text{ MJ kg}_{\text{ar}}^{-1}$ reported by Eckardt and Albers⁵². **Figure 5-73** and **Figure 5-74** illustrate the SRF Q statistics in relation to characteristic the power plant (lower range) and cement kiln (higher range) specifications.

SRF net calorific value vs. its material composition

Hence, the SRF is suitable for range of end-uses, marginally including cement kiln in fuel-only application if lower than the publically stated values are tolerable. The UK MBT plant A flowsheet enables most of the high calorific value waste components (plastic films: $30.7 \text{ MJ kg}_{\text{ar}}^{-1}$; other packaging plastic: $26.1 \text{ MJ kg}_{\text{ar}}^{-1}$) to be entirely incorporated into the SRF product, together accounting for 43.6% of the SRF load. The trommel and the air classifier allow only modest quantities of the combustible mass to leave the SRF process line ($14.3 \pm 2.8\%$ and $15.4 \pm 21\%$, respectively). Most of the combustible dry ash-free mass not incorporated into the SRF ($25.5 \pm 3.2\%$), is in the form of paper, which has considerably lower net calorific value ($13.0 \text{ MJ kg}_{\text{ar}}^{-1}$); increased reporting in the SRF output would result in further lowering of the net calorific value level, despite that on the whole more of the combustible matter would have been recovered by the plant. An increase in the $\langle Q_{\text{net,p,ar}} \rangle$ values would be necessary in order to bring it within the calorific ranges desirable for cement kilns. To achieve that, the general options would be: (1) mixing with higher in Q commercial waste (a solution followed by some SRF production plants, e.g., the Pirelli Ambiente Renewable Energy²⁰⁷ adding an mixture of plastic and tyres scraps to increase the $\langle Q_{\text{net,p,ar}} \rangle$ at $> 20 \text{ MJ kg}_{\text{ar}}^{-1}$ and (2) improve the drying performance of the biodrying section, since the

$Q_{\text{net,p}}$ values are highly dependent of the $\langle M_T \rangle$ level, as can be readily seen from its computation formula (**Equation [2-3]**) and **Figure 5-73** and **Figure 5-74**.

Mrotzek et al.³²¹ simulated SRF properties based upon characterisation and literature data, reporting that the development of a spreadsheet and database able to predict the SRF calorific value. Results of calorific indicate very good agreement between average experimentally measured and simulated values (0.3% relative difference). However no detailed information on methodology has been provided.

6.5.8 UK MBT plant A: SRF total nitrogen content

The principal issue associated with the $\langle \text{TN} \rangle$ levels of SRF is the emission of NO_x during thermal recovery²¹⁵. The fuel-related N contributes to NO_x formation along with thermal and prompt creation mechanisms. Typically primary and secondary APC measures (air staging, combustion-related properties adjustment, selective non-catalytic reduction, and selective catalytic reduction) enable to tolerate TN content in the fuel at levels times higher of the 0.6% w/w, which would be acceptable without any emission control in place: e.g., up to 3% w/w.

Results of total nitrogen on individual incremental (and composite) samples are presented in **Table 5-19** and plotted in **Figure 5-75**. Summary data and statistics are found in **Table 5-12** and **Table 5-13**, and presented in **Figure 5-76**.

Variability of total nitrogen

The repeatability of $\langle \text{TN} \rangle$, determined on 3 replicates of the GAS, (within-sample and analytical determination variability) can be assessed by the %CV(TN) (**Table 5-13**): it ranges from 13.1% to 1.1% for the L1+2+3 set of samples; and 7.6-1.1% for the L1+2+3-L3oult. The median values are respectively 3.3% and 2.6%. The between-incremental sample variability of $\langle \text{TN} \rangle$ can be evaluated by the %CV,

because the normality assumption is not violated ($p_{w-s} > 0.8$) (**Table 5-12**): 18.2% for L1+2+3-L3outl and 14.7% for L3-outl; when the atypical samples are included, higher between-sample variability is experienced (>20%).

Both the within-sample/analytical repeatability and the between-incremental sample variability are at acceptable levels; the between-incremental is less dominant, compared with other quantities ($\langle M_T \rangle$, $\langle Q_{net,p,ar} \rangle$). The low %CV(TN) of the triplicate determinations on just ca 0.25 mg aliquots of the SH0.5 GAS (L1+2+3-L3outl median at 2.6%), shows that the SRF samples are sufficiently homogenised for total nitrogen determination, despite the tiny quantity on which the test sample is performed; and that the CHN analyser operates consistently. Since there is no random uncertainty propagation in the computation of U_{95} , this directly mirrors the %CV values behaviour.

The between-incremental sample variability is on the higher end of the range for all the quantities considered: second most variable after $\langle M_T \rangle$; however, still within an acceptable range (below the arbitrary 20%). The L3 typical samples show less variability than the overall L1+2+3-L3outl, indicating that regarding $\langle TN \rangle$, the SRF output for consecutive summer-period days of trouble-free plant operation can be more stable than the year when wider periods are considered. **Figure 5-75** suggests that, with the exemption of L1_INC1, the L1+2 values are on average just slightly higher than L3-outl. Namely, there is no great difference between the winter and summer samples (whilst not enough winter samples are available for a statistically quantified comparison).

The between-incremental sample variability is generally higher than the within-sample/analytical variability, as anticipated. However, this does not pertain to the L3outl samples; and to certain cases (e.g., L3_INC10), given the only 3 replications,

the resultant $U_{95,2}(\langle \text{TN} \rangle)$ is comparable to the between-incremental sample variability (plant production and sampling variability).

Average and upper limit of total nitrogen

All four SRF sets of samples show very similar $\langle \text{TN} \rangle$ medians (0.9-1.0% w/w_d) **Table 5-19** (or 0.9% w/w_d if the individual replicates are used for their computation, as plotted in **Figure 5-76**). Given normality is not violated the $UCI_{95\%}(\langle \text{TN} \rangle)$ can be used to evaluate compliance with standards. For both L1+2+3-L3outl and L3-outl the $UCI_{95\%}(\langle \text{TN} \rangle)$ is similar (1.10% w/w_d and 1.08% w/w_d, respectively); and the $p_{80}(\langle \text{TN} \rangle)$ at 1.16% w/w_d and 1.12% w/w_d respectively.

The average $\langle \text{TN} \rangle$ quality for SRF achieved from the UK MBT plant is similar, or better, than other European biodrying MBT-derived SRF. It is very close to the value reported for the Eco-deco biodrying plant at Monatanaso Italy: 0.83% w/w (median of values reported¹³ for samples collected in 2003: reporting basis not stated). Considerably lower than older TN SRF data from biodrying MBT processes: (Nehlsen⁴³,³²⁵ Calobren: 1.5% w/w; and Herhof TST⁴³,³²⁴ from the Asslar plant: 1.7% w/w – reporting basis not stated).

The achieved $\langle \text{TN} \rangle$ level falls within the range of values reported for biofuels (0.5-3% w/w_{daf}), as detailed by Obernberger et al.²¹⁵ (for comparison on same reporting basis, conservatively assume a maximum of 20% higher values for the MBT plant A $\langle \text{TN} \rangle$ to convert from _d to _{daf} values). Indicative values for selected typical biofuels are plotted in the **Figure 5-76** to help visualise the comparison. In particular, the range of values is identical to that reported for waste wood³⁷². Similarly, for indicative coal types: the average (and the very close upper limit) $\langle \text{TN} \rangle$ level is typical of Spain and Russian anthracite (0.9% w/w_{daf} and 1.0% w/w_{daf} respectively), and lower than the German one

(1.4% w/w_{daf}); and within the range of average European lignite/ brown coals (0.5-1.4% w/w_{daf}).

The available SRF standards / end-user agreements do not specify any TN limits. A useful comparison can be made with the tolerable values for e.g., solid biofuels as discussed in detail by Obernberger et al.²¹⁵. The UCI_{95%}(<TN>) and p₈₀(<TN>) values for UK MBT plant A exceed the 0.6% w/w upper limit, which could enable combustion without specific APC measures in place. However, this is also the case for many solid biofuels. The maximum concentrations remain well within the emission mitigation capacity of the less costly selective non-catalytic reduction.

The atypical L3outl samples generally result in lower values than the typical (**Figure 5-75**); thus, they do not present a problem regarding <TN> quality.

7 CONCLUSIONS AND FUTURE WORK

The work presented here allows a series of conclusions to be drawn. Conclusions pertain to the objectives of this research. They are presented in the order they appear in the main text, as far as possible. Generally they stem from: (i) the critical review of SRF production and quality assurance in MBT plants, and (ii) the experimental body of work for the UK MBT plant A. General Comments in full text are followed by specific quantitative conclusions in the form of a list of bullet points.

7.1 Critical review conclusions

The critical review of the European experience in SRF production from MBT plants shows that, despite the fact that most of the unit operations currently used in SRF-producing MBT plants have an established track record, insufficient scientifically-derived data are available in the public domain on the performance of individual process unit operations that could inform the design of MBT plants, to meet the needs of the modern sustainable resource management agenda.

It might be technically challenging for many MBT plants to produce SRF of a suitably high quality, whether achieving the desirable target level of properties or low variability, especially for the more demanding thermal applications. A trade-off between achieving a high quality of recoverable outputs and the properties of reject materials is supported, e.g., a considerably high yield of rejects may be necessary to achieve an SRF with low total chlorine content. It is difficult to reduce the concentration of zinc and chlorine in SRF produced from residual MSW, because they are present at similar levels in many waste components. With the objective of high-grade SRF production, it is not sufficient to separate a comminuted coarse fraction just on a particle size distribution basis.

There is no satisfactory understanding of what constitutes appropriate data at the operational and regulatory level and suitable statistical analysis for MBT-derived

SRF and other waste-derived products to enable appropriate quality control of MBT-derived SRF production and harmonised, transparent and unambiguous reporting.

There is not satisfactory understanding of what constitutes suitable SRF quality for thermal recovery. For a series of potential thermal recovery applications technical issues have not been thoroughly investigated so far; and have resulted from only limited in time and extent of full-scale utilisation of MBT-derived SRF.

The critical review of the process science and engineering of biodrying bioreactors shows that biodrying demands different management of process control variables than composting, to fulfil different objectives. High aeration rates and limited biodegradation produce optimally biodried output, for further processing to SRF. Typical process times are 7-15 days, leading to weight loss of 25-30% w/w of the reactor input, mainly $\text{H}_2\text{O}_{(g)}$ and CO_2 . Modification of the psychrometric properties of input air and minimisation of matrix gradients for critical properties, such as moisture content, are critical aspects of optimisation. Inverted air and rotary drum reactor designs can improve uniformity of treatment and output quality, but they have still to be proven on a commercial scale.

The first available statistical overview of non-UK, European MBT-derived SRF, quality data indicates that MBT-derived SRF quality is within the range of potential applications, but for certain properties it is difficult to reach the standards set for the most demanding applications. Specific numeric conclusions:

- The SRF with the highest net calorific value median, on an as-received basis ($19.9 \text{ MJ kg}_{\text{ar}}^{-1}$) (**Table 5-1**) falls below the threshold for primary firing in cement kilns ($20.0 \text{ MJ kg}_{\text{ar}}^{-1}$) (**Figure 5-1**).

- The upper limit for ash content set for primary firing in cement kilns (15% w/w_d) is exceeded by more than 75% of the SRFs considered (**Table 5-1 - Figure 5-2**).
- Copper and lead have the highest potential to exceed the limits of the German SRF quality standard RAL-GZ 724 (upper quartile of all the SRF cases examined: 448 mg kg_d⁻¹ and 208 mg kg_d⁻¹, respectively) (**Table 5-1 - Figure 5-4**).

7.2 UK MBT plant A material flow analysis conclusions

A novel combination of a series of state-of-the-art methodological approaches was adopted in this research, some of them being applied for the first time ever in a waste management/MBT context:

- sampling of a full-scale commercial, fully operational MBT plant of the latest technology;
- sampling of inner process streams and the input in addition to the outputs (traditionally the only flows sampled);
- sampling plans following the principles of correct sampling according to the theory of sampling;
- sampling mass variable per sampling point theoretically calculated according to the ToS formulas;
- application of best available practices in sample preparation (sub-sampling and size reduction) following the ToS stipulations to maintain representativeness;

- application of the recently available, still under validation, CEN TC/343 methods particular to SRF characterisation;
- material flow analysis using data reconciliation software to overcome potential inconsistencies, and reduce uncertainty;
- proper quantification of the uncertainty regarding each measurement and propagation of it throughout the computations, including the material flow analysis.

These novel methodological approaches implemented in the experimental part have demonstrated for the first time that it is feasible to develop closing balances for mass, waste material components and preserved fuel-related properties, for the processing section of an SRF-producing MBT plant, enabling to be accurately reconstructed the material composition of a finely shredded SRF (<40 mm) (**Figure 5-21**), to gain a detailed understanding of all the main inner flows and, and to measure transfer coefficients of the process unit operations, whilst quantifying 95% confidence intervals around the mean reported values. In addition, based on characterisation results of SRF material components and the SRF composition reconstructed through material flow analysis it has been feasible to simulate the properties of the SRF at a reasonable level of accuracy.

The material flow analysis of the UK MBT plant A demonstrates that the majority of the combustible matter input to the processing section is incorporated into the SRF; yet around one quarter of the combustible dry ash-free mass is not thermally recovered. For the first time, data are reported for the biogenic content, determined by the selective dissolution method (DD CEN/TS 15440:2006), expressed on a dry ash-free basis. For the first time, a detailed characterisation of the waste components of the biodried fraction allows a thorough understanding of how the measured moisture

content results from the contribution of the individual waste components present in the SRF. Data valuable for establishing upper or lower control limits around target values for quality control of SRF production have been produced in this research. It is demonstrated that in general the SRF properties are relatively stable, for MSW-derived fractions. Specifically:

- For total chlorine content and moisture content, measured and simulated values were statistically indistinguishable (d.f. = 15, $\alpha = 0.05$) (**Table 5-11 - Figure 5-59**).
- For the net calorific value on an as-received basis and the ash content 11.7% underestimation and 14.9% overestimation relative to the measured value are evident respectively, the values being statistically different (**Table 5-11 - Figure 5-59**).
- The transfer coefficients (TC) from the processing section input to the SRF output are (**Table 5-4**): net calorific value, as-received $73.2 \pm 8.6\%$ (**Figure 5-53**); combustible mass, dry, ash-free: $74.5 \pm 3.2\%$ (**Figure 5-26**).
- The plant is slightly less effective in concentrating the paper into the SRF (TC dry basis: $80.0 \pm 5.7\%$) (**Figure 5-29**), than the plastics ($92.3 \pm 7.3\%$) (**Figure 5-35**) (**Table 5-4**).
- The rest of the paper reports to the reject fraction not lifted in the air classifier (TC to heavy air classifier output, as-received: $18.1 \pm 5.0\%$) (**Table 5-6 - Figure 5-29**).
- The total chlorine content (DD CEN/TS 15408:2006) of the UK MBT plant A SRF is suitable for the majority of thermal applications

($0.71 \pm 0.06\%$ w/w_d) (**Table 5-12**) and could potentially be classified as CEN CI class 3 (**Table 2-13 - Figure 5-64**).

- A considerable part of the total chlorine load present in the combustible mass is transported to the SRF (TC: $78.9 \pm 26.2\%$) (**Table 5-4**); plastics, along with shoes, contribute considerably (packaging plastic and plastic films: 62% of the specific load (**Table 5-10 - Figure 5-56**), despite comprising only 30% w/w_d of the SRF dry mass; shoes: 14.5%) (**Table_App F-19**).
- Determination of the total chlorine showed low repeatability (%CV: 8.1%) (**Table 5-13**) resulting in confidence limits (d.f. = 3, $\alpha = 0.05$) comparable with the between-day sample variability (**Figure 5-63**), not allowing its precise evaluation, suggesting that improvements are necessary and 3 replications are a practical minimum.
- The UK MBT plant A produces an SRF of biogenic content on a dry ash-free basis that is just above the 50% threshold that currently appeals to the cement industry ($x_{B,daf}$: $55.5 \pm 2.7\%$ w/w_{daf}) (**Table 5-12 - Figure 5-71**).
- This level of biogenic content is achieved despite the fact that almost all the plastics (non-biogenic) are incorporated into the SRF, whilst $20.0 \pm 5.7\%$ of the paper (biogenic) is not (**Table 5-4 - Figure 5-35 - Figure 5-29**).
- Of the biogenic content present in the processing input, $77.7 \pm 3.4\%$ is incorporated into the SRF output (**Table 5-4 - Figure 5-52**).

- Almost 50% w/w of the ash content (from biogenic, non-biogenic or inert origin) present in the SRF samples dissolves during the selective dissolution (**Figure 5-68**), which justifies the need for reporting on a dry ash-free basis, because at the moment a suitable correction cannot be applied.
- The ash content (DD CEN/TS 15403:2006), on a dry basis, of the SRF produced in the UK MBT plant A is at (arithmetic mean) $18.1 \pm 1.6\%$ w/w_d (**Table 5-12**) which is close to the average of the values reported for European MBT-derived SRF (**Table 5-1**).
- The ash content of the UK MBT plant A (**Table 5-12**) clearly exceeds (**Figure 5-67**) the upper limit of 15% w/w_d, suitable for primary firing in cement kilns (**Table 2-16**), and is just marginally within the limit of 20% applicable to thermal recovery in certain types of power plants.
- Only $37.8 \pm 3.1\%$ of the ash content of the combustible part of the biodried input reports to the SRF (**Table 5-4**).
- There is potential to lower the ash content by reducing the mass fraction of the incombustible impurities in the SRF, which, despite being relatively low ($3.5 \pm 1.2\%$ w/w_d) (**Table App F-19 - Figure 5-21**), contributes considerably to the overall ash load; the non-ferrous metals in particular account for 10% (**Table 5-10 - Figure 5-57**).
- For this to be achieved, the performance of the eddy-current separator should be improved, currently transferring $64.1 \pm 10.2\%$ of its non-ferrous metal input to the SRF output (**Table 5-9 - Figure 5-48**).

- Plastic materials, already fully incorporated into the SRF, have a beneficial impact due to their low ash content (plastic film: 7.6% w/w_d; other packaging plastic: 1.6% w/w_d) (**Table 5-10 - Figure 5-57**).
- Incorporation of more paper would not alter the ash content level considerably of the average SRF, because is almost identical tho the average SRF ash content level (17.5% w/w_d) (**Table 5-10 - Table 5-12 - Figure 5-57**).
- The moisture content (DD CEN/TS 15414-2:2006), on an as-received basis of the SRF of the UK MBT plant A (15.0±2.6% w/w_{ar}) (**Table 5-12 - Figure 5-67**) is at the upper level of what is acceptable for the most demanding application of primary firing in cement kilns (**Table 2-16**).
- The paper contribution to the SRF ash load is considerable (68.4%) (**Table 5-10 - Figure 5-57**), whilst the readily biodegradable fractions (biological, fines <10 mm) can account for only limited amounts (3.5% and 0.5%, respectively) (**Table 5-10 - Figure 5-57**).
- Because the moisture content of the paper (**Table 5-12**) is higher than that of the SRF average (20.6% w/w_d) (**Table 5-10 - Figure 5-55**), any further increase of its SRF mass fraction would result in increased moisture content for the SRF. As a result, it is suggested that further improvements in the moisture content level could be sought in the direction of optimising the performance of the biodrying reactor.
- The calorific value (DD CEN/TS 15400:2006) of the UK MBT plant A SRF, expressed as net calorific value on an as-received basis, can be

potentially classified as CEN class 3 or 4 (depending on the statistic applied) ($15.7 \pm 0.9 \text{ MJ kg}_{\text{ar}}^{-1}$) (**Table 5-12 - Figure 5-73**).

- This calorific value (**Table 5-12 - Figure 5-73**) is below the threshold necessary for use in cement kiln primary firing ($>20 \text{ MJ kg}_{\text{ar}}^{-1}$) (**Table 2-16**), but could be suitable for less demanding applications (**Table 2-15**).
- The UK MBT plant A flowsheet results in most of the high calorific value contained in the waste components (plastic films: $30.7 \text{ MJ kg}_{\text{ar}}^{-1}$; other packaging plastic: $26.1 \text{ MJ kg}_{\text{ar}}^{-1}$) (**Table 5-10 - Figure 5-58**) to be entirely incorporated into the SRF product (**Table 5-4 - Figure 5-53**), together accounting for 43.6% of the SRF load (**Table 5-10 - Figure 5-58**).
- The trommel (**Table 5-5**) and the air classifier (**Table 5-6**) allow only modest quantities of the combustible mass to leave the SRF process line ($14.3 \pm 2.8\%$ and $15.4 \pm 21\%$, respectively) (**Figure 5-58**).
- Most of the combustible dry ash-free mass not incorporated into the SRF ($25.5 \pm 3.2\%$) (**Table 5-4 - Figure 5-26**) is in the form of paper, which has a considerably lower net calorific value ($13.0 \text{ MJ kg}_{\text{ar}}^{-1}$) (**Table 5-10 - Figure 5-58**). Increased reporting in the SRF output would result in further lowering of the net calorific value level, although on the whole more of the combustible matter would have been recovered by the plant.
- With the two major potential contributors to high calorific value already fully included in the SRF output (plastic films (**Figure 5-30**) and other packaging plastics (**Figure 5-31**)), there is very limited potential to

increase it through changes in the plant flowsheet operation. Potential improvements might be sought in incorporating more plastics-rich commercial waste in the plant input, or in improving the drying performance of the biodrying reactor.

- The between-days variability of the SRF properties, reflecting the plant production variability (and all indistinguishable sources of uncertainty during sampling and determination) indicate the following ranking of reduced variability (excluding samples of problematic plant operation), as estimated by the coefficient of variation: moisture content (22.8%) < total chlorine < total nitrogen < net calorific value, as received < ash content < biogenic content, dry ash-free (6.9%) (**Table 5-12**).
- The variability increases considerably when ca 25% samples of atypical plant operation are included (maximum: moisture content 49.4%, minimum: ash content 14.2%) (**Table 5-12**); hence, it might be advisable that regular trouble-free operation of the UK MBT plant should be prioritised over other performance improvements.

Overall the UK MBT plant A is reasonably optimised, and further improvements might be difficult to implement. If improvements are thought necessary, insights developed in this thesis can be of use; particularly regarding the inevitable trade-offs occurring when prioritising the potential presence of certain components over others in the SRF. For the UK MBT plant A it is now feasible to explore possibilities through sensitivity analysis, using the reported waste component properties and transfer coefficients.

The methodological approach followed resulted in an in-depth analysis of the SRF quality produced by the UK MBT plant A and paves the way for similar work to be

implemented in similar cases. It has also led to novel results, providing both the research community and the stakeholders commercially involved or through the public sector with conclusions of high relevance and applicability.

7.3 Future research suggestions

Future research can be identified through three main routes. Firstly, through the key research gaps identified in the critical review but not have been explored due to the inevitable limitations of resources. Secondly, by investigating points for which enhanced methodological understanding would have been beneficial. Thirdly, through questions posed by the conclusions of this research and/or any methodological achievements. Key future research recommendations with wider implications are listed below:

- There is a need to gain concrete understanding of what could constitute suitable quality for SRF for a series of end-uses. This should probably involve long-term data, for a more extensive characterisation suite.
- It is necessary to merge the knowledge that is relevant to the SRF quality management, especially regarding the mathematical/statistical tools available: theory of sampling, traditional statistical quality control, compliance statistics, uncertainty quantification, error propagation, data reconciliation.
- The above knowledge could be combined with additional empirical and, if feasible, first principle modelling of the material flow performance of unit operations used in MBT plants. This would enable researchers and practitioners to eventually get effective probabilistic modelling for the

SRF production leading to huge benefits for producers, end-users and regulators.

- The combination of novel methodological principles applied here for the first time could be repeated for a series of other MBT/MRF plants producing additional empirical data, useful for an in-depth understanding of such plants.
- The moisture content is a critical parameter that affects all other SRF quality characteristics - the calorific value in particular. It is necessary to gain a greater understanding of how the moisture of SRF changes from the production to storage and final end-use and how these changes relate to the values reported in the laboratory analysis
- A variogram according to the theory of sampling could provide us with a solid understanding of the minimum inevitable heterogeneity of MBT-derived SRF and reveal any periodicities in its year-round production.
- A sensitivity analysis should be performed for the UK MBT plant A using the developed transfer coefficients to investigate potential trade-offs for the production of SRF of varying quality.
- Ways should be sought to improve calorific value, moisture content and ash content of the MBT-derived SRF.
- A detailed probabilistic modelling exercise could quantify what is the exact achievable quality for MBT-derived SRF, starting from a biodried residual waste input.

- Optimisation of the performance of the eddy current separator and further investigation of the necessity for the air drum separator classification could improve the performance of the MBT plant A.
- The extensive dataset produced could be used for systematic evaluation of the material flow management performance of MBT plants, by using any of the potentially suitable tools, such as life-cycle analysis.

REFERENCES

- [1] Velis, C.A., Wilson, D.C., and Cheeseman, C.R., 19th century London dust-yards: A case study in closed-loop resource efficiency, *Waste Management* 29 (4), 1282, 2009.
- [2] Wilson, D.C., Development drivers for waste management, *Waste Management and Research* 25 (3), 198, 2007.
- [3] Döberl, G., Huber, R., Brunner, P.H., Eder, M., Pierrard, R., Schönback, W., Frühwirth, W., and Hutterer, H., Long-term assessment of waste management options - a new, integrated and goal-oriented approach, *Waste Management and Research* 20 (4), 311, 2002.
- [4] Lisney, R., Riley, K., and Banks, C.J., Waste as a resource: a discussion paper on the changes needed for the development of a resource recovery based waste strategy, *CIVM Scientific & Technical Review* 5 (2), 11, 2004.
- [5] Enviros, Mechanical biological treatment & mechanical heat treatment of municipal solid waste, Department of Environment Food and Rural Affairs (DEFRA), UK, 2005.
- [6] Steiner, M., MBT in Europe: roles & perspectives (part 2), *Warmer Bulletin* 103 8, 2006.
- [7] Steiner, M., MBT in Europe: roles & perspectives, *Warmer Bulletin* 102 14, 2005.
- [8] Kuehle-Weidemeier, M., The current situation of MBT in Germany, In: *International Symposium MBT 2007, 22-24 May 2007, Hanover, Germany*, Kuehle-Weidemeier, M. (Ed.), Cuvillier Verlag, 2007.
- [9] Heermann, C., Using Mechanical-Biological Treatment for MSW in Europe, *BioCycle* 44 (10), 58, 2003.
- [10] TBU - Eunomia - Greenpeace, Cool waste management. A state-of-the-art alternative to incineration for residual municipal waste, February 2003, Greenpeace Environmental Trust, London, 2003.
- [11] Müller, W. and Bulson, H., Significance of bio-mechanical waste treatment in Europe, In: *Waste 2004 - Integrated Waste Management and Pollution Control: Policy and Practice, Research and Solutions*, 28-30 September 2004, Stratford-upon-Avon, UK, 2004.
- [12] Bardos, R.P., Composting of mechanically segregated fractions of municipal solid waste – a review, SITA Environmental Trust, contractor: r³ Environmental Technology, 2005.
- [13] Juniper, Mechanical-biological treatment: a guide for decision makers, processes, policies and markets, CD-ROM, v1, March 2005, Juniper Consultancy Services, UK, 2005.
- [14] Stegmann, R., Mechanical biological pre-treatment of municipal solid waste, In: *Proceedings Sardinia 2005. Tenth international waste management and landfill symposium*, 3-7 October 2005, S. Margherita di Pula, Cagliari, Italy, 2005.
- [15] Binner, E., Mechanical biological pre-treatment of residual waste in Austria, In: *Sustainable Waste Management, Proceedings of the International Symposium*, 9-11 September 2003, University of Dundee, Scotland, UK, Dhir, R.K., Newlands, M.D., and Dyer, T.D. (Eds.), 2003.
- [16] Neubauer, C., Mechanical-biological treatment of waste in Austria: current developments, In: *International Symposium MBT 2007, 22-24 May 2007, Hanover, Germany*, Kuehle-Weidemeier, M. (Ed.), Cuvillier Verlag, 2007.
- [17] Papadimitriou, E.K., Stentiford, E., and Barton, J.R., *Deploying mechanical biological treatment in the UK*, *Wastes Management*, p.2, 2002.

- [18] Ibbetson, C., UK market development of solid recovered fuel from MBT plants, In: *Waste 2006 - Sustainable waste and resource management*, 19-21 September 2006, Stratford-upon-Avon, UK, 2006.
- [19] Bayard, R., de Brauer, C., Ducom, G., Morais, J.d.A., Achour, F., Moretto, R., Naquin, P., Sarrazin, B., Gourco, J.P., Riquier, L., and Berthet, J., Mechanical biological treatment and residual waste landfill in France: a case study, In: *International Symposium MBT 2005*, 23-25 November 2005, Hanover, Kühle-Weidemeier, M. (Ed.), Cuvillier Verlag, Göttingen, Germany, 2005.
- [20] Haritopoulou, T. and Lasaridi, K., Mechanical-biological treatment experiences in Greece: problems, trends and perspectives, In: *International Symposium MBT 2007*, 22-24 May 2007, Hanover, Germany, Kuehle-Weidemeir, M. (Ed.), Cuvillier Verlag, 2007.
- [21] Pires, A., Martinho, M.G., and Silveira, A., Could MBT plants be the solution of fulfil Landfill Directive targets in Portugal?, In: *International Symposium MBT 2007*, 22-24 May 2007, Hanover, Germany, Kuehle-Weidemeir, M. (Ed.), Cuvillier Verlag, 2007.
- [22] Council of the European Union, Council Directive 1999/31/EC on the landfill of waste, L 182, 16-07-1999, European Commission - Official Journal of the European Communities, 1999.
- [23] GTZ, Sector project. Mechanical-biological waste treatment, Deutsche Gesellschaft für Technische Zusammenarbeit (GTZ), Division 44 - Environment & Infrastructure, Eschborn, Germany, 2003.
- [24] Lornage, R., Redon, E., Lagier, T., Hébé, I., and Carré, J., Performance of a low cost MBT prior to landfilling: study of the biological treatment of size reduced MSW without mechanical sorting, *Waste Management* 27 (12), 1755, 2007.
- [25] Pereira, C.J., Practical experience with MBT in emerging nations - example Brazil, In: *International Symposium MBT 2005*, 23-25 November 2005, Hanover, Kühle-Weidemeier, M. (Ed.), Cuvillier Verlag, Göttingen, Germany, 2005.
- [26] Tränkler, J., Visvanathan, C., and Kurupan, P., Mechanical biological waste treatment – the south-east Asian experiences, In: *Proceedings Sardinia 2005. Tenth international waste management and landfill symposium*, 3-7 October 2005, S. Margherita di Pula, Cagliari, Italy, 2005.
- [27] Raninger, B., Bidlingmaier, W., Rundong, L., and Qi, W., Management of municipal solid waste In China - mechanical biological treatment can be an option? The Sino-German RRU-BMW Research Project to apply BMW within the framework of waste management related policies, In: *International Symposium MBT 2005*, 23-25 November 2005, Hanover, Kühle-Weidemeier, M. (Ed.), Cuvillier Verlag, Göttingen, Germany, 2005.
- [28] Brunner, P.H. and Rechberger, H., *Practical handbook of material flow analysis*, Lewis Publishers, Washington, D.C., US, 2004.
- [29] European Commission, Communication from the Commission: towards a thematic strategy on the prevention and recycling of waste, COM(2003) 301 final, 27 May 2003, Brussels, 2003.
- [30] McDougal, F., White, P., Franke, M., and Hindle, P., *Integrated solid waste management: a life cycle inventory*, 2nd ed, Blackwell Science, Oxford, 2001.
- [31] Baccini, P. and Brunner, P.H., *Metabolism of the anthroposphere*, Springer, New York, 1991.
- [32] Braungart, M. and McDonough, W., *Cradle to cradle. Remaking the way we make things*, 2nd ed, Vintage books, London, 2009.

- [33] Ibbetson, C. and Wengenroth, K., Optimisation of fuels from MBT processes, In: *International Symposium MBT 2007*, 22-24 May 2007, Hanover, Germany, Kuehle-Weidemeir, M. (Ed.), Cuvillier Verlag, 2007.
- [34] Garg, A., Smith, R., Hill, D., Simms, N., and Pollard, S., Wastes as co-fuels: The policy framework for solid recovered fuel (SRF) in Europe, with UK implications, *Environmental Science and Technology* 41 (14), 4868, 2007.
- [35] Steiner, M., Status of mechanical-biological treatment of residual waste and utilization of refuse-derived fuels in Europe, In: *The future of residual waste management in Europe*, 17-18 November 2005, Luxembourg, ORBIT Association, Centre de Recherche Public Henri Tudor, 2005.
- [36] Greiner, T., Market research: development of plant capacities for refuse derived fuel plants as a market for high calorific MBT output in Germany, In: *International Symposium MBT 2007*, Hanover, Germany, Kuehle-Weidemeir, M. (Ed.), Cuvillier Verlag, 2007.
- [37] Greiner, T., Swings and roundabouts. Demand for RDF swells in Germany, *Waste Management World* May-June 33, 2007.
- [38] Roos, H.-J. and Peters, W., Advanced processing production of municipal solid waste for the of high-grade quality fuels, In: *Proceedings Sardinia 2007. Eleventh international waste management and landfill symposium*, 1-5 October 2007, S. Margherita di Pula, Cagliari, Italy, 2007.
- [39] Hill, D., Garg, A., Smith, R., Pollard, S.J.T., and Longhurst, P., Appraisal for options of solid recovered fuel (SRF) utilisation within the UK, In: *Venice 2006 - Biomass and Waste to Energy Symposium*, November 29 - December 1, 2006, Cini Foundation, Island of San Giorgio Maggiore, Venice, Italy, EuroWaste, 2007.
- [40] Kronberger, R., Waste to recovered fuel: cost-benefit analysis, April 2001, European Commission, Directorate-General for Energy and Transport, 2001.
- [41] European Committee for Standardisation, Solid recovered fuels, PD CEN/TR 14745:2003, European Committee for Standardisation (CEN), 2003.
- [42] European Recovered Fuel Organisation, BREF waste treatment. Solid recovered fuels, European Recovered Fuel Organisation (ERFO), IAR Aachen, 2003.
- [43] Gendebien, A., Leavens, A., Blackmore, K., Godley, A., Lewin, K., Whiting, K.J., Davis, R., Giegrich, J., Fehrenbach, H., Gromke, U., del Bufalo, N., and Hogg, D., Refuse derived fuel, current practice and perspectives, B4-3040/2000/306517/MAR/E3, WRc Ref: CO5087-4, July 2003, WRc for the European Commission-Directorate General Environment, WRc, IFEU, Ecotec, Eunomia, Brussels, 2003.
- [44] Schulz-Ellermann, H.-J., Production of RDF in Europe today and development of standard, In: *FEAD-Congress Entsorga 2003*, 24 September 2003, Cologne, Germany, European Federation of Wastes and Environmental Services (FEAD), 2003.
- [45] Wilén, C., Salokoski, P., Kurkela, E., and Sipilä, K., Finnish expert report on best available techniques in energy production from solid recovered fuels, The Finnish Environment 668, Finnish Environment Institute, Helsinki, Finland, 2004.
- [46] Oakdene Hollins, Quantification of the potential energy from residuals (EfR) in the UK, Commissioned by The Institution of Civil Engineers and The Renewable Power Association, March 2005, 2005.
- [47] Beckmann, M. and Thomé-Kozmiensky, H.C.K.J., Substitute fuels – potential applications | [Ersatzbrennstoffe - Einsatzmöglichkeiten], *Aufbereitungs Technik/Mineral Processing* 47 (5), 10, 2006.
- [48] Frigerio, M., High quality solid recovered fuel (HQ-SRF): international perspectives of potential use and cost ranking among renewable energy sources, In: *Proceedings*

- Sardinia 2007. Eleventh international waste management and landfill symposium*, 1-5 October 2007, S. Margherita di Pula, Cagliari, Italy, 2007.
- [49] Silva, R.B., Barreiro, F., Navais, J.M., M, C., and Martin Dias, S., Refuse derived fuel production and use in Portugal, In: *Proceedings Sardinia 2007. Eleventh international waste management and landfill symposium*, 1-5 October 2007, S. Margherita di Pula, Cagliari, Italy, 2007.
- [50] Glorius, T., van Tubergen, J., Thomas, P., Khoury, A., and Uepping, R., Solid recovered fuels. Contribution to BREF "Waste Treatment", European Recovered Fuel Organisation (ERFO), Institute of Processing and Recycling of Solid Waste (I.A.R.), RWTH Aachen, Undated.
- [51] Beckmann, M., Karl, H.C., and Thomé-Kozmiensky, H.C.K.J., Waste-derived fuels – opportunities and problems | [Ersatzbrennstoffe - Chancen und probleme], *Aufbereitungs Technik/Mineral Processing* 47 (4), 28, 2006.
- [52] Eckardt, S. and Albers, H., Specifying criteria for the utilisation of refuse derived fuels (RDF) in industrial combustion plants, In: *Proceedings Sardinia 2003, Ninth International Waste Management and Landfill Symposium*, 6-10 October 2003, S. Margherita di Pula, Cagliari, Italy, 2003.
- [53] von Blottnitz, H., Pehlken, A., and Pretz, T., The description of solid wastes by particle mass instead of particle size distributions, *Resources, Conservation and Recycling* 34 (3), 193, 2002.
- [54] Pretz, T. and Onasch, K.-J., Mechanical processing of municipal solid waste with modern sorting technologies, In: *Proceedings Sardinia 2003, Ninth International Waste Management and Landfill Symposium*, 6-10 October 2003, S. Margherita di Pula, Cagliari, Italy, 2003.
- [55] Rotter, V.S., Kost, T., Winkler, J., and Bilitewski, B., Material flow analysis of RDF-production processes, *Waste Management* 24 (10), 1005, 2004.
- [56] Zwisele, B., Material flow and process analysis in MBT plants, In: *International Symposium MBT 2005*, 23-25 November 2005, Hanover, Germany, Kuehle-Weidemeier, M. (Ed.), Cuvillier Verlag, Göttingen, Germany, 2005.
- [57] Brunner, P.H. and Stampfli, D.M., Material balance of a construction waste sorting plant, *Waste Management & Research* 11 (1), 27, 1993.
- [58] Kost, T., Rotter, S., and Bilitewski, B., Chlorine and heavy metal content in house-hold waste fractions and its influence on quality control in RDF production processes, In: *Sardinia 2001, Eighth International Waste Management and Landfill Symposium*, 1-5 October 2001, S. Margherita di Pula, Cagliari, Italy, CISA, Environmental Sanitary Engineering Centre, 2001.
- [59] Adani, F., Baido, D., Calcaterra, E., and Genevini, P., The influence of biomass temperature on biostabilization-biodrying of municipal solid waste, *Bioresource Technology* 83 (3), 173, 2002.
- [60] Rada, E.C., Franzinelli, A., Taiss, M., Ragazzi, M., Panaitescu, V., and Apostol, T., Lower heating value dynamics during municipal solid waste bio-drying, *Environmental Technology* 28 (4), 463, 2007.
- [61] Her Majesty's Stationery Office, The Landfill (England and Wales) (Amendment) Regulations 2004, 0110493168 Statutory Instrument 2004 No. 1375, The Stationery Office HMSO, 2004.
- [62] Heering, B.M., Heering, M., and Heil, J., Processing waste to useful fractions with the Herhof dry stabilization technique | [Aufbereitung von Restabfall zu verwertbaren Teilfraktionen mit dem Herhof-Trockenstabilatverfahren], *Aufbereitungs-Technik/Mineral Processing* 40 (1), 11, 1999.

- [63] Gaillarde, E., Carbon footprint of solid recovered fuel, In: *First UK conference on solid recovered fuels*, 6 November 2008, London, Strange, K. (Ed.), Resource Recovery Forum - ERFO, 2008.
- [64] Flamme, S., The biogenic content in substitute fuels | [Biogener Anteil in ersatzbrennstoffen], *Aufbereitungs-Technik/Mineral Processing* 47 (3), 40, 2006.
- [65] Mohn, J., Szidat, S., Fellner, J., Rechberger, H., Quartier, R., Buchmann, B., and Emmenegger, L., Determination of biogenic and fossil CO₂ emitted by waste incineration based on ¹⁴CO₂ and mass balances, *Bioresource Technology* 99 (14), 6471, 2008.
- [66] Staber, W., Flamme, S., and Fellner, J., Methods for determining the biomass content of waste, *Waste Management and Research* 26 (1), 78, 2008.
- [67] Herhof GmbH, *Reference plants*, [www page] Available at: <http://www.herhof.com/en/business-divisions/stabilat/reference-plants.html> Last update: 2007 (Retrieved on: 20-11-2008).
- [68] Shanks Waste Management Ltd, The intelligent transfer station. A method for the treatment of municipal solid waste, May 2007, Shanks, Sistema Ecodeco, UK, 2007.
- [69] Calcaterra, E., Baldi, M., and Adani, F., An innovative technology for municipal solid waste energy recovery In: *C.I.P.A. - Centro di Ingegneria per la Protezione dell' Ambiente*, CIPA (Ed.), C.I.P.A, Milano, Italy, 123, 2000.
- [70] Wiemer, K. and Kern, M., *Mechanical biological treatment of residual waste based on the dry stabilize method*, M.I.C. Baeza-Verlag, Witzenhausen, Germany, 1994.
- [71] Soyez, K. and Plickert, S., Material flux management of waste by mechanical biological pre-treatment, In: *Proceedings Sardinia 2003, Ninth International Waste Management and Landfill Symposium*, 6-10 October 2003, S. Margherita di Pula, Cagliari, Italy, 2003.
- [72] The Composting Association, A guide to in-vessel composting. Plus a directory of system suppliers, The Composting Association, Wellingborough, UK, 2004.
- [73] Meinel, A., History of screening technology: Screen sizing and separation from the 20th century BC to the early 20th century AD | [Zur Geschichte der Siebtechnik: Siebklassierung vom 20. Jh. v. Chr. bis zum Anfang des 20. Jh. n. Chr.], *Aufbereitungs-Technik/Mineral Processing* 49 (7), 6, 2008.
- [74] Shapiro, M. and Galperin, V., Air classification of solid particles: a review, *Chemical Engineering and Processing* 44 (2), 279, 2005.
- [75] Timmel, G., Air-flow separation for residual waste treatment | [Aerostromsortierung bei der Restabfallaufbereitung], *Aufbereitungs-Technik/Mineral Processing* 47 (4), 16, 2006.
- [76] Hasselriis, F., *Refuse-derived fuel processing*, Butterworth Publishers, Boston, MA, US, 1984.
- [77] Barton, J.R., Poll, A.J., Webb, M., and Whalley, L., *Waste sorting and RDF production in Europe*, Elsevier Applied Science Publishers, London, 1985.
- [78] Tchobanoglous, G., Theisen, H., and Vigil, S.A., *Integrated solid waste management: engineering principles and management issues*, Mc-Graw Hill, New York, 1993.
- [79] Manser, A.G.R. and Keeling, A.A., *Practical handbook of processing and recycling municipal waste*, CRC Press, Lewis Publishers, 1996.
- [80] Pichtel, J., *Waste management practices: municipal, hazardous, and industrial*, CRC Press, Taylor & Francis Group, Boca Raton, FL, US, 2005.
- [81] Porteous, A., *Refuse derived fuels*, Applied Science Publishers, Halsted Press, London, 1981.
- [82] Diaz, L.F. and Savage, G.M., Approaches to mechanical-biological treatment of solid wastes, In: *International Seminar and Workshop "The sustainable landfilling"*, 13-15

- June 2005, Abbey of Praglia (Padua), Italy, CISA, Sanitary Environmental Engineering Centre, 2005.
- [83] Barton, J.R., Mechanical processing - what it can do and cannot do, In: *DEn/DoE/DTI Integrated Municipal Waste Management Seminars*, 25 June 1992, Bristol, UK, 1992.
- [84] Schubert, G. and Bernotat, S., Comminution of non-brittle materials, *International Journal of Mineral Processing* 74 (Supplement 1), S19, 2004.
- [85] Pourghahramani, P. and Forsberg, E., Review of applied particle shape descriptors and produced particle shapes in grinding environments. Part I: particle shape descriptors, *Mineral Processing and Extractive Metallurgy Review* 26 (2), 145, 2005.
- [86] Hogg, R., Turek, M.L., and Kaya, E., The role of particle shape in size analysis and the evaluation of comminution processes, *Particulate Science and Technology* 22 (4), 355, 2004.
- [87] Allen, T., *Particle size measurement*, 5th ed, Chapman and Hall, London, 1997.
- [88] American Society for Testing and Materials, Manual on test sieving methods, 0803104766, American Society for testing and Materials (ASTM), Philadelphia, PA, US, 1985.
- [89] European Committee for Standardisation, Solid recovered fuels – quality management systems - particular requirements for their application to the production of solid recovered fuels, PD CEN/TR 15358:2006, European Committee for Standardisation (CEN), 2006.
- [90] Nakamura, M., Castaldi, M.J., and Themelis, N.J., Measurement of particle size and shape of New York city municipal solid waste and combustion particles using image analysis, In: *Proceedings of the 16th Japan Society of Waste Management Experts (JSMWE) Fall Conference*, Sendai, Japan, 2005.
- [91] Nakamura, M., Castaldi, M.J., and Themelis, N.J., Numerical analysis of size reduction of municipal solid waste particles on the travelling grate of a waste-to-energy combustion chamber, In: *Proceedings of the 14th Annual North American Waste to Energy Conference, NAWTEC14*, Tampa, FL, 2006.
- [92] Pehlken, A., Uepping, R., and Pretz, T., Process assessment and quality assurance in waste processing | [Prozessbewertung und Qualitätssicherung in der Abfallaufbereitung], *Aufbereitungs-Technik/Mineral Processing* 46 (5), 21, 2005.
- [93] Deutsches Institut für Normung e.V., Investigations of the raw material in hard-coal-mining; determination of the particle-size-distribution > 20 µm by sieve-analysis, 03-1985, Deutsches Institut für Normung e.V. (DIN), 1985.
- [94] Trezek, G.J., Savage, G.M., and Obeng, D.M., Size reduction in solid waste processing: 2nd year progress report 1972-1973, EPA Report under Grant No. EPA R-801218, 1973.
- [95] Trezek, G.J. and Savage, G.M., MSW component size distributions obtained from the Cal resource recovery system, *Resource Recovery and Conservation* 2 (1), 67, 1976.
- [96] Ruf, J.A., Particle size spectrum and compressibility of raw and shredded MSW, PhD Thesis, University of Florida, FL, US, 1974.
- [97] Miller, A.P. and Clesceri, N.L., *Waste sites as biological reactors. Characterization and modelling*, CRC Press, Lewis Publishers, Boca Raton, FL, US, 2003.
- [98] Pfannkuch, H.O. and Paulson, R., *Grain size distribution and hydraulic properties*, [www page] Available at: <http://web.cecs.pdx.edu/~ian/geology2.5.html> (Retrieved on: 15-12-2006).
- [99] Zwisele, B., The necessity of material flow and process analyses for the assessment and optimization of waste management plants | [Die Notwendigkeit von Stoffstrom- Und Prozessanalysen zur Beurteilung und Optimierung abfallwirtschaftlicher Anlagen], *Aufbereitungs-Technik/Mineral Processing* 46 (5), 34, 2005.

- [100] McCabe, W., Smith, J.C., and Harriott, P., *Unit operations of chemical engineering*, 6th ed, McGraw Hill, New York, 2001.
- [101] Spencer, D.B., Temple, J.W., Forsythe, D.M., and Bond, B.E., Large-scale rotary shear shredder performance testing, *Journal of Energy Resources Technology, Transactions of the ASME* 107 (2), 289, 1985.
- [102] Breuer, W., Experiences with the operation of the Nehlsen drying plant Stralsund, In: *International Symposium MBT 2007*, 22-24 May 2007, Hanover, Germany, Kuehle-Weidemeir, M. (Ed.), Cuvillier Verlag, 2007.
- [103] Campbell, G.M. and Webb, C., On predicting roller milling performance: part I: the breakage equation, *Powder Technology* 115 (3), 234, 2001.
- [104] King, R.P., *Modelling and simulation of mineral processing systems*, Butterworth-Heinemann Publications, Oxford, UK, 2001.
- [105] Husemann, K., Modeling of Comminution Processes | [Zur Modellierung von Zerkleinerungsprozessen], *Chemie Ingenieur Technik* 77 (3), 205, 2005.
- [106] van Schaik, A., Reuter, M.A., and Heiskanen, K., The influence of particle size reduction and liberation on the recycling rate of end-of-life vehicles, *Minerals Engineering* 17 (2), 331, 2004.
- [107] Tchobanoglous, G. and Kreith, F., *Handbook of solid waste management*, 2nd ed, McGraw Hill, New York, 2002.
- [108] Nikolov, S., Modelling and simulation of particle breakage in impact crushers, *International Journal of Mineral Processing* 74 (Supplement 1), S219, 2004.
- [109] Shiflett, G.R. and Trezek, G.J., Parameters governing refuse comminution, *Resource Recovery and Conservation* 4 (1), 31, 1979.
- [110] Savage, G.M., Diaz, L.F., and Trezek, G.J., On-site evaluation of municipal solid waste shredders, *Resource Recovery and Conservation* 5 (4), 343, 1981.
- [111] Vesilid, P.A., Rimer, A.E., and Worrell, W.A., Performance characteristics of a vertical hammermill shredder, In: *Proceedings 1980 ASME national waste processing conference*, Washington, D.C., US, ASME, 1980.
- [112] Savage, G.M., Claub, J.C., and Diaz, L.F., Models of unit operations used for solid-waste processing, ANL/CNSV-TM-152, September 1984, Argonne National Laboratory (ANL), Argonne, IL, US, 1984.
- [113] Geyer, H.K. and Grammel, S.J., Municipal solid waste processing systems computer model, ANL/ENG/TM-03 (draft), March 1985, Argonne National Laboratory (ANL), Argonne, IL, US, 1985.
- [114] Wheeler, P.A. and Barton, J.R., Evaluation of the GRAB refuse processing simulation program and its future potential. Final report, ETSU B 1180, June 1987, Department of Energy, contractor: Warren Spring Laboratory, 1990.
- [115] Woldt, D., Schubert, G., and Jäckel, H.G., Size reduction by means of low-speed rotary shears, *International Journal of Mineral Processing* 74 (Supplement 1), S405, 2004.
- [116] McCormick, P.G. and Froes, F.H., The fundamentals of mechanochemical processing, *JOM* 50 (11), 61, 1998.
- [117] Faculty of chemical technology. University of Split, *Ball mill. Chemistry dictionary and glossary*, [www page] Available at: http://www.ktf-split.hr/glossary/en_index.html Last update: 2005 (Retrieved on: 20-10-07).
- [118] Suryanarayana, C., *Mechanical alloying/milling* CRC Press, Taylor & Francis Group, Boca Raton, FL, US, 2004.
- [119] Koch, P., Werning, W., and Pickert, B., Treatment of domestic refuse and residuals using the modular Hese MBWT process | [Haus- und restmüllbehandlung mit dem

- modularen Hese-MBA-verfahren], *Aufbereitungs-Technik/Mineral Processing* 42 (6), 284, 2001.
- [120] Koch, P., The role of size reduction in facilities for mechanical-biological treatment of domestic refuse (MBWT) | [Die rolle der zerkleinerung in anlagen zur mechanisch-biologischen abfallbehandlung von hausmüll (MBA)], *Aufbereitungs-Technik/Mineral Processing* 43 (4), 25, 2002.
- [121] Schade-Dannewitz, S., Studies on the mechanical-biological treatment of northern Thuringian waste | [Untersuchungen zur mechanisch-biologischen Behandlung Nordthüringer Restabfälle], *Aufbereitungs-Technik/Mineral Processing* 46 (4), 12, 2005.
- [122] Koch, P., The role of selective size reduction in facilities for mechanical- biological treatment of domestic refuse | [Zum Einfluss der selektiven Zerkleinerung auf Entwurf und Betrieb von mechanisch-biologischen Abfallbehandlungsanlagen von Haus- und Restmüll], *Aufbereitungs-Technik/Mineral Processing* 45 (8-9), 13, 2004.
- [123] University of Southampton, *The effect of particle size on the bio-processing of wastes*, Pickering, J., (Ed.) Technologies Research and Innovation Fund (TRIF), TRIF event, 2006.
- [124] Jackson, D.V., The economics of recycling - the national field, In: *Waste recycling - the next steps for local authorities*, 1 November 1978, 1978.
- [125] Kohaupt, U., Metal sorting in waste treatment - improvement of quality and economic backbone, In: *International Symposium MBT 2007, 22-24 May 2007*, Hanover, Germany, Kuehle-Weidemeir, M. (Ed.), Cuvillier Verlag, 2007.
- [126] Rietema, K., On the efficiency in separating mixtures of two constituents, *Chemical Engineering Science* 7 (1-2), 89, 1957.
- [127] Klumpar, I., Measuring and optimizing air classifier performance, *Separations Technology* 2 (3), 124, 1992.
- [128] Worrell, W.A. and Vesilind, P.A., Testing and evaluation of air classifier performance, *Resource Recovery and Conservation* 4 (3), 247, 1979.
- [129] Vesilind, P.A. and Rimer, A.E., *Unit operations in resource recovery engineering*, Prentice Hall, Englewood Cliffs, NJ, US, 1981.
- [130] Everett, J.W. and Peirce, J.J., The development of pulsed flow air classification theory and design for municipal solid waste processing, *Resources, Conservation and Recycling* 4 (3), 185, 1990.
- [131] American Society for Testing and Materials, Standard test method for determination of the recovery of a product in a materials separation device, E 1108-828 (Reapproved 2004), July 1986, American Society for testing and Materials (ASTM), Philadelphia, PA, US, 1986.
- [132] Schweitzer, P.A., (Ed.) *Handbook of separation techniques for chemical engineers* 3rd ed. McGraw-Hill, 1997.
- [133] Wang, Q., Melaaen, M.C., and De Silva, S.R., Investigation and simulation of a cross-flow air classifier, *Powder Technology* 120 (3), 273, 2001.
- [134] American Society for Testing and Materials, Standard test method for composition or purity of a solid waste materials stream, E 889-82 (Reapproved 2004), May 1983, American Society for testing and Materials (ASTM), Philadelphia, PA, US, 1983.
- [135] Vesilind, P.A., Air classification of shredder refuse, *Conservation & Recycling* 9 (1), 35, 1986.
- [136] Rhyner, C.R., Schwartz, L.J., Wenger, R.B., and Kohrell, M.G., *Waste management and resource recovery*, CRC Press, Boca Raton, 1995.
- [137] Diaz, L.F., Savage, G.M., and Golueke, C.G., *Resource recovery from municipal solid wastes*, Vol. 1, CRC Press, Boca Raton, FL, US, 1982.

- [138] Caputo, A.C. and Pelagagge, P.M., RDF production plants: I. Design and costs, *Applied Thermal Engineering* 22 (4), 423, 2002.
- [139] Chang, Y.H., Chang, N.B., and Chen, W.C., Systematic evaluation and uncertainty analysis of the refuse-derived fuel process in Taiwan, *Journal of the Air and Waste Management Association* 48 (6), 537, 1998.
- [140] Zwisele, B., Rosenkranz, J., and Nordwig, A., Simulation of mechanical processing in waste management, In: *International Symposium MBT 2007, 22-24 May 2007*, Hanover, Germany, Kuehle-Weidemeir, M. (Ed.), Cuvillier Verlag, 2007.
- [141] Huang, W.L., Lin, D.H., Chang, N.B., and Lin, K.S., Recycling of construction and demolition waste via a mechanical sorting process, *Resources, Conservation and Recycling* 37 (1), 23, 2002.
- [142] Belevi, H. and Langmeier, M., Factors determining the element behavior in municipal solid waste incinerators. 2. Laboratory experiments, *Environmental Science and Technology* 34 (12), 2507, 2000.
- [143] Belevi, H. and Moench, H., Factors determining the element behavior in municipal solid waste incinerators. 1. Field studies, *Environmental Science and Technology* 34 (12), 2501, 2000.
- [144] Fehringer, R., Brandt, B., Brunner, P.H., Daxbeck, H., Neumayer, S., Smutny, R., Villeneuve, J., Michael, P., Kranert, M., Schultheis, A., and Steinbach, D., MFA manual. Guidelines for the use of material flow analysis (MFA) for municipal solid waste (MSW) management, Project AWAST, Contract title: EVK4-CT-2000-00015, Vienna University of Technology – Institute for Water Quality and Waste Management, Resource Management Agency, Bureau de Recherches Geologiques et Minieres, Stuttgart University – Institute for Water Quality and Waste Management, Undated.
- [145] Thomé-Kozmiensky, K.J., Processing concepts for substitute fuels | [Aufbereitungskonzepte für ersatzbrennstoffe], *Aufbereitungs-Technik/Mineral Processing* 43 (4), 11, 2002.
- [146] Hüttner, A., Maximum recovery of the outputs of MBT and AD plants treating grey fraction or combined MSW, In: *Biometa 05*, 14-15 November 2005, 2005.
- [147] HAASE, *Welcome to Luebeck MBT plant*, 2005.
- [148] Williams, E., Review of the literature on the use of trommels in waste processing and resource recovery, DOE Contract No. AGO 1-76CS20167, July 1981, National Centre for Resource Recovery, Washington, D.C., US, 1981.
- [149] Sullivan, J.W., Hill, R.M., and Sullivan, J.F., Place of the trommels in resource recovery, In: *Proceedings of National Waste Processing Conference*, Detroit, MI, US, ASME, 1992.
- [150] Lau, S.T., Cheung, W.H., Kwong, C.K., Wan, C.P., Choy, K.K.H., Leung, C.C., Porter, J.F., Hui, C.W., and Mc Kay, G., Removal of batteries from solid waste using trommel separation, *Waste Management* 25 (10), 1004, 2005.
- [151] Wheeler, P.A., Barton, J.R., and New, R., An empirical approach to the design of trommel screens for fine screening of domestic refuse, *Resources, Conservation and Recycling* 2 (4), 261, 1989.
- [152] Stessel, R.I., A new trommel model, *Resources, Conservation and Recycling* 6 (1), 1, 1991.
- [153] Stessel, R.I. and Cole, K., Laboratory investigation of a new trommel model, *Journal of the Air and Waste Management Association* 46 (6), 558, 1996.
- [154] Piekarczyk, M. and Ciurej, H., Trommel screens for waste utilization. Computer aided design, *Archives of Civil Engineering* 44 (1), 107, 1998.

- [155] Fricke, K. and Mueller, W., Stabilisation of residual waste by mechanical-biological treatment and consequences for landfills. Final report for the German Federal research project on mechanical-biological treatment of waste before landfill, IGW, Witzenhausen, 1999.
- [156] Pilz, G., Stoffstromtrennverfahren der Linde-KCA (In German) | [Material separation for Linde-KCA], In: *Reformbedarf in der Abfallwirtschaft | [Necessary reform for waste management]*, Thomé-Kozmiensky, K.J. (Ed.), TK Verlag, Neuruppin, Germany, 347, 2001.
- [157] Koch, P., Pickert, B., and Wayman, P., The role of selective size reduction in facilities for mechanical biological treatment of domestic refuse, In: *Biodegradable and residual waste management: 1st UK Conference and exhibition*, 18-19 February 2004., Harrogate, UK, E.K. Papadimitriou and E.I. Stentiford (Ed.), Cal Recovery Europe Ltd, 2004.
- [158] Delgenes, J.P., Penaud, V., and Moletta, R., Pretreatments for the enhancement of anaerobic digestion of solids wastes, In: *Biomethanization of the organic fraction of municipal solid wastes*, Mata-Alvarez, J. (Ed.), IWA Publishing, London, 201, 2003.
- [159] Palmowski, L.M. and Mueller, J.A., Anaerobic degradation of organic materials. Significance of the substrate surface area, *Water Science and Technology* 47 (12), 231, 2003.
- [160] Palmowski, L.M. and Mueller, J.A., Influence of the size reduction of organic waste on their anaerobic digestion, *Water Science and Technology* 41 (3), 155, 2000.
- [161] Baaden, A., Mundhenke, R., Mueller, J.A., and Schwedes, J., Physical properties and comminution behaviour of organic materials, In: *Reprints 10th European Symposium on Comminution*, Heidelberg, Germany, 2002.
- [162] Haug, R.T., *The practical handbook of compost engineering*, CRC Press, Lewis Publishers, Boca Raton, FL, USA, 1993.
- [163] Silvestri, S., Dallago, L., Odorizzi, G., Zorzi, G., Gardelli, G., and Ragazzi, M., Biological stabilization of residual solid waste: technologies and methods, In: *Proceedings Sardinia 2005. Tenth international waste management and landfill symposium*, 3-7 October 2005, S. Margherita di Pula, Cagliari, Italy, 2005.
- [164] Mueller, W., Niesar, M., and Turk, T., Optimized mechanical treatment and material segregation through ballistic separation within mechanical biological waste treatment, In: *Proceedings Sardinia 2003, Ninth International Waste Management and Landfill Symposium*, 6-10 October 2003, S. Margherita di Pula, Cagliari, Italy, 2003.
- [165] Peirce, J.J., Understanding technology: new concepts for air classification in waste processing and resource recovery, In: *Proceedings – Frontiers in Education Conference*, West Lafayette, IN, US, IEEE, 1991.
- [166] Savage, G., Diaz, L., and Goldstein, N., A compost screening primer, *BioCycle* 46 (5), 55, 2005.
- [167] He, Y.Q., Wang, H.F., Duan, C.L., and Song, S.L., Numerical simulation of airflow patterns within passive pulsing air classifiers, *Zhongguo Kuangye Daxue Xuebao/Journal of China University of Mining and Technology* 34 (5), 574, 2005.
- [168] Bartlett, J., The effect of moisture on air classification on municipal solid waste, MSc Thesis, Duke University, Durham, NC, US, 1983.
- [169] Taub, J., The effect of feed composition on air classifier performance, MSc Thesis, Duke University, Durham, NC, US, 1981.
- [170] Biddulph, M.W. and Connor, M.A., A method of comparing the performance of air classifiers, *Resources, Conservation and Recycling* 2 (4), 275, 1989.
- [171] Flitton, J.T., Refuse handling and processing by air classification, In: *Refuse Handling and Processing*, 11 May 1978, London, Institution of Mechanical Engineers, 1978.

- [172] Wakita, S., Recycling of waste plastics in NKK, *SEASI Quarterly (South East Asia Iron and Steel Institute)* 31 (4), 60, 2002.
- [173] Mitsubishi Rayon Engineering, *Ballistic sorter*, [www page] Available at: http://www.mrc.co.jp/mre/english/recycle/recycle_05.html Last update: 2004 (Retrieved on: 15-09-2007).
- [174] Bilitewski, B., Recyclinganlagen für Haus- Und Gewerbeabfall (In German) | [Recycling plants for household and commercial waste], *Müll & Abfall* Beiheft 21 1985.
- [175] O.Key Engineering, *Which screen do I need?*, [www page] Available at: http://www.okay.co.uk/products_mrf_s_which_one.htm (Retrieved on: 20-2-2007).
- [176] Harbeck, H. and Kroog, H., New developments in sensor-based sorting | [Neue Entwicklungen in der Sensorgestützten Sortierung], *Aufbereitungs-Technik/Mineral Processing* 49 (5), 4, 2008.
- [177] Zeiger, E., Sorting waste streams with mogensen X-ray sorting systems | [Sortierung verschiedener abfallströme mit mogensen-röntgensortiertechnik], *Aufbereitungs-Technik/Mineral Processing* 47 (3), 16, 2006.
- [178] Schirmer, M., Janz, A., Bilitewski, B., and Rotter, S., Sources of chlorine in MSW and RDF – species, analytical methods and requirements on improved separation methods, In: *Proceedings Sardinia 2005, Tenth International Waste Management and Landfill Symposium*, 3-7 October 2005, S. Margherita di Pula, Cagliari, Italy, 2005.
- [179] Ma, W. and Rotter, S., Overview on the chlorine origin of MSW and Cl-originated corrosion during MSW & RDF combustion process, In: *2nd International Conference on Bioinformatics and Biomedical Engineering, iCBBE 2008*, Shanghai, 2008.
- [180] Wengenroth, K., New developments in the dry stabilize process | [Neue Entwicklungen beim Trockenstabilat-Verfahren], *Aufbereitungs-Technik/Mineral Processing* 46 (3), 14, 2005.
- [181] Skutan, S. and Brunner, P.H., Stoffbilanzen mechanisch-biologischer anlagen zur behandlung von restmüll (SEMBA) (in German) | [Material balances for mechanical-biological facilities treating residual waste (SEMBA)], July 2006, Institute for Water Quality, Resources and Waste Management, Vienna University of Technology, Vienna, Austria, 2006.
- [182] Barton, J.R. and Wheeler, P.A., The benefits of front end trommelling in processing municipal solid wastes. Trials at the Byker plant, LR 661 (MR)M June 1987, Department of Trade and Industry, contractor: Warren Spring Laboratory, 1987.
- [183] Heilmann, A. and Bilitewski, B., High-grade fuel derived from residual waste, In: *Sardinia 1999, Seventh International Waste Management and Landfill Symposium*, 4-8 October 1999, S. Margherita di Pula, Cagliari, Italy, CISA, Environmental Sanitary Engineering Centre, 1999.
- [184] British Standards Institution, Quality management systems - fundamentals and vocabulary, BS EN ISO 9000:2005, British Standards Institution (BSI), 2005.
- [185] Valtanen, J., Alakangas, E., and Levlin, J.-E., Fuel quality assurance, In: *International Conference. Standardisation of solid biofuels*, 6-7 October 2004, Leipzig, Germany, Hein, M. and Kaltschmitt, M. (Eds.), Institute for Energy and Environment, 2004.
- [186] Cuperus, J.G. and van Dijk, E.A., Determination of the biomass fraction in solid recovered fuels, R003-3907341JGC-D01-D, 6 June 2002, TAUW, Deventer, The Netherlands, 2002.
- [187] Environment Agency, Compost quality protocol, Waste & Resources Action Programme (WRAP), Oxon, UK, 2007.
- [188] British Standards Institution, Specification for composted materials, BSI PAS 100:2005, 31 March 2005, British Standards Institution (BSI), 2005.

- [189] Mason, C., *Landspreading sewage sludge on agricultural land*, [www page] Available at: http://www.netregs.gov.uk/netregs/sectors/1770583/1771509/1774438/?version=1&lang=_e Last update: 16-07-2007 (Retrieved on: 15-09-2007).
- [190] Lasaridi, K., Protopapa, I., Kotsou, M., Pilidis, G., Manios, T., and Kyriacou, A., Quality assessment of composts in the Greek market: the need for standards and quality assurance, *Journal of Environmental Management* 80 (1), 58, 2006.
- [191] European Committee for Standardisation, Solid recovered fuels – specifications and classes, DD CEN/TS 15350:2006, European Committee for Standardisation (CEN), 2006.
- [192] Saft, R.J. and Elsinga, W., Source separation, composting a win for greenhouse gas reduction, *BioCycle* 47 (6), 50, 2006.
- [193] Ibbetson, C., Chappell, J., and Wengenroth, K., European market development - solid recovered fuel from MBT plants, In: *International Symposium MBT 2005*, 23-25 November 2005, Hanover, Kühle-Weidemeier, M. (Ed.), Cuvillier Verlag, Göttingen, Germany, 2005.
- [194] Garg, A., Smith, R., Hill, D., and Pollard, S.J.T., An integrated, quantitative appraisal of options for the utilisation of solid recovered fuel (SRF) from the mechanical-biological treatment of MSW, Report to Grantscape No. 760828/1, July 2007, Cranfield University, Integrated Waste Management Centre (IWMC), Cranfield, UK, 2006.
- [195] Michels, N., Tenders and contracts for the sale of RDF, In: *International Symposium MBT 2007*, 22-24 May 2007, Hanover, Germany, Kuehle-Weidemeir, M. (Ed.), Cuvillier Verlag, 2007.
- [196] Langheinrich, M. and Kaltschmitt, M., Implementation and application of quality assurance systems, In: *International Conference. Standardisation of solid biofuels*, 6-7 October 2004, Leipzig, Germany, Hein, M. and Kaltschmitt, M. (Eds.), Institute for Energy and Environment, 2004.
- [197] Alakangas, E., Lensu, T., Haglund, N., and Nitschke, M., Bioenergy 2003 – 2005. Action 2: Development of standards to achieve market harmonisation in the bioenergy field. Review of the present status and future prospects of standards and regulations in the bioenergy field, PRO2/P2031/05, 9-9-2005, VTT Processes, NAH Consulting, Elsam Engineering, 2005.
- [198] European Commission, IPPC draft reference document on best available techniques for waste treatment industries, MA/EIPPCB/WT_Draft_2, January 2004, Institute for Prospective Technological Studies, European IPPC Bureau, Seville, Spain, 2004.
- [199] Flamme, S., Quality certification mark for secondary fuels RAL-GZ 724 | [Gütezeichen für Sekundärbrennstoffe RAL-GZ 724], *ZKG International* 58 (8), 51, 2005.
- [200] American Society for Testing and Materials, Annual ASTM standards. Vol 11.04, Vol 11.04, American Society for testing and Materials (ASTM), Philadelphia, PA, US, 1985.
- [201] Alter, H., The history of refuse-derived fuels, *Resources and Conservation* 15 (4), 251, 1987.
- [202] European Association of Waste Thermal Treatment Companies for Specialised Waste, *Methodology for the determination of technical co-incineration criteria*, [www page] Available at: <http://www.eurits.org/pages/coincineration.asp#> (Retrieved on: 15-09-2007).
- [203] World Business Council for Sustainable Development, *Guidelines for the selection and use of fuels and raw materials in the cement manufacturing process*, Cement Sustainability Initiative (CSI), WBCSD, Geneva, Switzerland, 2005.
- [204] van Tubergen, J., Glorius, T., and Waeyenbergh, E., Classification of solid recovered fuels, February 2005, European Recovered Fuel Organisation (ERFO), 2005.

- [205] Finish Standards Association, Solid recovered fuel. Quality control system, 24-01-2000, Finish Standards Association (FSF), 2000.
- [206] German Institute for Quality Assurance and Certification, Solid recovered fuels. Quality assurance, RAL-GZ 724, June 2001, German Institute for Quality Assurance And Certification (RAL), 2001.
- [207] Zanotta, C., I.D.E.A. GRANDA: over 4 years experience of co-firing HQ-SRF in cement kiln, In: *Proceedings Sardinia 2007. Eleventh international waste management and landfill symposium*, 1-5 October 2007, S. Margherita di Pula, Cagliari, Italy, 2007.
- [208] Cuperus, J.G., van Dijk, E.A., and de Boer, R.C., Pre-normative research on SRF, R001-4271783EDA-rvb-V01-NL, 13 September 2005, TAUW, Deventer, The Netherlands, 2005.
- [209] Environment Agency, *Substitute fuels protocol for use in cement and lime kilns*, Environment Agency (EA), 2005.
- [210] European Committee for Standardisation, Key properties on solid recovered fuels to be used for establishing a classification system, PD CEN/TR 15508:2006, European Committee for Standardisation (CEN), 2006.
- [211] European Council, Directive 2000/76/EC of the European Parliament and of the Council of 4 December 2000 on the incineration of waste, L 332/92, 28-12-2000, 2000.
- [212] Niessen, W.P., *Combustion and incineration processes*, 3rd ed, Marcel Dekker, New York, 2002.
- [213] Hilber, T., Martensen, M., Maier, J., and Scheffknecht, G., A method to characterise the volatile release of solid recovered fuels (SRF), *Fuel* 86 (1-2), 303, 2007.
- [214] Hartmann, H., Physical-mechanical fuel properties - significance and impacts, In: *International Conference. Standardisation of solid biofuels*, 6-7 October 2004, Leipzig, Germany, Hein, M. and Kaltschmitt, M. (Eds.), Institute for Energy and Environment, 2004.
- [215] Obernberger, I., Brunner, T., and Baerenthaler, G., Chemical fuel properties - significance and impact, In: *International Conference. Standardisation of solid biofuels*, 6-7 October 2004, Leipzig, Germany, Hein, M. and Kaltschmitt, M. (Eds.), Institute for Energy and Environment, 2004.
- [216] Roberts, N., CEMEX UK Climafuel. Case study, In: *First UK conference on solid recovered fuels*, 6 November 2008, London, Stragne, K. (Ed.), Resource Recovery Forum - ERFO, 2008.
- [217] Achternbosch, M., Bräutigam, K.-R., Gleis, M., Hartlieb, N., Kupsch, C., Richers, U., and Stemmermann, P., Heavy metals in cement and concrete resulting from the co-incineration of wastes in cement kilns with regard to the legitimacy of waste utilisation, FZKA 6923, October 2003, Forschungszentrum Karlsruhe, Karlsruhe, Germany, 2003.
- [218] SINTEF, Formation and release of POPs in the cement industry, 2nd ed, 23 January 2006, World Business Council for Sustainable Development (WBCSD), Geneva, Switzerland, 2006.
- [219] Coda, B., Aho, M., Berger, R., and Hein, K.R.G., Behavior of chlorine and enrichment of risky elements in bubbling fluidized bed combustion of biomass and waste assisted by additives, *Energy and Fuels* 15 (3), 680, 2001.
- [220] Balampanis, D., Simms, N., and Villa, R., Transfer coefficients and organochloride load of a 'chlorine-class 2' solid recovered fuel in fluidized bed combustion, In: *Proceedings Venice 2008, Second International Symposium on Energy from Biomass and Waste*, Venice, Italy, CISA, Environmental Sanitary Engineering Centre, 2008.
- [221] Bøjer, M., Jensen, P.A., Frandsen, F., Dam-Johansen, K., Madsen, O.H., and Lundtorp, K., Alkali/Chloride release during refuse incineration on a grate: Full-scale experimental findings, *Fuel Processing Technology* 89 (5), 528, 2008.

- [222] Liu, G.-Q., Itaya, Y., Yamazaki, R., Mori, S., Yamaguchi, M., and Kondoh, M., Fundamental study of the behavior of chlorine during the combustion of single RDF, *Waste Management* 21 (5), 427, 2001.
- [223] Sorell, G., The role of chlorine in high temperature corrosion in waste-to-energy plants, *Materials at High Temperatures* 14 (3), 207, 1997.
- [224] Danuvola, L. and Freimann, W., Chlorine bypass, *World Cement* 37 (1), 107, 2006.
- [225] Opoczky, L. and Gavel, V., Effect of certain trace elements on the grindability of cement clinkers in the connection with the use of wastes, *International Journal of Mineral Processing* 74 (Supplement 1), S129, 2004.
- [226] Cozens, P., EfW - an alternative vision, In: *Biodegradable and residual waste management: 1st UK conference and exhibition*, 18-19 February 2004, Harrogate, UK, Papadimitriou, E.K. and Stentiford, E.I. (Eds.), Cal Recovery Europe Ltd, 2004.
- [227] Kakaras, E., Grammelis, P., Agraniotis, M., Derichs, W., Shchiffer, H.-P., Maier, J., Hilber, T., Glorius, T., and Becker, U., Solid recovered fuel as coal substitute in the electricity generation sector, *Thermal Science* 9 (2), 17, 2005.
- [228] Schultz, W., Einsatz von Sekundärbrennstoffen in Grosskraftwerken. Sekundärbrennstoffe und erneuerbare Energien (In German) | [Application of secondary fuels in main power stations. Secondary fuels and renewable energy], In: *Bundesgütegemeinschaft Sekundärbrennstoffe e.V., Entsorga 2003*, Clogne, 2003.
- [229] Beckmann, M. and Thomé-Kozmiensky, H.C.K.J., Das Ersatzbrennstoffproblem (In German) | [The waste-derived fuel problem], In: *Ersatzbrennstoffe 5 - Herstellung und Verwertung | [Waste-derived fuels 5 - production and utilisation]*, November 2005, Berlin, Germany, Neuruppin, S. (Ed.), TK-Verlag, 2005.
- [230] Fernandez, A., Wendt, J.O.L., Wolski, N., Hein, K.R.G., Wang, S., and Witten, M.L., Inhalation health effects of fine particles from the co-combustion of coal and refuse derived fuel, *Chemosphere* 51 (10), 1129, 2003.
- [231] Hamel, S., Hasselbach, H., Weil, S., and Krumm, W., Autothermal two-stage gasification of low-density waste-derived fuels, *Energy* 32 (2), 95, 2007.
- [232] Kobayashi, N., Itaya, Y., Piao, G., Mori, S., Kondo, M., Hamai, M., and Yamaguchi, M., The behavior of flue gas from RDF combustion in a fluidized bed, *Powder Technology* 151 (1-3), 87, 2005.
- [233] Jand, N., Brandani, V., and Foscolo, P.U., Thermodynamic limits and actual product yields and compositions in biomass gasification processes, *Industrial and Engineering Chemistry Research* 45 (2), 834, 2006.
- [234] Kilgallon, P., Simms, N.J., and Oakey, J.E., Fate of trace contaminants from biomass fuels in gasification systems, In: *Materials for advanced powered engineering 2002*, Lecomte-Beckers, J., Carton, M., Schubert, F., and Ennis, P. (Eds.), Forschungszentrum Juelin GmbH, Liege, France, 903, 2002.
- [235] Niederdränk, J., Wirtgen, C., and Heil, J., Studies of the thermal upgrading of mechanically and biologically treated waste, *Aufbereitungs-Technik/Mineral Processing* 44 (2), 2003.
- [236] Kock, O., Development of a characterization method for the combustion behavior of solid recovered fuels, *Chemical Engineering and Technology* 27 (7), 743, 2004.
- [237] Kehl, I.P., Scharf, K.-F., Scur, P., and Wirthwein, R., Die Betriebsergebnisse aus den ersten 30 Monaten mit der neuen Ofenlinie 5 im Zementwerk Rüdersdorf (In German) | [Results from the first 30 operating months of new stove line 5 in the cement works at Rüdersdorf], *ZKG International* 51 (8), 410, 1998.
- [238] Herhof Environmental, Biological-mechanical waste plant - Dresden, Saxony, Germany, Undated.

- [239] Herhof GmbH, Clean energy from waste, Undated.
- [240] European Committee for Standardisation, Solid recovered fuels. Report on relative difference between biodegradable and biogenic fractions of SRF, CEN/TR 14980:2004, European Committee for Standardisation (CEN), 2005.
- [241] Department of Trade and Industry, Renewables obligation order 2006 – final decisions, January 2006, Department of Trade and Industry (DTI), 2006.
- [242] Environmental Resources Management, Carbon balances and energy impacts of the management of UK waste streams, WR0602, 1 January 2006, Defra, contractor: Environmental Resources Management (ERM), Oxford, UK, 2005.
- [243] Energy Information Administration, Methodology for allocation municipal solid waste to biogenic and non-biogenic energy, 20585, May 2007, Energy Information Administration (EIA), U.S. Department of Energy, Washington, D.C., US, 2007.
- [244] European Committee for Standardisation, Solid recovered fuels – specifications and classes: final draft, CEN/TC 343/WG 2 N092 Final Draft, European Committee for Standardisation (CEN), Undated.
- [245] European Committee for Standardisation, Solid recovered fuels – ¹⁴C-based methods for the determination of the biomass content, DD CEN/TS 15747:2008, 31-03-2007, European Committee for Standardisation (CEN), 2008.
- [246] Ofgem, Renewables obligation: fuel measurement and sampling guidance, 57/07, 29-03-2007, Ofgem, London, 2007.
- [247] Fellner, J., Cencic, O., and Rechberger, H., A new method to determine the ratio of electricity production from fossil and biogenic sources in waste-to-energy plants, *Environmental Science and Technology* 41 (7), 2579, 2007.
- [248] Uerkvitz, R. and Goetz, D., Statistical estimation of chemical characteristics for dispersed solid matter, *Waste Management and Research* 16 (1), 83, 1998.
- [249] Chang, N.-B., Chang, Y.-H., and Chen, W.C., Evaluation of heat value and its prediction for refuse-derived fuel, *Science of The Total Environment* 197 (1-3), 139, 1997.
- [250] Montgomery, D.C., *Introduction of statistical quality control*, 6th ed, John Wiley & Sons, 2009.
- [251] StatSoft, Statistica 8. Data analysis software system, Version 8, 2008.
- [252] Ledolter, J. and Burrill, C.W., *Statistical quality control. Strategies and tools for continual improvement*, John Wiley & Sons, USA, 1999.
- [253] Glorius, T., Remondis - SRF in a German power plant, In: *First UK conference on solid recovered fuels*, 6 November 2008, London, Stragne, K. (Ed.), Resource Recovery Forum - ERFO, 2008.
- [254] Desimoni, E. and Brunetti, B., Uncertainty of measurement: approaches and open problems, *Annali di Chimica* 95 (5), 265, 2005.
- [255] Ellison, S.L.R. and Williams, A., Use of uncertainty information in compliance assessment, Eurachem/CITAC, 2007.
- [256] International Organization for Standardization / International Electrochemical Commission, Guide 98-3:2008, Uncertainty of measurement – Part 3: guide to the expression of uncertainty in measurement (GUM:1995), 98-3:2008, ISO/IEC, 2008.
- [257] Ellison, S.L.R., Rosslein, M., and Williams, A., *Quantifying uncertainty in analytical measurement*, 2nd ed, Eurachem/CITAC, 2000.
- [258] American Society of Mechanical Engineers, Guidelines for decision rules: considering measurement uncertainty in determining conformance with specifications, B89.7.3.1-2001, Reaffirmed 2006, American Society of Mechanical Engineers (ASME), Philadelphia, PA, US, 2001.

- [259] European Committee for Standardisation, Solid recovered fuels – specifications and classes, DD CEN/TC 343/WG2 N111, 12-11-2007, European Committee for Standardisation (CEN), 2007.
- [260] Dean, R.B. and Dixon, W.J., Simplified statistics for small numbers of observations, *Analytical Chemistry* 23 (4), 636, 1951.
- [261] Shapiro, S., Wilk, M., An analysis of variance test for normality, *Biometrika* 52 (3 and 4), 591, 1965.
- [262] Henderson, A.R., Testing experimental data for univariate normality, *Clinica Chimica Acta* 366 (1-2), 112, 2006.
- [263] Dieck, H.R., *Measurement uncertainty. Methods and applications*, 4th ed, ISA - The Instrumentation, Systems and Automation Society, NC, USA, 2007.
- [264] European Committee for Standardisation, Solid recovered fuels – methods for sampling, DD CEN/TS 15442:2006, 28-02-2007, European Committee for Standardisation (CEN), 2006.
- [265] CEMEX, Rugnby works permit BL7248. Application for a Variation under PPC to allow use of a fuel known as Climafuel, VARIATION REF: 2006/01, November 2006, CEMEX UK Cement Limited, 2006.
- [266] Undisclosed, *Biodryig MBT in-house SRF data*, Shanks Waste Management Ltd, 2007.
- [267] Gy, P., *Sampling for analytical purposes*, Wiley, 1998.
- [268] Gy, P., Sampling of discrete materials: III. Quantitative approach – Sampling of one-dimensional objects, *Chemometrics and Intelligent Laboratory Systems* 74 (1), 39, 2004.
- [269] Gy, P., Sampling of discrete materials: II. Quantitative approach – sampling of zero-dimensional objects, *Chemometrics and Intelligent Laboratory Systems* 74 (1), 25, 2004.
- [270] Gy, P., Sampling of discrete materials – a new introduction to the theory of sampling: I. Qualitative approach, *Chemometrics and Intelligent Laboratory Systems* 74 (1), 7, 2004.
- [271] Gy, P.M., *Sampling heterogeneous and dynamic material systems*, Elsevier Scientific Publishing, Amsterdam, 1992.
- [272] Gy, P.M., Introduction to the theory of sampling I. Heterogeneity of a population of uncorrelated units, *TrAC Trends in Analytical Chemistry* 14 (2), 67, 1995.
- [273] Horwitz, W., The certainty of uncertainty, *Journal of AOAC International* 86 (1), 109, 2003.
- [274] Lambkin, D., Nortcliff, S., and White, T., The importance of precision in sampling sludges, biowastes and treated soils in a regulatory framework, *TrAC Trends in Analytical Chemistry* 23 (10-11), 704, 2004.
- [275] Riber, C., Rodushkin, I., Spliid, H., and Christensen, T.H., Method for fractional solid-waste sampling and chemical analysis, *International Journal of Environmental Analytical Chemistry* 87 (5), 321, 2007.
- [276] la Cour Jansen, J., Spliid, H., Hansen, T.L., Svard, A., and Christensen, T.H., Assessment of sampling and chemical analysis of source-separated organic household waste, *Waste Management* 24 (6), 541, 2004.
- [277] Fricke, K., Santen, H., and Wallmann, R., Comparison of selected aerobic and anaerobic procedures for MSW treatment, *Waste Management* 25 (8), 799, 2005.
- [278] Wrisberg, N., Udo de Haes, H.A., Bilitewski, B., Bringezu, S., Bro-Rasmussen, F., Clift, R., Eder, P., Ekins, P., Frischknecht, R., and Triebswetter, U., Part 1: demand and supply of environmental information, In: *Analytical tools for environmental desing and*

- management in a systems perspective*, Wrisberg, N. and Udo de Haes, H.A. (Eds.), Kluwer Academic Publishers, Dordrecht, The Netherlands, 3, 2002.
- [279] Institute for Water Quality Resources and Waste Management TU-Wien, STAN2.0, Software for substance flow analysis, Institute for Water Quality, Resources and Waste Management, Vienna University of Technology 2009.
- [280] Biffa Leicester plant operator, *Monitoring properties for Biffa Bursom Leicester plant.*, 2006 personal communication,.
- [281] Tolvanen, M., Mass balance determination for trace elements at coal-, peat- and bark-fired power plants, PhD Thesis, University of Helsinki, Helsinki, 2004.
- [282] Van der Sloot, H.A., Developments in testing for environmental impact assessment, *Waste Management* 22 (7), 693, 2002.
- [283] European Committee for Standardisation, Solid recovered fuels – methods for the determination of the metallic aluminium, PD CEN/TR 15412:2006, European Committee for Standardisation (CEN), 2003.
- [284] van der Sloot, H.A., Meeussen, J.C.L., van Zomeren, A., and Kosson, D.S., Developments in the characterisation of waste materials for environmental impact assessment purposes, *Journal of Geochemical Exploration* 88 (1-3 SPEC. ISS.), 72, 2006.
- [285] Rupp, G.L. and Jones, R.R., *Heterogeneous wastes characterisation: methods and recommendations*, CRC Press, 1992.
- [286] Environmental Protection Agency, RCRA waste sampling - draft technical guidance. Planning, implementation and assessment, EPA530-D-02-002, August 2002, United States Environmental Protection Agency, Office of Solid Waste, Washington D.C., 2002.
- [287] Gerlach, R.W. and Nocerino, J.M., Guidance for obtaining representative laboratory analytical subsamples from particulate laboratory samples, EPA/600/R-03/027, November 2003, Environmental Protection Agency, 2004.
- [288] European Committee for Standardisation, Characterisation of waste – sampling of waste materials. Part 1: guidance on selection and application of criteria for sampling under various conditions, PD CEN/TR 15310:2006, European Committee for Standardisation (CEN), 2006.
- [289] Petersen, L., Minkkinen, P., and Esbensen, K.H., Representative sampling for reliable data analysis: theory of sampling, *Chemometrics and Intelligent Laboratory Systems* 77 (1-2 SPEC. ISS.), 261, 2005.
- [290] Pitard, F.F., *Pierre Gy's sampling theory and sampling practice. Heterogeneity, sampling correctness and statistical process control*, CRC Press, Boca Raton, 1993.
- [291] Gerlach, R.W., Nocerino, J.M., Ramsey, C.A., and Venner, B.C., Gy sampling theory in environmental studies: 2. subsampling error estimates, *Analytica Chimica Acta* 490 (1-2), 159, 2003.
- [292] Grigorieff, A., Costa, J.F., and Koppe, J., Quantifying the influence of grain top size and mass on a sample preparation protocol, *Chemometrics and Intelligent Laboratory Systems* 74 (1), 201, 2004.
- [293] Lyn, J.A., Ramsey, M.H., Damant, A.P., and Wood, R., Optimising uncertainty in physical sample preparation, *Analyst* 130 (11), 1507, 2005.
- [294] Séverin, M., *Improved methods for the determination of biogenic content in solid recovered fuels and related streams*, School of Applied Sciences, Cranfield University. MSc thesis, Cranfield, p.106, 2008.
- [295] Séverin, M., Velis, C.A., Longhurst, P.J., and Pollard, S.J.T., The biogenic content (χ_B) of process streams from mechanical-biological treatment plants producing solid

- recovered fuel. Do the manual sorting and selective dissolution methods for χ_B correlate?, *Waste management* 2010 - in press.
- [296] Nocerino, J.M., Schumacher, B.A., and Dary, C.C., Role of laboratory sampling devices and laboratory subsampling methods in representative sampling strategies, *Environmental Forensics* 6 (1), 35 2005.
- [297] Petersen, L., Dahl, C.K., and Esbensen, K.H., Representative mass reduction in sampling - a critical survey of techniques and hardware, *Chemometrics and Intelligent Laboratory Systems* 74 (1), 95, 2004.
- [298] Khuri, A.I., Designs for variance components estimation: Past and present, *International Statistical Review* 68 (3), 311, 2000.
- [299] Paakkunainen, M., Reinikainen, S.P., and Minkkinen, P., Estimation of the variance of sampling of process analytical and environmental emissions measurements, *Chemometrics and Intelligent Laboratory Systems* 88 (1), 26, 2007.
- [300] Dahlén, L. and Lagerkvist, A., Methods for household waste composition studies, *Waste Management* 28 (7), 1100, 2008.
- [301] American Society for Testing and Materials, Standard test method for determination of the composition of uprocessed municipal solid waste, D5231-92, American Society for testing and Materials (ASTM), Philadelphia, PA, US, 2003.
- [302] European Commission, *Methodology for the analysis of solid waste (SWA-tool)*, European Commission- 5th Framework Program, Vienna, Austria, 2004.
- [303] California Integrated Waste Management Board, Statewide waste characterisation study. Results and final report., 340-00-009, California Integrated Waste Management Board (CIWMB),
- [304] Maystre, L.Y. and Viret, F., A goal-oriented characterization of urban waste, *Waste Management and Research* 13 (3), 207, 1995.
- [305] Sharma, M. and McBean, E., A methodology for solid waste characterization based on diminishing marginal returns, *Waste Management* 27 (3), 337, 2007.
- [306] Scott, P.E., The International Energy Agency's (IEA) work in harmonising sampling and analytical protocols related to municipal solid waste (MSW) conversion to energy, *Biomass and Bioenergy* 9 (1-5), 415, 1995.
- [307] Sfeir, H., Reinhart, D.R., and McCauley-Bell, P.R., An evaluation of municipal solid waste composition bias sources, *Journal of the Air and Waste Management Association* 49 (9), 1096, 1999.
- [308] Klee, A.J. and Carruth, D., Sample weights in solid waste composition studies, *American Society of Civil Engineering, Journal of the Sanitary Engineering Division* 96 (5A), 945, 1970.
- [309] European Committee for Standardisation, Solid recovered fuels – method for the determination of the biomass content, DD CEN/TS 15440:2006, 28-02-2007, European Committee for Standardisation (CEN), 2006.
- [310] Pedersen, A.J., Frandsen, F.J., Riber, C., Astrup, T., Thomsen, S.N., Lundtorp, K., and Mortensen, L.F., A full-scale study on the partitioning of trace elements in municipal solid waste incinerations-Effects of firing different waste types, *Energy and Fuels* 23 (7), 3475, 2009.
- [311] Chancerel, P. and Rotter, S., Recycling-oriented characterization of small waste electrical and electronic equipment, *Waste Management* 29 (8), 2336, 2009.
- [312] Slack, R.J., Bonin, M., Gronow, J.R., Van Santen, A., and Voulvoulis, N., Household hazardous waste data for the UK by direct sampling, *Environmental Science and Technology* 41 (7), 2566, 2007.

- [313] Burnley, S.J., The use of chemical composition data in waste management planning - A case study, *Waste Management* 27 (3), 327, 2007.
- [314] Gidakos, E., Havas, G., and Ntzamilis, P., Municipal solid waste composition determination supporting the integrated solid waste management system in the island of Crete, *Waste Management* 26 (6), 668, 2006.
- [315] Hansen, T.L., Cour Jansen, J.I., Spliid, H., Davidsson, A., and Christensen, T.H., Composition of source-sorted municipal organic waste collected in Danish cities, *Waste Management* 27 (4), 510, 2007.
- [316] Riber, C., Fredriksen, G.S., and Christensen, T.H., Heavy metal content of combustible municipal solid waste in Denmark, *Waste Management and Research* 23 (2), 126, 2005.
- [317] Zhang, H., He, P.J., Shao, L.M., and Lee, D.J., Source analysis of heavy metals and arsenic in organic fractions of municipal solid waste in a mega-city (Shanghai), *Environmental Science and Technology* 42 (5), 1586, 2008.
- [318] Narasimhan, S. and Jordache, C., *Data reconciliation and gross error detection - an intelligent use of process data*, Gulf Professional Publishing, Houston, TX, USA, 2000.
- [319] Hartge, E.U., Pogodda, M., Reimers, C., Schwier, D., Gruhn, C., and Werther, J., SolidSim - A tool for the flowsheet simulation of solids processes | [SolidSim - Ein werkzeug für die fließschemasimulation von feststoffprozessen], *Aufbereitungs-Technik/Mineral Processing* 47 (1-2), 42, 2006.
- [320] Reimers, C., Werther, J., and Gruhn, G., Design specifications in the flowsheet simulation of complex solids processes, *Powder Technology* 191 (3), 260, 2009.
- [321] Mrotzek, A., Marzi, T., and Hiebel, M., Model-based material flow analysis of RDF-production, In: *Proceedings Venice 2008, Second International Symposium on Energy from Biomass and Waste*, 17-20 November 2008, Venice, Italy, CISA, Environmental Sanitary Engineering Centre, 2008.
- [322] Schirmer, M., Ma, W., Hoffmann, G., and Rotter, S., Origin and fate of chlorine in RDF production processes, In: *Proceedings Sardinia 2007. Eleventh international waste management and landfill symposium*, 1-5 October 2007, S. Margherita di Pula, Cagliari, Italy, 2007.
- [323] Paoli, P., Dell'Andrea, E., Brozzi, B., Teardo, G., and Casarin, F., Vesta Fusina RDF production plant and co-combustion in the ENEL power plant: experimentation and continued operation results, In: *Proceedings Sardinia 2007. Eleventh international waste management and landfill symposium*, 1-5 October 2007, S. Margherita di Pula, Cagliari, Italy, 2007.
- [324] Heering, B.-M., Untersuchungen zur herstellung von verwertbaren stoffen aus restabfall nach mechanisch-biologischer behandlung (In German) | [Investigations for the production of usable materials from the residues of mechanical-biological treatment], PhD Thesis, Rheinisch- Westfälische Technische Hochschule, Aachen, 2001.
- [325] Zeschmar-Lahl, B., Jager, J., and Ketelsen, K., (Eds.) *Mechanisch-biologische Abfallbehandlung in Europa / Verband der Kommunalen Abfallwirtschaft und Stadtreinigung (VKS) / Verbindung mit der Arbeitsgemeinschaft Stoffspezifische Abfallbehandlung (ASA) (In German) | [Mechanical-biological waste treatment in Europe / Association of Municipal Waste Management and City Cleaning (VKS) / In relation to the Registered Association for Material-Specific Waste Treatment (ASA)]*, Blackwell Wissenschafts-Verlag, Berlin, 2000.
- [326] Sokal, R. and Rolf, J., *Biometry: the principles and practice of statistics in biological research*, 3rd ed, W. H. Freeman, New York, 1995.
- [327] Williams, A., An alternative to the effective number of degrees of freedom *Accreditation and Quality Assurance* 4 (1-2), 14, 1999.

- [328] European Committee for Standardisation, Solid recovered fuels – method for the determination of the calorific value, DD CEN/TS 15400:2006, October 2006, European Committee for Standardisation (CEN), 2006.
- [329] European Committee for Standardisation, Solid biofuels – calculation of analyses to different bases, DD CEN/TS 15269:2006, 28 April 2006, European Committee for Standardisation (CEN), 2006.
- [330] European Committee for Standardisation, Solid recovered fuels — determination of moisture content using the oven dry method. Part 1: determination of total moisture by a reference method, DD CEN/TS 15414-1:2006, 30-11-2006, European Committee for Standardisation (CEN), 2006.
- [331] European Committee for Standardisation, Solid recovered fuels — determination of moisture content using the oven dry method. Part 2: determination of total moisture by a simplified method, DD CEN/TS 15414-2:2006, 30-11-2006, European Committee for Standardisation (CEN), 2006.
- [332] European Committee for Standardisation, Solid recovered fuels – methods for the determination of ash content, DD CEN/TS 15403:2006, 30-11-2006, European Committee for Standardisation (CEN), 2006.
- [333] European Committee for Standardisation, Solid recovered fuels — Method for the determination of carbon (C), hydrogen (H) and nitrogen (N) content, DD CEN/TS 15407:2006, 30-11-2006, European Committee for Standardisation (CEN), 2006.
- [334] Elementar, Vario EL III, Issue12/2000, Elemental GmbH, Hanau, Germany, 2000.
- [335] British Standards Institution, Guide for determination of calorific values of solid, liquid and gaseous fuels (including definitions), BS 7420:1991, 28 June 991, British Standards Institution (BSI), 1991.
- [336] Channiwala, S.A. and Parikh, P.P., A unified correlation for estimating HHV of solid, liquid and gaseous fuels, *Fuel* 81 (8), 1051, 2002.
- [337] British Standards Institution, Methods for analysis and testing of coal and coke. Part 100: general introduction and methods for reporting results, BS 1016-100:1994, 15 January 1994, British Standards Institution (BSI), 1994.
- [338] American Society for Testing and Materials, Standard test method for gross calorific value of coal and coke, D5865 - 07a American Society for testing and Materials (ASTM), Philadelphia, PA, US, 2007.
- [339] European Committee for Standardisation, Solid recovered fuels – determination of the biomass content based on the ¹⁴C method PD CEN/TR 15591:2007, 30-04-2007, European Committee for Standardisation (CEN), 2007.
- [340] Gawlik, B.M., Sobiecka, E., Vaccaro, S., and Ciceri, G., Quality management organisation, validation of standards, developments and inquiries for solid-recovered fuels-An overview on the QUOVADIS-Project, *Energy Policy* 35 (12), 6293, 2007.
- [341] QUOVADIS, Quality management, organisation, validation of standards, developments and inquiries for SRF, EIE 2003 031 PAD -775040, December 2007, CESI RICERCA Milano, Italy, 2007.
- [342] Fellner, J. and Rechberger, H., Abundance of 14C in biomass fractions of wastes and solid recovered fuels, *Waste Management* 29 (5), 1495, 2009.
- [343] American Society for Testing and Materials, Standard test methods for determining the biobased content of solid, liquid, and gaseous samples using radiocarbon analysis, D6866 - 08 ASTM International, West Conshohocken, PA, 2008.
- [344] European Committee for Standardisation, Solid recovered fuels — Methods for the determination of sulphur (S), chlorine(Cl), fluorine (F) and bromine (Br) content, DD CEN/TS 15408:2006, 31-10-2006, European Committee for Standardisation (CEN), 2006.

- [345] Flores, Á.M.M., Barin, J.S., Mesko, M.F., and Knapp, G., Sample preparation techniques based on combustion reactions in closed vessels - A brief overview and recent applications, *Spectrochimica Acta - Part B Atomic Spectroscopy* 62 (9), 1051, 2007.
- [346] Cortés-Peña, M.A., Pérez-Arribas, L.V., León-González, M.E., and Polo-Díez, L.M., Determination of chlorine and bromine in automotive shredder residues by oxygen bomb and ion chromatography, *Waste Management and Research* 20 (3), 302, 2002.
- [347] Ma, W., Rotter, S., Hoffmann, G., and Lehmann, A., Origins of chlorine in MSW and RDF: Species and analytical methods, In: *WIT Transactions on Ecology and the Environment*, Granada, 2008.
- [348] Dionex, High performance ion chromatograph, 2001.
- [349] Currie, L.A., Limits for qualitative detection and quantitative determination: Application to radiochemistry, *Analytical Chemistry* 40 (3), 586, 1968.
- [350] Currie, L.A., Nomenclature in evaluation of analytical methods including detection and quantification capabilities (IUPAC Recommendations 1995), *Analytica Chimica Acta* 391 (2), 105, 1999.
- [351] Jorhem, L., Certified reference materials as a quality tool in food control: much used - often misused - sometimes abused, *Accreditation and Quality Assurance* 9 (6), 305, 2004.
- [352] Scotti, S. and Minetti, G., Suitability of MBT facilities in treatment of different kinds of waste, In: *International Symposium MBT 2007, 22-24 May 2007*, Hanover, Germany, Kuehle-Weidemeir, M. (Ed.), Cuvillier Verlag, 2007.
- [353] Undisclosed, UK MBT plant A - operational data, 2008.
- [354] Diaz, L.F., Papadimitriou, E.K., Savage, G.M., Eggerth, L.L., and Stentiford, E.I., Selective aspects of the treatment of biodegradable waste in the European Union, In: *Proceedings. 2002 International symposium. Composting and compost utilisation*, 6-8 May 2002, Columbus, OH, USA, Frederick, C.M.J., Rynk, R., and Hoitink, H.A.J. (Eds.), 2002.
- [355] Kohaupt, U.W., Innovative sorting. An essential for economic improvements in waste handling, *Waste Management World* July-August 35, 2009.
- [356] Bartha, B. and Brummack, J., Investigations on the separability of dynamically dried municipal solid waste, In: *International Symposium MBT 2007, 22-24 May 2007*, Hanover, Germany, Kuehle-Weidemeir, M. (Ed.), Cuvillier Verlag, 2007.
- [357] Williams, P.T., *Waste treatment and disposal*, 2nd ed, Wiley, England, 2005.
- [358] Malhotra, S. and Godley, A.R., Application of the environment agency MBT monitoring guidance, In: *Waste 2006 - Sustainable waste and resource management*, 19-21 September 2006, Stratford-upon-Avon, UK, 2006.
- [359] Nicosia, S., Lanza, P.A., Spataro, G., and Casarin, F., Drawing the materials balance for an MBT cycle form routine process measures in MBT plant located in Venice, In: *International Symposium MBT 2007, 22-24 May 2007*, Hanover, Germany, Kuehle-Weidemeir, M. (Ed.), Cuvillier Verlag, 2007.
- [360] Gidaracos, E. and Simantiraki, F., RDF evaluation in the region of Chania, Crete, In: *Proceedings Venice 2008, Second International Symposium on Energy from Biomass and Waste*, Venice, Italy, CISA, Environmental Sanitary Engineering Centre, 2008.
- [361] Rada, E.C., Ragazzi, M., Panaitescu, V., and Apostol, T., Experimental characterization of municipal solid waste bio-drying, In: *WIT Transactions on Ecology and the Environment*, Malta, 2006.

- [362] Bonifazi, G., Serranti, S., and Rem, P.C., Hydrogen content and calorific value of municipal solid waste: Innovative quality control strategies of waste fed to incinerators, Granada, 2008.
- [363] Shanks Waste Management, Test results of Frog Island ITS SRF, Unpublished data, 2008.
- [364] Siskos, P., Scoullou, M., Zeri, C., Skordilis, A., Ziogas, C., Sakellari, A., Giannopoulou, K., Tsiolis, P., Mavroudeas, S., Argyropoulos, I., Roumeliotis, T., and Skiadi, O., Evaluation of the RDF from the mechanical biological treatment plant in Ano Liosia (in Greek) | [Η αξιολόγηση του RDF στο εργοστάσιο μηχανικής ανακύκλωσης και κομποστοποίησης 'Ανω Λιοσίων], In: *EEDSA workshop* - 28 May 2009, Athens, Greece, Hellenic Solid Waste Management Association, 2009.
- [365] Glorius, T., The EU-Project RECOFUEL, In: *QUOVADIS workshop*, 23-25 November 2007, Rome, 2007.
- [366] de Zorzi, P., Barbizzi, S., Belli, M., Barbina, M., Fajgelj, A., Jacimovic, R., Jeran, Z., Menegon, S., Pati, A., Petruzzelli, G., Sansone, U., and Van der Perk, M., Estimation of uncertainty arising from different soil sampling devices: The use of variogram parameters, *Chemosphere* 70 (5), 745, 2008.
- [367] Esbensen, K.H., Friis-Petersen, H.H., Petersen, L., Holm-Nielsen, J.B., and Mortensen, P.P., Representative process sampling - in practice: Variographic analysis and estimation of total sampling errors (TSE), *Chemometrics and Intelligent Laboratory Systems* 88 (1), 41, 2007.
- [368] Heikka, R. and Minkkinen, P., Comparison of some methods to estimate the limiting value of the variogram, $v(h)(j)$, for the sampling interval $j=0$ in sampling error estimation, *Analytica Chimica Acta* 346 (3), 277, 1997.
- [369] Ketelhut, R., Chlorine content of refuse derived fuels: is chemical analysis necessary?, In: *Reliable data for waste management*, 25-26 September 2008, Vienna, Austria, Institute for Water Quality, Resources and Waste Management - Vienna University of Technology, 2008.
- [370] Gascoyne, A., Shanks recovered fuel™. Fuelling a better environment, In: *First UK conference on solid recovered fuels*, 6 November 2008, London, Stragne, K. (Ed.), Resource Recovery Forum - ERFO, 2008.
- [371] Friedl, A., Padouvas, E., Rotter, H., and Varmuza, K., Prediction of heating values of biomass fuel from elemental composition, *Analytica Chimica Acta* 544 (1-2 SPEC. ISS.), 191, 2005.
- [372] Miller, B.G. and Tillman, D.A., Coal characteristics, In: *Combustion engineering issues for solid fuel systems*, Tillman, D.A. (Ed.), Elsevier, 33, 2008.
- [373] ANSI/ASME, Performance test code, instruments and apparatus. Part1, test uncertainty, PTC 19.1-2006, ANSI/ASME, 2006.
- [374] International Organization for Standardization / International Electrochemical Commission, Guide 98-3/Suppl.1:2008, Uncertainty of measurement – Part 3: guide to the expression of uncertainty in measurement (GUM:1995). Supplement 1: Propagation of distributions using a Monte Carlo method, 98-3/Suppl.1: 2008, ISO/IEC, 2008.
- [375] Brownlee, K.A., *Statistical theory and methodology in science and engineering*, 2nd ed, John Wiley & Sons, New York, 1967.
- [376] Ireland, S.N., McGrellis, B., and Harper, N., On the technical and economic issues involved in the co-firing of coal and waste in a conventional pf-fired power station, *Fuel* 83 (7-8), 905, 2004.
- [377] Shanks Waste Management Ltd, *Solid recovered fuel. An abundant and deliverable source of renewable energy*, Ecodeco, S., (Ed.) Shanks, UK, 2005.

- [378] Gy, P., Part IV: 50 years of sampling theory – a personal history, *Chemometrics and Intelligent Laboratory Systems* 74 (1), 49, 2004.
- [379] Smith, L.P., *A primer for sampling solids, liquids and gasses. Based on the seven sampling errors of Pierre Gy*, American Statistical Association (ASA), Society for Industrial and Applied Mathematics (SIAM). Lucbbock, Texas, 2001.
- [380] Svennmark, B., *Notes on Gy's formula*, University of Copenhagen, p.12, 2007.
- [381] Esbensen, K.H., Editorial, *Chemometrics and Intelligent Laboratory Systems* 74 (1), 1, 2004.
- [382] Petersen, I.F., Blending in circular and longitudinal mixing piles, *Chemometrics and Intelligent Laboratory Systems* 74 (1), 135, 2004.
- [383] Pitard, F.F., Effects of residual variances on the estimation of the variance of the Fundamental Error, *Chemometrics and Intelligent Laboratory Systems* 74 (1), 149, 2004.
- [384] Petersen, L. and Esbensen, K.H., Representative process sampling for reliable data analysis - a tutorial, *Journal of Chemometrics* 19 (11-12), 625, 2005.
- [385] Ketata, C. and Rockwell, M.C., Stream material variables and sampling errors, *Mineral Processing and Extractive Metallurgy Review* 29 (2), 104, 2008.
- [386] Carrasco, P., Carrasco, P., and Jara, E., The economic impact of correct sampling and analysis practices in the copper mining industry, *Chemometrics and Intelligent Laboratory Systems* 74 (1), 209, 2004.
- [387] Francois-Bongarcon, D., Theory of sampling and geostatistics: an intimate link, *Chemometrics and Intelligent Laboratory Systems* 74 (1), 143, 2004.
- [388] Holmes, R.J., Correct sampling and measurement--the foundation of accurate metallurgical accounting, *Chemometrics and Intelligent Laboratory Systems* 74 (1), 71, 2004.
- [389] Minkkinen, P., Practical applications of sampling theory, *Chemometrics and Intelligent Laboratory Systems* 74 (1), 85, 2004.
- [390] Mucha, J. and Szuwarzynski, M., Sampling errors and their influence on accuracy of zinc and lead content evaluation in ore from the Trzebionka mine (Silesian-Cracow Zn-Pb ore district, Poland), *Chemometrics and Intelligent Laboratory Systems* 74 (1), 165, 2004.
- [391] Robinson, G.K., How much would a blending stockpile reduce variation?, *Chemometrics and Intelligent Laboratory Systems* 74 (1), 121, 2004.
- [392] Minnitt, R.C.A., Rice, P.M., and Spangenberg, C., Part 1: Understanding the components of the fundamental sampling error: a key to good sampling practice, *Journal of The South African Institute of Mining and Metallurgy* 107 (8), 505, 2007.
- [393] Spanjer, M.C., Sampling for grain quality, *Stewart Postharvest Review* 3 (6), 2007.
- [394] Poll, A.J., Sampling and analysis of domestic refuse - a review of procedures at Warren Spring Laboratory, LR 667 (MR)M, September 1988, Warren Spring Laboratory, The Department Trade and Industry (dti), Stevenage, UK, 1988.
- [395] Moller, H., Sampling of heterogeneous bottom ash from municipal waste-incineration plants, *Chemometrics and Intelligent Laboratory Systems* 74 (1), 171, 2004.
- [396] Bareel, P.F., Bastin, D., Bodson, C., and Frenay, J., Sampling of Fine Shredder Residues (FSR) and characterisation oriented to physical separations, In: *2006 TMS Fall Extraction and Processing Division: Sohn International Symposium*, San Diego, CA, 2006.
- [397] Svennmark, B., *Notes on variances for ToS*, University of Copenhagen, p.11, 2007

APPENDICES

Appendix A - Terminology for MBT-derived fuels

MBT output fractions intended as secondary fuels fall into the category of WDFs, also referred to as solid waste fuels, secondary fuels, substitute fuels, or alternative fuels. In the absence of a legal definition or universally accepted term, the two most established terms relevant to thermally recoverable waste fractions are RDF and SRF. Many other partially overlapping terms exist and are discussed elsewhere^{13, 43, 201}. Conventionally, RDF refers to a combustible, high CV waste fraction (e.g., paper, card, wood and plastic) produced by the mechanical treatment of municipal or similar commercial/industrial waste.

SRF is a recently introduced term that denotes a WDF prepared to a quality specification. A technical committee of the European Committee for Standardisation (CEN) (CEN/TC 343) works to unify the various approaches to WDF, providing quality management guidance. According to DD CEN/TS 15359:2006, SRF should be²⁵⁹: *“solid fuel prepared from non-hazardous waste [as defined in Directive on hazardous waste (91/689/EEC); the input waste can be specific waste streams, municipal solid waste, industrial waste, commercial waste, construction and demolition waste, sewage sludge, etc.58] to be utilised for energy recovery in incineration or co-incineration plants, and meeting the classification and specification requirements laid down in CEN/TS WI00343003.”*

RDF or SRF may originate from sources other than MBT, such as source-segregated paper/card/plastic fractions. However, in this review these terms will refer to fuel produced by MBT plants, and for clarity a distinction is made between MBT-derived RDF and SRF. Figure A-1 shows the relationship between different terminologies.

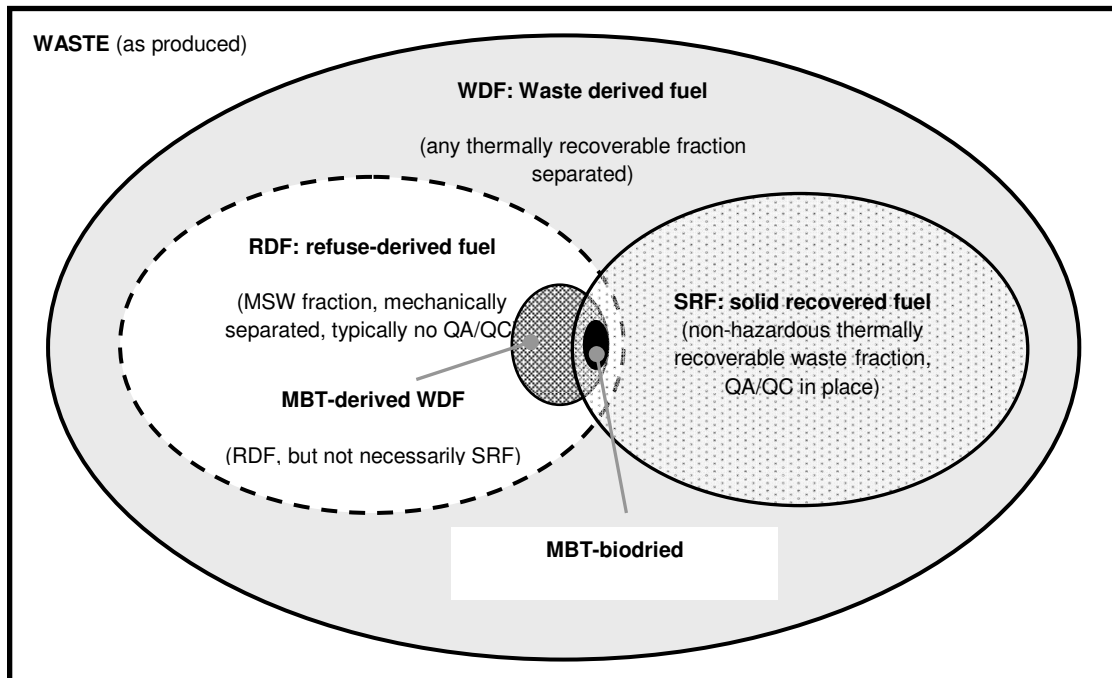


Figure A-1 Venn diagram exemplifying terminology used for thermally recoverable waste fractions in mechanical-biological treatment plants (MBT) and their quality assurance/quality control (QA/QC).

'SRF' is any MBT-derived WDF that follows (or can be reasonably anticipated to follow) the CEN quality management procedures. The WDF produced by biodrying is typically SRF. These processes are optimised to produce a partially stabilised fuel of consistent and high-quality composition as their primary output. Such MBT configurations could achieve CEN certification when trading the WDF in third party markets. 'RDF' is any MBT-derived WDF that was not, or could be reasonably anticipated to meet, the CEN quality management procedures in the immediate future. This might be any WDF produced as a co-product of MBT optimised for different primary products, such as biogas from anaerobic digestion (AD) or biostabilised output for landfill storage. Hence, we interpret SRF as a WDF following a quality management; but not necessarily exhibiting better quality compared with an RDF. However, because the quality management procedures relate to SRF production, much

higher reliabilities for SRF can be anticipated when compared to RDF. In the US, the term RDF has been applied to WDFs of standardised quality, according to ASTM standards²⁰¹. The term 'RDF/SRF' is used within this review.

Appendix B - Statistical approaches and descriptors

B.1 Variability in the measurement of waste-related properties

Here the various forms variability encountered in the waste and product quality characterisation are discussed. The result of each (chemical) measurement process (CMP) is subject to variability, which inevitably results in lack of certainty about the result. Hence, a quantitative estimation of the uncertainty related to the test result value is necessary. Such an 'uncertainty measurement' enables meaningful interpretation and use of the result, e.g., for compliance testing purposes. This research topic is covered by metrology. Simplifying, the measurement uncertainty can be separated into two general cases. This uncertainty measurement relates to the notion of CMP repeatability. Throughout the CMP for each waste property the uncertainty measurement is quantified, enabling to assess if a suitable level of precision is achieved. Such a quantity provides an indirect measure for the repeatability of the CMP, perceived as within-GAS and analytical sample variability. This information is critical also when in quality control one tries to assess compliance with specification limits.

There is paucity of information on the variability related to waste characterisation properties especially with regard to the computation of measurement uncertainty where error propagation applies. Additionally this is amongst the very first times that a series of determinations, recently specified by CEN, but still not fully validated, are applied to MBT-derived SRF and SRF upstream types of samples. The variability information produced here can prove valuable to the better implementation of these measurement standards in the future.

High variability is typically associated with sampling of a waste treatment plant process stream: e.g., temporal variability is encountered between results obtained during the measurement of a property as series of samples (increments) at separate time points. This between-sample variability (or between-incremental samples variability) reflects the variability in this part of the processing line, e.g. that of the SRF output of an MBT plant. Note that this variability is confounded with that related to the sampling scheme. Such production-line variability can be investigated by traditional statistical quality control approaches. However, simple statistical measures can be used in the evaluation of the between sample variability in the absence of detailed process information and long time-series of samples: e.g. coefficient of variation values (%CV), or ranges etc. The spread of the values is an integral part of any compliance decision rule, such as confidence limits around the mean. Hence, the between-sample variability of a production line is of paramount importance in establishing the quality of the product and in assessing its compliance with prescribed limits.

However, the between-incremental samples variability depends also on the uncertainty measurement characterising each of the individual incremental samples and the sub-sampling component of variability. Both the sub-sampling variability and the within-GAS and analytical determination variability should be small enough, enabling the relatively precise determination of the investigated property (under the selected number of replications). Low enough means that the resulting magnitude of measurement uncertainty values for the individual samples should be considerably smaller than the average between-sample variability. Otherwise, the between-sample variability is overshadowed by the within-sample and analytical variability. In this case, the encountered between-sample variability can be the result of imprecise measurement and not an indicator of the actual production line variability. Hence, a sufficiently low within-GAS and between-sub-samples variability is a prerequisite for

meaningfully monitoring the plant operation variability. Ideally, the within-GAS and analytical measurement variability should be incorporated into the computation of the average level of the incremental samples.

It is many expected that the widest variability of an SRF property is encountered for estimates sourced from various MBT plants, sampled and determined with diverse methods. This between-plants and determination methodologies variability is can be quantified as %CV and/or ranges of values by collating and statistically analysing published results on (European) MBT-derived SRF.

B.2 Measurement error, uncertainty and propagation

As a general principle, results of every measurement process of a property ('test result') should be accompanied by a quantitative estimation of the level of uncertainty related to it ('measurement uncertainty'). The measurement uncertainty is a way of quantifying the probability of making an incorrect decision when using the test result value²⁶³. Whilst usually the actual purpose of the measurement process is to obtain the test result value for a measurand (a well-defined physical property²⁵⁶), a statement pertaining to the uncertainty associated with it is necessary in order to meaningfully interpret the result, particularly as a part of any decision-making process²⁶³. This necessity for appropriate quantification and reporting of uncertainty for waste-related compliance testing has been recently widely acknowledged²⁷⁴.

Since around 1960, significant progress has been achieved in understanding and clearly describing the nature and mathematical formalism for evaluating measurement errors and the resultant uncertainty, along with standardising their presentation. Here, we follow the approach, terminology and nomenclature of Dieck's²⁶³ established textbook and reference manual. Notably, Dieck's approach spans the significant literature in the subject, including the ISO publications (guide to

the expression of uncertainty in measurement: GUM and supplements)²⁵⁶, and it incorporates recent developments as recommended by the ANSI/ASME³⁷³. In an analytical chemistry determinations context, guidance has been produced by EURACHEM/CITAC²⁵⁷; Desimoni and Brunetti²⁵⁴ presented a comprehensive review of the literature and critical evaluation of open questions.

‘Error’ is considered the difference of the unknown ‘true’ value from the measurement result obtained through the measurement process. This ‘true’ value is a hypothetical notion, never known. Hence, the error is by default impossible to accurately quantify. That said, an estimate of the limits within which we can anticipate the error to extend can be quantified (at a pre-determined, selected level of confidence), that is ‘uncertainty.’ According to Dieck²⁶³ a non-technical definition of measurement uncertainty could be: *“an interval about the data average that expresses the maximum possible error that may reasonably occur with some confidence. Errors larger than the measurement uncertainty should rarely occur.”* However, this approach implies that a high level of confidence has been selected; but the level of confidence should be fit-for-purpose and inevitably varies accordingly.

The sources of error can be separated into random (precision) and systematic (bias). These categories exclude any miss-readings resulting from mistakes (‘blunders’), which are assumed to have been avoided or corrected. Random errors cannot be predicted: they result in a spread (scatter) of the test results. Systematic errors are constant throughout the experiment (or are changing in a way causing a predictable effect on the measurand²⁵⁷) and cause a shift in the test result value, which however cannot be directly observed because the ‘true’ value remains unknown. Dieck²⁶³ defines 5 types of systematic errors, from which only those falling into the 5th type are to be included in the estimation of the measurement uncertainty: these are of unknown magnitude, cannot be eliminated by good engineering or calibration and are

not negligible. Other groupings of error sources are also proposed, mainly to facilitate their calculation and interpretation. ISO suggests 'Type A' and 'Type B' sources of error, the former includes cases where replication of the measurement enables a standard deviation s to be calculated and the latter the absence of data on repeatability gained directly through experiment replication²⁵⁶. The ANSI/ASME proposes the grouping of error sources into³⁷³: calibration, data acquisition (e.g., instrument reading error), data deduction (e.g., truncation, rounding), errors of method. Dieck²⁶³ maintains that these categorisations can be helpful but not essential in the evaluation of the measurement uncertainty, and hence are not discussed here further. Instead, Dieck follows the reasonable assumption that the systematic uncertainty b_R is Type B ISO and the random uncertainty s_R is Type A ISO: indeed in the case where no replication is available (Type B) the only contribution to the uncertainty estimate can come from its systematic part. The most critical property of a source of error is its systematic or random character - this property being irrespective of its type of source²⁶³.

The measurement uncertainty (U_R) combining both the random and systematic components of the uncertainty applicable to the determination of the property X (test result R), is modelled using the ASME U_{95} estimation formula³⁷³:

$$U_{R,95} = \pm t_{95,v} \times \left[(b_R)^2 + (s_{\bar{X},R})^2 \right]^{1/2} \quad \text{[0-1]}$$

Where,

$U_{R,95}$ measurement uncertainty of property X, with measure test result R at $p=0.05$

$t_{95,v}$ t-student statistic, at $p=0.05$ and d.f.: $v = N-1$

b_R standard systematic uncertainty

$s_{\bar{X},R}$ standard random uncertainty (standard error of the mean, SE)

The $t_{95,v}$ is the Student t-statistic for 95% level of confidence and v degrees of freedom (d.f.), equals N-1, (N number of observations) and practically interpreted as the “*amount of room left for error*”²⁶³. It is serving as a coverage factor (usually denoted k). The use of the t-statistic is, in practice, necessary when d.f.<30, i.e., less than 31 replications, as suggested by Dieck²⁶³, and the measurand can be assumed to be normally distributed. However, the Dieck suggests that for most practical cases the replacement of the multiplier with a coverage factor of 2 (the standardised z (Normal) value at 95% confidence) can also provide an estimate of the measurement uncertainty sufficient for most practical applications. Other potential choices, reflecting the actual or estimated type of PDF, are discussed for CMPs by EURACHEM/CITAC²⁵⁷.

The two components of U_R are (**Equation [2-1]**): (1) standard random uncertainty (also known as ‘standard error of the mean’):

$$s_{\bar{X},R} = s_X / \sqrt{N} \quad \text{[0-2]}$$

where,

$s_{\bar{X},R}$ standard random uncertainty (standard error of the mean, SE)

s_X standard deviation, sd (repeatability sd for a single laboratory)

N number of observations

The standard deviation of a data set (sample population) measuring property X is calculated using N observations (note that this s_x , when measurement is exclusively performed in a single laboratory, stands for the within-laboratory standard deviation, i.e., the method repeatability standard deviation).

$$b_R = \sqrt{\sum_i (b_i)^2} \quad \text{[0-3]}$$

where,

b_R standard systematic uncertainty

b_i Individual components of systematic uncertainty from different sources

i up to N observations

The component b_R is the standard systematic uncertainty. When more than one independent source contributes to the standard systematic uncertainty, the individual ('elemental') contributions b_i are correctly combined as in **Equation [0-3]**²⁶³. The assumption made is that the standard systematic uncertainties stem from error sources independently normally distributed, determined with infinite d.f.

Note that the various adjectives found in the literature qualifying the term uncertainty U_R are not used consistently - here the following meanings will be used: (1) 'combined' U_R : incorporating both random and systematic parts; (2) 'extended' U_R : combined U_R multiplied by a coverage factor (either 2 or $t_{95,v}$); (3) 'total' U_R : when uncertainty propagation calculations are necessary to incorporate more than one contribution of uncertainty, i.e., when a single output quantity is a function of a number of input quantities, each characterised by its own uncertainty measurement.

Propagation of uncertainty measurement estimates is necessary for incorporating the uncertainty contributions of many (denoted i) measured variables (denoted V) that combine through a mathematical formula ($R=f(V_i)$) to calculate the overall result (denoted R). Sophisticated and resource intensive methods such as 'dithering' and Monte Carlo simulation³⁷⁴ may be necessary for certain challenging engineering problems²⁶³. However, in our case the common approach of developing through a Taylor's series approximation can suffice. In most cases calculations can be

expressed as closed-form equations (i.e., mathematical formulas), hence a Taylor's series approximation is applicable. The total uncertainty measurement of the R (denoted U_R), assuming the systematic uncertainty measurements of the individual variables are statistically independent, and remembering that the random uncertainty measurements are by default independent, can be computed using:

$$U_R = \left[\sum_i \left[\left(\frac{\partial R}{\partial V_i} \right)^2 \times (U_i)^2 \right] \right]^{1/2} \quad \text{[0-4]}$$

where,

U_R uncertainty measurement of the R

$\partial R / \partial V_i$ partial derivative of R with respect to the variable V_i

U_i Individual components of uncertainty of variable V_i

i up to N variables

The partial derivative of R with respect to the variable V_i ($\partial R / \partial V_i$) has the physical meaning of the rate of change of R in the direction of V_i , as calculated in the vicinity of the specific value of R which is of interest. It functions as a weighting factor (influence or sensitivity coefficient), denoting the magnitude of the influence the uncertainty in V_i (U_i) has upon U_R . Knowledge of these weighting factors can potentially enable an 'uncertainty budget' to be computed during the experimental design stage: if the anticipated central tendencies and uncertainties are known before the experiment, evaluation of the relative contribution of each of the input quantities to the final measurand and focussing replication efforts to where most necessary and/or cost-efficient. Notwithstanding this, it is hardly ever practiced.

It might be anticipated that the random errors b_R during in materials encountered in most waste characterisation CMPs are negligible in comparison to their random counterparts. For waste-derived samples we speculate that it can be safely

assumed that in most of the cases the heterogeneity of the GAS remains high despite the effort for maximum homogenisation, (e.g., by shredding to 0.5 mm and thoroughly manually mixing the GAS before selecting an aliquot for each replicate test analysis). This, in combination with the random sources of variability pertaining to the measurement method, could typically result in random uncertainties orders of a magnitude higher than any systematic uncertainties, especially those stemming from the reading errors which are those that can be readily quantified.

Certain computational details deserve attention. Note that the correct estimation of the U_R is made separately for the systematic and random parts before finally combining the two attributes. The suitable d.f. should be used in each case to determine the t-statistic value for the random part of the uncertainty. When random uncertainty components from many sources have to be combined, the use of the Welch-Satterthwaite method (W/S) as detailed by Brownlee³⁷⁵ is suggested^{256, 263} in order to compute an 'effective number of d.f.' v_{eff} :

$$v_{\text{eff}} = \frac{\left[\sum_i \left(\frac{\partial R}{\partial V_i} \times s_i^2 \right) + \sum_i \left(\frac{\partial R}{\partial V_i} \times \left(\frac{b_i}{2} \right)^2 \right) \right]^2}{\left\{ \sum_i \left[\left(\frac{\partial R}{\partial V_i} \right)^2 \times s_i^4 / v_i \right] + \sum_i \left[\left(\frac{\partial R}{\partial V_i} \right)^2 \times \left(\frac{b_i}{2} \right)^4 / v_i \right] \right\}} \quad \text{[0-5]}$$

where,

- v_{eff} effective number of d.f.
- V_i variable V_i upon which R depends
- s_i standard random uncertainty of V_i
- b_i systematic uncertainty of V_i
- v_i number of d.f. with which the variable V_i is determined
- i up to N variables

Note that this formula is following Williams³²⁷ description of the W/S and differs from that quoted in Dieck²⁶³. Williams³²⁷ proposed a computationally simplified alternative to the W/C formula, leading to more conservative estimates for the coverage factor, especially for lower numbers of d.f.: but is applicable to input quantities with d.f.≥3.

In the computations performed in this research the W/S method is applicable when propagating the uncertainties of many input variables, each of them determined through repeated measurements²⁶³, whilst ignoring the systematic uncertainty contributions. Thus, typically:

$$v_{eff} = \left[\sum_i \left(\frac{\partial R}{\partial V_i} \times s_i^2 \right) \right]^2 / \sum_i \left[\left(\frac{\partial R}{\partial V_i} \right)^2 \times s_i^4 / v_i \right] \quad \text{[0-6]}$$

where, notation as in **Equation [0-5]**

To illustrate the computation of the uncertainties³²⁷, an output quantity calculated from two input quantities supposedly exhibiting equal weighing factors and random uncertainties, assuming $v_1 = v_2 = 3$ would result in $v_{eff} = 6$.

Finally, expressing the U_R as a percentage of R (percent or relative uncertainty % U_R) (**Equation [0-7]**) similarly to a coefficient of variation, can provide a readily comprehensible, scale-free measure of the precision that the property R is estimated (at the selected level of confidence, here consistently at 95%).

The repeatability of any CMP can be indirectly related to the uncertainty measurement. Assume that the investigated quantity is directly measured, i.e., it does not depend on the measurement of other quantities, and subsequent computations, and that any potential systematic error is ignored. Assuming destructive CMP, repeatability of the CMP has to be estimated indirectly by replication on aliquots from

the GAS. In this case the within-GAS variability cannot be separated from the determination method variability (analytical variability). Hence, %CV provides a measure of the repeatability of the CMP with the particular GAS (within-GAS and analytical determination variability). Moreover, the %U_R is directly reflecting the %CV (Equation [0-7])

However, if the quantity R depends on other quantities for its determination, the repeatability of the CMP cannot be estimated through the %CV, because it is impossible to define the %CV. Note that the computation of a %CV assumes there a well-defined standard deviation of the R population³²⁶. No single such statistic can be obtained here because there is no R population, because R is computed through the averages of other quantities. Instead, there can be standard error of its mean s(<R>), propagated through the computation, which with the effective number of d.f. enables the calculation of U_R. In this case, the %U_R can provide an indirect measure of the repeatability of the overall CMP.

$$\%U_R = (U_R / \langle R \rangle) \times 100 = \frac{t_{95,v} \times s(R)}{\langle R \rangle \times \sqrt{N}} = \%CV_R \times \frac{t_{95,v}}{\sqrt{N}} \quad [0-7]$$

where,

- %U_R relative or percent uncertainty for test result R
- U_R uncertainty measurement of the test result R
- %CV_R coefficient of variation for test result R
- <R> arithmetic mean of test result R
- N independent replicates of the determination of R
- s(R) standard random of test result for R (repeatability sd)
- t_{95,v} t-student statistic, at p=0.05 and d.f.: v = N-1

v_i number of d.f. with which the variable U_R is determined

Appendix C – Computations and statistical details for fuel characterisation properties

C.1 Moisture content (M)

For any computations, the discarded categories were considered 'inert' and 'dry' (i.e., $A = 100\% \text{ w/w}_d$, $\chi_{Bi} = 0\% \text{ w/w}_d$ and $M_T = 0\% \text{ w/w}_{ar}$). This approximation holds because: (i) non-shreddable waste fragments suffer relatively low contamination by non-inert adhesives; and (ii) the input to the mechanical processing of the MBT plant exhibits a reduced MT SP1 ($<20\% \text{ w/w}_{ar}$), whilst the non-shreddable fractions comprise materials with high bulk density (ferrous and non-ferrous metal, glass) and a limited ability to absorb/adsorb moisture, resulting in a very low M. Hence, each of the measured ar weight can be assumed as d without introducing significant bias.

Uncertainty propagation example: total moisture content (MT)

The uncertainty estimate related to the M_T is, thus, propagated from the test results of M_b and M_r . The random part of uncertainty: (1) the s_{M_r} can be estimated through replication: typically at least 3 replicates on aliquots of the GAS are performed; (2) on the other hand, in the bulk drying test there can be no replication: hence there is no direct estimate of the s_{M_r} . However, this is less of a problem because the whole sample is undergoing the analysis (drying). Hence, there is no within-sample variability, but just the analytical error, i.e., the part of the error introduced when aliquots of the sample, each constituting a small portion of the overall sample, whereas replicate analyses aimed at estimating the average across the overall sample, are not present here. The systematic parts of the uncertainty, from sources such as calibration of balances, (digital) reading errors, etc are generally orders of magnitude lower than the random errors, and hence they can be ignored during RSS calculations: (M_b : least

count (LC) (size of smallest division on a scale, typically higher than the instrument limit of error (ILE)): 0.01g) with typical weight readings involved ca 300-1200 g; and M_r : LC 0.0001, with typical weights 30-70 g and samples of 1-2 g).

However, other sources of error might need to be discussed/accounted for, notably fluctuations/trends on the last digits of the scales. Such fluctuations may result from the necessity to weigh the samples immediately after their removal from the 40°C and, especially, the 105°C drying ovens (or after ashing 60-70°C) (note however, that the CEN suggestion for measurement within 10-15 secs, is clearly impossible to perform because the heat transfer causes changes in the pressure within the measuring chamber of high accuracy balances). Rapid measurement is recommended in the relevant CEN document³³¹ to prevent the absorbance of moisture because the materials involved (SRF and similar streams) are highly hygroscopic. The use of desiccators is not suggested because the dried/ashed samples can absorb moisture from the desiccant; and the use of desiccators without desiccants, despite being suggested in CEN SRF-guidance of the determination of the ash content³³² is not a sufficient solution. Hence, the samples are left for a few minutes to cool down to temperatures so that they do not induce temperature and/or pressure changes in the weighing chamber (along with the use of T insulating intermediate materials on the weighing surface). Hence the actual uncertainty could be ca 0.0005 g for the M_r , when hot samples are measured. The above challenge, inevitably introduced a systematic error, as hot dry samples which spend more time between their exit from the oven and their moment of measurement re-absorb more moisture during the ca 10 minutes the measurement process (of ca 20 crucibles per batch) takes place. Whilst this trend could be potentially quantified and allocated for by a correction factor, the effort involved is not justified, because the gain in moisture for fully dried samples after ashing at 550°C is ca 0.0050 g in 10 min for samples of ca 2.000 with ca 3% w/w M,

i.e., 0.0050 g=1/12 of the 0.0600 g of M. Hence, correctly these could be allocated as part of a systematic error, but are ignored here, given their negligible influence on the overall M_T (or ash content A measurements). Indeed the differences due to the within GAS variability (i.e., of tests measured in almost identical conditions) are much higher, and even higher are the ones experienced between the increments (INCs) and lots (L), that they can be safely ignored.

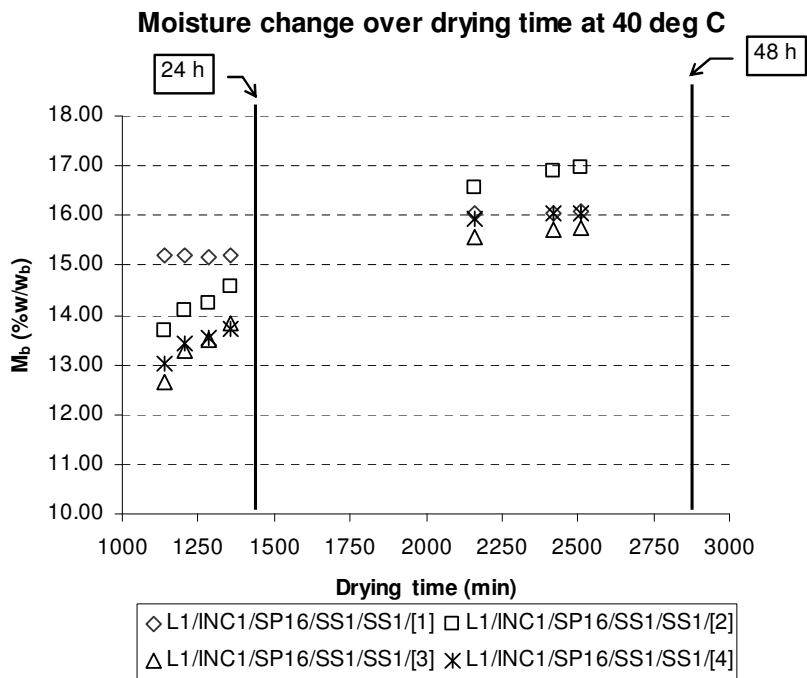
The absence of a direct estimate for sM_b is addressed here not by a detailed evaluation of sources and magnitudes of contributing parts, but by making a general conservative estimate for most of the cases. Note that the entire mass sample is measured, hence, this is an infrequent occurrence where there is no within-sample variability. Given the high sample mass (ca. 300-1200) involved, the systematic errors due to, for example, instrument readings are negligible. The U_{95, M_b} is estimated as 4% of the M_b for each GAS, and assumed to be all random. Note that this does not imply any form of heteroscedasticity: the population ('configuration space') here is the notional body of repetitions of the analytical determination (bulk drying) of each whole sample. The very different spread levels resultant among the M_T of each sample just reflect the fact that the measurement uncertainty of each sample corresponds to a different population/measurement, reflecting the inhomogeneity of each sample with regard to the measurand together with the rest of the measurement-related random variability. In the absence of any d.f. contributed from the M_b measurement, the effective d.f. is assumed the same as for the M_r - no separate calculation is done. With these assumptions, the uncertainty of the M_T can be computed as:

$$U_{M_T,95} = \left\{ \left[(1 - M_r / 100) \times U_{M_b} \right]^2 + \left[(1 - M_b / 100) \times U_{M_r} \right]^2 \right\}^{1/2} \quad [0-8]$$

where,

$U_{M,T,95}$ measurement uncertainty of total moisture computation

- $U_{M,b}$ measurement uncertainty of bulk moisture
- $U_{M,r}$ measurement uncertainty of residual moisture
- M_r residual moisture content (moisture of the GAS)
- M_b bulk moisture content



Figure_App C-1 Moisture change during bulk drying at 40°C for indicative samples

C.2 Ash content (A)

The mass percent of ash content was estimated as:

$$A = \frac{m_{ash}}{m_d} \times 100$$

[0-9]

where,

m_{ash} mass of the ashed sample, dry basis

m_d mass of the test sample, dry basis

C.3 Calorific (heating) value

From the $Q_{\text{gr},\text{v},\text{b}}$, measured on the bulk dried GAS, the $Q_{\text{net},\text{p},\text{d}}$ and $Q_{\text{net},\text{p},\text{ar}}$ were computed, using the formulas stipulated in DD CEN/TS 15400:2006³²⁸ and DD CEN/TS 15269:2006³²⁹.

$$\langle Q_{\text{gr},\text{v},\text{d}} \rangle = \langle Q_{\text{gr},\text{v},\text{b}} \rangle \times \frac{1}{1 - \langle M_r \rangle} \quad [0-10]$$

where,

$Q_{\text{gr},\text{v},\text{d}}$ gross calorific value, under constant volume, on a dry basis

$Q_{\text{gr},\text{v},\text{b}}$ gross calorific value, under constant volume, on a bulk dried basis

M_r residual moisture of a bulk dried sample

$$\langle Q_{\text{net},\text{p},\text{d}} \rangle = \langle Q_{\text{gr},\text{v},\text{d}} \rangle - 212.2 \times \langle TH_d \rangle - 0.8 \times [\langle TO_d \rangle + \langle TN_d \rangle] \quad [0-11]$$

where,

$Q_{\text{net},\text{p},\text{d}}$ net calorific value, under constant pressure, dry basis

$Q_{\text{gr},\text{v},\text{d}}$ gross calorific value, under constant volume, dry basis

TH_d total hydrogen, dry basis

TO_d total oxygen, dry basis

TN_d total nitrogen, dry basis

$$\langle Q_{\text{net},\text{p},\text{ar}} \rangle = \langle Q_{\text{net},\text{p},\text{d}} \rangle \times (1 - 0.01 \times \langle M_T \rangle) - 24.43 \times \langle M_T \rangle \quad [0-12]$$

where,

$Q_{\text{net,p,d}}$ net calorific value, under constant pressure, as received basis

$Q_{\text{net,p,d}}$ net calorific value, under constant pressure, dry basis

M_T Total moisture, dry basis, percent

Where, the TH, TN and TO are expressed as percents on a dry basis; the M_T is entered as percent; the TH includes both the hydrogen from the hydration of mineral mater and the part bound in the sample substance³²⁸.

As the standard practice is, the total oxygen has not been measured, because this would demand a separate determination, difficult to accurately measure, for a correction that is not of great importance: this can be readily seen by comparing the multipliers for the correction of TH (212.2) and TO (0.8). Typical products for SRF are respectively in the order of $212.2 \times 6.5 \approx 1400 \text{ KJ kg}_d^{-1}$ and $0.8 \times 30 \approx 24 \text{ KJ kg}_d^{-1}$. A maximum possible error of ± 15 (% w/w_d) in the estimation of TO can only lead to a percent bias of $\text{ca } 0.4\% = (15/(5000-1400))$ in the worst case of a minimum $\langle Q_{\text{net,p,d}} \rangle$ of $\text{ca } 5000 \text{ KJ kg}_d^{-1}$; and affect only negligible changes in the $U_{95,\text{veff}}(\langle Q_{\text{net,p,d}} \rangle)$. The TO varies significantly in the various materials/waste streams as can be seen in Ireland et al.³⁷⁶; here, it is globally estimated at 29.4 (%w/w_d) as reported for RDF/SRF by Cozens²²⁶, a value lower than older US RDF measurements (38.36 (% w/w_d))³³⁶, and higher than the recent German Remondis SBS[®] SRF (18.5 (% w/w))²²⁷; note the aspiration of Shanks/Ecodeco commercial leaflet for SRF at 25 (% w/w)³⁷⁷.

The total extended uncertainties are computed in accordance with the general **Equation [0-4]**, resulting in **Equations [0-13]** and **[0-14]**. The effective d.f. (v_{eff}) is computed according to the **Equation [0-6]** (exact formula not shown). In both cases the resultant v_{eff} is 1, dominated by the only one degree of freedom available for the

$Q_{gr,v,b}$ computed as the arithmetic mean of only two replications, resulting in the maximum possible coverage factor ($t_{95,1}=12.706$).

$$U_{95,veff}(<Q_{net,p,d}>) = t_{95,veff} \times \left[\left(\frac{1}{1-M_r} \times s(<Q_{gr,v,b}>) \right)^2 + \left(\frac{<Q_{gr,v,b}>}{(1-M_r)^2} \times s(<M_r>) \right)^2 + (2122 \times s(<TH_d>))^2 + 0.8^2 \times [s(<TO_d>)^2 + (s(<TN_d>))^2] \right]^{1/2} \quad [0-13]$$

where, as in previous equations

$$U_{95,veff}(<Q_{net,p,ar}>) = t_{95,veff} \times \left[\left((1-0.01 \times <M_T>) \times s(<Q_{net,p,d}>) \right)^2 + \left((0.01 \times Q_{net,p,d} + 23.43) \times s(<M_r>) \right)^2 \right]^{1/2} \quad [0-14]$$

where, as in previous equations

C.4 Biogenic content by selective dissolution

The χ_B by the SDM is determined on aliquots of the GAS. Note that here for the first time the correct way of computing the uncertainty pertaining to the individual samples of SRF is described and followed. The SD and subsequent ashing process involves the determination of the measurands necessary to compute the quantity

$$\left\langle \frac{m_{res+f,d} - m_{res+f,ashed,d}}{m_{ts,b}} \right\rangle, \text{ which stands for the ash fraction of the test samples}$$

dissolved, expressed on a bulk drying basis for the test sample mass, hereafter denoted: $\langle A_{ts,dis,d/b} \rangle$. In order to calculate the χ_B , the quantities of $\langle M_r \rangle$ and $\langle A_{ts,d} \rangle$ expressed as weight percentages are also needed, measured independently.

$$\langle \chi_{B,SHR,daf} \rangle = \left[1 - \left\{ \left\langle \frac{m_{res+f,d} - m_{res+f,ashed,d}}{m_{ts,b}} \right\rangle \times \frac{1}{\langle M_r \rangle} + \frac{\langle A_{ts,d} \rangle}{100} \right\} \right] \times 100 \quad [0-15]$$

where,

$X_{b,SRH,daf}$ biogenic content, of the shreddable part of sample on a dry ash-free basis

$M_{res+f,d}$ mass of dissolution residue and filter, dry basis

- $M_{res+f_ashed,d}$ mass of ashed dissolution residue and filter, dry basis
- $M_{ts,b}$ mass of test sample, bulk dry basis
- M_r residual moisture of bulk dried sample
- $A_{ts,d}$ ash content of test sample, dry basis

Given that the GAS represents only the shreddable/combustible part of the initial sample, a correction factor (cf) has to be applied to convert from the shreddable sample $\chi_{B,SHR,daf}$ to the global sample $\chi_{B,daf}$. It follows that cf is the ratio of the sum of shreddable sorting components over the sum of all sorting components, both expressed on a dry basis due to the d reporting basis of χ_B ; hence, needing to use also the M_T , as the sorting categories are measure of an ar basis. Hence:

$$\langle cf_d \rangle = \frac{\sum_i^{SHR} m_{d,i}}{\sum_i^{ALL} m_{d,i}} = \frac{1 - \langle M_T \rangle}{\frac{100}{\sum_i^{SHR} m_{ar,i}} - \langle M_T \rangle} \quad [0-16]$$

where,

- cf_d Correction factor for non-shreddable part, dry basis
- M_T Total moisture, dry basis
- $m_{d,i}$ Mass of non-shreddable component i, dry basis
- $M_{ar,i}$ Mass of non-shreddable component i, as-recieved basis

$$\langle \chi_{B,daf} \rangle = \langle \chi_{B,SHR,daf} \rangle \times \langle cf_d \rangle \quad [0-17]$$

where, As in previous equations

Or explicitly:

$$\langle \chi_{B,daf} \rangle = \left[1 - \left\{ \frac{m_{res+f,d} - m_{res+f_ashed,d}}{m_{ts,b}} \times \frac{1}{\langle M_r \rangle} + \frac{\langle A_{ts,d} \rangle}{100} \right\} \right] \times 100 \times \langle cf_d \rangle \quad [0-18]$$

where, As in previous equations

Note that for the L3 SRF samples the whole sample was shredded (not only the 'shreddable' part: for these, the computed $\chi_{B,SHR,daf}$ coincides with the needed $\chi_{B,daf}$).

The uncertainty propagation computations for the $\langle \chi_{B,SHR,daf} \rangle$, $\langle cf_d \rangle$ and $\langle \chi_{B,daf} \rangle$, according to **Equation [0-4]**, have as follows. For most of the SRF samples the v_{eff} for the $U(\langle \chi_{B,SHR,daf} \rangle)$ computation results in less than two and around 3 for certain other cases (according to the **Equation [0-6]**). An $v_{eff} = 2$ is adopted, which whilst not corresponding to the maximum conservative choice, serves the purpose of evaluating the d.f. with a single value for all the similar cases, facilitating their comparability, whilst still leads to a conservative estimate of the uncertainty.

$$U(\langle \chi_{B,SHR,daf} \rangle) = t_{95,v_{eff}} \times \left[\left(\frac{s(\langle A_{ts,disd/b} \rangle)}{1 - \langle M_r \rangle} \right)^2 + \left(\frac{\langle A_{ts,disd/b} \rangle}{(1 - \langle M_r \rangle)^2} \times s(\langle M_r \rangle) \right)^2 + \left(\frac{s(\langle A_{ts,d} \rangle)}{100} \right)^2 \right]^{1/2} \times 100 \quad [0-19]$$

where, as in previous equations

$$U(\langle cf_d \rangle) = t_{95,v_{eff}} \times \left[\left(\frac{-1}{\frac{100}{\sum_i^{SHR} m_{ar,i}} - \langle M_T \rangle} + \frac{1 - \langle M_T \rangle}{\left(\frac{100}{\sum_i^{SHR} m_{ar,i}} - \langle M_T \rangle \right)^2} \right)^2 \times (s(\langle M_T \rangle))^2 \right]^{1/2} \quad [0-20]$$

where, As in previous equations

Regarding the uncertainty of $\sum_i^{SHR} m_{ar,i}$, there is no random error estimate readily available, because no repetition of the sorting process has been feasible. This contribution is ignored, since the random standard uncertainty of MT is dominating the result. The two d.f. stemming from the $U(\langle M_T \rangle)$ computation is also used for the $U(\langle cf_d \rangle)$, since there is only the M_T contribution.

$$U(\langle \chi_{B,daf} \rangle) = t_{95,v_{eff}} \times \left[(\langle cf_d \rangle \times s(\langle \chi_{B,SHR,daf} \rangle))^2 + (s(\langle cf_d \rangle) \times \langle \chi_{B,SHR,daf} \rangle)^2 \right]^{1/2} \quad \text{[0-21]}$$

where, As in previous equations

In the two stage computation of uncertainty for $U(\langle \chi_{B,daf} \rangle)$, the d.f. is conservatively estimated as two, given the previous estimates of $v_{eff}(U(\langle cf_d \rangle)) = 2$, and $v_{eff}(U(\langle \chi_{B,SHR,daf} \rangle)) = 2$. This also renders the $U(\langle \chi_{B,daf} \rangle)$ and $U(\langle \chi_{B,SHR,daf} \rangle)$ readily (visually) comparable.

C.4.1 Standard operating procedure: Method for the determination of the biogenic content of solid recovered fuels (solid waste) in percent by weight using the selective dissolution method

The procedure is based on DD CEN/TS 15440:2006. The underlying principle is the hydrolysis and oxidation of the biogenic organic content of the test sample by sulphuric acid (H_2SO_4), followed by hydrogen peroxide (H_2O_2). The non-biogenic organic matter should be left behind, because generally biomass oxidises significantly more quickly than non-biomass. However, there are issues with certain fossil origin organic materials that do degrade under the test conditions, such as: plastics (nylon, polyurethane, silicon rubber); fossil fuels (coal, lignite). Care should be taken not to be present in significant amounts [**Note:** see DD CEN/TS 15440:2006 relative detailed guidance]. Procedure steps:

1. Prepare the general laboratory sample to an appropriate final fineness: shredded down to 1 mm nominal top particle size or less (see DD CEN/TS 15443:2006). **[Note:** shredding and sub-division takes place in Building 244 – sample preparation room].

2. Select a representative test sample quantity from the finely shredded general laboratory sample: i.e. perform correct sub-sampling according to the stipulations of the Theory of Sampling (see DD CEN/TS 15442:2006). Weigh 2 twin test samples (A and B) of 5 g each to 3 decimal places [i.e., 4 digits precision] - record measurements.

3. Determine the ash content A_{SRF} of the portion A according to CEN/TS 15403. **[Note:** Building 244]. **[Note:** Keep the ashes for determination of Total Carbon content (TC), when determination of biogenic content by TC is also performed.]

4. Dry and cool test sample B in a crucible at 105°C to constant weight, according to CEN/TS 15414-1:2006. Weigh dried test sample B to 3 decimal places accuracy - record measurement m_{SRF} .

5. Insert the entire test sample B into an empty and clean 500ml flask. Weigh the crucible (3 decimal places) after completely emptying it to correct for any material left on it (re-calculate m_{SRF} if necessary).

6. **[H&S Note:** carry out this analysis in a fume cupboard; take extreme care when handling and dispensing concentrated acid; wear acid resistant gloves; eye shield and lab coat; handle in fume cupboard with shield down]. Add carefully 150ml of 78% H_2SO_4 (w/w) (concentrated¹ sulphuric acid) to the flask. Use a volumetric tube and initially add around 120ml. Stir carefully, but thoroughly, by swirling the flask by hand.

¹ If concentrated 98% H_2SO_4 (w/w) is available instead, dilute to 150 ml of 84% (w/w) as follows: measure 30 ml deionised water in a robust glass volumetric tube and add carefully in a fume cupboard 120 ml of 98% (w/w) H_2SO_4 . This is slightly than the prescribed by the standard 78% w/w.

Make sure the entire sample is well dispersed and immersed in the acid. If any sample material has been attached to the walls add the rest acid in a way that brings the sample into solution.

Leave the flask for 16 [\pm 2] hours. [**H&S Note:** leave flasks in an acid resistant spill tray and put unattended operation warning notice]. [**Note:** e.g. if dissolution starts at 17:00 pm then next step has to take place around 9:00 am next day].

7. [**H&S Note:** as in 6]. After 16 [\pm 2] h add 30ml of 35% (w/w) H₂O₂ (concentrated hydrogen peroxide). Stir as in 6. Leave for 5 [\pm 1] h. [**Note:** e.g. this step at ca 9:00 am then next step at ca 14:00 am].

8. Dry (oven 105°C, until constant weight achieved) a GF 6 [or: GF/B] glass fibre filter (0.45µm pore size, retaining particles > 1µm; ϕ ca 90 mm, fully fitting the available Buchner funnel) and record its weight m_f .

9. After 5 [\pm 1] h add 300ml of deionised water to dilute the acid. [**H&S Note:** adding water to concentrated acid is dangerous, because the mixture will heat rapidly and spit. Therefore have the 300ml water in a separate flask and add about half the acid to the water. When is mixed the acidified water can be poured slowly into the remaining acid digestion flask.]

10. Filter the digest through the glass fibre in a Buchner funnel. Rinse both flasks repeatedly with 50ml doses of de-ionised water to ensure the entire solid sample residue is filtered. Rinse the filter with 6 doses of 50 ml of deionised water [**Note:** it might practically have to be e.g. 5 doses of 100ml, as the diameter of the funnel is 90mm and not all the solid residue is washed out by rinsing by 50ml each time]. Make sure the entire 50 [or 100] ml is removed before another dose is added. The last filtrated volume has a pH of at least 3.0. While each washing addition stir carefully the suspended solid

resides to facilitate their washing, e.g. with a spatula, taking extra care not to scrub any material of the glass filter.

11. Determine the DM of the filter+residue (oven 105°C, until constant weight achieved). Weigh dried filter+residue and record measurement m_{f+res} . Calculate the mass of residue: $m_{res} = m_{f+res} - m_f$

12. Brush off gently [**Note:** use soft brush, take extra care not to scrape any paper] the residue and retain as Residue B.

13. Determine the ash content of the residue of sample B $m_{res-ash}$ (by weight determination), (see step 3 for method).

14. Record results in paper and transfer to appropriate software template (e.g. Excel); determine the percentage of biogenic content by mass, according to the formula of DD CEN/TS 15440:2006 (formula B.1).

C.5 Total chlorine content

Uncertainty propagation formulas and conventions are used throughout. Where results are reported for the total chlorine concentration for the entire samples (biodried fraction, oversized heavy rejects: **Figure 5-15**) computed from the value measured for the shreddable-only part (excluding hazardous components) the correction factor detailed in the biogenic content determination applies (**Section 4.13.5**), along with a similar (generally negligible) correction for the hazardous items.

Appendix D – Sampling plan for UK MBT plant A

D.1 Introduction to the Gy's theory of sampling (ToS)

Lately it has become increasingly apparent to the scientific community that correct and representative sampling of solid heterogeneous streams can be designed according to the theory of sampling (ToS). ToS have been primarily developed by Pierre Gy over the last 50 years³⁷⁸. The key reason that the ToS should be applied is that it is the only theory that takes into account the heterogeneity of the material to be sampled in a quantitative way, derived from basic principles and by following a structured mathematical approach³⁷⁹. Basic merits of the ToS are that (1) offers a systematic approach to describe all errors encountered in sampling heterogeneous materials and provides the tools to evaluate and eliminate or minimise them²⁸⁹; (2) it can account for the heterogeneity due to the different concentration of the analyte under investigation in fragments of different mass, of which the lot to be sampled is composed of³⁸⁰; and (3) in practice, it allows to quantify (the order of magnitude of) the minimum mass sample to be taken as a representative sample of a population (lot), given a maximum level of relative standard deviation around the lot mean that has not to be exceeded, for a defined level of confidence²⁶⁷.

The increased recognition of the importance of ToS has resulted in many publications. A search in Scopus for the journal publications that cite the main book that provides guidance on how to put the ToS into practice²⁹⁰ returns 85 results. Relevant publications come in the form of books^{267, 271, 290, 379}; peer-reviewed papers discussing theory^{268, 381, 269, 270, 382, 383, 297, 289, 384, 385} and applications^{291-292, 299, 382, 386-393}.

Gy has clearly stated the great potential for application of the ToS in the waste management sector²⁷¹. Early applications of the ToS in the waste sampling and

characterisation have been discussed in the UK by Warren Spring Laboratories³⁹⁴ and in the US^{285, 290}. Recently the ToS has been included in the EPA guidance on waste sampling²⁸⁶ and sample preparation²⁸⁷ and the CEN guidance on waste²⁸⁸ and solid recovered fuels sampling²⁶⁴. Peer-reviewed research results on waste using the ToS have just started appearing^{208, 275, 289, 395-396}. Seminars have been delivered by chemometricians for the application of the ToS in a waste management context^{380, 397}.

A series of seven practical sampling principles summarise good practice in the technical aspects of a sampling plan²⁸⁹:

Principle No.	Description
PSP1	Always perform a heterogeneity characterisation of new materials
PSP2	Mix (homogenise) well before all further sampling steps
PSP3	Use composite sampling instead of premature focus on overall mass sample
PSP	Only use representative mass reduction
PSP5	Use comminution whenever necessary (reduction in fragment size)
PSP6	Perform variographic characterisation of 1-D heterogeneity
PSP7	Whenever possible turn 2-D and 3-D lots into 1-D equivalents

D.2 Application of theory of sampling to the UK MBT plant A

D.2.1 Calculation of lot sizes

The size of the lots (in mass or time) is arbitrarily defined by the objectives of each sampling plan. If the sampling plan aims at quality control, the lots should be sufficiently small to indicate changes in the product quality. Hence, the CEN/TS 343 guidance for SRF (15442:2006)²⁶⁴ demands that for this material flow the maximum weight of a lot should be no more than 1500 Mg or the 1/10th of the yearly production (for non-output flows could be: throughput) if that is less than 15,000 Mg.

In this example we arbitrarily (initially) define the lot to be the average mass quantity processed during one month, through each sampling point. Assuming 1 year =

356.5 calendar days; 1 month = 1 year / 12 it follows that: 1 month = 365.5/12 = 30.46 calendar days.

D.2.2 Calculation of the composite sample mass according to ToS: desirable vs. achievable precision

The formula below, based on Gy's theory of sampling as implemented by DD CEN/TS 15412:2006, provides the mass of the composite sample. (Names of the variables/parameters in this formula are explained in the **Table_App D-1**).

Formula for calculation of the minimum sampling mass,

$$M_s = \frac{1}{M_L + \frac{S(TE)^2}{2 \times \left[\left(\frac{1 - a_L}{a} \right) \times \rho_a + \left(1 - \frac{a_L}{a} \right) \times \rho_m \right] \times \left(\frac{d_0}{d_{95}} \right)^x \times f \times g \times d_{95}^3}} \quad [0-22]$$

Table_App D-1 Explanation and notes on the ToS sample mass formula

Property	Designation	Units	Formula or Determination method	Anticipated or nominal value	Comments
Nominal top particle size	d_{95}	mm	CEN/TS 15415 DD CEN/TS 15442:2006 dictates that for fluff-type SRF the value of $d_{95,l}$ should be used		
Maximum length of a fluff particle	$d_{95,l}$	mm			
Minimum particle size	d_{05}	mm	CEN/TS 15415		
Maximum volume of fluff particle	V_{95}	mm^3	$V = l \times b \times h$		
(SRF particle) Shape	s	mm^3/mm^3	$s = \frac{V_{95}}{d_{95,l}^3}$		DD CEN/TS 15442:2006 "Shape factor"

factor					generally increases if the material is comminuted”
SRF average density of particles	λ	g/mm ³ (ar)			
Distribution factor	g		DD CEN/TS 15442:2006 Table D.1 (p.31) $g = f\left(\frac{d_{95}}{d_{05}}\right)$	DD CEN/TS 15442:2006 “... fluff-type SRFs ... [have] generally a large distribution in the particle size. In many cases the distribution results in a g of 0.25 [i.e., $d_{95}/d_{05}>4$]”	Factor g is related to the typical mass-based grade efficiency descriptor, a measure of how much narrow or wide is the SRF PSD: see 7.3.1. Section LR
Factor-p	p	g/g		DD CEN/TS 15442:2006 If value not known or not-determined, then a fixed value of 0.10 shall be maintained	DD CEN/TS 15442:2006 “Fraction of the particles with a specific characteristic, such as contaminant” The 0.10 value presumably assumes a 10 % wt. contamination or 90 % wt. purity of SRF
Coefficient of variation	C_v			DD CEN/TS 15442:2006 With the above assumptions a value of	

				0.1 shall be maintained	
Minimum sample size	m_m	g (ar)	$m_m = \frac{\pi}{6} \times d_{95}^3 \times s \times \lambda \times g \times \frac{(1-p)}{(C_v)^2 \times p}$		
Minimum sample size	m_m	g (ar)	DD CEN/TS 15442:2006 Table D.2 (p.33)		Surrogate estimate, under certain assumptions for fluff-type SRF
(SRF) Bulk density	Φ_f	kg/m ³ (ar)	CEN/TS 15401		
Minimum sample volume	V_m	m ³	$V_m = \frac{m_m}{10^3 \times \Phi_f}$		

It is fundamental to note that the composite sample mass is calculated for a certain value of “total sampling error” (TSE) and it refers to a certain measurand (analyte concentration, e.g. Cd concentration). This error is a relative standard deviation: its value determines the reliability of the overall measurement process in terms of precision. Generally speaking, for a lot with defined characteristics, the bigger the composite sample mass, the lower the (TSE) and hence the higher the precision of the overall measurement process. Unfortunately, the very precise determination of inhomogeneously distributed trace analytes in residual municipal solid waste poses an almost unsolvable (at realistic cost and effort) sampling problem²⁶⁷. The masses necessary to sample for a precision of a relative standard deviation of 0.01 can be unmanageable.

An example on heterogeneity and precision is provided. Assuming a median concentration of Cd at ca. 1 mg/kg, a relative standard deviation of 0.5 would mean that the standard deviation is 0.5x1=0.5 mg/kg. Hence, assuming that the Cd concentration follows a normal distribution (assumed for simplicity), we would expect to find the Cd concentrations in the range of ± 2 standard deviations (2x0.5) around the

mean value, i.e. with a ca. 96 confidence interval. Namely, it would be: $[Cd] = 1 \pm 2 \times 0.5 = 1 \pm 1$ mg/kg. However, for this very low level of precision achieved by a 0.5 relative standard deviation we estimate that we need to collect a sample of ca 230 kg to represent the lot of the input material to the processing section if it was shredded to a nominal top size d95 of 150 mm, and a mass of ca 710 kg, if it was shredder to a d95 of ca 300 mm. A much higher level of precision would demand much higher composite mass samples for this material stream. The variance (standard deviation squared) is additive, hence other parts of the measurement, such as the analytical determination, will introduce a variance that has to be added to that of the primary sampling. However, the error due to the primary sampling is anticipated to be orders of magnitude larger than the analytical error^{267, 289}: hence, efforts should be concentrated into quantifying and minimising the variance of the primary sampling.

D.2.3 Parameters with critical impact on Ms

The critical parameters that have the most influence to the Ms as calculated by the above formula derived from Gy's sampling formula are:

(1) the nominal top size d95 of the fragments that constitute the lot (e.g. 30 cm for the shredded biodried input to the refinement section; 3 cm for the SRF) because it is raise to the third power. It is clear that the heterogeneity (measured as relative standard deviation) is dramatically reduced with the reduction of the nominal top size of the fragments, and hence the necessary sample mass. However, the power 2 has been proposed for flat shredded waste, but this theoretical assumption, stemming from the desire to produce manageable Ms has not been tested³⁹⁴.

(2) The relative ratio of the aL (average concentration of the analyte in the lot) and a (concentration of the analyte in the analyte containing fragments of the lot). Heterogeneity is much lower for analytes that are evenly distributed in the lot

fragments, compared to those for which most of their quantity is concentrated into small, not frequently encountered fragments.

Other researchers concluded that for waste the liberation factor might be of even more importance than the implied by the above formula, especially with matrices with high fractions of liberated solid metal²⁷⁵.

For each sampling point the parameters in the formula above should be estimated and the desired level of precision should be selected. It is outside the scope of this document to present the detailed calculations involved in the determination of Ms. A series of assumptions and estimations are necessary in order to quantify the sample masses theory of ToS, namely for deriving the above formula and for estimating the values of the properties that appear in the formula. Estimation of the variables/parameters can be based on similar plant SRF data, literature review MBT-derived SRF data, detailed review of existing literature on other properties, nominal values provided for the UK MBT plant A plant (primary and secondary comminution at 300 and 30 mm respectively), educated guesses and balancing calculations. Estimates of the necessary composite mass samples necessary to achieve the denoted level of relative standard deviation based cadmium (Cd) concentrations, calculated into easy to sample measures, can be found at the sampling SOPS.

D.3 Calculation of trommel input lot

Accurate calculation of the lot mass of the biodried fraction processed through the refinement section should be based on the mass flow data of the cranes that feed the refinement section. For instance, the in-feed of the refinement section for 14 operational days, from 21/10/07, 00:00:00 to 07/11/07, 23:59:59: was at 585.3 Mg for all types of input contracts included. How many (1) operational hours; (2) days of plant availability; and (3) days per calendar month does the 585.3 Mg correspond to?

In these 14 operational days the mean throughput of the mechanical section is 41.8 Mg /operational day. The median daily processes quantity is 41.0 Mg, (or 573.9 Mg sum) which is statistically sounder for performing calculations.

For a 30.46 days per month we can have two “end-of spectrum scenarios: a (1) 5 operating day out of 7 calendar day week (“5/7”) or a (2) (“6/7”). Calculations for these two scenarios can provide the range of possible values. We assume that a 6 day week will result in a higher processing mass: however, this might not be the case: the plant operator can chose to process less each day and spread over 6 days. We can see no apparent reason for this to happen but we have to consider it.

(1) 5/7 week: the 14 operating days are equivalent to $14 \times (7/5)$ calendar days = 19.6 days. Processing section input month lot mass: $ML(inp) = 573.9 \times 30.46 / 19.6 = 892$ Mg

(2) 6/7 week: the 14 operating days are equivalent to $14 \times (7/6)$ calendar days = 16.8 days. Processing section input month lot mass: $ML(inp) = 573.9 \times 30.46 / 16.8 = 1041$ Mg

Hence the monthly input mass lot belongs to the range of: [892, 1041] Mg, namely $ML(inp)$ is ca. 1 Mg (ton). Regarding the CEN QA/QC criterion for the 1/10th of the yearly production this is automatically met, as we have selected the lot to be the 1/12th of the yearly processed quantity.

D.3.1 Refining the estimates of sample masses through an iterative process

The production of sampling plan according to ToS is an iterative process. This first calculations are a desk-based study. Resultant mass of composite samples is an initial rough estimate, and hence should be treated as the first rough stage of a tiered approach to quantifying the heterogeneity of each lot. They should be revised as

conclusive results are obtained (evidence based on actual sampling and analysis). However, they constitute realistic values to allow the sampling process to start.

To accurately estimate the heterogeneity (variability) of the flows, it is necessary to conduct a variographic experiment. As stated by both academics and practitioners of the theory of sampling, such an experiment is a critical component of the heterogeneity characterisation process which is necessary to inform any sampling plan (see also **Section 2.5.3**)^{267, 379, 384}.

Results of the first full analysis of the first composite samples produced after proper sampling is established can be used to estimate the measured variance, e.g., by conduction a staggered nested design of analysis of variance²⁷⁵⁻²⁷⁶.

D.3.2 Incremental sampling frequency

The sample mass that represents the lot for each sampling point is collected in a series of incremental sampling actions. In each of them an incremental sample mass is collected. At the end of the collection period that represents each lot, all the incremental samples for the same material flow are combined together to create the composite sample mass. Compositing serves two critical objectives. It:

(1) averages quantities so as to be able to balance quantities before and after unit operations. This is necessary because in practice it is not possible sampling the same matrix quantity throughout an operational plant.

(2) reduces the grouping and segregation error (GSE) for our measurements²⁹⁰. To achieve this, sampling as often as possible is necessary, i.e. having the biggest number of increments possible. Indicatively, the CEN guidance for SRF QA/QC demands 24 increments per composite sample²⁶⁴. However, this is an arbitrary value and it constitutes a suitable compromise; not the result of scientific necessity. A much

greater number of increments may be necessary in order to minimise the grouping and segregation error (see for instance the measurements and theoretical calculations by TAUW)²⁰⁸.

The GSE error is minimised by reducing the incremental sample mass: this is why many increments, each of lower mass, are taken, rather than many increments of bigger mass (which to the limit of zero increments would mean taking just one big sample, i.e. not to create a composite sample). This explains why for a given composite sample mass, it is not a preferable option to reduce the number of increments and increase the mass we are sampling at each of them – exactly the opposite is desirable: sample as many times as we can, taking as small increments as we can.

D.3.3 Number of increments

In practice, the number of increments per lot will be determined by:

- (1) the duration (or overall mass) of the lot, and:
- (2) the sampling frequency that is practically achievable at a full scale commercial operational plant, without causing excessive downtime and cost.

For instance, an achievable sampling frequency for the case study of the UK MBT plant A is twice per calendar week. If the lots have been set to a calendar month (see 2.2.3) this would mean that in a calendar month the number of increments collected would be: $4.35 \times 2 = 8.7$ which rounds to the closed integral 9. For 9 increments per lot, collected twice per calendar week, the lot would be somewhat bigger than one month, equivalent to $4.5 \text{ weeks} = 7 \times 4.5 = 31.5$ calendar days. For this new duration of the lot the new ML(inp) range would be: [922, 1076] Mg. Again, a rough estimate for 1 Mg holds.

D.3.4 Temporal random stratified sampling

Lots to be sampled are either 1-D (conveyor belts/drop flows) or 4-D (stock piles). If temporal variation is ignored, i.e., autocorrelations are assumed to be negligible the 1-D lots can be sampled as practically zero-D and the 4-D as 3-D.

In accordance with the imperatives of ToS autocorrelations should be investigated by a variographic study and sampling provisions are corrected accordingly. In the absence of such information, the minimisation of the variance due to anticipated but unknown periodicities can be sought by following random stratified sampling for the time dimension. This means that each incremental sample should be taken at a randomly selected point of time, within the time period that is allowed to be taken (i.e., half a calendar week)²⁹⁰.

At finer detail, the temporally stratified random sampling should be distributed with equal probability over the mass flows processed rather than keeping a stable interval of calendar days. This may be necessary, to accommodate for varying flow-rates. The practical application of this guidance can be complicated for a fully operational MBT plant as it would demand to monitor the processed throughput and adapt the lot duration and the sampling frequency to any significant changes. Indicatively this could occur if significantly lower quantities are directed to the biodried bypass, i.e., much higher quantities are processed through the refinement section in the same time period.

For instance, fluctuations of daily flow rate are common, as is evident in Figure 3. (mass flow-rates at the feeding of the processing section varied from 23.2 Mg/d to 76.2 Mg/d; assuming that the mechanical processing section is not operating if it was not fed by the crane for more than 30 min). Additionally, change between a 5 and 6 day operational week will inevitably result in varying flow rates achieved in different days.

D.3.5 Contingency sampling

If for any reason an incremental sampling action cannot be performed during the planned time, it should be performed as soon as possible after the initially planned time and before the next planned increment. If convenient, the in-built flexibility within the temporal stratified sampling should be used to delay the following sample for a while to enable a more representative spread of these samples. If the sample is not taken at all within the allocated sampling time slot, then a new one should be taken at another convenient time. For certain flows (conveyor belts) it might not be possible to sample twice the incremental sample mass at the same sampling act. Other cases will be dealt with on a case by case basis.

D.4 Sampling plans prepared for the UK MBT plant A

The exact sampling plans prepared for sampling the UK MBT plant A are presented. The calculated sample masses per sampling point, are mentioned in the form of volume, converted using estimated bulk densities. However, these estimates were not always verified. In addition, for many sampling points the sample mass able to collect within the limitations of the sampling was considerably lower than the specified. As a result, this guidance was only partly implemented.

Preparations for sampling

Equipment necessary for sampling [required from UK MBT plant A where marked]

- Adhesive strip: Used for attaching the plastic collection sheet to the walls of the APC dust container.
- Collection tray: Container in which drop flows are initially collected in. It is mechanically supported and moved. It needs to be appropriately dimensioned. The mechanically supported collection tray should be sufficiently big to cover the whole cross-section (or footprint) of the flow at the height of sampling (flows spread as they fall and typically fragments segregate in various ways). Ideally the opening surface of the collection tray should be just a bit bigger than the surface of the drop flow footprint measured at the height of the collection tray opening. [MBT plant A]
- Cooling container: Used for preserving the incremental samples until the composite sample is created. Preservation bags that came from different sampling points are deposited at different locations, clearly marked.
- Stopwatch: operated by the sampler to accurately measure the sampling time during sampling of drop flows (precision sec).
- Hand heat-sealer: Machine that uses heat to seal the preservation bags, manually operated.
- Marked floor area: Clearly marked area at the biodried by-pass plant section, for the reception of the initial sample of flow 1. [MBT plant A]
- Personal protective equipment (PPE), as required and specified by the UK MBT plant A H&S department. [MBT plant A]
- Plastic collection sheet: Plastic sheet that is used to collect the APC dust sample (flow17).
- Preservation bag: Moisture-proof bags, used for the intermediate storage of the samples in the cooling container.
- Scale: A scale that can measure up to 30 kg with gram accuracy.
- Scoops: Necessary for transferring the sampled to the transfer container.
- Small brush: Used for transferring the finest fragments (fines, dust) of the sample to the transfer container.
- Squeegee: sampling tool for conveyor belts. There are 3 conveyor belt widths: (a) 120 mm; (b) 100 mm; and (c) 80 mm. For each conveyor belt width a separate squeegee will be used that meets its exact cross-section. These will be clearly marked. [MBT plant A]
- Tape measure: Used for measuring the length of the conveyor belt from which sample was removed (precision mm).
- Transfer container: Used for gathering the sample at the sampling point, transferring it to the weighing area and weighing it. Each of the 1-16 material flows has its own one, clearly marked. Lids or covers necessary.
- Water-proof permanent ink markers.
- Weighing and sub-sampling working area: Environmentally protected area, where samples mass contained in the sample container is weighed on a scale. Sub-sampling takes place there as well. [MBT plant A]

Before sampling:

- Bring with you: all necessary sampling equipment, Record Sheet (one for each sampling day), Sample Labels (one for each preservation bag).
- Fill in the relative information section of the form for each sampling material flow just before the sampling action and complete during and after sampling, immediately after a measurement is taken, or an observation is made.
- Weigh the clean transfer container beforehand once and mark the value on the container. If any container other than the usual, marked one is used, the weight of the container should be measured beforehand.
- Verify that all sampling equipment is clean and in good working order. It is necessary to thoroughly clean the collection trays and the transfer containers the before sampling of each flow, to avoid cross-contamination from residuals due to previous uses.
- Use all specified PPP and follow the H&S guidance.
- Carry with you and consult the sampling SOPs.

After sampling:

- If feasible, keep a duplicate safe copy (photocopy) of the Record Sheet.

SAMPLE LABEL

SAMPLER	
Sampling date	
Lot No.	
No. of incremental sample	
Sampling point number	
Number of preservation bag – part of same sample	
Humidity indication: initial / final	
Unusual observations	
Contingency sample	

KEY		
Sampler	e.g.: CV	Sampler's initials (E.g. for Costas Velis)
Sampling date	e.g.: 12-01-08	
Sampling location	1-17	See plant flow-sheet in sampling SOPs
Number of preservation bag - part of same sample	e.g.: 1/3	Leave blank if only one bag contains entire increment E.g.: 1/3 means bag No. 1 out of 3 that are part of the same sample
Lot No.	A, B, C, etc	Each lot represents the flow of around one month
Increment No.	1-9	Number of incremental sample within each certain lot For the APC: 1-4
Unusual observations	Y	Yes: if details given in sampling record sheet - otherwise leave blank
Contingency sample	Y	Yes: If it is a contingency sample - otherwise leave blank

SAMPLING RECORD SHEET	
Samples general code: (Reflect site location, project, serial number of sampling record): MBT plant A /CR/	
Date and Time of sampling:	
Plant lock-off time:	
Lot No.:	
GENERAL INFORMATION	
Material producer: Contact name:	Project Ref. No.: Contact name: Costas Velis
Site address:	Carried out by (Company): Cranfield University CRM&E and UK MBT plant A Sampler(s) (Full name and initials):
Reason samples required (sampling objective): Material flow analysis of the plant, whilst following stipulations of quality assurance and control	
MATERIAL DETAILS	
Material type: Biodried municipal solid waste (or as denoted in goods in) and subsequent sub-flows	
Description:(e.g.: colour, moisture content, odour, consistency/homogeneity/particle size - uniform or diverse) 17 selected flows (marked on plant flow-line) with different characteristics at locations before and after unit operations (see table below)	
Describe the process generating the material to be sampled: Biodrying MBT, mechanical processing - refinement section	
SAMPLING METHODOLOGY	
General: Following Gy's Theory of Sampling (TOS) for representative and correct sampling. Sampling of full cross-sections of lots treated as zero-dimension. 3-D lots sampled only if unavoidable.	
Equipment used: As detailed in sampling plan/Detail otherwise:	
Describe sampling procedure (i.e. how were the samples collected): As detailed in sampling plan/Detail otherwise:	
PACKAGING, PRESERVATION, STORAGE AND TRANSPORT DETAILS	
Packaging: Moisture-proof, high tear and puncture resistant bags (12PET/9ALU/12NYLON/100LDPE); heat-sealed/Detail otherwise:	
Preservation: n.a.	
Storage: Cooling refrigerated container (2±2 °C)	
Transport: After mixing and sub-sampling to composite samples	
UNUSUAL OBSERVATIONS AND DEVIATIONS FROM SAMPLING PLAN	
Record any deviations or 'out of norm' conditions 1. Was the plant process operating under 'typical' conditions for the increment to be sampled "steady state"), etc? Detail:	

2. **Observations during sampling:** (e.g. unusual nature of the sample composition, particle size etc.)Detail:

3. **Non-typical application of sampling plan.** Detail:

SIGNATURE OF SAMPLER(S):

1

2

COMMENTS ON THE TABLE

S: Collection tray starts entering drop flow

E: Collection tray has just fully exited drop flow

n.a.: non applicable

Highlighted with thicker red border: cells to be completed by the sampler (if applicable)

No.	Stream	Location	Sampling type	Sampler's initials	Increment number (within lot)	Time (see page 2)	Belt length sampled (mm)	Number of preservation bags per sample	Weighing container mass (g)	Sample + container mass (g)	Specified sample mass (kg)	Specified belt length (cm)	Specified numbers / parts of transfer containers
1	Primary shredder output	Shredder output [exact point to be identified]	Crane grub (C.)							Grabbed mass:	Grab: 100	Sub-sampling: 2 rows H=20 cm, W=60 cm L=350 cm	Final: 7 of 25 L
										Final 1:	Final: 20		
										2:			
										3:			
										4:			
										5:			
										6:			
7:													

No.	Stream	Location	Sampling type	Sampler's initials	Increment number (within lot)	Time (see page 2)	Belt length sampled (mm)	Number of preservation bags per sample	Weighing container mass (g)	Sample + container mass (g)	Specified sample mass (kg)	Specified belt length (cm)	Specified numbers / parts of transfer containers
2	Trommel 130 underflow	720 conveyor belt: upstream magnet 202	Stopped conveyor belt (A.)									150	3/4 of 25 L
3	Fe metals	910_C1 (place of collection skip)	Flowing stream (B.)			S:						n.a.	1 of 3 L
						E:							
4	Magnet 202 rejects	720 conveyor belt: downstream magnet 202	Stopped conveyor belt (A.)									150	3/4 of 25 L
5	-8 Fines	826_C1/2 (place of collection skip)	Flowing stream (B.)			S:						n.a.	1 of 3 L
						E:							
6	+8-20 Flip-flop 740 screen overflow	Small belt (784?) between 740 flip-flop and 780 drumscreen	Stopped conveyor belt (A.)									150	3/4 of 25 L

No.	Stream	Location	Sampling type	Sampler's initials	Increment number (within lot)	Time (see page 2)	Belt length sampled (mm)	Number of preservation bags per sample	Weighting container mass (g)	Sample + container mass (g)	Specified sample mass (kg)	Specified belt length (cm)	Specified numbers / parts of transfer containers
7	+8-20 Aggregates	825_C1/2 (place of collection skip)	Flowing stream (B.)			S:						n.a.	1/3 of 25 L
						E1:							
8	Trommel M130 overflow	140 conveyor belt	Stopped conveyor belt (A.)							Initial sum:		Initial :300	11 of 25 L
										Final 1:			
										2:			
										3:			
4:	Final: 4 of 25 L												
9	Windshift 150 high-gravity output	860 conveyor belt	Stopped conveyor belt (A.)							1:		100	4 of 25 L
										2:			
										3:			
										4:			
10	Secondary shredder	170 conveyor belt	Stopped conveyor								200	1 of 25 L	

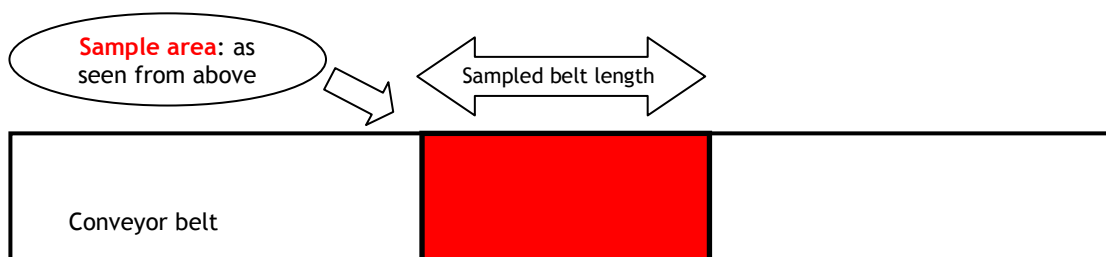
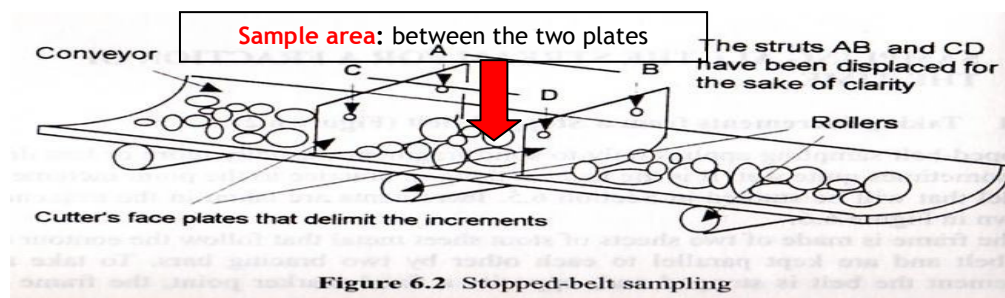
No.	Stream	Location	Sampling type	Sampler's initials	Increment number (within lot)	Time (see page 2)	Belt length sampled (mm)	Number of preservation bags per sample	Weighing container mass (g)	Sample + container mass (g)	Specified sample mass (kg)	Specified belt length (cm)	Specified numbers / parts of transfer containers
	output		or belt (A.)										
11	Magnet 201 rejects	180 conveyor belt: downstream magnet 201, upstream of addition of 781 belt stream	Stopped conveyor or belt (A.)						1:			300	1.5 of 25 L
									2:				
12	Eddy current separator 210 input	180 conveyor belt: downstream of addition of 781 belt stream	Stopped conveyor or belt (A.)									200	1 of 25 L
13	SRF	240 conveyor belt	Stopped conveyor or belt (A.)						1:			250	2 of 15 L
									2:				
14	Non-Fe metals	210_C1 (place of collection skip)	Flowing stream (B.)			S:						n.a.	1/3 of 15 L
						E:							

No.	Stream	Location	Sampling type	Sampler's initials	Increment number (within lot)	Time (see page 2)	Belt length sampled (mm)	Number of preservation bags per sample	Weighting container mass (g)	Sample + container mass (g)	Specified sample mass (kg)	Specified belt length (cm)	Specified numbers / parts of transfer containers
15	Eddy current separator 210 rejects	Eddy current rejects container [not stated in official flow-chart]	Flowing stream (B.)			S: E:						n.a.	1/2 of 15 l
16	+20-150 Rejects	870 conveyor belt	Stopped conveyor belt (A.)							1: 2: 3: 4:		100	4 of 25 L
17	Dust	Dust pipe [or dust collection container]	Flowing stream [or static pile] (D.)								0.4		n.a.

SOP A: Sampling from a stopped conveyor belt

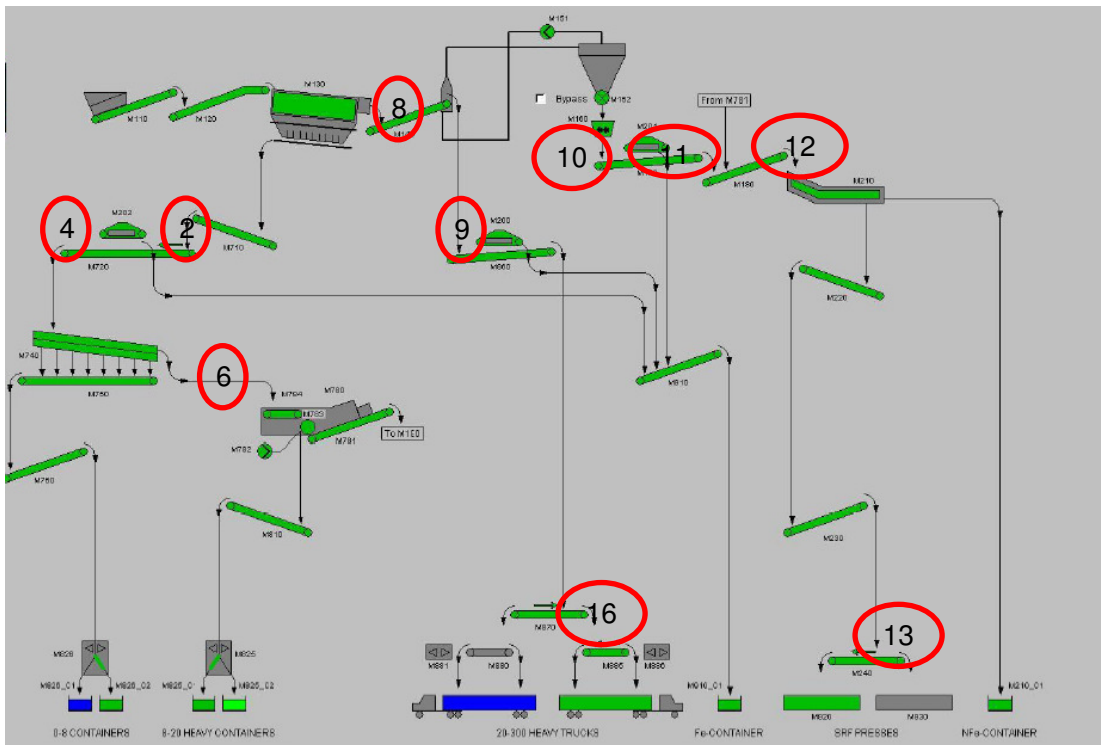
Lot duration	Around 1 month
Number of increments per lot	9 sample increments to form the composite sample for each lot
Sampling frequency	One sample every 2 nd day of plant operation
Sampling time	Any time within the sampling day Selected at random by the plant operator Refinement section should be operating at typical conditions for at least 30 min just before the sampling starts

1. **Lock-off the plant:** Check conveyor is stationary. Note the time on the *Record Sheet*.
2. **Access the sampling area** by lifting the conveyor belt cover, and removing guards and covers.
3. **Inspect the material:** If the mixture is unusual, note this on the *Record Sheet* and mark on the *Sample Label*.
4. **Identify the belt area to be sampled:** Always sample a full, symmetrical slice of the belt. The material falls between two lines across the belt. A starting line (CA), and an ending (DB).
5. **Separate the material to be sampled from the rest**, by applying the squeegee at these lines. Push away material that will NOT be sampled, i.e. material before and after these lines.



6. **Sample collection:** Collect ALL material in the isolated area. By using scoops, collect the material into suitable *transfer container(s)*. If needed, use the squeegee to reach far-off material. AVOID SPILLING any material outside the belt sides. Use brushes to transfer the very fine material.
7. **If the belt length sampled differs from the specified:** measure it in mm. Note on the *Record Sheet*.
8. **Transfer the sample** to the weighing point. Protect the sample by covering the *transfer container*.
9. **Weigh the gross mass of the collected sample:** Remove any cover or lid. Weight the *transfer container(s)* with the sample in grams. Note the value(s) on the *Record Sheet*.

10. **Record data and label the preservation bags:** Complete the *Record Sheet* and *Sample Label(s)*. Note any unusual conditions, sampling practices, observations, for this sampling action.
11. **Transfer the sample to the final preservation bag:** Immediately transfer the sample from the *transfer container* to the *preservation bag*. Transfer **ALL** material, especially the fines. Use more than 1 bag if needed. Complete a *Sample Label* for each bag. Note the number of the bags on the *Record Sheet*.
12. **Seal the preservation bag using the *hand heat sealer* equipment.**
13. **Sample storage:** Immediately store the *preservation bag* in the *cooling container* allocation marked for the sampling point.



Sampling points			Transfer containers		
Stream	Location	Stream number	Belt length (cm)	15L	25L
Trommel 130 underflow (Magnet 202 rejects)	720 conveyor belt: upstream magnet 202	2	150		¾
Magnet 202 reject (Flip-flop 740 screen input)	720 conveyor belt: downstream magnet 202	4	150		¾
+8-20 Flip-flop 740 screen overflow (Drumscreen air classifier 780 input)	Small belt (784) between 740 flip-flop and 780 drumscreen	6	150		¾
Trommel 130 overflow (Windshift air classifier 150 input)	140 conveyor belt	8*	300		11
Windshift air classifier 150 high-gravity output (Magnet 200 input)	860 conveyor belt		Final:		4
Windshift air classifier 150 low-gravity output shredded by 160 secondary shredder (Magnet 201 input)	170 conveyor belt	10	200		1
Magnet 201 rejects	180 conveyor belt: downstream magnet 201, upstream of addition of 781 belt stream	11	300		1.5
Eddy current separator 210 input (Mixed magnet 201 reject and drumscreen 780 high-gravity output - 781 belt)	180 conveyor belt: down stream of addition of 781 belt stream	12	200		1

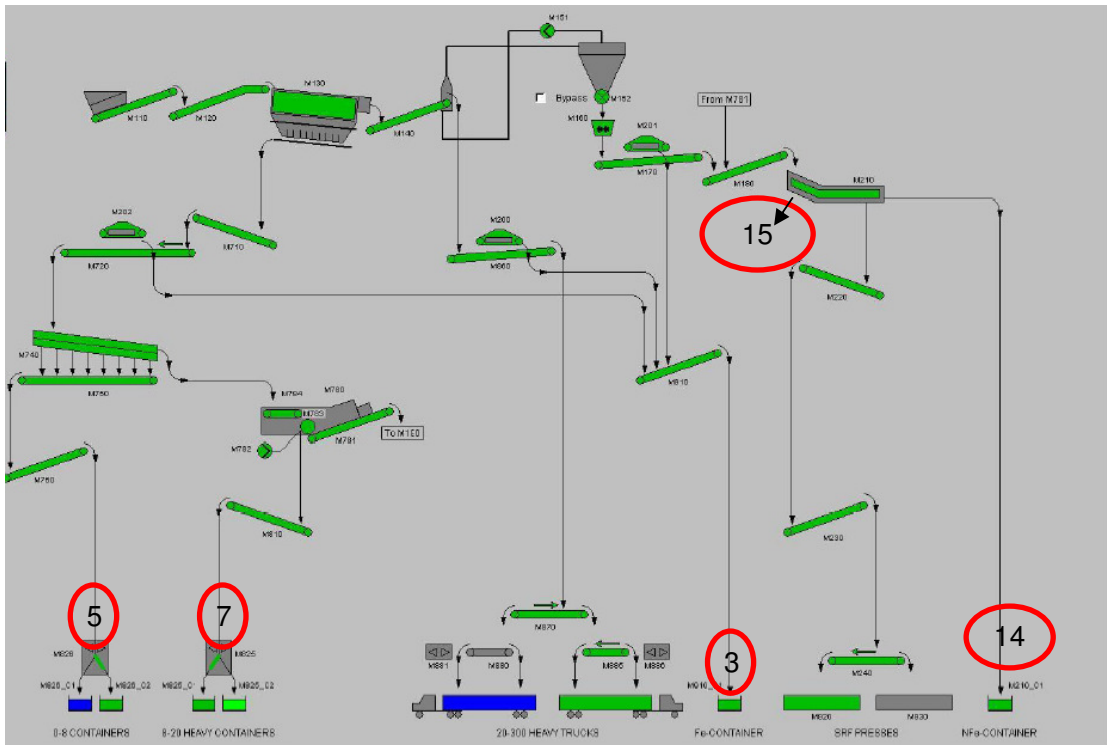
SRF (1 out of 3 of eddy-current 210 outputs)	240 conveyor belt	13	250	2	
+20-300 Rejects (Magnet 200 rejects)	870 conveyor belt	16	100		4

*Stream 8: the initially collected sample (300 cm of belt length, equivalent to 11 buckets of 25 L) will be sub-sampled following the procedure of step 4, SOP C. A final sample of 4 buckets will be stored.

SOP B: Sampling from a drop flow (final outputs)

Lot duration	Around 1 month
Number of increments per lot	9 sample increments to form the composite sample for each lot
Sampling frequency	One sample every 2 nd day of plant operation
Sampling time	Any time within the sampling day Selected at random by the plant operator Refinement section should be operating at typical conditions for at least 30 min just before the sampling starts

- 1 Access the sampling point by removing the skip.
- 2 Inspect the material by allowing for some material to drop to the ground. If the mixture is unusual, note this on the Record Sheet and mark on the Sample Label.
- 3 **Start sample collection:** Move the mechanically supported collection tray along the flow. Move the collection tray AT A CONSTANT SPEED under the flow, so that all parts of the cross-section of the drop flow are sampled for the same time period. The speed should be slow enough to allow for the collection of the entire specified sample mass (volume).
- 4 **Record the start time:** Accurately measure by an stopwatch in seconds the time the collection tray starts entering the flow (time: S).
- 5 **Complete sample collection:** Move only forwards, DO NOT REVERSE. Do so until the collection tray completely exits the flow.
- 6 **Record the end time:** Measure (as in step 5) the time the collection tray completely exits the flow (time: E). Note the values S and E on the Record Sheet.
- 7 **Beware:** While moving away from the collection area, do NOT gather any additional material in the collection tray. Do not accidentally place any part of it under the drop flow again.
- 8 **Upload the sample:** Immediately, within the plant, upload the sample from the collection tray to the transfer container(s). Transfer ALL material. Protect the sample from e.g. rainfall or snowfall by covering the transfer container.
- 9 Transfer the sample to the weighing point.
- 10 **Weigh the gross mass of the collected sample:** Remove any cover (or lid). Weight the transfer container(s) with the sample in grams. Note the value(s) on the Record Sheet.
- 11 **Record data and label the preservation bags:** Complete the Record Sheet and Sample Label(s). Note any unusual conditions, sampling practices, observations, for this sampling action.
- 12 **Transfer the sample to the final preservation bag:** Immediately transfer the sample from the transfer container to the preservation bag. Transfer ALL material, especially paying attention to the fines. Use more than 1 bag if needed. Complete a Sample Label for each bag. Note the number of the bags on the Record Sheet.
- 13 **Seal the preservation bag** using the hand heat sealer equipment.
- 14 **Sample storage:** Immediately store the preservation bag in the cooling container allocation marked for the sampling point.



Sampling point			Transfer container		
Stream	Location	Stream number	3L	15L	25L
Fe metal (Magnets 202, 201, 200 Fe output)	Under chute 910_C1	3	1		
-8 Fines (Flip-flop 740 screen underflow)	Under chute 826_C1/2	5	1		
+8-20 Aggregates ("Glass and stones")	Under chute 825_C1/2	7			1/3
Non-Fe metals ("Al")	Under chute 210_C1	14		1/3	
Eddy current separator 210 rejects	Under eddy-current reject chute	15		1/2	

SOP C: Sampling biodried material (flow No. 1)

Lot duration	Around 1 month
Number of increments per lot	9 sample increments to form the composite sample for each lot
Sampling frequency	One sample every 2 nd day of plant operation
Sampling time	Any time within the sampling day Selected at random by the plant operator Refinement section should be operating at typical conditions for at least 30 min just before the sampling starts

1. **Special features of the lot:** this flow is consists of the biodried material collected just before the input into the processing section. The shredded bio-dried material is transported to *in-feed hopper 110* by cranes 1 and 2. A crane is used for collecting the sample.
2. **Sample collection:** the crane operator grabs around 100 kg of the matrix (**initial sample mass**). Grab a sample randomly among the material which the processing section is fed with at that very moment. Note the automatically measured weight of the crane grab on the *Record Sheet*. This **initial sample mass** will be further reduced to a **final sample mass** (see step 4).
3. **Sample release:** Check that the marked floor area at the biodried by-pass area does is clean. Release the grab on it. Include ALL the released material in further procedures (even if it falls out of the exact limits of the marked floor area).
4. **Sub-sampling to the final sample mass**
 - a) Homogenise the released initial sample by thoroughly mixing with shovels.
 - b) Shape it into two long piles with a uniform section and of rectangular footprint. I.e., imagine each as a big chocolate bar with height H=20 cm, width W=60 cm and length L=around 3.5 m.
 - c) Separate each bar into 7 equal slices (“piece of cake”) of 50 mm length each.
 - d) **Create the final sample mass:** Randomly select 3 slices from the piles. Remove ALL their material, including fines. Gather all these 3 slices into transfer containers.

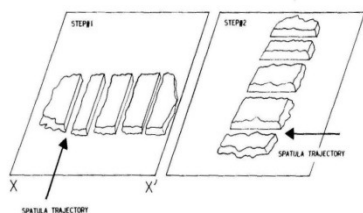
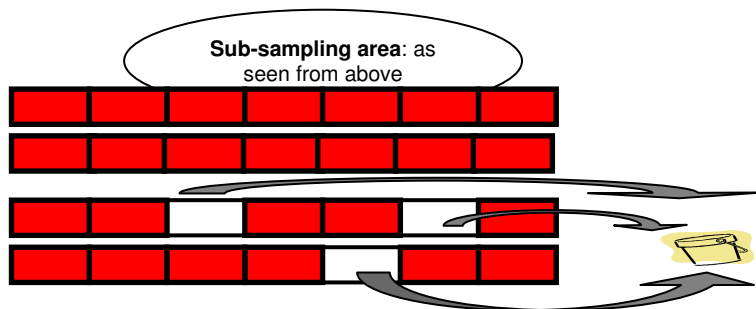
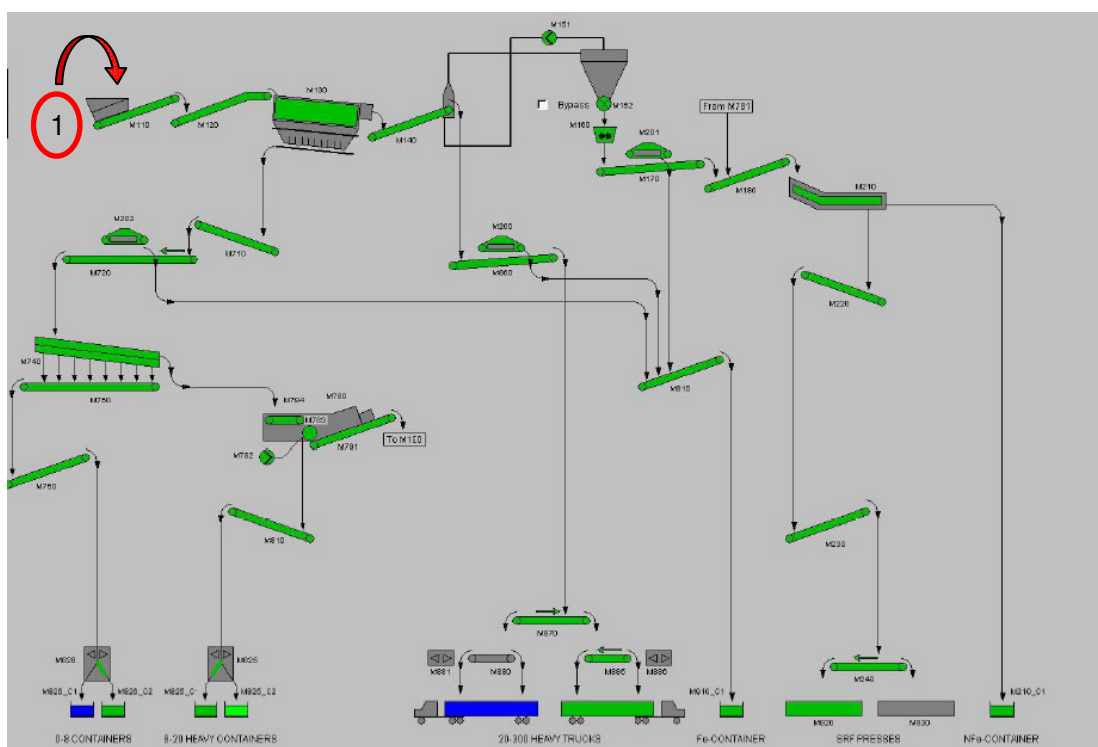


FIGURE 14.12. The one-dimensional Japanese slab-cakes. The increment delimitation can easily be performed correctly.



5. **Transfer the final sample** to the weighing point. Protect the sample by covering the transfer containers.

6. **Weigh the gross mass of the collected sample:** Remove any cover or lid. Weight the transfer containers with the sample in grams. Note the value(s) on the Record Sheet.
7. **Record data and label the preservation bags:** Complete the Record Sheet and Sample Label(s). Note any unusual conditions, sampling practices, observations, for this sampling action.
8. **Transfer the sample to the final preservation bags:** Immediately transfer the sample from the transfer containers to the preservation bags. Transfer ALL material, especially the fines. Complete a Sample Label for each bag. Note the number of the bags on the Record Sheet.
9. **Seal the preservation bags using the hand heat sealer equipment.**
10. **Sample storage:** Immediately store the preservation bags in the cooling container allocation marked for the sampling point 1.



Sampling point		Sub-sampling		
Stream	Location	Stream number	Initial sample (crane grab) (kg)	Final sample (transfer containers of 25 L)
Biodried material, processing section input	Feeding of processing section by cranes 1 or 2	1*	100	7

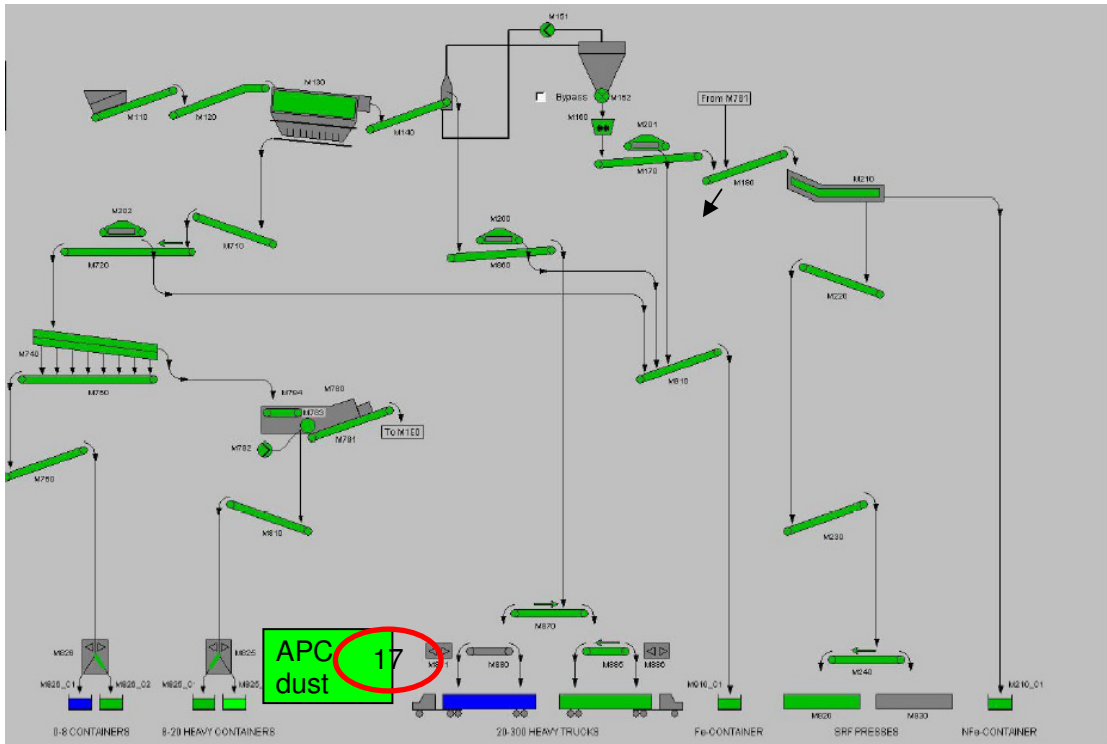
* The initial sample of the crane grab is sub-sampled to the final sample, during step 4.

SOP D: Sampling APC dust output (flow No. 17)

Lot duration	Around 1 month
Number of increments per lot	4 sample increments to form the composite sample for each lot
Sampling frequency	One sample every week of plant operation
Sampling time	Any time within the sampling day Selected at random by the plant operator Suitable weather conditions desirable Refinement section should be operating at typical conditions for at least 30 min just before the sampling starts

1. **Special features of the lot:** this flow consists of the air pollution control (APC) material as it is collected at the discharge of the de-dusting units. The matrix seems to be rather homogeneous, consisting of 2 types of fractions: a fluffy, cotton-like material and a very fine dust. The APC material flows through a piping system and is stored in a fully enclosed, secured dust container.
2. **Accessing the matrix**
 - a) Avoid sampling when raining or windy as dust can very easily become airborne and absorb moisture. Otherwise ensure that no water/moisture is absorbed by the sample and that dust is securely contained. Avoid introducing any agitation that could change the lot.
 - b) Stop the feeding operation of the dust container. An alarm will sound.
 - c) Disengage and slide the container away from the pipe.
 - d) Seal with a plastic collection sheet to separate the lot from the deposited flow. Attach the plastic collection sheet tightly to the walls of the container with an adhesive strip.
4. **Sample collection**
 - a) Re-engage the container. Start the flow (time S1). Take a measurement of the starting time (S1) and make a note on the Record Sheet and the Sample Label.
 - b) Allow the newly discharged material to accumulate above the plastic collection sheet for the specified time period. After the specified time repeat step 2. Report the end time (E1) that the flow was stopped.
 - c) Carefully remove the adhesive stripes that attach the plastic collection sheet to the walls of the container. Remove the plastic collection sheet and transfer the sample directly to the preservation bag (as opposed to a transfer container in other cases). Take care to include ALL material during the transfer. Perform the transfer indoors: step 2.1 precautions apply.
 - d) Immediately secure with adhesive stripe.
5. Transfer the preservation bag to the weighing point.
6. **Weigh the gross mass of the collected sample:** Weight the preservation bag with the sample in tenth of grams. Note the value on the Record Sheet.
7. **Record data and label the preservation bag:** Complete the Record Sheet and Sample Label. Note any unusual conditions, sampling practices, observations, for this sampling action.
8. **Transfer the sample to the final preservation bag:** Immediately transfer the sample from the transfer container to the preservation bag. Transfer ALL material, especially paying attention to the fines.
9. **Seal the preservation bag** using the hand heat sealer equipment.

10. **Sample storage:** Immediately store the *preservation bag* in the *cooling container* allocation marked for the sampling point 17.



Sampling point			Sample size	
Stream	Location	Stream number	Increment size (g)	Increment sampling time (t)
Dust (APC - de-dusting residue)	APC dust container	17	400	*

* Time period that corresponds to the specified sample mass will be identified by an initial measurement of the flow rate, during the first test run. The time period should be sufficient to collect both the dust and fibrous portions (which may be generated at different rates).

Appendix E – Analytical determinations and quality control

E.1 Cl determination by ion chromatography (IC)

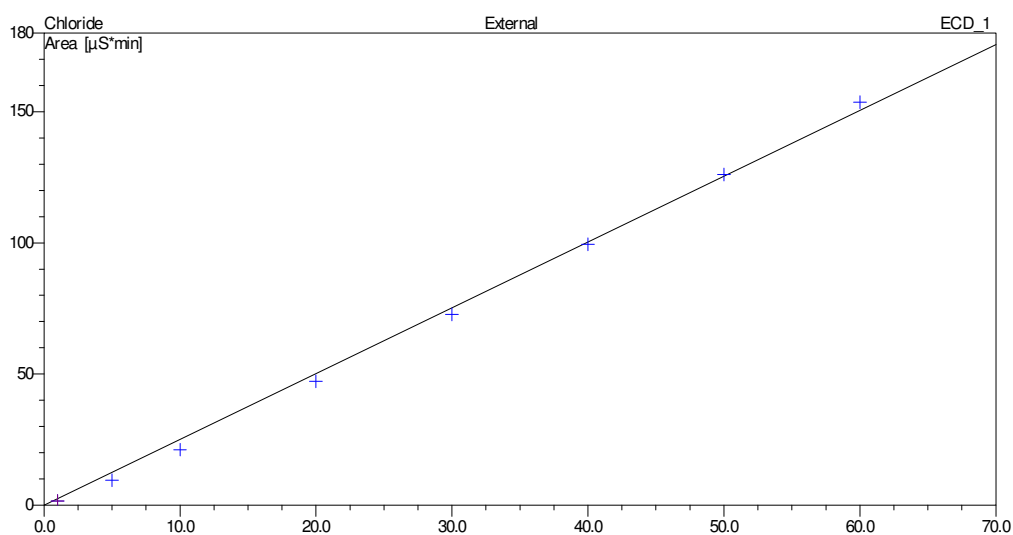


Figure 0-1 Typical calibration curve (generally $R^2 > 99.5$)

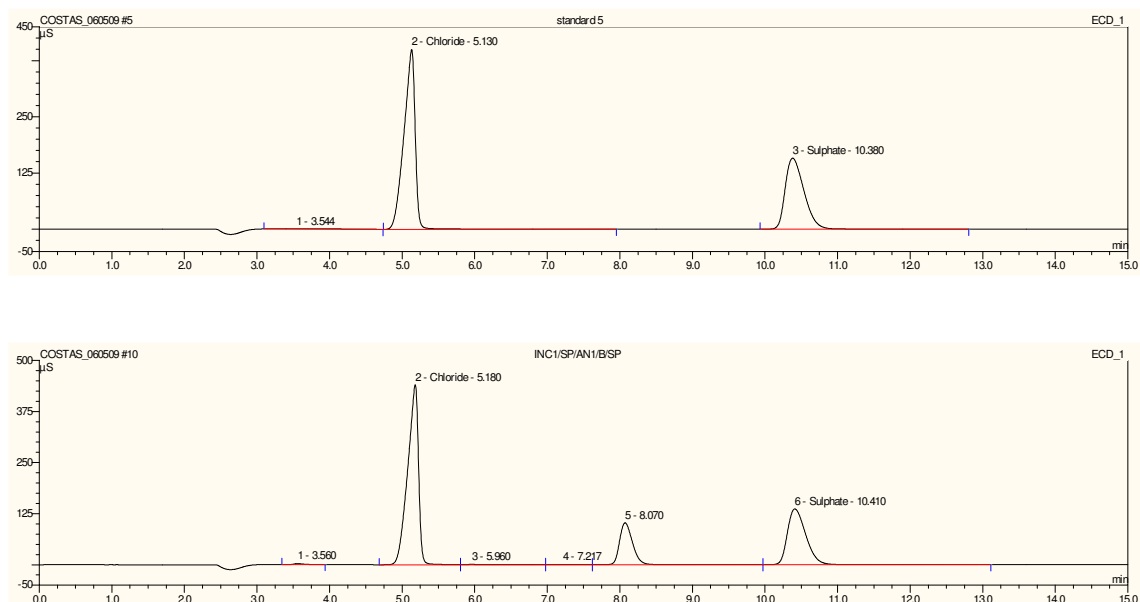


Figure 0-2 Typical chromatograms: upper: mid-range calibration standard; lower: typical sample biodried material. Generally peaks were sufficiently symmetrical.

E.2 Calorific value determination by oxygen bomb combustor

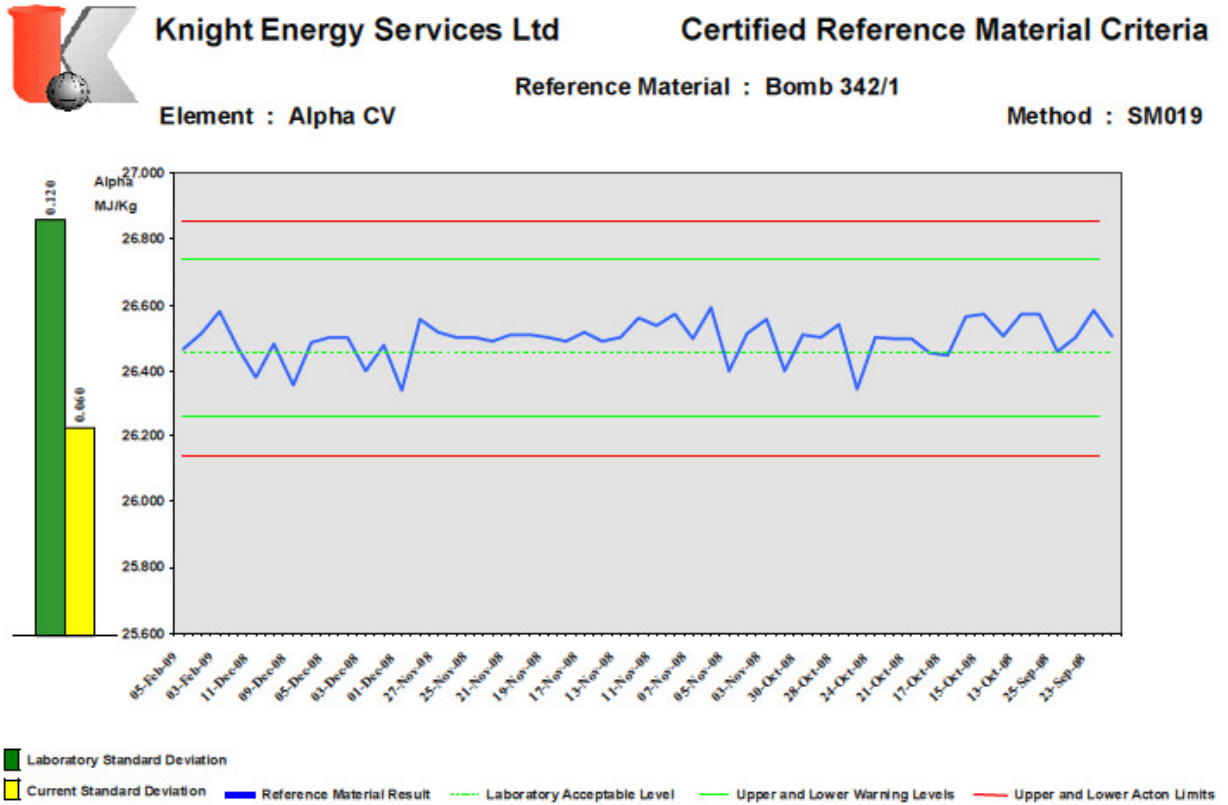


Chart Bomb 342/1 SM019 Alpha CV

Figure 0-3 In house quality control chart for the bomb calorimeter (Gross calorific value determinations)

Appendix F - Material flow analysis of UK MBT plant A

Table_App F-1 UK MBT plant A: raw results of manual sorting of process flows components. Starting point for developing the corrected (modelled) values serving as input to the STAN2[®] modelling. Sampling point 1 (SP1)

Sample ID	L1_INC1_SP1	L1_INC2_SP1	L1_INC3_SP1	L1_INC4_SP1	L1_INC5_SP1	L1_INC6_SP1	L2_INC1-7COMP_SP1	L2_INC8_SP1	ΣL	ΣL
Lot	L1	L1	L1	L1	L1	L1	L2	L2		
Increment	INC1	INC2	INC3	INC4	INC5	INC6	INC1-7COMP	INC8		
Sampling point	SP1	SP1	SP1	SP1	SP1	SP1	SP1	SP1		
Units	g (ar)	g (ar)	g (ar)	g (ar)	g (ar)	g (ar)	g (ar)	g (ar)	g (ar)	W/W _{ar}
Batteries	37.60	1.47	0.00	0.00	32.66	37.66	0.00	24.16	133.55	0.12
Biological	625.21	460.39	781.79	413.10	507.85	660.18	665.54	370.35	4484.41	3.93
Cables	18.59	4.84	9.35	1.23	11.76	0.00	302.90	34.92	383.59	0.34
Carpet/mats	86.84	7.14	331.84	0.43	271.18	366.97	134.83	0.00	1199.23	1.05
Cartons	216.02	55.15	118.46	129.66	86.82	129.77	82.03	75.35	893.26	0.78
Cinders	44.14	43.38	83.53	29.94	48.38	36.32	29.57	20.14	335.40	0.29
Composites	212.14	184.34	411.86	393.46	291.18	381.43	221.42	133.56	2229.39	1.95
Durable plastic	637.79	285.52	418.78	222.81	388.06	387.02	232.12	180.15	2752.25	2.41
Ferrous metal	471.31	637.92	413.41	833.42	1050.14	728.01	887.26	1123.23	6144.70	5.38
Fines < 10 mm	2303.70	1696.14	2760.20	2872.59	1630.66	4239.72	1663.24	935.90	18102.15	15.85
Fluff	14.67	12.21	0.00	12.23	0.00	0.00	369.20	0.00	408.31	0.36
Glass	1708.35	763.75	1326.56	933.40	930.88	1998.65	599.10	315.43	8576.12	7.51
Hazardous	225.70	1.83	83.45	3.89	76.29	74.69	111.90	61.37	639.12	0.56
Non-Fe metal	428.54	166.68	370.70	154.06	277.00	330.44	82.41	163.69	1973.52	1.73
Other	0.00	0.00	0.00	0.00	0.00	0.00	0.00	0.00	0.00	0.00
Other packaging plastic	1027.99	1041.85	1471.83	719.59	2339.73	1687.92	787.43	506.12	9582.46	8.39
Paper/card	4045.93	3723.17	4915.54	3835.72	4203.23	5018.32	2340.44	2681.61	30763.96	26.93
Plastic film	899.29	650.54	1244.34	692.18	2551.53	1417.02	588.49	426.88	8470.27	7.42
Rubber/leather	34.18	13.09	50.72	28.47	7.47	38.56	10.54	18.28	201.31	0.18
Sanitary products	23.37	260.32	172.29	290.45	0.00	214.93	137.37	111.57	1210.30	1.06
Shoes	707.37	0.00	731.94	0.00	725.01	0.00	227.20	0.00	2391.52	2.09

Stones/ceramic	874.48	494.99	534.60	593.57	332.52	937.36	734.66	260.57	4762.75	4.17
Textile/fabric	352.75	151.37	379.84	117.42	323.43	541.75	482.12	668.36	3017.04	2.64
Tissues	77.31	83.10	124.03	207.81	65.42	60.09	161.13	31.51	810.40	0.71
Treated wood	498.04	1040.94	526.79	636.86	669.73	742.77	421.62	224.04	4760.79	4.17
Overall	15571.31	11780.13	17261.85	13122.29	16820.93	20029.58	11272.52	8367.19	114225.80	100.00

Table_App F-2 UK MBT plant A: raw results of manual sorting of process flows components. Starting point for developing the corrected (modelled) values serving as input to the STAN2[®] modelling. Sampling point 2 (SP2)

Sample ID	L1_INC1_SP2	L1_INC2_SP2	L1_INC3_SP2	L1_INC4_SP2	ΣL	ΣL
Lot	L1	L1	L1	L1		
Increment	INC1	INC2	INC3	INC4		
Sampling point	SP2	SP2	SP2	SP2		
Units	g (ar)	g (ar)	g (ar)	g (ar)	g (ar)	w/w _{ar}
Batteries	0.00	0.00	0.00	0.00	0.00	0.00
Biological	66.12	25.27	78.43	36.42	206.24	6.37
Cables	1.42	0.00	0.17	0.00	1.59	0.05
Carpet/mats	0.00	0.06	0.00	0.00	0.06	0.00
Cartons	0.00	0.08	0.00	0.11	0.19	0.01
Cinders	14.34	3.53	0.00	1.07	18.94	0.58
Composites	8.82	0.30	3.26	1.18	13.56	0.42
Durable plastic	6.39	1.02	0.72	3.29	11.42	0.35
Ferrous metal	12.16	0.00	36.40	0.13	48.69	1.50
Fines < 10 mm	727.75	249.92	717.61	645.23	2340.51	72.28
Fluff	9.31	0.00	0.00	0.00	9.31	0.29
Glass	249.77	49.26	54.69	71.17	424.89	13.12
Hazardous	0.00	0.00	0.00	0.00	0.00	0.00
Non-Fe metal	2.11	0.71	4.09	0.98	7.89	0.24
Other	0.00	0.00	0.00	0.00	0.00	0.00
Other packaging plastic	4.05	0.61	4.21	0.00	8.87	0.27
Paper/card	22.34	7.40	23.36	12.20	65.30	2.02
Plastic film	9.11	1.59	7.84	2.13	20.67	0.64
Rubber/leather	0.00	0.00	0.59	0.91	1.50	0.05

Sanitary products	0.00	0.00	0.00	0.00	0.00	0.00
Shoes	0.00	0.00	0.00	5.98	5.98	0.18
Stones/ceramic	0.00	21.42	10.86	7.02	39.30	1.21
Textile/fabric	1.70	1.31	1.30	0.76	5.07	0.16
Tissues	0.00	0.00	0.56	0.00	0.56	0.02
Treated wood	2.53	1.57	3.30	0.00	7.40	0.23
Overall	1137.92	364.05	947.39	788.58	3237.94	100.00

Table_App F-3 UK MBT plant A: raw results on manual sorting of process flows components. Starting point for developing the corrected (modelled) values serving as input to the STAN2[®] modelling. Sampling point 3 (SP3)

Sample ID	L1_INC1_SP3	L1_INC2_SP3	L1_INC3_SP3	L1_INC4_SP3	ΣL	ΣL
Lot	L1	L1	L1	L1		
Increment	INC1	INC2	INC3	INC4		
Sampling point	SP3	SP3	SP3	SP3		
Units	L1_INC1_SP3	L1_INC2_SP3	L1_INC3_SP3	L1_INC4_SP3	g (ar)	w/w _{ar}
Batteries	0.00	14.26	0.00	0.00	14.26	0.12
Biological	0.77	0.04	0.00	1.31	2.12	0.02
Cables	0.00	9.08	0.00	0.00	9.08	0.08
Carpet/mats	0.00	0.00	0.00	1.02	1.02	0.01
Cartons	0.00	3.76	0.17	1.37	5.30	0.05
Cinders	0.00	0.00	0.00	0.00	0.00	0.00
Composites	9.02	3.97	9.39	7.21	29.59	0.25
Durable plastic	2.76	4.54	0.00	2.54	9.84	0.08
Ferrous metal	2985.12	2305.34	2258.48	2834.10	10383.04	88.42
Fines < 10 mm	257.04	229.96	250.84	120.59	858.43	7.31
Fluff	0.00	0.82	0.00	2.86	3.68	0.03
Glass	0.00	0.00	0.00	0.00	0.00	0.00
Hazardous	0.00	6.29	0.00	0.07	6.36	0.05
Non-Fe metal	0.00	0.00	0.00	0.00	0.00	0.00
Other	0.00	0.00	0.00	0.00	0.00	0.00
Other packaging plastic	7.05	18.98	8.48	19.67	54.18	0.46
Paper/card	15.06	53.15	46.65	47.10	161.96	1.38

Plastic film	41.85	41.09	36.16	23.74	142.84	1.22
Rubber/leather	0.00	0.08	0.00	1.19	1.27	0.01
Sanitary products	0.00	0.00	0.00	0.00	0.00	0.00
Shoes	0.00	0.00	0.00	0.00	0.00	0.00
Stones/ceramic	0.00	3.38	18.49	0.00	21.87	0.19
Textile/fabric	12.00	11.62	0.00	9.90	33.52	0.29
Tissues	0.00	0.34	0.00	0.73	1.07	0.01
Treated wood	0.00	1.79	0.00	1.61	3.40	0.03
Overall	3330.67	2708.49	2628.66	3075.01	11742.83	100.00

Table_App F-4 UK MBT plant A: raw results on manual sorting of process flows components. Starting point for developing the corrected (modelled) values serving as input to the STAN2[®] modelling. Sampling point 4 (SP4)

Sample ID	L1_INC2_SP4	L1_INC3_SP4	L1_INC4_SP4	ΣL	ΣL
Lot	L1	L1	L1		
Increment	INC2	INC3	INC4		
Sampling point	SP4	SP4	SP4		
Units	g (ar)	g (ar)	g (ar)	g (ar)	w/w _{ar}
Batteries	0.00	0.00	0.00	0.00	0.00
Biological	32.67	46.23	15.45	94.35	5.64
Cables	0.00	0.25	0.00	0.25	0.01
Carpet/mats	0.00	0.00	0.00	0.00	0.00
Cartons	0.00	0.00	0.10	0.10	0.01
Cinders	0.00	0.00	0.26	0.26	0.02
Composites	0.00	0.80	0.63	1.43	0.09
Durable plastic	0.32	2.67	1.57	4.56	0.27
Ferrous metal	6.43	0.00	0.89	7.32	0.44
Fines < 10 mm	511.76	390.81	353.00	1255.57	75.03
Fluff	0.00	0.00	2.36	2.36	0.14
Glass	70.73	66.35	65.60	202.68	12.11
Hazardous	0.00	0.46	0.00	0.46	0.03
Non-Fe metal	0.15	0.00	0.70	0.85	0.05
Other	0.00	0.00	0.00	0.00	0.00

Other packaging plastic	0.00	1.33	0.23	1.56	0.09
Paper/card	11.69	10.89	8.60	31.18	1.86
Plastic film	3.29	2.34	1.40	7.03	0.42
Rubber/leather	0.00	0.08	0.36	0.44	0.03
Sanitary products	0.00	0.00	0.00	0.00	0.00
Shoes	0.00	0.00	0.00	0.00	0.00
Stones/ceramic	21.64	21.59	13.17	56.40	3.37
Textile/fabric	0.95	0.55	0.34	1.84	0.11
Tissues	0.00	0.00	0.00	0.00	0.00
Treated wood	0.00	3.61	1.18	4.79	0.29
Overall	659.63	547.96	465.84	1673.43	100.00

Table_App F-5 UK MBT plant A: raw results on manual sorting of process flows components. Starting point for developing the corrected (modelled) values serving as input to the STAN2[®] modelling. Sampling point 5 (SP5)

Sample ID	L1_INC1_SP5	L1_INC2_SP5	L1_INC3_SP5	L1_INC4_SP5	L1_INC9_SP5	ΣL	ΣL
Lot	L1	L1	L1	L1	L1		
Increment	INC1	INC2	INC3	INC4	INC9		
Sampling point	SP5	SP5	SP5	SP5	SP5		
Units	g (ar)	g (ar)	g (ar)	g (ar)	g (ar)	g (ar)	w/w_{ar}
Batteries	0.00	0.00	0.00	0.00	0.00	0.00	0.00
Biological	26.36	32.86	24.27	38.27	26.11	147.87	2.51
Cables	0.00	0.00	0.00	0.00	0.00	0.00	0.00
Carpet/mats	0.00	0.00	0.00	0.00	0.00	0.00	0.00
Cartons	0.00	0.00	0.00	0.00	0.32	0.32	0.01
Cinders	0.00	1.18	3.87	0.87	1.35	7.27	0.12
Composites	0.64	0.33	1.10	2.31	2.07	6.45	0.11
Durable plastic	0.00	4.08	8.39	2.28	1.58	16.33	0.28
Ferrous metal	0.00	0.00	0.18	0.47	0.00	0.65	0.01
Fines < 10 mm	917.26	689.24	1187.74	1422.27	1160.52	5377.03	91.22
Fluff	0.00	0.00	11.68	12.32	0.00	24.00	0.41

Glass	11.46	88.43	52.39	18.61	29.78	200.67	3.40
Hazardous	0.00	0.84	0.00	0.00	0.00	0.84	0.01
Non-Fe metal	0.00	0.11	0.00	0.51	0.00	0.62	0.01
Other	0.00	0.00	0.00	0.00	0.00	0.00	0.00
Other packaging plastic	0.75	2.63	0.73	1.67	0.56	6.34	0.11
Paper/card	8.30	1.58	10.41	11.96	6.33	38.58	0.65
Plastic film	1.50	1.72	1.62	3.06	3.23	11.13	0.19
Rubber/leather	0.00	0.00	0.00	0.00	0.00	0.00	0.00
Sanitary products	0.00	0.00	0.00	0.00	0.00	0.00	0.00
Shoes	0.00	0.00	0.00	0.00	0.00	0.00	0.00
Stones/ceramic	1.24	20.40	11.75	2.51	8.29	44.19	0.75
Textile/fabric	2.04	0.00	0.35	1.56	0.48	4.43	0.08
Tissues	0.00	0.90	0.31	0.49	0.00	1.70	0.03
Treated wood	0.86	0.34	1.64	1.69	1.74	6.27	0.11
Overall	970.41	844.64	1316.43	1520.85	1242.36	5894.69	100.00

Table_App F-6 UK MBT plant A: raw results on manual sorting of process flows components. Starting point for developing the corrected (modelled) values serving as input to the STAN2[®] modelling. Sampling point 6 (SP6)

Sample ID	L1_INC1_SP6	L1_INC2_SP6	L1_INC3_SP6	L1_INC4_SP6	L1_INC9_SP6	ΣL	ΣL
Lot	L1	L1	L1	L1	L1		
Increment	INC1	INC2	INC3	INC4	INC9		
Sampling point	SP6	SP6	SP6	SP6	SP6		
Units	g (ar)	g (ar)	g (ar)	g (ar)	g (ar)	g (ar)	w/w_{ar}
Batteries	0.00	0.00	0.00	0.00	0.00	0.00	0.00
Biological	24.68	45.15	48.43	52.85	44.67	215.78	9.24
Cables	0.00	0.00	0.00	0.00	0.00	0.00	0.00
Carpet/mats	0.00	0.00	0.06	0.00	0.00	0.06	0.00
Cartons	0.00	0.00	0.00	1.36	1.08	2.44	0.10
Cinders	3.75	8.45	25.11	19.28	9.22	65.81	2.82
Composites	4.85	3.61	9.44	13.03	10.82	41.75	1.79

Durable plastic	2.34	6.69	8.83	25.65	11.09	54.60	2.34
Ferrous metal	0.00	0.00	0.00	2.19	10.85	13.04	0.56
Fines < 10 mm	35.68	64.61	86.10	173.50	125.81	485.70	20.79
Fluff	0.00	1.54	4.94	7.97	6.69	21.14	0.90
Glass	67.63	65.09	188.49	267.95	174.12	763.28	32.67
Hazardous	0.00	0.00	0.76	0.83	0.51	2.10	0.09
Non-Fe metal	0.00	0.00	0.77	0.37	1.33	2.47	0.11
Other		0.00	0.00	21.23	0.00	21.23	0.91
Other packaging plastic	2.14	3.04	4.10	5.33	3.52	18.13	0.78
Paper/card	9.52	21.31	46.22	28.30	39.51	144.86	6.20
Plastic film	1.61	5.89	6.09	9.28	10.53	33.40	1.43
Rubber/leather	0.00	1.53	0.00	0.00	1.23	2.76	0.12
Sanitary products	0.00	0.00	0.00	0.00	0.00	0.00	0.00
Shoes	0.00	0.00	0.00	0.00	0.00	0.00	0.00
Stones/ceramic	38.69	48.24	94.46	143.03	79.02	403.44	17.27
Textile/fabric	0.56	1.50	2.99	1.25	1.96	8.26	0.35
Tissues	0.00	0.00	2.38	0.79	0.00	3.17	0.14
Treated wood	0.86	6.40	12.18	7.43	5.70	32.57	1.39
Overall	192.31	283.05	541.35	781.62	537.66	2335.99	100.00

Table_App F-7 UK MBT plant A: raw results on manual sorting of process flows components. Starting point for developing the corrected (modelled) values serving as input to the STAN2[®] modelling. Sampling point 7 (SP7)

Sample ID	L1_INC1_SP7	L1_INC2_SP7	L1_INC3_SP7	L1_INC4_SP7	L1_INC9_SP7	ΣL	ΣL
Lot	L1	L1	L1	L1	L1		
Increment	INC1	INC2	INC3	INC4	INC9		
Sampling point	SP7	SP7	SP7	SP7	SP7		
Units	g (ar)	g (ar)	g (ar)	g (ar)	g (ar)	g (ar)	w/w_{ar}
Batteries	0.00	0.00	0.00	0.00	7.93	7.93	0.10
Biological	54.02	206.10	62.89	83.88	89.62	496.51	6.40
Cables	0.00	0.09	0.76	0.00	11.08	11.93	0.15

Carpet/mats	0.00	0.00	0.00	0.00	0.00	0.00	0.00
Cartons	1.04	0.00	0.00	1.26	0.00	2.30	0.03
Cinders	26.69	60.42	53.35	43.60	85.56	269.62	3.47
Composites	7.16	9.68	8.09	13.48	6.91	45.32	0.58
Durable plastic	14.73	31.73	26.65	26.37	44.15	143.63	1.85
Ferrous metal	16.11	14.54	6.62	11.65	10.48	59.40	0.77
Fines < 10 mm	164.71	184.01	301.55	527.81	118.35	1296.43	16.71
Fluff	0.75	0.00	0.00	6.45	0.00	7.20	0.09
Glass	554.01	699.57	689.60	801.59	517.12	3261.89	42.04
Hazardous	0.00	4.04	3.44	5.21	0.00	12.69	0.16
Non-Fe metal	5.04	7.73	2.98	2.47	13.96	32.18	0.41
Other	5.00	0.00	0.00	5.31	0.00	10.31	0.13
Other packaging plastic	1.98	13.30	3.60	2.61	1.31	22.80	0.29
Paper/card	24.63	134.37	37.94	24.43	39.54	260.91	3.36
Plastic film	0.00	11.59	3.63	7.76	0.51	23.49	0.30
Rubber/leather	0.00	5.79	0.00	3.61	1.76	11.16	0.14
Sanitary products	0.00	0.00	0.00	0.00	0.00	0.00	0.00
Shoes	0.00	0.00	0.00	0.00	0.00	0.00	0.00
Stones/ceramic	271.93	306.58	315.94	306.44	482.82	1683.71	21.70
Textile/fabric	0.46	0.00	2.92	1.25	0.76	5.39	0.07
Tissues	0.00	0.61	0.00	0.82	1.00	2.43	0.03
Treated wood	5.02	25.55	16.60	11.10	33.70	91.97	1.19
Overall	1153.28	1715.70	1536.56	1887.10	1466.56	7759.20	100.00

Table_App F-8 UK MBT plant A: raw results on manual sorting of process flows components. Starting point for developing the corrected (modelled) values serving as input to the STAN2[®] modelling. Sampling point 10 (SP10)

Sample ID	L1_INC1_SP10	L1_INC2_SP10	L1_INC3_SP10	L1_INC4_SP10	ΣL	ΣL
Lot	L1	L1	L1	L1		
Increment	INC1	INC2	INC3	INC4		
Sampling point	SP10	SP10	SP10	SP10		

Units	g (ar)	g (ar)	g (ar)	g (ar)	g (ar)	w/w _{ar}
Batteries	0.00	0.00	0.00	0.00	0.00	0.00
Biological	2.00	2.67	3.19	2.64	10.50	0.50
Cables	0.00	0.00	0.00	0.00	0.00	0.00
Carpet/mats	1.48	1.35	1.70	0.94	5.47	0.26
Cartons	3.86	3.81	1.05	1.99	10.71	0.51
Cinders	0.00	0.00	0.91	0.00	0.91	0.04
Composites	19.81	10.71	7.34	7.81	45.67	2.16
Durable plastic	6.42	5.99	6.40	11.82	30.63	1.45
Ferrous metal	5.77	14.33	12.71	6.58	39.39	1.86
Fines < 10 mm	273.44	224.58	252.04	137.75	887.81	41.91
Fluff	7.41	8.94	14.75	10.93	42.03	1.98
Glass	0.00	0.98	1.32	2.66	4.96	0.23
Hazardous	0.00	0.34	0.30	0.14	0.78	0.04
Non-Fe metal	8.23	5.40	9.59	6.05	29.27	1.38
Other	0.00	0.00	0.00		0.00	0.00
Other packaging plastic	36.35	50.41	30.32	33.38	150.46	7.10
Paper/card	111.95	165.39	176.09	84.32	537.75	25.39
Plastic film	44.01	37.62	70.09	24.41	176.13	8.32
Rubber/leather	0.80	3.97	0.14	1.42	6.33	0.30
Sanitary products	0.00	0.00	0.00	1.36	1.36	0.06
Shoes	0.00	0.00	0.00	0.31	0.31	0.01
Stones/ceramic	0.00	3.83	14.88	0.00	18.71	0.88
Textile/fabric	26.23	16.62	13.91	13.40	70.16	3.31
Tissues	0.00	1.51	1.58	0.64	3.73	0.18
Treated wood	8.64	14.74	11.24	10.48	45.10	2.13
Overall	556.40	573.19	629.55	359.03	2118.17	100.00

Table_App F-9 UK MBT plant A: raw results on manual sorting of process flows components. Starting point for developing the corrected (modelled) values serving as input to the STAN2[®] modelling. Sampling point 11 (SP11)

Sample ID	L1_INC1_SP11	L1_INC2_SP11	L1_INC3_SP11	L1_INC9_SP11	ΣL	ΣL
Lot	L1	L1	L1	L1		
Increment	INC1	INC2	INC3	INC9		
Sampling point	SP11	SP11	SP11	SP11		
Units	g (ar)	g (ar)	g (ar)	g (ar)	g (ar)	w/w _{ar}
Batteries	0.00	0.00	0.00	0.00	0.00	0.00
Biological	1.61	2.62	1.97	1.95	8.15	0.44
Cables	0.00	0.00	0.00	0.35	0.35	0.02
Carpet/mats	1.94	4.04	2.12	1.23	9.33	0.50
Cartons	1.46	2.44	1.21	4.71	9.82	0.53
Cinders	0.00	0.56	0.38	0.00	0.94	0.05
Composites	7.95	4.51	7.41	6.31	26.18	1.41
Durable plastic	9.74	2.10	1.48	4.29	17.61	0.95
Ferrous metal	0.87	0.00	1.45	0.13	2.45	0.13
Fines < 10 mm	219.44	169.76	185.74	164.14	739.08	39.72
Fluff	9.34	7.82	5.63	6.27	29.06	1.56
Glass	0.72	1.50	1.12	0.00	3.34	0.18
Hazardous	0.00	0.36	0.24	0.00	0.60	0.03
Non-Fe metal	0.97	10.02	7.72	5.68	24.39	1.31
Other	0.00	0.00	0.00	0.00	0.00	0.00
Other packaging plastic	23.70	30.61	46.49	37.72	138.52	7.44
Paper/card	143.22	180.52	200.49	76.74	600.97	32.30
Plastic film	37.78	45.16	48.24	18.48	149.66	8.04
Rubber/leather	1.66	1.70	0.77	1.36	5.49	0.30
Sanitary products	0.00	0.00	0.00	0.00	0.00	0.00
Shoes	0.00	0.00	0.00	0.00	0.00	0.00
Stones/ceramic	0.00	0.00	3.32	0.00	3.32	0.18
Textile/fabric	21.10	8.61	17.09	12.18	58.98	3.17
Tissues	0.00	0.91	1.10	0.37	2.38	0.13
Treated wood	6.58	6.02	11.73	5.81	30.14	1.62

Overall	488.08	479.26	545.70	347.72	1860.76	100.00
----------------	--------	--------	--------	--------	---------	---------------

Table App F-10 UK MBT plant A: raw results on manual sorting of process flows components. Starting point for developing the corrected (modelled) values serving as input to the STAN2[®] modelling. Sampling point 12 (SP12)

Sample ID	L1_INC1_SP12	L1_INC2_SP12	L1_INC3_SP12	L1_INC4_SP12	L1_INC9_SP12	ΣL	ΣL
Lot	L1	L1	L1	L1	L1		
Increment	INC1	INC2	INC3	INC4	INC9		
Sampling point	SP12	SP12	SP12	SP12	SP12		
Units	g (ar)	g (ar)	g (ar)	g (ar)	g (ar)	g (ar)	w/w _{ar}
Batteries	0.00	0.00	0.00	0.00	0.00	0.00	0.00
Biological	3.82	5.92	6.42	6.53	1.90	24.59	1.11
Cables	0.00	0.65	0.00	0.32	0.79	1.76	0.08
Carpet/mats	0.62	0.67	0.81	1.19	4.21	7.50	0.34
Cartons	4.09	1.01	3.18	2.59	2.95	13.82	0.62
Cinders	0.00	0.00	0.00	0.00	0.00	0.00	0.00
Composites	7.71	6.49	5.27	10.65	12.62	42.74	1.93
Durable plastic	5.24	5.48	11.47	11.40	6.50	40.09	1.81
Ferrous metal	1.71	11.52	2.97	5.30	3.96	25.46	1.15
Fines < 10 mm	204.21	211.94	225.27	141.00	213.57	995.99	44.95
Fluff	5.96	3.35	5.51	17.94	4.84	37.60	1.70
Glass	0.00	6.98	2.22	0.46	0.00	9.66	0.44
Hazardous	0.02	0.62	0.16	0.32	0.17	1.29	0.06
Non-Fe metal	2.99	2.71	6.72	3.48	9.18	25.08	1.13
Other	0.00	0.00	0.00	0.58	0.00	0.58	0.03
Other packaging plastic	23.98	28.43	37.86	27.66	32.76	150.69	6.80
Paper/card	104.66	159.06	143.56	90.17	45.32	542.77	24.49
Plastic film	31.96	33.69	29.01	18.01	26.65	139.32	6.29
Rubber/leather	1.01	1.24	3.59	2.01	3.20	11.05	0.50
Sanitary products	0.00	0.00	0.00	0.00	0.00	0.00	0.00
Shoes	0.00	0.00	0.00	0.00	0.00	0.00	0.00

Stones/ceramic	0.00	0.00	0.00	2.01	0.00	2.01	0.09
Textile/fabric	24.31	13.18	14.59	21.44	18.69	92.21	4.16
Tissues	0.00	0.30	1.81	0.35	0.00	2.46	0.11
Treated wood	5.91	10.32	15.42	12.03	5.66	49.34	2.23
Overall	428.20	503.56	515.84	375.44	392.97	2216.01	100.00

Table App F-11 UK MBT plant A: raw results on manual sorting of process flows components. Starting point for developing the corrected (modelled) values serving as input to the STAN2[®] modelling. Sampling point 13 (SP13)

Sample ID	L1_INC1_SP13	L1_INC6_SP13	L1_INC8_SP13	L2_INC1-7COMP_SP13	L2_INC8_SP13	ΣL	ΣL
Lot	L1	L1	L1	L2	L2		
Increment	INC1	INC6	INC8	INC1-7COMP	INC8		
Sampling point	SP13	SP13	SP13	SP13	SP13		
Units	g (ar)	g (ar)	g (ar)	g (ar)	g (ar)	g (ar)	w/w_{ar}
Batteries	0.00	0.00	0.00	0.00	0.00	0.00	0.00
Biological	4.78	7.38	2.44	0.00	9.36	23.96	1.07
Cables	1.80	0.03	0.59	0.28	1.46	4.16	0.19
Carpet/mats	0.00	2.86	5.50	1.18	0.73	10.27	0.46
Cartons	8.20	1.45	4.04	2.97	3.27	19.93	0.89
Cinders	0.00	0.00	0.00	0.43	0.48	0.91	0.04
Composites	18.09	7.37	10.85	10.65	7.18	54.14	2.42
Durable plastic	7.28	0.00	15.09	18.86	6.73	47.96	2.14
Ferrous metal	2.11	0.00	0.00	0.52	0.00	2.63	0.12
Fines < 10 mm	154.55	203.71	211.17	220.86	132.72	923.01	41.27
Fluff	12.85	13.45	28.02	16.37	13.79	84.48	3.78
Glass	0.00	0.00	0.71	0.20	0.00	0.91	0.04
Hazardous	0.83	0.10	0.63	0.09	0.45	2.10	0.09
Non-Fe metal	5.80	0.20	1.73	7.15	5.59	20.47	0.92
Other	0.00	4.36	0.62	0.62	1.33	6.93	0.31
Other packaging plastic	36.10	13.31	24.28	39.86	33.43	146.98	6.57
Paper/card	161.55	68.14	134.77	106.66	88.87	559.99	25.04

Plastic film	35.85	16.92	31.51	19.20	15.41	118.89	5.32
Rubber/leather	1.26	0.81	1.58	0.72	0.08	4.45	0.20
Sanitary products	0.00	0.00	2.13	0.69	1.24	4.06	0.18
Shoes	0.00	0.00	0.59	3.21	0.73	4.53	0.20
Stones/ceramic	0.00	1.80	1.30	1.50	2.31	6.91	0.31
Textile/fabric	38.10	14.92	36.65	21.37	15.92	126.96	5.68
Tissues	1.90	0.48	1.43	2.61	1.43	7.85	0.35
Treated wood	8.38	8.03	12.40	13.08	12.34	54.23	2.42
Overall	499.43	365.32	528.03	489.08	354.85	2236.71	100.00

Table_App F-12 UK MBT plant A: raw results on manual sorting of process flows components. Starting point for developing the corrected (modelled) values serving as input to the STAN2[®] modelling. Sampling point 14 (SP14)

Sample ID	L1_INC1_SP14	L1_INC2_SP14	L1_INC3_SP14	L1_INC4_SP14	ΣL	ΣL
Lot	L1	L1	L1	L1		
Increment	INC1	INC2	INC3	INC4		
Sampling point	SP14	SP14	SP14	SP14		
Units	g (ar)	g (ar)	g (ar)	g (ar)	g (ar)	w/w _{ar}
Batteries	0.71	0.00	0.00	0.00	0.71	0.02
Biological	7.42	2.30	5.39	10.43	25.54	0.60
Cables	1.21	1.26	0.85	0.38	3.70	0.09
Carpet/mats	0.00	2.82	0.00	0.13	2.95	0.07
Cartons	1.26	0.00	0.17	0.79	2.22	0.05
Cinders	0.00	0.00	0.00	0.82	0.82	0.02
Composites	5.33	2.48	7.98	4.15	19.94	0.47
Durable plastic	18.28	13.43	19.15	19.25	70.11	1.64
Ferrous metal	0.00	0.00	0.00	0.41	0.41	0.01
Fines < 10 mm	82.48	76.10	113.45	116.73	388.76	9.10
Fluff	0.00	0.00	0.00	0.00	0.00	0.00
Glass	0.65	0.00	5.39	7.60	13.64	0.32
Hazardous	0.00	0.00	0.00	0.91	0.91	0.02
Non-Fe metal	692.54	882.36	957.62	876.33	3408.85	79.81

Other	0.00	0.00	0.00	1.31	1.31	0.03
Other packaging plastic	29.49	27.25	36.68	26.32	119.74	2.80
Paper/card	37.57	27.13	22.62	22.97	110.29	2.58
Plastic film	2.77	4.54	1.73	7.45	16.49	0.39
Rubber/leather	2.66	0.52	0.82	0.96	4.96	0.12
Sanitary products	0.00	0.00	0.00	0.00	0.00	0.00
Shoes	0.00	0.00	0.00	0.93	0.93	0.02
Stones/ceramic	4.14	9.09	13.27	4.73	31.23	0.73
Textile/fabric	1.98	1.94	0.86	0.61	5.39	0.13
Tissues	0.00	0.00	0.00	0.12	0.12	0.00
Treated wood	9.67	8.81	11.23	12.54	42.25	0.99
Overall	898.16	1060.03	1197.21	1115.87	4271.27	100.00

Table_App F-13 UK MBT plant A: raw results on manual sorting of process flows components. Starting point for developing the corrected (modelled) values serving as input to the STAN2[®] modelling. Sampling point 15 (SP15)

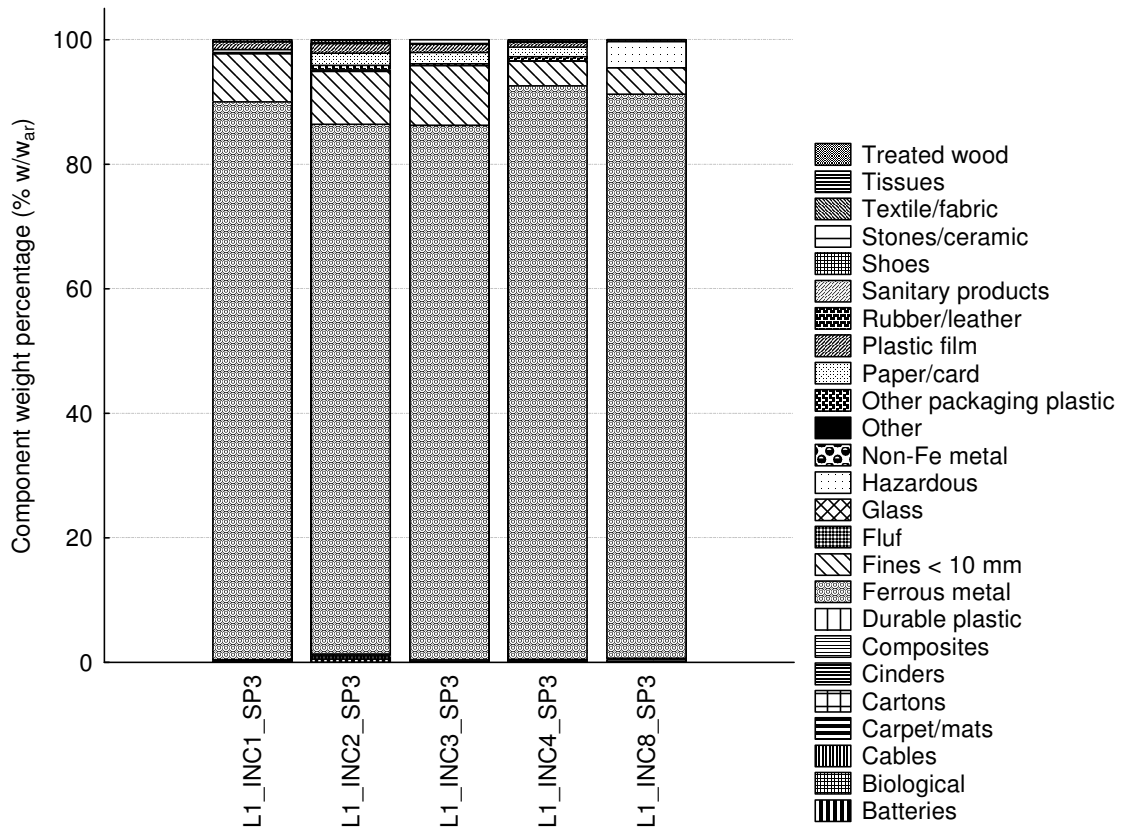
Sample ID	L1_INC1_SP15	L1_INC2_SP15	L1_INC3_SP15	L1_INC4_SP15	ΣL	ΣL
Lot	L1	L1	L1	L1		
Increment	INC1	INC2	INC3	INC4		
Sampling point	SP15	SP15	SP15	SP15		
Units	g (ar)	g (ar)	g (ar)	g (ar)	g (ar)	w/W _{ar}
Batteries	0.00	0.00	0.00	0.00	0.00	0.00
Biological	0.63	0.19	0.88	0.88	2.58	0.11
Cables	0.20	0.00	0.00	0.00	0.20	0.01
Carpet/mats	0.00	0.25	0.00	0.05	0.30	0.01
Cartons	0.00	0.09	0.06	0.47	0.62	0.03
Cinders	0.00	0.00	0.00	0.00	0.00	0.00
Composites	2.36	1.17	1.97	2.48	7.98	0.33
Durable plastic	0.00	2.13	0.22	0.00	2.35	0.10
Ferrous metal	279.90	283.31	636.33	228.49	1428.03	59.46
Fines < 10 mm	158.89	173.14	271.17	180.44	783.64	32.63
Fluff	3.81	3.14	6.65	5.51	19.11	0.80
Glass	0.69	0.00	0.00	0.00	0.69	0.03
Hazardous	0.00	0.00	1.92	0.31	2.23	0.09
Non-Fe metal	0.41	2.21	0.20	0.00	2.82	0.12
Other	0.00	0.00	0.00	0.00	0.00	0.00
Other packaging plastic	1.46	1.99	0.97	1.25	5.67	0.24
Paper/card	20.66	18.54	17.97	17.25	74.42	3.10
Plastic film	8.29	6.12	8.18	7.38	29.97	1.25
Rubber/leather	0.17	0.84	0.64	0.00	1.65	0.07
Sanitary products	0.00	0.00	0.00	1.01	1.01	0.04
Shoes	0.00	0.00	0.00	0.63	0.63	0.03
Stones/ceramic	0.00	0.00	0.00	0.00	0.00	0.00
Textile/fabric	6.10	10.31	7.97	11.17	35.55	1.48
Tissues	0.00	0.73	0.07	0.41	1.21	0.05

Treated wood	0.00	0.24	0.43	0.40	1.07	0.04
Overall	483.57	504.40	955.63	458.13	2401.73	100.00

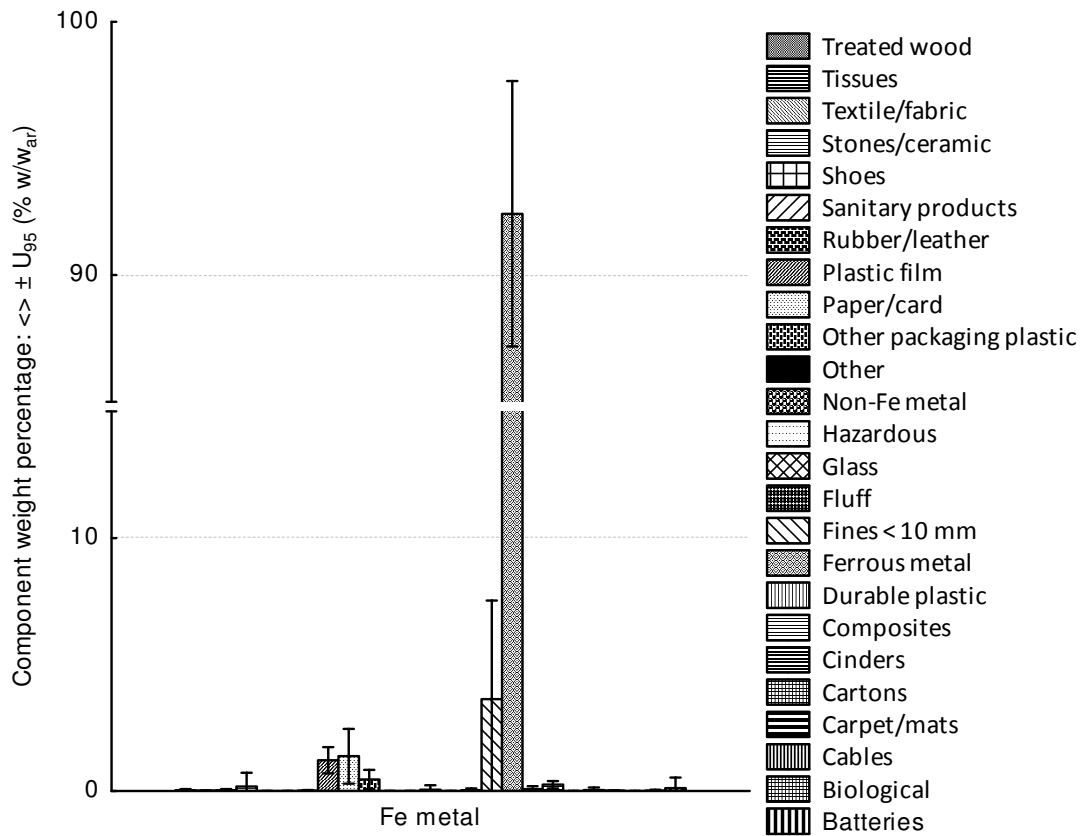
Table_App F-14 UK MBT plant A: raw results on manual sorting of process flows components. Starting point for developing the corrected (modelled) values serving as input to the STAN2[®] modelling. Sampling point 16 (SP16)

Sample ID	L1_INC1_SP1 6	L1_INC2_SP1 6	L1_INC3_SP1 6	L1_INC4_SP1 6	L1_INC5_SP1 6	L1_INC6_SP1 6	L1_INC9_SP1 6	L2_INC1- 7COMP_SP1 6	L2_INC8_SP1 6	ΣL	ΣL
Lot	L1	L1	L1	L1	L1	L1	L1	L2	L2		
Increment	INC1	INC2	INC3	INC4	INC5	INC6	INC9	INC1- 7COMP	INC8		
Sampling point	SP16	SP16	SP16	SP16	SP16	SP16	SP16	SP16	SP16		
Units	g (ar)	g (ar)	g (ar)	g (ar)	g (ar)	g (ar)	g (ar)	g (ar)	g (ar)	g (ar)	W/W_{ar}
Batteries	117.99	0.00	74.93	30.09	0.00	0.00	0.00	85.94	92.91	401.86	0.18
Biological	290.47	650.97	1928.79	742.66	790.67	476.60	840.00	239.81	944.99	6904.96	3.08
Cables	114.49	95.92	265.17	159.11	87.05	921.50	228.60	260.52	21.88	2154.24	0.96
Carpet/mats	0.00	773.52	208.13	161.06	122.08	469.88	60.00	185.96	441.81	2422.44	1.08
Cartons	82.21	0.00	0.00	24.21	75.12	16.03	180.00	57.68	0.00	435.25	0.19
Cinders	0.00	0.00	0.00	5.37	8.03	0.00	7.56	48.88	14.76	84.60	0.04
Composites	2.84	1.80	5.26	9.24	131.39	850.37	125.00	33.69	8.59	1168.18	0.52
Durable plastic	102.50	794.34	308.06	765.91	525.12	958.88	880.00	876.50	294.71	5506.02	2.45
Ferrous metal	1996.61	319.16	3255.96	1895.99	234.26	2428.57	2000.00	912.66	774.44	13817.65	6.16
Fines < 10 mm	16.29	11.56	14.11	28.35	6.42	34.50	33.70	134.04	132.64	411.61	0.18
Fluff	0.00	4.53	0.00	0.00	0.00	0.00	0.00	0.00	0.00	4.53	0.00
Glass	13.28	5.75	5.41	8.27	32.61	1.74	154.00	183.53	269.91	674.50	0.30
Hazardous	644.53	253.55	60.71	1.70	77.19	1127.58	242.00	324.31	127.88	2859.45	1.27
Non-Fe metal	906.02	931.20	3763.40	443.41	1266.53	565.51	1640.00	239.36	101.80	9857.23	4.39
Other	0.00	0.00	0.00	0.00	0.00	0.00	0.00	200.00	0.00	200.00	0.09
Other packaging plastic	887.62	599.73	1217.53	731.02	521.75	550.25	820.00	512.15	251.41	6091.46	2.72
Paper/card	13599.98	19835.03	9446.89	14348.39	16340.16	15372.81	5340.00	4584.36	1811.15	100678.7	44.88

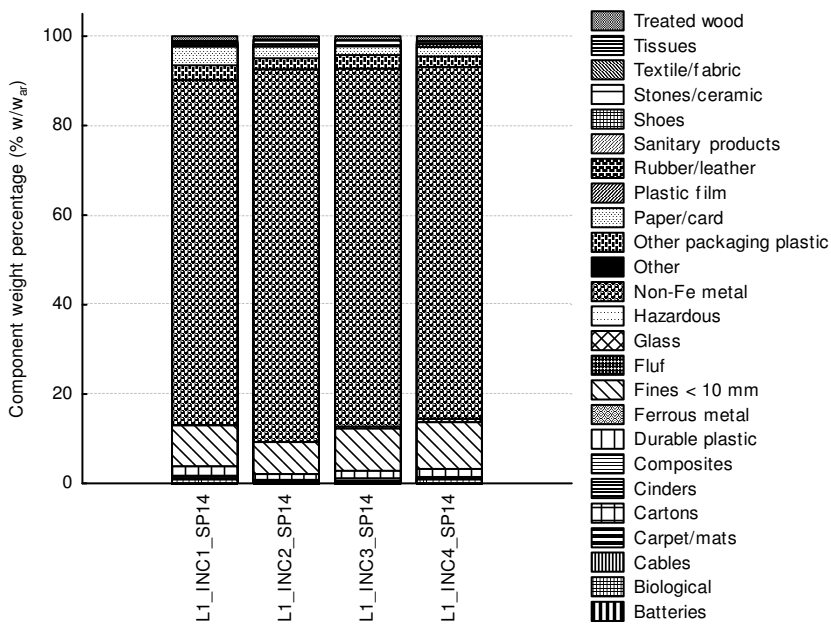
											7	
Plastic film	161.47	473.27	171.50	160.72	97.59	325.16	96.00	74.12	78.31	1638.14	0.73	
Rubber/leather	434.79	197.04	200.84	59.57	8.48	12.11	3.36	53.59	140.49	1110.27	0.49	
Sanitary products	953.50	892.97	189.44	698.95	832.80	917.80	860.00	157.76	0.00	5503.22	2.45	
Shoes	2456.81	1852.66	7404.48	1751.02	2367.17	3317.69	1160.00	1394.96	1310.58	23015.37	10.26	
Stones/ceramic	640.85	426.22	2394.93	2254.84	1810.26	853.04	3360.00	7263.99	2283.34	21287.47	9.49	
Textile/fabric	171.10	0.00	0.00	352.72	2.36	334.77	17.00	21.98	53.98	953.91	0.43	
Tissues	0.00	0.00	0.00	12.41	37.03	2.45	0.00	11.69	24.09	87.67	0.04	
Treated wood	1256.46	1233.61	2136.41	3677.26	784.88	2457.47	2500.00	1717.30	1312.78	17076.17	7.61	
Overall	24849.81	29352.83	33051.95	28322.27	26158.95	31994.71	20547.22	19574.78	10492.45	224344.97	100.00	



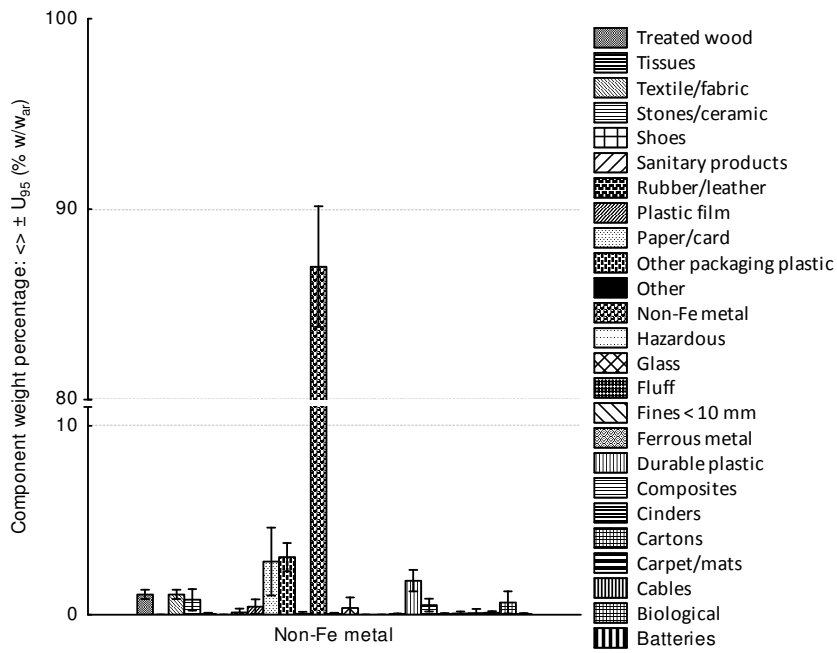
Figure_App F-1



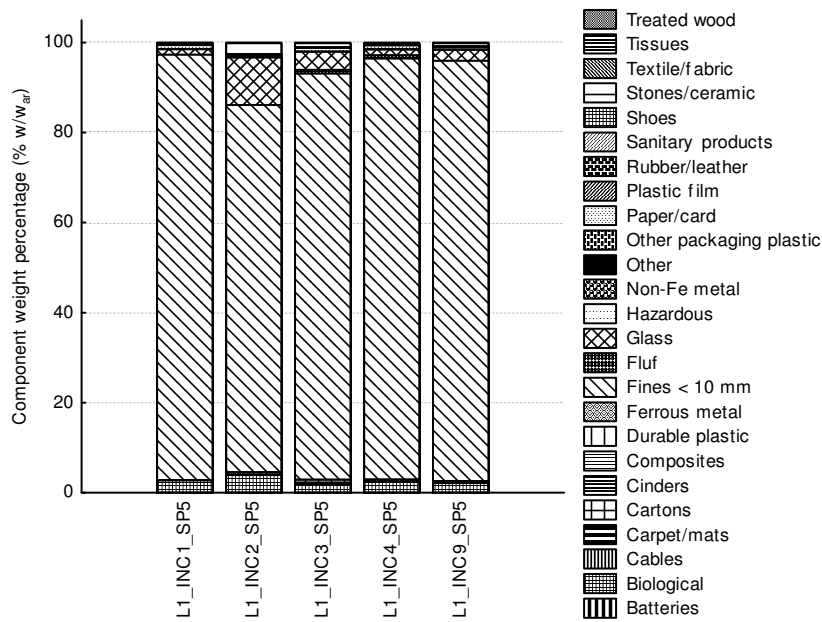
Figure_App F-2



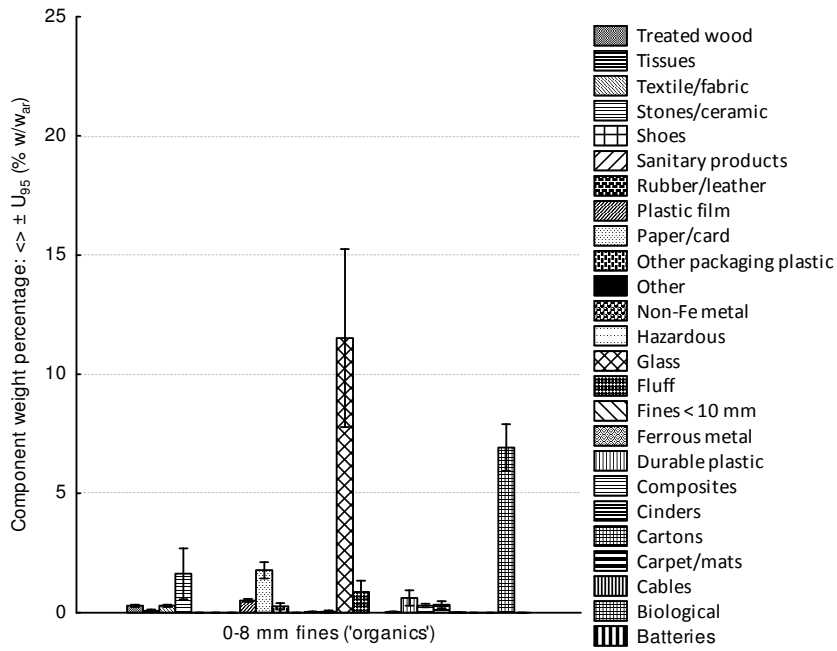
Figure_App F-3



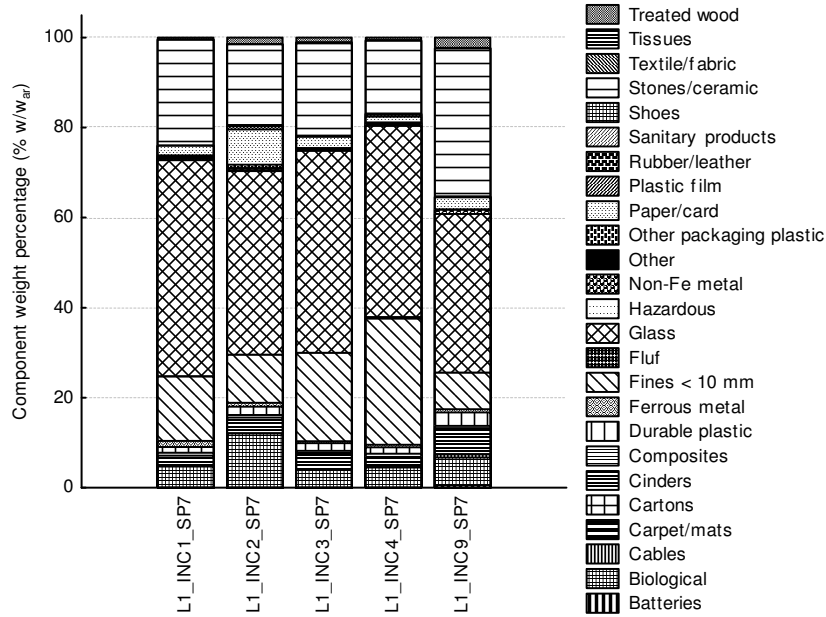
Figure_App F-4



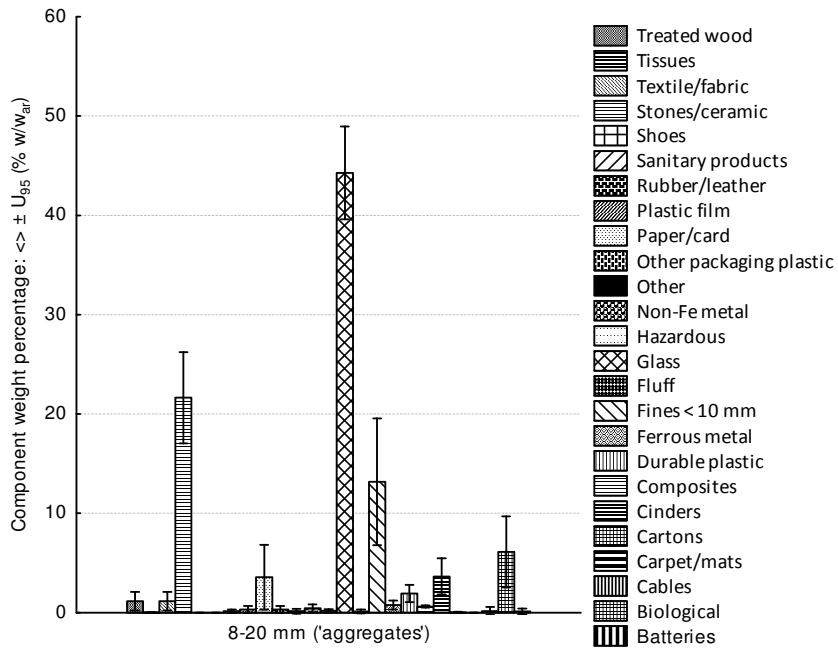
Figure_App F-5



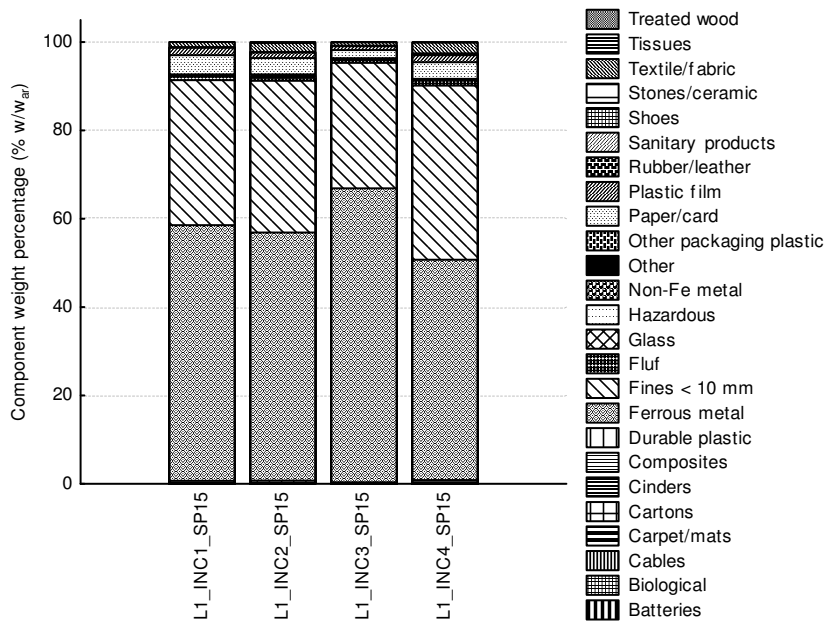
Figure_App F-6



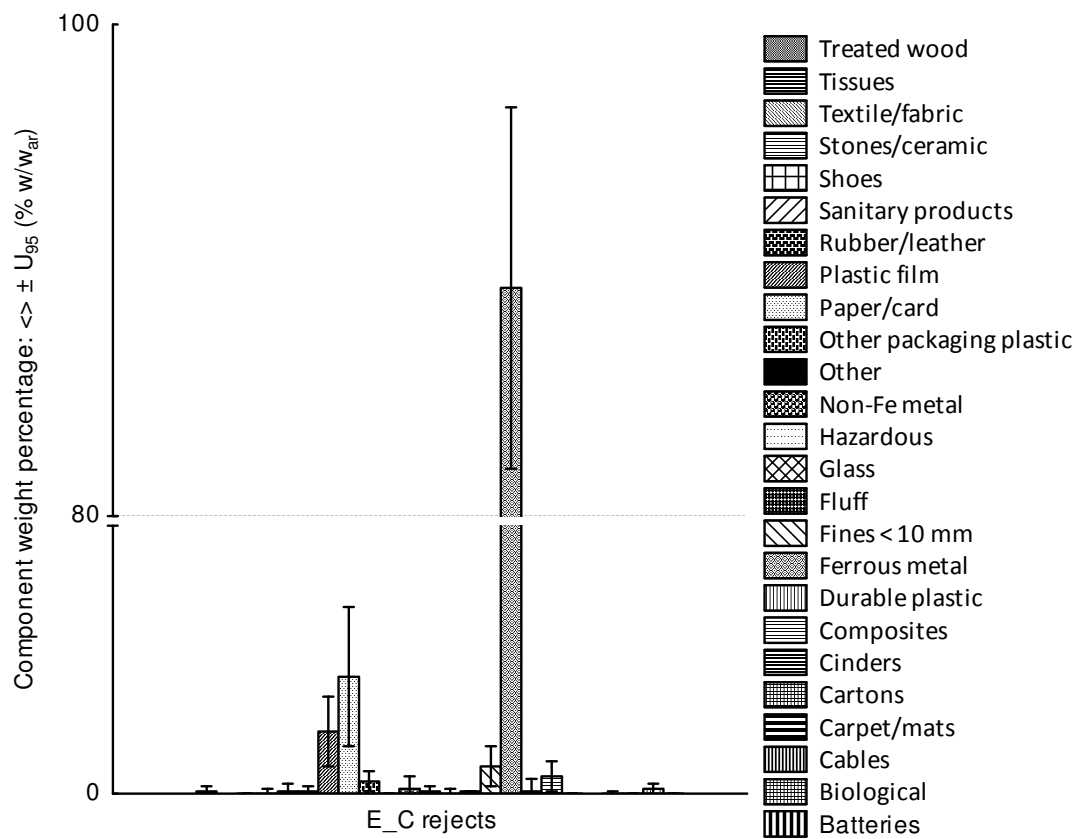
Figure_App F-7



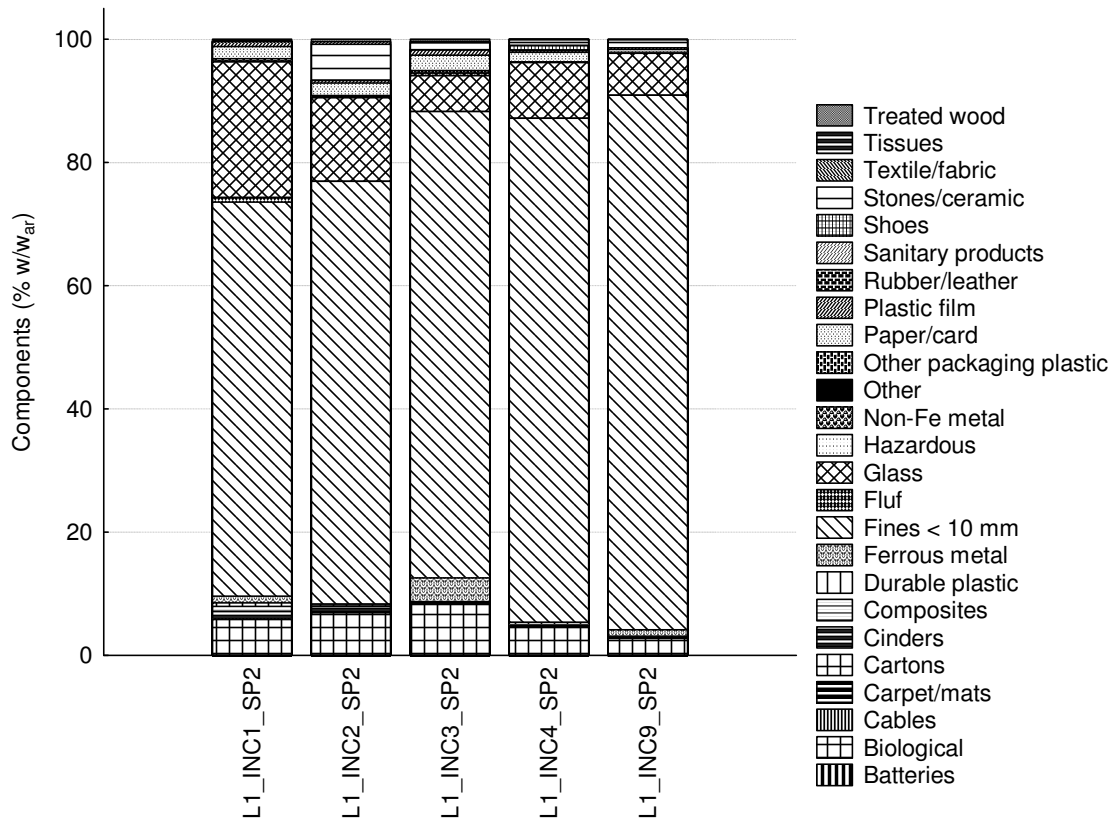
Figure_App F-8



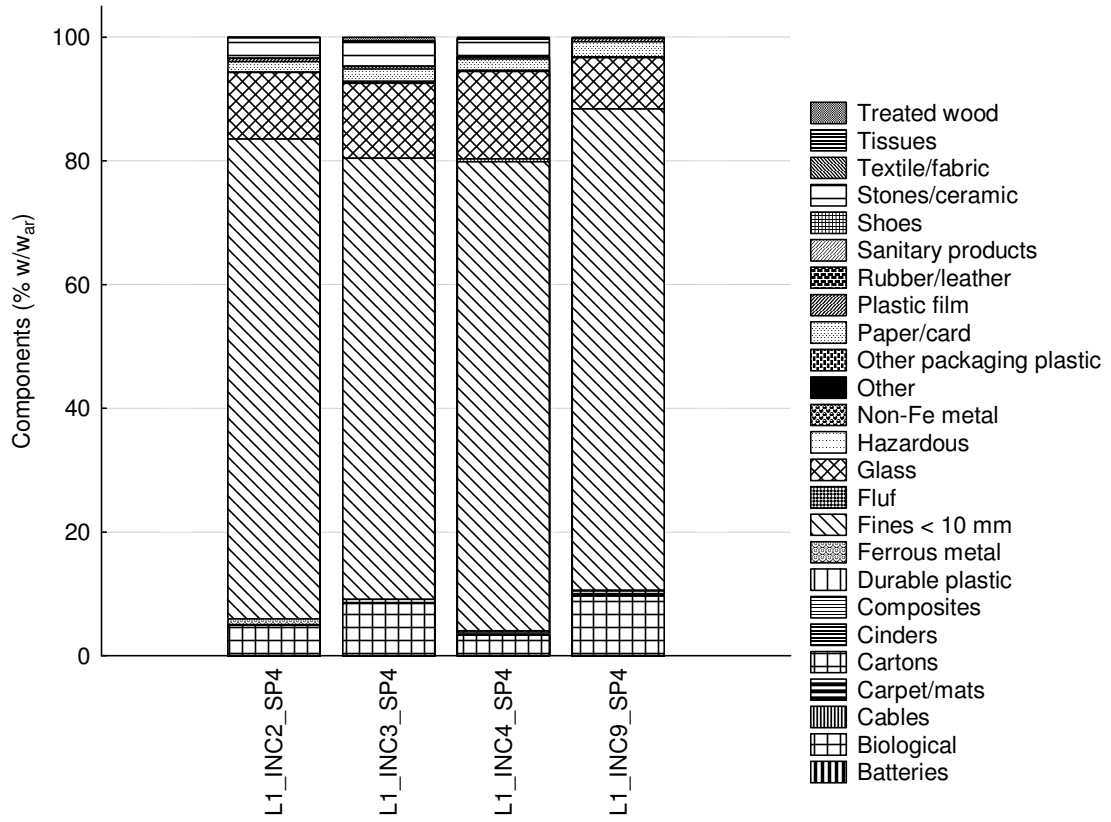
Figure_App F-9



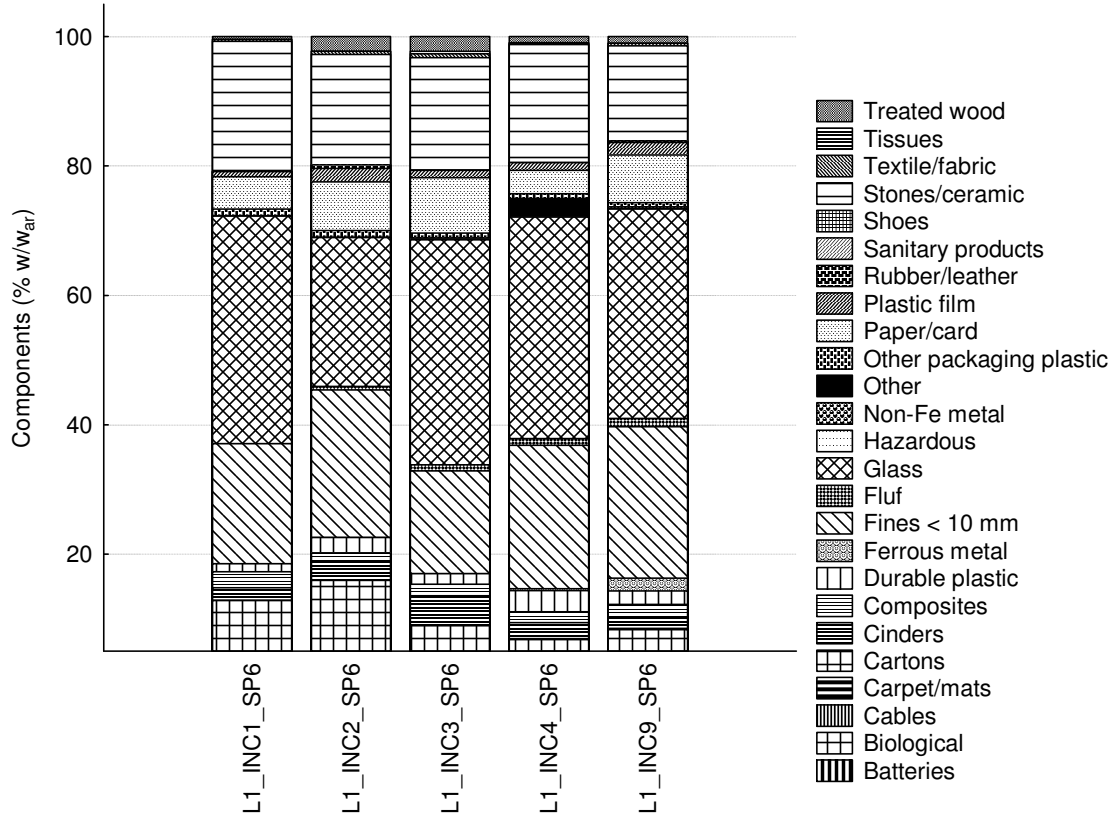
Figure_App F-10



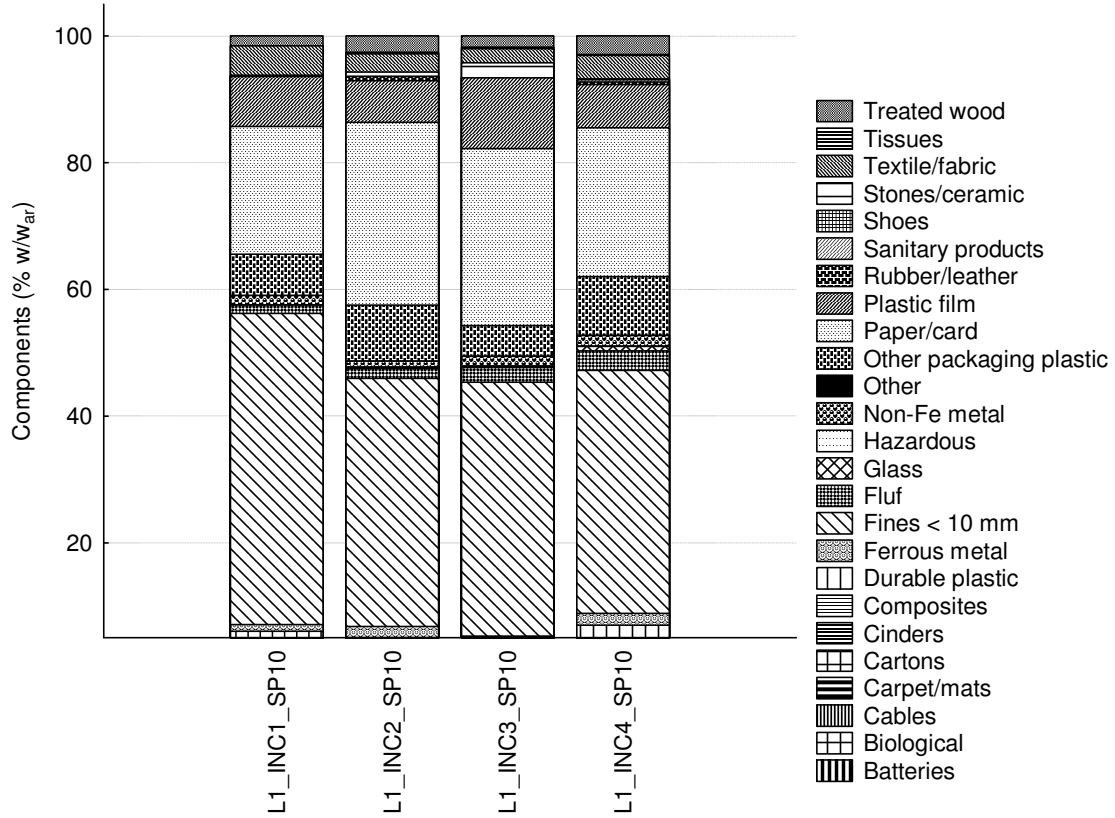
Figure_App F-11



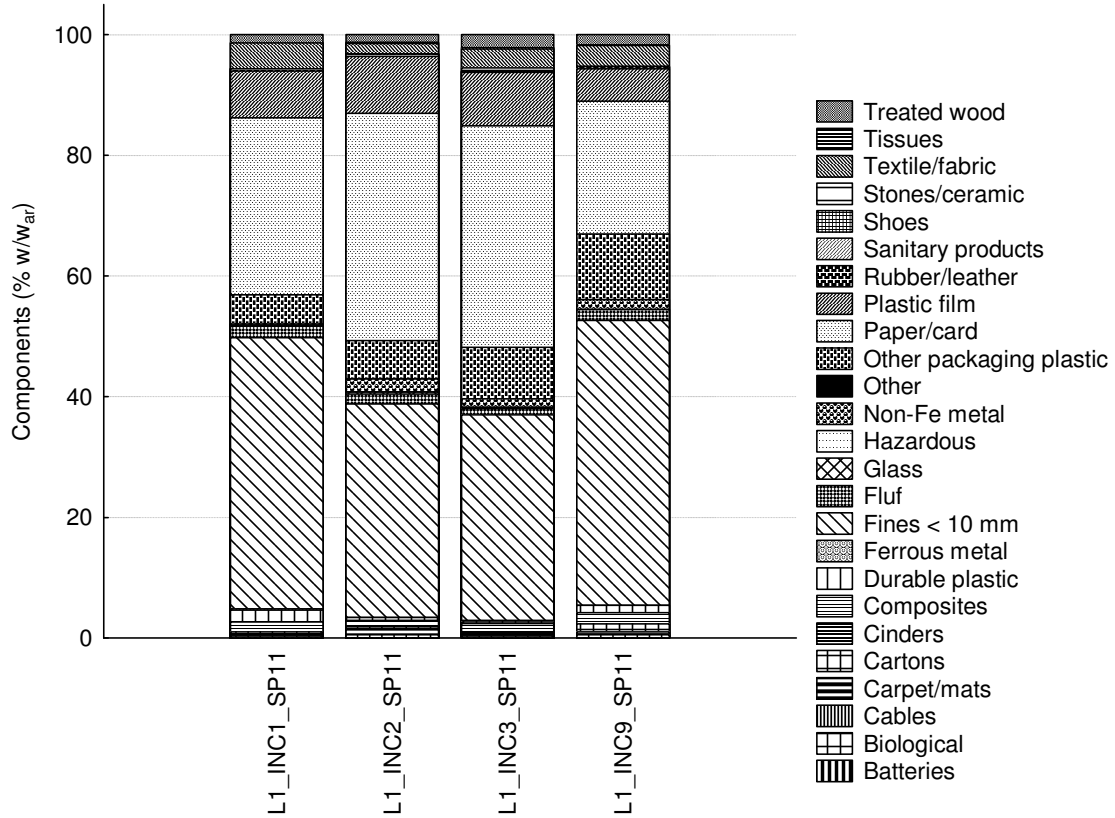
Figure_App F-12



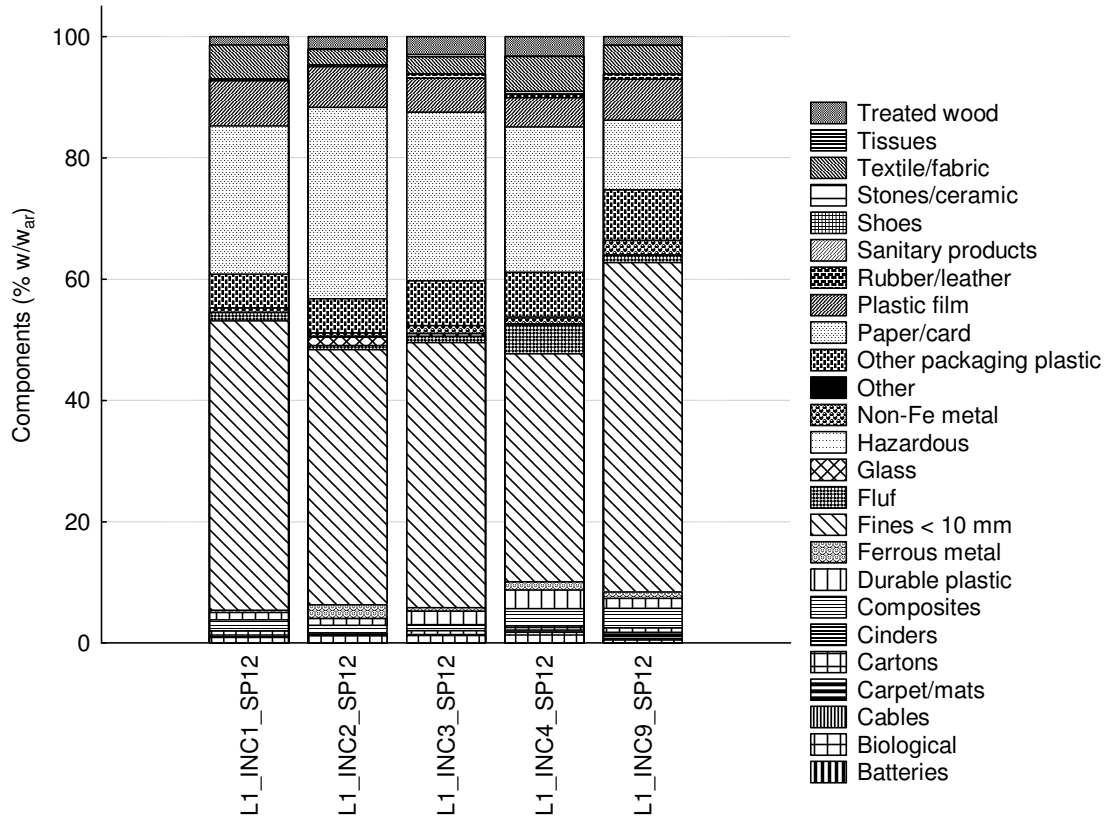
Figure_App F-13



Figure_App F-14



Figure_App F-15



Figure_App F-16

Table_App F-15 Comparison of two different statistical estimates of the average percent mass fraction for each component and sampled process flow (SP)

Component	SP1			SP2			SP3			SP4			SP5		
	Med (m)	m/Σm	%[Δ(Med-m/Σm)]/Med	Med (m)	m/Σm	%[Δ(Med-m/Σm)]/Med	Med (m)	m/Σm	%[Δ(Med-m/Σm)]/Med	Med (m)	m/Σm	%[Δ(Med-m/Σm)]/Med	Med (m)	m/Σm	%[Δ(Med-m/Σm)]/Med
Batteries	0.10	0.12	-16.63	0.00	0.00	-	0.00	0.12	-	0.00	0.00	-	0.00	0.00	-
Biological	3.96	3.93	0.90	5.81	6.37	-9.62	0.00	0.02	-1122.45	6.69	5.64	15.78	2.52	2.51	0.31
Cables	0.06	0.34	-441.30	0.00	0.05	-	0.00	0.08	-	0.01	0.01	-27.73	0.00	0.00	-
Carpet/mats	0.88	1.05	-19.73	0.00	0.00	-	0.00	0.01	-	0.00	0.00	-	0.00	0.00	-
Cartons	0.71	0.78	-10.61	0.00	0.01	-	0.01	0.05	-597.89	0.00	0.01	-	0.00	0.01	-
Cinders	0.27	0.29	-7.60	0.14	0.58	-331.10	0.00	0.00	-	0.03	0.02	44.33	0.11	0.12	-13.50
Composites	1.82	1.95	-7.37	0.15	0.42	-179.87	0.27	0.25	6.95	0.14	0.09	39.23	0.08	0.11	-30.95
Durable plastic	2.23	2.41	-8.05	0.28	0.35	-25.88	0.08	0.08	-1.12	0.37	0.27	26.38	0.15	0.28	-84.79
Ferrous metal	5.83	5.38	7.71	1.06	1.50	-41.33	89.63	88.42	1.34	0.17	0.44	-160.48	0.00	0.01	-
Fines < 10 mm	14.77	15.85	-7.26	75.75	72.28	4.57	7.72	7.31	5.28	76.68	75.03	2.15	93.41	91.22	2.35
Fluff	0.05	0.36	-667.08	0.00	0.29	-	0.00	0.03	-	0.00	0.14	-	0.00	0.41	-
Glass	6.80	7.51	-10.44	9.03	13.12	-45.40	0.00	0.00	-	11.42	12.11	-6.10	2.40	3.40	-42.02
Hazardous	0.47	0.56	-19.43	0.00	0.00	-	0.00	0.05	-2279.21	0.03	0.03	-5.01	0.00	0.01	-
Non-Fe metal	1.65	1.73	-4.82	0.19	0.24	-31.41	0.00	0.00	-	0.01	0.05	-346.74	0.00	0.01	-
Other	0.00	0.00	-	0.00	0.00	-	0.00	0.00	-	0.00	0.00	-	0.00	0.00	-
Other packaging plastic	7.71	8.39	-8.86	0.17	0.27	-63.49	0.32	0.46	-43.02	0.06	0.09	-54.52	0.08	0.11	-39.16
Paper/card	27.23	26.93	1.09	1.96	2.02	-2.72	1.53	1.38	9.95	1.92	1.86	2.79	0.79	0.65	16.77
Plastic film	5.65	7.42	-31.27	0.44	0.64	-46.16	1.26	1.22	3.19	0.46	0.42	9.25	0.20	0.19	6.16
Rubber/leather	0.20	0.18	13.92	0.02	0.05	-115.08	0.00	0.01	-	0.02	0.03	-23.89	0.00	0.00	-
Sanitary products	1.15	1.06	7.53	0.00	0.00	-	0.00	0.00	-	0.00	0.00	-	0.00	0.00	-
Shoes	1.01	2.09	-107.76	0.00	0.18	-	0.00	0.00	-	0.00	0.00	-	0.00	0.00	-
Stones/ceramic	4.36	4.17	4.43	1.15	1.21	-5.88	0.00	0.19	-	3.05	3.37	-10.36	0.67	0.75	-12.35
Textile/fabric	2.23	2.64	-18.29	0.14	0.16	-14.11	0.32	0.29	11.34	0.09	0.11	-16.06	0.04	0.08	-94.51
Tissues	0.60	0.71	-18.06	0.00	0.02	-	0.00	0.01	-	0.00	0.00	-	0.02	0.03	-22.47
Treated wood	3.72	4.17	-11.91	0.22	0.23	-2.79	0.00	0.03	-	0.18	0.29	-57.46	0.11	0.11	4.28

-: Computation not feasible; Med: median of component mass fraction (percentages) over all increments (INCs); m/Σm: mass fraction using sum of mass over all INCs; %[Δ(Med-m/Σm)]

/Med: percent relative difference of the two statistics; highlighted results: relative difference >20, or <-20

Component	SP6			SP7			SP10			SP11			SP12		
	Med (m)	m/Σm	%[Δ(Med -m/Σm)] /Med	Med (m)	m/Σm	%[Δ(Med -m/Σm)] /Med	Med (m)	m/Σm	%[Δ(Med -m/Σm)] /Med	Med (m)	m/Σm	%[Δ(Med -m/Σm)] /Med	Med (m)	m/Σm	%[Δ(Med -m/Σm)] /Med
Batteries	0.00	0.00	-	0.00	0.10	-	0.00	0.00	-	0.00	0.00	-	0.00	0.00	-
Biological	8.95	9.24	-3.25	4.68	6.40	-36.61	0.49	0.50	-1.94	0.45	0.44	3.49	1.18	1.11	5.61
Cables	0.00	0.00	-	0.01	0.15	-2831.04	0.00	0.00	-	0.00	0.02	-	0.09	0.08	6.82
Carpet/mats	0.00	0.00	-	0.00	0.00	-	0.26	0.26	2.15	0.39	0.50	-27.59	0.16	0.34	-115.54
Cartons	0.00	0.10	-	0.00	0.03	-	0.61	0.51	17.04	0.40	0.53	-30.59	0.69	0.62	9.60
Cinders	2.47	2.82	-14.21	3.47	3.47	-0.08	0.00	0.04	-	0.03	0.05	-45.09	0.00	0.00	-
Composites	1.74	1.79	-2.49	0.56	0.58	-3.52	2.02	2.16	-6.64	1.49	1.41	5.79	1.80	1.93	-7.12
Durable plastic	2.06	2.34	-13.32	1.73	1.85	-6.73	1.10	1.45	-31.53	0.84	0.95	-13.21	1.65	1.81	-9.37
Ferrous metal	0.00	0.56	-	0.71	0.77	-7.13	1.93	1.86	3.44	0.11	0.13	-22.12	1.01	1.15	-14.01
Fines < 10 mm	22.20	20.79	6.33	14.28	16.71	-16.99	39.61	41.91	-5.82	40.19	39.72	1.17	43.67	44.95	-2.92
Fluff	0.91	0.90	0.83	0.00	0.09	-	1.95	1.98	-1.69	1.72	1.56	9.07	1.23	1.70	-37.76
Glass	34.28	32.67	4.69	42.48	42.04	1.03	0.19	0.23	-23.04	0.18	0.18	-1.77	0.12	0.44	-255.79
Hazardous	0.09	0.09	5.23	0.22	0.16	26.95	0.04	0.04	15.00	0.02	0.03	-46.63	0.04	0.06	-34.56
Non-Fe metal	0.05	0.11	-123.37	0.44	0.41	5.10	1.50	1.38	7.95	1.52	1.31	14.00	0.93	1.13	-22.10
Other	0.00	0.91	-	0.00	0.13	-	0.00	0.00	-	0.00	0.00	-	0.00	0.03	-
Other packaging plastic	0.76	0.78	-2.48	0.17	0.29	-71.15	7.66	7.10	7.31	7.45	7.44	0.12	7.34	6.80	7.35
Paper/card	7.35	6.20	15.61	2.47	3.36	-36.18	25.73	25.39	1.32	33.04	32.30	2.25	24.44	24.49	-0.21
Plastic film	1.19	1.43	-20.43	0.24	0.30	-28.15	7.35	8.32	-13.07	8.29	8.04	2.98	6.69	6.29	6.03
Rubber/leather	0.00	0.12	-	0.12	0.14	-19.85	0.27	0.30	-10.83	0.35	0.30	15.07	0.54	0.50	6.86
Sanitary products	0.00	0.00	-	0.00	0.00	-	0.00	0.06	-	0.00	0.00	-	0.00	0.00	-
Shoes	0.00	0.00	-	0.00	0.00	-	0.00	0.01	-	0.00	0.00	-	0.00	0.00	-
Stones/ceramic	17.45	17.27	1.02	20.56	21.70	-5.53	0.33	0.88	-164.39	0.00	0.18	-	0.00	0.09	-
Textile/fabric	0.36	0.35	3.00	0.05	0.07	-34.05	3.32	3.31	0.11	3.32	3.17	4.45	4.76	4.16	12.51
Tissues	0.00	0.14	-	0.04	0.03	11.92	0.21	0.18	17.95	0.15	0.13	13.66	0.06	0.11	-86.33
Treated wood	1.06	1.39	-31.52	1.08	1.19	-9.72	2.18	2.13	2.26	1.51	1.62	-7.30	2.05	2.23	-8.64

Component	SP13			SP14			SP15			SP16		
	Med (m)	m/Σm	%[Δ(Med-m/Σm)]/Med	Med (m)	m/Σm	%[Δ(Med-m/Σm)]/Med	Med (m)	m/Σm	%[Δ(Med-m/Σm)]/Med	Med (m)	m/Σm	%[Δ(Med-m/Σm)]/Med
Batteries	0.00	0.00	-	0.00	0.02	-	0.00	0.00	-	0.11	0.18	-68.60
Biological	0.96	1.07	-11.92	0.64	0.60	6.30	0.11	0.11	3.38	2.62	3.08	-17.38
Cables	0.11	0.19	-66.45	0.09	0.09	8.75	0.00	0.01	-	0.56	0.96	-70.93
Carpet/mats	0.24	0.46	-90.31	0.01	0.07	-1085.67	0.01	0.01	-128.90	0.63	1.08	-71.47
Cartons	0.77	0.89	-16.46	0.04	0.05	-22.30	0.01	0.03	-114.04	0.09	0.19	-126.96
Cinders	0.00	0.04	-	0.00	0.02	-	0.00	0.00	-	0.02	0.04	-98.89
Composites	2.05	2.42	-17.80	0.48	0.47	3.28	0.36	0.33	7.70	0.08	0.52	-536.03
Durable plastic	1.90	2.14	-13.06	1.66	1.64	1.26	0.01	0.10	-750.04	2.71	2.45	9.31
Ferrous metal	0.00	0.12	-	0.00	0.01	-	57.02	59.46	-4.27	7.38	6.16	16.55
Fines < 10 mm	39.99	41.27	-3.19	9.33	9.10	2.44	33.59	32.63	2.87	0.10	0.18	-83.29
Fluff	3.68	3.78	-2.59	0.00	0.00	-	0.74	0.80	-7.25	0.00	0.00	-
Glass	0.00	0.04	-	0.26	0.32	-22.22	0.00	0.03	-	0.05	0.30	-462.59
Hazardous	0.12	0.09	21.31	0.00	0.02	-	0.03	0.09	-174.43	1.18	1.27	-8.22
Non-Fe metal	1.16	0.92	21.19	79.26	79.81	-0.69	0.05	0.12	-122.14	3.17	4.39	-38.50
Other	0.13	0.31	-144.41	0.00	0.03	-	0.00	0.00	-	0.00	0.09	-
Other packaging plastic	7.23	6.57	9.09	2.82	2.80	0.49	0.29	0.24	17.85	2.58	2.72	-5.20
Paper/card	25.04	25.04	0.03	2.31	2.58	-11.83	3.72	3.10	16.72	48.05	44.88	6.60
Plastic film	4.63	5.32	-14.76	0.37	0.39	-4.81	1.41	1.25	11.63	0.57	0.73	-28.67
Rubber/leather	0.22	0.20	10.27	0.08	0.12	-50.30	0.05	0.07	-34.54	0.27	0.49	-80.77
Sanitary products	0.14	0.18	-28.66	0.00	0.00	-	0.00	0.04	-	2.87	2.45	14.49
Shoes	0.11	0.20	-81.26	0.00	0.02	-	0.00	0.03	-	9.05	10.26	-13.37
Stones/ceramic	0.31	0.31	-0.73	0.66	0.73	-10.91	0.00	0.00	-	7.25	9.49	-30.95
Textile/fabric	4.49	5.68	-26.52	0.13	0.13	0.97	1.65	1.48	10.44	0.11	0.43	-278.67
Tissues	0.38	0.35	7.75	0.00	0.00	-	0.05	0.05	-4.07	0.01	0.04	-410.32
Treated wood	2.35	2.42	-3.24	1.01	0.99	1.80	0.05	0.04	3.75	7.68	7.61	0.90

Table_App F-16 UK MBT plant A process flows: average (<>) component mass percentages (w/w_{ar}) and their U_{95,v}; corrected (modelled) values, input data to the initial stage of STAN2[®] (R1) for data reconciliation, and rest internal flows and TCs computation with uncertainty propagation

Component	SP1		SP2		SP3		SP4		SP5		SP6		SP7	
	<>	±U _{95,8}	<>	±U _{95,3}	<>	±U _{95,3}	<>	±U _{95,2}	<>	±U _{95,4}	<>	±U _{95,4}	<>	±U _{95,4}
Batteries	0.12	0.10	0.00	0.00	0.12	0.42	0.00	0.00	0.00	0.00	0.00	0.00	0.11	0.30
Biological	3.93	0.79	11.73	2.49	0.02	0.03	10.25	6.50	6.59	0.98	9.97	4.66	6.61	4.10
Cables	0.34	0.77	0.09	0.10	0.08	0.27	0.03	0.07	0.00	0.00	0.00	0.00	0.16	0.41
Carpet/mats	1.05	0.70	0.00	0.01	0.01	0.03	0.00	0.00	0.00	0.00	0.00	0.01	0.00	0.00
Cartons	0.78	0.25	0.01	0.02	0.05	0.10	0.01	0.03	0.01	0.01	0.11	0.13	0.03	0.05
Cinders	0.29	0.08	1.08	0.98	0.00	0.00	0.03	0.08	0.32	0.14	3.04	1.44	3.59	1.79
Composites	1.95	0.44	0.77	0.50	0.25	0.14	0.16	0.20	0.29	0.07	1.93	0.57	0.60	0.12
Durable plastic	2.41	0.61	0.65	0.33	0.08	0.11	0.50	0.55	0.73	0.33	2.52	0.98	1.91	0.85
Ferrous metal	5.38	2.94	2.77	2.88	92.08	5.24	0.80	1.28	0.03	0.02	0.60	1.09	0.79	0.45
Fines < 10 mm	15.85	3.57	51.79	12.50	3.66	3.90	55.70	8.01	71.36	6.60	14.99	4.00	12.31	9.82
Fluff	0.36	0.96	0.53	0.65	0.03	0.07	0.26	0.73	1.07	0.58	0.98	0.60	0.10	0.18
Glass	7.51	2.02	24.16	11.16	0.00	0.00	22.02	4.19	8.95	4.81	35.25	6.34	43.40	5.94
Hazardous	0.56	0.40	0.00	0.00	0.05	0.18	0.05	0.12	0.04	0.06	0.10	0.08	0.17	0.17
Non-Fe metal	1.73	0.52	0.45	0.22	0.00	0.00	0.09	0.20	0.03	0.02	0.11	0.13	0.43	0.40
Other	0.00	0.00	0.00	0.00	0.00	0.00	0.00	0.00	0.00	0.00	0.98	1.51	0.14	0.25
Other packaging plastic	8.39	2.21	0.50	0.32	0.46	0.38	0.17	0.32	0.28	0.14	0.84	0.27	0.30	0.35
Paper/card	26.93	3.18	3.71	0.60	1.38	1.07	3.39	0.27	1.72	0.35	6.69	2.53	3.47	3.22
Plastic film	7.42	2.83	1.18	0.44	1.22	0.51	0.76	0.25	0.50	0.06	1.54	0.68	0.31	0.35
Rubber/leather	0.18	0.07	0.09	0.09	0.01	0.03	0.05	0.10	0.00	0.00	0.13	0.30	0.15	0.18
Sanitary products	1.06	0.68	0.00	0.00	0.00	0.00	0.00	0.00	0.00	0.00	0.00	0.00	0.00	0.00
Shoes	2.09	1.81	0.34	0.60	0.00	0.00	0.00	0.00	0.00	0.00	0.00	0.00	0.00	0.00
Stones/ceramic	4.17	1.23	2.23	4.21	0.19	0.53	6.13	1.39	1.97	1.16	18.63	2.45	22.40	8.19
Textile/fabric	2.64	1.90	0.29	0.19	0.29	0.30	0.20	0.09	0.20	0.10	0.38	0.20	0.07	0.09
Tissues	0.71	0.41	0.03	0.05	0.01	0.02	0.00	0.00	0.08	0.05	0.15	0.24	0.03	0.04
Treated wood	4.17	1.64	0.42	0.30	0.03	0.06	0.52	0.83	0.28	0.05	1.50	1.02	1.22	0.93
Overall	100.00		102.81		100.00		101.11		94.43		100.44		98.30	
Σ(SHR)	82.76	2.90	72.49	11.24	7.59	4.39	72.16	2.86	83.20	6.06	43.01	7.46	28.03	8.43
Σ(non-SHR)	19.53	2.62	30.78	11.24	92.46	4.49	29.10	2.86	11.30	6.01	57.64	7.42	70.87	8.59
Σ(combustibles)	81.10	2.37	73.11	10.20	7.54	4.66	72.04	2.80	83.46	5.95	45.84	7.39	31.02	7.71

Σ(non-combustibles)	19.24	2.37	29.70	10.20	92.46	4.66	29.07	2.80	10.97	5.95	54.60	7.39	67.28	7.71
Σ(P/C+TIS+CAR)	28.42	3.13	3.76	0.63	1.43	1.15	3.40	0.27	1.81	0.30	6.95	2.59	3.53	3.20
Σ(C/M+FL+S_P+SH+T/F)	7.20	2.52	1.16	0.63	0.33	0.34	0.46	0.66	1.27	0.57	1.36	0.64	0.17	0.20
Σ(COM+D_P+O_P_P+P_F)	20.17	4.88	3.10	1.21	2.01	0.57	1.58	0.95	1.79	0.36	6.83	0.90	3.13	0.91
Total chlorine content (SHR,d)	100.00	68.95	8.27	1.84	0.45	0.28	5.22	7.68	4.45	9.47	5.19	4.03	1.52	0.77
Net calorific value (SHR,ar)	15032	2310	1978	389	78	18	1990	609	1876	2393	730	72	479	196
Biogenic content (SHR,daf)	5104.93	1612.75	432.16	76.24	37.70	6.31	350.39	109.19	286.44	90.61	143.28	31.78	116.75	29.72
Ash content (SHR,d)	2831.2	821.5	1516.5	163.5	4.7	1.9	1836.5	112.9	1368.9	124.1	221.7	47.0	125.5	18.0

Component	SP10		SP11		SP12		SP13		SP14		SP15		SP16	
	<>	±U _{95,3}	<>	±U _{95,3}	<>	±U _{95,4}	<>	±U _{95,4}	<>	±U _{95,3}	<>	±U _{95,3}	<>	±U _{95,8}
Batteries	0.00	0.00	0.00	0.00	0.00	0.00	0.00	0.00	0.02	0.07	0.00	0.00	0.18	0.24
Biological	0.94	0.39	0.81	0.42	2.22	0.86	2.37	2.89	0.66	0.59	0.22	0.23	3.08	1.98
Cables	0.00	0.00	0.04	0.16	0.15	0.23	0.29	0.35	0.09	0.08	0.01	0.05	0.96	0.64
Carpet/mats	0.47	0.09	0.86	0.53	0.70	1.13	0.97	1.07	0.07	0.22	0.02	0.06	1.08	1.04
Cartons	0.90	0.75	0.94	1.69	1.17	0.72	1.47	0.70	0.06	0.11	0.04	0.13	0.19	0.22
Cinders	0.07	0.20	0.08	0.14	0.00	0.00	0.07	0.13	0.02	0.07	0.00	0.00	0.04	0.07
Composites	4.34	3.95	2.67	1.65	4.12	2.91	5.12	1.14	0.52	0.35	0.68	0.58	0.52	0.66
Durable plastic	2.51	2.95	1.71	2.49	3.27	1.55	3.67	3.37	1.81	0.58	0.15	0.50	2.45	1.03
Ferrous metal	3.20	1.41	0.22	0.32	2.06	1.56	0.18	0.33	0.01	0.03	87.40	7.17	6.16	2.57
Fines < 10 mm	0.00	0.00	0.00	0.00	0.98	1.95	0.61	1.35	0.00	0.00	1.09	0.81	0.18	0.33
Fluff	0.30	0.19	0.23	0.09	0.25	0.31	0.28	0.19	0.00	0.00	0.12	0.00	0.00	0.00
Glass	0.39	0.87	0.29	0.33	0.75	1.25	0.07	0.12	0.35	0.57	0.04	0.17	0.30	0.66
Hazardous	0.06	0.07	0.05	0.09	0.10	0.10	0.15	0.12	0.02	0.07	0.13	0.21	1.27	0.90
Non-Fe metal	2.44	1.02	2.16	2.17	2.16	2.09	1.53	1.44	87.79	3.20	0.18	0.50	4.39	2.71
Other	0.00	0.00	0.00	0.00	0.04	0.14	0.65	1.43	0.03	0.10	0.00	0.00	0.09	0.26
Other packaging plastic	13.67	5.65	13.81	9.32	14.21	4.64	13.78	4.44	3.09	0.76	0.49	0.40	2.72	0.63
Paper/card	44.18	7.60	53.74	11.51	43.87	13.96	43.14	3.37	2.84	1.83	4.65	2.78	44.88	14.23
Plastic film	16.07	6.51	14.65	3.45	13.19	4.25	11.32	2.77	0.43	0.39	2.53	1.37	0.73	0.30
Rubber/leather	0.51	0.78	0.51	0.37	0.93	0.71	0.35	0.25	0.13	0.20	0.10	0.17	0.49	0.48
Sanitary products	0.11	0.51	0.00	0.00	0.00	0.00	0.34	0.39	0.00	0.00	0.08	0.29	2.45	1.16
Shoes	0.02	0.12	0.00	0.00	0.00	0.00	0.36	0.63	0.02	0.07	0.04	0.18	10.26	4.00

Stones/ceramic	1.49	3.08	0.27	0.75	0.15	0.49	0.58	0.59	0.80	0.57	0.00	0.00	9.49	8.99
Textile/fabric	4.14	2.28	3.89	2.20	5.20	2.27	7.33	2.06	0.13	0.13	1.87	1.36	0.43	0.37
Tissues	0.29	0.33	0.20	0.23	0.19	0.32	0.60	0.32	0.00	0.01	0.08	0.17	0.04	0.06
Treated wood	3.88	1.52	2.87	1.07	4.28	1.57	4.75	1.68	1.09	0.26	0.05	0.12	7.61	2.90
Overall	100.00		100.00		100.00		100.00		100.00		99.96		100.00	
Σ(SHR)	94.91	3.86	99.16	2.34	97.00	3.01	98.96	1.78	98.72	3.57	12.64	7.22	84.15	10.18
Σ(non-SHR)	7.59	3.82	3.05	2.28	5.27	2.94	2.72	1.76	89.09	3.56	87.63	7.08	21.52	10.17
Σ(combustibles)	92.48	3.64	97.03	2.16	94.73	2.74	97.35	1.45	10.93	3.59	12.33	7.09	78.52	10.07
Σ(non-combustibles)	7.52	3.64	2.97	2.16	5.27	2.74	2.65	1.45	89.07	3.59	87.63	7.09	21.48	10.07
Σ(P/C+TIS+CAR)	45.38	7.46	54.88	10.04	45.23	13.67	45.22	3.72	2.90	1.91	4.77	2.90	45.11	14.16
Σ(C/M+FL+S_P+SH+T/F)	5.05	2.51	4.98	1.83	6.16	2.86	9.29	2.13	0.23	0.27	2.13	1.76	14.22	3.47
Σ(COM+D_P+O_P_P+P_F)	36.59	7.57	32.84	8.18	34.79	10.15	33.89	4.05	5.84	1.32	3.84	2.18	6.42	1.26
Total chlorine content (SHR,d)	51.14	20.29	84.91	32.35	54.18	31.45	78.91	6.19	0.23	0.19	0.03	0.03	16.39	35.20
Net calorific value (SHR,ar)	10829	3567	10915	2407	11871	1731	9823	1477	12	3	3	0	2047	641
Biogenic content (SHR,daf)	4016.51	211.25	4250.89	387.94	4421.95	233.93	4169.74	471.16	5.93	1.19	3.64	0.52	833.25	92.86
Ash content (SHR,d)	1100.0	66.2	1010.4	175.6	1059.6	99.0	1230.4	420.8	3.3	1.0	1.3	0.5	190.5	43.2

Table_App F-17 Results of sensitivity analysis for balances of the adjusted (modelled) waste components – UK MBT plant A

Mass balance scenario	L				M				H			
	Component	m(l)	Σm(E)	% Σm(E)/ m(l)	% Σm(E)/- m(l)	Σm(E)	% Σm(E)/ m(l)	% Σm(E)/- m(l)	Σm(E)	% Σm(E)/ m(l)	% Σm(E)/- m(l)	
Batteries	11.69	3.69	31.57	-68.43	4.21	36.03	-63.97	4.77	40.80	-59.20		
Biological	392.59	359.97	91.69	-8.31	348.10	88.67	-11.33	334.02	85.08	-14.92		
Cables	33.58	29.54	87.98	-12.02	33.56	99.93	-0.07	37.16	110.66	10.66		
Carpet/mats	104.99	65.19	62.09	-37.91	70.15	66.82	-33.18	74.47	70.93	-29.07		
Cartons	78.20	81.84	104.66	4.66	82.71	105.76	5.76	83.40	106.65	6.65		
Cinders	29.36	42.59	145.05	45.05	35.03	119.30	19.30	28.99	98.73	-1.27		
Composites	195.17	291.91	149.56	49.56	292.70	149.97	49.97	293.16	150.21	50.21		
Durable plastic	240.95	259.93	107.88	7.88	266.06	110.42	10.42	271.19	112.55	12.55		
Ferrous metal	537.94	474.71	88.24	-11.76	438.45	81.50	-18.50	461.83	85.85	-14.15		
Fines < 10 mm	1584.77	1629.95	102.85	2.85	1464.10	92.39	-7.61	1267.97	80.01	-19.99		
Fluff	35.75	38.17	106.79	6.79	35.89	100.42	0.42	33.08	92.55	-7.45		
Glass	750.80	575.39	76.64	-23.36	473.30	63.04	-36.96	387.05	51.55	-48.45		
Hazardous	55.95	26.72	47.75	-52.25	32.07	57.32	-42.68	36.82	65.81	-34.19		
Non-Fe metal	172.77	184.17	106.60	6.60	203.32	117.68	17.68	220.19	127.44	27.44		
Other	0.00	37.00	-	-	37.18	-	-	37.33	-	-		
Other packaging plastic	838.91	780.76	93.07	-6.93	792.58	94.48	-5.52	802.28	95.63	-4.37		
Paper/card	2693.26	2940.36	109.17	9.17	3135.94	116.44	16.44	3305.94	122.75	22.75		
Plastic film	741.54	631.19	85.12	-14.88	632.88	85.35	-14.65	634.09	85.51	-14.49		
Rubber/leather	17.62	26.46	150.15	50.15	28.43	161.32	61.32	30.19	171.29	71.29		
Sanitary products	105.96	49.30	46.53	-53.47	60.46	57.06	-42.94	70.27	66.32	-33.68		
Shoes	209.37	148.86	71.10	-28.90	195.47	93.36	-6.64	236.50	112.96	12.96		
Stones/ceramic	416.96	390.15	93.57	-6.43	384.92	92.32	-7.68	384.35	92.18	-7.82		
Textile/fabric	264.13	402.45	152.37	52.37	404.17	153.02	53.02	405.27	153.43	53.43		
Tissues	70.95	34.49	48.61	-51.39	34.49	48.61	-51.39	34.41	48.50	-51.50		
Treated wood	416.79	366.37	87.90	-12.10	398.26	95.56	-4.44	426.18	102.25	2.25		
Σ(components)	10000.00	9871.15	98.71	-1.29	9884.43	98.84	-1.16	9900.91	99.01	-0.99		
Σ(SHR)	8275.61	8381.79	101.28	1.28	8547.03	103.28	3.28	8633.58	104.33	4.33		
Σ(non-SHR)	1953.12	1700.24	87.05	-12.95	1572.80	80.53	-19.47	1524.34	78.05	-21.95		
Σ(combustibles)	8109.83	8213.50	101.28	1.28	8346.66	102.92	2.92	8405.56	103.65	3.65		
Σ(non-combustibles)	1923.75	1657.65	86.17	-13.83	1537.77	79.94	-20.06	1495.35	77.73	-22.27		
Σ(P/C+TIS+CAR)	2842.41	3056.69	107.54	7.54	3253.13	114.45	14.45	3423.75	120.45	20.45		

$\Sigma(C/M+FL+S_P+SH+T/F)$	720.19	703.97	97.75	-2.25	766.14	106.38	6.38	819.59	113.80	13.80
$\Sigma(COM+D_P+O_P_P+P_F)$	2016.56	1963.78	97.38	-2.62	1984.22	98.40	-1.60	2000.72	99.21	-0.79

m(l): specific mass load of waste component at the refinement section input (overall 10000 mass units): mass percentage times 100 mass units

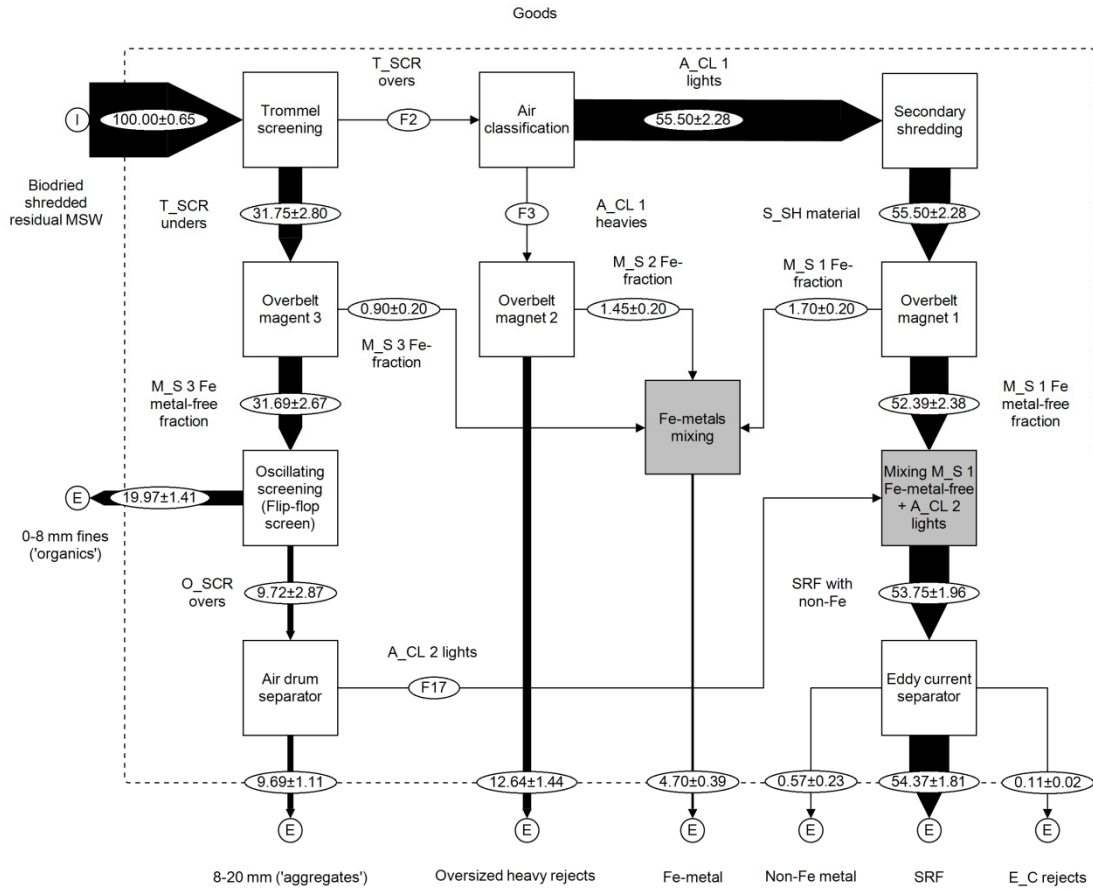
$\Sigma m(E)$: sum of specific mass load of waste component over the plant outputs; at each output : adjusted (modelled) mass percentage times the mass units as reconciled by STAN2 after the mass balance scenario (L, M, H)

% $\Sigma m(E)$ / m(l)

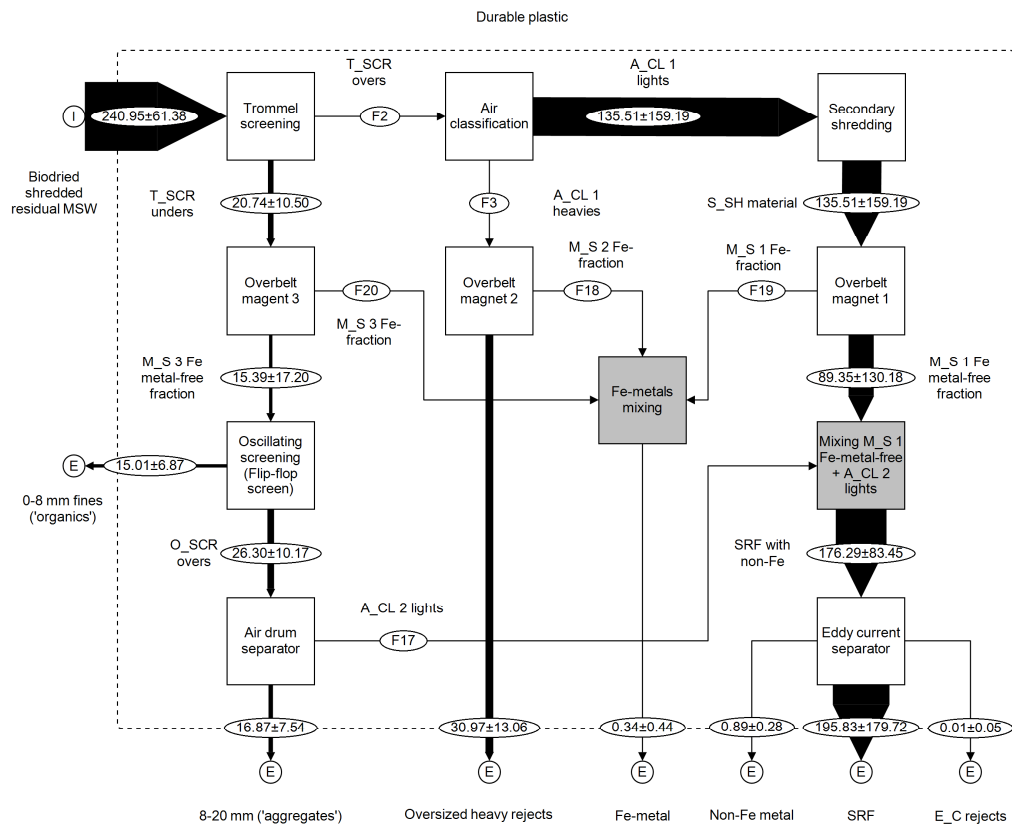
L, M, H: mass balance scenarios codes, according to the assumed level of oversized heavy rejects (SP16): liw, medium and high accordingly (See [TableXXX](#))

Table_App F-18 UK MBT plant A process flows: average (<>) dry mass percentages (w/w_d) and U₉₅, before and after reconciliation by STAN2®

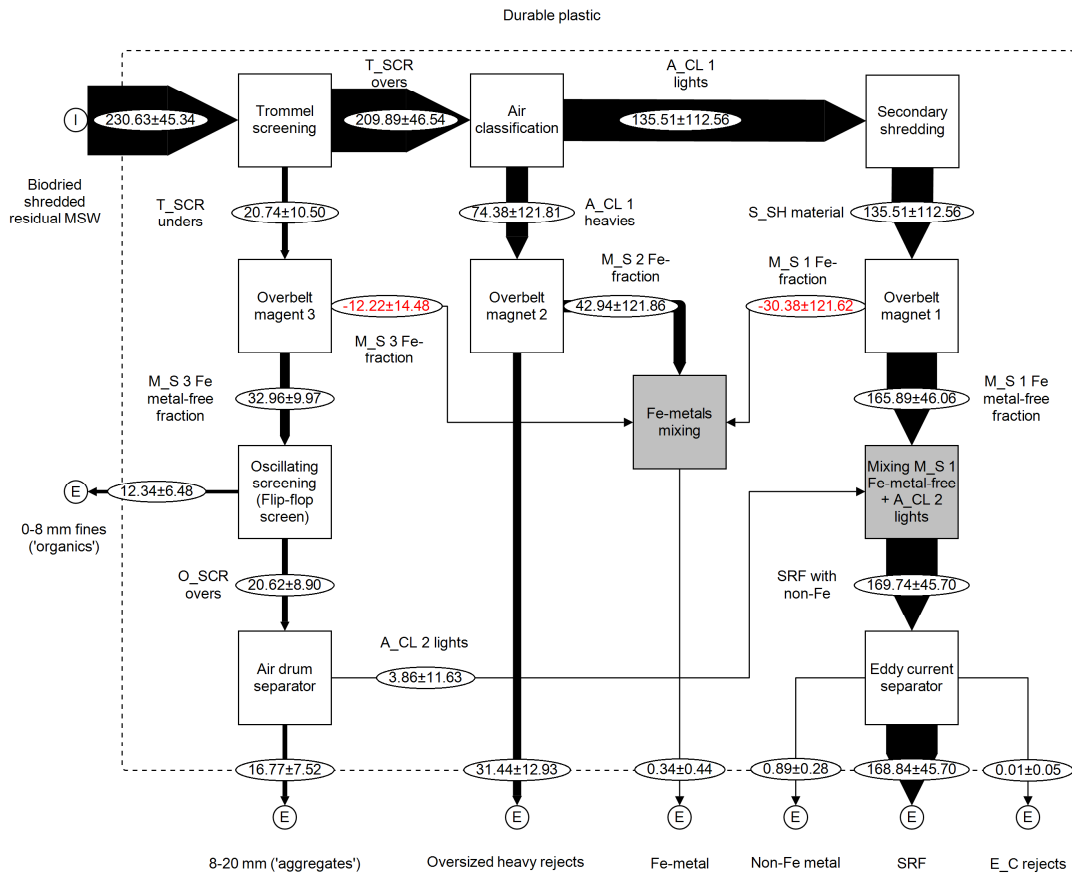
Flow	Sampling point ID	Flow description	<Input to STAN2>	$\pm U_{95}$	<STAN2 output>	$\pm U_{95}$
			(% w/w _d)	(% w/w _d)	(% w/w _d)	(% w/w _d)
F1	SP1	Biodried shredded residual MSW	100.00	0.65	100.10	0.62
F10	SP15	E_C rejects	0.11	0.02	0.11	0.02
F11	SP14	Non-Fe metal	0.57	0.23	0.56	0.23
F12	SP2	T_SCR unders	31.75	2.80	31.49	1.27
F13	SP4	M_S 3 Fe metal-free fraction	31.69	2.67	30.50	1.27
F14	SP5	0-8 mm fines ('organics')	19.97	1.41	19.90	1.14
F15	SP6	O_SCR overs	9.72	2.87	10.59	1.39
F16	SP7	8-20 mm ('aggregates')	9.69	1.11	9.52	0.99
F17		A_CL 2 lights			1.08	1.42
F18		M_S 2 Fe-fraction	1.45	0.20	1.54	0.18
F19		M_S 1 Fe-fraction	1.70	0.20	1.80	0.18
F2		T_SCR overs			68.61	1.31
F20		M_S 3 Fe-fraction	0.90	0.20	0.99	0.18
F21	SP3	Fe-metal	4.70	0.39	4.33	0.26
F3		A_CL 1 heavies			13.69	1.12
F4		Oversized heavy rejects	12.64	1.44	12.15	1.11
F5		A_CL 1 lights	55.50	2.28	54.92	1.11
F6	SP10	S_SH material	55.50	2.28	54.92	1.11
F7	SP11	M_S 1 Fe metal-free fraction	52.39	2.38	53.12	1.11
F8	SP12	SRF with non-Fe metals	53.75	1.96	54.20	1.12
F9	SP13	SRF	54.37	1.81	53.53	1.12



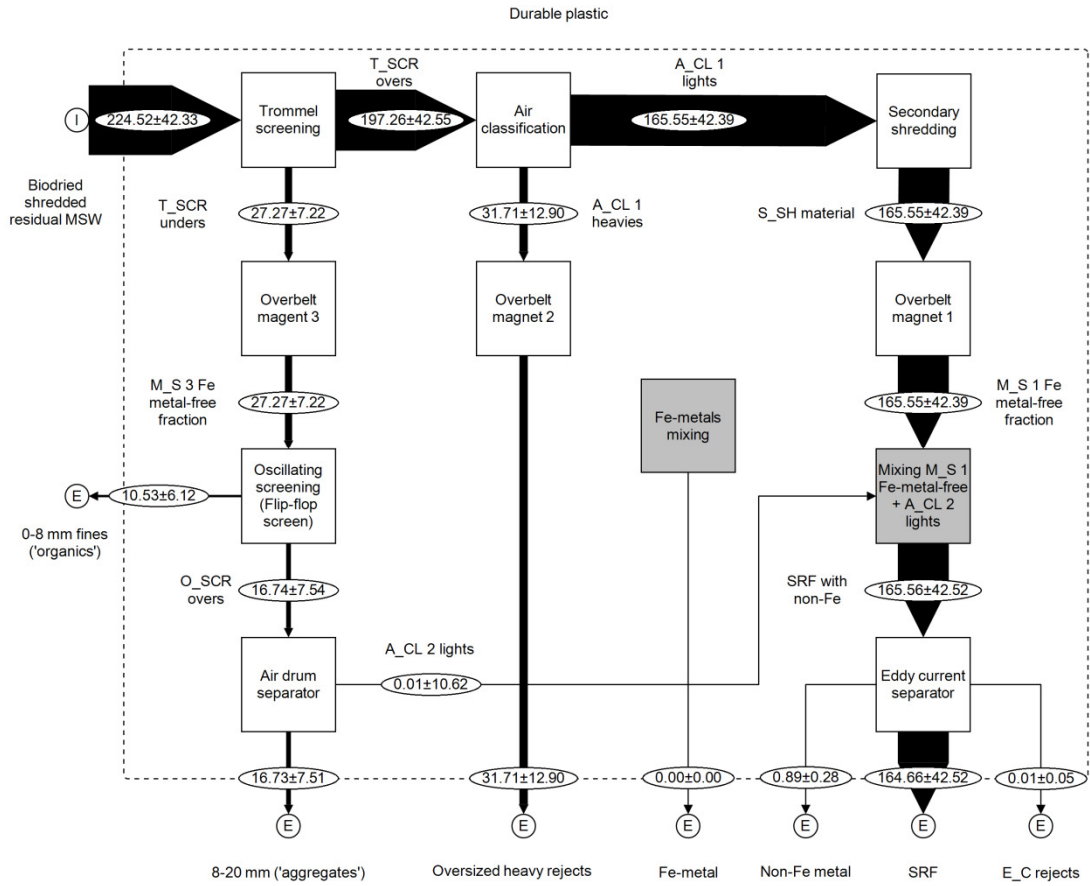
Figure_App F-17 Entire mass, dry basis data input to STAN2[®] for reconciliation



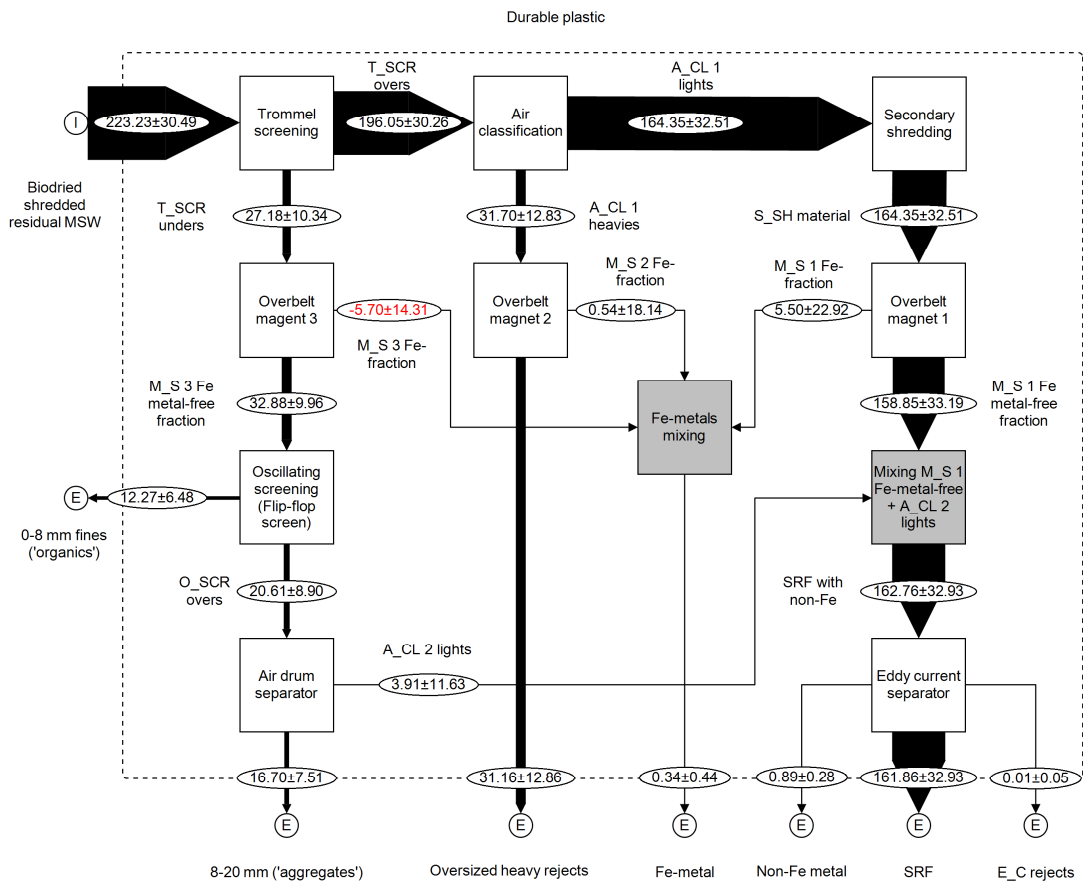
Figure_App F-18: input data



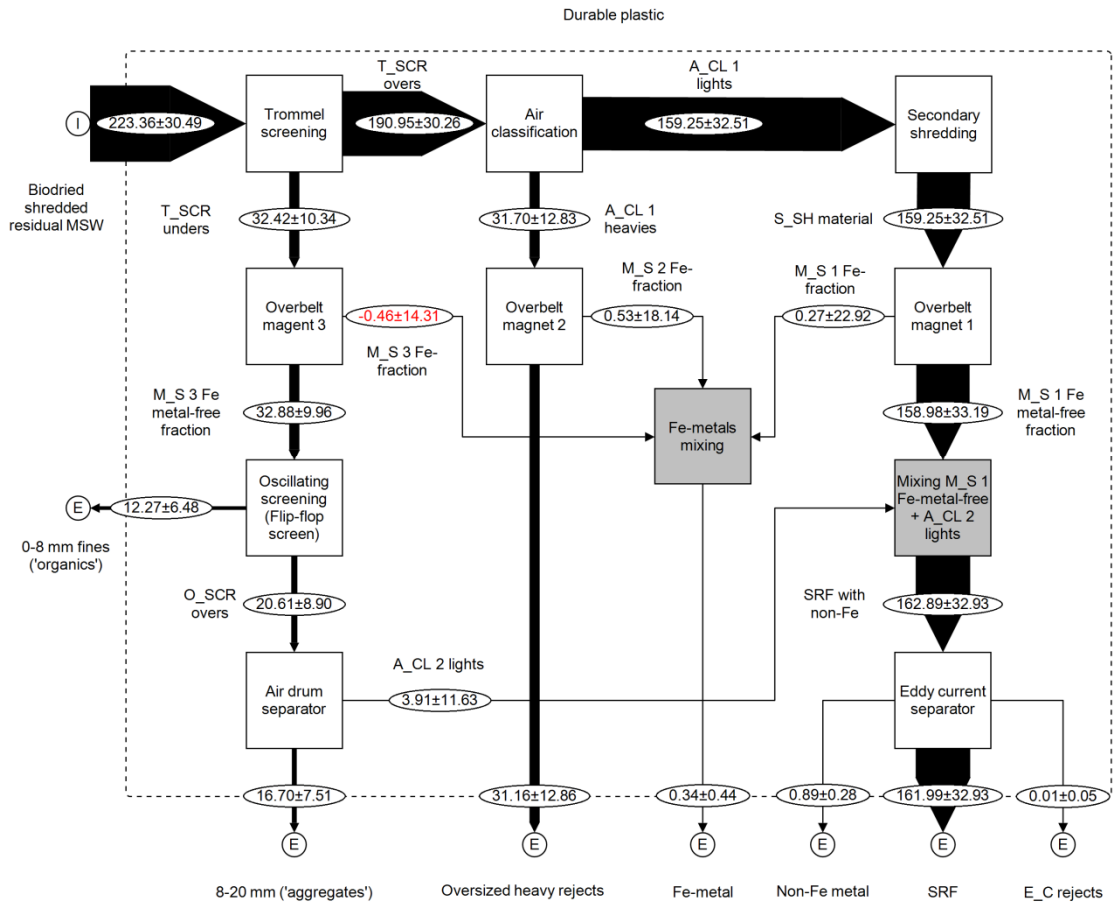
Figure_App F-19: R1output



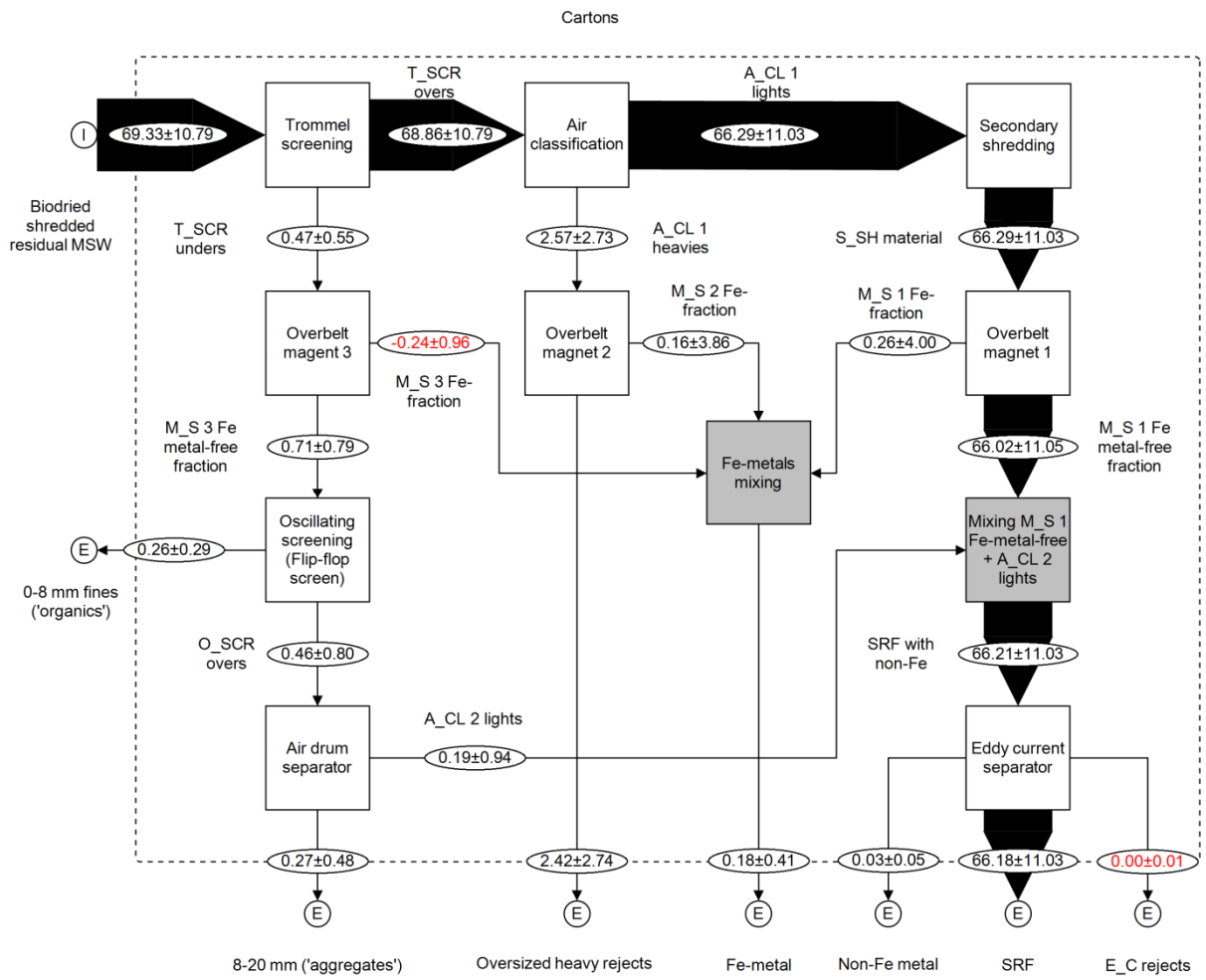
Figure_App F-20: R2 input



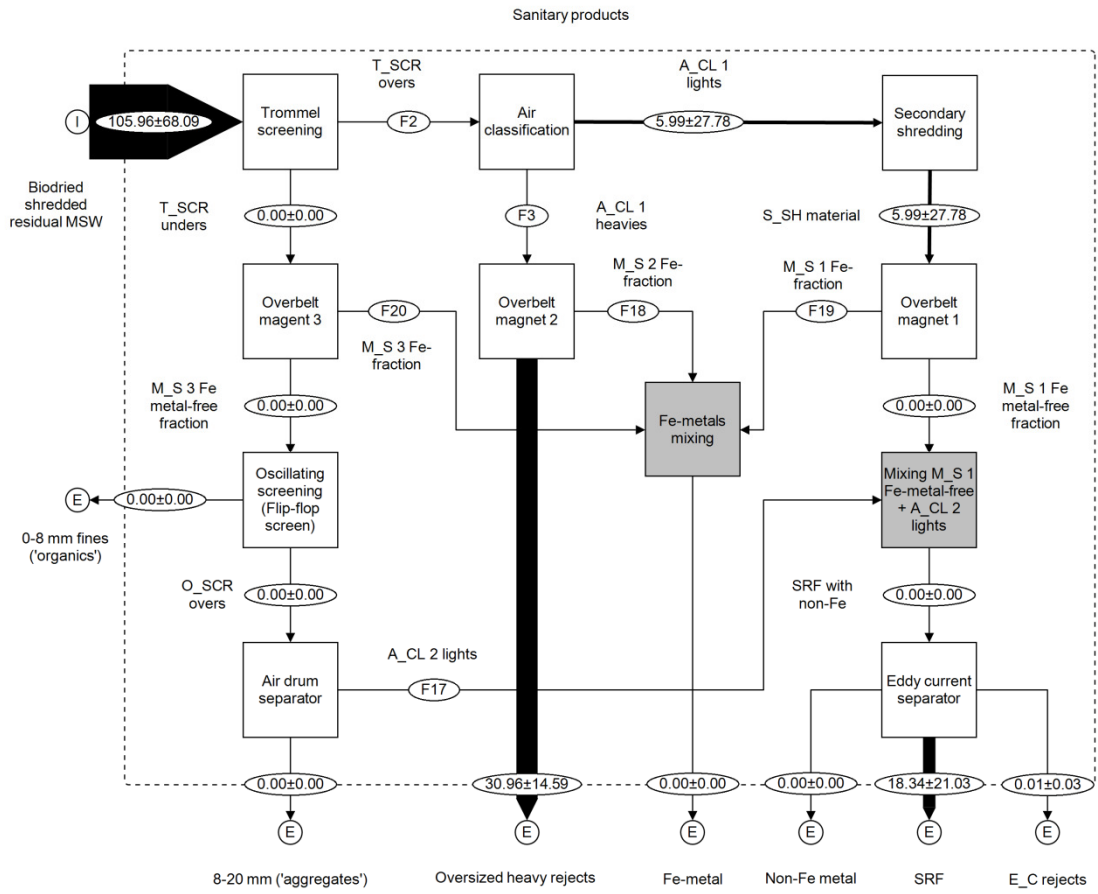
Figure_App F-21: R3 input



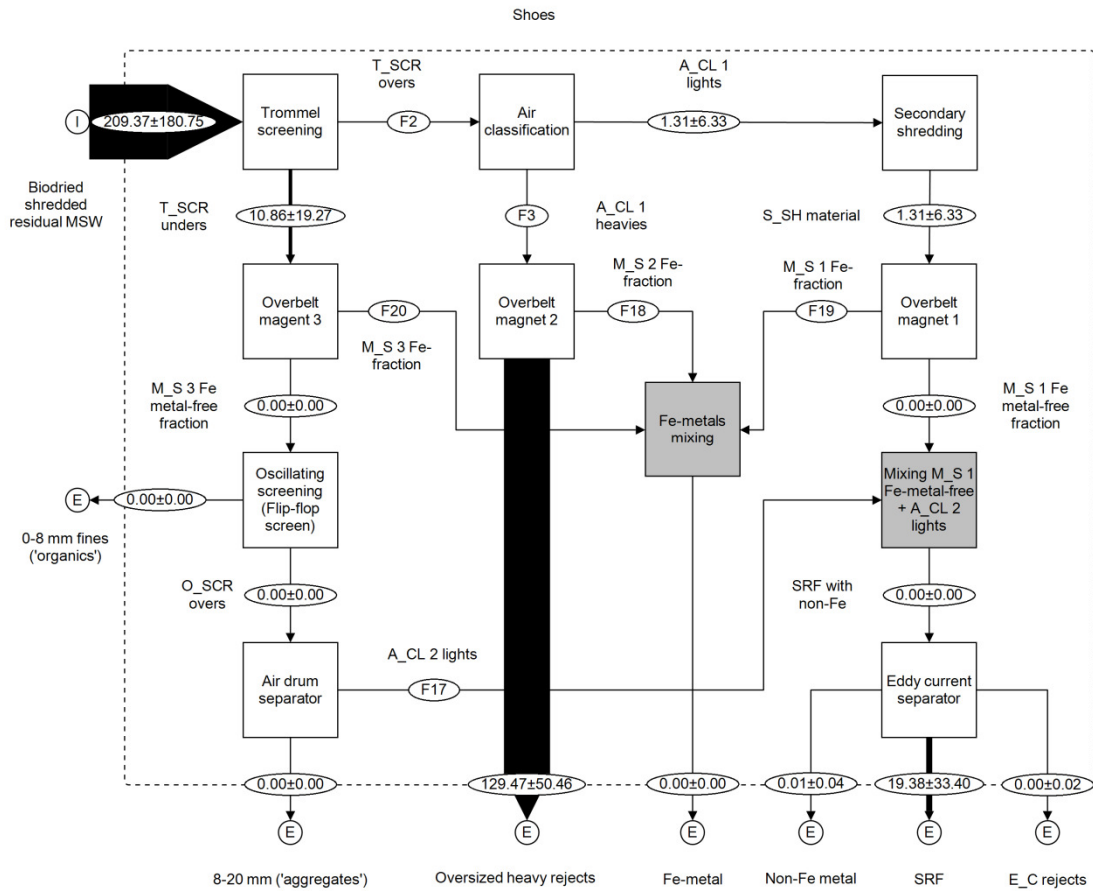
Figure_App F-22: R4



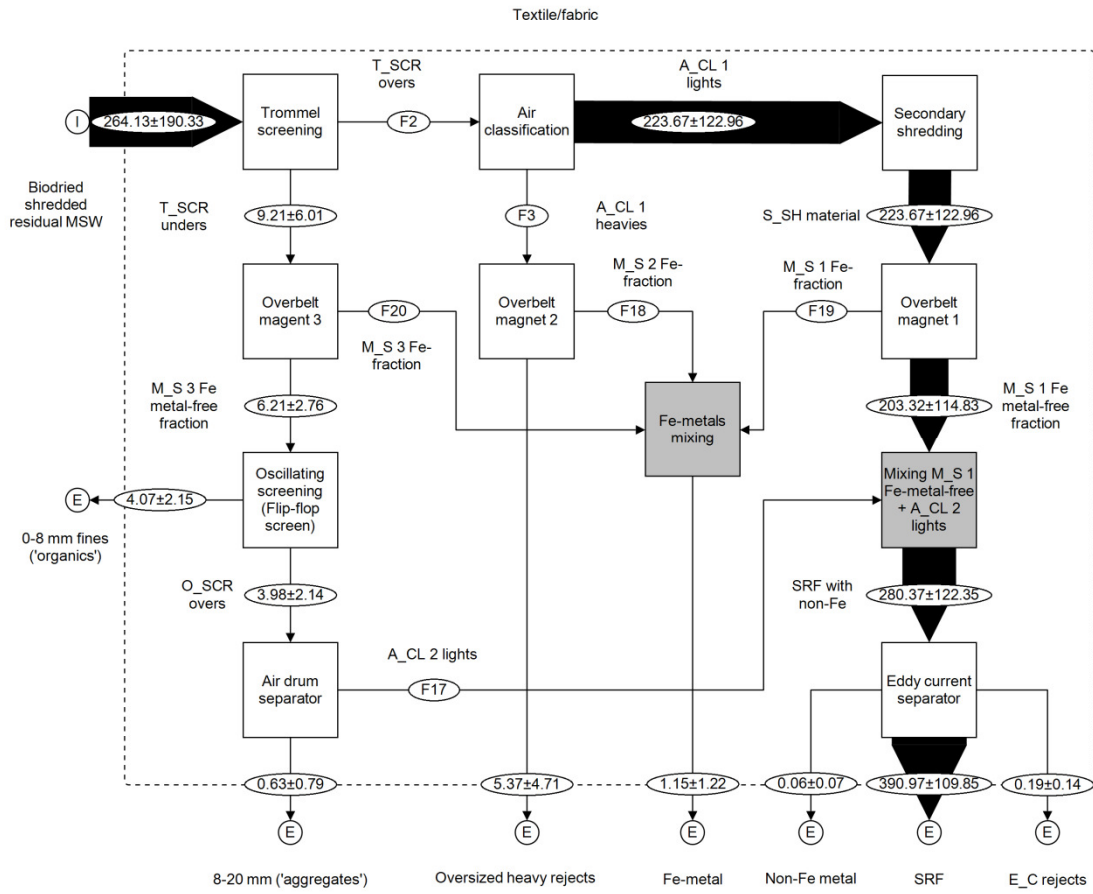
Figure_App F-23



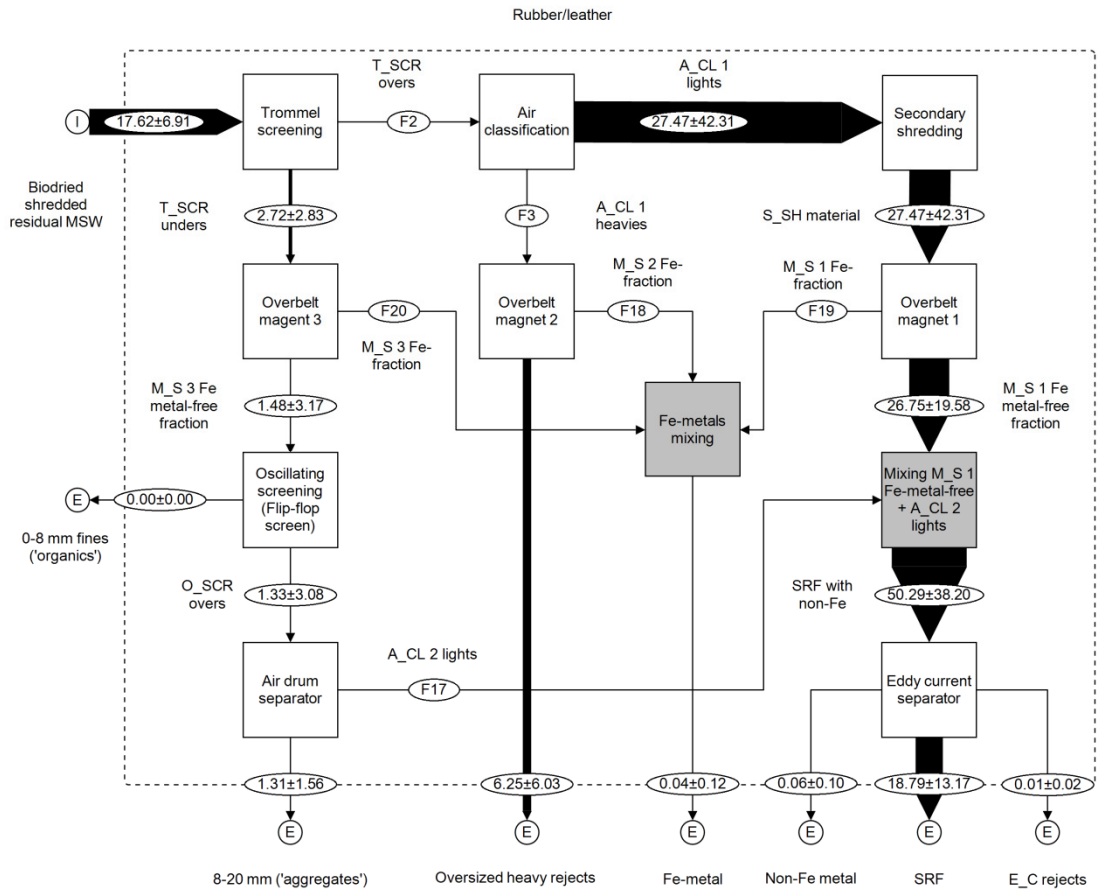
Figure_App F-24 Flows of waste component sanitary products as corrected for the secondary shredding effect. Not reconciled by STAN2 application.



Figure_App F-25 Flows of waste component shoes as corrected for the secondary shredding effect. Not reconciled by STAN2 application.



Figure_App F-26 Flows of waste component textile/fabric as corrected for the secondary shredding effect. Not reconciled by STAN2 application.



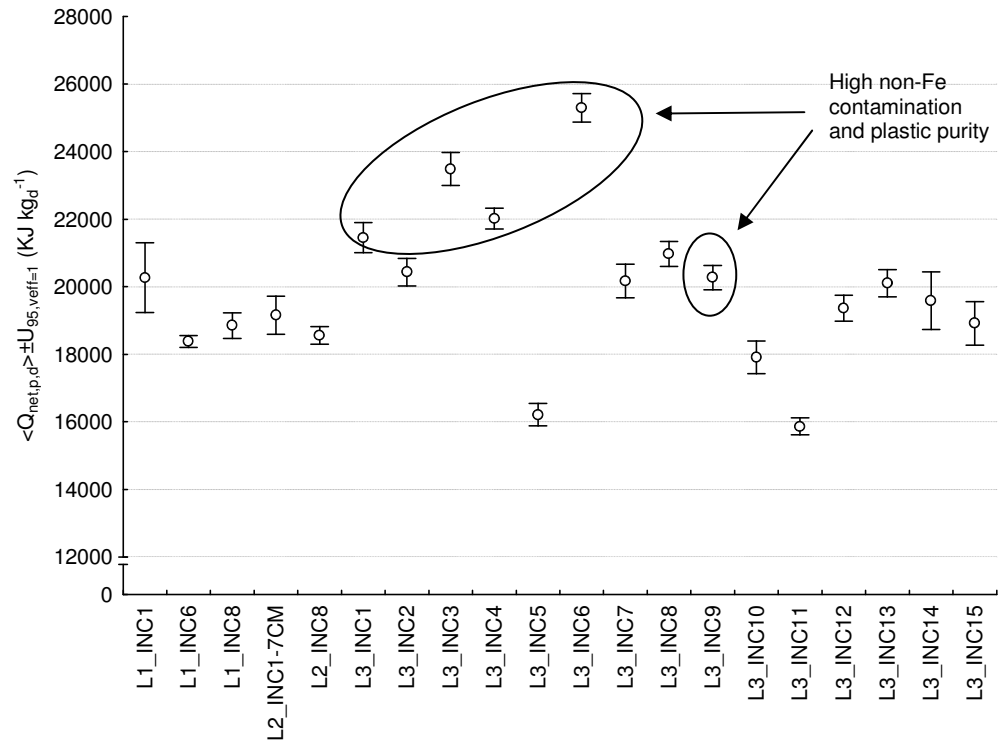
Figure_App F-27 Flows of waste component rubber/leather as corrected for the secondary shredding effect. Not reconciled by STAN2 application.

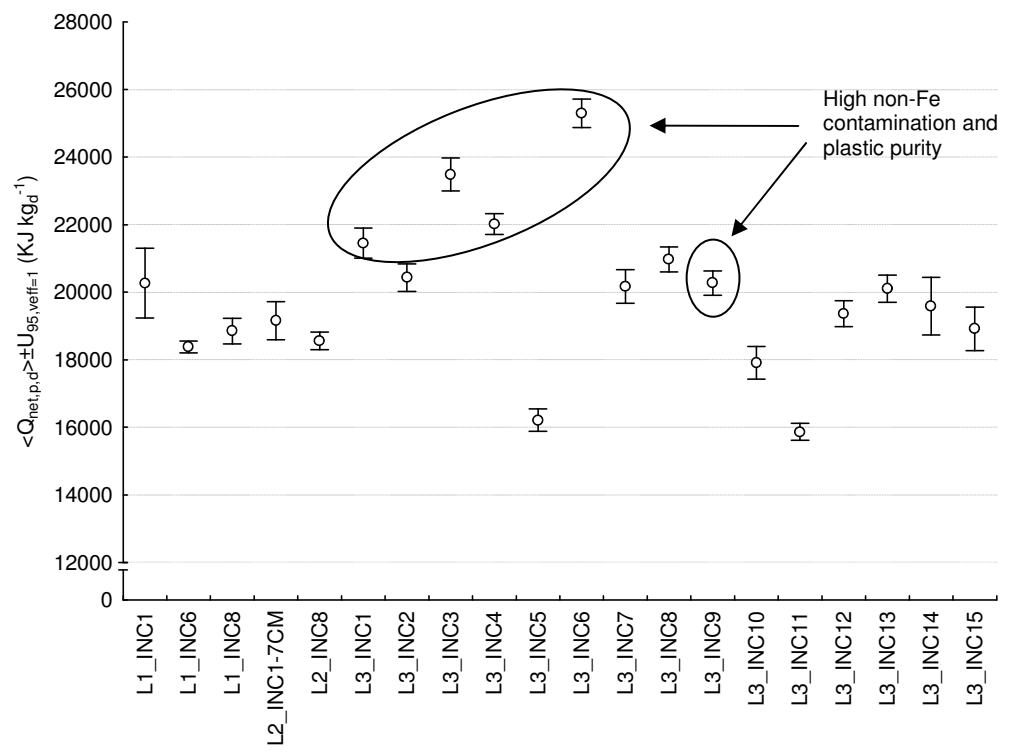
Table_App F-19 Reconstructed SRF material composition on dry mass basis for the UK MBT plant A

Waste component	Component ID	Waste particular component characterisation ID	Mb (w/war)	Mlr (w/wb)	<Mir> (w/wb)	Reconstructed SRF composition (% w/war)	±U95(%m) w/war	Reconstructed SRF composition d (not 100 adding)	Reconstructed SRF composition d (% w/wd)
Biological	BIO	BL/ST1	16.2	6.39	5.81	2.16	0.6	1.69	2.0
		BL/ST2		5.24			6		
Carpet/mats	C/M	C+M/ST1	3.11	1.81	1.81	0.99	1.1	0.94	1.1
Cartons	CAR	CRT/ST1	8.76	4.57	4.57	1.27	0.2	1.11	1.3
		CA/ST3					1		
Composites	COM	CMP/ST1	5.12	5.46	5.07	3.51	1.1	3.15	3.6
		CMP/ST3		4.69			7		
Durable plastic	D_P	H+DPL/ST1/SH1	0.31	0.98	0.98	3.12	0.6	3.08	3.6
		H+DPL/ST2					3		
Fines <10 mm	F<10	L1/INC1/SP1/F	5.23	3.38	3.23	0.80	0.9	0.74	0.9
		L1/INC4/SP1/F		3.09			7		
Other	OTH		0.00	0.00	0.00	0.67	1.4	0.67	0.8
Fluff	FL		3.64		0.00	0.34	0.1	0.33	0.4
Other packaging plastic	O_P_P	OPL/ST2	3.36	0.67	0.60	14.13	4.5	13.57	15.7
		OPPL/ST2/SH1		0.52			6		
Paper/card	P/C	P+C/ST1	16.5	4.89	4.34	44.54	2.6	35.35	40.8
		PC/ST2		3.19			2		
Plastic film	P_F	FPL/ST3/SH1	2.98	1.67	1.67	13.40	1.2	12.79	14.8
Rubber/leather	R/L		4.95	0.00	0.00	0.36	0.2	0.34	0.4
Sanitary products	S_P	SNP/ST1	45.0	18.8	18.8	1.44	0.4	0.64	0.7
Shoes	SH	SHS/ST1	6	8	8		0		
			4.48	2.03	2.03	1.54	0.6	1.44	1.7
Textile/fabric	T/F	FB+TXT/ST3	5.39	3.29	3.29	3.83	0.6	3.51	4.1
Tissues	TIS		6.94		0.00	1.33	0.3	1.24	1.4
Treated wood	T_W	TW/ST1	10.3	3.82	4.66	3.87	0.6	3.34	3.9
		TW/ST1*	6	6.27			4		

Waste component	Component ID	Waste particular component characterisation ID	Mb (w/war)	Mlr (w/wb)	<Mr> (w/wb)	Reconstructed SRF composition (% w/war)	±U95(%m) w/war	Reconstructed SRF composition d (not 100 adding)	Reconstructed SRF composition d (% w/wd)
		TW/ST3		3.89					
Batteries	BAT		0.52		0.00	0.00	0.00	0.00	0.00
Cables	CAB		0.00	0.00	0.00	0.20	0.17	0.20	0.20
Cinders	CIN		3.55	4.59	4.59	0.07	0.14	0.07	0.10
Ferrous metal	Fe_M		0.85	0.00		0.18	0.25	0.18	0.20
Glass	GL		0.02	0.00	0.00	0.29	0.28	0.29	0.30
Hazardous	HAZ	HAZ/T6/SH1	0.00	2.86	1.40	0.16	0.12	0.15	0.20
		HAZ/T7/SH1		0.43					
		HAZ/T12/SH1		0.90					
		HAZ/T13/SH1		0.78					
		VT		0.00					
		PWB/SH1		1.59					
Non-ferrous metal	nFe_M		1.02	0.00	0.00	1.48	0.65	1.46	1.70
Stones/ceramics	S/C		0.84	0.00	0.00	0.32	0.38	0.31	0.40
Total sum						100.00		86.57	100.0

Appendix G - SRF characterisation – UK MBT plant A





Table_App G-1 Results on SRF characterisation for TC TH TN

Sample ID	<TC>	s(TC)	%CV(<TC >)	s(<TC >)	±U _{95,2} (<TC>)	%U _{95,2} (<TC>)	<TH>	s(TH)	%CV(<TH >)	s(<TH >)	±U _{95,2} (<TH>)	%U _{95,2} (<TH>)
	% w/w _d	% w/w _d	%	% w/w _d	% w/w _d	% w/w _d	% w/w _d	% w/w _d	%	% w/w _d	% w/w _d	% w/w _d
L1_INC1	47.57	1.138	2.4	0.657	2.828	5.9	6.59	0.160	2.4	0.092	0.397	6.0
L1_INC6	46.43	0.337	0.7	0.195	0.838	1.8	6.00	0.049	0.8	0.028	0.122	2.0
L1_INC8	47.66	0.841	1.8	0.486	2.089	4.4	6.34	0.104	1.6	0.060	0.258	4.1
L2_INC1- 7CM	45.99	0.297	0.6	0.171	0.737	1.6	5.99	0.079	1.3	0.046	0.196	3.3
L2_INC8	46.72	0.134	0.3	0.077	0.333	0.7	6.21	0.050	0.8	0.029	0.124	2.0
L3_INC1	56.44	0.994	1.8	0.574	2.469	4.4	6.42	0.209	3.2	0.120	0.518	8.1
L3_INC2	50.76	1.763	3.5	1.018	4.379	8.6	7.24	0.215	3.0	0.124	0.535	7.4
L3_INC3	55.92	1.508	2.7	0.871	3.747	6.7	6.89	0.209	3.0	0.121	0.519	7.5
L3_INC4	54.26	0.549	1.0	0.317	1.364	2.5	6.91	0.096	1.4	0.056	0.239	3.5
L3_INC5	49.25	0.785	1.6	0.453	1.951	4.0	6.85	0.113	1.7	0.065	0.281	4.1
L3_INC6	56.76	0.640	1.1	0.369	1.589	2.8	6.78	0.068	1.0	0.039	0.168	2.5
L3_INC7	48.36	0.377	0.8	0.218	0.937	1.9	6.82	0.013	0.2	0.007	0.031	0.5
L3_INC8	52.79	0.940	1.8	0.543	2.335	4.4	7.29	0.124	1.7	0.072	0.308	4.2
L3_INC9	53.39	0.313	0.6	0.181	0.778	1.5	7.25	0.087	1.2	0.051	0.217	3.0
L3_INC10	46.75	1.198	2.6	0.691	2.975	6.4	6.55	0.102	1.6	0.059	0.254	3.9
L3_INC11	47.48	0.238	0.5	0.137	0.590	1.2	6.69	0.029	0.4	0.016	0.071	1.1
L3_INC12	48.79	0.425	0.9	0.245	1.055	2.2	6.79	0.040	0.6	0.023	0.100	1.5
L3_INC13	47.02	0.146	0.3	0.084	0.362	0.8	6.56	0.026	0.4	0.015	0.066	1.0
L3_INC14	48.27	0.945	2.0	0.546	2.348	4.9	6.72	0.145	2.2	0.084	0.361	5.4
L3_INC15	45.85	0.317	0.7	0.183	0.788	1.7	6.38	0.053	0.8	0.031	0.132	2.1

Appendix H – Publications

Refereed journals: published/accepted for publication

- Velis C.A., Longhurst, P.J., Drew, G.H., Smith, R., Pollard, S.J.T., (In press). Production and quality assurance of solid recovered fuels using mechanical-biological treatment (MBT) of waste: a comprehensive assessment. *Critical Reviews in Environmental Science and Technology*.
- Velis C.A., Longhurst, P.J., Drew, G.H., Smith, R., Pollard, S.J.T., (2009). Biodrying for mechanical-biological treatment of wastes: A review of process science and engineering. *Bioresource Technology*, 100, 2747-2761.
- Séverin M., Velis, C.A., Longhurst, P.J., Pollard, S.J.T., (2010). The biogenic content (χ_B) of process streams from mechanical-biological treatment plants producing solid recovered fuel. Do the manual sorting and selective dissolution methods for χ_B correlate? *Waste management*. doi:10.1016/j.wasman.2010.01.012

Refereed international conferences

- Velis C.A., Longhurst, P.J., Pollard, S.J.T., (2009). Biodrying for mechanical-biological Treatment (MBT): achievements and challenges. 3rd International conference HSWMA: solid waste management - towards a zero waste society, 30-31 October 2009, Evgenidou Foundation, Athens, Greece, Hellenic Solid Waste Management Association.
- Séverin M., Velis, C.A., Longhurst, P.J., Pollard, S.J.T., (2009). Do the manual sorting and selective dissolution methods for biogenic content correlate for solid recovered fuels (SRF)? 14th European Biosolids and Organic Resources Conference and Exhibition, Leeds, UK.
- Velis, C.A., Longhurst, P.J., Pollard, S.J.T., (Submitted, 2010). Biodried MSW characterisation - how much upgrade is needed to produce a solid recovered fuel (SRF) of suitable quality? ORBIT 10th Organic Resources in the Carbon Economy, Heraclion, Greece.

Reports

- Velis C., Smith, R., Pollard, S.T.J., Longhurst, P., Drew, G.H., (2008). The mechanical biological treatment (MBT) of municipal solid wastes (MSW): Part 2. Review of mechanical processing and SRF quality. Cranfield University report to GrantScape No. CU/MBT/REP/2. Centre for Resource Management and Efficiency, Cranfield University, Cranfield, UK.
- Velis C., Smith, R., Pollard, S.T.J., Longhurst, P., Drew, G.H., (2008). The mechanical biological treatment (MBT) of municipal solid wastes (MSW): Part 3. Review of biodrying. Cranfield University report to GrantScape No. CU/MBT/REP/3.

Centre for Resource Management and Efficiency, Cranfield University,
Cranfield, UK.

Poster presentations

Velis C., Smith, R., Garg, A., Pollard, S.J.T., Hill, D., (2005). Mechanical biological treatment of wastes: overcoming barriers and reducing risk in the UK. International Symposium MBT 2005, 23-25 November 2005, Hanover, Cuvillier Verlag, Göttingen, Germany.

In preparation

A series of refereed journal publications, reporting results from this PhD research

Appendix I – Biodrying: critical review



Review

Biodrying for mechanical–biological treatment of wastes: A review of process science and engineering

C.A. Velis, P.J. Longhurst, G.H. Drew, R. Smith, S.J.T. Pollard *

Cranfield University, Centre for Resource Management and Efficiency, School of Applied Sciences, Cranfield, Bedfordshire MK43 0AL, UK

ARTICLE INFO

Article history:

Received 8 October 2008
Received in revised form 9 December 2008
Accepted 15 December 2008
Available online 11 February 2009

Keywords:

Biodrying
Mechanical–biological treatment
Solid recovered fuel
Biomass
Composting

ABSTRACT

Biodrying is a variation of aerobic decomposition, used within mechanical–biological treatment (MBT) plants to dry and partially stabilise residual municipal waste. Biodrying MBT plants can produce a high quality solid recovered fuel (SRF), high in biomass content. Here, process objectives, operating principles, reactor designs, parameters for process monitoring and control, and their effect on biodried output quality are critically examined. Within the biodrying reactors, waste is dried by air convection, the necessary heat provided by exothermic decomposition of the readily decomposable waste fraction. Biodrying is distinct from composting in attempting to dry and preserve most of biomass content of the waste matrix, rather than fully stabilise it. Commercial process cycles are completed within 7–15 days, with mostly $\text{H}_2\text{O}_{(\text{g})}$ and CO_2 losses of ca. 25–30% w/w, leading to moisture contents of <20% w/w. High airflow rate and dehumidifying of re-circulated process air provides for effective drying. We anticipate this review will be of value to MBT process operators, regulators and end-users of SRF.

© 2009 Elsevier Ltd. All rights reserved.

1. Introduction

Biodrying (biological drying) is an option for the bioconversion reactor in mechanical–biological treatment (MBT) plants, a significant alternative for treating residual municipal solid waste (MSW). Waste treatment plants defined as MBT integrate mechanical processing, such as size reduction and air classification, with bioconversion reactors, such as composting or anaerobic digestion. Over the last 15 years MBT technologies have established their presence in Europe (Binner, 2003; Haritopoulou and Lasaridi, 2007; Ibbetson, 2006; Juniper, 2005; Neubauer, 2007; Pires et al., 2007; Stegmann, 2005; Steiner, 2005, 2006), with 6,350,000 Mg a^{-1} of residual waste currently treated in Germany alone (Kuehle-Weidemeier, 2007). MBT is emerging as an attractive option for developing countries as well (GTZ, 2003; Lornage et al., 2007; Pereira, 2005; Raninger et al., 2005; Tränkler et al., 2005).

To our knowledge, the term “biodrying” was coined by Jewell et al. (1984) whilst reporting on the operational parameters relevant for drying dairy manure. Here, the term “biodrying” denotes: (1) the bioconversion reactor within which waste is processed; (2) the physiochemical process, which takes place within the reactor;

and (3) the MBT plants that include a biodrying reactor: “biodrying MBT,” hereafter. Typically, the biodrying reactor within MBT plants receives shredded unsorted residual MSW and produces a biodried output which undergoes extensive mechanical post-treatment. Within the biodrying bioreactor the thermal energy released during aerobic decomposition of readily degradable organic matter is combined with excess aeration to dry the waste (Fig. 1).

This is attractive for MBT plants established to produce solid recovered fuel (SRF) as their main output, because removing the excessive moisture of the input waste facilitates mechanical processing and improves its potential for thermal recovery (Rada et al., 2007b). A major benefit of SRF production in MBT with biodrying is the opportunity to incorporate the biogenic content of the input waste, a carbon dioxide (CO_2)-neutral, alternative energy source (Flamme, 2006; Mohn et al., 2008; Staber et al., 2008), into a fuel product. This produces an SRF low in CO_2 specific emission loading (Heering et al., 1999), mitigating the waste management contribution to climate change. As result, there is high interest in biodrying MBT plants: 20 commercial references are currently operational in Europe, with overall capacity of ca. 2,000,000 Mg a^{-1} (Herhof GmbH, 2008; Shanks, 2007).

However, biodrying remains a relatively new technology and published research is limited. Experience from commercial full-scale application of biodrying MBT plants spans only over the last decade. The first plants that became operational were the Eco-deco in Italy (1996) using the “BioCubi[®]” aerobic drying process; and the Herhof process in Asslar, Germany (1997), using the “Rotteboxes[®].” Despite having been subject to research (Calcaterra

Abbreviations: APC, air pollution control; CV, calorific value; EC, energy content; MBT, mechanical–biological treatment; MC, moisture content; MSW, municipal solid waste; NVC, net calorific value; OFMSW, organic fraction of municipal solid waste; SRF, solid recovered fuel; RDB, rotary bio-dryer; VS, volatile solids.

* Corresponding author. Tel.: +44 01 234 754101; fax: +44 01 234 751671.

E-mail address: s.pollard@cranfield.ac.uk (S.J.T. Pollard).

Nomenclature

Properties

EMC	equilibrium moisture content
ERH	equilibrium relative humidity
Q_{air}	inlet airflow rate
K	permeability
m	mass
MC	moisture content
O_2	molecular oxygen
rH	relative humidity
T	temperature

Subscripts

air	air flowing through waste matrix
initial	initial plant or process input values
max	maximum value
MSW	municipal solid waste
out	outlet (exhaust) air
TS	total solids
VS	volatile solids
waste	waste matrix

General

%	percent
\emptyset	diameter
Δ	difference
®	proprietary

Selected units

ar	reporting basis: as received (i.e., wet)
d or DM	reporting basis: dry matter
d	days
Mg	mega gram (or metric ton)
Mg a^{-1}	mega gram per year (or tpa: ton per annum)
Nm^3	normal cubic meters
Scfm	standard cubic feet per minute
Rpm	rotations per minute
w	weeks
w/w	weight fraction or percent
v/v	volume fraction or percent
$^{\circ}\text{C}$	degrees celsius

et al., 2000; Wiemer and Kern, 1994), is neither fully understood nor optimised (Adani et al., 2002).

This review presents and evaluates the process science and engineering available for optimal SRF production through biodrying in MBT plants. It places biodrying in context with composting and similar bioconversion applications. Experience from full-scale biodrying in commercial MBT plants is also included. A separate publication that compliments this is in press, covering the assessment of SRF quality, and mechanical processing necessary to be coupled with biodrying for SRF production in MBT plants (Velis et al., in press). In order to understand the science and engineering of biodrying processes adequately, it is necessary to make reference to commercially available technologies and the grey literature. Technologies are described according to the manufacturer or trade name. The authors have no interest in promoting or endorsing specific technologies.

2. Biodrying for MBT in context with similar bioconversion drying applications

Biodrying reactors use a combination of engineered physical and biochemical processes. Reactor design includes a container

coupled with an aeration system; containers can be either enclosed (Fig. 1), or open tunnel-halls, or rotating drums (Fig. 2). On the biochemical side, aerobic biodegradation of readily decomposable organic matter occurs. On the physical side, convective moisture removal is achieved through controlled, excessive aeration. Whilst the general reactor configuration and physiobiochemical phenomenon is similar to composting, the exact way in which it is operated is significantly different.

Composting is a widely studied and largely understood natural process, controlled for specific objectives within waste management. It refers to the aerobic biodegradation and stabilisation of mixed organic matter substrates by micro-organisms, under conditions that allow development of thermophilic temperatures (de Bertoldi et al., 1996; Epstein, 1997; Haug, 1993; Insam and de Bertoldi, 2007). During multiple cycles of biodegradation, a widely diverse population of micro-organisms catabolises substrates through complex biochemical reactions to satisfy metabolic and growth needs, gradually leading to mineralisation of organic substances (Richard, 2004). The most important parameters that affect composting are substrate composition, carbon–nitrogen ratio (C/N), oxygen content, substrate temperature, moisture content (MC), hydrogen ion concentration (pH), aeration and the matrix

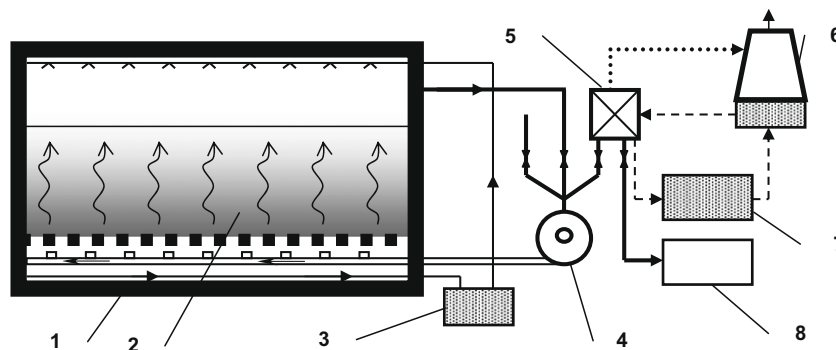


Fig. 1. Schematic of biodrying box with process air circulation and dehumidification based on a Herhof system: (1) enclosed box; (2) air forced through the waste matrix, heated by the exothermic aerobic biodegradation of readily decomposable waste fragments; (3) leachate collection and circulation system; (4) forced aeration system with partial air recirculation, mixing ambient air and conditioned process air; (5) heat exchanger; (6) cooling tower; (7) water (vapour condensate); (8) exhaust air treatment through biofilter or regenerative thermal oxidation (RTO). Appropriate conditions for microbial activity allow for the biodegradation of the waste placed within the bioreactor, providing the necessary heat to evaporate moisture from the waste fragments. Evaporated moisture is removed by the air convection, achieved by forced aeration. The exhaust air is going through various treatment stages that improve its drying capacity (ability to carry moisture) before it is partly re-circulated into the reactor, after being mixed with ambient air. Redrawn from Herhof Environmental (Undated).

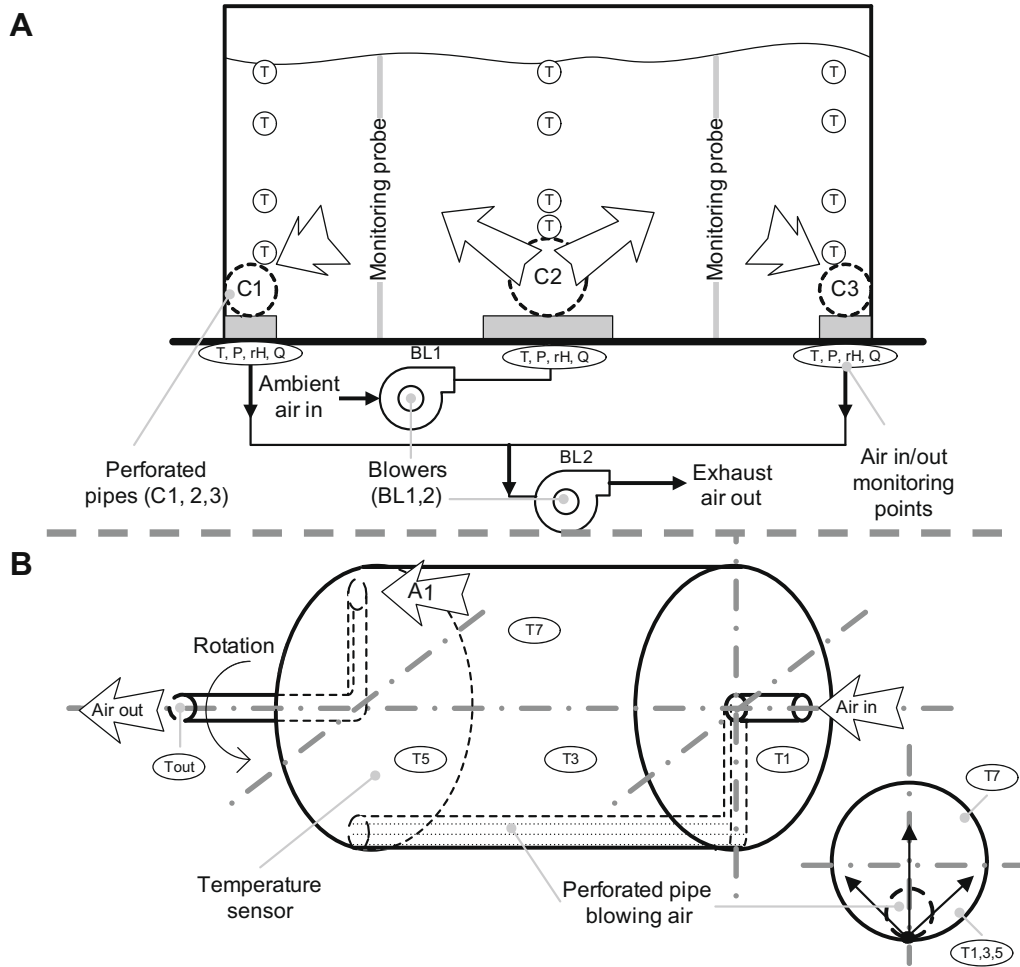


Fig. 2. Simplified schematics of bench/pilot-scale biodrying reactor designs, among else aiming to mitigate the uneven drying of matrix. Reactor A: static enclosed cell. The central perforated pipe (C2) alternates between blowing and pulling air through the matrix, whilst the peripheral pipes (C1, C3) operate conversely. Reactor B: cylindrical rotating drum with one perforated pipe. Certain monitoring points are shown: T: temperature: 1–7 internal, out: exhaust air; P: pressure; rH: relative humidity; Q: airflow rate. BL: blower. For A1 refer to Fig. 3. Redrawn from A: Frei et al. (2004b) and B: Bartha (2008).

characteristics of mechanical strength, particle size distribution (PSD), bulk density, air-filled porosity, and permeability (K). Their influence on composting systems has been discussed elsewhere (Diaz and Savage, 2007; Haug, 1993; Schulze, 1961; Richard, 2004).

Biodrying as a variation of composting has been described for applications, other than MBT, including the composting of high MC materials, such as manure (Choi, 2001; Richard and Choi, 1997; Wright, 2002), and of sludge from pulp and paper wastewater treatment intended for combustion in wood-waste furnaces (Frei et al., 2004a; Frei et al., 2004b; Navaee-Ardeh et al., 2006; Roy, 2005). Ragazzi et al. (2007) investigated at bench-scale the co-digestion of dewatered and treated sewage sludge with municipal waste.

Research relevant to biodrying has been also conducted for near-ambient grain drying for food preservation (Brazier, 1996; Nellist and Brook, 1987), and for the combined drying and storage of forest residues (Nellist et al., 1993). Near-ambient air drying (or bulk storage drying) uses the flow of air through harvested grains or forest residues in deep beds to dry and preserve them (Nellist, 1998). Matrix temperatures up to 5 °C above ambient are reached. The critical operational and state parameters are matrix-related (MC, equilibrium MC, safe storage time, and pressure resistance to airflow) and air-related (airflow rate and psychrometric properties, i.e., properties referring to the thermodynamic and physical relationship between air and water vapour, such as relative humid-

ity, temperature, etc.). Careful management of the process and suitable climatic conditions are critical for successful near-ambient air drying.

Biodrying differs from composting and near-ambient air drying in terms of the objectives of each process. Composting produces a humus-like “compost” that can be beneficially and safely applied to land, subject to regulatory approval. Composting is also used to stabilise the biodegradable organic material of MSW prior to landfill disposal, minimising leachate and landfill gas formation. Near-ambient air drying: (1) dries grains or forestry residues before storage to prevent spoilage; (2) achieves low specific energy consumption; and (3) reduces the risk of over-drying, as opposed to heated dryers, by using air temperatures close to the ambient level (Nellist, 1998; Nellist et al., 1993).

In contrast, the biodrying reactor aims to pre-treat waste at the lowest possible residence time in order to produce a high quality SRF. This is achieved by: (1) increasing the energy content (EC) (Adani et al., 2002) by maximising removal of moisture present in the waste matrix and preserving most of the gross calorific value of the organic chemical compounds through minimal biodegradation; (2) facilitating the incorporation of the partly preserved biogenic content into the SRF; and (3) rendering the output more suitable for mechanical processing by reducing its adhesiveness.

Secondary benefits are also achieved. Biodrying renders the material more suitable for short-term storage and transport both

Table 1
Objectives and features of biodrying in comparison with other similar drying bioconversion technologies.

Process feature	Drying process			
	Composting (intensive) (de Bertoldi et al., 1996; Epstein, 1997; Haug, 1993; Richard, 2004)	Sludge dewatering by composting (Frei et al., 2004a; Frei et al., 2004b; Navaee-Ardeh et al., 2006; Roy, 2005)	Grain and forest residues air drying (Brazier, 1996; Nellist and Brook, 1987; Nellist et al., 1993)	Biodrying in MBT (Adani et al., 2002; Rada et al., 2007a; Hood et al., 2008; Sugni et al., 2005; Wiemer and Kern, 1994)
Objectives	Production of a compost, largely stabilised material Apply beneficially on-land or dispose of in landfill	Reduce sludge volume Dry and partially stabilise sludge	Food preservation (dry grains before storage to prevent proliferation of spoilage agents, including biodegradation)	Produce a high quality SRF Partially stabilise output and inhibit further biodegradation rendering it suitable for short-term storage Preserve biogenic content of substrate Output suitable for subsequent mechanical processing (improve flowability) Residual unsorted MSW Mechanically separated OFMSW ^h Fully enclosed bio-cells/rotating drums or enclosed in tunnel Depending on degree of sophistication of reactor design Reduce MC from ca. 40% to 20% w/w ar or less
Matrix type	Organic waste material	Sludge (biosolids)	Grain harvest Forest residues Outdoors design	
Degree of reactor enclosure	Outdoors or indoors in fully enclosed cells	Enclosed cells		
Dependence on meteorological conditions	Depending on reactor type	No	Influx air T, rH dependent on meteorological conditions	
Moisture content management	Limited removal or addition of water to keep MC within optimum range of ca. 50–70% w/w ar ^{a,b}	Reduce MC from an indicative 80 to ca. 40% w/w ar ^d	Reduce MC to 14.5% w/w ar ^f	
Residence time	10–12 w of intensive decomposition	ca. 10 d	Months	Static, commercial designs: 5–15 d Longer for higher input MC ^g Pilot-scale rotating drum: 2–3 d ^h 0.023.1 m ³ kg _{TS} ⁻¹ h ⁻¹
Airflow rate	Batch systems peak: 4–14 O ₂ g _{VS} h ⁻¹ at T 45–65 °C (under certain assumptions equivalent to: 125–460 m ³ h ⁻¹ (metric ton of feed solids) ⁻¹) ^c Continuous systems: average demand ca. 1660 m ³ h ⁻¹ (dry metric ton of feed solids per day) ⁻¹) ^c	ca. 42.5 ± 3.4 N m ³ h ⁻¹ (25 ± 2 scfm) ^e		Increasing over time (for high-MC input): ca.11.5 Nm ³ kg _{MSW} ⁻¹ after two weeks; up to ca.14.5 Nm ³ kg _{MSW} ⁻¹ after 4 weeks ^g RDB cooling cycle: 0.120–0.150 m ³ h ⁻¹ kg ⁻¹ h

General references are presented in the column titles. Reference to specific values are denoted by Latin letters below. MBT: mechanical–biological treatment. MC: moisture content. MSW: municipal solid waste. RDB: Rotary bio-dryer. scfm: standard cubic feet per minute. SRF: solid recovered fuel

^a Regan et al. (1973).

^b Richard (2004).

^c Haug (1993).

^d Navaee-Ardeh et al. (2006).

^e Frei et al. (2004b).

^f Brazier (1996).

^g Rada et al. (2007a).

^h Hood et al. (2008).

ⁱ Adani et al. (2002).

by partially biostabilising it and by reducing its MC below the necessary threshold for biodegradation to occur. Partial sanitisation of the output is also accomplished (Adani et al., 2002; Calcaterra et al., 2000; Rada et al., 2005; Sugni et al., 2005; Wiemer and Kern, 1994); for the bulk of the biodried product sanitisation to high standards is not necessary, because most of it is not intended to be applied on land but to be thermally recovered.

Table 1 summarises process objectives and typical parameter values for biodrying and similar bioconversion technologies. Notwithstanding that technology transfer could be feasible, wide differences are evident. Hence, uncritical extrapolation of results to

different reactor designs, scales, substrates, and operating regimes may be misleading.

3. Biodrying process science fundamentals and engineering

3.1. Operating principles of biodrying: drying

Drying technology generally reduces the MC of a matrix by the application of heat, causing water to evaporate into the air phase (vapour), and produce dried outputs of desired characteristics (Dufour, 2006). Drying phenomena have been widely researched (Hall, 2007). However, the micro-scale mechanisms of drying are highly

complex and not fully understood (Konvalov, 2005). Drying technology has been developed within the scope of food, agricultural, pharmaceutical, pulp and paper, and many other industries (Mujumdar, 2004, 2007). For environmental engineering applications, dryers using external sources of heat have been used for refuse-derived fuel (RDF) drying (e.g., rotary cascade and thermopneumatic) (Manser and Keeling, 1996) and sludge dewatering (Chen et al., 2002).

In biodrying, the main drying mechanism is convective evaporation, using heat from the aerobic biodegradation of waste components and facilitated by the mechanically supported airflow. The MC of the waste matrix is reduced through two main steps: (1) water molecules evaporate (i.e., change phase from liquid to gaseous) from the surface of waste fragments into the surrounding air; and (2) the evaporated water is transported through the matrix by the airflow and removed with the exhaust gasses. Limited amount of free water may seep through the waste matrix and be collected at the bottom of the biodrying reactor as leachate.

3.2. The drying phenomenon

In biodrying, air convection and molecular diffusion are the main transport mechanisms responsible for moisture flow through the matrix (Frei et al., 2004b). Air convection, induced by engineered airflow through the matrix, is almost exclusively responsible for the water losses. Here, air carries the water evaporated from the surface of matrix particles (free moisture) with which is in contact. Removal of water content from the waste matrix (desorption) by convective evaporation is governed by the thermodynamic equilibrium between the wet waste matrix (solid state) and the air flowing through the matrix (gaseous phase). Mujumdar (1997) provided an extensive list of the psychrometric properties (thermodynamic and transport phenomena related) of the air pertaining to drying. Pakowski et al. (1991) reported the engineering properties of humid air.

Whilst no relevant research particular to biodrying is available, relative science has been summarised elsewhere for the cases of drying of foods (Basu et al., 2006), grains (Mujumdar and Beke, 2003) and wood (Krupinska et al., 2007). The vapour-carrying capacity of air is limited at each T_{air} and reached at saturation point, after which condensation occurs. At a given level of relative humidity (rH) of air (rH_{air}) the mass of water vapour the air can hold increases with the temperature. rH_{air} has been used in near-ambient drying modelling to estimate the distance from saturation point of inlet air, i.e., can be simplistically perceived as a surrogate measure of its drying potential.

For desorption to happen the rH_{air} has to be lower than the equilibrium relative humidity (ERH_{air}), i.e., the rH_{air} value at which the MC of air-vapour mixture (MC_{air}) is in equilibrium with the MC of the matrix (MC_{waste}). This is also expressed as the equilibrium MC of the waste (EMC_{waste}) and depends on temperature and pressure (Mujumdar, 1997). The inverse phenomenon may also happen, where air of sufficiently high humidity moistens the matrix particle surfaces (adsorption), case evident in inverted aeration configurations of biodrying reactors (Fig. 2A) (Frei et al., 2004b; Sugni et al., 2005).

The rH_{air} and EMC_{waste} relationship can be expressed through equilibrium moisture curves called sorption (adsorption/desorption) isotherms. They are temperature dependent, reflecting the temperature dependence of rH_{air} . In principle, experimentally identified and/or mathematically simulated desorption/adsorption isotherms for biodrying of residual waste matrices could potentially be used to model and optimise the drying process, practice established in the wider drying research and engineering. For instance, for grain drying, some of sorption isotherms exhibit an S-

curve shape and a hysteresis effect appears between adsorption and desorption (Basu et al., 2006).

The form in which the water is present within the solid fragments of the matrix has a decisive influence on the drying phenomenon. Different regions of the sorption isothermal curves correspond to drying involving moisture present in different states (e.g., free or capillary, bound, etc.), governed by different physical mechanisms, as described elsewhere (Basu et al., 2006; Brazier, 1996; Mujumdar and Beke, 2003; Tsang and Vesilind, 1990). Air convection may eventually dry the surface of the particle, reaching the hygroscopic limit, i.e., leaving no surface areas saturated with water, resulting in less water to evaporate. For further drying, additional moisture has to migrate from the particle interior (bound moisture) to its surface, process governed by diffusion mechanisms (Roy et al., 2006); e.g., during the drying of hygroscopic porous media, such as wood (Stanish et al., 1986).

3.3. Energy balance of biodrying reactors

The energy necessary for evaporation to occur (vaporisation latent heat, or enthalpy of vaporisation) and any additional if the hygroscopic limit is reached, is provided mainly by aerobic biodegradation. In contrast, conventional drying employs external sources of heat. The aerobic decomposition of organic matter by micro-organisms is an exothermic biochemical transformation that can rapidly raise matrix temperatures to the thermophilic range. In composting, maximum temperatures of 50–62 °C for small-scale systems or up to 70 °C for larger reactors have been reported (Richard, 2004). Roy et al. (2006) reported average rates of energy production due to bioconversion at 23–29 W kg_{DM}⁻¹ during biodrying of pulp and paper mill sludge. This energy usually constitutes a sufficient source for drying, despite heat losses from convection, radiation and sensible heating of both the outlet air and any discharged leachate. A small part of the significant external energy needed for aeration is converted to heat flow through the frictional losses caused by the mechanically supported flow of air through the waste. In near-ambient grain drying, this results in an anticipated typical rise in the grain temperature between 0.5 °C and 2 °C (Nellist, 1998); however, the rise may vary according to the exact ambient atmospheric and matrix conditions.

Results of heat transfer studies have established the ability in commercial, large-scale applications to control heat losses and subsequently matrix temperature through increased aeration. For the industrial-scale and fully enclosed Herhof-Rottebox[®] cells (Fig. 1) conduction by aeration (and hence water evaporation) was found to contribute more than 75% to the heat transfer (Weppen, 2001). This indicated limited heat losses by conductance through vessel walls and open surfaces. Instead, the most significant heat fluxes were attributed to sensible heat removed by ventilation, energy storage by change in sensible heat of matrix and vessel, and micro-organism needs. This result is in agreement with similar investigations in composting operations (Bach et al., 1987; Themelis, 2005).

3.4. Process design, monitoring and control

Optimal biodrying can be achieved through effective reactor design and conditioning of the input material, combined with suitable process monitoring and control. Control can be exercised by adjusting the level of operational variables (suitable to directly manipulate), informed by process state variables (suitable to monitor and evaluate). Typical design and operational choices involve:

1. matrix conditioning through mechanical pre-processing, e.g., comminution and/or mixing, affecting the physical properties of the matrix, such as the resistance to airflow;

2. type of containment of waste matrix, e.g., in enclosed boxes (or “bio-cells”) (Fig. 1) or piling in tunnel windrow systems, affecting drying mechanisms including insulating effect and degree of compaction;
3. use of mixing/agitation/rotation of the waste matrix in dynamic reactors to homogenise it, i.e., achieve uniform conditions: e.g., by rotating drum reactors (Fig. 2B) (Bartha and Brummack, 2007; Bartha, 2008; Skourides et al., 2006); however, most of the existing commercial designs are static;
4. aeration system design: inverted aeration systems have been tested (Fig. 2A), intending to reduce gradients experienced in prevalent unidirectional designs (Frei et al., 2004b; Sugni et al., 2005);
5. management of the aeration rate of the waste matrix, by control of the inlet airflow rate (Q_{air}), to remove water vapour and off-gasses and control state process parameters, such as substrate temperature and oxygen availability;
6. external systems for controlling the psychrometric properties of the inlet air (e.g., temperature, dew point, relative humidity), by cooling and dehumidifying of the process air to enhance its capacity to hold water vapour, combined with partial process air recirculation; and,
7. residence time within the reactor, affecting the degree of completion of biochemical and physical processes.

Application of process control engineering in biodrying is challenging. The main difficulty is the twofold role of the waste matrix, being both (1) the mass to be dried, and (2) the substrate supporting the microbial activity, which in turn provides for the source of heat necessary for the drying. Another difficulty is the inherent high heterogeneity of the residual waste, compared with, for instance, food grains. These main differences impede direct technology transfer from other control applications.

However, control for biodrying could potentially benefit from the recent advances in general drying technology and composting applications. Control engineering for drying technology is applied mainly in the food industry, but also increasingly in painting, pharmaceuticals and paper/wood applications, and has advanced with the application of open and closed loop optimal controllers. However, generally first principle models of drying are still lacking outside the food industry (Dufour, 2006). Software packages for drying have been developed (Devahastin, 2006; Gong and Mujumdar, 2008; Kemp, 2007; Menshutina and Kudra, 2001; Wang et al., 2004).

Both simple and complex process control strategies are employed in commercial bioreactor systems treating biodegradable waste. Ward et al. (2008) reviewed control systems for anaerobic digestion reactors: their general suggestions, including the importance of *in situ* on-line monitoring and control, largely apply to all waste treatment technologies. For composting aeration systems, the emphasis is upon providing sufficient oxygen (O_2) for aerobic biodegradation (de Guardia et al., 2008), whilst simultaneously meeting the requirements of the process air clean up. A general list of control approaches for composting aeration can be found in Haug (1993). Commercially available computerised systems developed for composting complex aeration control have been reviewed by Goldstein (2006).

Theoretically, many process state variables can be used for biodrying monitoring to inform the control of operational variables, such as airflow rate. However, this demands substantial understanding and modelling of the process science which has not yet been achieved. Leonard et al. (2005) examined the effect of inlet air temperature, superficial velocity and humidity on the drying kinetics of convective drying of wastewater sludge in a microdryer using a 3^3 factorial design experiment. The inlet air temperature had the greatest influence. Roy et al. (2006) suggested that for bio-

drying process control purposes the outlet air temperature should be used – not the average matrix temperature, as is often the case with biostabilisation.

Certain commercial applications use advanced control systems, including control loops. Bartha (2008) developed a fuzzy-logic process control system for a biodrying rotating drum reactor. A Herhof European patent for continuous bio-cell biodrying opts for control of the air supply so that the CO_2 content in the exhaust air is kept within a range of 0.05–0.4% v/v (Hansjoerg et al., 2004). Segmental air supply is blown through a floor plate and automatically adjusted by on-line measurements of heat quantity, exhaust air and matrix temperatures, air permeability of matrix, and CO_2 exhaust concentration. Process air is cooled and dehumidified by a heat exchanger, and re-circulated until a certain CO_2 limit is met.

3.5. Matrix physical–mechanical properties

Biodrying is heavily dependent on the physical process of convective evaporation, so it can be assumed that physical–mechanical matrix properties are critical for process optimisation. Scholwin et al. (2003) stressed the importance of physical–mechanical properties of waste matrices for effective process modelling and control in the case of organic substrate composting. The relevant parameters that could impact on effective bioconversion were grouped into three classes, related to material, packed bed and flow pattern. Understanding of relevant issues has been advanced for composting substrates (Barrington et al., 2002; Das and Keener, 1997; Richard et al. 2004). Properties such as MC, air-filled porosity, permeability, mechanical strength, and compaction of matrix, have the potential to affect the resistance to flow of air and, in turn, the level of airflow rate necessary for effective biodrying. Some of these properties could be beneficially conditioned by pre-processing the biodrying input to the bioreactor. Currently, the pre-processing strategy in most biodrying MBT plants is limited to coarse shredding, e.g., at 300–150 mm maximum particle size.

3.6. Aeration system type

Mechanically supported aeration of waste is critical for biodrying. It provides a mass and energy flow media, enabling: (1) water content removal; (2) heat transfer redistribution, removing excessive heat and, adjusting the matrix temperature; and (3) O_2 delivery to meet the stoichiometric demand for aerobic decomposition.

Extensive research and experience on aeration is available for composting operations (Keener et al., 2005; Keener et al., 1997; Sessay et al., 1998), but limited for biodrying. In composting, positive and negative pressure, hybrid, inverted and re-circulating airflow designs have been implemented. Chiumenti et al. (2005) has shown that with static piles, as used in tunnel designs, negative pressure aeration achieves more homogeneous air distribution, reducing the problem of preferential air paths that may create anaerobic pockets. In enclosed bio-cells, the usual configuration is positive pressure, forcing air through the matrix flooring and collecting off-gasses through openings located at the top.

Air management in biodrying varies according to reactor design and process complexity. The bottom of a commercial biodrying bio-cell (Herhof Rottebox[®]) is divided into 12 parts enabling airflow to vary in each segment, facilitating control of matrix temperature (Nicosia et al., 2007). Air partial recirculation systems are often used in biodrying to reduce the volume of exhaust air requiring treatment; especially if air pollution control (APC) is accomplished through high cost equipment, such as regenerative thermal oxidation (RTO), necessitated by stringent legislative requirements in Austria and Germany (Breuer, 2007).

3.7. Uneven drying and solutions

One-way airflow through the waste matrix in static bed systems (e.g., enclosed halls) has been shown to cause gradients in the vertical profile of process state variables in both composting and biodrying. The uneven drying is also well known in grain drying, where a drying zone is established around the air supply.

VanderGheynst et al. (1997) investigated temperature and moisture profiles of an in-vessel pilot-scale reactor composting synthetic food waste with initial MC 45% ar and 55% ar. They observed maximum temperature differences to occur together with significant MC differences; and differences in maximum temperatures in the vertical (ΔT_{\max}) to be less than for higher aeration rates ($\Delta T_{\max} = 32\text{ }^{\circ}\text{C}$ at $0.06\text{ l min}^{-1}\text{ kg}_{\text{initial DS}}^{-1}$ and $\Delta T_{\max} = 29\text{ }^{\circ}\text{C}$ at $0.6\text{ l min}^{-1}\text{ kg}_{\text{initial DS}}^{-1}$).

In bench-scale biodrying experiments, matrix temperature differences as high as $30\text{ }^{\circ}\text{C}$ from the top to the bottom of a 800 mm high container have been observed during the initial high-microbial activity phase (Adani et al., 2002; Sugni et al., 2005). The T_{matrix} values converged as the biodegradation ceased (Fig. 3A), but the moisture gradient persisted. In turn, these gradients lead to heterogeneous biodried output. Sugni et al. (2005) speculated that air flowing through the lower layers of the matrix had already reached saturation point and hence could not remove additional moisture. This could be in agreement with the higher temperature measured at this layer, as the limited heat removal would result in a higher matrix temperature. However, it is worth considering the possibility of moisture accumulation in the lower layer due to gravitational flow of free water. Whilst some authors do not consider (Adani et al., 2002; Sugni et al., 2005), or exclude (Navaee-Ardeh et al., 2006) this possibility, in both commercial biodrying systems based on halls (e.g., Eco-deco) or bio-cells (e.g., Herhof), a small amount of leachate is collected (Herhof Environmental, Undated).

In order to overcome the uneven drying of grain matrix recirculation or continuous flow mixing systems are used. For biodrying, alternative aeration systems and non-static designs have been proposed to overcome gradient formation aiming at a homogenised output. Two types of improved designs are (1) rotating drum reactors (Bartha and Brummack, 2007; Bartha, 2008; Skourides et al., 2006) and (2) inverted airflow designs (Fig. 2). Sugni et al. (2005) experimented with a reactor that simulated daily inverted airflow by exchanging positions of the upper and lower reactor layers. They observed a mitigation of the matrix temperature gradient (Fig. 3B) and a more homogeneous content in terms of moisture and energy, compared with the unidirectional flow. However, this arrangement did not achieve early convergence with the ambient temperatures as in the unidirectional experiments, indicating the necessity for a prolonged residence time; and the impact of solid and moisture substrate flows introduced by the exchanging of the reactor layers remain uncertain.

Frei et al. (2004b) tested a sophisticated three perforated pipe, inverted airflow system for biodrying of a sludge/wood mixture (Fig. 2A). This system employed a central conduit either pumping or pulling air, whilst the other two pipes were on invert airflow, and operated at a set-point airflow rate of $ca. 42.5 \pm 3.4\text{ Nm}^3\text{ h}^{-1}$ ($ca. 25 \pm 2\text{ scfm}$ (standard cubic feet per minute)). The configuration was criticised for removing water from the wet portion and depositing it in the dry portion of the matrix; this then favoured biodegradation rather than biodrying (Navaee-Ardeh et al., 2006). Inverting the airflow led to a drop in relative humidity of the outlet air for the next 10–20 h, indicating that the matrix was re-wetted by the humid inlet air. This was accompanied by increased matrix temperatures (Fig. 3B), possibly reflecting a rise in biodegradation activity due to partial restoration of MC. However, as this phenomenon was more acute during the earlier per-

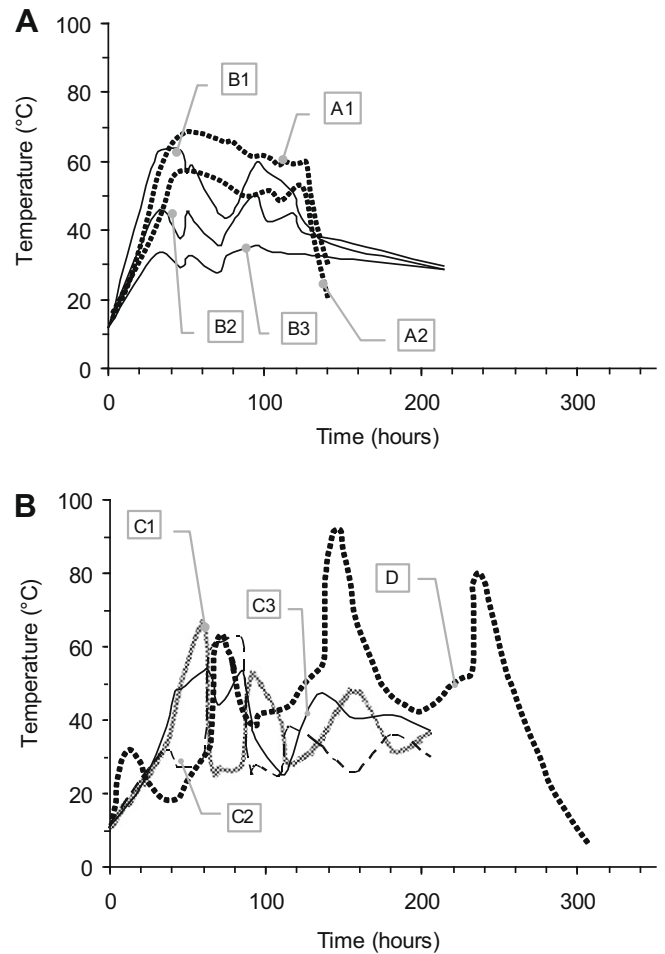


Fig. 3. Various matrix temperatures and process completion times during biodrying bench/pilot-scale reactor experiments, reflecting different reactor designs, control mechanisms, operation regimes and matrices. Part A: (i) curves B1–3: bottom, middle and upper layer T , respectively, of enclosed cell reactor (Adani et al., 2002; Sugni et al., 2005). Airflow direction from upper to bottom layer. T differences resulting in uneven drying; (ii) curves A1–2: rotary drum reactor (Fig. 2, reactor B) (Bartha, 2008). Range of temperatures inside reactor walls at T1/3/5/7 points. A1 curve shows T_7 , almost identical with T_{out} (Fig. 2). Part B: airflow inversion designs, abrupt T increase denotes inversion of flow: (i) reactor as in part 1(i), curves C1–3: bottom, middle and upper layer T respectively (Sugni et al., 2005); (ii) curve D, (Fig. 2, reactor A), matrix mixture of sludge/wood, average matrix T (Frei et al., 2004b). Redrawn from the above indicated sources.

iod when the substrate was relatively wet, it is less important for residual waste treatment, because of the much lower MC of the residual waste substrate (initial $ca. 40\text{ w/w ar}$) compared with the pulp sludge (final $ca. 40\text{ w/w ar}$). Exhaust air became saturated once matrix temperature exceeded $ca. 40\text{ }^{\circ}\text{C}$.

The biodried output resulting from the same experiment (Frei et al., 2004b) was generally homogeneously dried. However, the lower part of the matrix was slightly drier, a result converse to the effect observed by Sugni et al. (2005), who used a different process of inverted flow. Frei et al. (2004b) attributed the differentiated drying of the lower layer to preferential airflow within the matrix via the shortest routes between the inlet and outlet air ports. Drying of the matrix led to a significant increase in matrix permeability resulting in lower pressure across the matrix, reducing the preferential flow in the lower part of the reactor (Hoffmann, 2005). A continuous vertical reactor configuration with segmented air flows reducing downwards (from the upper inlet to the lower outlet) was proposed as a potential solution for less preferential drying (Navaee-Ardeh et al., 2006).

In a pilot-scale rotating drum (Fig. 2B) (Bartha, 2008), temperature differences among the T_{out} and various points within the reactor were evident, but smaller compared with other static single-direction flow designs (Fig. 3).

3.8. Aeration rate and air properties

Aeration rate is the main operational variable used for process control in biodrying, both in laboratory (Adani et al., 2002; Navae-Ardeh et al., 2006; Sugni et al., 2005) and commercial applications. The inlet airflow rate can be manipulated to control matrix temperature, in turn affecting the air dew point and biodegradation kinetics. A high airflow rate is necessary for the production of a sufficiently high in calorific value (CV) SRF, through preserving most of the biogenic content. In a comprehensive study Adani et al. (2002) used static, adiabatic reactors fed on the fine fraction of shredded MSW ($\phi < 50$ mm). Trials were conducted on set-points of middle layer matrix temperature, controlled manually by adjusting the airflow rate. It was established that high airflow rate is necessary for effective and fast drying, result in agreement with Roy (2005). However, further studies with the same sample revealed a low reproducibility of EC and CV, these properties being highly dependant on the laboratory employed to measure them (Sugni et al., 2005).

The oxygen stoichiometric demand for aerobic decomposition is satisfied by O_2 provided by the high aeration rate necessary for effective drying (Epstein, 1997; Rada et al., 2007a; Themelis, 2005). According to Epstein (1997) the aeration rate necessary for moisture removal in composting is 6–10 times higher than that necessary for biological activity. Rada et al. (2007a) measured the O_2 concentration in the process outlet air at above 15% (generally >20%). Use of air recirculation systems results in low O_2 concentration in the inlet air: the rotary drum reactor tested by Bartha and Brummack (2007) was operated with O_2 concentration up to 3% v/v.

In biodrying, optimisation of the drying potential of the input air can be achieved by adjusting its psychrometric properties. This is attained through (1) dehumidification of the exhaust air by cooling in a heat exchanger and cooling tower and (2) subsequent partial recirculation of it after mixing with ambient air, achieving an input air mixture of the desirable temperature and absolute humidity (Herhof Environmental, Undated) (Fig. 1).

3.9. Moisture content and losses

MC of the waste matrix is the single most important variable for evaluating the performance of biodrying processes. In waste management the MC is typically measured by gravimetric water content methods and expressed as a percentage of water for the wet weight of the material (wet basis: ar) (Tchobanoglous et al., 1993). A more accurate biophysical parameter relevant to the microbial activity is the water matric potential, denoting the energy with which water is held in a sample against the force of gravity (Miller, 1989).

In biodrying, the MC can be reduced from ca. 35–55% w/w ar (Thomé-Kozmiesky, 2002) to 20–10% w/w ar. During aerobic biodegradation around 0.5–0.6 g of metabolic water is produced per g of VS decomposed (Miller, 1989, 1991). However, water losses during biodrying are much greater than the gains of metabolic water, resulting in a dried matrix (Nakasaki et al., 1987b; Richard, 2004). Water losses can be estimated using values of airflow rate and inlet-outlet air conditions, i.e., absolute humidity (Richard, 2004). Mass balance of MC should include both metabolic water gains and evaporation–convection losses. Rada et al. (2007b) consider overall weight losses of 25% w/w as typical. The authors, in test-scale biodrying experiments with artificial MSW of high moisture

input (MC: 50% w/w ar) and 50% w/w organic material, reported similar time dependent curves for both the water and VS losses, with most losses attributable to moisture removal (ratio of weight losses between VS and condensed moisture: 1:7). The drying rate in sludge biodrying was reported to correlate mainly with airflow rate and outlet air temperature, which in turn was found to depend on the degree of biological activity close to the air outlets (Navae-Ardeh et al., 2006; Roy, 2005).

MC critically influences the dynamics of biodegradation during composting. Optimal moisture conditions for composting range significantly, change during the process (either increase or decrease) and vary with substrate (Richard and Choi, 1997; Richard et al., 2002). Regan et al. (1973) reported an optimal MC range for cellulose degradation at 50–70% w/w. Relevant overviews for waste substrates have been provided by Epstein (1997), Richard (2004), and Liang et al. (2003). Liang et al. (2003) used factorial design experiments to investigate the influence of temperature and MC on microbial activity, measured as O_2 uptake rate ($mg\ g^{-1}\ h^{-1}$) during composting of biosolids, showing that MC is more influential than temperature. In practice, biodegradation may stop during biodrying, or its rate may be significantly reduced, due to complete decomposition of readily biodegradable VS (degradation effect), or, more possibly, due to water stress where low moisture conditions inhibit microbial activity and movement (drying effect) (Griffin, 1981; Miller, 1989).

For biodrying processes, the minimum MC below which the biodegradation process is inhibited has not been identified. The rate of heat production by microbial activity can be anticipated to decline as the MC of the matrix approaches the water stress limit, affecting the drying mechanism. From composting studies it is evident that below 20% w/w very little or no microbial activity occurs (Haug, 1993).

3.10. Air and matrix temperatures for optimal biodrying

Conflicting evidence is available for the temperature range that optimises drying. Whilst some modelling studies for aerobic biodegradation indicate highest moisture removal at matrix temperatures at or slightly above the peak of biodegradation rate, experimental evidence supports maximum drying for much lower temperatures, which delay biodegradation. We speculate this contradiction can partly be attributed to confusion concerning the temperature referred to or measured, which could include the varying or set-point, biodegradation reaction, air outlet, matrix average or in various points within the matrix. Further, results from composting models rarely allow for high or constant airflow rates, typical in biodrying. Comparative interpretation of results is not helped by the wide variety of units used for reporting aeration rates.

Most evidence indicates that comparatively effective heat removal can be achieved by higher aeration rates resulting in lower matrix temperatures (Adani et al., 2002; Skourides et al., 2006; VanderGheynst et al., 1997), with an optimal T_{waste} as low as ca. 45 °C. In batch-scale biodrying of pulp and paler sludge, Roy et al. (2006) reported higher drying rates (volume of removed moisture per time) for higher airflow rates; the curves of the T_{out} and Q_{air} followed the same trends. This is in agreement with Adani et al. (2002) who achieved best drying results for the highest specific airflow rates they used ($0.023\ m^3\ kg_{RS}^{-1}\ h^{-1}$) allowing for a mid-layer matrix set-point temperature of 45 °C, whilst they even higher airflow rates for more effective drying.

Skourides et al. (2006) investigated the agitated biodrying of the organic fraction of municipal solid waste in a semi-industrial rotary drum. Similarly, results showed maximum drying rate achieved for the highest aeration rates used ($120\ m^3\ h^{-1}$), leading to lower final MC levels (20% w/w from an initial 40% w/w) with

a shorter retention time (< 7 d). This agrees with results reported by Macgregor et al. (1981) for field-scale, open static pile composting of sewage sludge and wood chip mixture, aerated by a blower and two perforated ducts system at the pile base. Lower set-point substrate temperatures (45 °C, as compared with 55 °C and 65 °C) achieved by longer blower operation, resulted in more effective drying (from 75% w/w to ca. 20% w/w, as compared to ca. 40% w/w, respectively).

However, a model of semi-batch stationary composting based upon heat and mass balance, and validated with laboratory and commercial scale experiments on mixtures of dewatered sewage sludge, seed and rice husks, reached conflicting conclusions (Nakasaka et al., 1987a). The optimal MC removal (from 60.3% w/w to 44.8% w/w) was achieved at a set-point substrate temperature of 60 °C with an average specific airflow rate of $0.0143 \text{ m}^3 \text{ h}^{-1} \text{ kg}_{\text{initial}}^{-1}$ after 150 h of operation, whilst a minimum set temperature of 50 °C, demanding the highest average specific airflow rate of $0.0164 \text{ m}^3 \text{ h}^{-1} \text{ kg}_{\text{initial}}^{-1}$, reduced MC only to 48.6% w/w. The model predicted that the optimum temperature for biodegradation coincided with the optimum temperature for drying, a result verified for a series of biodegradation kinetics models examined by Richard and Choi (1997). However, this model enabled varying airflow rates, a condition which does not correspond to usual biodrying practice. Jewell et al. (1984) reported maximum moisture removal rates at 46 °C, but maximum degradation at 60 °C, whilst studying biodrying of dairy manure.

Most commercial biodrying processes operate in the temperature range of 40–70 °C for outlet air T_{out} , for most of the residence time (Herhof Environmental, Undated; Juniper, 2005). A typical temperature profile for the Nehlsen process is available (Juniper, 2005). Herhof Rottebox® applies a staged T_{out} control, consisting of four phases over one week: (1) start up and biomass acclimatization: 40 °C; (2) degradation: 40–50 °C; (3) sanitisation and drying: 50–60 °C; (4) cooling to room temperature (60 °C to ambient T) (Nicosia et al., 2007).

3.11. Microbial activity

Microbial processes during biodrying should be suitably harnessed for the generation of the heat necessary for effective drying, along with limited biodegradation of waste substrates. Substrate temperature T_{waste} is the most critical factor affecting the microbial growth (Miller, 1996), because, *inter alia*, provides ideal conditions for proliferation of certain types of micro-organisms, e.g., mesophilic or thermophilic. In turn, this affects the type of organic matter that can be degraded. In composting, at $T_{\text{waste}} > 60$ °C cellulose and lignin are largely preserved, as the thermophilic fungi die-off, but waxes, proteins and hemicelluloses are readily metabolised by spore-forming bacteria and actinomycetes (Lester and Birckett, 1999).

The wider influence of substrate temperature on composting microbial population dynamics has been discussed elsewhere, including Miller (1996), Epstein (1997), and Liang et al. (2003). Overviews of microbial community dynamics, including group succession and utilisable substrate for different process stages and temperature ranges, can be found in Marshall et al. (2004) and Insam and de Bertoldi (2007). However, biodrying of MSW is operated within a MC range typically lower than the optimal composting and the T_{waste} profile is managed differently: therefore, biodegradation behaviour may be atypical compared with composting research results (Adani et al., 2002).

During biodrying of a high MC matrix of pulp and paper sludge, Roy et al. (2006) identified three separate drying stages, which correlated with microbial population growth periods: (1) acclimatisation of microbes resulting in an exponentially increasing drying rate; (2) exponential decrease of the drying rate due to insufficient

availability for nutrients for microbe consumption, and (3) constant drying rate, corresponding to the fluctuations of the Q_{air} . If a similar dynamic applies to the much drier substrates of residual MSW it would indicate that after some point biodrying is less dependent on the microbial activity, increasingly impeded by water stress; becoming, instead, just a physical process (air convection). It is not clear how this would affect the energy balance of the process.

3.12. Degree of biostabilisation at process completion

Fast and effective biodrying, optimised for SRF production, can be achieved at the expense of a low degree of biostabilisation for the organic substrate. Because the thermal energy for drying results from the decomposition of organic matter, a degree of biostabilisation is anticipated to have occurred at the end of the process. Regarding SRF product quality, the desirable degree of biostabilisation will generally be low, as this would preserve carbonaceous matter, reserving CV and biogenic content. Conversely, where the SRF is not used immediately, biostabilisation to a limited degree is desirable, because this would reduce any potential storage and environmental problems caused by further biodegradation.

There is evidence that the degree of substrate biostabilisation is inversely correlated to a fast-rate, producing high EC output biodrying (Adani et al., 2002). Adani et al. (2002) showed in comparative laboratory tests that the highest airflow rate enabled the fastest SRF production (ca. 150 h), along with the highest EC. Using lower airflow rates, the process took more than 250 h to complete and the end occurred because of sufficient biodegradation of readily decomposable organic matter. This resulted in much higher losses of VS, leading to much lower final EC, rendering it unsuitable for SRF production.

A further experiment under different process parameters showed that microbial activity ceased after about 200 h, as verified by the final temperatures, which converged with ambient values (Sugni et al., 2005). Thus, under controlled laboratory conditions, fully enclosed biodrying can be effectively completed within 8–9 d. However, Rada et al. (2007a) in test-scale biodrying of high MC input (MC_{waste} ca. 50% ar) observed longer times for the process completion of up to 4 w, using increased aeration over the time (ca. $11.5 \text{ Nm}^3 \text{ kg}_{\text{MSW}}^{-1}$ after two weeks of treatment and ca. $14.5 \text{ Nm}^3 \text{ kg}_{\text{MSW}}^{-1}$ after four weeks).

3.13. Biodrying configured for biostabilisation

Some advocates of biodrying consider it feasible to use biodrying reactors for effective intensive composting, based on the similarities between biodrying and in-vessel composting. This capability would theoretically enable the process to be adapted for stabilising organic material intended for landfill, thereby achieving regulatory compliance. Such an operational mode could be adopted until a robust market for SRF was secured, as market availability is challenging under current conditions (Juniper, 2005; Maunder, 2005). However, further evidence is required before such process resilience can be guaranteed.

Regarding full-scale reactors, the Eco-deco biodrying plants in Corteolona and Bergamo, Italy, have previously operated with the objective to minimise biodegradability, producing a fully biostabilised output (Juniper, 2005). Scotti and Minetti (2007) presented Eco-deco data from the Montanaso plant showing the ability of the process to operate in “high speed process management” mode, intending to achieve a higher level of weight loss in fewer days (typical weight loss of 28% w/w ar of input waste reached in ca. 5 d instead of ca. 14 d; final losses of ca. 38% were achieved in 14 d). The authors argue, but have not quantified, that such an operational mode leads to higher final stability for the biodried output.

However, it is evident that biostabilisation demands a very different operational mode than biodrying. Rada et al. (2007b) based on respirometric index measurements argued that a biodrying operation mode is capable of achieving only partial final output stability, compared with biostabilisation through composting. Input waste of 50% in organic content reached $500 \text{ mg O}_2 \text{ kg}_{\text{TS}}^{-1} \text{ h}^{-1}$ after ca. 200 h residence time (typical limit in Italy (Scotti and Minetti, 2007): at $< 1000 \text{ mg O}_2 \text{ kg}_{\text{VS}}^{-1} \text{ h}^{-1}$).

3.14. Modelling of biodrying processes

Limited modelling attempts for MBT-related biodrying processes exist in the peer-reviewed literature. However, composting processes have been extensively modelled (Mason, 2006; Mason and Milke, 2005a; Mason and Milke, 2005b). Particularly relevant are attempts to model moisture-dependent aerobic biodegradation (Higgins and Walker, 2001; Pommier et al., 2008); however, evaporation phenomena were excluded. Brazier (1996) reviewed modelling efforts for near-ambient drying and developed a validated simulation model from first principles. The wider modelling and simulation research on grain drying has been reviewed by Parde et al. (2003). Nakasaki et al. (1987a) modelled a generic composting process to explore the relationship between aeration and drying, reaching results that contradict recent biodrying experiments.

Rada et al. (2007a) provided initial biodrying modelling results focusing on simulation of lower heating value (LHV) (or net calorific value, (NCV)) dynamics, volatile solids (VS) consumption, waste MC dynamics, and nitrogen compounds release. The overall loss in EC of the input waste matrix was 3% w/w and most of the change in the NVC was accomplished within the two first weeks of the process. The energy produced from the bio-oxidation of the readily decomposable VS was dominant in the energy balance, compared with the enthalpy of the input at ambient T .

Nicosia et al. (2007) combined both experimental data and theoretical calculations to provide simplistic mass and energy balances for a fully operational biodrying bio-cell. The process losses (37% w/w of input) were simulated with 80% accuracy, stressing the importance of more accurate estimates for matrix biochemical composition and actual amount of heat generated during biodegradation. Frei et al. (2004b) modelled the matrix pneumatic behaviour of their complex inverted airflow configuration for biodrying of paper and pulp wastewater. Navaee-Ardeh et al. (2006) adopted a stepwise approach to model, at an introductory level, a vertical continuous biodrying reactor for sludge drying, with perpendicular forced aeration diversified within four compartments. Bartha (2008) extensively modelled properties of a bench-scale rotary drum biodrying reactor, including its biodegradation behaviour, for process control purposes.

4. Commercial biodrying-MBT applications

Commercial, proprietary applications of biodrying within MBT plants are described. Indicative flow-sheets for some of these plants can be found in the related MBT review (Velis et al., in press). Following sections provide comparative data on operating parameters from commercial biodrying processes in full-scale plants summarised in Table 2 and Table 3. Almost all data have necessarily been collected from the grey literature supplied by process providers.

4.1. Technology provider: Eco-deco

Eco-deco is an Italian company that developed biodrying in the mid 1990s and operates 10 plant plants in Italy, the UK, and Spain with an overall capacity of ca. $900,000 \text{ Mg a}^{-1}$ (Shanks, 2007). The

core biological process is marketed as “BioCubi[®]” in Italy, and the overall plant as the “Intelligent Transfer Station (ITS)” under licence by Shanks in the UK (Juniper, 2005). Scotti and Minetti (2007) provide a recent account of the commercial reference plants of Eco-deco.

Eco-deco plant configurations differ according to the available options for outputs. They are fully enclosed and equipped with APC systems. Various process flow-lines have been described in detail elsewhere (Cozens, 2004; Environment Agency, 2007; Juniper, 2005). Waste input is shredded to ca. 200–300 mm, with the aim of homogenisation and size reduction to improve efficiency of subsequent aerobic fermentation. Biodrying occurs in an enclosed hall, with comminuted input automatically stockpiled by crane in adjoining windrows. These are divided for process control purposes into a virtual grid that provides on-line data to a computerised control system.

Air suction is applied through the waste matrix, through the vents of a pre-cast perforated floor and is directed to the APC system. The airflow rate is automatically adjusted depending on the exhaust air temperature. Various optimal temperature ranges have been reported in the literature, namely 55–70 °C (Juniper, 2005); 50–60 °C (Environment Agency, 2007); and ca. 65 °C (Cozens, 2004). Residence time within the biodrying unit is 12–15 d.

4.2. Technology provider: Entsorga

The technology is marketed as “H.E.BIO.T.[®],” (“High Efficiency Biological Treatment”) (Entsorga, Undated). Entsorga will be commissioning a MBT plant to treat $60,000 \text{ Mg a}^{-1}$ at Westbury, UK (Hill, 2005). No data on the exact process configuration and anticipated performance are yet available in the public domain.

4.3. Technology provider: Future Fuels

Future Fuels have recently applied for an international patent of a biodrying method (Hood et al., 2008), building upon pilot-scale research and development by Skourides et al. (2006). The concept uses an inclined rotating drum (“Rotary bio-dryer,” (RBD)) to process a mechanically separated organic fraction of MSW (OFMSW), potentially mixed with selected commercial waste. The RDB is operated in alternate cooling and heating cycles, using consecutive rotating and static intervals, and variable airflow rates. The process control strategy aims to keep the temperature inside the bioreactor optimised for aerobic biodegradation (upper mesophilic to thermophilic range: 40–55 °C). According to the process developers, the RDB can achieve fast and homogeneous drying of the OFMSW, reducing its MC from 35–40% w/w ar to 10–15% w/w ar within 3 d. Table 3 includes further process details.

4.4. Technology provider: Herhof

Herhof developed biodrying in 1995 (Wengenroth, 2005; Wiemer and Kern, 1994) and the first commercial plant to operate was in Asslar, Germany, in 1997 (Juniper, 2005). Herhof operates 8 plants in Germany, Italy and Belgium, with overall operational capacity ca. $1,085,000 \text{ Mg a}^{-1}$. Their processes differ slightly, to adapt to local conditions or due to evolving optimisation. Plant configurations have been described elsewhere (Diaz et al., 2002; Herhof Environmental, Undated; Juniper, 2005). The plants are fully enclosed, automated and equipped with APC systems.

Rotary shredders are used for mechanical pre-treatment (Rennrod: $< 150 \text{ mm}$; Dresden: $< 200 \text{ mm}$). Downstream a magnetic conveyor belt removes the ferrous material. The comminuted free output is biodried within air- and liquid-tight boxes (“Herhof-Rotteboxes[®]”) with capacity of 600 m^3 , receiving around 280 Mg of waste each. Filling/unloading of material and handling of

Table 2
Indicative mass balances of commercial MBT processes using biodrying reactors.

Material fraction/recovery	Process provider							
	Eco-deco		Entsorga	Herhof		Nehlsen		Wehrle Werk
	Frog Island plant	General process	Indicative process	Rennerod plant	Dresden plant	Rugen plant	Stralsund plant	General process
	(Scotti and Minetti, 2007)	(Cozens, 2004; Environment Agency, 2007; Juniper, 2005)	(Entsorga, Undated)	(Diaz et al., 2002) ^{a,b}	(Diaz et al., 2002) ^c	(Juniper, 2005) ^e	(Breuer, 2007)	(Juniper, 2005)
SRF (% w/w input)	39	ca. 53 49.5 ^f	46.0–53.5	53	50	ca. 55	50.7	ca. 35 ^g
Fe (% w/w input)	2.6	3.3	5–10 ^h	4	4	4		
Fe recovery (% w/w)				85 ^d				
Non-Fe (% w/w input)	0.3	0.4		1 ^d	1	1	2.3	
Non-Fe recovery (% w/w)				60 ^d			0.9	
CLO ⁱ (% w/w input)	11 (–8 mm)	17 (+20 mm)	5–10					
Sum of mineral fraction (% w/w input)				15	10			
Sum of mineral fraction recovery				95 ^d				
Aggregates (sand, stones, ceramics, porcelain) (% w/w input)	1.6 (+8–20 mm) ^j	5 ^j		4				
Glass (% w/w input)				4				
Batteries (% w/w input)				0.05	0.05			
Losses (CO ₂ + H ₂ O _(g)) (%w/w input)	28.4	Typical: 25 Range: 20–28	29.0–31.5	30 ^k	30 ^k	25–30	16.2	ca. 15 ^l
Liquid effluent (% w/w input)		>1						
Solid reject fraction (% w/w input)	17.5	17 (+20 mm)	10–15	4 ^m	5 ^m	15	Landfill: 22.7 WIP: 7.4	

General references are presented in the column titles. Reference to specific values are denoted by Latin letters below. APC: air pollution control. CLO: compost-like output. WIP: waste incineration plant.

^a Typical approximate values. APC residue/light reject fraction pelletised and used with SRF.

^b 70% residual (high kerbside segregation) 30% commercial.

^c Approximate values. Mass balance not closing; insufficient data. Less kerbside segregation than and advanced post-refinement compared to Rennerod. APC residue/light reject fraction pelletised and used with SRF.

^d Juniper (2005).

^e Use in cement kilns.

^f Possibly including the processed oversized trommel fraction and rich-in-plastics contaminants of the aggregate fraction.

^g Various grades.

^h Both Fe and non-Fe metals.

ⁱ Not fully stabilised. Needs further composting to CLO markets or to landfill disposal with low biodegradability.

^j Both aggregates and glass.

^k Partly re-circulated.

^l Biodrying reactor is fed with a fraction of plant input.

^m Light densimetric fraction + APC residue.

the box lid is handled automatically by crane. The biodrying reactor residence time ranges from 5 to 10 d, with 7 d the most common (Herhof Environmental, Undated; Herhof GmbH, Undated; Juniper, 2005).

The mass losses in the biodrying stage are around 30% w/w input. The initial MC of 42% is reduced to 12% after six days biodrying in the Rennerod facility. APC residue (dust) from the bag-filter (ca. 4% w/w input) is pelletised and mixed with the SRF. High effectiveness has been reported for the mechanical post-biodrying at the Rennerod-Asslar plant, with typical purity of the final “Dry Stabilat[®]” over 99%, i.e., < 1% impurities with a yield of around 50% of plant input. Recovery of the combustible mass content of the input waste is much higher.

4.5. Technology provider: Nehlsen

Nehlsen developed a biodrying process during the mid-1990s in Germany, marketed as “Mechanical–Biological Stabilisation” (MBS) and the SRF as “Calobren[®]”. The process configuration is similar to Herhof, using biodrying containers with underflow of partially circulated process air. In the past, plant capacities were lower and the mechanical refinement stage less sophisticated than other biodrying providers (Juniper, 2005). Breuer (2007) reported on recent operation experience of the Stralsund plant. This facility

is diversifying its production lines and SRF outputs to secure multiple market outlets.

4.6. Technology provider: Wehrle Werk

The Wehrle Werk system is operated on mixed MSW. It uses mechanical pre-treatment followed by percolation (“Bio-percolat”) and anaerobic digestion, aiming at easily degradable materials (Juniper, 2005). Solid residuals from the percolator are dewatered by a screw press to about 40% MC. This is fed into closed tunnel biodrying reactors with matrix circulation known as “Percotry[®]”. Output MC is reduced to below 15%. Sieving of the biodried output could produce an SRF that is around 35% w/w of input waste. Overall process losses are around 15% w/w.

5. Conclusions and recommendations

Biodrying for MBT is a versatile bioconversion process that can improve the fuel characteristics of its output, or partially biostabilise it, according to end-use. Few providers of commercial biodrying processes dominate the market, but research and development on process variations is continued. Most of this research is proprietary and has not yet reached the public domain. There are limited experimental results on the physiobiochemical fundamentals and

Table 3
Comparison of selected process elements and parameters for biodrying commercial processes.

Process feature	Process provider					
	Eco-deco (Cozens, 2004; Environment Agency, 2007; Juniper, 2005)	Entsorga (Entsorga, Undated; Hill, 2005)	Future Fuels (Hood et al., 2008)	Herhof (Diaz et al., 2002; Herhof Environmental, Undated; Juniper, 2005)	Nehlsen (Breuer, 2007; Juniper, 2005)	Wehrle Werk (Juniper, 2005) ^a
Biodrying reactor type	BioCubi [®] Windrows in enclosed hall. Downward air suction through matrix	H.E.BIO.T. [®] Enclosed hall	Rotary bio-dryer (RDB), with internal lifters: circular cylindrical drum Inclined 7° Ø 4 m Length 25 m Airflow rate Drum rotation pH of RDB input: 6.0–8.5, by recirculation of 10–20% w/w of biodried output Heating cycle for $T < 40$ °C: 30–35 m ³ h ⁻¹ Mg ⁻¹ Reactor static for 1–2 h; rotating for 10–15 min Cooling cycle, for $T > 55$ °C: 120–150 m ³ h ⁻¹ Mg ⁻¹ Reactor rotating at 0.5 rpm T: 5 thermocouples, kept within 40–55 °C Exhaust air rH	Herhof-Rotteboxes [®] Air and liquid-tight boxes. Upward blowing of circulated dehydrated air through matrix	Bio-cells, air and liquid-tight	Percotry [®] Enclosed tunnels with waste circulation
Operational variables (manipulated)	Airflow rate			Airflow rate 12 segments in bio-cell bottom ^c		
State variables (to inform control)	Exhaust air T			Heat quantity, matrix temperature, air permeability of matrix, CO ₂ exhaust concentration ca. 50 Staged approach, 40–60 ^{b,c}	Up to 70	
Biodrying unit outlet air temperature T _{out} (°C)	50–70					
Residence time	12–15 d	14 d	Aeration bay: 14–72 h RDB: 2 d: for MC reduction from 35 3 d: MC reduction to 10 OFMWS, mechanically separated from residual unsorted MSW	5–10 d	ca. 7 d	
Input to the biodrying reactor	Residual unsorted MSW					Dry residuals of MSW percolation, dewatered to MC 40% ar
Mechanical pre-treatment	Shredding 200–300 mm	Trommel	Bag splitter Primary shredding to 80–120 mm (Aeration bay) Trommel at 80 mm underflow fed to RDB Metal separation of trommel overflow and secondary shredding at 80 mm, fed to RDB	Hammermill < 200/150 mm	Shredding <300 mm Single shaft cutting mills suitable for high plastic film content ^d	
Biodrying losses (% w/w)	ca. 30			20–28 Typical 30; specific case reported 37 ^c	ca. 25 ca. 30 of input to the biodrying unit ^d	ca. 15 of plant input
Liquid effluent	<1%			Condensate treated or evaporated		
Process air management	Negative pressure Selective airflow treatment		Possible pre-heating of RBD inlet air by air-to-air heat exchanger using heat from aeration bays	Partial circulation for biodrier process air Circulation of cleaned fabric filter air Airlocks in discharge area Enclosed conveying LARA [®] RTO Fabric-filter for densimetric separation	Partial circulation of screening and refining process air after cleaning Negative pressure	
Air pollution control	Biofilter for biodrying Fabric-filter for air classification	Biofilter	Biofilter		Previously biofilter; upgraded to RTO to meet German 30th BImSchV	

General references are presented in the column titles. Reference to specific values are denoted by Latin letters below. MC: moisture content. MSW: Municipal solid waste. OFMWS: organic fraction of municipal solid waste. RBD: Rotary bio-dryer. RTO: regenerative thermal oxidation.

^a Mass balance values as percentages of plant 100% input: biodrying reactor is fed with a fraction of plant input.

^b See Section 3.10. for details.

^c Nicosia et al. (2007).

^d Stralsund plant Breuer (2007).

dynamics of biodrying reactors; and few modelling results have been published.

This said, this review provides a critique of the current state-of-the-art. Evidence suggests that effective biodrying demands different management of process control variables than composting, to fulfil different objectives. High aeration rates and limited biodegradation produce optimally biodried output, for further processing to SRF. Typical process times are 7–15 days, leading to weight loss of 25–30% w/w of the reactor input, mainly $H_2O_{(g)}$ and CO_2 . Modification of the psychrometric properties of input air and minimisation of matrix gradients for critical properties, such as MC, are crucial aspects of optimisation. Inverted air and rotary drum reactor designs can improve uniformity of treatment and output quality, but they have still to be proven on a commercial scale. Integration into the wider MBT plants flow-line deserves more attention, especially pre-conditioning for optimal airflow through the matrix.

Additional modelling efforts could explain the prevailing process dynamics and evaluate the relative role and contribution to drying of the bio-conversion vs. the physical mechanism of aeration. Process control can be improved. Suitability of state and operational process variables used for process monitoring and control respectively should be further investigated. Knowledge transfer from the traditional drying applications can be sought for both modelling and control purposes.

Research should seek to examine the possible trade-offs in process performance, enabling optimisation in line with site-specific desired output quality and wider process objectives, eventually further increasing market confidence in biodrying MBT plants.

Acknowledgements

The funding for this project is made possible by donations from Waste Recycling Group Limited through the Landfill Communities Fund of Grantscape. Additional donations have been made from the following organisations for which the project team is grateful: Biffa Waste Services Ltd, Cambridgeshire County Council, Cemex, Defra, Donarbon Ltd, Dorset County Council, Enviros, Luton Borough Council, Norfolk Environmental Waste Services, SITA, Summerlease Ltd, Sustainable Development Research Centre, Viridor and Wasteology Systems Ltd. We would like to express our gratitude to the members of the project steering group. The comments and views herein are the authors' alone.

References

- Adani, F., Baido, D., Calcaterra, E., Genevini, P., 2002. The influence of biomass temperature on biostabilization–biodrying of municipal solid waste. *Bioresour. Technol.* 83, 173–179.
- Bach, P.D., Nakasaki, K., Shoda, M., Kubota, H., 1987. Thermal balance in composting operations. *J. Ferment. Technol.* 65, 199–209.
- Barrington, S., Choinière, D., Trigui, M., Knight, W., 2002. Compost airflow resistance. *Biosyst. Eng.* 81, 433–441.
- Bartha, B.K., 2008. Entwicklung einer steuerungsstrategie für die biologische abfallbehandlung im dynamischen reaktor. In: *Development of a Control Strategy for the Treatment of Biological Waste in a Dynamic Reactor*. Ph.D. Thesis, Technische Universität Dresden, Dresden, p. 265 (in German).
- Bartha, B., Brummack, J., 2007. Investigations on the separability of dynamically dried municipal solid waste. In: Kuehle-Weidemeir, M. (Ed.), *International Symposium MBT 2007*. Hanover, Germany 22–24 May 2007, pp. 350–360.
- Basu, S., Shivhare, U.S., Mujumdar, A.S., 2006. Models for sorption isotherms for foods: a review. *Dry. Technol.* 24, 917–930.
- Binner, E., 2003. Mechanical–biological pre-treatment of residual waste in Austria. In: Dhir, R.K., et al. (Eds.), *In: Proceedings of the International Symposium, Sustainable Waste Management*. University of Dundee, Scotland, UK 9–11 September 2003, pp. 213–224.
- Brazier, K.J., 1996. Verification and Parameter Optimisation of a Simulation of Near-Ambient Grain Drying. Ph.D. Thesis, Cranfield University, Silsoe, UK, p. 224.
- Breuer, W., 2007. Experiences with the operation of the Nehlsen drying plant Stralsund. In: Kuehle-Weidemeir, M. (Ed.), *International Symposium MBT 2007*, Hanover, Germany 22–24 May 2007, pp. 128–142.
- Calcaterra, E., Baldi, M., Adani, F., 2000. An innovative technology for municipal solid waste energy recovery. In: CIPA (Ed.), *CIPA – Centro di Ingegneria per la Protezione dell' Ambiente*. CIPA, Milano, Italy, pp. 123–135.
- Chen, G., Yue, P.L., Mujumdar, A.S., 2002. Sludge dewatering and drying. *Dry. Technol.* 20, 883–916.
- Chiumenti, A., Chiumenti, R., Diaz, L.F., Savage, G.M., Eggerth, L.L., Goldstein, N., 2005. Modern composting technologies. The JG Press Emmaus, PA, USA.
- Choi, H.L., 2001. Composting high moisture materials: biodrying poultry manure in a sequentially fed reactor. *Compost Sci. Util.* 9, 303–311.
- Cozens, P., 2004. EFW – an alternative vision. In: Papadimitriou, E.K., Stentiford, E.I. (Eds.), *Biodegradable and Residual Waste Management: First UK Conference and Exhibition*. Harrogate, UK, 18–19 February 2004, pp. 464–472.
- Das, K., Keener, H.M., 1997. Moisture effect on compaction and permeability in composts. *J. Environ. Eng. ASCE* 123, 275–281.
- de Bertoldi, M., Sequi, P., Lemmes, B., Papi, T. (Eds.), 1996. *The Science of Composting: Part 1*. Chapman and Hall, London.
- de Guardia, A., Petiot, C., Rogeau, D., 2008. Influence of aeration rate and biodegradability fractionation on composting kinetics. *Waste Manage.* 28, 73–84.
- Devahastin, S., 2006. Software for drying/evaporation simulations: simprosys. *Dry. Technol.* 24, 1533–1534.
- Diaz, L.F., Papadimitriou, E.K., Savage, G.M., Eggerth, L.L., Stentiford, E.I., 2002. Selective aspects of the treatment of biodegradable waste in the European Union. In: Frederick, C.M.J., et al. (Eds.), *Proceedings 2002 International Symposium. Composting and Compost Utilisation*, Columbus, OH, USA, 6–8 May 2002, pp. 428–441.
- Diaz, L.F., Savage, G.M., 2007. Factors that affect the process. In: Diaz, L.F. et al. (Eds.), *Compost Science and Technology*. Elsevier, pp. 49–65.
- Dufour, P., 2006. Control engineering in drying technology: review and trends. *Dry. Technol.* 24, 889–904.
- Entsorga, Undated. H.E.BIO.T (High efficiency biological treatment). RS 100 HEBIOT MBT Technology – ENG revD, Entsorga Italia, Tortona, Italy, p. 18.
- Environment Agency, 2007. Eco-deco. Available at: <http://www.environment-agency.gov.uk/wtd/679004/679026/679079/973452/?version=1&lang=_e> (Retrieved: 15.09.2007).
- Epstein, E., 1997. *The Science of Composting*. CRC Press, Technomic Publishing, Lancaster, PA, USA.
- Flamme, S., 2006. The biogenic content in substitute fuels. *Biogener anteil in ersatzbrennstoffen. Aufbereitungs-Tech./Mineral Process.* 47, 40–45.
- Frei, K., Roy, G., Stuart, P., Pelletier, M.A., 2004a. Drying pulp and paper mill mixed sludges for combustion using a novel biodrying process. In: *Paper 2004: Conferences, Energy and Carbon Management*, Helsinki, Finland, 1–3 June 2004, pp. 77–84.
- Frei, K.M., Stuart, P.R., Cameron, D., 2004b. Novel drying process using forced aeration through a porous biomass matrix. *Dry. Technol.* 22, 1191–1215.
- Goldstein, N., 2006. Knowledge is power in compost process control. *Biocycle* 47, 36–40.
- Gong, Z.X., Mujumdar, A.S., 2008. Software for design and analysis of drying systems. *Dry. Technol.* 26, 884–894.
- Griffin, D.M., 1981. Water and microbial stress. In: Alexander, M. (Ed.), *Advances in Microbial Ecology*. Plenum Press, New York, pp. 91–136.
- Hall, C.W., 2007. Reviews on drying: 1982–2006. *Dry. Technol.* 25, 19–28.
- Hansjoerg, H., Boeddeker, H.-J., Gurudas, S., Schaefer, K., Roth, B., Roth, J., 2004. Process and Apparatus for Biological Drying of Residual Waste, Sewage Sludge and/or Biomass. European Patent EP1408021, 14-04-2004, European Patent Office, p. 5.
- Haritopoulou, T., Lasaridi, K., 2007. Mechanical–biological treatment experiences in Greece: problems, trends and perspectives. In: Kuehle-Weidemeir, M. (Ed.), *International Symposium MBT 2007*. Hanover, Germany, 22–24 May 2007, pp. 51–62.
- Haug, R.T., 1993. *The Practical Handbook of Compost Engineering*. CRC Press, Lewis Publishers, Boca Raton, FL, USA.
- Heering, B.M., Heering, M., Heil, J., 1999. Processing waste to useful fractions with the Herhof dry stabilization technique. *Aufbereitung von Restabfall zu verwertbaren Teilfraktionen mit dem Herhof-Trockenstabilisierverfahren. Aufbereitungs-Tech./Mineral Process.* 40, 11–18.
- Herhof Environmental, Undated. *Biological–Mechanical Waste Plant – Dresden*. Saxony, Germany, p. 12.
- Herhof GmbH, 2008. Reference Plants. Available at: <<http://www.herhof.com/en/business-divisions/stabilat/reference-plants.html>> (Retrieved: 20.11.2008).
- Herhof GmbH, Undated. *Clean Energy from Waste*, p. 14.
- Higgins, C.W., Walker, L.P., 2001. Validation of a new model for aerobic organic solids decomposition: simulations with substrate specific kinetics. *Process. Biochem.* 36, 875–884.
- Hill, D., 2005. Entsorga Set to Build the First High Efficiency Mechanical–Biological Treatment Process in Wiltshire. November 2005, Entsorga, p. 2.
- Hoffmann, B., 2005. New possibilities and limitations for the processing of waste from human settlements. *Neue möglichkeiten der aufbereitung von siedlungsabfällen und ihre grenzen. Aufbereitungs-Tech./Mineral Process.* 46, 8–29.
- Hood, P., Smith, S.R., Skourides, I., 2008. A Method and System for Treating Mixed Municipal and Selected Commercial Waste. International Publication Number: WO 2008/065452 A2, 5-06-08, World Intellectual Property Organisation, p. 17.
- Ibbetson, C., 2006. UK market development of solid recovered fuel from MBT plants. In: *Waste 2006 – Sustainable Waste and Resource Management*, Stratford-upon-Avon, UK, 19–21 September 2006, Paper 2B–15.00.
- Insam, H., de Bertoldi, M., 2007. Microbiology of the composting process. In: Diaz, L.F. et al. (Eds.), *Compost Science and Technology*. Elsevier, pp. 25–48.

- Jewell, W.J., Dondero, N.C., van Soest, P.J., Cummings, R.T., Vegara, W.W., Linkenheil, R., 1984. High Temperature Stabilization and Moisture Removal from Animal Wastes for By-Product Recovery. Final Report for the Cooperative State Research Service, SEA/CR 616-15-168, USDA, Washington, DC, USA, p. 169.
- Juniper, 2005. Mechanical–Biological Treatment: A Guide for Decision Makers, Processes, Policies and Markets. CD-ROM, v1, March 2005, Juniper Consultancy Services, UK.
- Keener, H.M., Hansen, R.C., Elwell, D.L., 1997. Airflow through compost: design and cost implications. *Appl. Eng. Agric.* 13, 377–384.
- Keener, H.M., Ekinci, K., Michel, F.C., 2005. Composting process optimization – using on/off controls. *Compost Sci. Util.* 13, 288–299.
- Kemp, I.C., 2007. Drying software: past, present, and future. *Dry. Technol.* 25, 1249–1263.
- Konovalov, V.I., 2005. Drying R&D needs: basic research in drying of capillary-porous materials. *Dry. Technol.* 23, 2307–2311.
- Krupinska, B., Strømmen, I., Pakowski, Z., Eikevik, T.M., 2007. Modelling of sorption isotherms of various kinds of wood at different temperature conditions. *Dry. Technol.* 25, 1463–1470.
- Kuehle-Weidemeier, M., 2007. The current situation of MBT in Germany. In: Kuehle-Weidemeier, M. (Ed.), *International Symposium MBT 2007*. Hanover, Germany, 22–24 May 2007, pp. 187–202.
- Leonard, A., Blacher, S., Marchot, P., Pirard, J.P., Crine, M., 2005. Convective drying of wastewater sludges: influence of air temperature, superficial velocity, and humidity on the kinetics. *Dry. Technol.* 23, 1667–1679.
- Lester, J.N., Birckett, J.W., 1999. *Microbiology and Chemistry for Environmental Scientists and Engineers*, second ed. E & FN Spon, London and New York.
- Liang, C., Das, K.C., McClendon, R.W., 2003. The influence of temperature and moisture contents regimes on the aerobic microbial activity of a biosolids composting blend. *Bioresour. Technol.* 86, 131–137.
- Lornage, R., Redon, E., Lagier, T., Hébé, I., Carré, J., 2007. Performance of a low cost MBT prior to landfilling: study of the biological treatment of size reduced MSW without mechanical sorting. *Waste Manage.* 27, 1755–1764.
- Macgregor, S.T., Miller, F.C., Psarianos, K.M., Finstein, M.S., 1981. Composting process-control based on interaction between microbial heat output and temperature. *Appl. Environ. Microbiol.* 41, 1321–1330.
- Manser, A.G.R., Keeling, A.A., 1996. *Practical Handbook of Processing and Recycling Municipal Waste*. CRC Press, Lewis Publishers.
- Marshall, M.N., Reddy, A.P., VanderGheynst, J.S., 2004. Microbial ecology of compost. In: Lens, P. et al. (Eds.), *Resource Recovery and Reuse in Organic Solid Waste Management*. IWA Publishing, London, pp. 193–224.
- Mason, I.G., 2006. Mathematical modelling of the composting process: a review. *Waste Manage.* 26, 3–21.
- Mason, I.G., Milke, M.W., 2005a. Physical modelling of the composting environment: a review. Part 1: reactor systems. *Waste Manage.* 25, 481–580.
- Mason, I.G., Milke, M.W., 2005b. Physical modelling of the composting environment: a review. Part 2: simulation performance. *Waste Manage.* 25, 501–509.
- Maunder, D., 2005. Delivering the solutions? Financing 'new technologies'. In: *Official Proceedings, Raising the Standard, CIWM Conference 2005*, Paignton, Torbay, UK, 14–17 June 2005. Thursday Conference Session 5, Paper 4, pp. 1–6.
- Menshutina, N.V., Kudra, T., 2001. Computer aided technologies. *Dry. Technol.* 19, 1825–1849.
- Miller, F.C., 1989. Matrix water potential as an ecological determinant in compost, a substrate dense system. *Microb. Ecol.* 18, 59–71.
- Miller, F.C., 1991. Biodegradation of solid wastes by composting. In: Martin, A.M. (Ed.), *Biological Degradation of Wastes*. Elsevier Applied Science, London, pp. 1–31.
- Miller, F.C., 1996. Composting of municipal solid waste and its components. In: PalmisanoBarlaz, A.C., Barlaz, M.A. (Eds.), *Microbiology of Solid Waste*. CRC Press, Boca Raton, USA, pp. 115–144.
- Mohn, J., Szidat, S., Fellner, J., Rechberger, H., Quartier, R., Buchmann, B., Emmenegger, L., 2008. Determination of biogenic and fossil CO₂ emitted by waste incineration based on ¹⁴C₂O and mass balances. *Bioresour. Technol.* 99, 6471–6479.
- Mujumdar, A.S., 1997. Drying fundamentals. In: Baker, C.G.J. (Ed.), *Industrial Drying of Foods*. Blackie Academic and Professional, pp. 7–30.
- Mujumdar, A.S., 2004. Research and development in drying: recent trends and future prospects. *Dry. Technol.* 22, 1–26.
- Mujumdar, A.S., 2007, third ed. *Handbook of Industrial Drying*. CRC Press, Taylor and Francis Group, Boca Raton, FL, USA.
- Mujumdar, A.S., Beke, J., 2003. Grain drying: basic principles. In: Chakraverty, A. et al. (Eds.), *Handbook of Postharvest Technology*. Marcel Dekker, New York, pp. 119–138.
- Nakasaki, K., Kato, J., Akiyama, T., Kubota, H., 1987a. A new composting model and assessment of optimum operation for effective drying of composting material. *J. Ferment. Technol.* 65, 441–447.
- Nakasaki, K., Nakano, Y., Akiyama, T., 1987b. Oxygen diffusion and microbial activity in the composting of dehydrated sewage sludge cakes. *J. Ferment. Technol.* 65, 43–48.
- Navaee-Ardeh, S., Bertrand, F., Stuart, P.R., 2006. Emerging biodyring technology for the drying of pulp and paper mixed sludges. *Dry. Technol.* 24, 863–878.
- Nellist, M.E., 1998. Bulk Storage Drying of Grain and Oilseeds. No. 38, September 1998, Silsoe Research Institute, Cranfield University, Silsoe, UK, p. 59.
- Nellist, M.E., Brook, R.C., 1987. Drying Wheat by Continuous Ventilation with Unheated Air in a Favourable Location. AFRC Institute of Engineering Research, Silsoe, UK, p. 18.
- Nellist, M.E., Lamond, W.J., Pringle, R.T., Burfort, D., 1993. Storage and Drying of Comminuted Forest Residues. AFRC Silsoe Research Institute, Silsoe, UK, p. 82.
- Neubauer, C., 2007. Mechanical–biological treatment of waste in Austria: current developments. In: Kuehle-Weidemeier, M. (Ed.), *International Symposium MBT 2007*. Hanover, Germany 22–24 May 2007, pp. 105–115.
- Nicosia, S., Lanza, P.A., Spataro, G., Casarin, F., 2007. Drawing the materials balance for an MBT cycle from routine process measures in MBT plant located in Venice. In: Kuehle-Weidemeier, M. (Ed.), *International Symposium MBT 2007*. Hanover, Germany 22–24 May 2007, pp. 116–127.
- Pakowski, Z., Bartzak, Z., Strumillo, C., Stenstrom, S., 1991. Evaluation of equations approximating thermodynamic and transport properties of water, steam and air for use in CAD for drying processes. *Dry. Technol.* 9, 753–773.
- Parde, S.R., Jayas, D.S., White, N.D.G., 2003. Grain drying: a review. *Sci. Aliment.* 23, 589–622.
- Pereira, C.J., 2005. Practical experience with MBT in emerging nations – example Brazil. In: Kuehle-Weidemeier, M. (Ed.), *International Symposium MBT 2005*. Hanover, 23–25 November 2005, pp. 42–50.
- Pires, A., Martinho, M.G., Silveira, A., 2007. Could MBT plants be the solution of fulfil landfill directive targets in Portugal? In: Kuehle-Weidemeier, M. (Ed.), *International Symposium MBT 2007*. Hanover, Germany, 22–24 May 2007, pp. 63–72.
- Pommier, S., Chenu, D., Quintard, M., Lefebvre, X., 2008. Modelling of moisture-dependent aerobic degradation of solid waste. *Waste Manage.* 28, 1188–1200.
- Rada, E.C., Ragazzi, M., Panaitescu, V., Apostol, T., 2005. An example of collaboration for a technology transfer: municipal solid waste biodyring. In: Margherita di Pula, S. (Ed.), *Proceedings Sardinia 2005*. Tenth International Waste Management and Landfill Symposium. Cagliari, Italy, 3–7 October 2005, Paper 044.
- Rada, E.C., Franzinelli, A., Taiss, M., Ragazzi, M., Panaitescu, V., Apostol, T., 2007a. Lower heating value dynamics during municipal solid waste biodyring. *Environ. Technol.* 28, 463–469.
- Rada, E.C., Ragazzi, M., Apostol, T., Panaitescu, V., 2007b. Critical analysis of high moisture MSW biodyring: the Romanian case. In: Kuehle-Weidemeier, M. (Ed.), *International Symposium MBT 2007*. Hanover, Germany, 22–24 May 2007, pp. 440–551.
- Ragazzi, M., Rada, E.C., Fortarel, L., Antolini, D., 2007. Co-biodyring of municipal solid waste and sludge. In: Margherita di Pula, S. (Ed.), *Proceedings Sardinia 2007*. Eleventh International Waste Management and Landfill Symposium, Cagliari, Italy, 1–5 October 2007, Paper 015.
- Raninger, B., Bidlingmaier, W., Rundong, L., Qi, W., 2005. Management of municipal solid waste in China – mechanical–biological treatment can be an option? The Sino-German RRU-BMW research project to apply BMWM within the framework of waste management related policies. In: Kuehle-Weidemeier, M. (Ed.), *International Symposium MBT 2005*. Hanover 23–25 November 2005, pp. 72–88.
- Regan, R., Jeris, A.S., Bassar, R., McCann, K., Hudek, J., 1973. Cellulose Degradation in Composting. EPA-R3-73-029, PB 215 722, USEPA, Washington, DC, USA, p. 142.
- Richard, T.L., 2004. Fundamental parameters of aerobic solid-state bioconversion processes. In: Lens, P. et al. (Eds.), *Resource Recovery and Reuse in Organic Solid Waste Management*. IWA Publishing, London, pp. 262–277.
- Richard, T.L., Choi, H.L., 1997. Optimizing the composting process for moisture removal. *Kor. J. Animal Sci.* 39, 446–456.
- Richard, T.L., Silva, T., Hamelers, H.V.M.B., Veeken, A., 2002. Moisture relationships in composting processes. *Compost Sci. Util.* 10, 286–302.
- Richard, T.L., Veeken, A.H.M., De Wilde, V., Hamelers, H.V.M., 2004. Air-filled porosity and permeability relationships during solid-state fermentation. *Biotechnol. Progr.* 20, 1372–1381.
- Roy, G., 2005. Modélisation technique et économique d'un réacteur de bioséchage discontinue. Technical and Economic Modelling of a Biodyring Batch reactor. MSc. Thesis, Ecole Polytechnique de Montréal, Montréal, Canada, (in French).
- Roy, G., Jasmin, S., Stuart, P.R., 2006. Technical modelling of a batch biodyring reactor for pulp and paper mill sludge. In: CHISA 2006 – 17th International Congress of Chemical and Process Engineering. Prague, Paper H6.2 14:20.
- Scholwin, F., Kraft, E., Bidlingmaier, W., 2003. Physical properties of organic waste – a key factor for successful control of aerobic biological waste treatment processes. In: Dhir, R.K., et al. (Eds.), *Recycling and Reuse of Waste Materials*, Proceedings of the International Symposium. Dundee, UK, 9–11 September 2003, pp. 205–211.
- Schulze, K.L., 1961. Aerobic Decomposition of Organic Waste Materials. Final Report. Project RG-4180 (C5R4), National Institute of Health, Washington DC, USA.
- Scotti, S., Minetti, G., 2007. Suitability of MBT facilities in treatment of different kinds of waste. In: Kuehle-Weidemeier, M. (Ed.), *International Symposium MBT 2007*. Hanover, Germany 22–24 May 2007, pp. 220–231.
- Sesay, A.A., Lasaridi, K.E., Stentiford, E.I., 1998. Aerated static pile composting of municipal solid waste (MSW): a comparison of positive pressure aeration with hybrid positive and negative aeration. *Waste Manage. Res.* 16, 264–272.
- Shanks, 2007. The intelligent Transfer Station. A Method for the Treatment of Municipal Solid Waste. Shanks, Sistema Eco-deco, UK, p. 6.
- Skourides, I., Theophilou, C., Loizides, M., Hood, P., Smith, S.R., 2006. Optimisation of advanced technology for production of consistent auxiliary fuels from biodegradable municipal waste for industrial purposes. In: *Waste 2006* –

- Sustainable Waste and Resource Management. Stratford-upon-Avon, UK, 19–21 September 2006, Paper 2B-14.40.
- Staber, W., Flamme, S., Fellner, J., 2008. Methods for determining the biomass content of waste. *Waste Manage. Res.* 26, 78–87.
- Stanish, M.A., Schajer, G.S., Kayihan, F., 1986. Mathematical model of drying for hygroscopic porous media. *AIChE J.* 32, 1301–1311.
- Stegmann, R., 2005. Mechanical–biological pre-treatment of municipal solid waste. In: Margherita di Pula, S. (Ed.), *Proceedings Sardinia 2005. Tenth International Waste Management and Landfill Symposium*. Cagliari, Italy, 3–7 October 2005, Paper 612.
- Steiner, M., 2005. MBT in Europe: roles and perspectives. *Warmer Bull.* 102, 14–17.
- Steiner, M., 2006. MBT in Europe: roles and perspectives (part 2). *Warmer Bull.* 103, 8–11.
- Sugni, M., Calcaterra, E., Adani, F., 2005. Biostabilization–biodrying of municipal solid waste by inverting air-flow. *Bioresour. Technol.* 96, 1331–1337.
- Tchobanoglous, G., Theisen, H., Vigil, S.A., 1993. *Integrated Solid Waste Management: Engineering Principles and Management Issues*. Mc-Graw Hill, New York.
- Themelis, N.J., 2005. Control of heat generation during composting. *Biocycle* 46, 28–30.
- Thomé-Kozmiensky, K.J., 2002. Processing concepts for substitute fuels. *Aufbereitungskonzepte für ersatzbrennstoffe. Aufbereitungs-Tech./Mineral Process.* 43, 11–20.
- Tränkler, J., Visvanathan, C., Kurupan, P., 2005. Mechanical–biological waste treatment – the south-east Asian experiences. In: Margherita di Pula, S. (Ed.), *Proceedings Sardinia 2005. Tenth International Waste Management and Landfill Symposium*. Cagliari, Italy, 3–7 October 2005, Paper 617.
- Tsang, K.R., Vesilind, P.A., 1990. Moisture distribution in sludges. *Water Sci. Technol.* 22, 135–142.
- GTZ, 2003. Sector project. Mechanical–biological waste treatment. *Deutsche Gesellschaft für Technische Zusammenarbeit (GTZ), Division 44 – Environment and Infrastructure, Eschborn, Germany*, p. 87.
- VanderGheynst, J.S., Gossett, J.M., Walker, L.P., 1997. High-solids aerobic decomposition: pilot-scale reactor development and experimentation. *Process Biochem.* 32, 361–375.
- Velis, C.A., Longhurst, P.J., Drew, G.H., Smith, R., Pollard, S.J.T., in press. Production and quality assurance of solid recovered fuels using mechanical–biological treatment (MBT) of waste: a comprehensive assessment. *Crit. Rev. Env. Sci. Tech.*
- Wang, D.-C., Fon, D.-S., Fang, W., 2004. Development of SAPGD – a simulation software regarding grain drying. *Dry. Technol.* 22, 609–625.
- Ward, A.J., Hobbs, P.J., Holliman, P.J., Jones, D.L., 2008. Optimisation of the anaerobic digestion of agricultural resources. *Bioresour. Technol.* 99, 7928–7940.
- Wengenroth, K., 2005. New developments in the dry stabilate process. *Neue Entwicklungen beim Trockenstabilat-Verfahren. Aufbereitungs-Tech./Mineral Process.* 46, 14–27.
- Weppen, P., 2001. Process calorimetry on composting of municipal organic wastes. *Biomass Bioenerg.* 21, 289–299.
- Wiemer, K., Kern, M., 1994. *Mechanical–Biological Treatment of Residual Waste Based on the Dry Stabilate Method*. M.I.C. Baeza-Verlag, Witzhausen, Germany.
- Wright, P., 2002. Biodrying dairy manure. In: *International Symposium on Composting and Utilisation*. Columbus, OH, USA, 6–8 May 2002, pp. 996–1007.